# STRUCTURAL DESIGN MANUAL

## VOLUME I


CONTENTS

# TABLE OF CONTENTS

TABLE OF CONTENTS (Cont'd.)

TABLE OF CONTENTS (Cont'd.)

TABLE OF CONTENTS (Cont'd.)

TABLE OF CONTENTS (Cont'd.)

TABLE OF CONTENTS (Cont'd.)

TABLE OF CONTENTS (Cont'd.)

# PURPOSE

# TABLE OF CONTENTS

## A1.0.0 Purpose

This manual is issued to the personnel of the Structural Design Group to provide uniform methods of design and ready reference data.

The manual is controlled within the Structural Design Group. Additions, revisions, and improvement changes by the designers are encouraged. Submit all suggestions to group supervision for evaluation and incorporation into the manual.

# SCOPE

# TABLE OF CONTENTS

## A2.0.0 Scope

The information contained in this manual is separated into five basic sections:

Section A - Introduction
Section B - Structure Design
Section C - Detail Design
Section D - Loads and Requirements
Section E - Reference Data

Generally, these sections are a condensation of material published by scientific journals, aircraft and missile industries, text books, and government agencies. In addition, basic design experience and philosophy that has evolved over a period of years at the Douglas Aircraft Company has been incorporated in the manual.

Methods of analysis and the use of design curves and tables are illustrated wherever such is considered necessary. Limitations on the procedures and the range of applicability of the data are indicated wherever possible.

Not all subjects in the Table of Contents are included in the body of the manual; some sections remain to be developed in the future. New subjects will be added as the demand arises. Revisions and replacements are to be incorporated as they become necessary.

# DESIGN PROCESS

TABLE OF CONTENTS

## A3.0.0 Design Process

The structural design process can be divided into four broad classifications: (1) definition of the problem, (2) solution search and selection, (3) completion of the design, and (4) follow-on. These classifications are detailed in the accompanying Design Procedure Check List and Flow Chart.

The designer must pay particular attention to the function "Safety" under the Design Procedure Check List. At DAC, this function is considered so important that a separate manual has been created; "Engineering Safety Manual", MDC J7411, March 1977 (revised 1982), to summarize the design practices engineers are expected to follow throughout the design phase of parts, components and systems. The manual provides guidance and source material, much of it drawn from existing practices and procedures, for safety program plans to ensure that all DAC products are designed for safety in all phases throughout their intended lives.

Not shown in the Design Procedure Check List and Flow Chart, and possibly one of the more important concepts of design to grasp, is that the design procedure is an iterative process. Our academic training too often forces us into a pattern of "given" and "find". The designer function is to "find". However, unlike in the academic world, the "given" changes throughout the design phase. It is the designer's responsibility to be aware of these changes and react to them as required.

MCDONNELL DOUGLAS CORPORATION

# DESIGN PROCEDURE CHECK LIST

## DEFINITION OF PROBLEM

**A. SCHEDULE**

1. ENGINEERING
2. MANUFACTURING, PROCUREMENT
3. TEST
4. MOCK-UP

**B. APPLICABLE SPECS**

1. GOVERNMENT
2. COMMERCIAL
3. SUPERVISORY DIRECTIVES
4. DOUGLAS

**C. STRENGTH & RIGIDITY**

1. STATIC (TIME-INDEPENDENT)
   a. AIR
   b. GROUND
   c. THERMAL EFFECTS
   d. PRESSURE
   e. CONTROL REVERSAL, DIVERGENCE
2. DYNAMIC (TIME-DEPENDENT)
   a. FATIGUE
   b. IMPACT
   c. THERMAL EFFECTS
   d. CREEP
   e. VIBRATION (NOISE)
   f. PRESSURE
   g. AEROELASTIC (FLUTTER, BUFFET)

**D. AERODYNAMIC**

1. GEOMETRY (LOFTED SHAPE)
2. CONTROL SURFACE TRAVEL
3. ALLOWABLE DEFORMATION
4. TOLERANCES (GAPS, CONTOURS)
5. SEALING

**E. WEIGHT**

1. TARGET
2. DISTRIBUTION
3. GROWTH ALLOWANCE

**F. FUNCTIONAL & OPERATIONAL**

1. MAINTENANCE
   a. ACCESSABILITY
   b. STD. TOOLS & PARTS
   c. SIMPLE ADJUSTMENTS
   d. INTERCHANGEABILITY
   e. REPLACEABILITY
   f. FREQUENCY OF REPLACEMENT OR EXPECTED DAMAGE
2. WEAR
3. TOLERANCES
4. SEALING, DRAINAGE, VENTING
5. OPERATING FORCES
6. MOTIONS
7. DEFLECTIONS (TOTAL & RELATIVE)
8. HUMAN FACTORS
9. MURPHY'S LAW
10. FRICTION & LUBRICATION
11. RELIABILITY ANALYSIS
12. MANHANDLING OF STRUCTURE, HAND & FOOT HOLDS
13. ELECTRICAL BONDING

**G. ENVIRONMENTAL**

1. TEMPERATURE
2. PRESSURE
3. RADIATION, SUNSHINE
4. CORROSION, EROSION
5. ACOUSTIC
6. ATMOSPHERIC CONSTITUENTS
7. ICE, RAIN, HUMIDITY, FUNGUS
8. CHEMICAL
9. SAND AND DUST
10. EXPLOSION
11. ELECTRICAL
12. GRAVITATIONAL

**H. LIFE**

1. SERVICE LIFE
2. PART REPLACEMENT TIME

**I. SAFETY**

1. RELIABILITY CONCEPT
2. FAIL-SAFE PHILOSOPHY
3. MURPHY'S LAW
4. ESCAPE PROVISIONS
5. SPECIAL COND. (CRASH, DITCH, WIND, RADIATION)
6. PROTRUSIONS, SHARP CORNERS
7. WATER TRAPS (FREEZING)

**J. PRODUCIBILITY**

1. COST
2. QUANTITY
3. PRODUCTION RATE

**PRODUCIBILITY (CONT)**

4. ASSEMBLY SEQUENCE
5. FABRICATION METHODS
6. MATL. SELECTION AND PROCUREMENT
7. TOLERANCES
8. STANDARDS
9. PROTECTIVE & SURFACE FINISHES
10. MANUFACTURING PROCESSES
11. ACCESSABILITY
12. ADJUSTABILITY

**K. APPEARANCE**

## SOLUTION SEARCH & SELECTION

**A. OBTAIN KNOWNS**

1. USE WORK (PROJECT) BOOK PROCEDURES
2. LIST INFORMATION KNOWN
3. DESIGN CARRY-OVER
4. LITERATURE SURVEY

**B. PLAN LAYOUT**

1. DETERMINE SCOPE
2. ESTABLISH LOCAL GEOMETRY
3. RELEASE LOFT INFO REQUESTS
4. CHECK FOR CLEARANCES
5. INCLUDE COMPONENTS FROM OTHER SECTIONS

**C. DEVELOP IDEAS**

1. USE LAID-OVER LAYOUT PROCEDURE
2. USE MODELS, MOCK-UPS, TRIAL PARTS

**D. COORDINATE WITH**

1. OTHER DESIGN SECTIONS
2. TECHNICAL SERVICE SECTIONS
3. LOFT
4. MOCK-UP
5. TOOLING, PLANNING, MANUFACTURING
6. SERVICE
7. MATL. & PROCESS ENGINEERING

**E. REFINE IDEAS**

1. SIMPLIFY
2. IMPROVE
3. OPTIMIZE

**F. RECOMMEND SOLUTION**

**G. OBTAIN GO-AHEAD**

## COMPLETION OF DESIGN

**A. COMPLETE LAYOUT**

1. LAYOUT SKETCHES
2. CHECK CLEARANCES (UNDER LOAD & NO LOAD CONDITIONS) SHOW ALL POSITIONS OF MOVING PARTS
3. SHOW LOADS
4. USE SIMPLIFIED CALCULATIONS
5. PROCESS FROM MAJOR COMPONENT TO DETAIL PARTS
6. SHOW ADEQUATE DETAIL
7. RECORD DECISIONS
8. CONSIDER ASSY SEQUENCE
9. GIVE PROPOSED METHODS OF FABRICATION
10. SHOW GRAIN FLOW AS NECESS.
11. GIVE MATLS., H, T., GAGES & SPECS
12. GIVE FINISHES (MACHINE, PROTECTIVE)
13. SHOW FITS AND TOLERANCES
14. GIVE FASTENER TYPES-SIZES
15. SHOW TYPES OF WELDS
16. REFERENCE RELATED LAYOUTS
17. INITIATE ADVANCE MATL. ORDERS
18. CHECK TOPIC AND COMPONENT CHECK LISTS
19. COORDINATE

**B. OBTAIN APPROVAL**

**C. INITIATE TESTS**

**D. DRAWING RELEASE**

1. MOCK-UP
2. PRODUCT., SPEC., STD.
3. ADVANCE TO AFFECTED GROUPS
4. REQUESTED CHANGES

## FOLLOW-ON

**A. SUPPLEMENTARY ENGINEERING**

1. LISTS (LUBE, NON-STD. PARTS, INTERCHANGEABILITY
2. HANDBOOKS
3. SPEC CHANGES & DEVIATIONS (MODEL, GOVT., CONTROL)
4. INSTL. & INSPEC. INSTRUCTIONS
5. DPS REVISIONS
6. DETAIL BREAKDOWN

**B. CORRECTIONAL CHANGES**

**C. LIAISON**

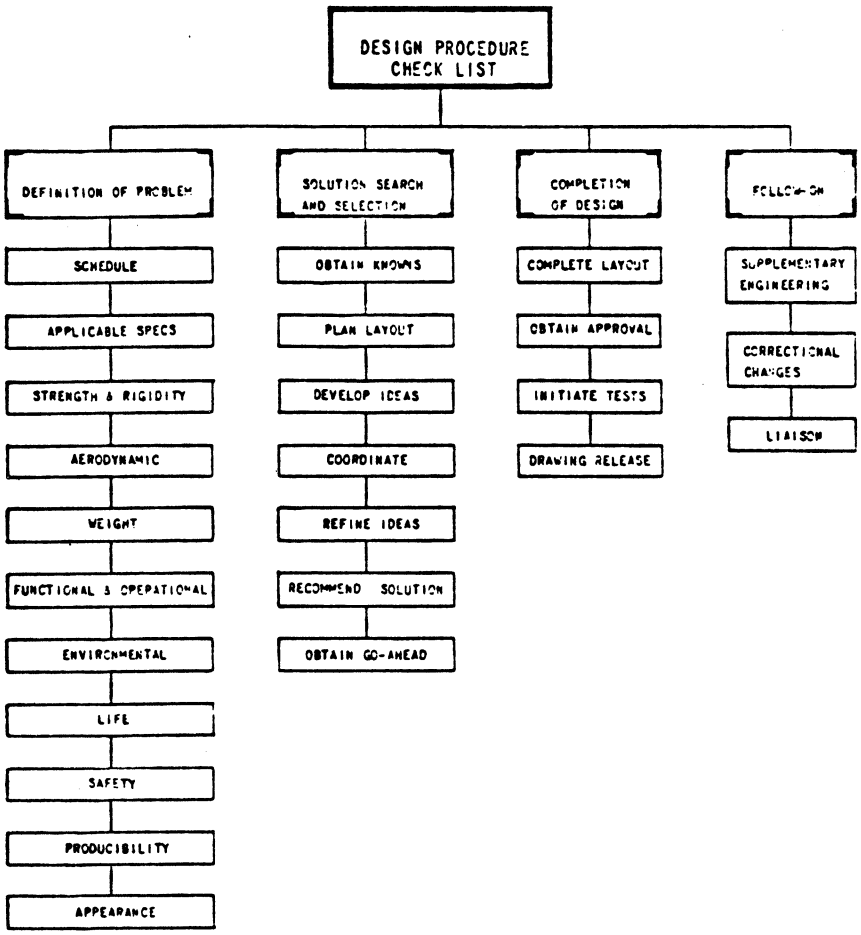
DESIGN PROCEDURE CHECK LIST
DEFINITION OF PROBLEM
SCHEDULE
APPLICABLE SPECS
STRENGTH & RIGIDITY
AERODYNAMIC
WEIGHT
FUNCTIONAL & OPERATIONAL
ENVIRONMENTAL
LIFE
SAFETY
PRODUCIBILITY
APPEARANCE
SOLUTION SEARCH AND SELECTION
OBTAIN KNOWNS
PLAN LAYOUT
DEVELOP IDEAS
COORDINATE
REFINE IDEAS
RECOMMEND SOLUTION
OBTAIN GO-AHEAD
COMPLETION OF DESIGN
COMPLETE LAYOUT
OBTAIN APPROVAL
INITIATE TESTS
DRAWING RELEASE
FOLLOW-ON
SUPPLEMENTARY ENGINEERING
CORRECTIONAL CHANGES
LIAISON

A4

# DOCUMENTATION

# TABLE OF CONTENTS

## A4.0.0 Documentation

The basic form of documentation to the designer is the layout. The function of the layout is to record on paper a complete picture of a piece of structure or assembly of parts in such a way that working shop drawings may be made.

In addition to providing the source for the detail drawings, the completed layout and the associated sketches is a design history of the particular problem it sets out to solve. As the layout develops from the first blank piece of paper to the final form, loads, stress analysis, manufacturing details, coordination and clearance problems, etc., become apparent and are indicated on the drawing.

At any future time, it should be possible to look at a layout and determine just what thinking influenced the design, what design loads were used, what coordinations were involved during the design, and the coordination requirements. When this is true, future designers working on the same part, or in the same region, will be guided as to what to look for and may have much of their coordination done for them.

It is the purpose of this section to present a systematic check list or procedure which, if followed, will help the designer increase his speed, reduce the number of false starts and omissions and, in general, improve the usefulness of his final layout.

Documentation of a structural design parallels the design process and similarly breaks down into the previously noted categories: (1) definition of the problem, (2) solution search and selection, (3) completion of the design.

## A4.1.0 Definition of the Problem

### A4.1.1 Record Book

Obtain a Technical Record Book (Form X60-1262 [4-68]) from the numbers clerk. The detail instructions on maintenance of this book are on the inside cover. You will need it immediately for all the information concerning the job, such as: reference drawing numbers, stress calculations, tolerance checks, information from vendors, and for the following definition of the problem.

A4.1.2 Statement of the Problem

A. Geometry - Within what region of the airplane is the problem located: What station numbers? What X, Y, Z dimensions are involved? Locate your space available in the airplane mockup, if one is available. What possible interferences are involved?

B. Function - What is the design required to do? How are other groups affected?

C. Weight - What is your weight allowance? Sometimes it is useful to set yourself a target weight somewhat lower than the allowance. Experience has shown that even after the layout is complete and the weight calculated, the final part in the airplane will be 3 to 5% heavier than the calculations.

D. Cost - Production design information. How many airplanes are to be made?

E. Strength - Load factors. Are loads available from Structural Mechanics Group?

F. Schedule - This is based on layouts being made as fast as possible consistent with the complexity of the design. Only by very careful work planning can this tight schedule be met. Engineering estimates are factual dates utilized by the Manufacturing Division in scheduling material, tooling, manufacturing, and final delivery of the airplane to the customer.

G. Coordinate.

A4.2.0 Solution Search

A. Choose a vellum size for your layout. Estmate what views will be needed by planning on a small sheet of paper. A few minutes spent doing this will save hours later when views won't quite fit into remaining space. In general, it has proved best to use full width, 36-inch, paper with a drawing number for the layout.

B. Accurately "spot in" on your layout vellum, all the known centerlines, station lines, contour lines, (10" grid lines, especially for wing sections), etc., that you will need. Generally, structures or mechanisms are viewed from the left-hand side of the airplane. Cross-sectional views are usually shown as viewed from aft looking forward. Scale of the layout should be as large as possible; limited only by the size of the vellum.

C. Determine approximate loading conditions and loads critical for the problem.

D. Search for the solution.

1. "Design carry-over" is fundamental in our design. The Douglas Aircraft Company sold billions of dollars worth of airplanes, entirely on the basis of our "know how". If every bit of the company's accumulated knowledge is not brought to bear on each problem, the designer is not doing his job. There are few problems on an airplane that are so new and different that some part of our past experience cannot be applied. The designer is obligated to know, before he starts his own solution, how similar problems were solved, both well and poorly, on all past commercial and military aircraft produced by McDonnell Douglas, as well as other manufacturers, where possible. Even more important than the physical solution that can be seen on current airplanes and drawings, is the "know how" to be gained by talking to the people that were involved in earlier designs. This includes service engineers, manufacturing and process people, as well as designers. Many of these men are no longer designing old aircraft parts and have moved to new jobs in other groups and other parts of the company, so it may take some leg work to find them. A few hours, or even a few days, spent chasing leads who may know something good or bad about a certain fitting or joint can be every bit as useful as sitting at table working in a vacuum. In addition, of course, to this (best) source of knowledge, the library has NACA data and technical publications and our own manuals have formalized much of this history. Every brain that can be "picked" must be expored before the designer can claim to have sufficient knowledge to solve his problem.

2. Place a generous sized sheet of sketching vellum over the layout and rough in outlines. Sketch in your first solution, selecting supporting structure consistent with loads. Determine a suitable space framework which satisfies the space and installation limitations. Sketch several rough solutions to your problem using your creative ability and ideas expressed by your supervisory engineers. A feeling of constructive discontent must be nurtured. Develop the habit of asking yourself: "How can it be done more simply?" "What other ways can we do this?" "How can we improve this?" "Can we reduce the number of parts or cost?"

3. Think in three dimensions. Many times a two-dimensional approach fails to reveal critical clearances or functional difficulties, which later may become embarrassingly apparent. Perspective sketching, clay molding, or the construction of simple cardboard or wooden models greatly aid in defining the geometry of the problem. They also save time when the problem is discussed. A good picture is truly worth a thousand words when one is trying to explain a problem so that others may offer help or when obtaining final approval.

A4.4.0 Completion of Design

Having the ideas fairly complete and approved, the designer can proceed with the layout design.

A. Put all loads on your layout as it progresses, preferably in colored pencil, with arrows showing direction of loads and points of application. This aids in visualizing the load paths and required member sizes to resist them, as well as helping to select the best attachment locations. It points up moments and eccentricities and saves time for others using your layout.

Often the Structural Mechanics Group will not have had time to obtain loads for your design problem at the time your layout is scheduled to begin. A good designer will proceed with such loads as are available, using his own short cut calculations or his supervisor's experienced guess at assumptions. More often than not, such procedure results in a design completed weeks or even months earlier, and requires only minor correction to modify it to the final loads.

Simplified methods should be used for stress calculations to determine sizes and to optimize structure for minimum weight. Calculations should not be over-refined.

Start with the major components and those that are critical for location of other parts. The designing of detail parts should not be commenced until overall structural arrangement is well along.

B. Continue the use of "laid over layout" vellum sketches to arrive at satisfactory solutions to the detail design of fittings, joints and mechanical components. These sketches, expressing several ideas on each detail, should be evaluated by yourself and design supervisor before incorporation on layout.

C. Contact other people and groups for pertinent information required to complete drawing. This requires consistent effort. Prod them to supply this information and also to keep you up to date on any changes that may affect your layout.

It is especially important, when your layout design is finished, to recheck the other design groups for changes that could affect your design.

D. Determine who will detail the design. Layout design completeness as to notes, dimensions and tolerances, design details, etc., will vary with the capabilities of the personnel who will detail your design. If you should detail it yourself, its completeness can be considerably lessened. Much time can be wasted showing unnecessary detail, such as rivets, bolts, etc. - they should be shown only where necessary for clearance checks.

E. Use colored pencils to clarify your layout drawing.

F. Institute tests, where required, to verify design decisions whether these be simple matters of geometry where a wood mockup clarifies a problem, a production matter, or a strength test.

G. Show the outlines of all surrounding parts or equipment and note clearance. Moving parts should be shown in all critical positions, and the clearances on nearby or surrounding structure or parts indicated. Deflections under applied loads where clearances may become critical should be noted.

H. List on the layout a practical sequence of assembly when the assembly consists of many parts.

I. Note the proposed method of fabrication. Consult with Production Design, Tooling Division, and Manufacturing.

J. Note the grain flow on highly stressed parts.

K. Give enough information on the layout to enable the detailer to detail the parts without any additional layout or research. Essential information includes: materials, gauges and specifications, heat treat notes, special finishes, important fits and tolerances, rivet and bolt types and sizes, type of welding, type of fittings (i.e., forging, casting), etc.

L. Make reference to all related layouts in the various sections (i.e., Structural, Mechanical, Equipment, and Power Plant) giving layout numbers and titles. Drawing numbers of the finished details should be noted on the layout of the detail by the detailer.

M. Get signatures of layout men from other groups when changes made on layouts affect them.

N. Get lofting started as soon as possible, if loft work is involved.

## A4.5.0 Layout Check List

Included in this section is a copy of the "Layout Check List". This is simply a compilation of items that, while they are small, may loom very important in the finished airplane. This list is of use to the designer when the layout is near completion. When the layout is ready for final approval, it should be checked against this list to see that these details have not been overlooked. Because this check sheet contains much information that should be recorded, the supervisor will keep a file of one such list for every layout. Copies of these sheets will be made available.

# LAYOUT CHECK LIST

DRAWING NO.:_____ TITLE:_____

DESIGNER: _____ DATE CHECKED: _____

## GENERAL:

1. Stress analysis - are loads on layout?_____ Book No._____
2. Has model, or mockup been made?_____ Photo Nos._____
3. Has test been made?_____ Test Report No._____
4. Date A.M.O._____and L.I.R._____released.

## WEIGHT ITEMS:

1. Allowance _____.
2. Are uncritical portions of structure trimmed away?
3. Can scarfs be made longer? (This usually does not cost any more.)
4. Can lightening holes be put in minimum gauge sheet?
5. Is minimum gauge a true "minimum" or is it arbitrary? Can it be less?
6. Can more "facets" be cut on machined fittings?
7. Can corners be "clipped" or "rounded"? (This often does not cost more).
8. Are thickness dimensions and angles arbitrarily set at even numbers (.125 - .250 or 90° - 45° etc.) or are they justified?
9. Actual weight _____ saving _____.

## FATIGUE ITEMS:

1. Are redundancy and multiple load paths provided in critical members? (No "single bolt" fittings?)
2. Are any eccentricities or notches present? Are they adequately protected with proper stress levels?
3. Are tapered or scalloped doublers, integral fittings, etc., used to minimize concentrations and eccentricities?
4. Are edge distances adequate? Will shop tolerances reduce edge distances to dangerous levels?

5. Every nut-plate makes three holes. Do patterns of nut-plates perforate the parts? Do not allow nut-plates to be rotated on installation allowing rivets to have inadequate edge distance. (See Structures Manual)
6. Are proper fits of bolts in holes provided.

MISCELLANEOUS ITEMS:

1. Have proper materials and heat treatment been specified?
2. Can the part, especially fatigue sensitive parts, be inspected and repaired easily?
3. Are clearances and adjustment ranges included on layout?
4. Are parts sealed against rain?
5. Is ventilation provided in closed bays?
6. Is drainage provided?
7. Will tolerances affect aerodynamic smoothness?

COORDINATION:

Are the following groups affected?

Tooling _____ Aero._____ A.C._____ Value Eng._____ Equip._____

Wt._____ Grd. Support_____ Hydr._____ Bio-Mech_____ M.C._____

P.P._____ ASM_____ Process_____ Service_____

# STRUCTURAL DESIGN PRACTICES

TABLE OF CONTENTS

## A5.0.0 Structural Design Practices

The structural design practices in this section have been generated from experience on past Douglas Aircraft designs and customer requirements. Adherence to these practices and requirements will provide improved structure with reduced life cycle costs for future designs.

Reference in this section to specific types of construction for the structural components of the airplane apply only to large transport type aircraft. These types of construction may be modified for future designs as the state-of-the-art is advanced.

## A5.1.0 General Practices

A. Where practical, structure shall be fail-safe; i.e., multiple, mutually independent load paths.

B. Where multiple load path structure is not practical, stress levels shall be established at a sufficiently low level to restrict rate of crack growth to be not critical within a stated inspection interval.

C. Structural members shall be open cross sections to facilitate attachment installation, inspection, and compartment sealing.

D. The design shall account for structural deflections of primary members such that:

   1. Secondary stresses are provided for or are not induced in adjacent structure (including preloads at installation).

   2. Interference does not occur which prevents actuation of doors or control surfaces.

E. In shear panels, fastener pattern allowables shall equal the shear strength of the thinnest attached sheet; i.e., fuselage, wing, and stabilizer skin panels.

F. Holes for pin joint fasteners shall be bushed or shall permit the installation of bushings having a wall thickness of at least .06 inch.

G. Bushing installation design shall permit the installation of oversize bushings up to .04 inch greater in wall thickness than the original.

H. Pin joints shall be designed to ensure that inadvertent rotation of bearings and bushings will not preclude proper lubrication of the pin or bearing journals.

I. To facilitate pin removal, metal-to-metal joints with single pins one inch in diameter or over, excluding pins for anti-friction type bearings, shall contain lubrication fittings and grease grooves and the pins shall be chrome plated or made of corrosion-resistant material.

J. Skin thickness and fastening system shall be selected to prevent feather edging of countersinks for attachments.

K. Fillets, fairings, and aerodynamic seals shall be removable without removing other structural components.

L. Fillet, fairing, and seal attachments shall be screw-type and chafing-protection shall be provided. (Consult with M&PE for material selection.)

M. Chafing-protection material shall be applied to the faying surface of the fixed structure for nonstructural access doors and landing gear doors and wherever seals may contact the structure. (Consult with M&PE for material selection.)

N. Chafing-protection material shall be attached to the primary structure. (Consult with M&PE for material selection.)

O. Flight control surfaces and adjacent fixed structure shall be protected from chafing. (Consult with M&PE for material selection.)

P. Edges of all fatigue critical machined parts should have .030 R ± .015; not chamfered or standard edge break.

Q. Service doors, filler caps, liquid drains, and other local ice accretion areas of the wings, fuselage, and engines shall be located and fabricated such that foreign object damage, as a consequence of ice shedding, shall be minimized.

R. Snap rings shall not be used to retain plugs, bearings and similar parts where applied load is against the snap ring.

S. Where bearings are retained by staking, the staking shall be continuous roll staking of the bearing outer race and not the housing material.

T. Alclad aluminum material will be used for all sheet stock unless machine tapering is required for weight savings or joint load transfer.

U. Locate tooling holes in non-critical areas or on tabs external to the part. Plug tooling holes when required for fatigue or damage tolerance.

V. The following will be used on new designs only with design supervision approval:

1. Cold Bonding.
2. Steel H.T. above 200,000 psi.
3. Blind Attachments.
4. Dimpled Attachments.
5. Castings.
6. Chemical Milling.
7. Flush Type Lube Fittings.
8. Welded Aluminum.
9. Spotwelds.
10. Miniature "Mickey Mouse" Type Nutplates.
11. Bolts Less than 3/16 dia. and 3/16 dia. bolts which are not in multiple bolt patterns.
12. Rivets 3/32 dia. or less (except for attaching nutplates and nutstrips).
13. Aluminum Bolts or Nuts, and Aluminum Lockbolts.
14. Tapped Holes in Aluminum.
15. Snap Rings.
16. Clip Nuts.
17. Attachments Not Listed in the Fastener Usage Policy Book for the applicable airplane model.

18. Lightening Holes Without Return Lip.

19. Teflon-Lined Bearings.

W. Shear carrying quick operating fasteners shall not be used.

A5.2.0 Structural Component Design Practices

A5.2.1 Wing Box

Wing boxes shall consist of upper and lower skin panels, front and rear spars, chordwise ribs and bulkheads, concentrated load fittings, and other members as required for local reinforcement.

A. Upper and lower skin panels shall consist of machine tapered aluminum plate stiffened with spanwise machine tapered aluminum stringers mechanically fastened to the skins.

B. Wing skin panels shall not be integrally stiffened.

C. Spars shall be built-up structures composed of machined extruded or forged spar caps (b/t values should be between 6 to 10) with separate webs and extruded stiffeners. Stiffeners shall be located, in general, on the external side of the spar webs if the box is a fuel tank.

D. Ribs and bulkheads shall be designed from machined extruded caps, and extrusion-stiffened sheet metal webs with flanged return lip lightening holes. The preferred orientation is 90 degrees to the rear spar.

E. Stringers shall be open section "Jay's" or "Zee's" for ease of attachment, installation, and inspection.

F. Stringers shall run parallel to each other to minimize shear clip configurations and parallel to one spar (usually the rear spar) to minimize runout problems, except that a "common" stringer (on which the other stringers end) shall be used aft of the front spar or forward of the rear spar to permit assembly of the skin panel outside of the tank jig.

G. All stringers shall be flanged in the same direction (preferrably forward) to facilitate skin panel installation.

H. A fused breakaway shall be provided for flap hinges, pylons, and landing gear support structure to prevent rupture of the fuel tank following an accidental contact with the ground or ground vehicles.

I. Spar caps shall be protected from fatigue damage due to discontinuities of leading and trailing edges; usually by a separate continuous doubler (attached to the spar caps with interference fit fasteners).

J. If the wing has a change in shape (i.e., thickness/chord ratio) the change shall be defined with a 5000 inch minimum radius if practical rather than a sharp break. This can eliminate mechanically formed stringers and may eliminate stringer and spar cap splices.

K. Drain holes and vent holes shall be provided in the wing box in nonfueled areas.

L. Jack points shall be provided on left and right sides, preferrably along the front or rear spar. (Coordinate with Ground Handling.)

A5.2.2 Wing Leading Edge (With Slats)

A. Leading edges shall be structurally independent of pylons and fuselage.

B. Leading edge skins shall be a minimum of .050 inch thick, stiffened with ribs approximately 6 inches on center, to resist erosion and hail damage and bird impact (4 lb.).

C. Upper leading edge skins shall be stiffened between ribs with doublers incorporating spanwise square ended beads to keep skins buckle-free at 1-1/4g wing deflections.

D. Hinged and latched non-stressed doors shall be provided on both inboard and outboard sides of slat track supports to facilitate track rigging, lubrication, and inspection.

E. For all hinged doors, hinges shall be located on the forward edge of the doors. (Airflow will move the doors toward a closed position.)

F. Stressed, screw attached, leading edge doors shall be installed on the lower surface for access to aircraft systems.

G. Pressure relief panels shall be installed in the leading edge to prevent over-pressure of the leading edge in the event of a burst pneumatic duct.

H. Leading edges shall be vented to prevent the accumulation of potentially flammable vapors.

I. Drain holes shall be located in the lower surface and periodic sealant dams shall be used to direct liquids to the drain holes to prevent a fuel leak from traversing the entire leading edge or into the fuselage.

J. Slat track support structure shall consist of pairs of ribs supporting individually replaceable lubable track roller bearings, guides, and stops.

K. Sufficient space shall be allowed between slat track support ribs (hand room) to permit roller and stop replacement and slat track adjustment.

L. Slat track fuel tank recess cans shall be large enough to provide track clearance for all possible track attitudes, including nominal misrigging. Cans shall be gravity drained of liquids.

M. Slat track stops shall be installed on both inboard and outboard sides of the track. Each single stop shall be capable of resisting the total stop design limit load at that station.

N. Slat tracks shall be interchangeable, non-handed, machined, annealed 6AL-4V titanium forgings (or equivalent) to resist corrosion.

O. Slat tracks shall have tungsten carbide hardcoat, .004 to .006 inches thick applied to the roller contact area for wear resistance.

P. Slat tracks shall contain an integral boss forward of the most forward support roller to prevent the inadvertent puncturing of the slat track tank recess can.

Q. The size of cutouts in the upper surface of the leading edge to accommodate the slat tracks shall be kept to a minimum to reduce aerodynamic drag. If cutouts are judged by Aerodynamics to be unacceptably large, spring loaded sealing doors shall be installed.

R. Chafing protection shall be installed on the upper surface of the leading edge in the area of slat trailing edges and seals. (Consult with M&PE for material selection.)

S. Track rollers shall be MS24466 double row, heavy duty sealed needle bearings, or equivalent, for main track rollers, and single row MS24465, or equivalent, for side rollers. .

T. Slat drive actuation shall be located as near to the centroid of the slat segment airload as possible, regardless of wing box rib locations.

A5.2.3 Slats

A. Slat shell shall be constructed of aluminum alloy skins supported by chordwise ribs and spanwise spars or intercostals.

B. If slat is hot air anti-iced, 2219 aluminum (or equivalent) shall be used for elevated temperatures above 250°F.

C. Machined ribs shall be employed at track support and drive stations.

D. The slat lower surface shall be installed with a minimum number of blind fasteners per the Fastener Usage Policy.

E. The minimum number of track supports shall be three per slat segment to control slat shape with respect to the deflected wing shape.

F. Slat-to-track attachment shall contain adjustment for vertical, fore, and aft directions.

G. Slats shall be aerodynamically sealed to the wing leading edge, both chordwise and spanwise when retracted.

H. Seals shall be easily replaceable.

I. Slat segments shall be individually interchangeable and contain provisions for hoisting.

J. The spanwise overhang beyond the most extreme support shall not exceed one slat chord length.

A5.2.4 Fuel Tanks (also see Section C6)

A. All overlapping surfaces of fuel tank boundary walls shall have both faying surface seals and fillet seals.

B. Multiple rows of interference fit attachments shall be installed in all tank boundary member splice joints.

C. All fasteners that penetrate the tank wall through non-interference holes shall be installed with wet sealant.

D. Stringers and stiffeners on skin panel, and spars shall be attached with machine installed fasteners to provide complete and uniform hole filling.

E. Stringers shall provide skin line drainage slots at the low point of each tank to allow complete chordwise drainage to sump areas.

F. All aluminum parts installed within fuel tanks shall be anodized and coated prior to assembly with a two-part polyurethane anti-corrosion material.

G. Load-carrying standard access doors shall generally be employed to add stiffness at high loads (deflections). The skin area removed for these doors will be replaced plus 25 percent minimum additional area along the door edges.

H. Tank access doors should be on the upper (compression) surface to the most outboard point where entry into the tank with the whole body is possible (20" box depth). Outboard of this point access doors should be on the lower (tension) surface for ease of access during maintenance.

I. Lower surface access door shall be located so that all areas within the fuel tank shall be within arms' reach to insure proper employment of assembly, sealing, and inspection practices.

J. A vapor barrier shall be provided on the fuel tank boundaries within the fuselage pressurized area.

K. Minimum skin gauges for fuel tanks shall be .080 in primary lightning strike zones to protect against lightning burn-through.

L. Safety wire and cotter pins shall not be used in fuel tanks.

A5.2.5 Fuselage

A. The fuselage shall be of semimonocoque construction.

B. Each fuselage shall be pressure checked at 1.33 times the maximum pressure relief valve setting per FAR 25.365d and 25.843a. This is limit pressure. Ultimate pressure is (1.5)(1.33)(p) = 2p.

C. Minimum diameter of rivets in pressurized skins is 5/32 inch., unless otherwise approved by design supervision. Rivets under

this diameter do not swell to fill the holes which can create a fatigue problem.

D. A jack point shall be provided near the forward end of the fuselage and at the cabin aft pressure bulkhead.

E. Pressure relief provisions shall be provided between pressurized fuselage compartments, unless it can be shown that adequate structural strength exists to accommodate the maximum differential pressure load due to an opening in the shell.

F. The pressure relief provisions shall be located to not interfere with passenger seating, routine maintenance or cargo loading. They shall be permanently attached to the structure.

G. The pressure relief provisions shall be located to preclude collection of dirt and debris.

H. If exterior skin lap splices are used, forward sheets of single lap lateral splices shall overlap the aft sheet.

I. If exterior skin lap splices are used, the upper sheet of single lap longitudinal splices shall overlap the lower skin.

J. Seals along the lower centerline shall be Skydrol resistant.

K. The main cabin aft pressure bulkhead shall be a flat design if it contains an access or passenger door.

A5.2.6 Fuselage Doors

A. Pressurized doors shall withstand internal air pressure in flight and external water pressure during ditching.

B. Doors shall be designed for twice cabin differential pressure as an ultimate load.

C. Doors shall be tested on the aircraft at 1.33 times maximum pressure relief valve setting, including tolerance.

D. Seals shall preclude the entry of rain water with the cabin unpressurized.

E. Doors and door jambs shall contain drain provisions to prevent the accumulation of fluids which might freeze and hamper safe door actuation.

F. A vent door system shall be provided for all outward opening cargo doors to prevent pressurization of the aircraft until the door latching system is safely locked.

G. Barrier nets shall be installed at cargo doorways to restrain loose cargo where displacement of cargo could prevent the door

from being opened. These nets are the responsibility of Mechanical Engineering.

H. Cargo doors shall have jambs free of protuberances and sharp corners which might damage cargo or injure personnel.

I. The cargo compartment door sill shall be flush with, or lower than, the flat portion of the compartment floor.

J. Support structure shall be provided for "Door Closed and Latched" switches at all pressurized fuselage doors, including the entrance doors, service doors, cargo compartment doors, access, and emergency doors.

K. Switch supports shall be located to permit switch adjustment or removal without disassembly of adjacent structure.

L. The switch location shall be chosen to preclude collection of dirt, moisture, snow, or other contamination.

M. Drain gutters, or equivalent, which will prevent water or other drainage from dripping onto the passenger entryway, shall be installed above passenger doors.

N. In so far as practical, the design of cargo doors shall include protection of door, door jamb, switches, and operating mechanisms from damage by cargo or cargo loading systems.

O. The door operating mechanism shall be replaceable without disassembly of permanent door or fuselage structure.

P. Access shall be provided for lubrication and rigging of the door operating mechanism, including limit switches.

Q. Door seals shall be designed and located to minimize damage from normal service and shall be attached by mechanical means which will permit rapid replacement of the seal. Seals should be installed on the door if practical.

R. Scuff plates shall be provided at passenger entry and cargo door openings.

S. The scuff plates shall be designed to protect jamb and adjacent fuselage skin up to the upper tangent point of lower corner radius.

T. Scuff plate attachments shall be screws.

U. Screw spacing at the scuff plate edges shall be designed to ensure aerodynamic smoothness.

V. Sealant shall be used in the scuff plate faying surface.

W. All external doors using handles or lever-type latches for operating or securing purposes will be designed so that the handle or lever cannot be stowed in its recessed position unless the door is closed and properly latched.

X. External recessed handles for pressurized doors shall be designed to remain recessed when the door is closed, latched, and under pressure.

Y. All cabin doors should have adjustable hinges (for rigging purposes).

A5.2.7 Floors

A. Floor panels shall be sandwich construction composed of fiberglass, graphite-epoxy or aluminum face sheets stiffened with a Nomex honeycomb core.

B. Individual floor panels shall be interchangeable.

C. Inserts shall be flush with the upper surface of the panel.

D. Panels shall not be "layered" such that the removal of one panel requires the removal of, or rework to, an adjacent panel.

E. Panels shall be secured to the substructure by screws installed through clip nuts. The clip nuts shall be nylon coated (or equivalent) to prevent scratching of the structure when the clip nuts are installed.

F. Fiberglass or graphite-epoxy face sheets shall be used in walkways, entrances, and under galleys and lavatories for corrosion resistance.

G. Additional mylar sheets shall be used over the floors under galleys and lavatories.

H. Faying surface seal with a parting agent on the panels shall be installed between the floor panels and the supporting structure.

I. Edges of adjacent panels shall be butt sealed with low adhesion sealant over nylon stripper cord. (End of cords at panel corners.)

J. Attaching screws shall be installed with wet sealant.

K. A design goal shall be commonality of panel assemblies and maximum size panels to reduce the number of seams.

A5.2.8 Cargo Compartment Liners

A. Liners shall be sheet laminated fiberglass, thick enough to resist cargo handling damage.

B. Liner materials shall be fire resistant.

C. Liner panels shall be replaceable.

D. The joints between adjacent liners shall be sealed with tape to attain an FAR Class D cargo compartment air leakage limitation.

A5.2.9 Transparencies (Windows) (also see Section B12)

A. Flight Compartment

1. The visibility envelope shall be established in accordance with FAR 25.

2. The forward windshields and clearview windows shall be designed to provide sufficient up-vision when banking the airplane that overhead windows are not required.

3. A minimum of twenty degrees unobstructed over-the-nose down-vision from the design eye position shall be designed into the windshields.

4. The parked windshield wipers shall not obstruct pilot's down-vision during approach and landing.

5. There shall be a minimum of seven inches head clearance from the design eye position to the posts and ceiling.

6. A two-panel windshield shall be installed.

7. Each windshield panel shall be of glass and plastic interlayer material laminated construction.

8. The windshield, together with its supporting structure, shall withstand, without penetration, the impact of a four-pound bird at an airplane speed of $V_{cruise}$ at sea level per FAR paragraph 25.775.

9. Anti-icing of the windshields shall be accomplished by electrical heating.

10. Separate automatic temperature controls shall be provided for each windshield.

11. Redundant internal sensing elements for the windshields shall be provided.

12. For each electrical coating bus bar, there shall be a minimum of two attachments for anti-icing.

13. Exposed interior surfaces of the fixed windshield panels will be scratch-resistant.

14. Anchor nuts will be used for windshield attachment and nut elements will be individually replaceable without removal of instrument panels or control columns.

15. The windshield shall be designed for dispatch for speeds to $V_{Cruise}$ at sea level with windshield heating inoperative and with either anti-icing or defogging pane cracked.

16. The cockpit trim in the area of the windshield will be removable and replaceable to permit anchor nut replacement.

17. Provisions for hoisting the windshield panels and fixed windows will be incorporated in the design.

18. The windshield and window seals shall be dry gasket types designed to prevent pressurization leaks and prevent water from entering the flight compartment.

19. The windshield and window seals shall provide smooth aerodynamic surface.

20. It shall be possible to replace a front windshield or fixed window panel within a period of two hours, using two men.

21. All windshield and fixed window flush head attaching screws of a given diameter shall be the same length.

22. Each windshield and each cockpit window shall be designed and manufactured for a minimum of 6,000 hours service life.

23. Defogging of the windshields and clearview windows shall be accomplished by electrical heating.

24. Two openable clearview windows shall be installed, one on each side adjacent of the windshields per FAR paragraphs 25.771, 25.773, and 25.775.

25. Each clearview window panel shall be of laminated stretched acrylic construction.

26. A wire heating element grid system shall not be used as a means for defogging in any window.

27. Internal sensing elements in the clearview window shall be redundant.

28. Separate automatic temperature controls shall be provided for each clearview window.

29. Each clearview window shall be designed for dispatch with speeds up to $V_{Cruise}$ at sea level with defog heat inoperative.

30. The opening mechanism shall be designed to prevent the clearview window from rubbing the interior lining when translating.

31. Each clearview window shall provide sufficient opening size to provide emergency exit per FAR 25.

32. Two fixed windows, aft of and adjacent to the clearview windows, shall be provided.

33. Each fixed window shall be of laminated stretched acrylic construction.

B. Cabin Windows

1. The windows shall be approximately 10 x 14 inches spaced between frames.

2. Main cabin entrance doors shall have viewing panels approximately seven inches in diameter.

3. The window seal design will limit fogging, frosting, staining, and accumulation of dirt and dust on the surfaces between the panes.

4. The window design will incorporate a dry seal.

5. To prevent leakage and extrusion into the windstream, the seal will be fabricated from materials which have demonstrated resistance to environmental deterioration.

6. The windows will be double pane construction, with either pane capable of carrying full pressurization loads to meet FAR fail-safe requirements.

7. The outer pane will be designed as the primary load-carrying panel by placing a .098 inch diameter hole in the inner pane.

A5.2.10 Control Surface Design

The design of control surfaces or slats and wing flaps shall be such that the aircraft may continue safe flight with any single hinge support failed. Where this is not practical, redundant or damage tolerant, fail-safe design must be used.

The following is a list of design features required for flaps, slats, and control surfaces. These design concepts have been established from past service experience and from acoustical development tests. Although all items apply to metallic construction, many of the items will also apply to composite construction.

A. Formed ribs, skins, and doublers shall be made from 2024 material (or equivalent) for best resistance to fatigue due to jet engine and boundary layer noise.

B. Principal bending material structure, such as spar caps, spar webs, leading edge stringers, and aft closing channels shall be made from 7075 (or equivalent) material (because of the higher allowables).

C. For rib-stiffened skin designs, the scalloped bonded doubler design shall be used for the aft skin panels (see Section D4.3.1.2).

D. Beads or pillows shall not be used in formed ribs, since cracks develop early at the bead ends when they are subjected to moderate-to-severe acoustic noise environment.

E. For acoustic fatigue resistance, flange bend reliefs are not to be used. Separate attach angles shall be used to avoid bend reliefs.

F. Integrally formed rib flanges contacting the skins shall be the return lip type to provide improved skin acoustic fatigue resistance.

G. Angle clips and attach angles, such as rib-to-spar attachment, shall be made from extrusions for acoustic fatigue resistance.

H. Sufficient clearance shall be provided at spar and aft closing channel to permit moving the aft ribs forward or aft in the assembly jig for contour adjustment. Sufficient edge distance must be provided for attachments at the spar and closing channel to accommodate this movement. Movement of ± 1/8 inch is usually considered adequate; however, this should be checked with Tooling Department involved.

I. Spacing of the aft ribs is established by acoustic fatigue requirements (see Section D4.3.1.2) where minimum gauge skin and doublers are used (.016 skin and .012 doubler). A rib spacing of approximately 5 inches should be used.

J. The closing channel forward of a trailing edge cutout, such as for tabs, should extend approximately two rib-bays beyond the ends of the cutout. (This has been an area of fatigue problems on previous airplanes.)

K. Shrouds should be provided around tab push-rods to prevent the end of a broken push-rod from jamming the surface.

L. Tab hinges should be flexible in a spanwise direction to prevent induced axial hinge loads from control surface bending. The side load should be taken at the horn-hinge point.

M. The horns for operating tabs shall be enclosed in fairings on the fixed structure of the surface. This eliminates two-piece sliding fairings which could cause friction, become damaged, and jam the surface, or collect moisture and freeze together. The fairings should be located on the upper surface to prevent collecting moisture which may freeze.

N. The trailing edge "V", except on honeycomb tabs, shall be designed from fiberglass to resist impact loads and provide for easy repairs. These members shall be attached by bonding and riveting.

O. The hinge bearings for surfaces shall be the integral eye-bolt type and shall be removable without removing the surface. The hinge line shall be forward of the spar to permit the hinge bolt to be easily removed. Access doors shall provide for bearing removal.

P. The hinge eye-bolts are designed with the threads on the shank approximately 1/16 smaller in diameter than the shank. This is used as a gauge of permissable hinge and hinge support misalignment. If the threads of the eye-bolt can be easily installed, it is permissible to draw the hinge support into alignment by torqueing the nut on the eye-bolt. The "A" frame hinge supports must be analyzed for loads resulting from this deflection.

Q. One hinge support shall be designed to resist side load; the other supports shall be flexible in the spanwise direction.

R. Special bushings shall be used at all control surface hinge points. These bushings are designed to have a minimum of 3/32 radial shoulder contact area on the lugs. Bushings with less contact areas have caused service problems by brinelling the aluminum lugs when the hinge bolt is torqued. Special large diameter steel washers shall be used under bolt head and nut at bushed hinge joints to provide a minimum of 3/32 radial bearing area around the bushed hole.

S. The control surfaces are weather sealed at all external seams and joints, and drain holes are added in the lower surface at the inboard forward and aft corners of each bay, which could trap moisture from leakage or condensation. The sealing is controlled by DPS and the drain holes are called for on the Assembly Drawing.

T. The attachment of the mass balance weights shall be designed and tested for loads (per FAR or Mil-A-8866) normal to the control surface hinge line. For commercial aircraft, this load is usually 60 g's.

U. Return lip lightning hole flanges shall be on the opposite side of the rib web from return lip rib cap flanges to prevent damage to the lightning hole flange when drilling and upsetting rivets through the cap flange.

V. The design requirements for wing flap and primary flight control surface fail-safe hinge supports follows: (The design goal is 120,000 hours and 100,000 landings which is twice the service life goal.)

Requirements for the areas noted in Figure A5.2.10-1 are as follows:

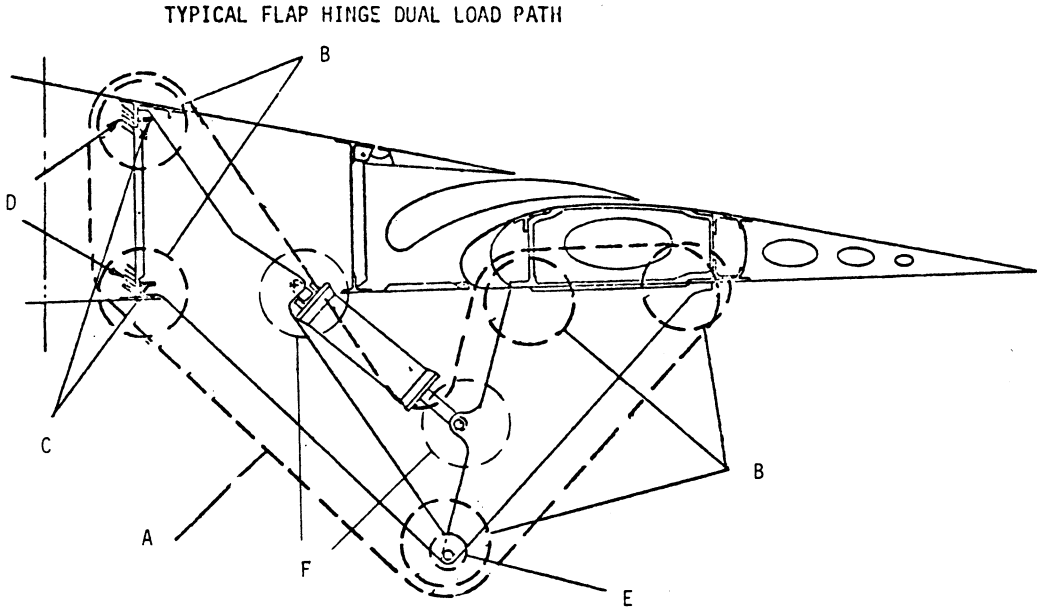


Figure A5.2.10-1 Flap Hinge Bracket

1. Area (A) Fitting:

   a. Dual load path - no failure

| | |
|---|---|
| Design ult. load | = limit x $1.5^{(1)}$ x $1.15^{(2)}$ |
| Allowable | = material ult. or 1.5 x yield |
| Fatigue condition | = fatigue spectrum (no factor) |
| Goal | = fatigue stress at 120,000 hrs. and 100,000 landings for average scatter on s-n curve |

   b. Dual load path - one path failed

(1) Factor of safety.
(2) Fitting factor.

Fail-safe ult. load = limit x 1.15(2)

Allowable = material ultimate

2. Area (B) Fitting:

   a. If single load path - no failure

      Design ult. load = limit x 1.5(1) x 1.25(3)

      Allowable = material ult. or 1.5 x yield

      Fatigue condition = fatigue spectrum (no factor)

      Goal = fatigue stress at 120,000 hrs. and 100,000 landings for average scatter on s-n curve

3. Area (C) Attach Bolts:

   a. Breakaway on wheels-up landing

      Design ult. load = limit x 1.5 x 1.25

      Allowable = material ult.

4. Area (D) Wing Tank Side of Joint

   a. No failure when area (C) fails

      Design ult. load = limit x 1.5 x 1.25 x 1.15(4)

      Allowable = material ult.

5. Area (E) Bearing:

   Spherical bearing considered anti-friction

   Static means no rotation

(1) Factor of safety.

(2) Fitting factor.

(3) Special factor in lieu of 1.15 fitting factor.

(4) Breakaway factor.

Dynamic means during rotation

| | |
|---|---|
| Static des. ult. load | = limit x 1.5 x 1.25 |
| Ult. static allowable | = manufacturer's static allowable x 1.5 |
| Dynamic des. load | = limit |
| Dynamic allowable | = 2/3 manufacturer's static allowable or life data if available for 50,000 flight cycles |

TFE lined spherical bearings: max $f_{br}$ for outer race projected area at limit load = 10,000 psi static and dynamic.

All-metal lubricated spherical bearing max $f_{br}$ for outer race projected area at limit load

Bronze outer race

Static } = 30,000 psi
Dynamic }

Steel outer race

Static = manufacturer's static allowable

Dynamic = 30,000 psi

6. Area (F) Drive Cylinder Attachment:

| | |
|---|---|
| Design ult. load | = limit x 1.5 x 1.25(5) x 1.15 or cylinder piston area x max. relief valve setting x 1.5 x 1.15 |
| Allowable | = material ultimate or yield x 1.5 |

(5)Hinge moment factor per FAR 25.395.

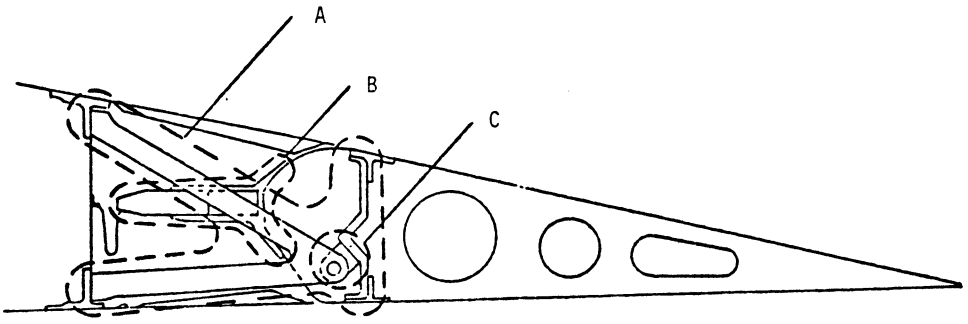


Figure A5.2.10-2 Primary Flight Control Surface Hinge

Requirements for the areas noted in Figure A5.2.10-2 are as follow:

1. Area (A) Frame and Hinge Fitting - Single Load Path:

   a. Single load path - no failure

| | |
|---|---|
| Design ult. load | = limit x 1.5 x 1.25 |
| Allowable | = material ult. or 1.5 x yield |
| Fatigue condition | = fatigue spectrum (no factor) |
| Goal | = fatigue stress at 120,000 hrs. and 100,000 landings for average scatter on s-n curve |

   b. Single load path - one hinge failed

| | |
|---|---|
| Fail-safe ult. load | = limit one hinge failed load x 1.15 |
| Allowable | = material ultimate |

2. Area (A) Frame and Hinge Fitting - Dual Load Path:

   a. Dual load path - no failure

| | |
|---|---|
| Design ult. load | = limit x 1.5 x 1.15 |
| Allowable | = material ult. or 1.5 x yield |
| Fatigue condition | = fatigue spectrum (no factor) |

Goal = fatigue stress at 120,000 hrs. and 100,000 landings for average scatter on s-n curve

b. Dual load path - one hinge failed

Fail-safe ult. load = limit x 1.15

Allowable = material ultimate

3. Area (B) Balance Weights and Attach:

a. Design ult. load = 60g's x wt.

Allowable = material ult. or 1.5 x yield

4. Area (C) Eye-Bolt Bearing (self-aligning roller) - Single Load Path Static means No Rotation; Dynamic Means during Rotation

a. No failure

Static des. ult. load = limit x 1.5 x 1.25

Ult. static allowable = manufacturer's static nonbrinell allowable x 1.5

Dynamic design load = limit spectrum load

Dynamic allowable = 2/3 manufacturer's static allowable or life data if available for 50,000 flt. cycles

b. One hinge failed

Design ult. load = limit load for one hinge failed x 1.15

Ult. allowable = manufacturer's static nonbrinell allowable x 1.5

5. Area (C) (Dual Load Path):

a. No failure

| | |
|---|---|
| Static des. ult. load | = limit x 1.5 x 1.15 |
| Ult. static allowable | = manufacturer's static nonbrinell allowable x 1.5 |
| Dynamic design load | = limit spectrum load |
| Dynamic allowable | = 2/3 manufacturer's static allowable or life data if available for 50,000 flt. cycles |

b. One load path failed

| | |
|---|---|
| Fail-safe ult. load | = limit x 1.15 |
| Allowable | = manufacturer's static nonbrinell allowable x 1.5 |

6. For Drive Cylinder Attachment (bolt and lug):

| | |
|---|---|
| a. Static des. ult. load | = limit x 1.5 x 1.25 x 1.15 or cylinder area x max pressure relief valve setting x 1.5 x 1.15 |
| Allowable | = material ult. or 1.5 x yield |

A5.2.11 Pylons (Wing)

(Note: Fuselage mounted pylons, DC-9 style, are similar.)

A. The pylon shall be a box beam structure suspended from the wing to support the engine.

B. Pylon structure shall be non-handed with wing contour differences between LH and RH side accommodated by separate fairings.

C. Pylon design shall satisfy both strength and stiffness requirements.

D. Pylon-to-wing attachment shall be such that pylon deflections shall not induce secondary stresses in wing structure.

E. Pylon-to-wing attachment shall be fail-safe and shall allow for easy pylon removal and replacement following engine removal.

F. Materials for the pylon shall consider temperature and corrosion resistance in an elevated temperature environment.

G. The lower spar of the pylon shall be the primary firewall protecting the wing and pylon structure from the engine fire zone. This firewall shall be light-tight, vapor-tight, and capable of withstanding a 2000°F flame for 15 minutes (.025 titanium or .016 stainless steel will accomplish this).

H. Engine mount fittings below the firewall shall be designed to withstand fires and engine induced temperatures.

I. Engine to engine-mount fittings shall be attached with tension bolts in 1/16 diameter over size holes to facilitate engine removal and replacement. There shall be no more than one shear pin or shear carrying bushing.

J. Engine mount bolts shall assist in engine alignment during installation.

K. Drain paths and sealing shall be provided in the pylon so that liquids drain overboard and not onto the engine.

L. The pylon shall be vented to expel any potentially flammable vapors.

M. Access panels shall be provided to systems within the pylon structure and to the wing-to-pylon attachments.

N. There shall be a secondary fire barrier between the pylon and the wing structure to protect the wing if the primary firewall is penetrated by engine disintegration.

O. The pylon and its attachment to the wing shall be designed such that, in case of a wheels-up landing or ground accident, the engine and/or pylon will separate from the wing without rupture of the fuel tank.

P. The pylons shall contain provisions for the attachment of a "boot-strap" engine hoist.

Q. The pylons shall contain pressure relief panels which will prevent over-pressure within the pylon in the event of a burst pneumatic duct.

A.5.2.12 Empennage Structure

In general, most of the requirements for wing box structure and wing leading edge structure apply except that:

A. The horizontal stabilizer skin panel shall be integrally stiffened machine tapered from stress corrosion resistant material unless damage requirements dictate separate skin and stringers (military transports). Then requirements of Section A5.2.1A and E and G apply.

B. For low tails, the vertical stabilizer may be multi-spar construction.

C. The empennage structure must be designed to assure capability of continued safe flight and landing of the airplane after impact with an 8 pound bird, per FAR 25.631.

A5.3.0 Detail Design Practice

A5.3.1 Welding

A. Spotwelding shall not be used in joints of primary or secondary aircraft structure.

B. Structural seam welding is permitted in 6061 aluminum alloy for complex contours of wing tips and fairings, but is not allowed in load-carrying applications.

C. Welding of steel and titanium is permitted in structural applications, but each welded assembly is required to undergo a 100% limit load proof test to qualify the weld.

D. Welded steel tubular structure shall be fabricated of chrome molybdenum alloy, or equivalent, and internally treated or hermetically sealed against corrosion.

A5.3.2 Fastener Usage (also see Section C1)

A. To minimize the types of fasteners and their installation variables, the appropriate "Structural Fastener Usage Policy" shall be used. A separate fastener usage policy shall be provided for each project.

B. Bolts, screws, lockbolts, and Hi-Lok type pins used in structural applications shall have a minimum ultimate tensile strength of 160 ksi.

C. High-strength tension bolts which are not torqued to a high preload (nonfatigue-critical applications), shall be 220-240 ksi UTS, H-11 steel, cadmium plated.

D. High-strength tension bolts which are torqued to a high preload for fatigue critical applications or are subject to high temperatures shall be 180-200 ksi UTS, unplated Inconel 718.

E. High-strength shear bolts shall be 132 ksi minimum ultimate shear strength H-11 steel diffused nickel-cadmium plated.

F. 3/16 diameter, or larger, permanently installed bolts, screws, lockbolts, and Hi-Lok type pins of 160-180 ksi UTS shall be 6A1-4V titanium unplated.

G. Threaded fasteners less than 3/16 diameter shall not be used in structural applications.

H. Access door flush-head screws shall be A-286, 160-180 ksi, tension head, cadmium plated, in aluminum alloy structure.

I. Thickness of material being countersunk shall preclude "knife edges".

J. Dimples shall not be used for aluminum alloys.

K. Shear-carrying, quick-disconnect fasteners shall not be used.

L. Lockbolts and Hi-Lok type pins shall be installed in interference fit holes in aluminum structure. See Drafting Manual and Fastener Usage Policy for other material.

M. For clearance fit applications, bolts and screws shall be used.

N. For general usage, dry film lubricated, alloy steel nuts shall be used.

O. Miniature nutplates shall not be used.

P. Nutplates and gang channels shall be of the replaceable nut element type.

Q. Use of "DD" (2024) type rivet shall be avoided.

R. NAS 446 type nuts and sheet metal screws shall not be used.

S. Attachments for wing-to-fuselage fillet fairings shall not penetrate fuel tanks.

T. The use of blind fasteners shall be avoided wherever possible.

U. When blind fasteners are used, positive locking features shall be demonstrated.

V. Blind rivets shall employ corrosion resistant stems.

W. Jo-bolts and riv-nuts shall not be employed.

X. Blind rivets shall not be employed in engine inlets. Nuts and bolts shall not be used in inlets wherever they may loosen or fail and then be ingested.

Y. The design shall permit machine installed rivets wherever possible for uniformity of hole preparation and hole filling.

Z. All bolted connections shall provide self-locking features.

AA. All permanent fasteners shall permit the installation of oversize salvage fasteners.

BB. For fasteners in graphite composites:

1. Aluminum alloy or cadmium plated steel fasteners shall not be used.

2. A ply of fiberglass shall be incorporated into the laminate along the fastener row to provide galvanic isolation to the substrate.

3. Interference fit fasteners shall not be used.

A5.3.3 Structural Joints (also see Section C2)

A. The design goal shall be the fewest possible structural joints.

B. The design goal shall be to design and verify by test all joints to a life equal to, or greater than, that of the unjoined structure.

C. The joint shall be designed such that crack initiation occurs away from the joint and shall be easily detectable.

D. Where possible, joining members shall be locally thickened to reduce the stress level in the vicinity of the first joint fasteners.

E. Where possible, joint shall be balanced symmetrically and parts loaded in double shear.

F. The joint design shall minimize eccentricities and geometric stress risers.

G. Joints shall employ gentle thickness buildups instead of sharp radii.

H. Joints shall employ interference fit fasteners where possible, otherwise, cold working of fastener holes shall be employed.

A5.3.4 Shims

A. Design practice shall lead to assembly sequences and structure which is adjustable for tolerances during assembly to minimize the need for shims.

B. Where fully machined parts must conform to lofted contours or station planes, shims shall be employed to account for manufacturing tolerances.

C. The design shall always account for a zero-to-positive thickness shim. The design shall not permit reworking parts to provide clearance on assembly.

D. Shims shall be constant thickness instead of tapered whenever possible because of cost considerations.

E. Epoxy or other cast-in-place shims will not be used.

F. Shims shall pick up a minimum of two fasteners and shall be compatible from a dissimilar metals standpoint with the adjacent structure.

G. Aluminum shims shall be anodized and primed.

H. Thick shims shall be avoided (to prevent them from picking up load).

A5.3.5 Piano Hinges (also see Section C8)

A. Piano-type hinge installations shall be designed to permit hinge or hinge pin removal without disassembly of adjoining parts.

B. Piano-type hinge installations shall provide a mechanical means of hinge pin retention without crimping the hinge lobes.

C. As a design objective, piano-type hinges that are difficult to replace shall be designed to permit installation of bushings. Difficult-to-replace piano-type hinges are defined as those bonded into structure assemblies or requiring disassembly of other primary structure for replacement.

D. Aluminum alloy piano-type hinges using 3/16-inch diameter or larger hinge pins shall be bushed.

E. Piano-type hinges that are over 18 inches in length and are difficult to replace shall have four or five lobes at each end bushed or constructed of material equivalent in wear resistance to steel.

A5.4.0 Ventilation, Dams and Drains

A. Adequate ventilation will be provided to prevent accumulation of hazardous vapors which could cause bodily harm or explosion.

B. Dams and drains shall be provided in the aircraft to control migration of fluids within the aircraft and to drain fluids overboard.

C. Exterior drains shall not drip on passenger entry areas, established service areas or engine cowling.

D. Fluids shall drain away from engines, tailpipes, exhausts, and locations where the fluids can re-enter the aircraft.

E. Vents and drains for flammable fluids shall prevent entry of the fluids into the aircraft.

F. Electronic and electrical equipment, including rotating beacon lights, shall be located or protected so that fluids or hazardous vapors cannot enter the equipment.

A5.5.0 Maintainability/Access

A. The structure shall contain hinged and latched access doors for the inspection and replacement of Line Replaceable Units (LRU's).

B. Adequate means of inspection (without aircraft disassembly) shall be provided for all compartments and zones within the aircraft.

C. Door sizes shall be determined to ensure that the maintenance tasks can be performed.

D. Routinely opened stressed doors shall, within each door, have fasteners standardized in grip, diameter, and recess type. Where different grip screws are a necessity, different diameter screws shall be employed.

E. Attaching hardware fastener part numbers shall be stenciled on the inner surface of each access door.

F. Doors shall never be "layered" such that the removal of one panel requires the disassembly of an adjacent panel.

G. Outward opening hinged external access doors shall have a tendency to close from forces of the airstream.

H. Attach provisions for hoisting shall be provided on the following aircraft components:

1. Wing flaps.
2. Engine pylons.
3. Vertical stabilizer.
4. Horizontal stabilizer.
5. Elevators.
6. Rudders.
7. Ailerons.
8. Slats.
9. Tail cone.
10. Cargo compartment doors.
11. Passenger compartment doors.
12. Empennage leading edges.
13. Radome.

I. Permanent station identification numbers at significant locations shall be provided.

A5.6.0 Repairability

A. The design shall consider ease of structural repair using conventional inventory tools and hardware.

B. Wear limits shall be specified and mechanical joints shall be bushed where wear could result in untimely maintenance costs.

C. Repair procedures shall be documented for both conventional and composite structure.

D. All seals shall be friction retained or attached with screws to facilitate replacement.

E. Sufficient material shall be allotted around each bushed hole, such that the bushing may be replaced with a salvage bushing with an outer diameter .08 inch oversize to the original bushing.

# BEAMS

TABLE OF CONTENTS

## B1.0.0 Beams

## B1.1.0 Simple Beams

### B1.1.1 Shear, Moment, and Deflection

The general equations that relate load, shear, bending moment and deflection are given in Table B1.1.1-1 in terms of deflection and bending moment.

Table B1.1.1-1 General Equations for Load, Shear, Bending Moment, and Deflection

| Title | y | M |
|---|---|---|
| Deflection | $\Delta = y$ | $\Delta = \iint \frac{M}{EI} dx\, dx$ |
| Slope | $\theta = dy/dx$ | $\theta = \int \frac{M}{EI} dx$ |
| Bending Moment | $M = EI\, d^2y/dx^2$ | M |
| Shear | $V = EI\, d^3y/dx^3$ | $V = dM/dx$ |
| Load | $W = EI\, d^4y/dx^4$ | $W = dv/dx = d^2M/dx^2$ |

The limiting assumptions for these relationships are:

- The material follows Hooke's Law
- Plane cross sections remain plane
- Shear deflections are negligible
- The deflections are small

If the beam length-to-depth ratio is small, then deflections due to shear may become important. For a rectangular beam having a length-to-depth ratio of 10.0, the effect of the shearing force on the deflection is about 3.0 percent.

Beam deflections are considered small when the maximum beam slope angle in radians, as defined in Table B1.1.1-1, is equal approximately to the tangent of the beam slope angle.

Sign convention for simple beams is generally taken as follows:

- x is positive to the right
- y is positive upward
- M is positive when the compressed fibers are at the top
- W is positive in the direction of negative y
- V is positive when the part of the beam to the left of the section tends to move upward under the action of the resultant of the vertical forces

Table B1.1.1-2 gives Shear, Moment, and Deflections for simple beams loaded and supported in various manners.

# Table B1.1.1-2 Shear, Moment, and Deflection Formulas for Simple Beams

## CONCENTRATED LOAD AT CENTER

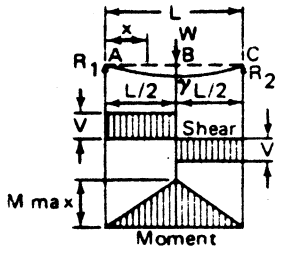


$R_1 = R_2 = V_1 = V_2 = \frac{P}{2}$

$M_{max}$ (at point of load) $= \frac{PL}{4}$

$M_x$ ( when $x < \frac{L}{2}$ ) $= \frac{Px}{2}$

$y_{max}$ (at point of load) $= \frac{-PL^3}{48\,EI}$

$y_x$ (when $x < \frac{L}{2}$ ) $= \frac{-Px}{48\,EI}(3L^2 - 4x^2)$

$\theta_A = \frac{-PL^2}{16\,EI}$

$\theta_C = -\theta_A$

## CONCENTRATED LOAD AT ANY POINT

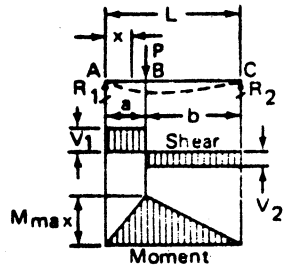


$R_1 = V_1$ (max when $a < b$) $= \frac{Pb}{L}$

$R_2 = V_2$ (max when $a > b$) $= \frac{Pa}{L}$

$M_{max}$ (at point of load) $= \frac{Pab}{L}$

$M_x$ (when $x < a$) $= \frac{Pbx}{L}$

$y_{max}$ (at $x = \sqrt{\frac{a(a+2b)}{3}}$ when $a > b$) $= \frac{-Pab(a+2b)\sqrt{3a(a+2b)}}{27\,EI\,L}$

$y_a$ (at point of load) $= \frac{-Pa^2b^2}{3EI\,L}$

$y_x$ (when $x < a$) $= \frac{-Pbx}{6\,EI\,L}(L^2 - b^2 - x^2)$

$\theta_A = -\frac{1}{6}\frac{W}{EI}(bL - \frac{b^3}{L})$

$\theta_C = +\frac{1}{6}\frac{W}{EI}(2bL + \frac{b^3}{L} - 3b^2)$

## Table B1.1.1-2 Shear, Moment, and Deflection Formulas for Simple Beams (Cont.)

**TWO EQUAL CONCENTRATED LOADS SYMMETRICALLY PLACED**

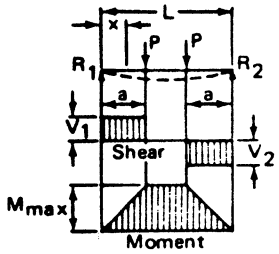


$R_1 = V_1 = R_2 = V_2 = P$

$V_x = P$ (when $x < a$) $= 0$ when $a < x < (a + b)$

$V_x = P$ (when $x > (a + b)$)

$M_{max}$ (between loads) $= Pa$

$M_x$ ($x < a$) $= Px$

$y_{max}$ (at center) $= \frac{-Pa}{24EI}(3L^2 - 4a^2)$

$y_x$ (when $x < a$) $= \frac{-Px}{6EI}(3La - 3a^2 - x^2)$

$y_x$ (when $x > a$ and $< (L - a)$) $= \frac{-Pa}{6EI}(3Lx - 3x^2 - a^2)$

$\theta = \frac{-Pa}{2EI}$ $(L - a)$ at left end

**TWO EQUAL CONCENTRATED LOADS UNSYMMETRICALLY PLACED**

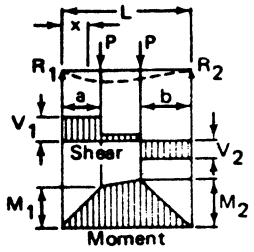


$R_1 = V_1$ ( max when $a < b$ ) $= \frac{P}{L}(L - a + b)$

$R_2 = V_2$ (max when $a > b$) $= \frac{P}{L}(L - b + a)$

$V_x$ = (when $x > a$ and $< (L - b)$) $= \frac{P}{L}(b - a)$

$V_x$ = ($x < a$) $= \frac{P}{L}(L - a + b)$

$M_1$ = (max when $a > b$) $= R_1 a$

$M_2$ = (max when $a < b$) $= R_2 b$

$M_x$ (when $x < a$) $= R_1 x$

$M_x$ (when $x > a$ and $< (L - b)$) $= R_1 x - P(x - a)$

$y = -\frac{1}{6}\frac{P}{EI}(x^3 - 3L^2x + 2L^3)$

$\theta_1 = +\frac{1}{2}\frac{PL^2}{EI}$

# Table B1.1.1-2 Shear, Moment, and Deflection Formulas for Simple Beams (Cont.)

## TWO UNEQUAL CONCENTRATED LOADS UNSYMMETRICALLY PLACED

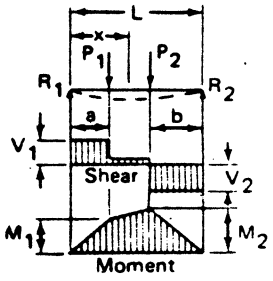


$R_1 = V_1 = \dfrac{P_1(L-a) + P_2 b}{L}$

$R_2 = V_2 = \dfrac{P_1 a + P_2 (L-b)}{L}$

$V_x$ (when $x > a$ and $< (L-b)$) $= R_1 - P_1$

$M_1$ (max when $R_1 < P_1$) $= R_1 a$

$M_2$ (max when $R_2 < P_2$) $= R_2 b$

$M_x$ (when $x < a$) $= R_1 x$

$M_x$ (when $x > a$ and $< (L-b)$) $= R_1 x - P_1 (x-a)$

$$(x < a),\ \theta_1 = \frac{1}{EI}\left[\frac{P_1 x^2}{2} - \frac{P_1 a x^2}{2L} + \frac{P_2 b x^2}{2L} + \frac{P_1 a^2}{2} - \frac{P_1 a^3}{6L} - \frac{P_2 L b}{6} - \frac{P_2 b^3}{6L} - \frac{P_1 a L}{3}\right]$$

$$y = \frac{1}{EI}\left[\frac{P_1 x^3}{6} - \frac{P_1 a x^3}{6L} + \frac{P_2 b x^3}{6L} + \frac{P_1 a^2 x}{2} - \frac{P_1 a^3 x}{6L} - \frac{P_2 L b x}{2} - \frac{P_2 b^3 x}{6L} - \frac{P_1 a L x}{3}\right]$$

$$(a < x < L-b),\ \theta_1 = \frac{1}{EI}\left[\frac{P_2 b x^2}{2L} - \frac{P_1 a x^2}{2L} + P_1 a x - \frac{P_1 a^3}{6L} - \frac{P_2 L b}{6} - \frac{P_2 b^3}{6L} - \frac{P_1 a L}{3}\right]$$

$$y = \frac{1}{EI}\left[\frac{P_2 b x^3}{6L} - \frac{P_1 a x^3}{6L} + \frac{P_1 a x^2}{2} - \frac{P_1 a^3 x}{6L} - \frac{P_2 L b x}{6} - \frac{P_2 b^3 x}{6L} - \frac{P_1 a L x}{3} + \frac{P_1 a^3}{6}\right]$$

$$L-b < x < L \quad \theta_1 = \frac{1}{EI}\left[P_1 a x + P_2 L x - P_2 b x - \frac{P_1 a x^2}{2L} - \frac{P_2 x^2}{2} + \frac{P_2 b x^2}{2L} - \frac{P_1 a^3}{6L} - \frac{P_2 L^2}{2} + \frac{5 P_2 L b}{6} - \frac{P_2 b^2}{2} - \frac{P_2 b^3}{6L} - \frac{P_1 a L}{3}\right]$$

$$y = \frac{1}{EI}\left[\frac{P_1 a x^2}{2} + \frac{P_2 L x^2}{2} - \frac{P_2 b x^2}{2} - \frac{P_1 a x^3}{6L} - \frac{P_2 x^3}{6} + \frac{P_2 b x^3}{6L} - \frac{P_1 a^3 x}{6L} - \frac{P_2 L^2 x}{2} + \frac{5 P_2 L b x}{6} - \frac{P_2 b^2 x}{2} - \frac{P_2 b^3 x}{6L} - \frac{P_1 a L x}{3} + \frac{P_1 a^3}{6} + \frac{P_2 L^3}{6} - \frac{P_2 L^2 b}{2} + \frac{P_2 L b^2}{2} - \frac{P_2 b^3}{6}\right]$$

## UNIFORMLY DISTRIBUTED LOAD

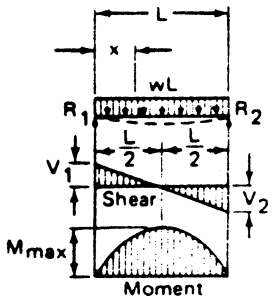


$R_1 = V_1 = R_2 = V_2 = \dfrac{wL}{2}$

$V_x = w\left(\dfrac{1}{2} - x\right)$

$M_{max}$ (at center) $= \dfrac{wL^2}{8}$

$M_x = \dfrac{wx}{2}(L-x)$

$y_{max}$ (at center) $= \dfrac{-5wL^4}{384\,EI}$

$y_x = \dfrac{-wx}{24EI}(L^3 - 2Lx^2 + x^3)$

$\theta_1 = -\dfrac{wL^3}{24EI}$

# Table B1.1.1-2 Shear, Moment, and Deflection Formulas for Simple Beams (Cont.)

## UNIFORM LOAD PARTIALLY DISTRIBUTED

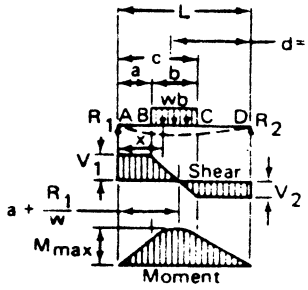


$W = wb$

$R_1 = V_1$ (A to B) $= \frac{Wd}{L}$

$R_2 = V_2 = \frac{W}{L}\left(a + \frac{b}{2}\right)$

$V_x$ (B to C) $= R_1 - w\frac{(x-a)}{b}$

$V_x$ (C to D) $= R_1 - W$

$M_{max}$ (at $x = a + \frac{R_1}{W}$) $= R_1\left(a + \frac{R_1}{2W}\right)$

$M_x$ (A to B) $= R_1 x$

$M_x$ (B to C) $= R_1 x - \frac{w}{2C}(x-a)^2$

$M_x$ (C to D) $= W\frac{d}{L}\left(a + \frac{bd}{2L}\right)$ at $x = a + \frac{bd}{L}$

$$y\ (A \text{ to } B) = \frac{-1}{48EI}\left\{8R_1(x^3 - L^2x) + Wx\left[\frac{8d^3}{L} - \frac{2cb^2}{L} + \frac{b^3}{L} + 2b^2\right]\right\}$$

$$y\ (B \text{ to } C) = \frac{-1}{48EI}\left\{8R_1(x^3 - L^2x) + Wx\left[\frac{8d^3}{L} - \frac{2cb^2}{L} + \frac{b^3}{L} + 2b^2\right] - 2W\frac{(x-a)^4}{b}\right\}$$

$$y\ (C \text{ to } D) = \frac{-1}{48EI}\left\{8R_1(x^3 - L^2x) + Wx\left[\frac{8d^3}{L} - \frac{2cb^2}{L} + \frac{b^3}{L}\right] - 8W\left(x - \frac{a}{2} - \frac{c}{2}\right)^3 + W(2cb^2 - b^3)\right\}$$

$$\theta_A = \frac{1}{48}EI\left[-8R_1L^2 + W\left(\frac{8d^3}{L} - \frac{2bc^2}{L} + \frac{c^3}{L} + 2c^2\right)\right]$$

$$\theta_B = \frac{1}{48}EI\left[16R_1L^2 - W\left(24d^2 - \frac{8d^3}{L} + \frac{2bc^2}{L} - \frac{c^3}{L}\right)\right]$$

## UNIFORM LOAD PARTIALLY DISTRIBUTED AT ONE END

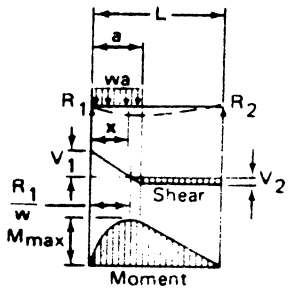


$W = wa$

$R_1 = V_{1max} = \frac{wa}{2L}(2L - a)$

$R_2 = -V_2 = \frac{wa^2}{2L}$

$V$ (when $x < a$) $= R_1 - wx$

$M_{max}$ (at $x = \frac{R_1}{W}$) $h = \frac{R_1^2}{2w}$

$M_x$ (when $x < a$) $= R_1 x - \frac{wx^2}{2}$

$M_x$ (when $x > a$) $= R_2(L - x)$

$y_x$ (when $x < a$) $= \frac{-wx}{24EIL}(a^2(2L-a)^2 - 2ax^2(2L-a) + Lx^3)$

$y_x$ (when $x > a$) $= \frac{-wa^2(L-x)}{24EIL}(4xL - 2x^2 - a^2)$

$\theta_1 = \frac{w}{24EIL}[-4Lx^3 + 6ax^2(2L-a) - a^2(2L-a)^2]$ $x < a$

$\theta_1 = \frac{wa^2}{24EIL}[-6x^2 + 12Lx - 4L^2 - a^2]$, $x > a$

## Table B1.1.1-2 Shear, Moment, and Deflection Formulas for Simple Beams (Cont.)

### UNIFORM LOAD PARTIALLY DISTRIBUTED AT EACH END

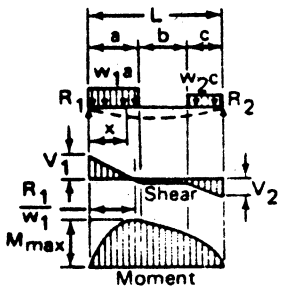


$$R_1 = V_1 = \frac{w_1a\,(2L - a) + w_2c^2}{2L}$$

$$R_2 = V_2 = \frac{w_2c\,(2L - c) + w_1a^2}{2L}$$

$V_x$ (when $x < a$) $= R_1 - w_1x$

$V_x$ (when $x < a$ and $< (a + b)$) $= R_1 - R_2$

$V_x$ (when $x > (a + b)$) $= R_2 - w_1\,(L - x)$

$M_{max}$ (at $x = \frac{R_1}{w_1}$ when $R_1 < w_1a$) $= \frac{R_1^2}{2w_1}$

$M_{max}$ (at $x = L - \frac{R_2}{w_2}$ when $R_2 < w_2c$) $= \frac{R_2^2}{2w_2}$

$M_x$ (when $x < a$) $= R_1x - \frac{w_1x^2}{2}$

$M_x$ (when $x > a$ and $< (a + b)$) $= R_1x - \frac{w_1^2}{2}\,(2x - a)$

$M_x$ (when $x > (a + b)$) $= R_2\,(L - x) - \frac{w_2(L - x)^2}{2}$

$$(x < a),\quad \theta = \frac{1}{EI}\left[-\frac{w_1x^3}{6} + \left(\frac{w_1a}{2} - \frac{w_1a^2}{4L} + \frac{w_2c^2}{4L}\right)x^2 + C_3\right]$$

Where $C_3$ = a Constant of Integration, C = Length of Loaded Span at Right End

$$y = \frac{1}{EI}\left[-\frac{w_1x^4}{24} + \left(\frac{w_1a}{6} - \frac{w_1a^2}{12L} + \frac{w_2c^2}{12L}\right)x^3 + C_3x\right]$$

$$(a < x < a + b),\quad \theta = \frac{1}{EI}\left[\left(\frac{w_2c^2 - w_1a^2}{4L}\right)x^2 + \frac{w_1a^2}{2}x + C_3 - \frac{w_1a^3}{6}\right]$$

$$y = \frac{1}{EI}\left[\left(\frac{w_2c^2 - w_1a^2}{12L}\right)x^3 + \frac{w_1a^2x^2}{4} - \frac{w_1a^3x}{6} + C_3x + \frac{w_1a^4}{24}\right]$$

$$(a + b < x < L),\quad \theta = \frac{1}{EI}\left[-\frac{w_2x^3}{6} + \left(\frac{w_2c^2 - w_1a^2}{4L} + \frac{w_2\,(a + b)}{2}\right)x^2 + \left(\frac{w_1a^2 - w_2\,(a+b)^2}{2}\right)x + \frac{w_2\,(a + b)^3}{6} - \frac{w_1a^3}{6} + C_3\right]$$

$$y = \frac{1}{EI}\left[-\frac{w_2x^4}{24} + \left(\frac{w_2c^2 - w_1a^2}{12L} + \frac{w_2\,(a + b)}{6}\right)x^3 + \left(\frac{w_1a^2 - w_2(a+b)^2}{4}\right)x^2 + \left(\frac{w_2\,(a + b)^3 - w_1a^3}{6} + C_3\right)x + \frac{w_1a^4}{24} - \frac{w_2\,(a + b)^4}{24}\right]$$

$$C_3 = \frac{w_2L^3}{24} - \left[\frac{w_2c^2 - w_1a^2}{12L} + \frac{w_2\,(a + b)}{6}\right]L^2 - \left(\frac{w_1a^2 - w_2\,(a + b)^2}{4}\right)L - \frac{w_2\,(a + b)^3}{6} + \frac{w_1a^3}{6} - \frac{w_1a^4}{24L} + \frac{w_2\,(a + b)^4}{24L}$$

## Table B1.1.1-2 Shear, Moment, and Deflection Formulas for Simple Beams (Cont.)

### PARABOLIC DISTRIBUTED LOAD

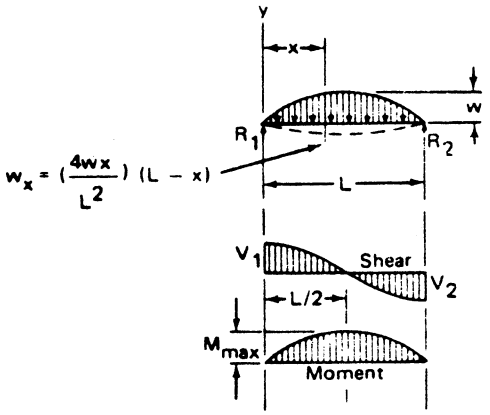


$$W = \frac{2wL}{3}$$

$$R_1 = R_2 = \frac{Lw}{3} = V_1 = V_2$$

$$V_x = \frac{w}{3L^2}(L^3 - 6x^2L + 4x^3)$$

$$M_x = w\left(\frac{Lx}{3} - \frac{2x^3}{3L} + \frac{x^4}{3L^2}\right)$$

$$M_{max} @ \text{℄} = \frac{5wL^2}{48} = \frac{5RL}{32}$$

$$\theta = \frac{w}{EI}\left[\frac{Lx^2}{6} - \frac{x^4}{6L} + \frac{x^5}{15L^2} - \frac{L^3}{30}\right]$$

$$y_x = \frac{w}{EI}\left[\frac{x^6}{90L^2} - \frac{x^5}{30L} + \frac{Lx^3}{18} - \frac{L^3x}{30}\right]$$

$$= \frac{wx(x-L)}{90L^2EI}\left[x^4 - 2x^3L - 2x^2L^2 + 3xL^3 + 3L^4\right]$$

### SINUSOIDAL DISTRIBUTED LOAD

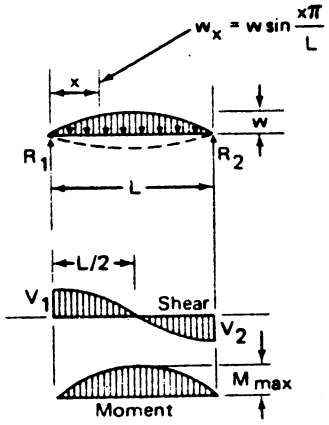


$$W = \frac{2wL}{\pi}$$

$$R_1 = R_2 = \frac{wL}{\pi} = V_1 = V_2$$

$$V_x = \left(\frac{wL}{\pi}\right)\left(\cos\frac{\pi x}{L}\right)$$

$$M_x = \left(\frac{wL^2}{\pi^2}\right)\left(\sin\frac{\pi x}{L}\right)$$

$$M_{\text{℄}} = M_{max} = \frac{wL^2}{\pi} = \frac{RL}{2\pi}$$

$$\theta_1 = -\left(\frac{wL^3}{\pi^3 EI}\right)\left(\cos\frac{\pi x}{L}\right)$$

$$y_x = -\left(\frac{wL^4}{\pi^4 EI}\right)\left(\sin\frac{\pi x}{L}\right)$$

### LOAD INCREASING UNIFORMLY TO CENTER

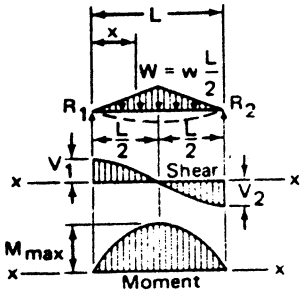


$$R_1 = V_1 = R_2 = V_2 = \frac{W}{2}$$

$$V_x \left(\text{when } x < \frac{L}{2}\right) = \frac{W}{2L^2}(L^2 - 4x^2),$$

$$x > \frac{L}{2} = -\frac{W}{2}\left[1 - 4\frac{(L-x)^2}{L^2}\right]$$

$$M_{max} \text{ (at center)} = \frac{WL}{6}$$

$$M_x \left(\text{when } x < \frac{L}{2}\right) = Wx\left(\frac{L}{2} - \frac{2x^2}{3L^2}\right),$$

$$\left(\text{when } x > \frac{L}{2}\right) = \frac{W}{6}\left[3(L-x) - \frac{4(L-x)^3}{L^2}\right]$$

$$y_{max} \text{ (at center)} = \frac{WL^3}{60EI}$$

$$y_x = \frac{-Wx}{420\,EI\,L^2}(5L^2 - 4x^2)^2$$

$$\vartheta = \frac{\pm 5WL^2}{96\,EI} \text{ @ ends}$$

## Table B1.1.1-2 Shear, Moment, and Deflection Formulas for Simple Beams (Cont.)

### LOAD INCREASING UNIFORMLY TO ONE END

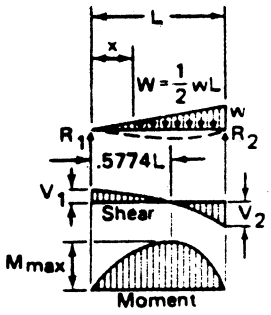


$R_1 = V = \frac{W}{3}$

$R_2 = V_2 = \frac{2W}{3}$

$V_x = \frac{W}{3} - \frac{Wx^2}{L^2}$

$V_{max} = V_2$

$M_{max}$ (at $x = \frac{L}{\sqrt{3}} = .5774L$) $= \frac{2WL}{9\sqrt{3}} = .1283\,WL$

$M_x = \frac{Wx}{3L^2}(L^2 - x^2)$

$y_{max}$ (at $x = .519L$) $= -.01304\,\frac{WL^3}{EI}$

$y_x = -\frac{Wx}{180EI\,L^2}(3x^4 - 10L^2x^2 + 7L^4)$

$\theta = \frac{+8WL^2}{180\,EI}$ @ $x = L$, $\quad \theta = -\frac{7WL^2}{180\,EI}$ @ $x = 0$

---

### UNIFORMLY VARYING DISTRIBUTED LOAD

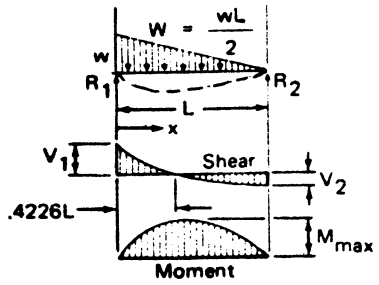


$R_1 = \frac{2W}{3}$

$R_2 = \frac{W}{3}$

$V_x = \frac{W}{3L^2}(2L^2 - 6Lx + 3x^2)$

$M_x = \frac{Wx}{3L^2}(2L^2 - 3Lx - x^2)$

$M_{max} = \frac{2WL}{9\sqrt{3}} = -0.1283WL$ (at $x = .4226L$)

$\theta = \frac{8WL^2}{180\,EI}$ (at left end)

$\theta = \frac{7WL^2}{180\,EI}$ (at right end)

$y_x = \frac{-Wx}{180\,EI\,L^2}(8L^4 - 20L^2x^2 + 15Lx^3 - 3x^4)$

$y_{max} = -.01304\,\frac{WL^3}{EI}$ (at $x = .4807L$)

# Table B1.1.1-2 Shear, Moment, and Deflection Formulas for Simple Beams (Cont.)

## END SUPPORTS, PARTIAL TRIANGULAR LOAD

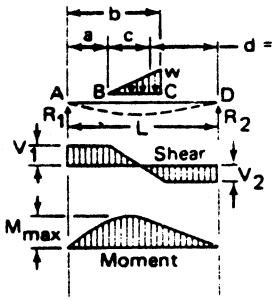


$$W = \frac{w}{3}(b - a)$$

$$R_1 = W\frac{d}{L}\ ;\ R_2 = W\frac{L-d}{L}\ ;\ \text{(A to B)}\ V = +R_1.$$

$$\text{(B to C)}\ V = R_1 - \left(\frac{x-a}{c}\right)^2 W;\ \text{(C to D)}\ V = R_1 - W$$

$$\text{(A to B)}\ M = R_1 x;\ \text{(B to C)}\ M = R_1 x - W\frac{(x-a)^3}{3c^2}$$

$$\text{(C to D)}\ M = R_1 x - \frac{W}{3}(3x - a - 2b):$$

$$\text{Max } M = \left[\frac{Wd}{L}\left(a + \frac{2c}{3}\sqrt{\frac{d}{L}}\right)\right] @\ x = a + c\sqrt{\frac{d}{L}}$$

$$\text{(A to B)}\ y = \frac{1}{6EI}\left\{R_1(x^3 - L^2x) + Wx\left[\frac{d^3}{L} + \frac{c^2}{6}\left(1 - \frac{b}{L}\right) + \frac{17}{120}\frac{c^3}{L}\right]\right\}$$

$$\text{(B to C)}\ y = \frac{1}{6EI}\left[R_1(x^3 - L^2x) - \frac{W}{10c^2}(x-a)^5 + Wx\left(\frac{d^3}{L} + \frac{c^2}{6} - \frac{c^2 b}{6L} + \frac{17c^3}{120L}\right)\right];$$

$$\text{(C to D)}\ y = \frac{1}{6EI}\left\{R_1(x^3 - L^2x) - W\left[\left(x - \frac{a}{3} - \frac{2b}{3}\right)^3 - \frac{d^3 x}{L} - \frac{bc^2}{6}\left(1 - \frac{x}{L}\right) + \frac{17c^3}{270}\left(1 - \frac{x}{L}\right)\right]\right\}$$

$$\theta_A = \frac{1}{6EI}\left[-R_1L^2 + W\left(\frac{d^3}{L} + \frac{c^2}{6} + \frac{17c^3}{270L} - \frac{c^2 b}{6L}\right)\right]$$

$$\theta_D = \frac{1}{6EI}\left[2R_1L^2 + W\left(\frac{d^3}{L} + \frac{17c^3}{270L} - \frac{c^2 b}{6L} - 3d^2\right)\right]$$

## END REACTION, PARTIAL TRIANGULAR LOAD

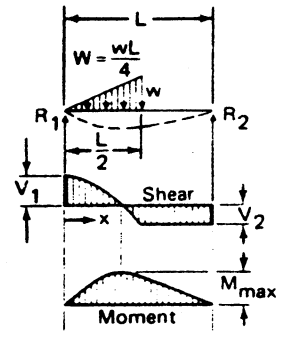


$$R_1 = \frac{2W}{3},\ R_2 = \frac{W}{3}$$

$$V_x = \frac{2W}{3} + \frac{4Wx^2}{L^2}\ \left(\text{when } x < \frac{L}{2}\right)$$

$$V_x = \frac{W}{3}\ \left(\text{when } x > \frac{L}{2}\right)$$

$$M_x = \frac{2Wx}{3L^2}(L^2 - 2x^2)\ \left(\text{when } x < \frac{L}{2}\right)$$

$$M_x = \frac{W}{3}(L - x)\ \left(\text{when } x > \frac{L}{2}\right)$$

$$M_{max} = \frac{4ML}{9\sqrt{6}} - .181WL\ \left(\text{at } x = \frac{L}{\sqrt{6}} = .408L\right)$$

$$y_x = \frac{W}{6EI}\left[\frac{2x^3}{3} - \frac{2x^5}{5L^2} - \frac{xL^2}{120}\right] @\ x < \frac{L}{2}$$

$$y_x = \frac{W}{6EI}\left[.0339L^3 - .706\,x\,L^2 - \frac{x^3}{3}\right] @\ x > \frac{L}{2}$$

$$\theta_1 = -(.342)\frac{WL^2}{6EI} @\ x = 0$$

$$\theta_1 = (.283)\frac{WL^2}{6EI} @\ x = L$$

## Table B1.1.1-2 Shear, Moment, and Deflection Formulas for Simple Beams (Cont.)

### PARTIAL TRIANGULAR LOAD AT END

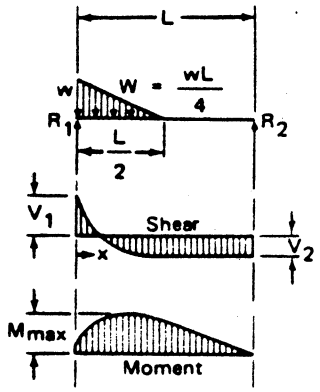


$$R_1 = \frac{5W}{6} \quad R_2 = \frac{W}{6}$$

$$V_x = \frac{5W}{6} - \frac{4Wx}{L^2} \quad (L - x) \quad (\text{when } x < \frac{L}{2})$$

$$V_x = \frac{-W}{6} \quad (x > \frac{L}{2})$$

$$M_x = \frac{W}{6} (L - x) \quad (\text{when } x > \frac{L}{2})$$

$$M_x = \frac{Wx}{6L^2} (5L^2 - 121x + 8x^2) \quad (\text{when } x < \frac{L}{2})$$

$$M_{max} = 0.106\ WL \quad (\text{at } x = 0.296\ L)$$

$$y_x = \frac{W}{36\ EI\ L^2} [\ 2.4x^5 - 6x^4L + 5x^3L^2 - 1.325\ L^4x\ ] \qquad x < \frac{L}{2}$$

$$y_x = \frac{W}{36\ EI} [\ -x^3 + 3Lx^2 - 2.075L^2x + .075L^3\ ] \qquad x > \frac{L}{2}$$

$$\theta_1 = \frac{W}{12\ EI\ L^2} [\ 4x^4 - 8Lx^3 + 5x^2L^2 - .442\ L^4\ ] @\ x < \frac{L}{2}$$

$$\theta_1 = \frac{W}{12\ EI} [\ -x^2 + 2Lx - .692L^2\ ] \qquad x > \frac{L}{2}$$

---

### LOAD DECREASING UNIFORMLY – ENDS TO ℄

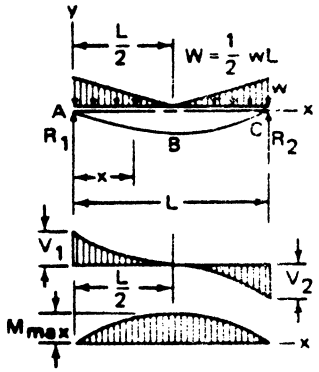


$$R_1 = \frac{W}{2}; \quad R_2 = \frac{W}{2}$$

$$(x < L/2)\ V = \frac{W}{2} (\frac{L - 2x}{L})^2$$

$$(x > L/2)\ V = \frac{-W}{2} (\frac{2x - L}{L})^2$$

$$(x < L/2)\ M = \frac{W}{2} (x - \frac{2x^2}{L} + \frac{4x^3}{3L^2})$$

$$(x > L/2)\ M = \frac{W}{2} [\ (L - x) - \frac{2\ (L - x)^2}{L} + \frac{4\ (L - x)^3}{3L^2}\ ]$$

$$\text{MAX } M = \frac{WL}{12} \text{ AT B}$$

$$(x < L/2)\ y = \frac{W}{12\ EI} (x^3 - \frac{x^4}{L} + \frac{2x^5}{5L^2} - \frac{3L^2x}{8})$$

$$\text{MAX } y = -\frac{3WL^3}{320\ EI} \text{ AT B}$$

$$\theta = -\frac{WL^2}{32\ EL} \text{ AT A}; \quad \theta = \frac{WL^2}{32\ EI} \text{ AT C}$$

## Table B1.1.1-2 Shear, Moment, and Deflection Formulas for Simple Beams (Cont.)

### END COUPLE

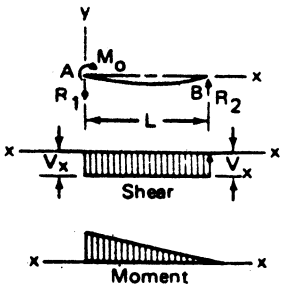


$$R_1 = -\frac{M_o}{L};\ R_2 = \frac{M_o}{L};\ V_x = R_1$$

$$M_x = M_o - R_1 x,\ M_{max} = M_o$$

$$y_x = \frac{M_o}{6EI}\left(3x^2 - \frac{x^3}{L} - 21x\right);\ y_{max} = -0.0642\frac{M_o L^2}{EI} \text{ @ } x = .422L$$

$$\theta = -\frac{M_o L}{3EI} \text{ at } x = 0;\quad \theta = +\frac{M_o L}{6EI} \text{ @ } x = L$$

### INTERMEDIATE COUPLE

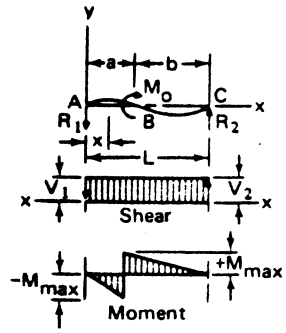


$$R_1 = -\frac{M_o}{L};\ R_2 = \frac{M_o}{L};\ V = +R_1;\ M = +R_1 x \text{ (A to B)}$$

$$M = +R_1 x + M_o \text{ (B to C)}$$

Max. (−M) = $+R_1 a$ just left of B; Max. (+M) = $+M_o$ just right of B

$$y_{max} = \frac{Mx^3}{3EIL} \text{ @ } x = \frac{\sqrt{L2}}{3} - b^2 \text{ when } a < b$$

$$\text{(A to B) } y = \frac{M_o}{6EI}\left[\left(6a - \frac{3a^2}{L} - 2L\right)x - \frac{x^3}{L}\right]$$

$$\text{(B to C) } y = \frac{M_o}{6EI}\left[3a^2 + 3x^2 - \frac{x^3}{L} - \left(2L + \frac{3a^2}{L}\right)x\right]$$

$$\theta = -\frac{M_o}{6EI}\left(2L - 6a + \frac{3a^2}{L}\right) \text{ at A};\quad \theta = \frac{M_o}{6EI}\left(L - \frac{3a^2}{L}\right) \text{ at C}$$

$$\theta = \frac{M_o}{EI}\left(a - \frac{a^2}{L} - \frac{L}{3}\right) \text{ at +B}$$

### UNEQUAL END COUPLES

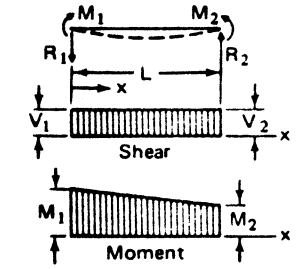


$$R_1 = \frac{M_2 - M_1}{L} \qquad R_2 = \frac{M_1 - M_2}{L}$$

$$V_x = \frac{M_2 - M_1}{L} = V_1 = V_2$$

$$M_x = M_1 + \frac{(M_2 - M_1)\,x}{L}$$

$$M_{max} = M_1 \quad (M_1 > M_2)$$

$$y_x = \frac{x(x - L)}{EI}\left[\frac{M_1}{2} + \frac{(M_2 - M_1)}{6L}(x + L)\right]$$

$$\theta = -\frac{L}{6EI}(2M_1 + M_2) \text{ (left end)};\quad \theta = \frac{L}{6EI}(M_1 + 2M_2) \text{ (right end)}$$

NOTE: Direction of $R_1$ and $R_2$ determined by relationship of $M_1$ and $M_2$ signs and values shown are for $M_1 > M_2$.

# Table B1.1.1-2 Shear, Moment, and Deflection Formulas for Simple Beams (Cont.)

## CONCENTRATED LOAD AT CENTER AND VARIABLE END MOMENTS

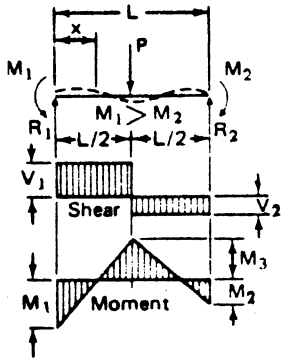


$$R_1 = V_1 = \frac{P}{2} + \frac{M_1 - M_2}{L}$$

$$R_2 = V_2 = \frac{P}{2} - \frac{M_1 - M_2}{L}$$

$$M_3 \text{ (At center)} = \frac{PL}{4} - \frac{M_1 + M_2}{2}$$

$$M_x \left(\text{When } x < \frac{L}{2}\right) = \left(\frac{P}{2} + \frac{M_1 - M_2}{L}\right) x - M_1$$

$$M_x \left(\text{When } x > \frac{L}{2}\right) = \frac{P}{2}(L - x) + \frac{(M_1 - M_2)x}{L} - M_1$$

$$y_x \left(\text{When } x < \frac{L}{2}\right) = \frac{Px}{48EI}\left\{(3L^2 - 4x^2) - \left[\frac{8(L - x)}{PL}\right]\left[M_1(2L - x) + M_2(L + x)\right]\right\}$$

$$y_x \left(x > \frac{L}{2}\right) = \frac{P}{48EI}\left\{-x(2x - 3L)^2 + L^3 + \frac{8x}{PL}(x - L)\left[M_1(x - 2L) - M_2(x + L)\right]\right\}$$

$$\theta \left(@\ x < \frac{L}{2}\right) = \frac{P}{48EI}\left\{3(2x - L)(2x + L) + \frac{8}{PL}\left[M_1(3x^2 - 6xL + 2L^2) - M_2(3x^2 - L^2)\right]\right\}$$

$$\theta \left(@\ x > \frac{L}{2}\right) = \frac{P}{48EI}\left\{-3(2x - 3L)(2x - L) + \frac{8}{PL}\left[M_1(3x^2 - 6xL + 2L^2) - M_2(3x^2 - L^2)\right]\right\}$$

## UNIFORMLY DISTRIBUTED LOAD AND VARIABLE END MOMENTS

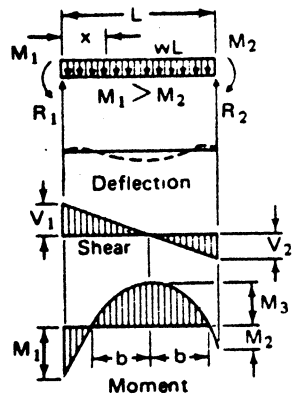


$$R_1 = V_1 = \frac{wL}{2} + \frac{M_1 - M_2}{L}; \quad R_2 = V_2 = \frac{wL}{2} - \frac{M_1 - M_2}{L}$$

$$V_x = w\left(\frac{L}{2} - x\right) + \frac{M_1 - M_2}{L}; \quad V_1 = R_1 + \frac{(M_1 - M_2)}{L}$$

$$M_3 \left(\text{at } x = \frac{L}{2} + \frac{M_1 - M_2}{wL}\right) = \frac{wL^2}{8} - \frac{M_1 + M_2}{2} + \frac{(M_1 - M_2)^2}{2wL^2}$$

$$M_x = \frac{wx}{2}(L - x) + \left(\frac{M_1 - M_2}{L}\right) x - M_1$$

$$\text{To locate b(inflection points)} = \sqrt{\frac{L^2}{4} - \left(\frac{M_1 + M_2}{w}\right) + \left(\frac{M_1 - M_2}{wL}\right)^2}$$

$$y_x = \frac{wx}{24EI}\left[x^2 - \left(2L + \frac{4M_1}{wL} - \frac{4M_2}{wL}\right)x^2 + \frac{12M_1}{w}x + L^3 - \frac{8M_1L}{w} - \frac{4M_2L}{w}\right]$$

$$\theta_x = \frac{1}{EI}\left[\frac{M_1}{2}(2x - L) - \frac{V_1}{6}(3x^2 - L^2) + \frac{w}{24}(4x^3 - L^3)\right]$$

## Table B1.1.1-2 Shear, Moment, and Deflection Formulas for Simple Beams (Cont.)

### UNIFORMLY INCREASING LOAD VARIABLE END MOMENTS

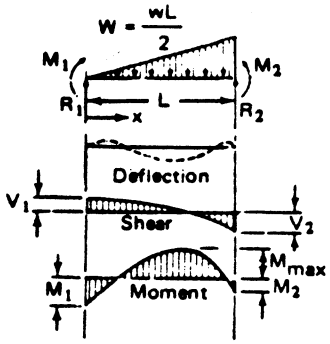


$$R_1 = \frac{M_2 - M_1}{L} + \frac{wL}{6} \qquad R_2 = \frac{M_1 - M_2}{L} + \frac{wL}{3}$$

$$V_1 = R_1 \qquad V_x = V_1 - \frac{wx^2}{2L}$$

$$M_x = M_1 + V_1 x - \frac{wx^3}{6L}$$

$$\theta_x = \frac{1}{EI}\left[\frac{M_1}{2}(2x - L) + \frac{V_1}{6}(3x^2 - L^2) - \frac{w}{120L}(5x^4 - L^4)\right]$$

$$y_x = \frac{x(x - L)}{EI}\left[\frac{M_1}{2} + \frac{V_1}{6}(x + L) - \frac{w}{120L}(x + L)(x^2 + L^2)\right]$$

### TRIANGULAR LOAD WITH APPLIED END MOMENTS

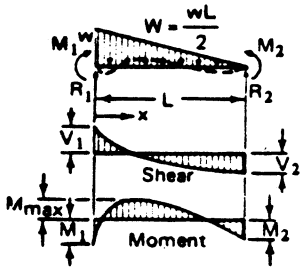


$$R_1 = \frac{M_2 - M_1}{L} + \frac{wL}{3}; \quad R_2 = \frac{M_1 - M_2}{L} + \frac{wL}{6}$$

$$V_x = V_1 - wx + \frac{wx^2}{2L}$$

$$M_x = M_1 + V_1 x - \frac{wx^2}{2} + \frac{wx^3}{6L}$$

$$\theta_x = \frac{1}{EI}\left[\frac{M_1}{2}(2x - L) + \frac{S_1}{6}(3x^2 - L^2) + \frac{w}{120L}(5x^4 - 20Lx^3 + 4L^4)\right]$$

$$y_x = \frac{x(x - L)}{EI}\left[\frac{M_1}{2} + \frac{v_1}{6}(x + L) - \frac{W}{30}(x^2 + xL + L^2) + \frac{Wx^3}{120L}\right]$$

### INTERMEDIATE LOAD WITH APPLIED END MOMENTS

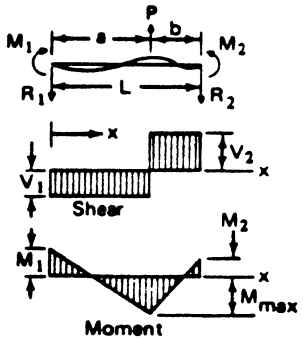


$$R_1 = \frac{M_2 - M_1}{L} - \frac{Pb}{L}; \qquad R_2 = \frac{M_1 - M_2}{L} - \frac{Pa}{L}$$

$$V_x = \frac{M_2 - M_1}{L} - \frac{Pb}{L} \text{ (when } x < a\text{)}; \quad V_x = \frac{M_1 - M_2}{L} - \frac{Pa}{L} \text{ (when } x > a\text{)}$$

$$M_x = M_1 + V_1 x \text{ (when } x < a\text{)}; \quad M_x = M_1 + V_1 x + P(x - a) \text{ (when } x > a\text{)}$$

$$\theta_x = \frac{1}{EI}\left[\frac{M_1}{2}(2x - L) + \frac{V_1}{6}(3x^2 - L^2) - \frac{Pb^3}{6L}\right] \text{ (when } x < a\text{)}$$

$$\theta_x = \frac{1}{EI}\left[\frac{M_1}{2}(2x - L) + \frac{V_1}{6}(3x^2 - L^2) + \frac{P}{6}3(x - a)^2 - \frac{b^3}{L}\right] \text{ (when } x > a\text{)}$$

$$y_x = \frac{x(x - L)}{EI}\left[\frac{M_1}{2} + \frac{V_1}{6}(x + L) - \frac{Pb^3}{6L(x - L)}\right] \text{ (when } x < a\text{)}$$

$$y_x = \frac{x(x - L)}{EI}\left[\frac{M_1}{2} + \frac{V_1}{6}(x + L) - \frac{P}{6(x - L)}\left(\frac{b^3}{L} - \frac{(x - a)^3}{x}\right)\right] \text{ (when } x > a\text{)}$$

# Table B1.1.1-2 Shear, Moment, and Deflection Formulas for Simple Beams (Cont.)

## BEAM OVERHANGING ONE SUPPORT – UNIFORMLY DISTRIBUTED LOAD

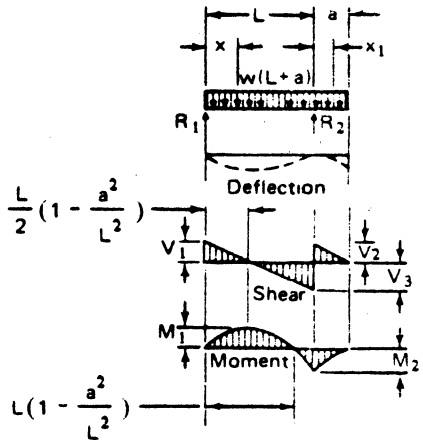


$$R_1 = V_1 = \frac{w}{2L}(L^2 - a^2) \qquad R_2 = V_2 + V_3 = \frac{w}{2L}(L + a)^2$$

$$V_2 = wa; \qquad V_3 = \frac{-w}{2L}(L^2 + a^2)$$

$$V_x \text{ (between supports)} = R_1 - wx; \quad V_{x_1} \text{ (for overhang)} = w(a - x_1)$$

$$M_1 \text{ (at } x = \frac{L}{2}\left[1 - \frac{a^2}{L^2}\right]) = \frac{w}{8L^2}(L + a)^2 (L - a)^2$$

$$M_2 \text{ (at } R_2) = \frac{-wa^2}{2}$$

$$M_x \text{ (between supports)} = \frac{wx}{2L}(L^2 - a^2 - xL)$$

$$M_{x_1} \text{ (for overhang)} = \frac{-w}{2}(a - x_1)^2$$

$$y_x \text{ (between supports)} = \frac{wx}{24EIL}(L^4 - 2L^2x^2 + Lx^3 - 2a^2L^2 + 2a^2x^2)$$

$$y_{x_1} \text{ (for overhang)} = \frac{-wx_1}{24EI}(4a^2L - L^3 + 6a^2x_1 - 4ax_1^2 + x_1^3)$$

---

## BEAM OVERHANGING ONE SUPPORT – UNIFORMLY DISTRIBUTED LOAD ON OVERHANG

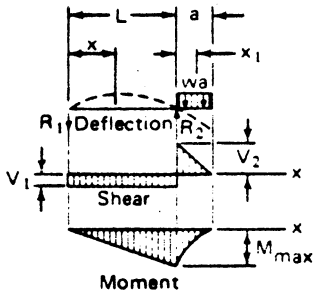


$$R_1 = V_1 = \frac{-wa^2}{2L} \qquad R_2 = V_1 + V_2 = \frac{wa}{2L}(2L + a)$$

$$V_2 = wa; \qquad V_{x_1} \text{ (for overhang)} = w(a - x_1)$$

$$M_{max} \text{ (at } R_2) = \frac{-wa^2}{2}$$

$$M_x \text{ (between supports)} = \frac{-wa^2x}{2L}$$

$$M_{x_1} \text{ (for overhang)} = \frac{-w}{2}(a - x_1)^2$$

$$y_{max} \text{ (between supports at } x = \frac{L}{\sqrt{3}}) = \frac{wa^2L^2}{18\sqrt{3}\,EI} = .03208\,\frac{wa^2L^2}{EI}$$

$$y_{max} \text{ (for overhang at } x_1 = a) = \frac{-wa^3}{24EI}(4L + 3a)$$

$$y_x \text{ (between supports)} = \frac{wa^2x}{12EIL}(L^2 - x^2)$$

$$y_{x_1} \text{ (for overhang)} = \frac{-wx_1}{24EI}(4a^2L + 6a^2x_1 - 4ax_1^2 + x_1^3)$$

# Table B1.1.1-2 Shear, Moment, and Deflection Formulas for Simple Beams (Cont.)

## BEAM OVERHANGING ONE SUPPORT – UNIFORMLY DISTRIBUTED LOAD BETWEEN SUPPORTS

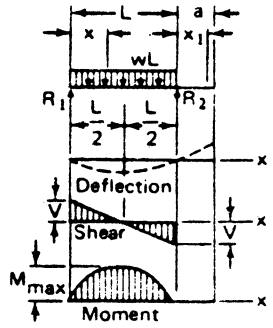


$$R_1 = V_1 = R_2 = V_2 = \frac{wL}{2}$$

$$V_x = w\left(\frac{L}{2} - x\right)$$

$$M_{max}\ \text{(at center)} = \frac{wL^2}{8} \qquad M_x = \frac{wx}{2}(L - x)$$

$$y_{max}\ \text{(at center)} = \frac{-5wL^4}{384EI}$$

$$y_x = \frac{wx}{24EI}(L^3 - 2Lx^2 + x^3)$$

$$y_{x_1} = \frac{wl^3 x_1}{24EI}$$

## BEAM OVERHANGING ONE SUPPORT – CONCENTRATED LOAD AT END OF OVERHANG

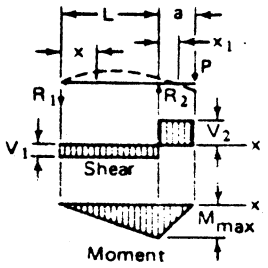


$$R_1 = V_1 = \frac{Pa}{L}; \qquad R_2 = V_1 + V_2 = \frac{P}{L}(L + a); \qquad V_2 = P$$

$$M_{max}\ (\text{at } R_2) = -Pa; \qquad M_x\ \text{(between supports)} = \frac{Pax}{L}$$

$$M_{x_1}\ \text{(for overhang)} = P(a - x_1)$$

$$y_{max}\ \text{(between supports at } x = \frac{L}{\sqrt{3}}) = \frac{PaL^2}{9\sqrt{3}EI} = .06415\frac{PaL^2}{EI}$$

$$y_{max}\ \text{(for overhang at } x_1 = a) = \frac{Pa^2}{3EI}(L + a)$$

$$y_x\ \text{(between supports)} = \frac{Pax}{6EIL}(L^2 - x^2)$$

$$y_{x_1}\ \text{(for overhang)} = \frac{-Px_1}{6EI}(2aL + 3ax_1 - x_1^2)$$

## BEAM OVERHANGING ONE SUPPORT – CONCENTRATED LOAD AT ANY POINT BETWEEN SUPPORTS

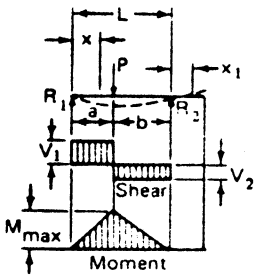


$$R_1 = V_1\ (\text{max. when } a < b) = \frac{Pb}{L}; \quad R_2 = V_2\ (\text{max. when } a > b) = \frac{Pa}{L}$$

$$M_{max}\ \text{(at point of load)} = \frac{Pab}{L}; \qquad M_x\ (\text{when } x < a) = \frac{Pbx}{L}$$

$$y_{max}\ \left(\text{at } x = \sqrt{\frac{a(a+2b)}{3}}\ \text{when } a > b\right) = \frac{-Pab(a+2b)\sqrt{3a(a+2b)}}{27EIL}$$

$$y_a\ \text{(at point of load)} = \frac{-Pa^2b^2}{3EIL}$$

$$y_x\ (\text{when } x < a) = \frac{-Pbx}{6EIL}(L^2 - b^2 - x^2)$$

$$y_x\ (\text{when } x > a) = \frac{-Pa(L - x)}{6EIL}(2Lx - x^2 - a^2); \quad y_{x_1} = \frac{+Pabx_1}{6EIL}(L + a)$$

# Table B1.1.1-2 Shear, Moment, and Deflection Formulas for Simple Beams (Cont.)

## CONCENTRATED LOAD AT FREE END

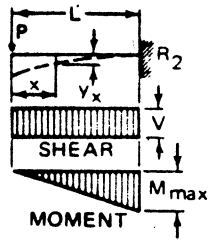


$R_2 = V_2 = P$

$M_{max}$ (AT FIXED END) $= -PL$

$M_x = -Px$

$y_{max}$ (AT FREE END) $= \dfrac{-PL^3}{3EI}$

$y_x = \dfrac{-P}{6EI}(2L^3 - 3L^2x + x^3)$

$\theta = \dfrac{1}{2}\dfrac{PL^2}{EI}$ @ $x = 0$

## CONCENTRATED LOAD AT ANY POINT

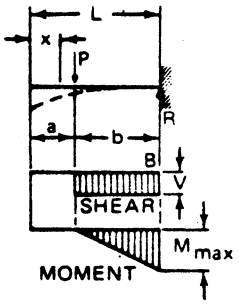


$R = V$ (WHEN $x > a$) $= P$

$M_{max}$ (AT FIXED END) $= -Pb$

$M_x$ (WHEN $x > a$) $= -P(x - a)$

$y_{max}$ (AT FREE END) $= \dfrac{-Pb^2}{6EI}(3L - b)$

$y_a$ (AT POINT OF LOAD) $= \dfrac{-Pb^3}{3EI}$

$y_x$ (WHEN $x < a$) $= \dfrac{-Pb^2}{6EI}(3L - 3x - b)$

$y_x$ (WHEN $x > a$) $= \dfrac{-P(L - x)^2}{6EI}(3b - L + x)$

$\theta_1 = \dfrac{1}{2}\dfrac{Pb^2}{EI}$, $a < x < b$

## END COUPLE

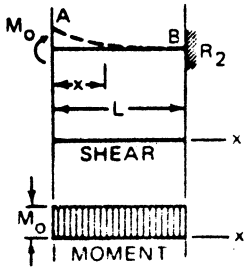


$R_2 = 0$ ; $V_x = 0$

$M_x = M_o$ ; $M_{max} = M_o$

$y_x = \dfrac{1}{2}\dfrac{M_o}{EI}(L^2 - 2Lx + x^2)$

$y_{max} = \dfrac{1}{2}\dfrac{M_o L^2}{EI}$ @ A

$\theta = \dfrac{M_o L}{EI}$ @ A

## Table B1.1.1-2 Shear, Moment, and Deflection Formulas for Simple Beams (Cont.)

### INTERMEDIATE COUPLE

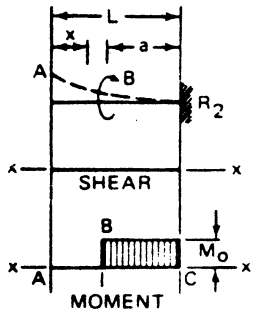


$R_2 = 0$; $V = 0$;

(A TO B) $M = 0$; (B TO C) $M = M_o$; $M_{max} = M_o$

(A TO B) $y = \frac{(M_o)a}{EI}\left(L - \frac{1}{2}a - x\right)$

(B TO C) $y = \frac{1}{2}\frac{M_o}{EI}\left[(x - L + a)^2 - 2a(x - L + a) + a^2\right]$

$y_{max} = \frac{(M_o)a}{EI}\left(L - \frac{1}{2}a\right)$ AT A

$\theta = \frac{(M_o)a}{EI}$ (A TO B)

### UNIFORMLY DISTRIBUTED LOAD

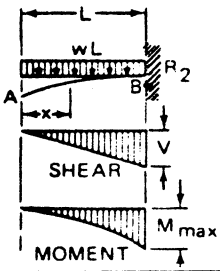


$R = V = wL$; $V_x = -wx$

$M_{max}$ (AT FIXED END) $= \frac{-wL^2}{2}$; $M_x = \frac{-wx^2}{2}$

$y_{max}$ (AT FREE END) $= \frac{-wL^4}{8EI}$ $y_x = \frac{-w}{24EIL}(x^4 - 4L^3x + 3L^4)$

$\theta = +\frac{1}{6}\frac{wL^3}{EI}$ @ A

### PARTIAL UNIFORM INTERMEDIATE LOAD

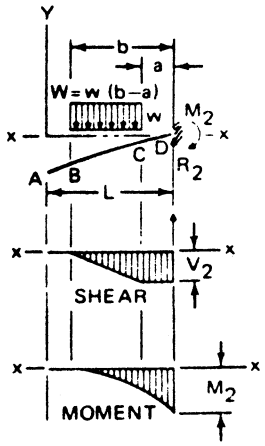


$R_2 = +W$; (A TO B) $V = 0$;

(B TO C) $V = -\frac{W}{b-a}(x - L + b)$; (C TO D) $V = -W$; $V = W$

(A TO B) $M = 0$; (B TO C) $M = -\frac{1}{2}\frac{W}{b-a}(x - L + b)^2$

(C TO D) $M = -\frac{1}{2}W(2x - 2L + a + b)$

max M $= -\frac{1}{2}W(a + b)$ AT D

(A TO B) $Y = -\frac{1}{24}\frac{W}{EI}\left[4(a^2 + ab + b^2)(L - x) - a^3 - ab^2 - a^2b - b^3\right]$

(B TO C) $Y = -\frac{1}{24}\frac{W}{EI}\left[6(a + b)(L - x)^2 - 4(L - x)^3 + \frac{(L - x - a)^4}{b-a}\right]$

(C TO D) $Y = -\frac{1}{12}\frac{W}{EI}\left[3(a + b)(L - x)^2 - 2(L - x)^3\right]$

max Y $= -\frac{1}{24}\frac{W}{EI}\left[4(a^2 + ab + b^2)L - a^3 - ab^2 - a^2b - b^3\right]$ AT A

$\theta = +\frac{1}{6}\frac{W}{EI}(a^2 + ab + b^2)$ (A TO B)

## Table B1.1.1-2 Shear, Moment, and Deflection Formulas for Simple Beams (Cont.)

### PARTIAL UNIFORM END LOAD

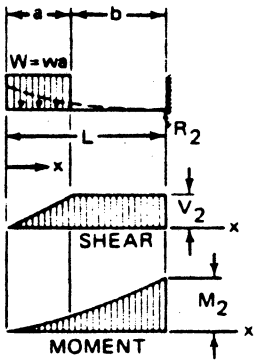


$R_2 = +W = V_2$

$V_x = -W\frac{x}{a}$ (WHEN $x < a$)

$V_x = -W$ (WHEN $x > a$)

$M_x = \frac{-Wx^2}{2a}$ (WHEN $x < a$)

$M_{max} = -W\left(\frac{a}{2} + b\right)$ (AT FIXED END)

$M_x = -W\left(x - \frac{a}{2}\right)$ (WHEN $x > a$)

$y_{max} = \frac{-W}{24EIa}\left(3L^4 - 4a^3L + a^4\right)$ (AT FREE END)

$\theta = +\frac{W}{6EI}\left(a^2 + 3ab + 3b^2\right)$ (AT FREE END)

---

### PARTIAL TRIANGULAR LOAD – DECREASING TOWARDS SUPPORT

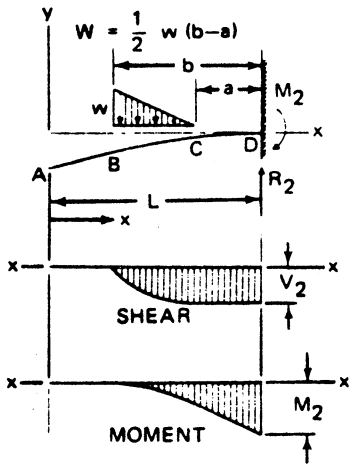


$R_2 = +W$

(A TO B) $V = 0$; (B TO C) $V = -W\left[1 - \frac{(L-a-x)^2}{(b-a)^2}\right]$; (C TO D) $V = -W$

(A TO B) $M = 0$; (B TO C) $M = -\frac{1}{3}W\left[\frac{3(x-L+b)^2}{b-a} - \frac{(x-L+b)^3}{(b-a)^2}\right]$

(C TO D) $M = -\frac{1}{3}W(-3L + 3x + 2b + a)$

Max $M = -\frac{1}{3}W(2b + a)$ @ D

(A TO B) $y = -\frac{1}{60}\frac{W}{EI}\left[(5a^2 + 10ab + 15b^2)(L-x) - a^3 - 2a^2b - 3ab^2 - 4b^3\right]$

(C TO D) $y = -\frac{1}{6}\frac{W}{EI}\left[(a + 2b)(L-x)^2 - (L-x)^3\right]$

(B TO C) $y = -\frac{1}{60}\frac{W}{EI}\left[\frac{(L-x-a)^5}{(b-a)^2} - 10(L-x)^3 + (10a + 20b)(L-x)^2\right]$

Max $y = -\frac{1}{60}\frac{W}{EI}\left[(5a^2 + 10ab + 15b^2)L - a^3 - 2a^2b - 3ab^2 - 4b^3\right]$ @ A

$\theta_x = +\frac{1}{12}\frac{W}{EI}\left(a^2 + 2ab + 3b^2\right)$ (A TO B)

## Table B1.1.1-2 Shear, Moment, and Deflection Formulas for Simple Beams (Cont.)

### PARTIAL TRIANGULAR LOAD – INCREASING TOWARDS SUPPORT

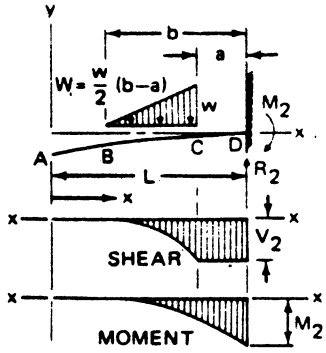


$R_2 = +W$; (A TO B) $V = 0$

(B TO C) $V = -\dfrac{W(x-L+b)^2}{(b-a)^2}$; (C TO D) $V = -W$

(A TO B) $M = 0$; (B TO C) $M = -\dfrac{1}{3}\dfrac{W(x-L+b)^3}{(b-a)^2}$

(C TO D) $M = -\dfrac{1}{3}W(3x-3L+b+2a)$;

Max $M = -\dfrac{1}{3}W(b+2a)$ @ D

(A TO B) $y = -\dfrac{1}{60}\dfrac{W}{EI}\left[(5b^2+10ba+15a^2)(L-x)-4a^3-2ab^2-3a^2b-b^3\right]$

(B TO C) $y = -\dfrac{1}{60}\dfrac{W}{EI}\left[(20a+10b)(L-x)^2-10(L-x)^3+5\dfrac{(L-x-a)^4}{b-a}-\dfrac{(L-x-a)^5}{(b-a)^2}\right]$

(C TO D) $y = -\dfrac{1}{6}\dfrac{W}{EI}\left[(2a+b)(L-x)^2-(L-x)^3\right]$

Max $y = -\dfrac{1}{60}\dfrac{W}{EI}\left[(5b^2+10ba+15a^2)L-4a^3-2ab^2-3ab^2b-b^3\right]$ @ A

$\theta = +\dfrac{1}{12}\dfrac{W}{EI}(3a^2+2ab+b^2)$ (A TO B)

### TRIANGULAR LOAD

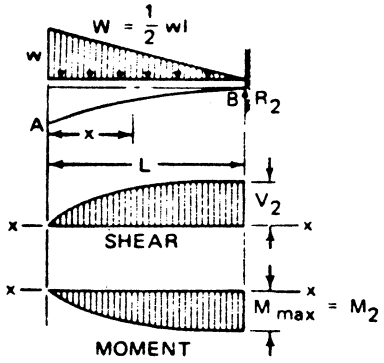


$R_2 = +W$; $V_x = -W\left(\dfrac{2Lx-x^2}{L^2}\right)$

$M_x = -\dfrac{1}{3}\dfrac{W}{L^2}(3Lx^2-x^3)$

$M_{max} = -\dfrac{2}{3}WL$ @ B

$y_x = -\dfrac{1}{60}\dfrac{W}{EIL^2}(-x^5-15L^4x+5Lx^4+11L^5)$

$y_{max} = -\dfrac{11}{60}\dfrac{WL^3}{EI}$ @ A

$\theta = \dfrac{1}{4}\dfrac{WL^2}{EI}$ @ A

### TRIANGULAR LOAD INCREASING UNIFORMLY TO FIXED END

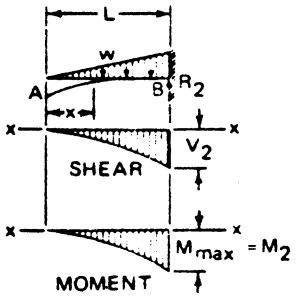


$R_2 = V_2 = W = \dfrac{wL}{2}$; $V_x = -W\dfrac{x^2}{L^2}$

$M_{max}$ (AT FIXED END) $= \dfrac{-WL}{3}$

$y_{max}$ (AT FREE END) $= \dfrac{-WL^3}{15EI}$; $M_x = \dfrac{-Wx^3}{3L^2}$

$y_x = \dfrac{-W}{60EIL^2}(x^5-5L^4x+4L^5)$

$\theta = \dfrac{1}{12}\dfrac{WL^2}{EI}$ @ A

# Table B1.1.1-2 Shear, Moment, and Deflection Formulas for Simple Beams (Cont.)

## CONCENTRATED LOAD AT CENTER

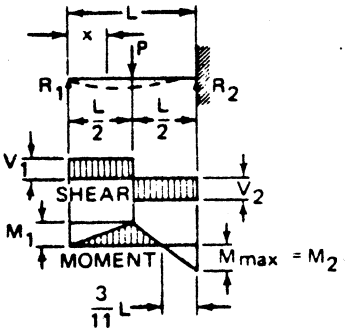


$R_1 = V_1 = \frac{5P}{16}$; $R_2 = V_2 = \frac{11P}{16}$

$M_{max}$ (AT FIXED END) $= \frac{3PL}{16}$; $M_1$ (AT POINT OF LOAD) $= \frac{5PL}{32}$

$M_x$ (WHEN $x < \frac{L}{2}$) $= \frac{5x}{16}$; $M_x$ (WHEN $x > \frac{L}{2}$) $= P\left(\frac{L}{2} - \frac{11x}{16}\right)$

$y_{max}$ (AT $x = L\sqrt{\frac{1}{5}} = 0.4472L$) $= \frac{-PL^3}{48EI\sqrt{5}} = 0.009317\frac{PL^3}{EI}$

$y_x$ (AT POINT OF LOAD) $= \frac{-7PL^3}{768EI}$

$y_x$ (WHEN $x < \frac{L}{2}$) $= \frac{-Px}{96EI}(3L^2 - 5x^2)$

$y_x$ (WHEN $x > \frac{L}{2}$) $= \frac{-P}{96EI}(x-L)^2(11x - 2L)$

$\theta_1 = \frac{1}{32}\frac{PL^2}{EI}$

## INTERMEDIATE LOAD

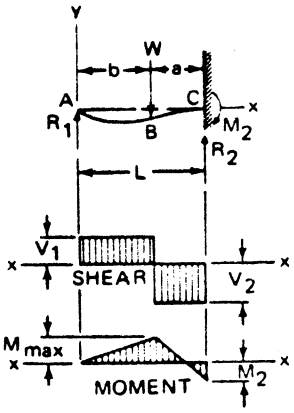


$R_1 = \frac{W}{2}\left(\frac{3a^2L - a^3}{L^3}\right)$; $R_2 = W - R_A$

(A TO B) $V = R_1$; (B TO C) $V = R_1 - W$; $M_2 = \frac{W}{2}\left(\frac{a^3 + 2aL^2 - 3a^2L}{L^2}\right)$

(A TO B) $M = R_1 x$; (B TO C) $M = R_1 x - W(x - L + a)$;

MAX. (+M) $= R_1(L - a)$ @ B (B to C) $V = R_1 - W$;
MAX. POSSIBLE VALUE = 0.174 WL
WHEN a = 0.634 L

MAX. (−M) $= -M_c$ @ C
MAX. POSSIBLE VALUE = −0.1927 WL
WHEN a = 0.4227 L

(A TO B) $y = \frac{-1}{6EI}\left[R_1(x^3 - 3L^2x) + 3Wa^2x\right]$

(B TO C) $y = \frac{-1}{6EI}\left\{R_1(x^3 - 3L^2x) + W\left[3a^2x - (x-b)^3\right]\right\}$

IF $a < 0.586$ L, MAX. y IS BETWEEN A AND B @ $x = L\sqrt{1 - \frac{2L}{3L - a}}$

IF $a > 0.586$ L, MAX. y IS @ $x = \frac{L(L^2 + b^2)}{3L^2 - b^2}$

IF $a = 0.586$ L, MAX. y IS @ B AND $= -0.0098\frac{WL^3}{EI}$, MAX. POSSIBLE DEFLECTION

$\theta = \frac{-W}{4EI}\left(\frac{a^3}{L} - a^2\right)$ @ A

# Table B1.1.1-2 Shear, Moment, and Deflection Formulas for Simple Beams (Cont.)

## UNIFORMLY DISTRIBUTED LOAD

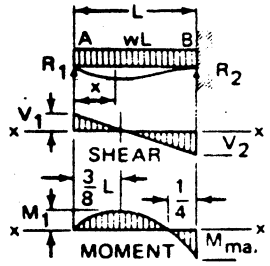


$R_1 = V_1 = \frac{3wL}{8}$

$R_2 = V_{2\,max} = \frac{5wL}{8}$

$V_x = R_1 - wx$

$-M_{max} = \frac{-wL^2}{8}$ @ B

$+M_{max}$ (AT $x = \frac{3}{8}$ L) $= \frac{9}{128}\,wL^2$

$M_x = R_1 x - \frac{wx^2}{2}$

$y_{max}$. (AT $x = \frac{1}{16}(1 + \sqrt{33}) = 0.4215$ L) $= \frac{-wL^4}{185EI}$

$y_x = \frac{-wx}{48EI}(L^3 - 3Lx^2 + 2x^3)$

$\theta = -\frac{wL^2}{48EI}$ @ A

## PARTIAL LOAD AT FIXED END

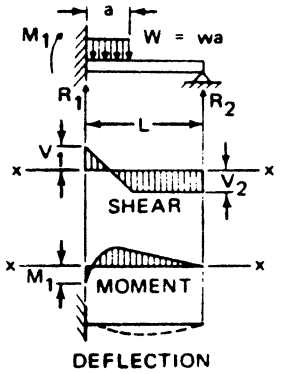


$R_1 = \frac{+wa^2}{8L^3}\left[\,a^2 - 4aL + \frac{8L^3}{a}\,\right]$

$R_2 = \left[\,+\frac{wa^3}{8L^3}(4L - a)\,\right]$

$M_1 = \frac{wa^2(2L - a)^2}{8L^2}$

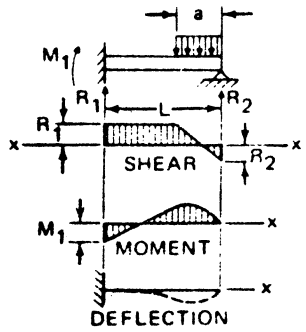


$R_1 = +\frac{wa^2}{8L^3}\left[\,6L^2 - a^2\,\right]$

$R_2 = +\frac{wa^2}{8L^3}\left[\,a^2 + \frac{8L^3}{a} - 6L^2\,\right]$

$M_1 = \frac{wa^2(2L^2 - a^2)}{8L^2}$

# Table B1.1.1-2 Shear, Moment, and Deflection Formulas for Simple Beams (Cont.)

## PARTIAL UNIFORM LOAD

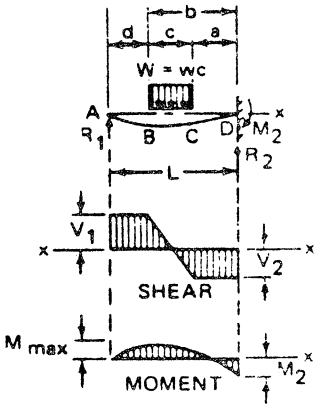


$R_1 = \frac{W}{8L^3}\left[4L(a^2 + ab + b^2) - a^3 - ab^2 - a^2b - b^3\right]$, $R_2 = W - R_1$

$M_2 = -R_1L + \frac{W}{2}(a + b)$; (A TO B) $V = R_1$, (B TO C) $V = R_1 - W\left(\frac{x-d}{c}\right)$

(C TO D) $V = R_1 - W$; (A TO B) $M = R_1 x$

(B TO C) $M = R_1 x - \frac{W(x-d)^2}{2c}$; (C TO D) $M = R_1 x - W\left(x - d - \frac{c}{2}\right)$

Max. $(+M) = R_1\left(d + \frac{R_1 c}{W}\right)$ AT $x = \left(d + \frac{R_1 c}{W}\right)$; Max. $(-M) = -M_2$

(A TO B) $y = \frac{1}{EI}\left[R_1\left(\frac{x^3}{6} - \frac{L^2x}{2}\right) + Wx\left(\frac{a^2}{2} + \frac{ac}{2} + \frac{c^2}{6}\right)\right]$

(B TO C) $y = \frac{1}{EI}\left[R_1\left(\frac{x^3}{6} - \frac{L^2x}{2}\right) + Wx\left(\frac{a^2}{2} + \frac{ac}{2} + \frac{c^2}{6}\right) - \frac{W(x-d)^4}{24c}\right]$

(C TO D) $y = \frac{1}{EI}\left\{R_1\left(\frac{x^3}{6} - \frac{L^2x}{2} + \frac{L^3}{3}\right) + W\left[\frac{1}{6}\left(a + \frac{c}{2}\right)^3 - \frac{1}{2}\left(a + \frac{c}{2}\right)^2 L - \frac{1}{6}\left(x - d - \frac{c}{2}\right)^3 + \frac{1}{2}\left(a + \frac{c}{2}\right)^2 x\right]\right\}$

$\theta = -\frac{1}{EI}\left[\frac{R_1 L^2}{2} - W\left(\frac{a^2}{2} + \frac{ac}{2} + \frac{c^2}{6}\right)\right]$ @ A

## TRIANGULAR LOAD – INCREASING TOWARDS FIXED END

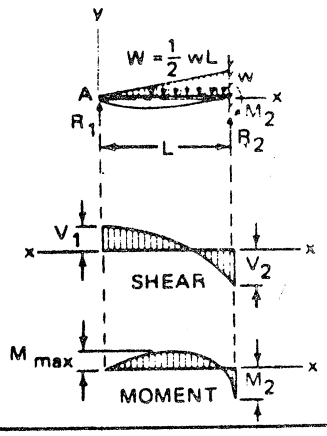


$R_1 = \frac{W}{5}$; $R_2 = \frac{4W}{5}$; $V = W\left(\frac{1}{5} - \frac{x^2}{L^2}\right)$

$M_2 = \frac{2WL}{15}$; $M = W\left(\frac{x}{5} - \frac{x^3}{3L^2}\right)$

Max. $(+M) = 0.06\,WL$ AT $x = 0.4474L$, Max. $(-M) = -M_2$

$y = \frac{-W}{60EIL}\left(2Lx^3 - L^3x - \frac{x^5}{L}\right)$

Max. $y = -0.00477\frac{WL^3}{EI}$ @ $x = L\sqrt{\frac{1}{5}}$

$\theta = -\frac{WL^2}{60EI}$ @ A

## TRIANGULAR LOAD – DECREASING TOWARDS FIXED END

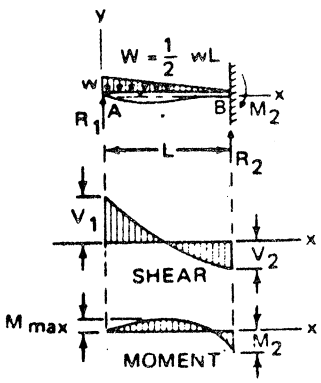


$R_1 = \frac{11W}{20}$; $R_2 = \frac{9W}{20}$; $V = W\left(\frac{11}{20} - \frac{2x}{L} + \frac{x^2}{L^2}\right)$

$M_2 = \frac{7WL}{60}$; $M = W\left(\frac{11x}{20} - \frac{x^2}{L} + \frac{x^3}{3L^2}\right)$

Max. $(+M) = 0.0846\,WL$ @ $x = 0.329\,L$; Max. $(-M) = -\frac{7WL}{60}$ @ B

$y = \frac{-W}{120EIL}\left(11Lx^3 - 3L^3x - 10x^4 + \frac{2x^5}{L}\right)$

Max $y = -0.00609\frac{WL^3}{EI}$ @ $x = 0.402L$

$\theta = -\frac{WL^2}{40EI}$ @ A

## Table B1.1.1-2 Shear, Moment, and Deflection Formulas for Simple Beams (Cont.)

### PARTIAL TRIANGULAR LOAD – CASE 1

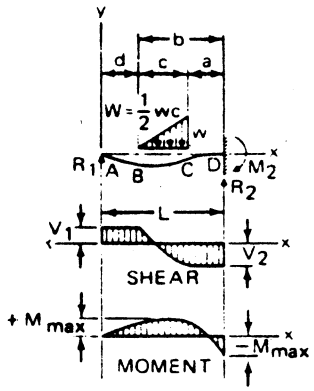


$$R_1 = \frac{1}{20}\frac{W}{L^3}[(10ab + 15a^2 + 5b^2)L - 4a^3 - 2ab^2 - 3a^2b - b^3]; \quad R_2 = W - R_1$$

$$\text{(A TO B) } V = R_1; \quad \text{(B TO C) } V = R_1 - W\left(\frac{x-d}{c}\right)^2; \quad \text{(C TO D) } V = R_1 - W$$

$$M_2 = -R_1L + \frac{1}{3}W(2a + b); \quad \text{(A TO B) } M = R_1x$$

$$\text{(B TO C) } M = R_1x - \frac{1}{3}W\frac{(x-d)^3}{c^2}; \quad \text{(C TO D) } M = R_1x - W\left(x - d - \frac{2}{3}c\right)$$

$$\text{Max} - M = R_1\left(d + \frac{2}{3}c\sqrt{\frac{R_1}{W}}\right) \text{ AT } x = d + c\sqrt{\frac{R_1}{W}} \qquad \text{Max} - M = -M_2$$

$$\text{(A TO B) } y = \frac{1}{EI}\left[R_1\left(\frac{1}{6}x^3 - \frac{1}{2}L^2x\right) + Wx\left(\frac{1}{2}a^2 + \frac{1}{3}ac + \frac{1}{12}c^2\right)\right]$$

$$\text{(B TO C) } y = \frac{1}{EI}\left[R_1\left(\frac{1}{6}x^3 - \frac{1}{2}L^2x\right) + Wx\left(\frac{1}{3}a^2 + \frac{1}{3}ac + \frac{1}{12}c^2\right) - W\frac{(x-d)^5}{60c^2}\right]$$

$$\text{(C TO D) } y = \frac{1}{EI}\left\{R_1\left(\frac{1}{6}x^3 - \frac{1}{2}L^2x + \frac{1}{3}L^3\right) + W\left[\frac{1}{2}\left(a + \frac{1}{3}c\right)^2x - \frac{1}{6}\left(x - d - \frac{2}{3}c\right)^3 + \frac{1}{6}\left(a + \frac{1}{3}c\right)^3 - \frac{1}{2}\left(a + \frac{1}{3}c\right)^2L\right]\right\}$$

$$\theta = -\frac{1}{EI}\left[\frac{1}{2}R_1L^2 - W\left(\frac{1}{12}c^2 + \frac{1}{3}ac + \frac{1}{2}a^2\right)\right] \text{ @ A}$$

### PARTIAL TRIANGULAR LOAD – CASE 2

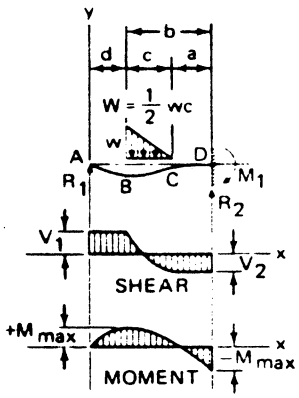


$$R_1 = \frac{1}{20}\frac{W}{L^3}(10ab + 5a^2 + 15b^2)\,L - c^3 - 2a^2b - 3ab^2 - 4b^3); \quad R_2 = W - R_1$$

$$\text{(A to B) } V = R_1; \quad \text{(B to C) } V = R_1 - \frac{2(x-d)}{c}W + \frac{(x-d)^2}{c^2}W; \quad \text{(C to D) } V = R_1 - W$$

$$M_2 = -R_1L + \frac{1}{3}W(a + 2b); \quad \text{(A to B) } M = R_1x$$

$$\text{(B to C) } M = R_1x - \frac{(x-d)^2}{c}W + \frac{(x-d)^3}{3c^2}W$$

$$\text{(C to D) } M = R_1x - W\left(x - d - \frac{1}{3}c\right)$$

$$\text{Max} + M = R_1\left(d + c - c\sqrt{1 - \frac{R_1}{W}}\right) - \frac{1}{3}Wc\left(1 - \sqrt{1 - \frac{R_1}{W}}\right)^2\left(2 + \sqrt{1 - \frac{R_1}{W}}\right) \quad @\ x = d + c\left(1 - \sqrt{1 - \frac{R_1}{W}}\right)$$

$$\text{Max} - M = -M_2 \text{ @ D}; \qquad \text{(A to B) } y = \frac{1}{EI}\left\{R_1\left(\frac{1}{6}x^3 - \frac{1}{2}L^2x\right) + Wx\left(\frac{1}{2}a^2 + \frac{2}{3}ac + \frac{1}{2}c^2\right)\right.$$

$$\text{(B to C) } y = \frac{1}{EI}\left\{R_1\left(\frac{1}{6}x^3 - \frac{1}{2}L^2x\right) + W\left[\frac{1}{60}\frac{(x-d)^5}{c^2} - \frac{1}{12}\frac{(x-d)^4}{c} + \left(\frac{1}{2}a^2 + \frac{2}{3}ac + \frac{1}{2}c^2\right)x\right]\right\}$$

$$\text{(C to D) } y = \frac{1}{EI}\left\{R_1\left(\frac{1}{6}x^3 - \frac{1}{2}L^2x + \frac{1}{3}L^3\right) - \frac{1}{2}W(L-x)^2\left[\left(a + \frac{2}{3}c\right) - \frac{L-x}{3}\right]\right\}$$

$$\theta = -\frac{1}{EI}\left[\frac{1}{2}R_1L^2 - W\left(\frac{1}{2}a^2 + \frac{2}{3}ac + \frac{1}{4}c^2\right)\right] \text{ @ A}$$

## Table B1.1.1-2 Shear, Moment, and Deflection Formulas for Simple Beams (Cont.)

### PARTIAL TRIANGULAR LOAD-CASE 3

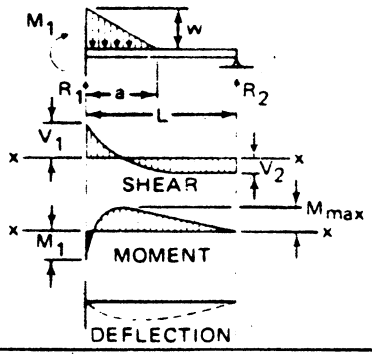


$$R_1 = + \frac{wa^2}{120L^3} \left( 3a^2 - 15aL + \frac{60L^3}{a} \right)$$

$$R_2 = + \frac{wa^2}{120L^3} \left( 15aL - 3a^2 \right)$$

$$M_1 = \frac{wa^2 (3a^2 - 15aL + 20L^2)}{120L^2}$$

### PARTIAL TRIANGULAR LOAD-CASE 4

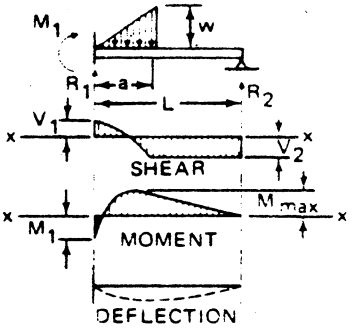


$$R_1 = + \frac{wa^2}{40L^3} \left( 15aL - 4a^2 \frac{20L^3}{a} \right)$$

$$R_2 = + \frac{wa^2}{40L^3} \left( 15aL - 4a^2 \right)$$

$$M_1 = \frac{wa^2 (40L^2 - 45aL + 12a^2)}{120L^2}$$

### PARTIAL TRIANGULAR LOAD-CASE 5

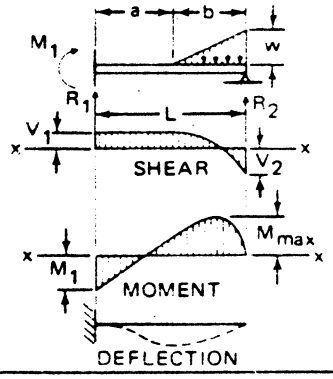


$$R_1 = + \frac{wb^2}{40L^3} \left( b^2 - 10L^2 \right)$$

$$R_2 = + \frac{wb^2}{40L^3} \left( b^2 - 10L^2 \right) - \frac{wb}{2}$$

$$M_1 = \frac{wb^2 (10L^2 - 3b^2)}{120L^2}$$

### PARTIAL TRIANGULAR LOAD-CASE 6

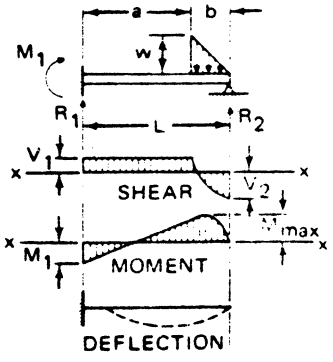


$$R_1 = + \left( \frac{M}{L} + \frac{3b^2}{3L} \right)$$

$$R_2 = + \left[ \left( L - \frac{2b}{3} \right) \left( \frac{bw}{2L} \frac{M}{L} \right) \right]$$

$$M_1 = \frac{w(2L^5 - 15a^2 L^2 + 25a^3 L^2 - 15a^4 L + 3a^5)}{30bL^2}$$

## Table B1.1.1-2 Shear, Moment, and Deflection Formulas for Simple Beams (Cont.)

BEAM FIXED AT ONE END, FREE TO DEFLECT VERTICALLY BUT NOT ROTATE AT OTHER
CONCENTRATED LOAD AT DEFLECTED END

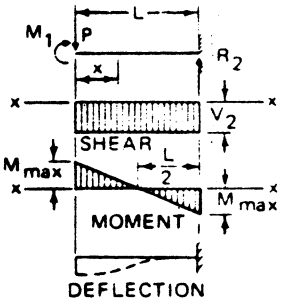


$R_2 = P$

$M_x = P\left(\frac{L}{2} - x\right)$

$M_{max}$ (AT BOTH ENDS) $= \frac{PL}{2}$

$y_x = \left[\frac{-P(L-x)^2}{12EI}\right](L + 2x)$

$y_{max}$ (AT DEFLECTED END) $= \frac{-PL^3}{12EI}$

---

FIXED AT ONE END, FREE TO DEFLECT VERTICALLY BUT NOT ROTATE AT OTHER
–UNIFORMLY DISTRIBUTED LOAD

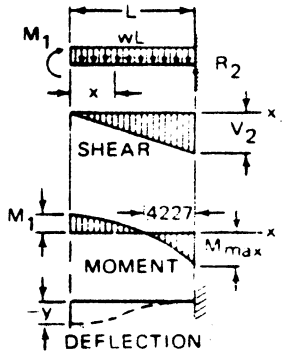


$R_2 = V = wL$

$V_x = wx$

$M_1$ (AT DEFLECTED END) $= \frac{wL^2}{6}$

$M_x = \frac{w}{6}(L^2 - 3x^2)$

$M_{max}$ (AT FIXED END) $= \frac{wL^2}{3}$

$y_x = \frac{-w(L^2 - x^2)^2}{24EI}$

$y_{max}$ (AT DEFLECTED END) $= \frac{-wL^4}{24EI}$

---

FIXED AT ONE END – SUPPORTED AT OTHER WITH APPLIED END MOMENT $M_o$

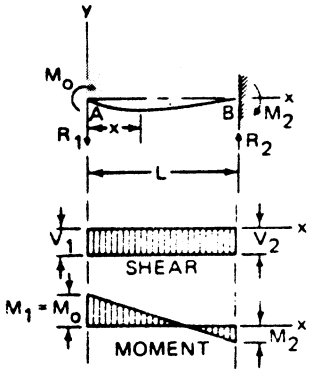


$R_A = -\frac{3M_o}{2L}$ ; $R_B = \frac{3M_o}{2L}$

$V = -\frac{3M_o}{2L}$

$M_1 = M_o$ $M_B = \frac{M_o}{2}$

$M_x = \frac{M_o}{2}\left(2 - \frac{3x}{L}\right)$

Max. (+M) $= M_o$ @ A

Max. (–M) $= -\frac{M_o}{2}$ @ B

$y_x = \frac{M_o}{4EI}\left(2x^2 - \frac{x^3}{L} - Lx\right)$

Max. y $= -\frac{M_o L^2}{27EI}$ @ $x = \frac{L}{3}$

$\theta = -\frac{M_o L}{4EI}$ @ A

## Table B1.1.1-2 Shear, Moment, and Deflection Formulas for Simple Beams (Cont.)

FIXED AT ONE END SUPPORTED AT OTHER WITH APPLIED INTERMEDIATE MOMENT, $M_0$

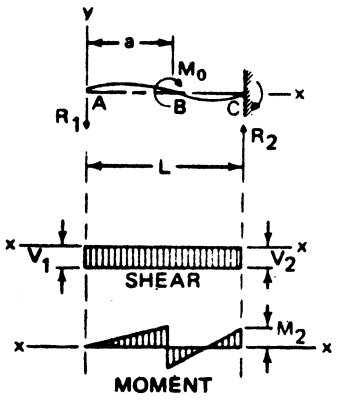


$$R_1 = -\frac{3M_0}{2L}\left(\frac{L^2 - a^2}{L^2}\right)$$

$$R_2 = \frac{3M_0}{2L}\left(\frac{L^2 - a^2}{L^2}\right)$$

(A TO B) $V = +R_1$

(B TO C) $V = +R_1$

$$M_2 = \frac{M_0}{2}\left(1 - \frac{3a^2}{L^2}\right)$$

(A TO B) $M = +R_1 x$

(B TO C) $M = +R_1 x + M_0$

Max $(+M) = M_0\left[1 - \frac{3a(L^2 - a^2)}{2L^3}\right]$ JUST TO THE RIGHT OF B

Max $(-M) = -M_2$ AT C WHEN $a < 0.275\,L$

Max $(-M) = R_1\,a$ TO THE LEFT OF B WHEN $a > 0.275\,L$

(A TO B) $y = \frac{M_0}{EI}\left[\frac{L^2 - a^2}{4L^3}(3L^2 x - x^3) - (L - a)x\right]$

(B TO C) $y = \frac{M_0}{EI}\left[\frac{L^2 - a^2}{4L^3}(3L^2 x - x^3) - Lx + \frac{(x^2 + a^2)}{2}\right]$

$$\theta = \frac{M_0}{EI}\left(a - \frac{L}{4} - \frac{3a^2}{4L}\right) \text{ @ A}$$

## Table B1.1.1-2 Shear, Moment, and Deflection Formulas for Simple Beams (Cont.)

### CONCENTRATED LOAD AT CENTER

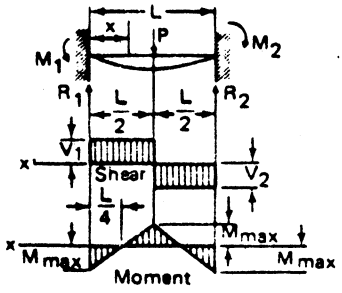


$R = V = \frac{P}{2}$

$M_{max}$ (at center and ends) $= \frac{PL}{8}$

$M_x$ (when $x < \frac{L}{2}$) $= \frac{P}{8}(4x - L)$

$y_{max}$ (at center) $= \frac{-PL^3}{192EI}$

$y_x = \frac{-Px^2}{48EI}(3L - 4x)$

### CONCENTRATED LOAD AT ANY POINT

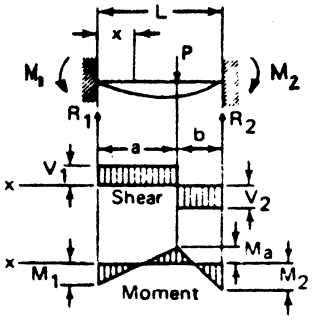


$R_1 = V_1$ (max when $a < b$) $= \frac{Pb^2}{L^3}(3a + b)$

$R_2 = V_2$ (max when $a > b$) $= \frac{Pa^2}{L^3}(a + 3b)$

$M_1$ (max when $a < b$) $= \frac{Pab^2}{L^2}$

$M_2$ (max when $a > b$) $= \frac{Pa^2b}{L^2}$

$M_a$ (at point of load) $= \frac{2Pa^2b^2}{L^3}$

$M_x$ (when $x < a$) $= R_1x - \frac{Pab^2}{L^2}$

$y_{max}$ (when $a > b$ at $x = \frac{2aL}{3a + b}$) $= \frac{-2Pa^3b^2}{3EI(3a + b)^2}$

$y_a$ (at point of load) $= \frac{-Pa^3b^3}{3EIL^3}$

$y_x$ (when $x < a$) $= \frac{-Pb^2x^2}{6EIL^3}(3aL - 3ax - bx)$

### UNIFORMLY DISTRIBUTED LOADS

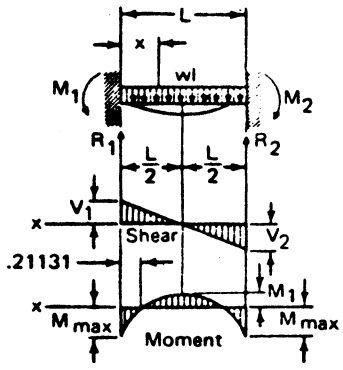


$R_1 = V_1 = R_2 = V_2 = \frac{wL}{2}$

$V_x = w(\frac{L}{2} - x)$

$M_{max}$ (at ends), $M_1$ & $M_2$ $= \frac{wL^2}{12}$

$M_1$ (at center) $= \frac{wL^2}{24}$

$M_x = \frac{w}{12}(6Lx - L^2 - 6x^2)$

$y_{max}$ (at center) $= \frac{-wL^4}{384EI}$

$y_x = \frac{-wx^2}{24EI}(L - x)^2$

# Table B1.1.1-2 Shear, Moment, and Deflection Formulas for Simple Beams (Cont.)

## STATICALLY INDETERMINATE BEAMS – PARTIAL UNIFORM LOAD

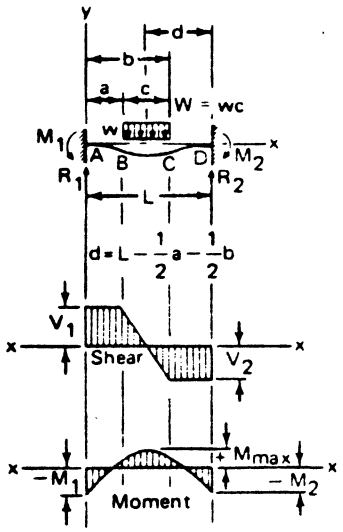


$$R_1 = \frac{W}{4L^2}\left(12d^2 - \frac{8d^3}{L} + \frac{2bc^2}{L} - \frac{c^3}{L} - c^2\right); \quad R_2 = W - R_1$$

(A to B) $V = R_1$; (B to C) $V = R_1 - W\left(\frac{x-a}{c}\right)$; (C to D) $V = R_1 - W$

$$M_1 = -\frac{W}{24L}\left(\frac{23d^3}{L} - \frac{6bc^2}{L} + \frac{3c^3}{L} + 4c^2 - 24d^2\right)$$

$$M_2 = \frac{W}{24L}\left(\frac{24d^3}{L} - \frac{6bc^2}{L} + \frac{3c^3}{L} + 2c^2 - 48d^2 + 24dL\right)$$

(A to B) $M = M_1 + R_1x$; (B to C) $M = -M_1 + R_1x - W\frac{(x-a)^2}{2c}$

(C to D) $M = -M_1 + R_1x - W(x - L + d)$

Max (+M) is between B and C at $x = a + \frac{R_1c}{W}$

Max (−M) = $-M_1$ when $a < (L - b)$; Max (−M) = $-M_2$ when $a > (L - b)$

(A to B) $y = \frac{1}{6EI}(R_1x^3 - 3M_1x^2)$

(B to C) $y = \frac{1}{6EI}\left(R_1x^3 - 3M_1x^2 - \frac{W(x-a)^4}{4c}\right)$

(C to D) $y = \frac{1}{6EI}\left[R_2(L-x)^3 - 3M_2(L-x)^2\right]$

## TRIANGULAR LOAD

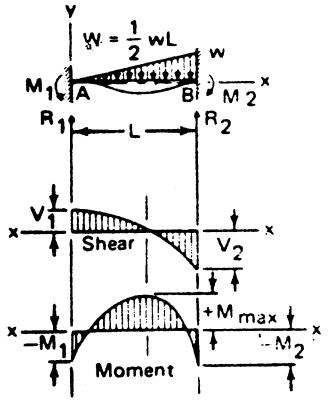


$$R_1 = \frac{3W}{10}$$

$$R_2 = \frac{1W}{10}$$

$$M_1 = \frac{WL}{15}$$

$$M_2 = \frac{WL}{10}$$

$$V_x = W\left(\frac{3}{10} - \frac{x^2}{L^2}\right)$$

$$M_x = W\left(\frac{3x}{10} - \frac{L}{15} - \frac{x^3}{3L^2}\right)$$

Max (+M) = 0.043 WL @ x = 0.548 L

Max (−M) = $-\frac{WL}{10}$ at B

$$y_x = \frac{W}{60EI}\left(3x^3 - 2Lx^2 - \frac{x^5}{L^2}\right)$$

Max y = $-0.002617\frac{WL^3}{EI}$ @ x = 0.525 L

# Table B1.1.1-2 Shear, Moment, and Deflection Formulas for Simple Beams (Cont.)

## STATICALLY INDETERMINATE BEAMS – PARTIAL TRIANGULAR LOAD

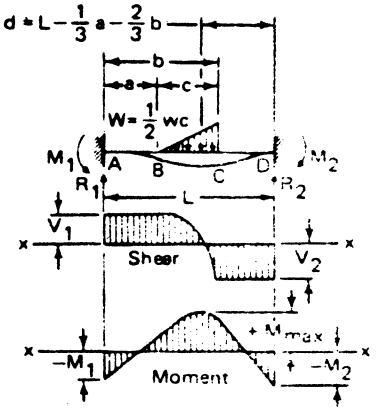


$$R_1 = \frac{W}{L^2}\left[3d^2 - \frac{1}{6}c^2 + \left(\frac{1}{3}\right)\left(\frac{6c^2}{L}\right) - \left(\frac{17}{135}\right)\left(\frac{c^3}{L}\right) - 2\frac{d^3}{L}\right]$$

$$R_2 = W - R_1$$

$$M_1 = -\frac{W}{L}\left[\frac{d^3}{L} + \frac{1}{9}c^2 + \left(\frac{51}{810}\right)\left(\frac{c^3}{L}\right) - \left(\frac{1}{6}\right)\left(\frac{c^3 b}{L}\right) - d^2\right]$$

$$M_2 = \frac{W}{L}\left[\frac{d^3}{L} + \frac{c^2}{18} + \left(\frac{51}{810}\right)\left(\frac{c^3}{L}\right) - \left(\frac{1}{6}\right)\left(\frac{c^2 b}{L}\right) - 2d^2 + dL\right]$$

Max + M at $x = a + c\sqrt{\frac{R_1}{W}}$

Max − M = $M_1$ when $d > \frac{L}{2}$, $M_2$ when $d < \frac{L}{2}$

(A to B)

$V = R_1$; $M = -M_1 + R_1 x$ $\qquad y = \frac{1}{6EI}(R_1 x^3 - 3M_1 x^2)$

(B to C)

$$V = R_1 - W\frac{(x-a)^2}{c^2} \qquad M = -M_1 + R_1 x - W\frac{(x-a)^3}{3c^2} \qquad y = \frac{1}{EI}\left(\frac{1}{6}R_1 x^3 - \frac{1}{2}M_1 x^2 - \frac{1}{60}W\frac{(x-a)^5}{c^2}\right)$$

(C to D)

$V = R_1 - W$; $M = M_1 + R_1 x - W(x - L + d)$

$$y = \frac{1}{6EI}\left\{R_1(x^3 - 3L^2 x + 2L^3) - 3M_1(L-x)^2 + W\left[3d^2 x + d^3 - 3d^2 L - (x - L + d)^3\right]\right\}$$

## STATICALLY INDETERMINATE BEAMS – INTERMEDIATE COUPLE

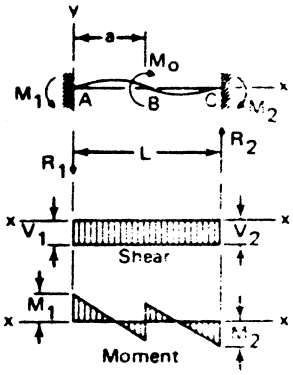


$$R_1 = -\frac{6M_o}{L^3}(aL - a^2); \qquad R_2 = \frac{6M_o}{L^3}(aL - a^2)$$

$$V = +R_1$$

$$M_1 = -\frac{M_o}{L^2}(4La - 3a^2 - L^2)$$

$$M_2 = \frac{M_o}{L^2}(2La - 3a^2)$$

(A to B) $M = -M_1 + R_1 x$; (B to C) $M = -M_1 + R_1 + M_o$

Max (+M) $= M_o\left(\frac{4a}{L} - \frac{9a^2}{L^2} + \frac{6a^3}{L^3}\right)$ just to the right of B

Max (−M) $= M_o\left(\frac{4a}{L} - \frac{9a^2}{L^2} + \frac{6a^3}{L^3} - 1\right)$ just to the left of B

(A to B) $y = -\frac{1}{6EI}(3M_1 x^2 - R_1 x^3)$

(B to C) $y = \frac{1}{6EI}\left[(M_o - M_1)(3x^2 - 6Lx + 3L^2) - R_1(3L^2 x - x^3 - 2L^3)\right]$

Max (+y) $= \frac{2M_1}{R_1}$ if $a > \frac{L}{3}$ $\qquad$ Max (−y) $= L - \frac{2M_2}{R_2}$ if $a < \frac{2L}{3}$

## B1.2.0 Curved Beams

When a curved beam is bent in the plane of initial curvature, plane sections remain plane, but because of the different lengths of fibers on the inner and outer sides of the beam the distribution of strain is not linear; the neutral axis therefore does not pass through the centroid of the section. If (K) denotes a correction factor, the stress at the extreme fiber of a curved beam is given by the equation.

$$\sigma = K\,(Mc/I) \qquad \text{(B1-1)}$$

Values of (K) are always less than 1.0 for the outer side of the curved beam. They are always greater than 1.0 for the inner side of the curved beam. In the limit as the radius of curvature becomes large, K approaches a value of 1.0 which represents a straight beam.

Values of K are given in Table B1.2.0-1 for various shaped beams. For shapes not covered in the table, K may be computed for the inside (concave) fibers by the approximate expression:

$$K = 1. + a\,\frac{I}{bc^2}\left[\frac{1}{R-c} + \frac{1}{R}\right] \qquad \text{(B1-2)}$$

where

a = 1.05 circular or eliptical sections
1.50 rectangular sections

b = Section maximum width for circular or eliptical sections
Section inside width for rectangular sections

c = Distances from centroidal axis to extreme fiber on concave side of beam, in.

I = Section moment of inertia, $in^4$

R = Radius of curvature measured to centroid of section, in.

The outer fiber is generally not important since its K value is always less than 1.0

## Table B1.2.0-1 Values of K for Curved Beams

| Section | $\frac{R}{c}$ | Factor K | |
|---|---|---|---|
| | | Inside Fiber | Outside Fiber |
| 1. 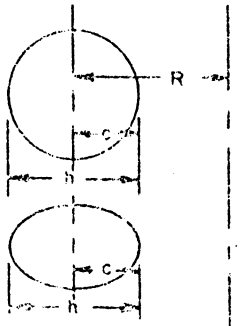  K the same for circle and ellipse and independent of dimensions. | 1.2 | 3.41 | 0.54 |
| | 1.4 | 2.40 | 0.60 |
| | 1.6 | 1.96 | 0.65 |
| | 1.8 | 1.75 | 0.68 |
| | 2.0 | 1.62 | 0.71 |
| | 3.0 | 1.33 | 0.79 |
| | 4.0 | 1.23 | 0.84 |
| | 6.0 | 1.14 | 0.89 |
| | 8.0 | 1.10 | 0.91 |
| | 10.0 | 1.08 | 0.93 |
| 2. 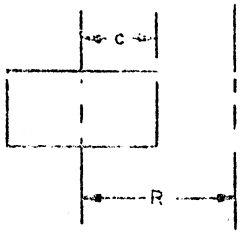  K independent of section dimensions | 1.2 | 2.89 | 0.57 |
| | 1.4 | 2.13 | 0.63 |
| | 1.6 | 1.79 | 0.67 |
| | 1.8 | 1.63 | 0.70 |
| | 2.0 | 1.52 | 0.73 |
| | 3.0 | 1.30 | 0.81 |
| | 4.0 | 1.20 | 0.85 |
| | 6.0 | 1.12 | 0.90 |
| | 8.0 | 1.09 | 0.92 |
| | 10.0 | 1.07 | 0.94 |
| 3. 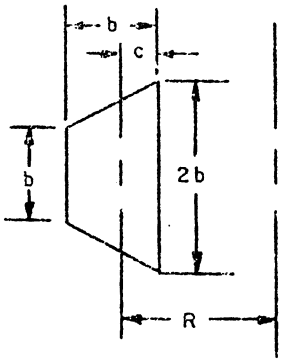  | 1.2 | 3.01 | 0.54 |
| | 1.4 | 2.18 | 0.60 |
| | 1.6 | 1.87 | 0.65 |
| | 1.8 | 1.69 | 0.68 |
| | 2.0 | 1.58 | 0.71 |
| | 3.0 | 1.33 | 0.80 |
| | 4.0 | 1.23 | 0.84 |
| | 6.0 | 1.13 | 0.88 |
| | 8.0 | 1.10 | 0.91 |
| | 10.0 | 1.08 | 0.93 |

## Table B1.2.0-1 Values of K for Curved Beams (Cont.)

| Section | R/c | Factor K | |
|---|---|---|---|
| | | Inside Fiber | Outside Fiber |
| 4. 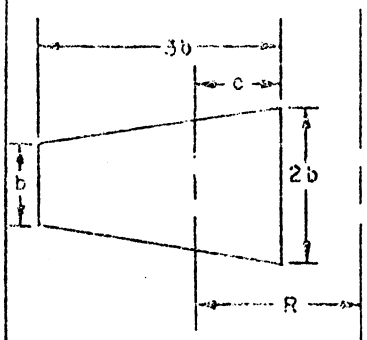  | 1.2 | 3.09 | 0.56 |
| | 1.4 | 2.25 | 0.62 |
| | 1.6 | 1.91 | 0.66 |
| | 1.8 | 1.73 | 0.70 |
| | 2.0 | 1.61 | 0.73 |
| | 3.0 | 1.37 | 0.81 |
| | 4.0 | 1.26 | 0.86 |
| | 6.0 | 1.17 | 0.91 |
| | 8.0 | 1.13 | 0.94 |
| | 10.0 | 1.11 | 0.95 |
| 5. 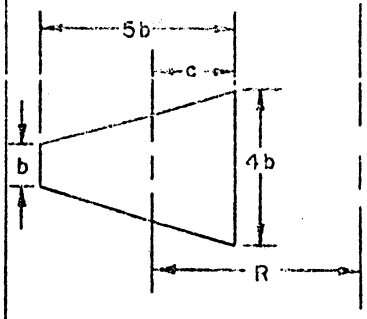  | 1.2 | 3.14 | 0.52 |
| | 1.4 | 2.29 | 0.54 |
| | 1.6 | 1.93 | 0.62 |
| | 1.8 | 1.74 | 0.65 |
| | 2.0 | 1.61 | 0.69 |
| | 3.0 | 1.34 | 0.76 |
| | 4.0 | 1.24 | 0.82 |
| | 6.0 | 1.15 | 0.87 |
| | 8.0 | 1.12 | 0.91 |
| | 10.0 | 1.10 | 0.93 |
| 6. 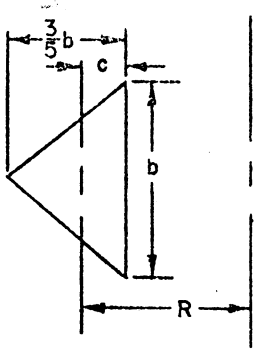  | 1.2 | 3.26 | 0.44 |
| | 1.4 | 2.39 | 0.50 |
| | 1.6 | 1.99 | 0.54 |
| | 1.8 | 1.78 | 0.57 |
| | 2.0 | 1.66 | 0.60 |
| | 3.0 | 1.37 | 0.70 |
| | 4.0 | 1.27 | 0.75 |
| | 6.0 | 1.16 | 0.82 |
| | 8.0 | 1.12 | 0.86 |
| | 10.0 | 1.09 | 0.88 |

## Table B1.2.0-1 Values of K for Curved Beams (Cont.)

| Section | $\frac{R}{c}$ | Factor K | |
|---|---|---|---|
| | | Inside Fiber | Outside Fiber |
| 7. 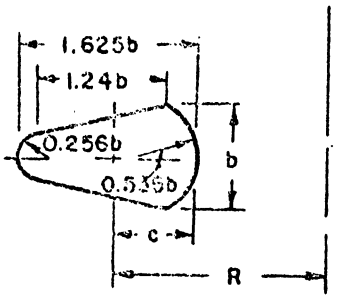  $A = 1.05b^2$ $I = 0.18b^4$ $C = 0.70b$ | 1.2 | 3.65 | 0.53 |
| | 1.4 | 2.50 | 0.59 |
| | 1.6 | 2.08 | 0.63 |
| | 1.8 | 1.85 | 0.66 |
| | 2.0 | 1.69 | 0.69 |
| | 2.5 | 1.49 | 0.74 |
| | 3.0 | 1.38 | 0.78 |
| | 4.0 | 1.27 | 0.83 |
| | 6.0 | 1.19 | 0.90 |
| | 8.0 | 1.14 | 0.93 |
| | 10.0 | 1.12 | 0.96 |
| 8. 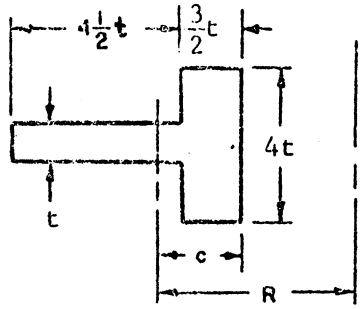  | 1.2 | 3.63 | 0.58 |
| | 1.4 | 2.54 | 0.63 |
| | 1.6 | 2.14 | 0.67 |
| | 1.8 | 1.89 | 0.70 |
| | 2.0 | 1.73 | 0.72 |
| | 3.0 | 1.41 | 0.79 |
| | 4.0 | 1.29 | 0.83 |
| | 6.0 | 1.18 | 0.88 |
| | 8.0 | 1.13 | 0.91 |
| | 10.0 | 1.10 | 0.92 |
| 9. 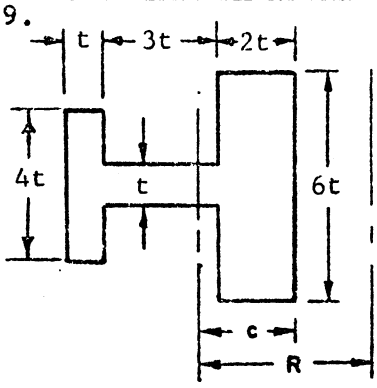  | 1.2 | 3.55 | 0.67 |
| | 1.4 | 2.48 | 0.72 |
| | 1.6 | 2.07 | 0.76 |
| | 1.8 | 1.83 | 0.78 |
| | 2.0 | 1.69 | 0.80 |
| | 3.0 | 1.38 | 0.86 |
| | 4.0 | 1.26 | 0.89 |
| | 6.0 | 1.15 | 0.92 |
| | 8.0 | 1.10 | 0.94 |
| | 10.0 | 1.08 | 0.95 |

## Table B1.2.0-1 Values of K for Curved Beams (Cont.)

| Section | $\frac{R}{c}$ | Factor K | |
|---|---|---|---|
| | | Inside Fiber | Outside Fiber |
| 10. 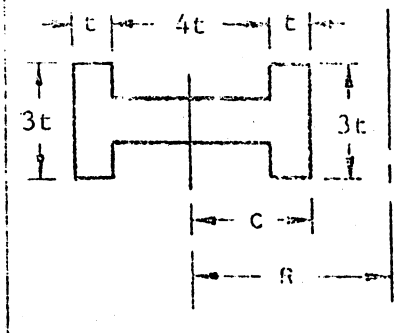  | 1.2 | 2.52 | 0.67 |
| | 1.4 | 1.90 | 0.71 |
| | 1.6 | 1.63 | 0.75 |
| | 1.8 | 1.50 | 0.77 |
| | 2.0 | 1.41 | 0.79 |
| | 3.0 | 1.23 | 0.86 |
| | 4.0 | 1.16 | 0.89 |
| | 6.0 | 1.10 | 0.92 |
| | 8.0 | 1.07 | 0.94 |
| | 10.0 | 1.05 | 0.95 |
| 11. 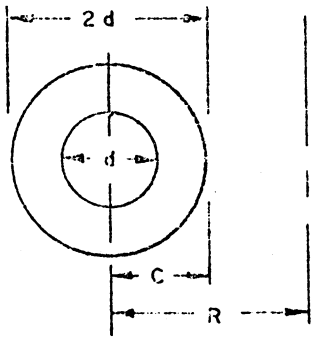  | 1.2 | 3.28 | 0.58 |
| | 1.4 | 2.31 | 0.64 |
| | 1.6 | 1.89 | 0.68 |
| | 1.8 | 1.70 | 0.71 |
| | 2.0 | 1.57 | 0.73 |
| | 3.0 | 1.31 | 0.81 |
| | 4.0 | 1.21 | 0.85 |
| | 6.0 | 1.13 | 0.90 |
| | 8.0 | 1.10 | 0.92 |
| | 10.0 | 1.07 | 0.93 |
| 12. 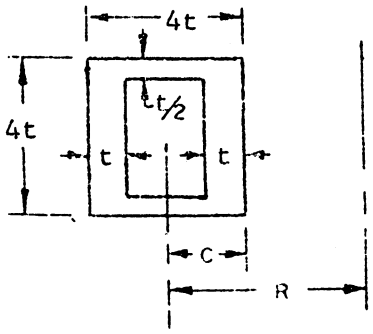  | 1.2 | 2.63 | 0.68 |
| | 1.4 | 1.97 | 0.73 |
| | 1.6 | 1.66 | 0.76 |
| | 1.8 | 1.51 | 0.78 |
| | 2.0 | 1.43 | 0.80 |
| | 3.0 | 1.23 | 0.86 |
| | 4.0 | 1.15 | 0.89 |
| | 6.0 | 1.09 | 0.92 |
| | 8.0 | 1.07 | 0.94 |
| | 10.0 | 1.06 | 0.95 |

Aircraft structural beams usually are made up of thin walled elements. If a cross section of a curved beam has flanges of considerable width, then their distortion under bending stresses may become important. The distortion is caused because the longitudinal bending stresses in the flanges give components in a radial direction which tend to produce bending in the flanges. This bending results in some diminishing of the longitudinal bending stresses in portions of the flanges at a considerable distance from the web.

The distribution of longitudinal stress in curved beam flanges of I beams is given in Figure B1.2.0-1 . In using this figure, an effective flange width must be determined as given in Figure B1.2.0-2. The value for K may be taken from Table B1.2.0-1 or computed from Equation B1-2.

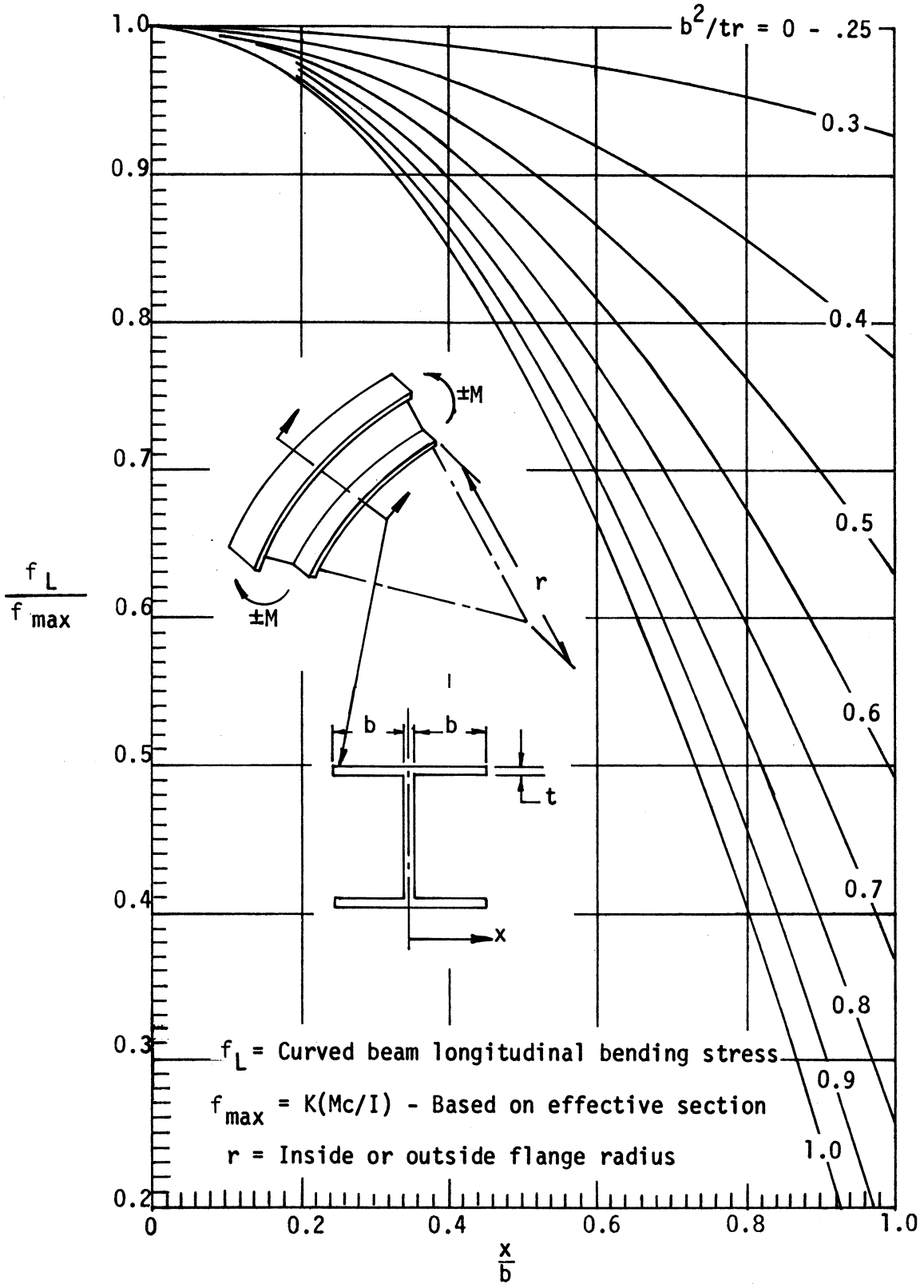


Figure B1.2.0-1 Longitudinal Stress Variation Across Flange of a Curved Beam in Bending

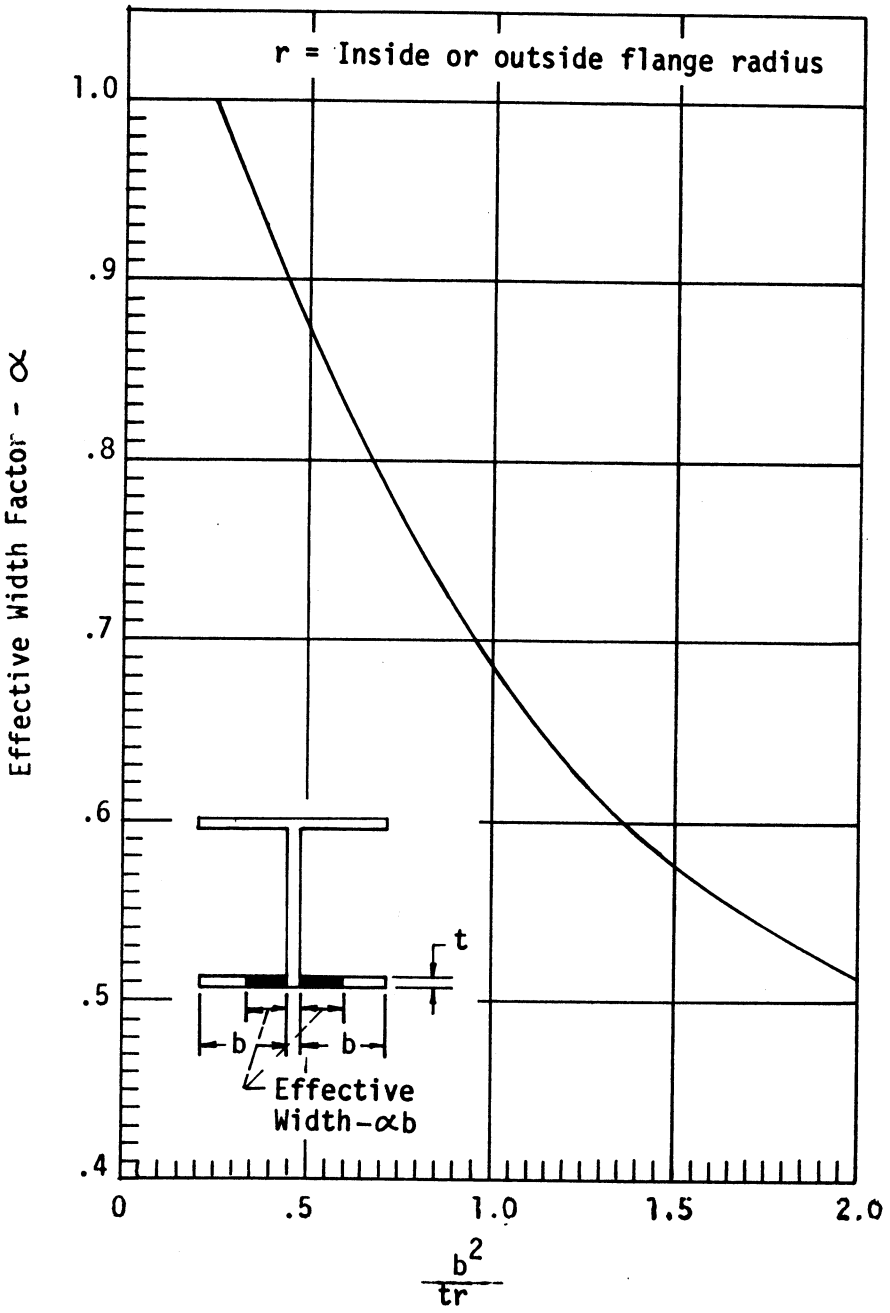


Figure B1.2.0-2 Effective Width of a Curved Beam in Bending

## B1.3.0 Continuous Beams

The three-moment equation is useful in the solution of problems involving continuous beams with relatively few redundant supports. The general equation is

$$\frac{M_a L_1}{I_1} + \frac{2M_b L_1}{I_1} + \frac{2M_b L_2}{I_2} + \frac{M_c L_2}{I_2} =$$

$$K_1 + K_2 + \frac{6E}{L_1}(Y_a - Y_b) + \frac{6E}{L_2}(Y_c - Y_b) \quad \text{(B1-3)}$$

where $K_1$ and $K_2$ are functions of loading on spans $L_1$ and $L_2$ respectively. Figure B1.3.0-1 gives geometry and moment definitions. Values for $K_1$ and $K_2$ are given in Table B1.3.0-1 for various types of loading.

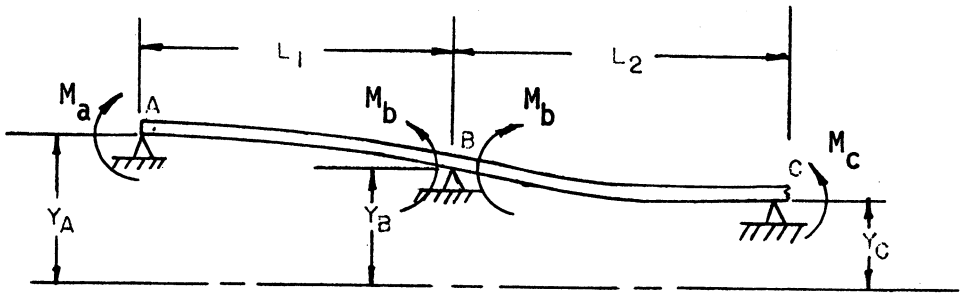


Figure B1.3.0-1 Geometry and Moment Definition for a Continuous Beam

In using Equation B1-3, one equation must be written for each intermediate support. The system of simultaneous equations is then solved for the moments at the intermediate supports. Support reactions can then be determined based on equilibrium considerations.

## Table B1.3.0-1 K Factors for Continuous Beams

| Type of Loading | Left Bay - $K_1$ | Right Bay - $K_2$ |
|---|---|---|
| 1. 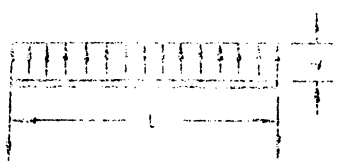 | $\frac{+w_1L_1^3}{4I_1}$ | $\frac{+w_2L_2^3}{4I_2}$ |
| 2. 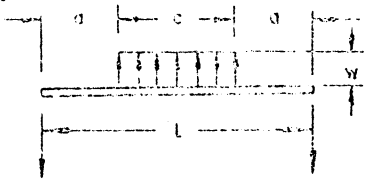 | $\frac{+w_1c_1\,(3L_1^2-c_1^2)}{8I_1}$ | $\frac{+w_2c_2\,(3L_2^2-c_2^2)}{8I_2}$ |
| 3. 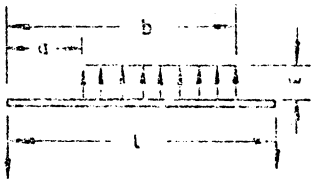 | $K_1 = +\frac{w_1\left[b_1^2(2L_1^2-b_1^2)-a_1^2(2L_1^2-a_1^2)\right]}{4I_1L_1}$ <br> $K_2 = +\frac{w_2\left[b_2^2(2L_2^2-b_2^2)-a_2^2(2L_2^2-a_2^2)\right]}{4I_2L_2}$ | |
| 4. 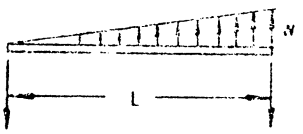 | $\frac{+2w_1L_1^3}{15I_1}$ | $\frac{+7w_2L_2^3}{60\,I_2}$ |
| 5. 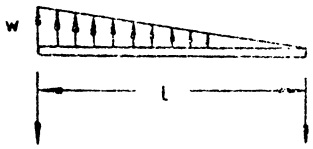 | $\frac{+7w_1L_1^3}{60I_1}$ | $\frac{+2w_2L_2^3}{15I_2}$ |
| 6. 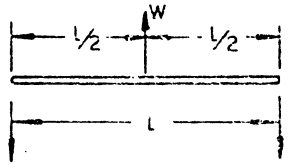 | $\frac{+3L_1^2w_1}{8I_1}$ | $\frac{+3L_2^2w_2}{8I_2}$ |

## Table B1.3.0-1 K Factors for Continuous Beams (Cont.)

| Type of Loading | Left Bay - $K_1$ | Right Bay - $K_2$ |
|---|---|---|
| 7. 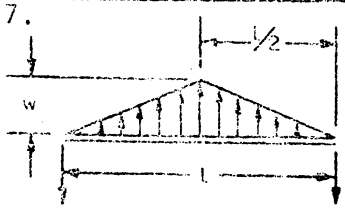  | $\frac{+5w_1L_1^3}{32I_1}$ | $\frac{+5w_2L_2^2}{32I_2}$ |
| 8. 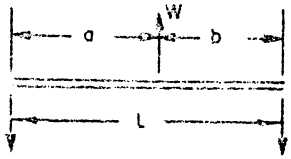  | $\frac{+w_1a_1\left(L_1^2-a_1^2\right)}{I_1L_1}$ | $\frac{+w_2b_2\left(L_2^2-b_2^2\right)}{I_2L_2}$ |
| 9. 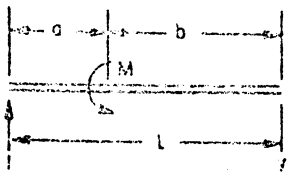  | $+\frac{M_1}{I_1}\left(L_1-\frac{3a_1^2}{L_1}\right)$ | $+\frac{M_2}{I_2}\left(\frac{3b_2^2}{L_2}-L_2\right)$ |
| 10. 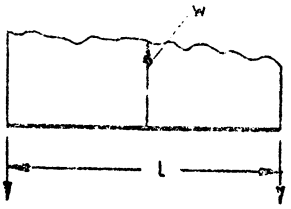  | $K_1=\frac{6}{I_2L_2}\int_0^L M_1\,x_1\,dx_1$ <br> $K_2=\frac{6}{I_2L_2}\int_0^L M_2\,x_2\,dx_2$ <br> Where M is the bending moment. | |

Figures B1.3.0-2 and B1.3.0-3 give shears and moments for uniformly loaded continuous beams with two and three intermediate supports. As the number of support increases, the moments at the supports approach that of a simple beam clamped at its ends ($M = -.0833\ wL^2$).

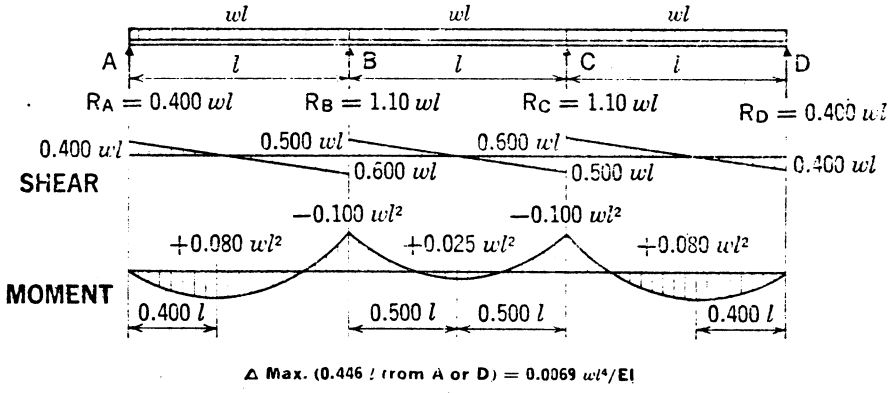


Figure B1.3.0-2 Uniformly Loaded Continuous Beam Two Intermediate Supports

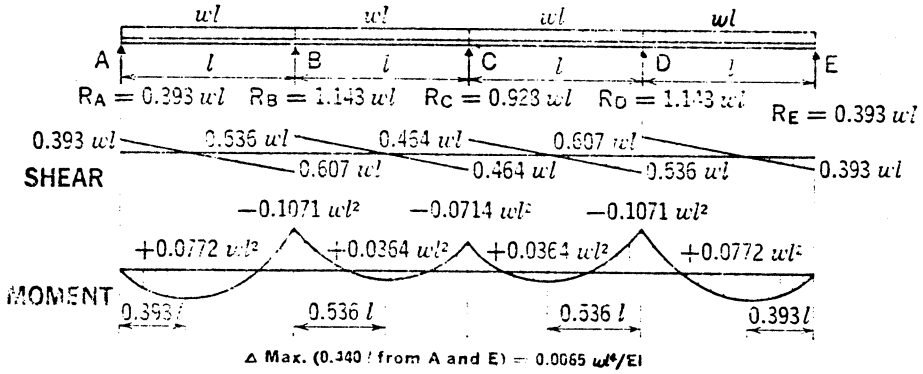


Figure B1.3.0-3 Uniformly Loaded Continuous Beam Three Intermediate Supports

## B1.4.0 Modulus of Rupture

| SECTION | K |
|---|---|
| | 1.0 |
| | 1.5 |
| | THIN — THICK WEB 1.0 — 1.5 |
| | THIN — THICK WEB 1.0 — 1.5 |
| | RING — SOLID 1.25 — 1.70 |
| | 2.0 |
| | THIN — THICK WEB 1.5 — 2.0 |
| | 4/3 |

Allowable $\frac{Mc}{I}$ vs. K curve is envelope of curves derived from ultimate allowable or 1.5 times yield allowable, whichever is less.

Local crippling may be critical but is not considered in this chart.

See ANC-5a for modulus of rupture value of round tubing.

Legend: $(F_{ty})\ F_{tu}$ - Minimum guaranteed value in Kips

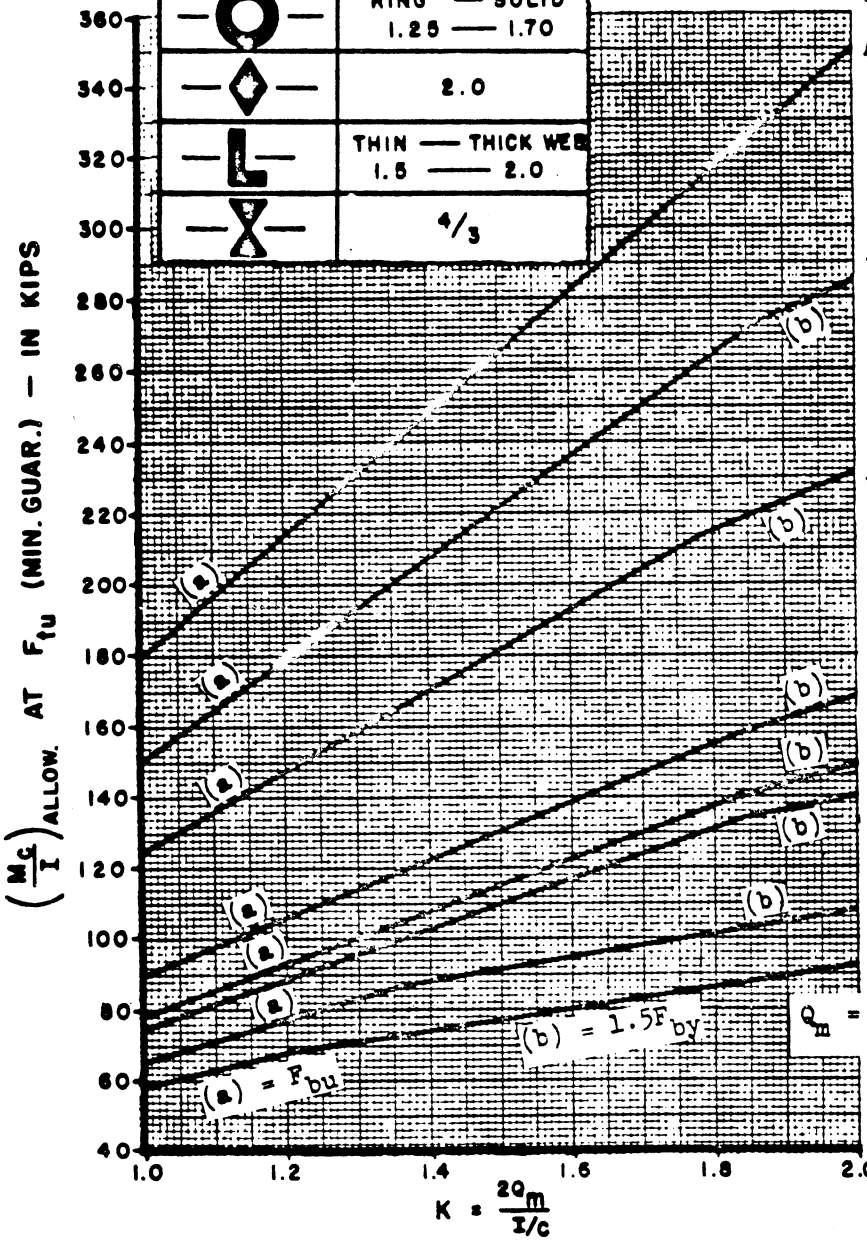


Alloy Steel (165) 180

Alloy Steel (135) 150
4330XX Steel Cast. (135) 150
X4130 Steel Forging (135) 150

Alloy Steel (100) 125

Alloy Steel (70) 90

75ST Bar or Extrusion (70) 78
75ST Forging (65) 75

14ST Forging (50) 65

24ST Extrusion (42) 58

$Q_m$ = Static moment, about neutral axis, of area between extreme compression fiber or extreme tension fiber and the neutral axis.

| SECTION | K |
|---|---|
| | 1.0 |
| | 1.5 |
| | THIN — THICK WEB 1.0 — 1.5 |
| | THIN — THICK WEB 1.0 — 1.5 |
| | RING — SOLID 1.25 — 1.70 |
| | 2.0 |
| | THIN — THICK WEB 1.5 — 2.0 |
| | 4/3 |

Allowable $\frac{Mc}{I}$ vs. K for minimum quaranteed values of $F_{tu}$ and $F_{ty}$. Local crippling may be critical but is not considered in this chart.

Legend: —— Ultimate
- - - Yield
($F_{ty}$) $F_{tu}$ - in Kips

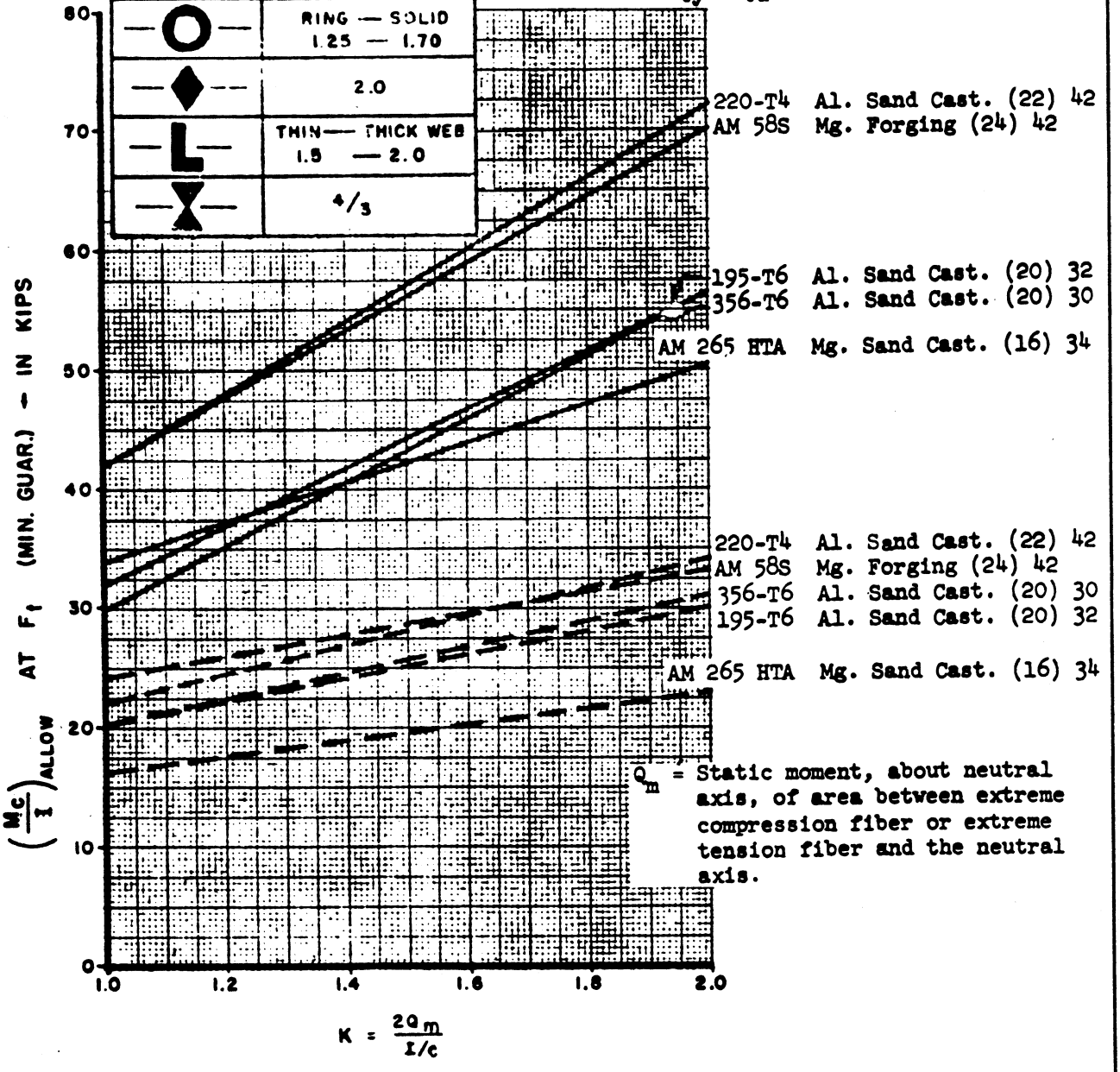


$Q_m$ = Static moment, about neutral axis, of area between extreme compression fiber or extreme tension fiber and the neutral axis.

## References

B1-1 Timoshenko, S. Strength of Materials, Part II, Advanced Theory and Problems, Second Edition, Van Nostrand Co., N.Y., 1941.

# FRAMES

## B2.0.0 Frames

## B2.1.0 Circular Rings

### B2.1.1 Introduction

When shell-supported rings are externally loaded, the applied loading is resisted primarily by shearing forces within the shell. The VQ/I and T/2A shear-flow distribution, frequently used in past analyses, is consistent with the assumption that the ring being loaded is rigid. For small diameter shells with sturdy rings, this distribution has proved reasonably satisfactory for design purposes. However, as the size of the airplane increases the rings become relatively more flexible so that the assumption of infinite ring stiffness may sometimes introduce errors of several hundred percent in ring design. Therefore, the necessity for a more accurate analysis becomes apparent. Design charts are presented in Figure B2.1.7-2 through B2.1.7-25 that include the ring and shell finite stiffness effects.

### B2.1.2 Theory

The theory upon which the design charts are based is presented in detail in Reference B2-1. Essentially, the analysis consists of the development and solution in closed form of a fourth-order finite-difference equation. The development is based upon the maintenance of continuity of deformation between reinforcing rings and the sheet of a circular semimonocoque cylinder. Only external forces acting in the plane of the ring are considerered. The following basic assumptions apply:

- The structure considered is a circular cylinder consisting of bays of identical construction and extending longitudinally to infinity in both directions from a loaded ring
- The reinforcing rings are of constant moment of inertia and are attached continuously along their periphery to the external skin. The radius of the neutral axis of each ring coincides with the radius to the middle of the skin.
- That part of the external skin area which is considered to resist overall fuselage bending is added to the stringer area and the combination is uniformly distributed about the periphery of the cylinder. This resulting combination gives an effective skin thickness, $t_e$ which resists the overall fuselage bending. The actual skin area is considered capable of supporting only shear stresses.

- Young's modulus, E, and the shear modulus, G, are constant throughout the cylinder.
- Radial deformation of rings and external skins causes no circumferential extension of these elements.

B2.1.3 Application

To apply the charts, a relative stiffness parameter (A/B) must be computed from the equation

$$A/B = \left[\frac{G}{E}\right](t_e)\left[\frac{R^3}{I}\right] \qquad \text{(B2-1)}$$

where

G = Shear modulus

E = Young's modulus

$t_e$ = thickness of all material carrying overall fuselage bending stresses in cylinder if uniformly distributed around the fuselage perimeter (effective skin)

R = radius of cylinder and ring (see second basic assumption)

I = moment of inertia of ring cross section

Equation B2-1 may be evaluated with the aid of Figure B2.1.7-1. For A/B = 0, the rings are considered rigid which corresponds to the assumption often used in previous analyses.

The proper design chart (Figures B2.1.7-2 through B2.1.7-25) is selected based on the external loads; either radial load, tangential load, or moment. The coefficient for bending moment, transverse shear, or axial load should be obtained for the desired angle by interpolating between the curves for the computed relative stiffness parameter, A/B. The bending moment, transverse shear, or axial load can then be computed based on the equation given on the figure. Sign convention is noted on each figure.

B2.1.4 Scope

Although the theory from which the charts are drawn is based on an infinitely long cylinder, loads and shear flows determined from the charts compare favorably with those obtained from experiment and from an exact analysis for cylinders of finite length, provided that the

rings loaded are at least two bays from external restraints.

The reference literature mentions another structural parameter,

$$A = R^6 t_e/(IL^3) \qquad \text{(B2-2)}$$

where L = distance between rings

R, $t_e$, and I are as mentioned before

The variation of this parameter was not included in preparing the graphs because large variations in "A" (i.e. $A = 2 \times 10^2$, $A = 2 \times 10^4$, $A = 2 \times 10^6$) have little effect in the resulting values of the coefficients.

Design charts are given not only for the loaded ring but also for the adjacent ring on either side. In case of several adjacent identical rings similarly loaded, the load distribution in and around the inner rings will approach that of a rigid ring (i.e. A/B = 0).

B2.1.5 Practical Designs

In practical designs, the rings are usually located inside the skin. Therefore, the radius of the centroidal axis of the ring is not equal to the radius to the middle of the skin. (Note the ring cross-section centroid is meant to include all the material which takes bending in the ring). For this case, in order to obtain section centroid moments, the ring bending moments must first be determined at the middle of the skin from the proper chart and then corrected by the addition of a moment equal to the axial load in the ring multiplied by the difference between the two radii mentioned above. Here, as in other cases in which there are multiple loads on a ring or on adjacent rings, the principle of superposition holds.

The case of a ring with a varying moment of inertia is approximated by determining an equivalent moment of inertia (I') from the equation

$$I' = \frac{\text{length of arc}}{\sum ds/I} \qquad \text{(B2-3)}$$

where the "length of arc" and $\sum ds/I$ are continued over only the region of appreciable bending moment. This region may be approximately located by using an estimated relative stiffness parameter (A/B) and referring to the appropriate curve. Ring loading coefficients are then determined by assuming the I' is constant around the ring.

The preceding approximation will work only if the moment of inertia distribution is symmetrical about some ring diameter and if the loads are applied where the axis of symmetry intersects the ring. If these conditions are not met, the equivalent moment of inertia method will give results which vary as much as two hundred percent from the results of a more exact strain energy analysis.

Even in the case of a symmetrically distributed moment of inertia with loads applied on the axis of symmetry, this approximate method gives results which differ by as much as twenty percent from the results of a strain energy analysis. Consequently the method should be used only for preliminary design.

B2.1.6 Example Problems

A. Constant Section Frame - Determine the magnitude and sign of the bending moment, axial load transverse shear, and ring-skin shear flow in the center ring for the constant section frames shown in Figure B2.1.6-1.

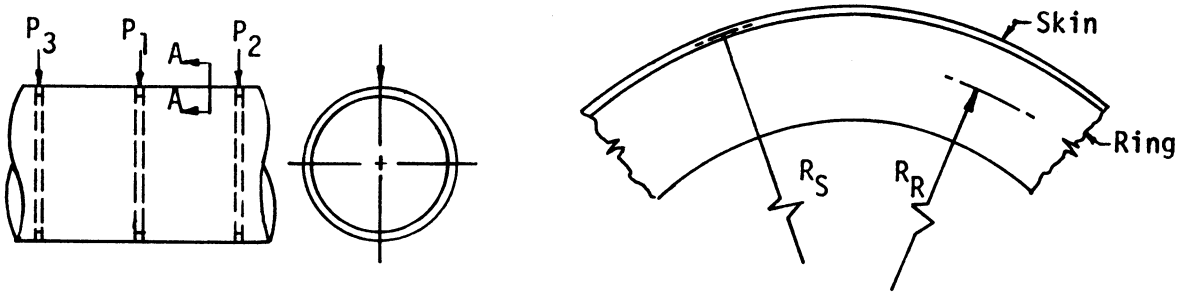


Figure B2.1.6-1 Constant Section Frame

Given: $P_1 = P_2 = P_3 = 10000$ lbs

$I = 2.9$ in$^4$

$t_e = 0.08$ in.

$G/E = 0.40$ in.

$R_s = 45.00$ in.

$R_R = 43.50$ in.

Compute: $A/B = \dfrac{(.40)(.08)(45)^3}{2.9} = 1000 \longrightarrow$ Equation B2-1

Note that $\phi$ is measured clockwise from load #1 (right end view).

Thus, for $\phi = 0°$, one obtains from Figures B2.1.7-2, -4,-6, and -8 the following values:

$$C_{mr} = 0.115;\ C_{ar} = -0.965;\ C_{sr} = -05.00;\ C_{qr} = 0.0$$

For load #1, one then computes, for example:

$$M_{\phi_1} = C_{mr}\ P_o\ R = 0.115 \times 10{,}000 \times 45 = 51{,}700 \text{ in. lbs.}$$

$$H_{\phi_1} = C_{ar}\ P_o = -0.965 \times 10{,}000 = 9650 \text{ lbs.}$$

With a similar procedure for various values of $\phi$. The process is repeated for the remaining loads, and the result is summed.

B. Variable Section Frames - Determine the magnitude and sign of the bending moment, axial load, transverse shear and the ring-skin shear flow for the frame shown in Figure B2.1.6-2. Variable geometry is provided in Table B2.1.6-1.

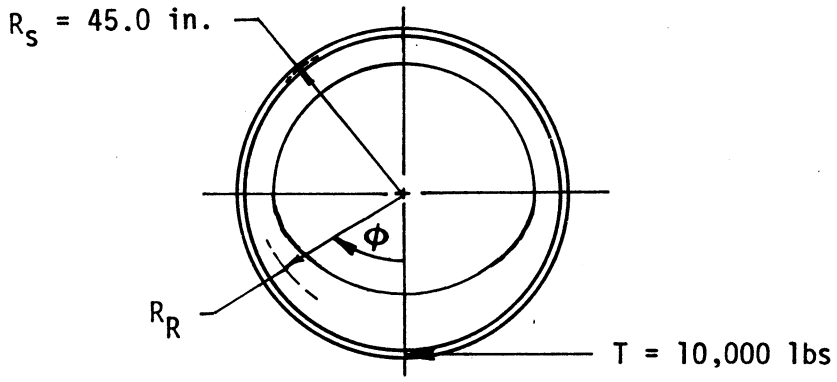


Figure B2.1.6-2 Variable Section Frame

Table B2.1.6-1 Variation of Ring Centroid Radius and Moment of Inertia with

| $\pm\phi$ Degrees | $R_R$ Inches | I Inches$^4$ |
|---|---|---|
| 0 | 41.76 | 10.0 |
| 20 | 41.82 | 9.5 |
| 40 | 42.52 | 4.5 |
| 60 | 43.24 | 1.6 |
| 80 → 180 | 43.50 | 1.0 |

Given: $A/B = 100$ for $I = 1.0\ in^4$
Since: $A/B \approx 1/I$
Then: $A/B = 10$ for $I = 10.0\ in^4$

A/B is assumed equal to 30. For this value, the region of maximum bending may be located from Figure B2.1.7-10. This region extends from -70° to -10° and from +10° to +70°. Since the ring is symmetrical about the point of loading, only the positive angle region of maximum moment need be considered in evaluating the equivalent moment of inertia I'.

$$I' = \frac{\text{length of arc}}{\sum ds/I} = \frac{2\pi R\left|\frac{\theta_1 - \theta_2}{360°}\right|}{2\pi R\,\frac{\Delta\theta}{360°}\left(\sum \frac{1}{I_N}\right)} = \frac{\left|\theta_1 - \theta_2\right|}{\Delta\theta\left(\sum \frac{1}{I_N}\right)}$$

where $\theta_1 = 10°$ (Note that angular measurements are absolute such
$\theta_2 = 70°$ that I' will always have a positive value)
$\Delta\theta$ = angular interval = 2.5° (This interval is arbitrary.)
$I_n$ = moment of inertia in the $n^{th}$ interval

$$I' = \frac{\left|10° - 70°\right|}{2.5°\left(\frac{1}{10} + \frac{1}{10} + \ldots + \frac{1}{1.4} + \frac{1}{1.2}\right)} = 5.30\ in^4$$

$$A/B \approx \frac{1}{I}$$

$$\therefore (A/B)_{equivalent} = 100\left(\frac{1.0}{5.30}\right) = 18.9$$

The method is an approximate one and should be used for preliminary estimates only. In any instance, however, it is necessary that the external load be applied along an axis of symmetry. If this requirement cannot be met, the method should not be used, since gross errors may occur.

B2.1.7 Design Charts

The following design charts should be used for determining the bending moments, transverse shear, and axial loads in circular rings caused by externally applied radial loads, tangential loads, and moments. The shear flow between the ring and the skin for a cylindrical skin reinforced by circular rings of constant or variable cross-section may also be determined.

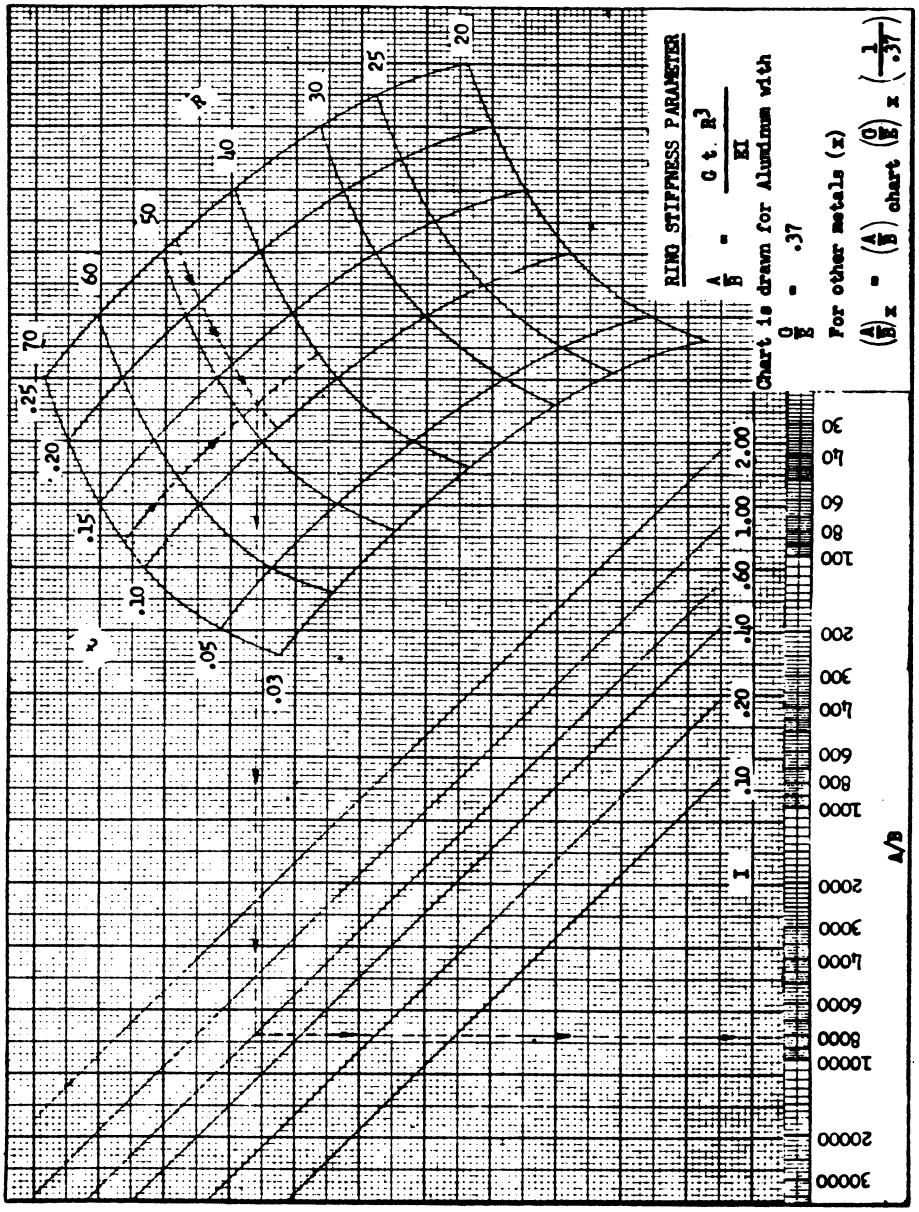


Figure B2.1.7-1 Ring Stiffness Parameter

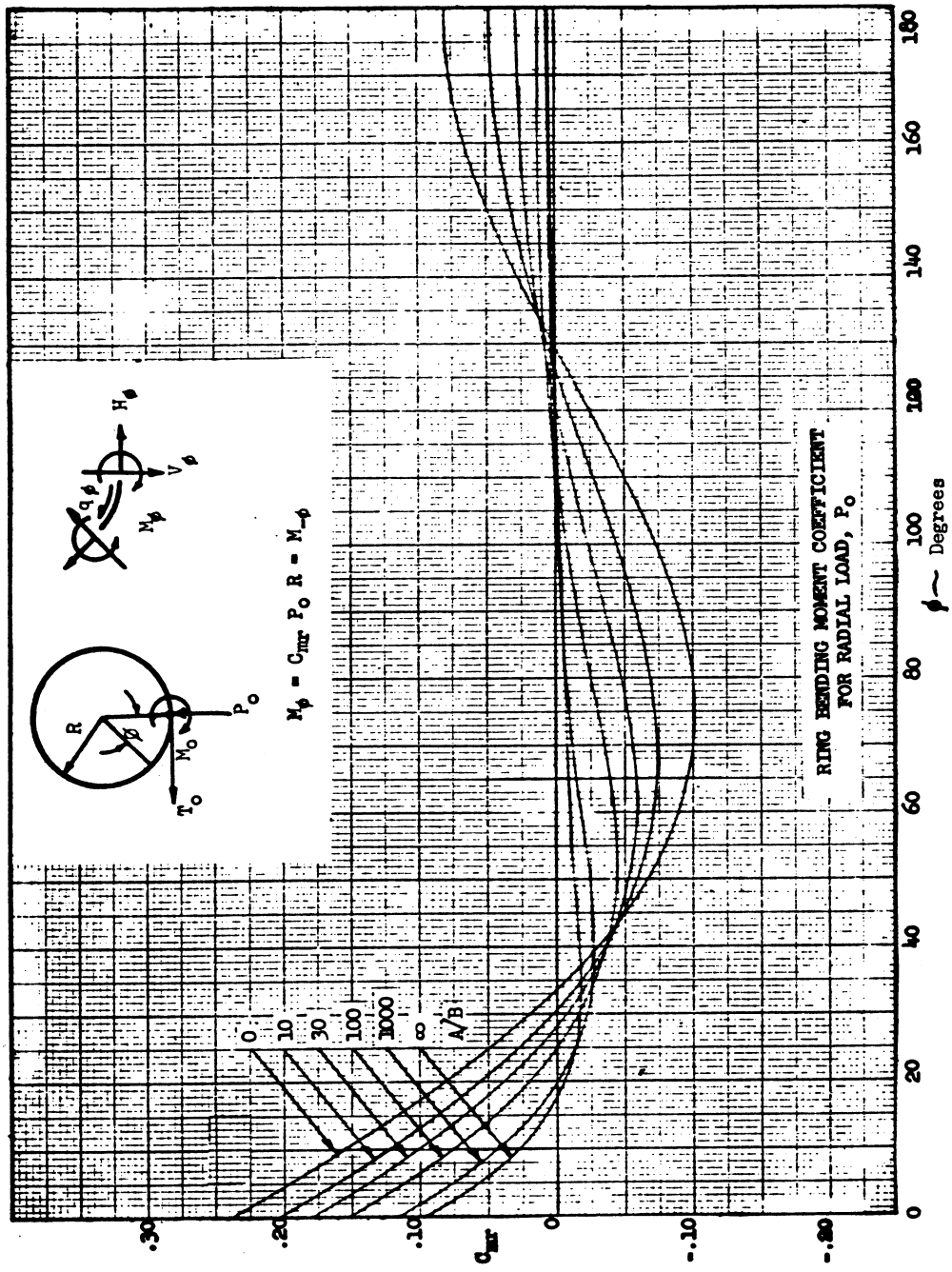


Figure B2.1.7-2 Ring Bending Coefficient for Radial Load, $P_o$

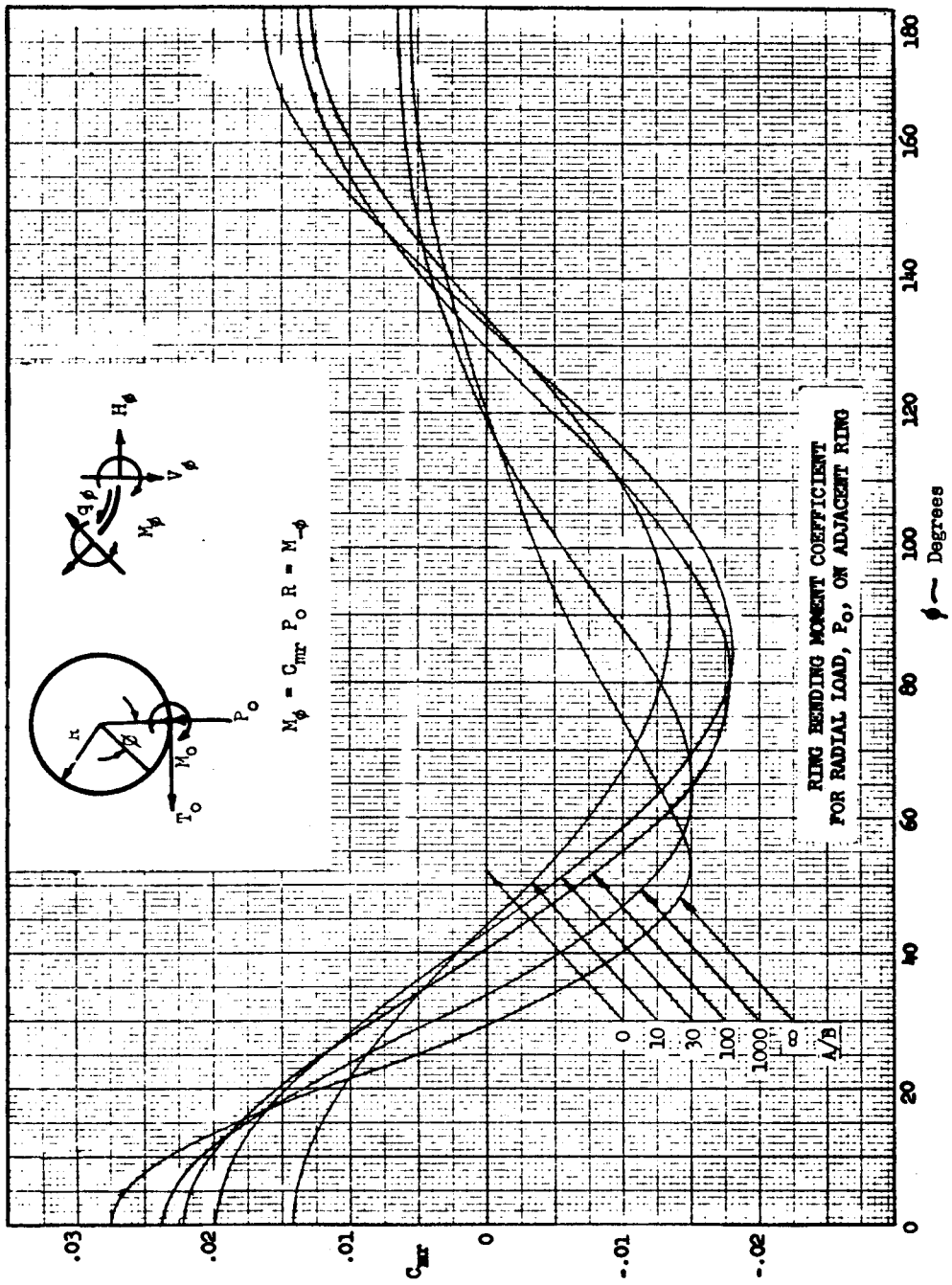


Figure B2.1.7-3 Ring Bending Moment Coefficient for Radial Load, $P_o$, On Adjacent Ring

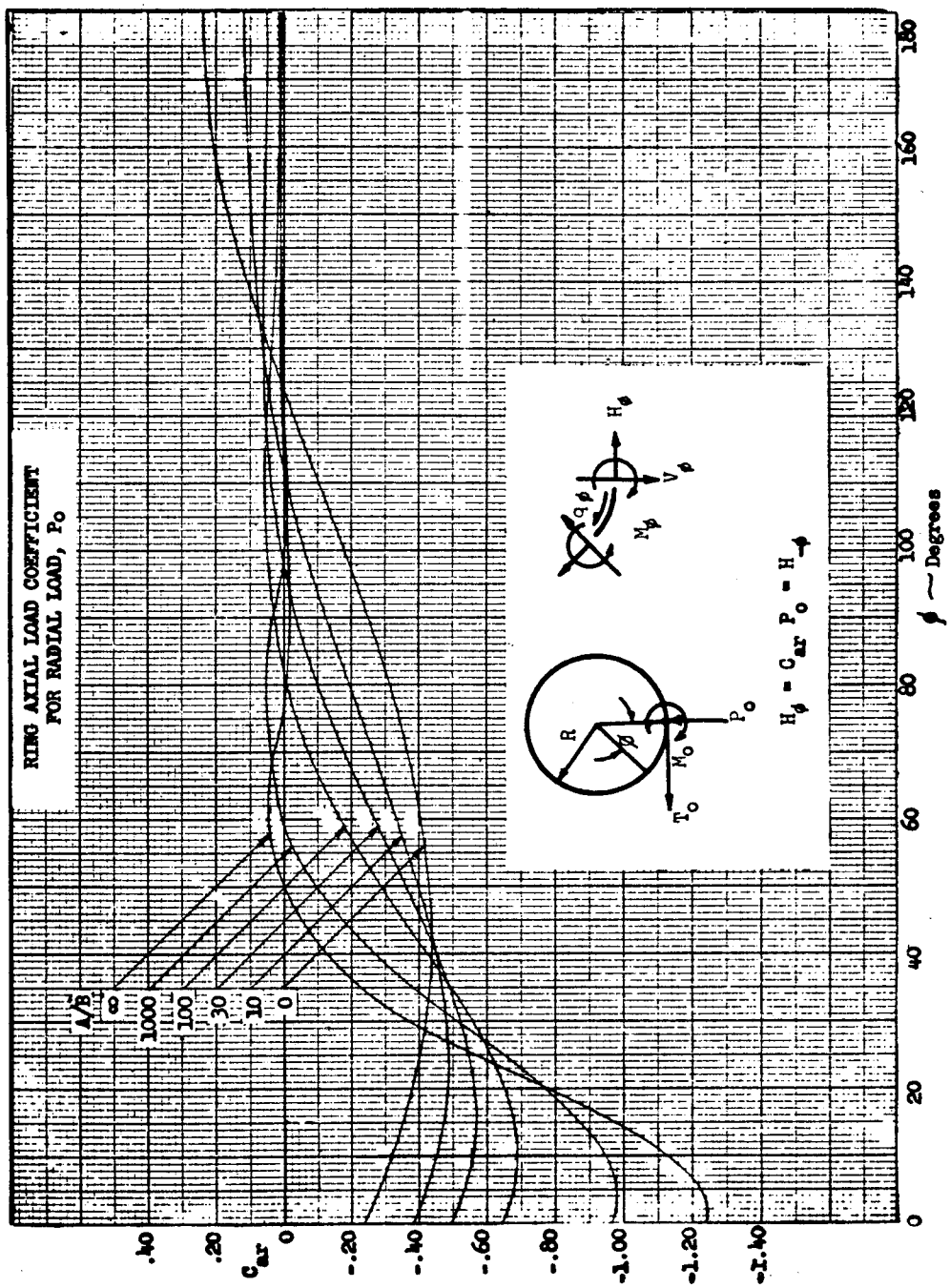


Figure B2.1.7-4 Ring Axial Load Coefficient for Radial Load, $P_o$

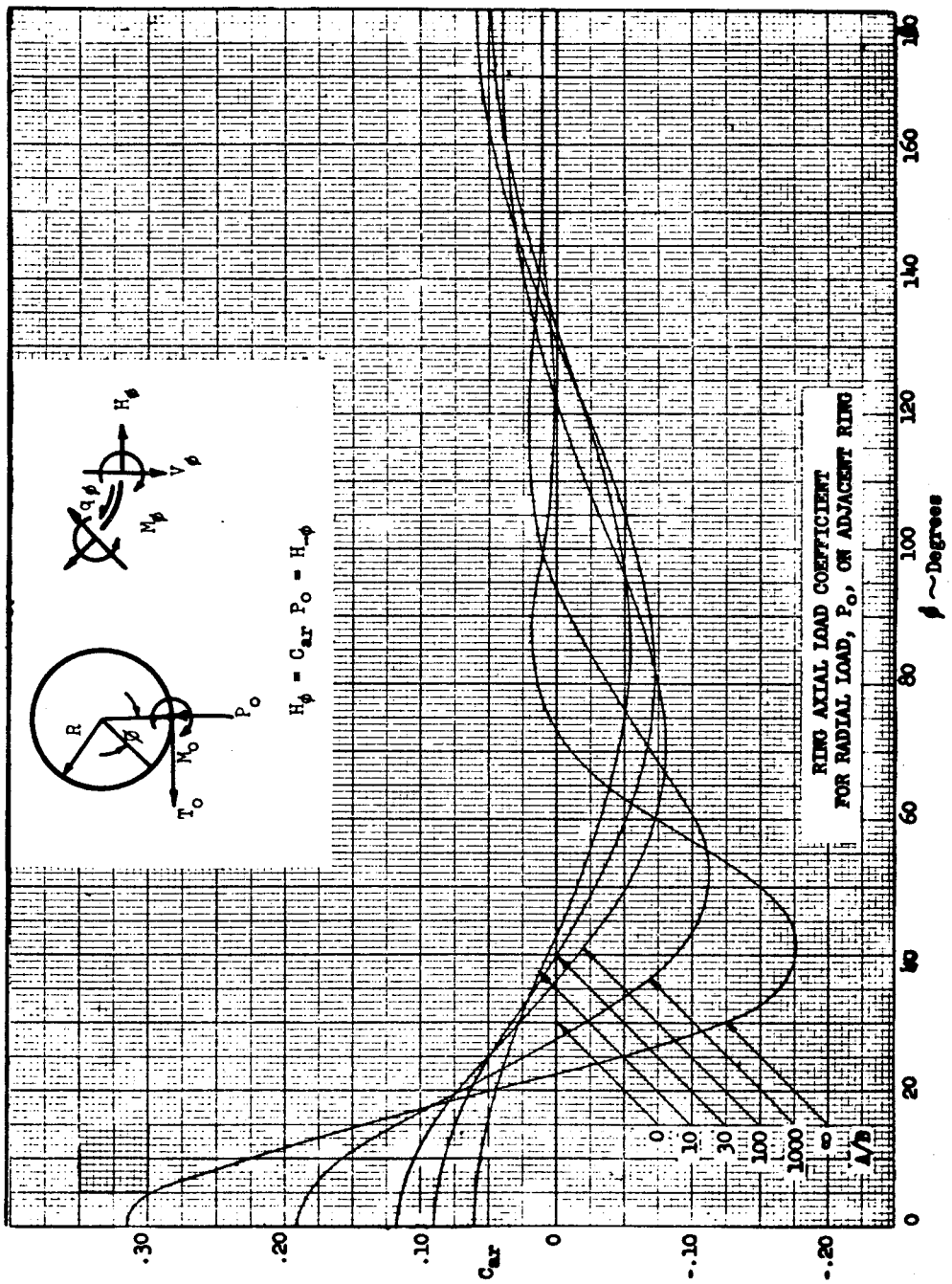


Figure B2.1.7-5 Ring Axial Load Coefficient for Radial Load, $P_o$, on Adjacent Ring

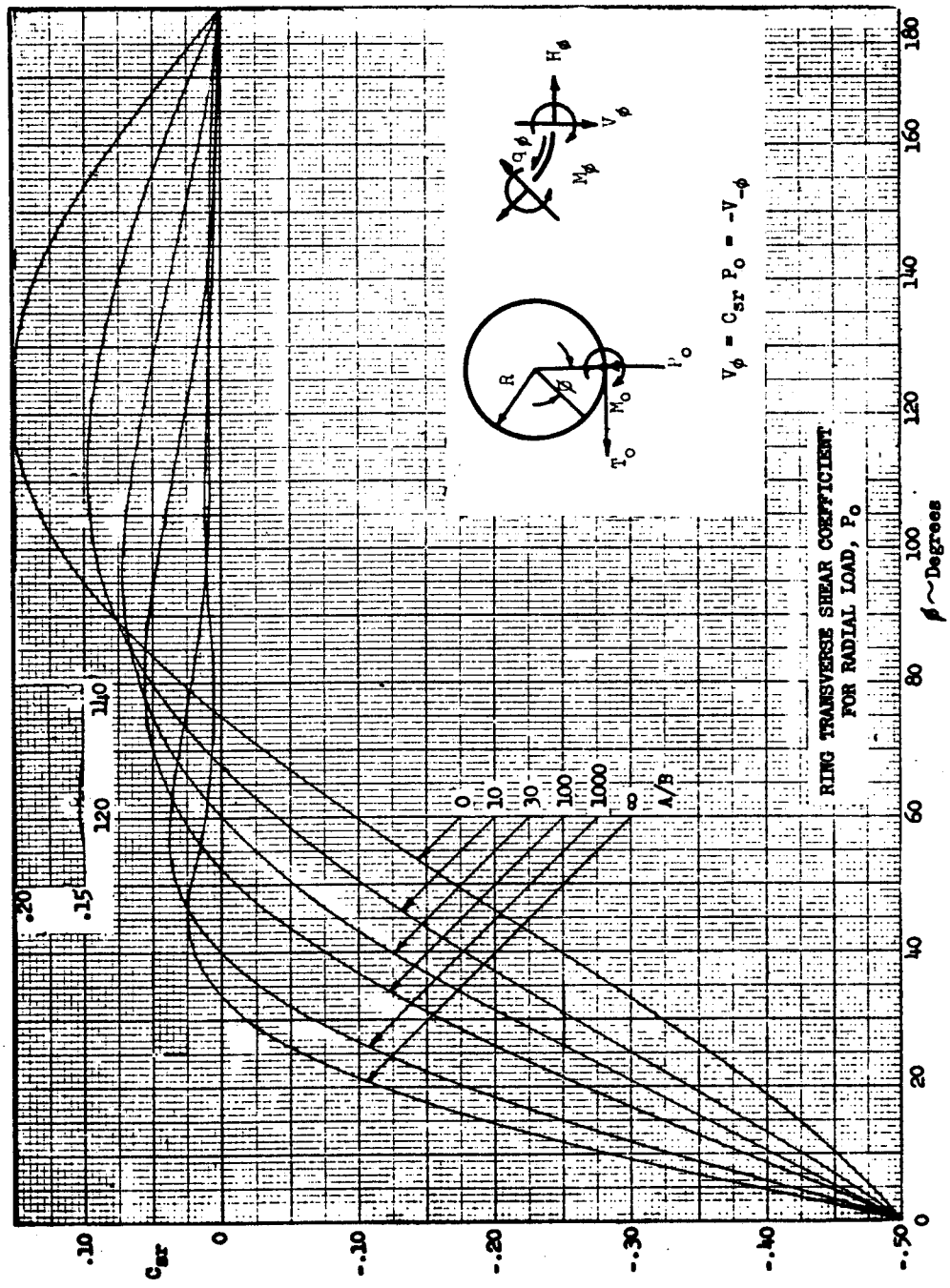


Figure B2.1.7-6 Ring Transverse Shear Coefficient for Radial Load, $P_o$

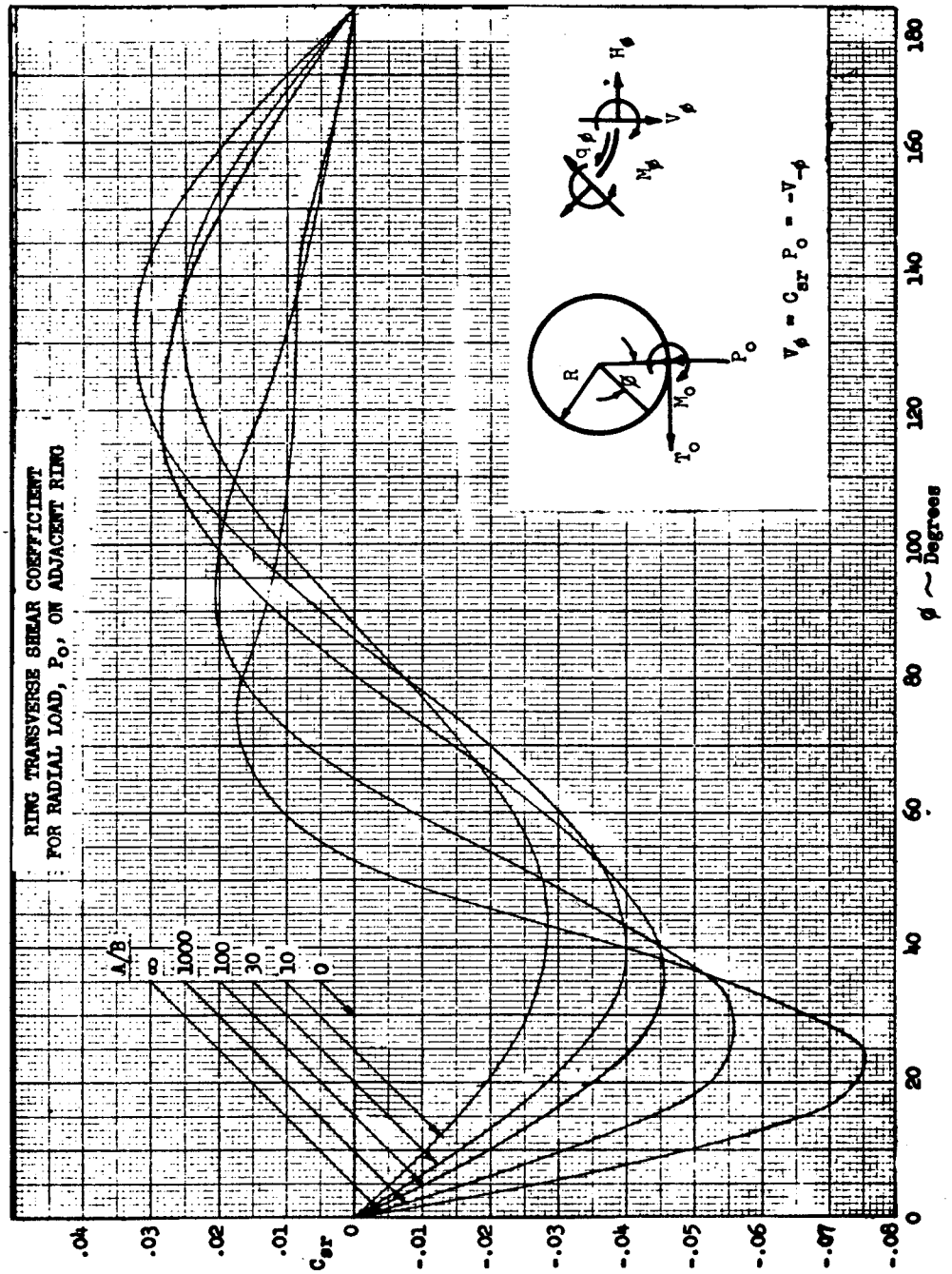


Figure B2.1.7-7 Ring Transverse Shear Coefficient for Radial Load, $P_o$, on Adjacent Ring

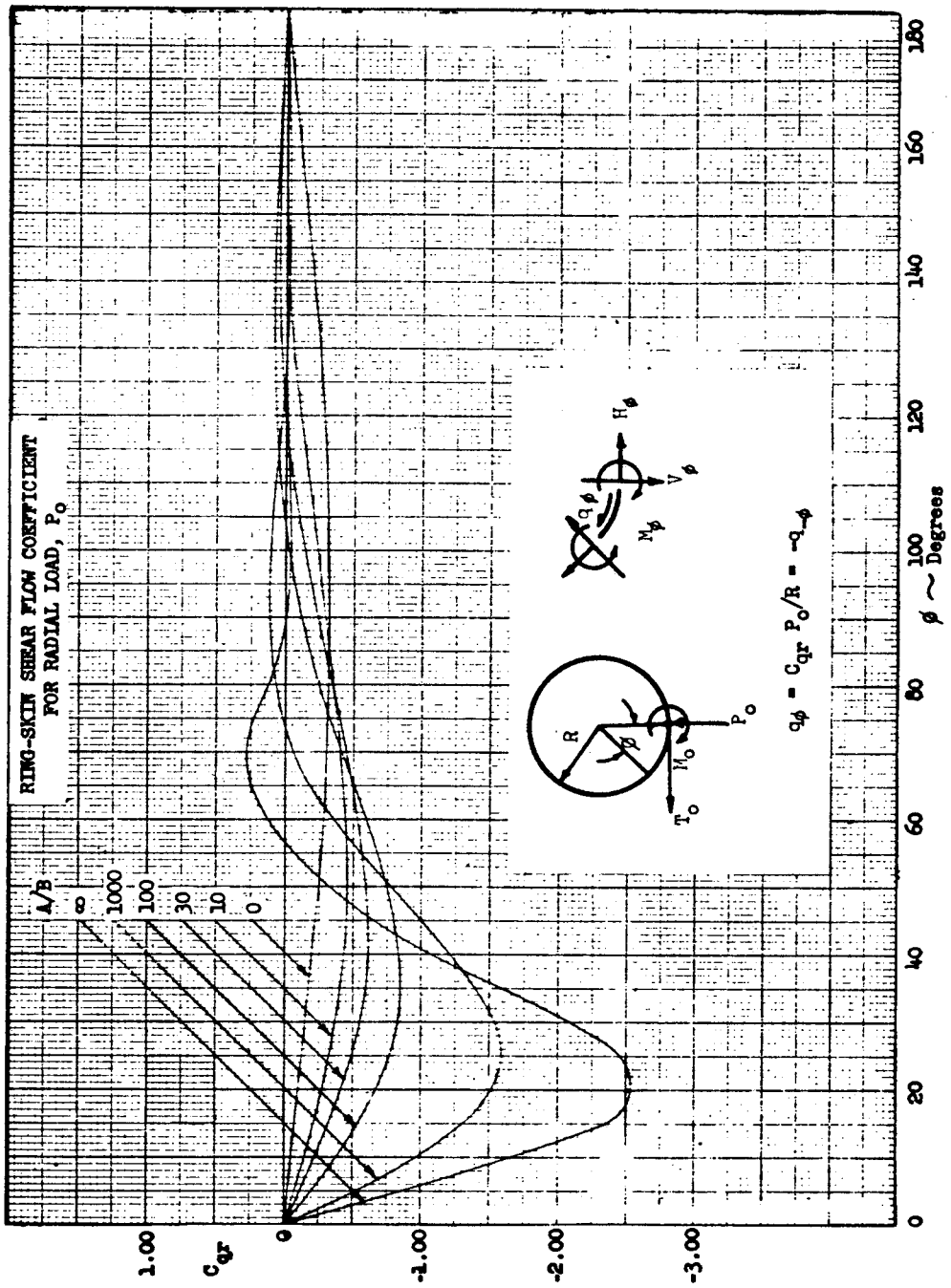


Figure B2.1.7-8 Ring-Skin Shear Flow Coefficient for Radial Load, $P_o$

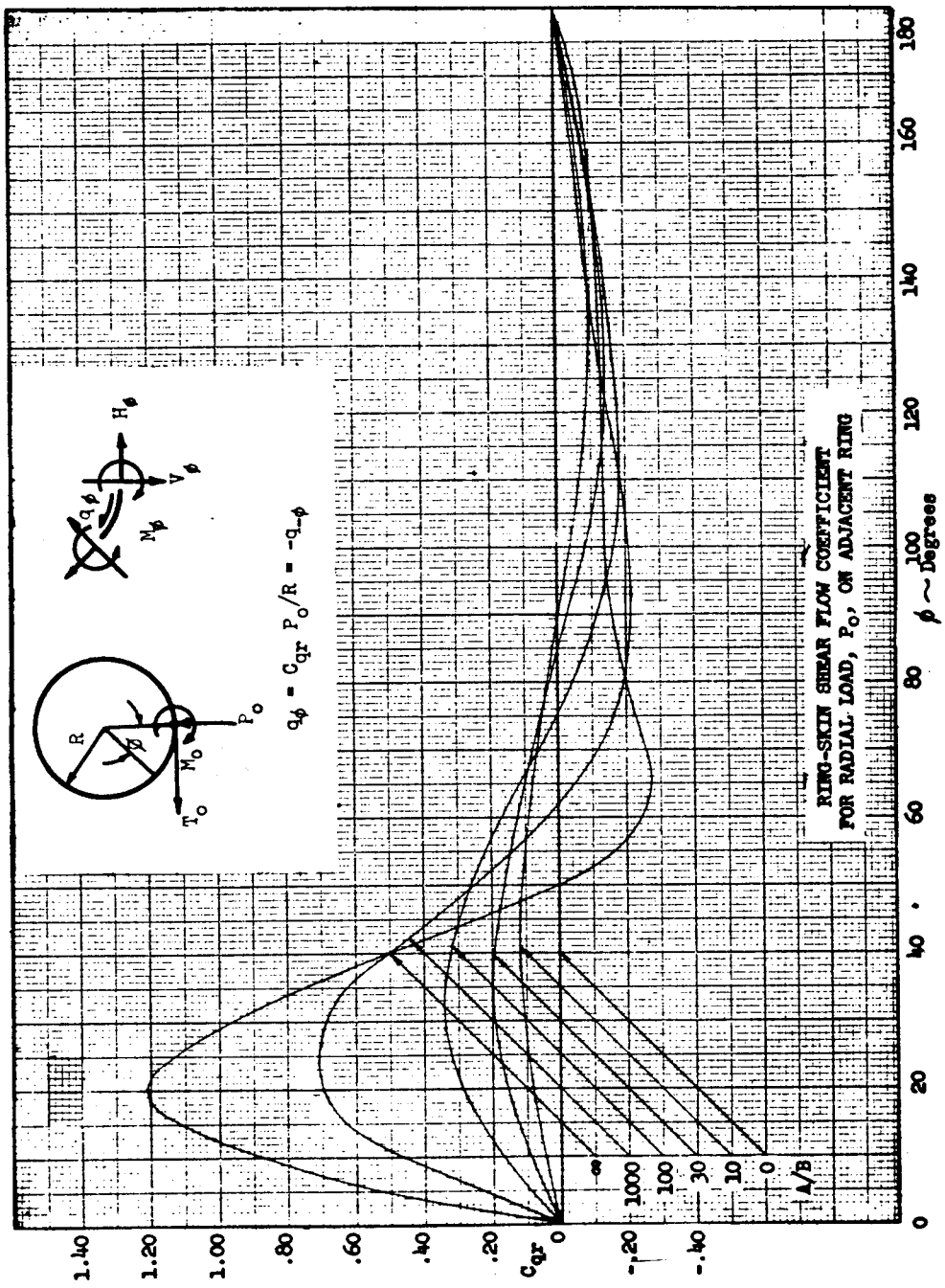


Figure B2.1.7-9 Ring-Skin Shear Flow Coefficient for Radial Load, $P_o$, on Adjacent Ring

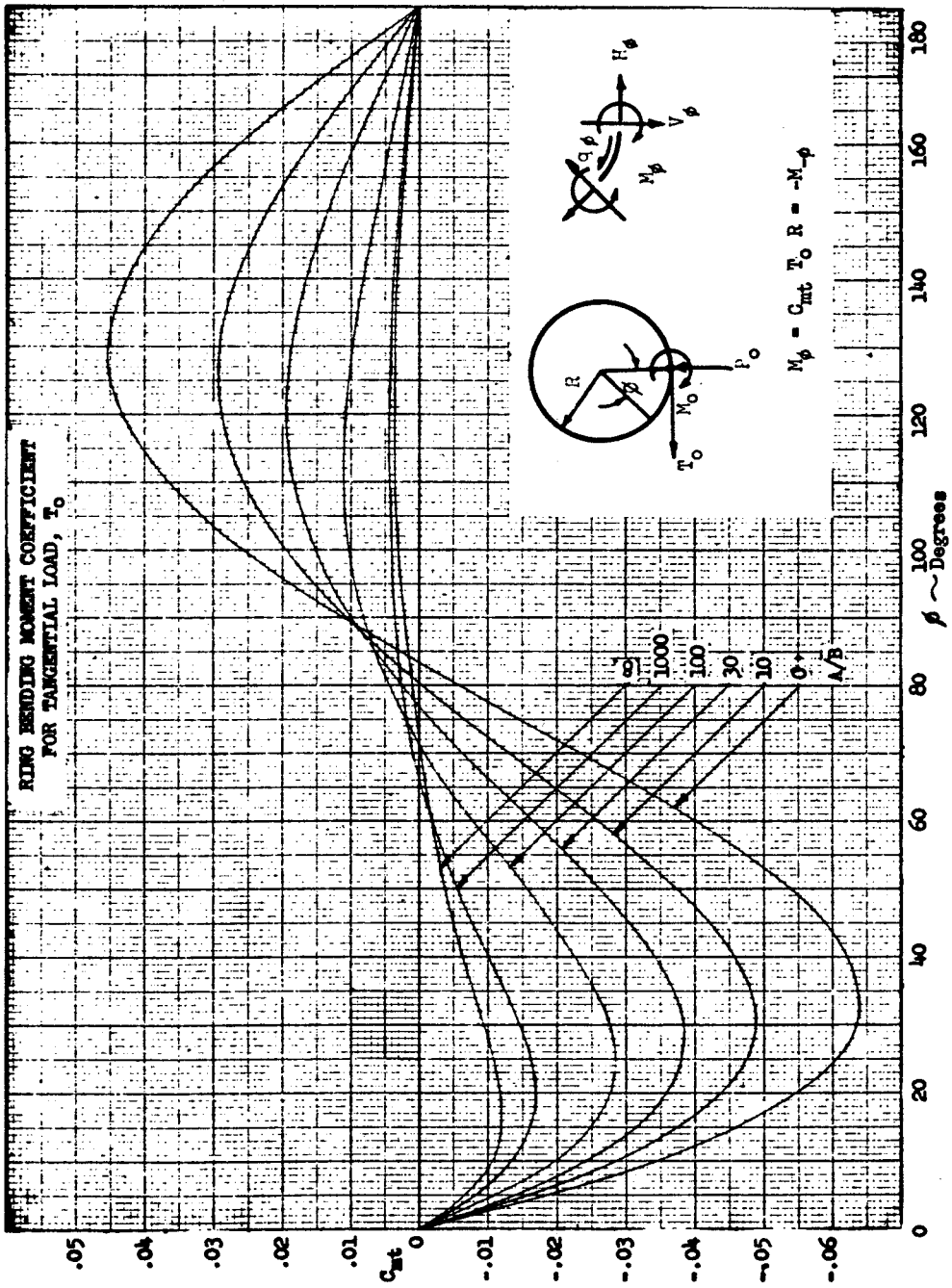


Figure B2.1.7-10 Ring Bending Moment Coefficient for Tangential Load, $T_o$

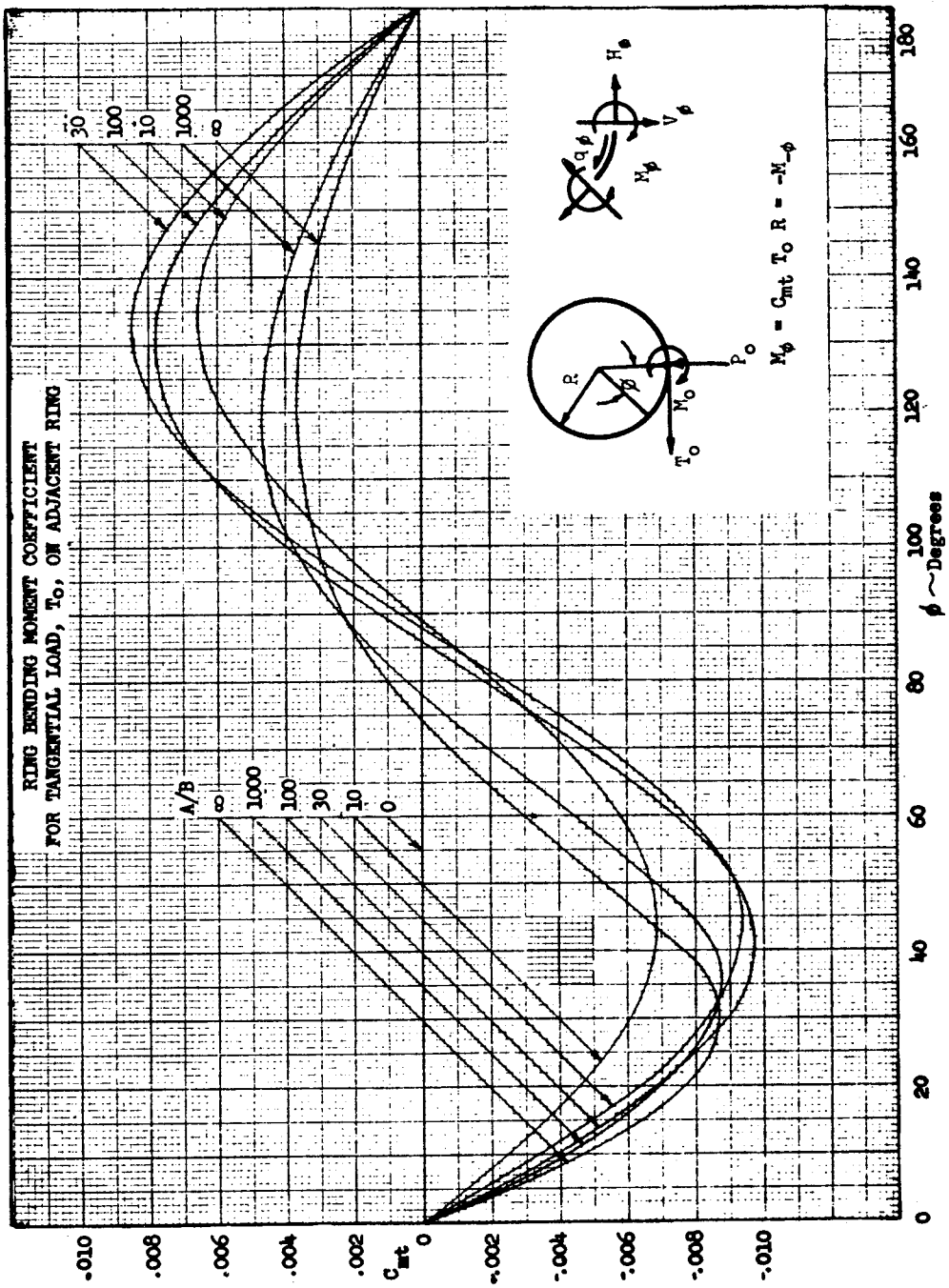


Figure B2.1.7-11 Ring Bending Moment Coefficient for Tangential Load, $T_o$, on Adjacent Ring

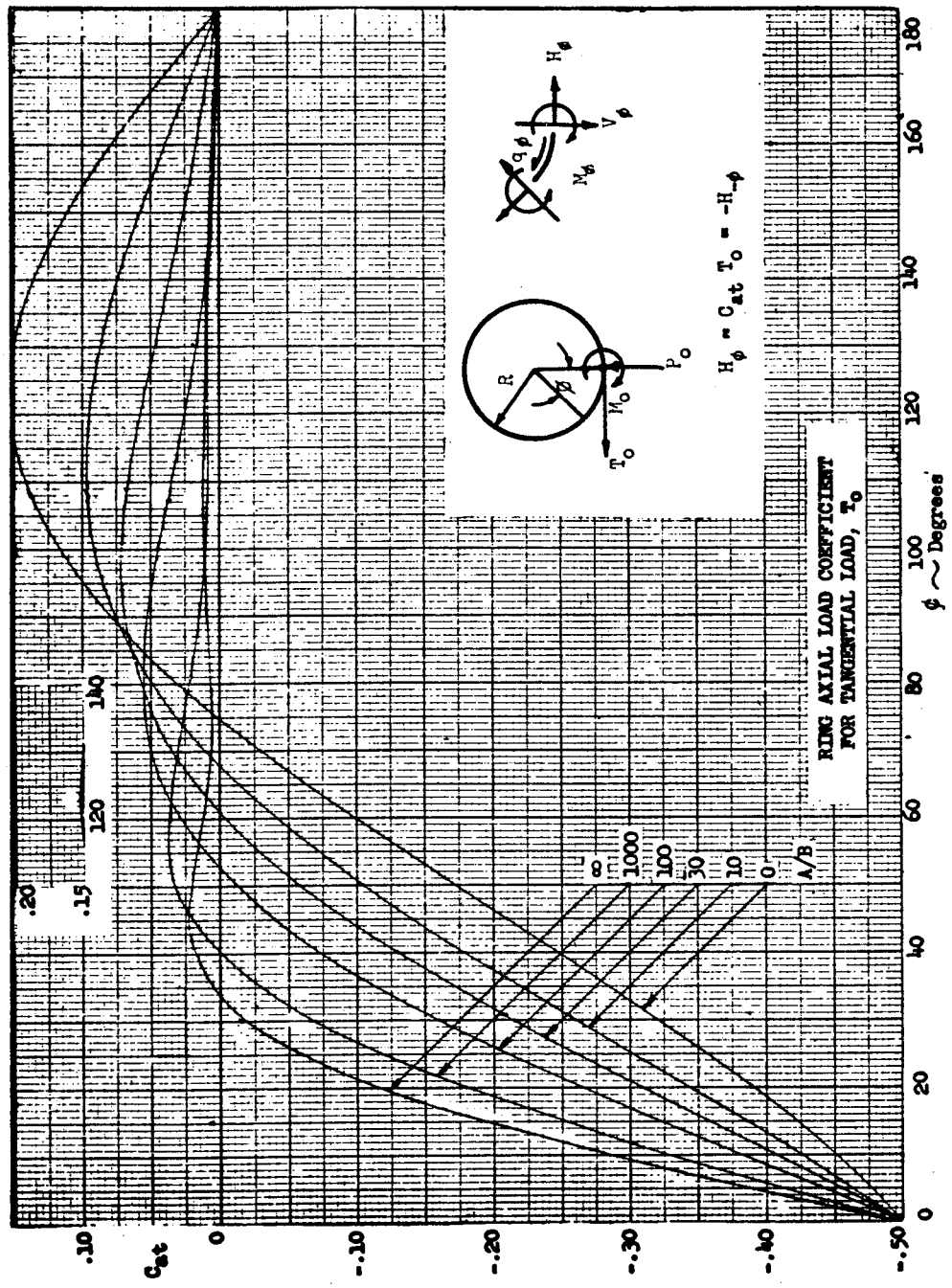


Figure B2.1.7-12 Ring Axial Load Coefficient for Tangential Load, $T_o$

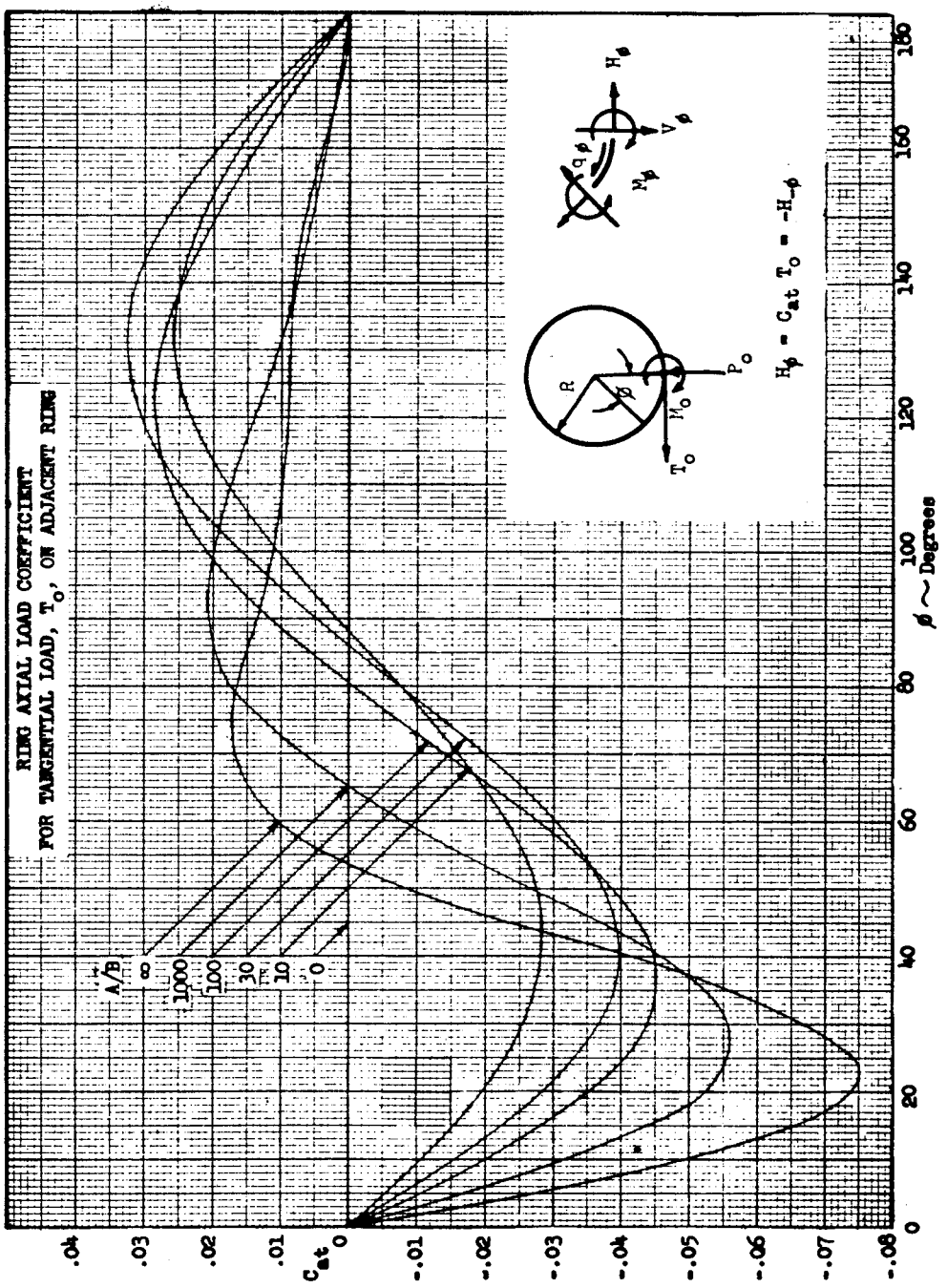


Figure B2.1.7-13 Ring Axial Load Coefficient for Tangential Load, $T_o$, on Adjacent Ring

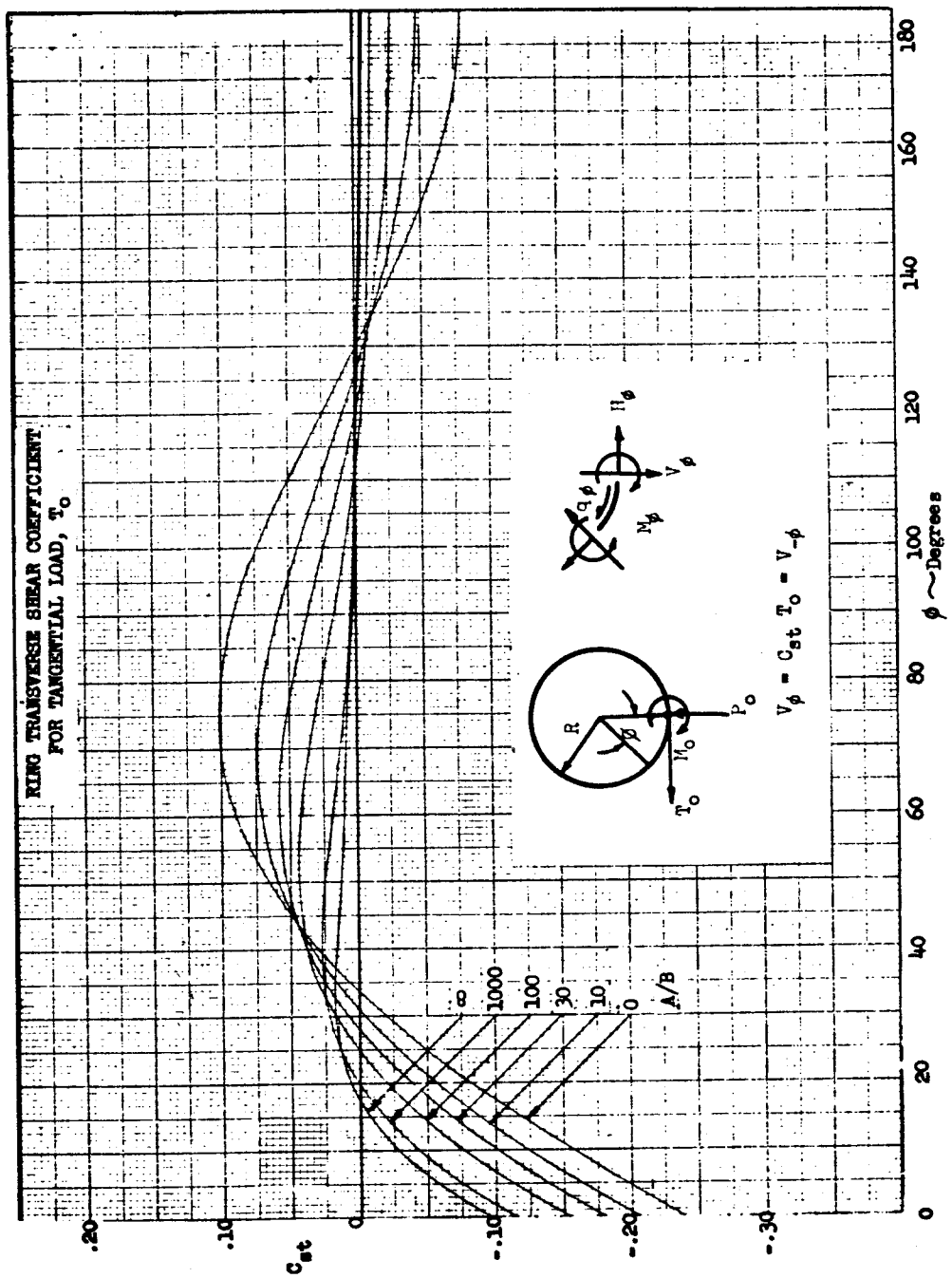


Figure B2.1.7-14 Ring Transverse Shear Coefficient for Tangential Load, $T_o$

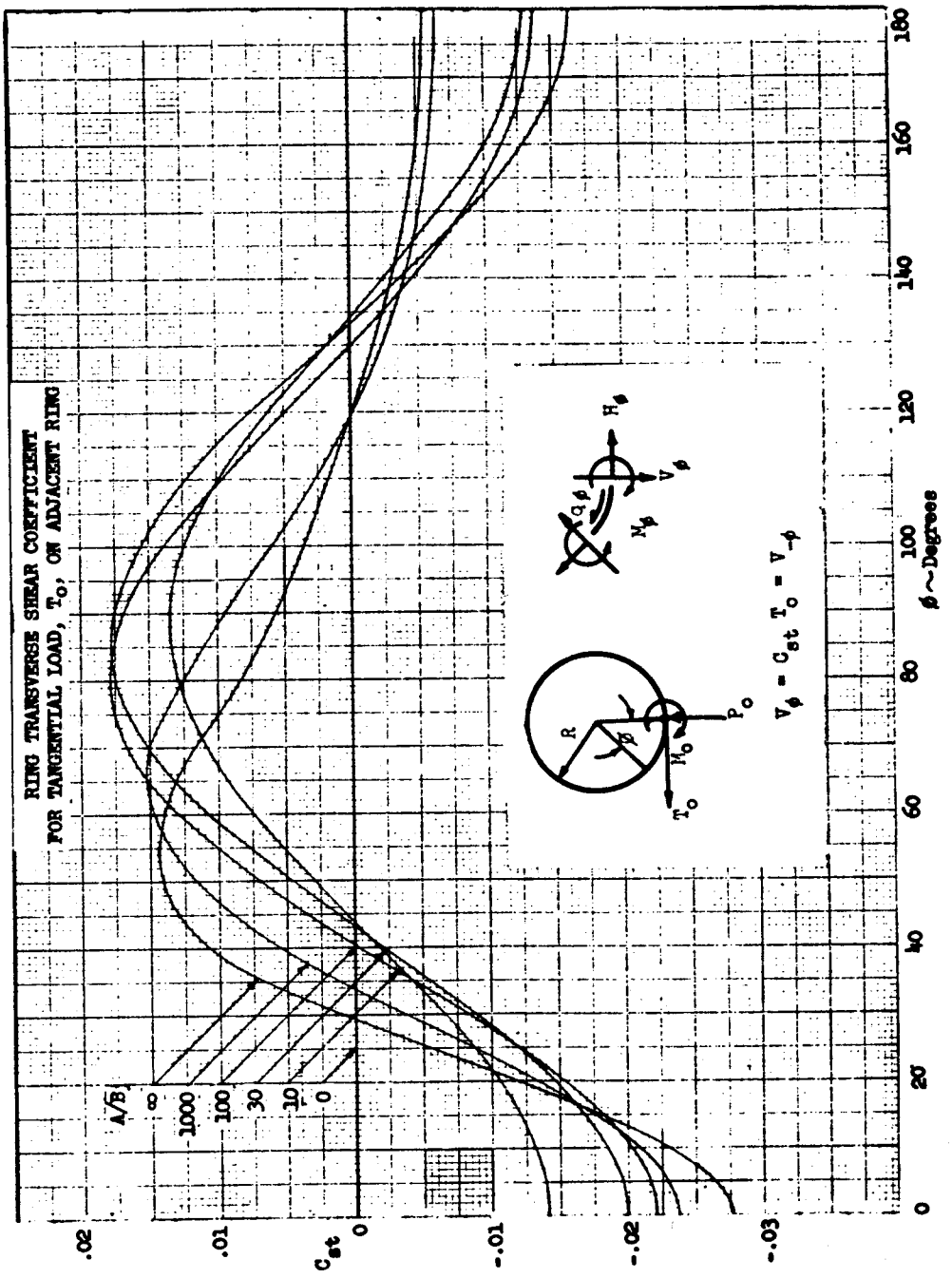


Figure B2.1.7-15 Ring Transverse Shear Coefficient for Tangential Load, $T_o$, on Adjacent Ring

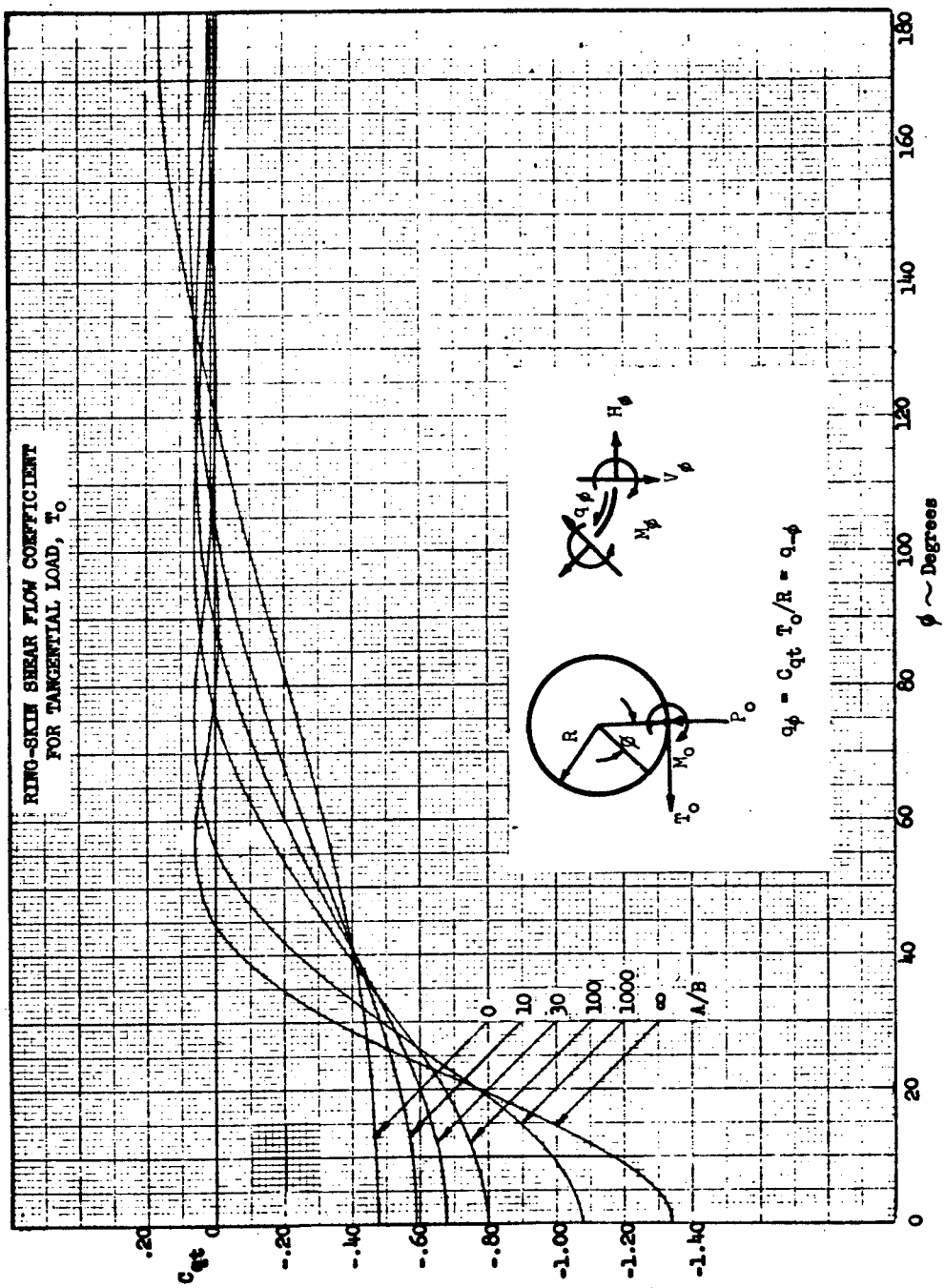


Figure B2.1.7-16 Ring-Skin Shear Flow Coefficient for Tangential Load, $T_o$

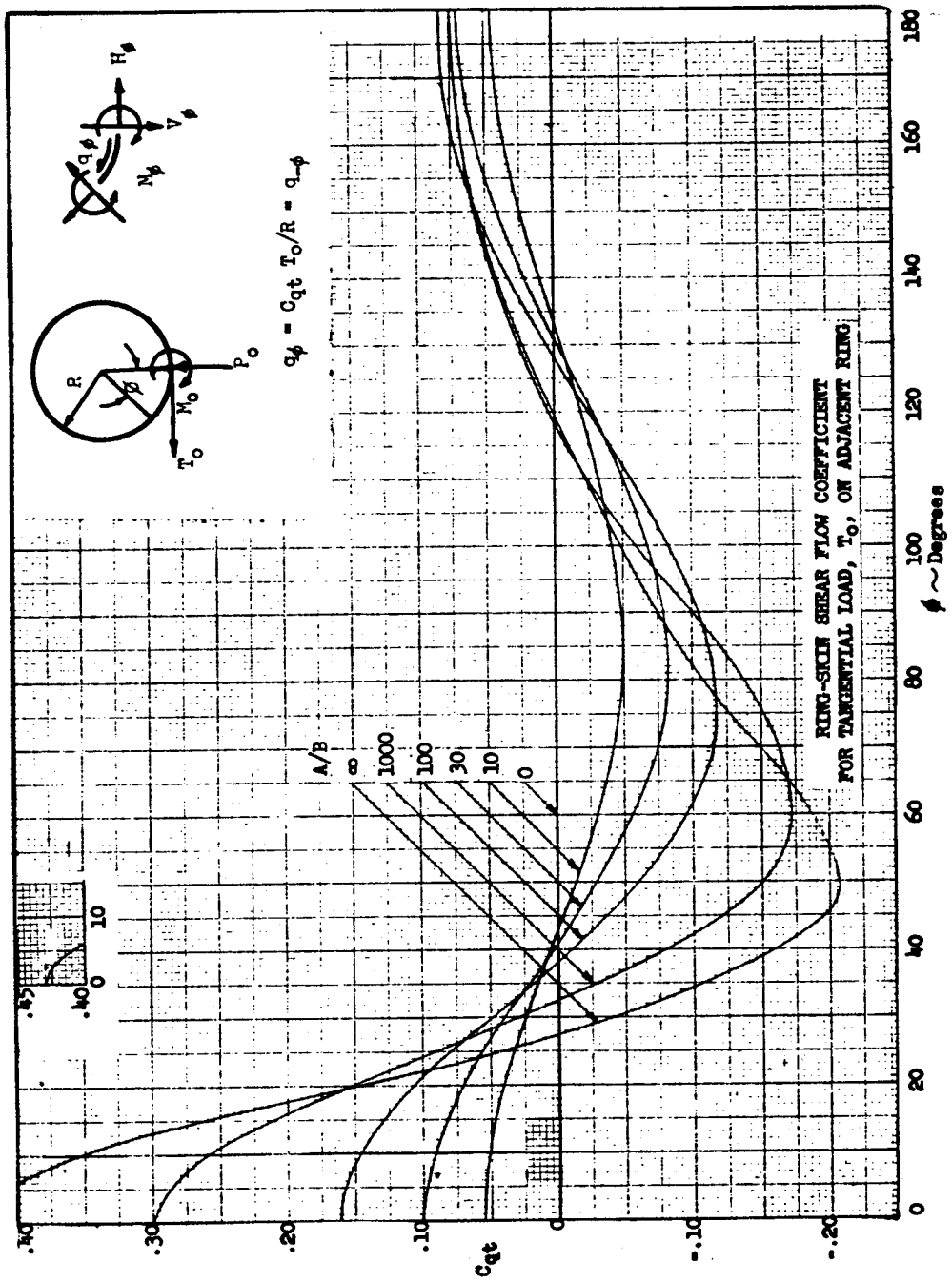


Figure B2.1.7-17 Ring-Skin Shear Flow Coefficient for Tangential Load, $T_o$, on Adjacent Ring

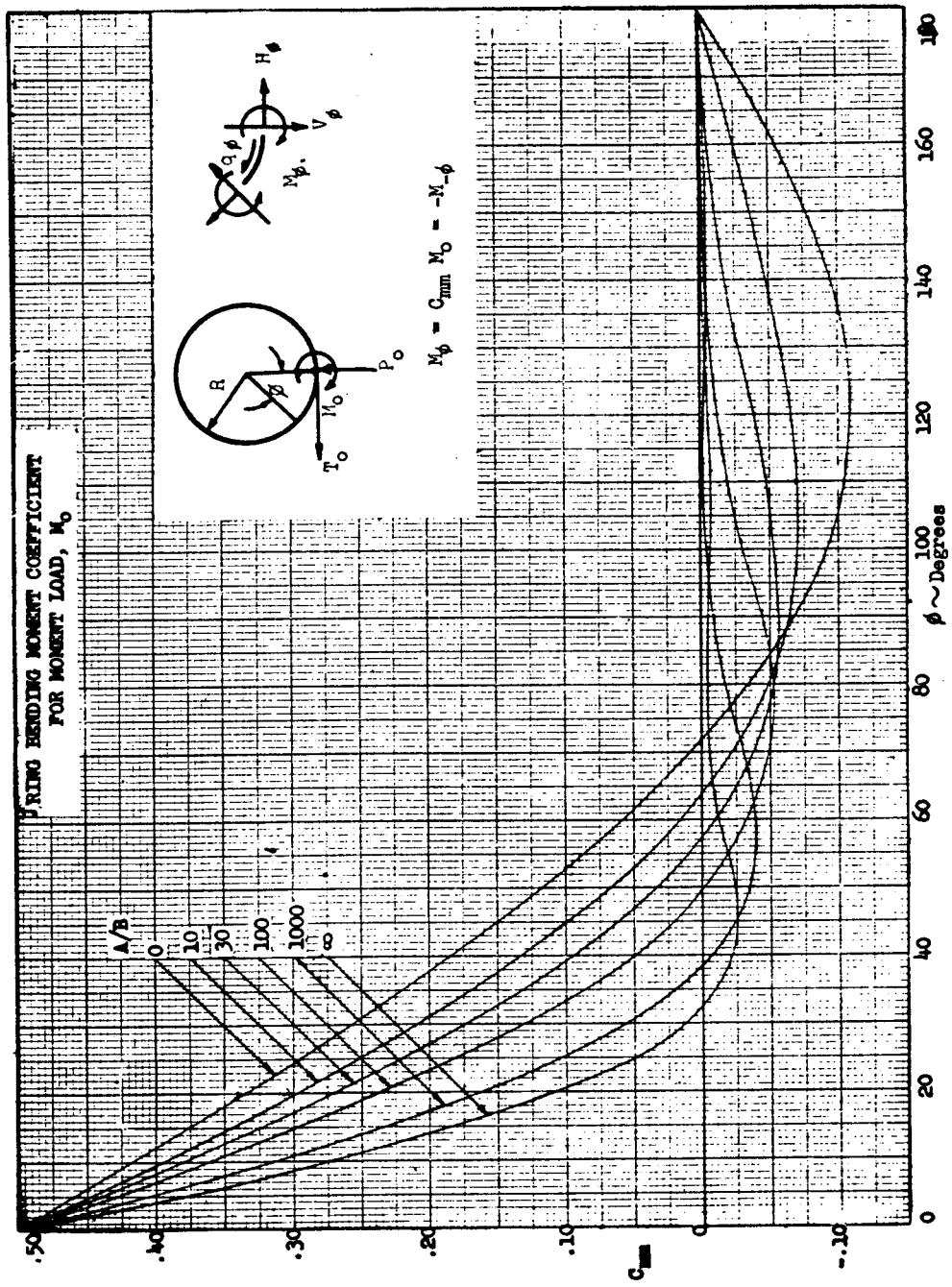


Figure B2.1.7-18 Ring Bending Moment Coefficient for Moment Load, $M_o$

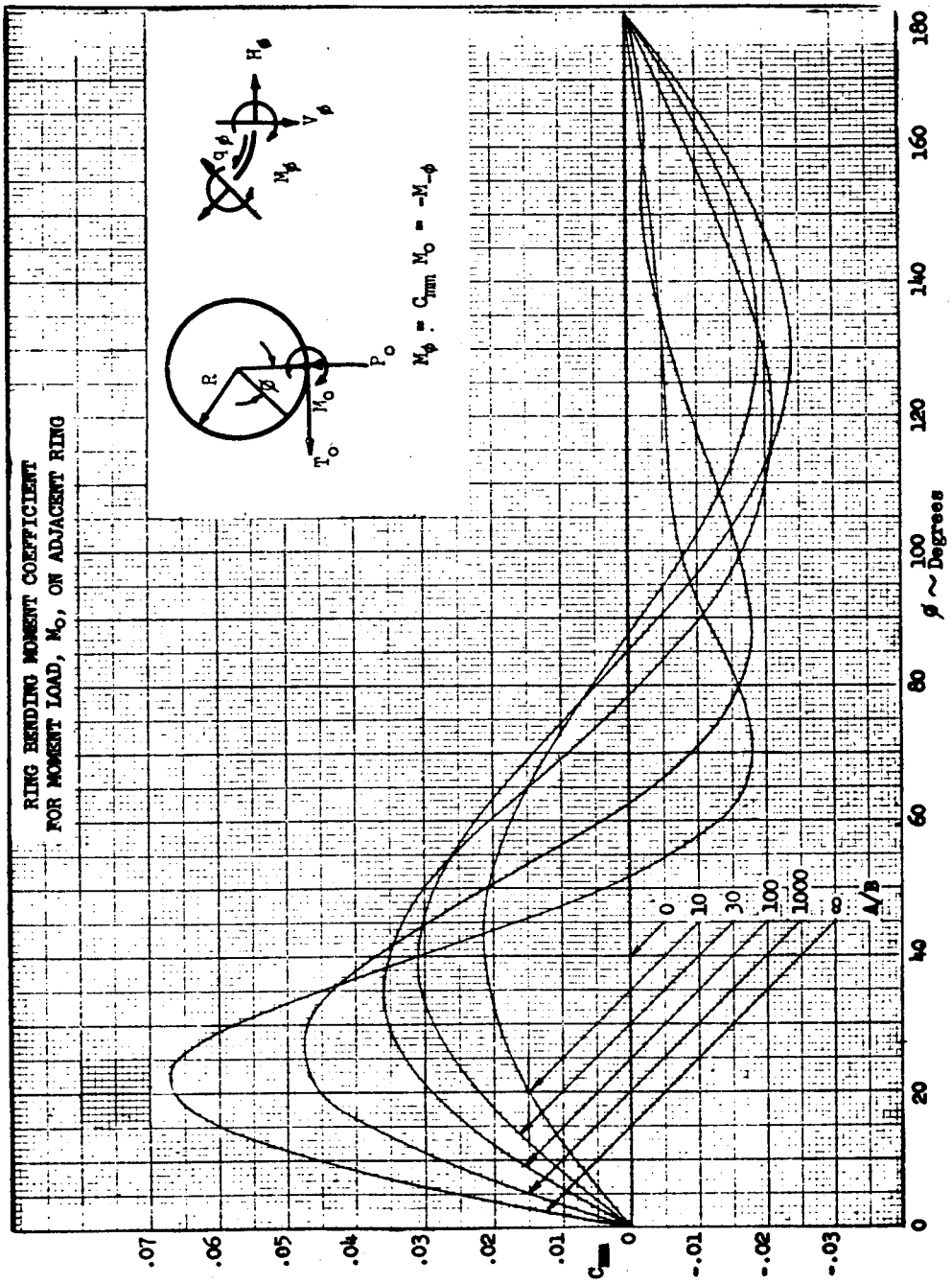


Figure B2.1.7-19 Ring Bending Moment Coefficient for Moment Load, $M_o$, on Adjacent Ring

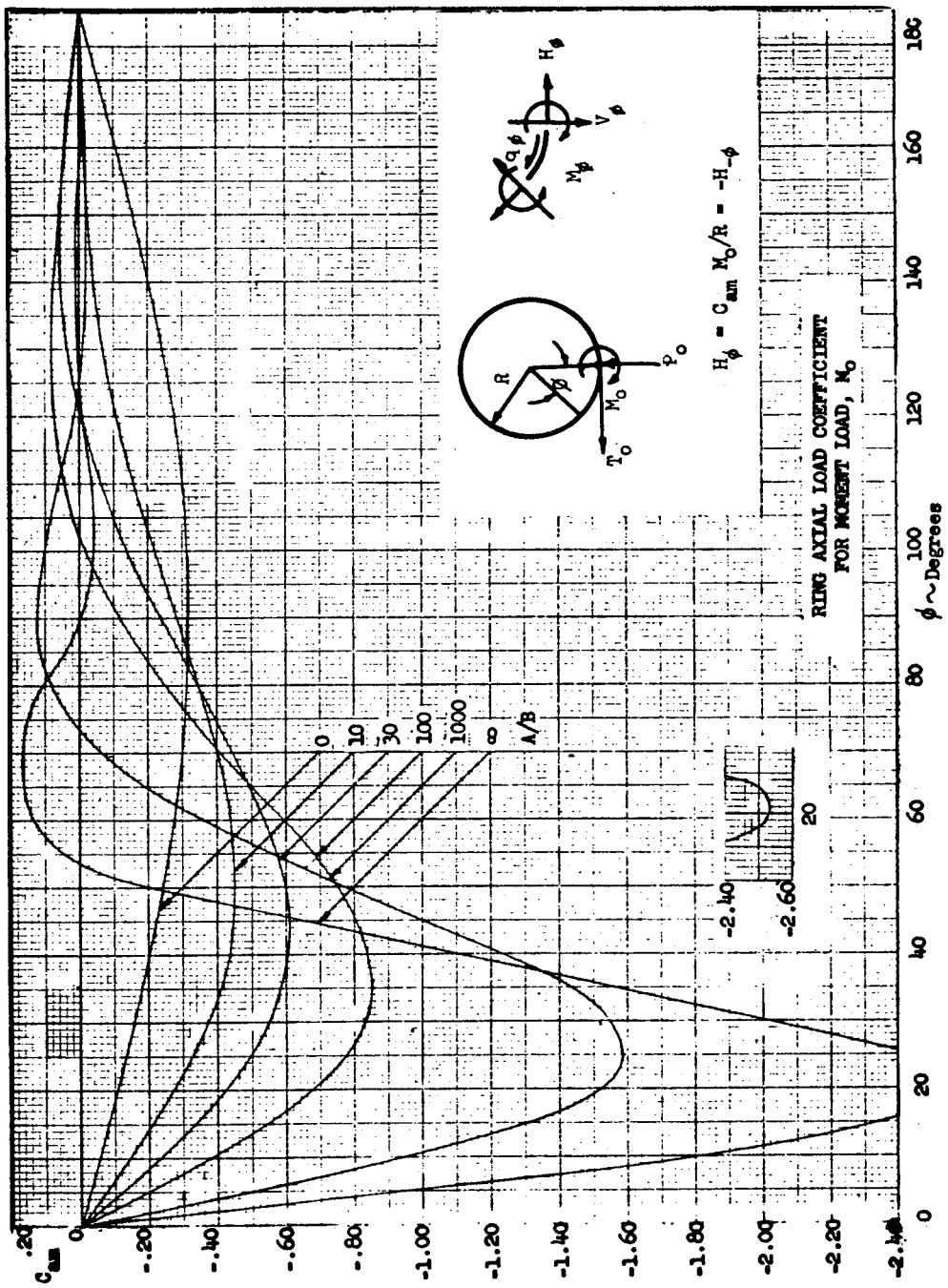


Figure B2.1.7-20 Ring Axial Load Coefficient for Moment Load, $M_o$

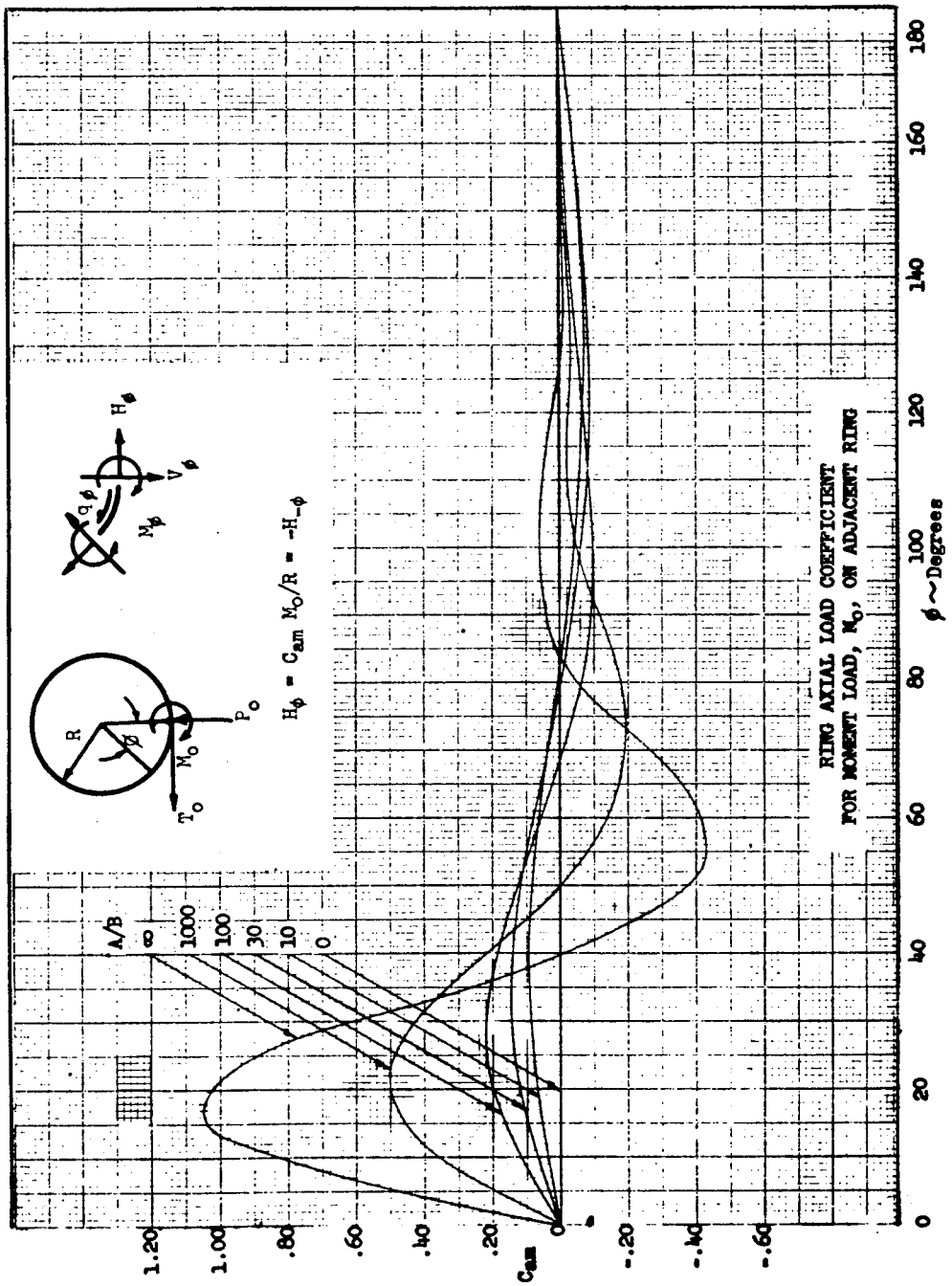


Figure B2.1.7-21 Ring Axial Load Coefficient for Moment Load, $M_o$, on Adjacent Ring

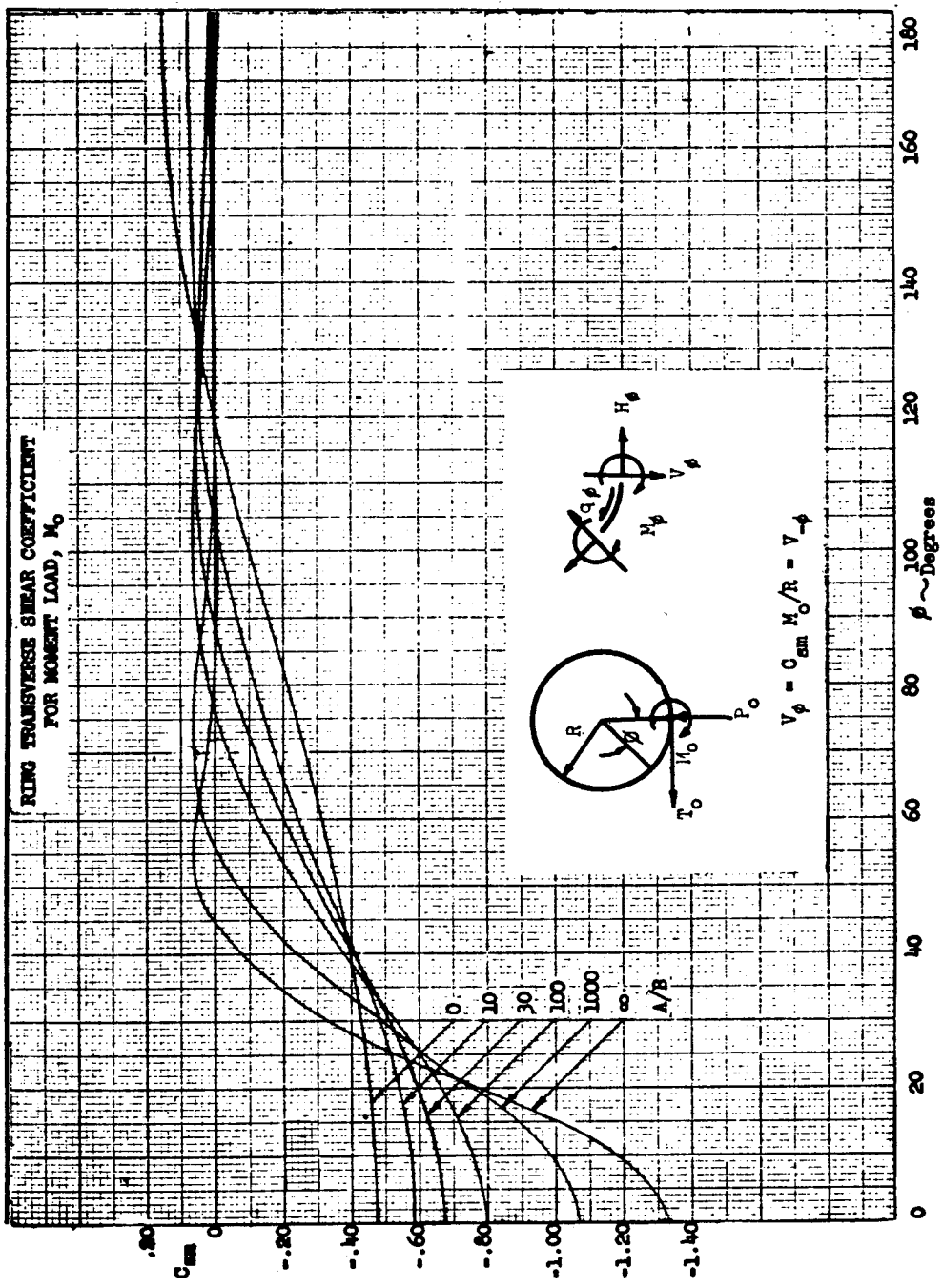


Figure B2.1.7-22 Ring Transverse Shear Coefficient for Moment Load, $M_o$

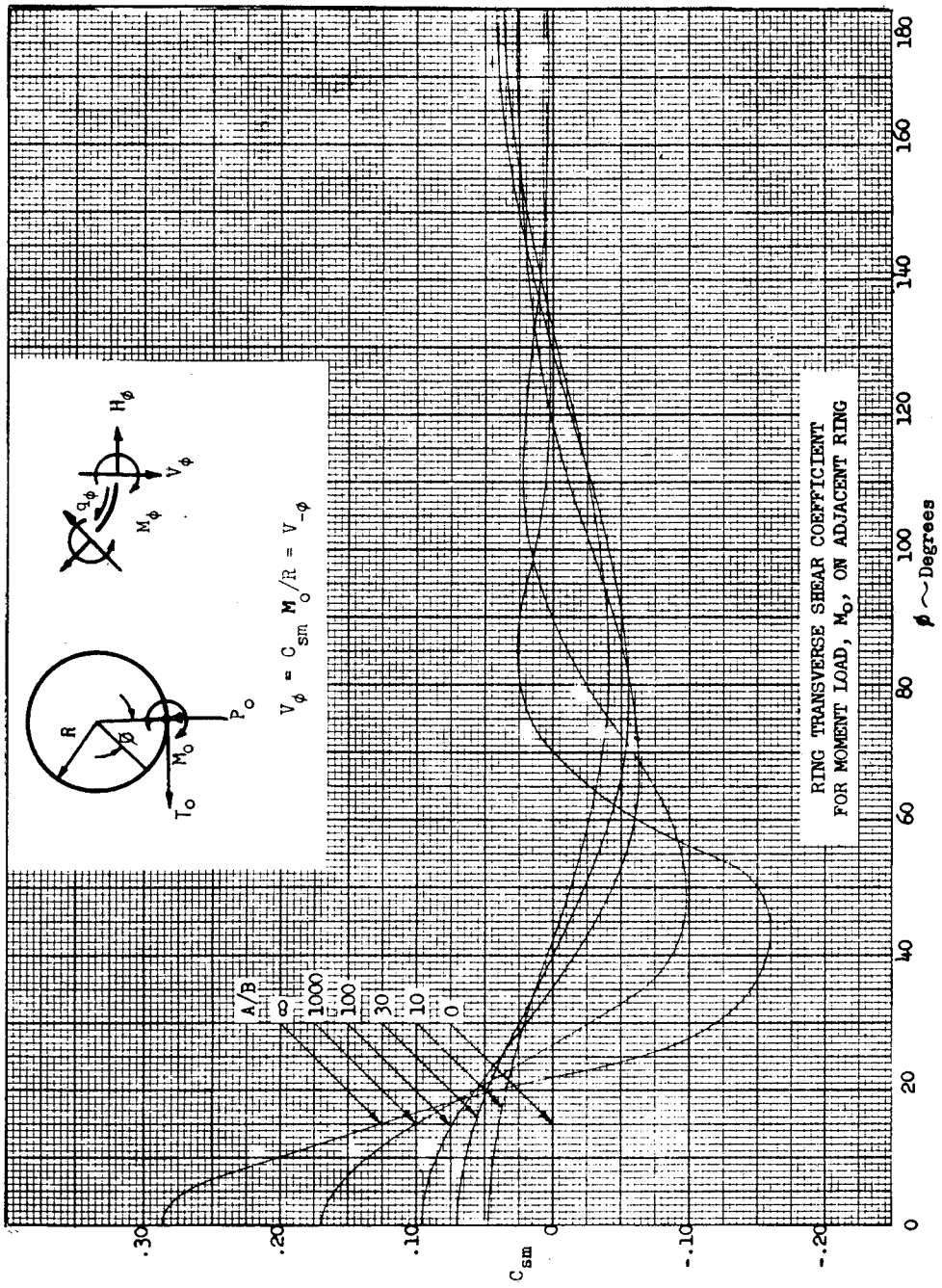


Figure B2.1.7-23 Ring Transverse Shear Coefficient for Moment Load $M_o$, on Adjacent Ring

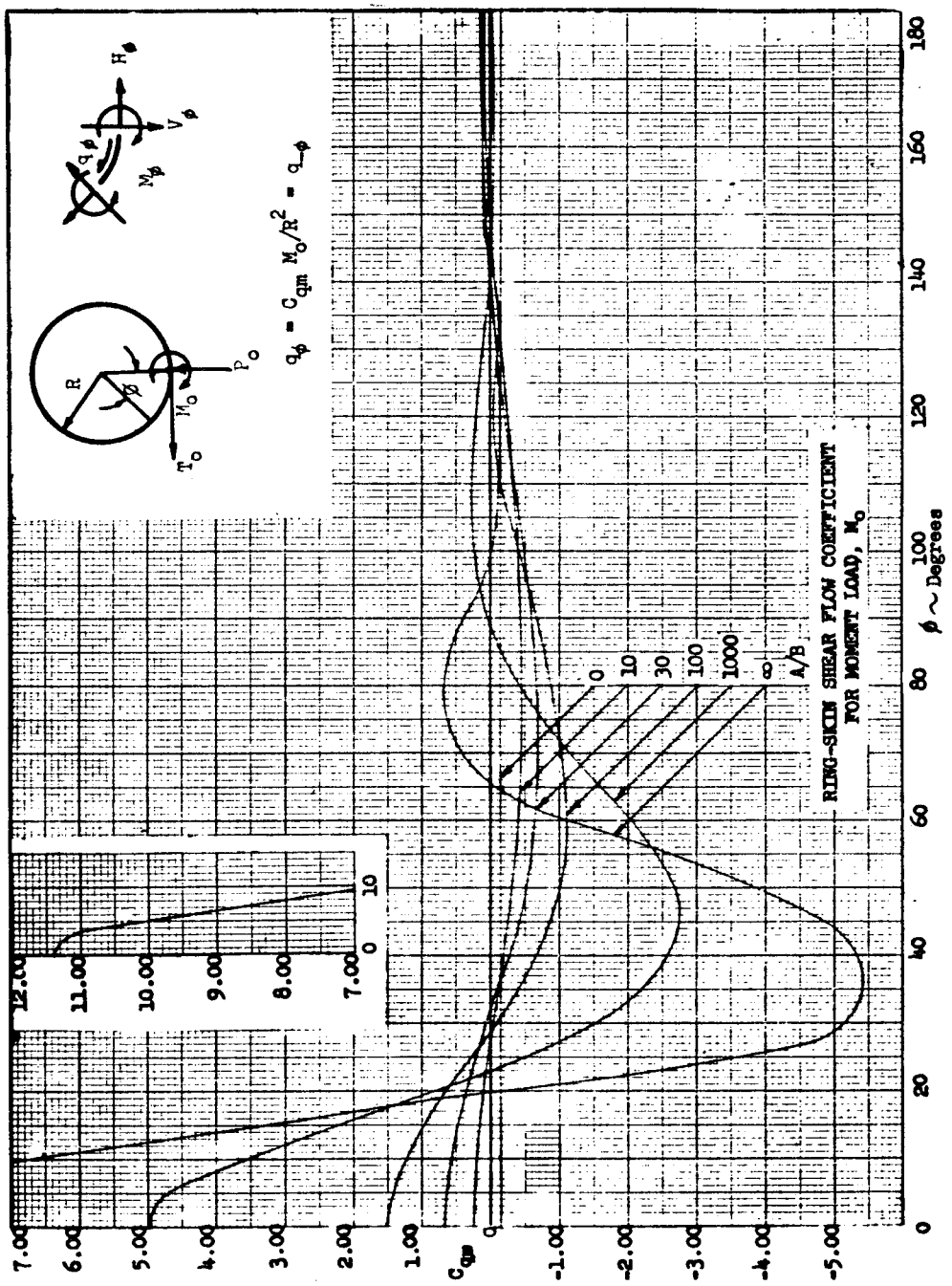


Figure B2.1.7-24 Ring-Skin Shear Flow Coefficient for Moment Load, $M_o$

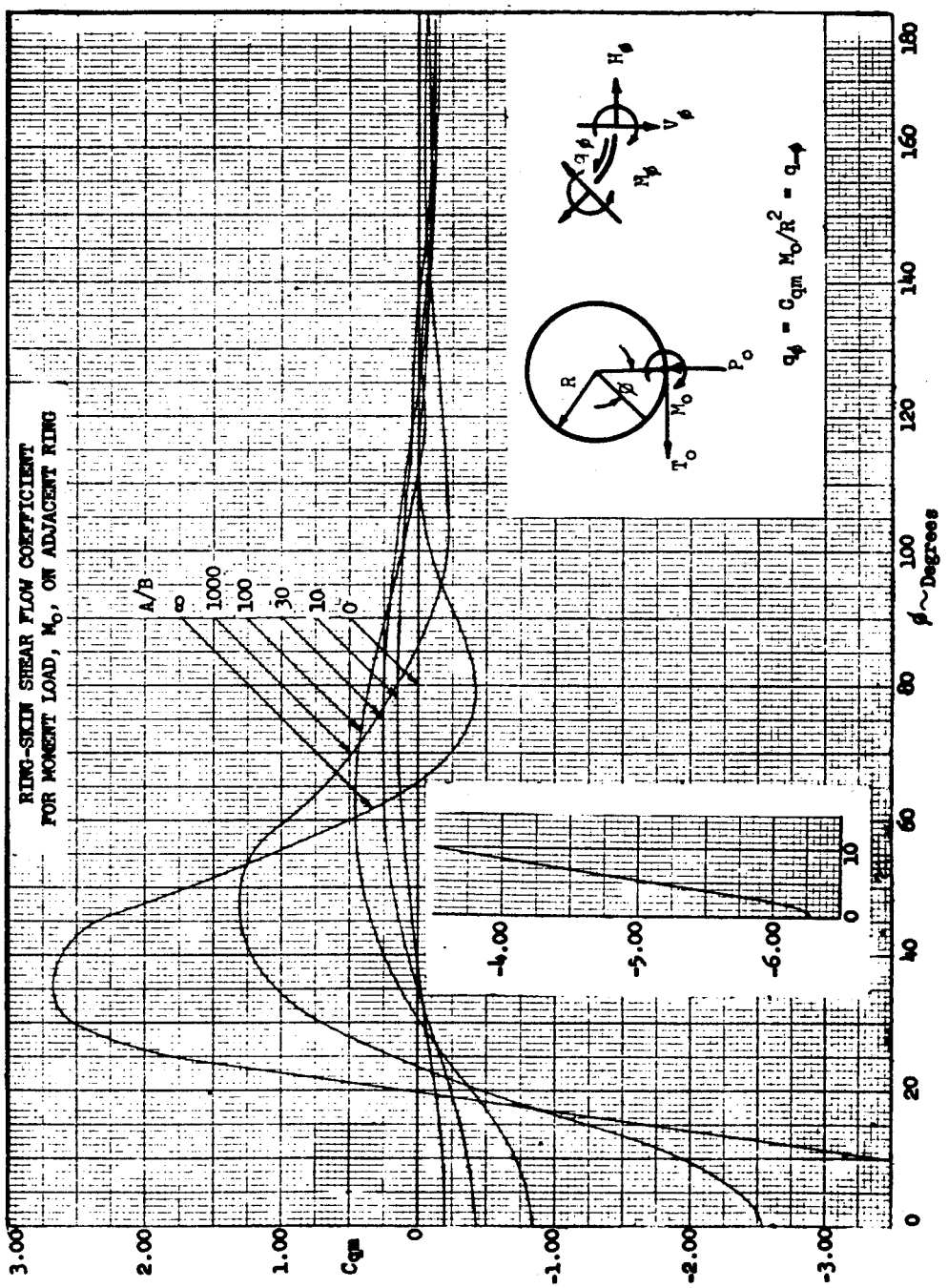


Figure B2.1.7-25 Ring-Skin Shear Flow Coefficient for Moment Load, $M_o$, on Adjacent Ring

## B2.2.0 Arches

In Table B2.2.0-1 formulas are given for arches with sinusoidal and uniform normal pressure. In all cases, constraining moments, reactions, and applied loads are positive when acting as shown.

Table B2.2.0-1 Formulas for Arches

| | |
|---|---|
| 1. SINUSOIDAL NORMAL PRESSURE 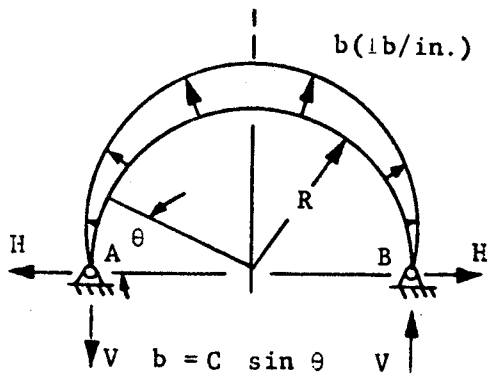  | $V = \frac{C\pi R}{4}$<br>$H = \frac{CR}{4}$<br>$M_\theta = \frac{CR^2}{4}\left[(\pi-2\theta)\cos\theta - \pi + 3\sin\theta\right]$<br>(Positive moment acts clockwise on section ahead.) |

## Table B2.2.0-1 Formulas for Arches (Cont)

| | |
|---|---|
| 2. SINUSOIDAL NORMAL PRESSURE 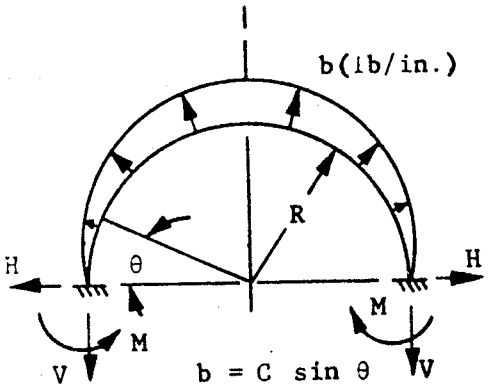  | $V = \frac{C\pi R}{4}$ <br> $H = \frac{CR}{4}\left[\frac{3\pi^2 - 32}{8 - \pi^2}\right] = .31974CR$ <br> $M = \frac{CR^2}{4}\left[\frac{\pi^3 - 10\pi}{8 - \pi^2}\right] = .05478CR^2$ <br> $M_\theta = CR^2\left[.81974 \sin\theta - .84018 + \frac{\cos\theta}{2}\left(\frac{\pi}{2} - \theta\right)\right]$ <br> (Positive moment acts clockwise on section ahead.) |
| 3. UNIFORM NORMAL PRESSURE 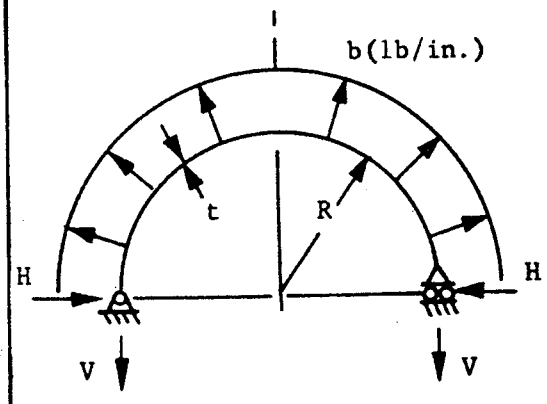  | M = 0 at all points since pin points permit a uniform hoop tension. T, where: <br> T = V = bR <br> H = 0 |

## B2.3.0 Bents

### B2.3.1 Rectangular Bents

In Table B2.3.1-1 formulas are given for rectangular bents with various type of loadings. In all cases, constraining moments, reactions, and applied loads are positive when acting as shown. The value for K should be computed by the equation

$$K = \frac{I_2 h}{I_1 L} \qquad \text{(B2-4)}$$

## Table B2.3.1-1 Formulas for Rectangular Bents

### 1. VERT. CONCENTRATED LOAD

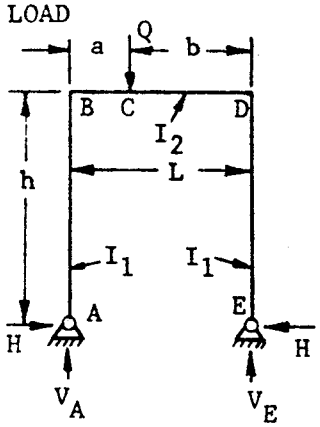


$$V_A = \frac{Qb}{L} \qquad V_E = Q - V_A$$

$$H = \frac{30ab}{2Lh(2K + 3)}$$

FOR SPECIAL CASE: $a = b = \frac{L}{2}$

$$V_A = V_E = \frac{Q}{2}$$

$$H = \frac{3QL}{8h(2K + 3)}$$

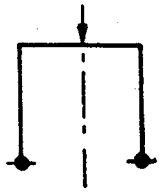

### 2. VERT. CONCENTRATED LOAD

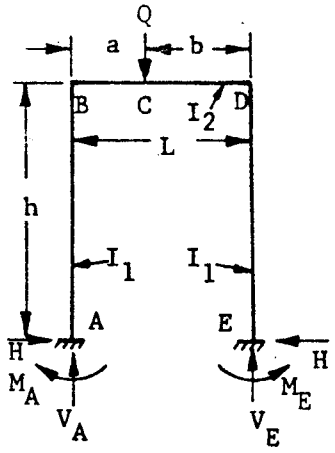


$$V_A = \frac{Qb}{L}\left[1 + \frac{a(b - a)}{L^2(6K + 1)}\right] \qquad V_E = Q - V_A$$

$$H = \frac{3Qab}{2Lh(K + 2)}$$

$$M_A = \frac{Qab}{L}\left[\frac{1}{2(K + 2)} - \frac{(b - a)}{2L(6K + 1)}\right]$$

$$M_E = \frac{Qab}{L}\left[\frac{1}{2(K + 2)} + \frac{(b - a)}{2L(6K + 1)}\right]$$

FOR SPECIAL CASE: $a = b = \frac{L}{2}$

$$V_A = V_E = \frac{Q}{2} \qquad M_A = M_E = \frac{QL}{8(K + 2)}$$

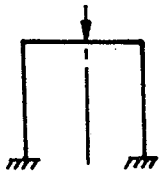

### 3. HORIZ. CONCENTRATED LOAD

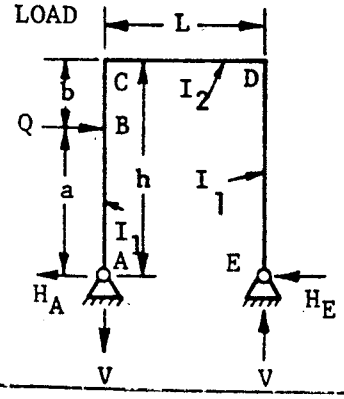


$$V = \frac{Qa}{L} \qquad H_A = Q - H_E$$

$$H_E = \frac{Qa}{2h}\left[\frac{bK(a + h)}{h^2(2K + 3)} + 1\right]$$

FOR SPECIAL CASE: $b = 0, \quad a = h$

$$V = \frac{Qh}{L}$$

$$H_E = H_A = \frac{Q}{2}$$

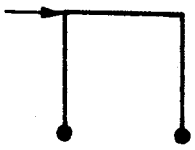

## Table B2.3.1-1 Formulas for Rectangular Bents (Cont)

### 4. HORIZ. CONCENTRATED LOAD

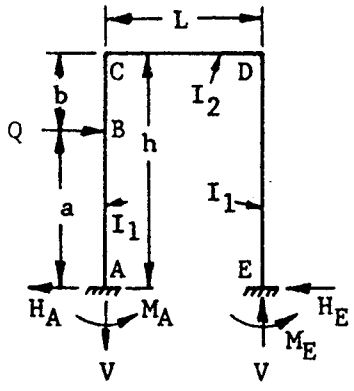


$$V = \frac{3Qa^2K}{Lh(6K+1)} \qquad H_A = Q - H_E$$

$$H_E = \frac{Qab}{2h^2}\left[\frac{h}{b} - \frac{h+b+K(b-a)}{h(K+2)}\right]$$

$$M_A = \frac{Qa}{2h}\left[\frac{b(h+b+bK)}{h(K+2)} + h - \frac{3aK}{(6K+1)}\right]$$

$$M_E = \frac{Qa}{2h}\left[\frac{-b(h+b+bK)}{h(K+2)} + h - \frac{3aK}{(6K+1)}\right]$$

FOR SPECIAL CASE: $b = 0,\ a = h$

$$V = \frac{3QhK}{L(6K+1)}$$

$$H_A = H_E = \frac{Q}{2}$$

$$M_A = M_E = \frac{Qh(3K+1)}{2(6K+1)}$$

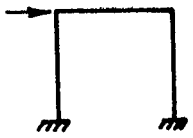

### 5. VERT. UNIFORM RUNNING LOAD

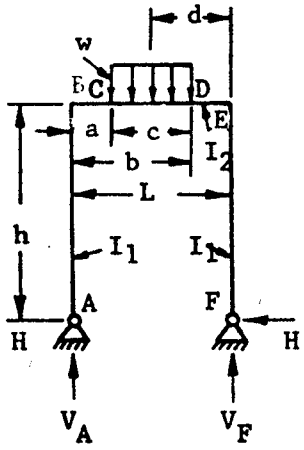


$$d = L - \frac{a}{2} - \frac{b}{2}$$

$$V_A = \frac{wcd}{L}$$

$$V_F = wc - V_A = \frac{wc}{L}\left(a + \frac{c}{2}\right) = wc\left(1 - \frac{d}{L}\right)$$

$$H = \frac{3}{2h}\left[\frac{x_1 + x_2}{2K+3}\right] = \frac{3wc}{24Lh(2K+3)}\left[12dL - 12d^2 - c^2\right]$$

where:

$$X_1 = -\frac{wc}{24L}\left[24\frac{d^3}{L} - 6\frac{bc^2}{L} + 3\frac{c^2}{L} + 4c^2 - 24d^2\right]$$

$$X_2 = \frac{wc}{24L}\left[24\frac{d^3}{L} - 6\frac{bc^2}{L} + 3\frac{c^3}{L} + 2c^2 - 48d^2 + 24dI\right]$$

FOR SPECIAL CASE: $a = 0,\ c = b = L,\ d = \frac{L}{2}$

$$V_A = V_F = \frac{wL}{2}$$

$$H = \frac{wL^2}{4h(2K+3)}$$

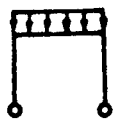

## Table B2.3.1-1 Formulas for Rectangular Bents (Cont)

### 6. VERT. UNIFORM RUNNING LOAD

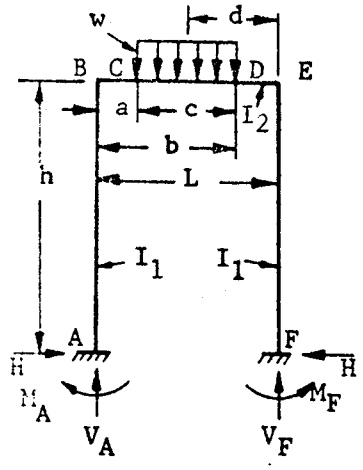


$$d = L - \frac{a}{2} - \frac{b}{2}$$

$$V_A = \frac{wcd}{L} + \frac{X_1 - X_2}{L(6K + 1)}$$

$X_1$ and $X_2$ are given in case 5

$$V_F = wc - V_A$$

$$H = \frac{3(X_1 + X_2)}{2h(K + 2)} \qquad M_A = \frac{X_1 + X_2}{2(K + 2)} - \frac{X_1 - X_2}{2(6K + 1)}$$

$$M_F = \frac{X_1 + X_2}{2(K + 2)} + \frac{X_1 - X_2}{2(6K + 1)}$$

FOR SPECIAL CASE: $a = 0,\ c = b = L,\ d = \frac{L}{2}$

$$V_A = V_F = \frac{wL}{2}$$

$$H = \frac{wL^2}{4h(K + 2)} \qquad M_A = M_F = \frac{wL^2}{12(K + 2)}$$

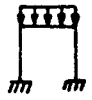

### 7. VERT. TRIANGULAR RUNNING LOAD

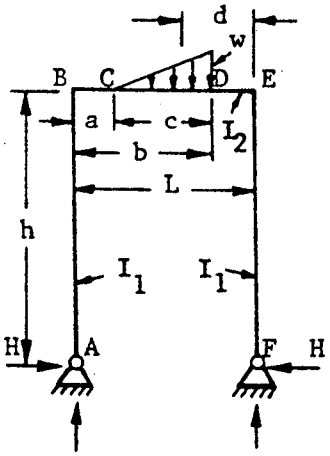


$$d = L - \frac{a}{3} - \frac{2b}{3}$$

$$V_A = \frac{wcd}{2L}$$

$$V_F = \frac{wc}{2} - V_A = \frac{wc}{2L}\left(a + \frac{2c}{3}\right)$$

$$H = \frac{3}{2h}\left[\frac{X_3 + X_4}{2K + 3}\right] = \frac{3wc}{4Lh(2K + 3)}\left[dL - \frac{c^2}{18} - d^2\right]$$

WHERE:

$$X_3 = -\frac{wc}{2L}\left[\frac{d^3}{L} + \frac{c^2}{9} + \frac{51c^3}{810L} + \frac{c^2b}{6L} - d^2\right]$$

$$X_4 = \frac{wc}{2L}\left[\frac{d^3}{L} + \frac{c^2}{18} + \frac{51c^3}{810L} - \frac{c^2b}{6L} - 2d^2 + dL\right]$$

FOR SPECIAL CASE: $a=o,\ c=b=L,\ d = \frac{L}{3}$

$$V = \frac{wL}{6}$$

$$H = \frac{wL^2}{8h(2K + 3)}$$

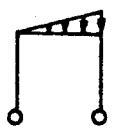

## Table B2.3.1-1 Formulas for Rectangular Bents (Cont)

### 8. VERT. TRIANGULAR RUNNING LOAD

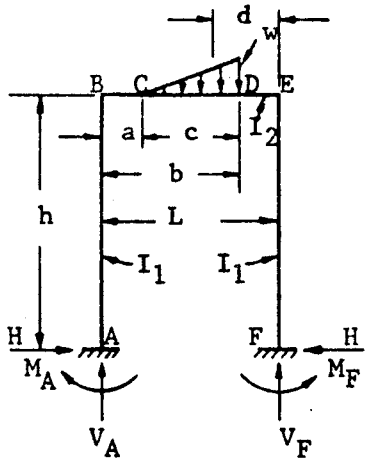


$$d = L - \frac{a}{3} - \frac{2h}{3}$$

$$V_A = \frac{wcd}{2L} + \frac{X_3 - X_4}{L(6K + 1)}$$

$X_3$ and $X_4$ are given in case 7

$$V_F = \frac{wc}{2} - V_A \qquad H = \frac{3(X_3 + X_4)}{2h(K + 2)}$$

$$M_A = \frac{X_3 + X_4}{2(K + 2)} - \frac{X_3 - X_4}{2(6K + 1)}$$

$$M_F = \frac{X_3 + X_4}{2(K + 2)} + \frac{X_3 - X_4}{2(6K + 1)}$$

FOR SPECIAL CASE: a=o, c=b=L, $d = \frac{L}{3}$

$$V_A = \frac{wL}{6}\left[1 - \frac{1}{10(6K + 1)}\right]$$

$$V_F = \frac{wL}{3}\left[1 + \frac{1}{20(6K + 1)}\right]$$

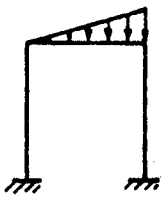

$$H = \frac{wL^2}{8h(K + 2)}$$

$$M_A = \frac{wL^2}{120}\left[\frac{5}{K + 2} + \frac{1}{6K + 1}\right]$$

$$M_F = \frac{wL^2}{120}\left[\frac{5}{K + 2} - \frac{1}{6K + 1}\right]$$

### 9. HORIZ. UNIFORM RUNNING LOAD

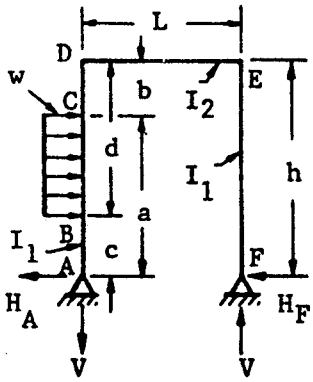


$$V = \frac{w(a^2 - c^2)}{2L} \qquad H_A = w(a - c) - H_F$$

$$H_F = \frac{w(a^2 - c^2)}{4h} + \frac{K\left[w(a^2-c^2)(2h^2-a^2-c^2)\right]}{8h^3(2K + 3)}$$

FOR SPECIAL CASE: c=o, b=o, a=d=h

$$V = \frac{wh^2}{2L}$$

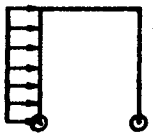

$$H_A = wh - H_F$$

$$H_F = \frac{wh}{4}\left[1 + \frac{K}{2(2K + 3)}\right]$$

## Table B2.3.1-1 Formulas for Rectangular Bents (Cont)

10. HORIZ. UNIFORM RUNNING LOAD

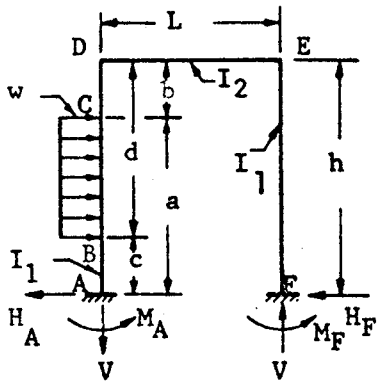


$$V = \frac{w(a^2 - c^2)}{2L} - \frac{M_A}{L} - \frac{M_F}{L}$$

$$H_A = w(a - c) - H_F$$

$$H_F = \frac{w(a^2 - c^2)}{4h} - \frac{X_5}{2h} + \frac{X_6(K - 1)}{2h(K + 2)}$$

WHERE:

$$X_5 = \frac{w}{12h^2}\left[d^3(4h - 3d) - b^3(4h - 3b)\right]$$

$$X_6 = \frac{w}{12h^2}\left[a^3(4h - 3a) - c^3(4h - 3c)\right]$$

$$M_A = \frac{(3K + 1)\left[\frac{w(a^2 - c^2)}{2} - X_5\right]}{2(6K + 1)} + \frac{X_6}{2}\left[\frac{1}{K + 2} + \frac{3K}{6K + 1}\right] + X_5$$

$$M_F = \frac{(3K + 1)\left[\frac{w(a^2 - c^2)}{2} - X_5\right]}{2(6K + 1)} - \frac{X_6}{2}\left[\frac{1}{K + 2} - \frac{3K}{6K + 1}\right]$$

FOR SPECIAL CASE: c=o, b=o, a=d=h:

$$V = \frac{wh^2K}{L(6K + 1)} \qquad H_A = wh - H_F$$

$$H_F = \frac{wh(2K + 3)}{8(K + 2)} \qquad M_F = \frac{wh^2}{24}\left[\frac{18K + 5}{6K + 1} - \frac{1}{K + 2}\right]$$

$$M_A = \frac{wh^2}{24}\left[\frac{30K + 7}{6K + 1} + \frac{1}{K + 2}\right]$$

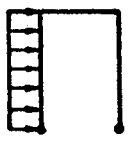

## Table B2.3.1-1 Formulas for Rectangular Bents (Cont)

### 11. HORIZ. TRIANGULAR RUNNING LOAD

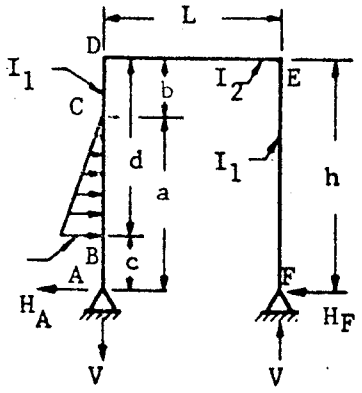


$$V = \frac{w}{6L}(a^2 + ac - 2c^2) \qquad H_A = \frac{w(a-c)}{2} - H_F$$

$$H_F = \frac{VL}{2h} + \frac{KX_7}{(2K+3)h} \qquad \text{WHERE:}$$

$$X_7 = \frac{w}{120h^2(d-b)}\left[3(4d^5+b^5) - 15h(3d^4+b^4) + 20h^2(2d^3+b^3) - 15bd^2(2h-d)^2\right]$$

FOR SPECIAL CASE: b=c=o, a=d=h:

$$V = \frac{wh^2}{6L} \qquad H_A = \frac{wh}{2} - H_F$$

$$H_F = \frac{wh}{12}\left[1 + \frac{7K}{10(2K+3)}\right]$$

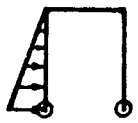

### 12. HORIZ. TRIANGULAR RUNNING LOAD

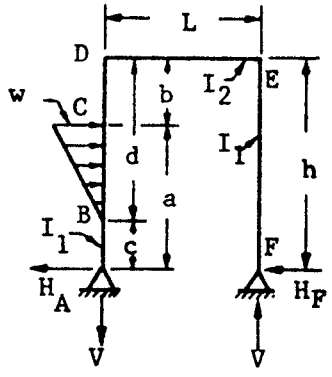


$$V = \frac{w}{6L}(2a + c)(a - c)$$

$$H_A = \frac{w(a-c)}{2} - H_F \qquad H_F = \frac{VL}{2h} + \frac{KX_{10}}{h(2K+3)}$$

WHERE:

$$X_{10} = \frac{w}{120h^2(a-c)}\left[-30h^2c(a^2-c^2) + 20h^2(a^3-c^3) + 15c(a^4-c^4) - 12(a^5-c^5)\right]$$

FOR SPECIAL CASE: b=c=o, a=d=h:

$$V = \frac{wh^2}{3L}$$

$$H_A = \frac{wh}{2} - H_F$$

$$H_F = \frac{wh}{10}\left[\frac{4K+5}{2K+3}\right]$$

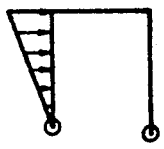

## Table B2.3.1-1 Formulas for Rectangular Bents (Cont)

13. HORIZ. TRIANGULAR RUNNING LOAD

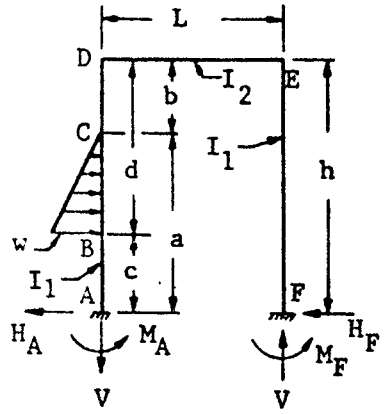


$$V = \frac{w(a^2 + ac - 2c^2)}{6L} - \frac{M_A}{L} - \frac{M_F}{L}$$

$$H_A = \frac{w(a - c)}{2} - H_F$$

$$H_F = \frac{w(a^2 + ac - 2c^2)}{12h} - \frac{X_8}{2h} + \frac{X_9(K-1)}{2h(K+2)}$$

WHERE:

$$X_8 = \frac{w}{60h^2(d-b)}\left[15(h+b)(d^4-b^4) - 12(d^5-b^5) - 20bh(d^3-b^3)\right]$$

$$X_9 = \frac{w}{60h^2(d-b)}\left[10d^2h^2(2d-3b) + 10bh(4d^3+b^2h-b^3) - d^4(30h+15b) + 12d^5 + 3b^5\right]$$

$$M_A = \frac{(3K+1)\left[\frac{w(a^2 + ac - 2c^2)}{6} - X_8\right]}{2(6K+1)} + \frac{X_9}{2}\left[\frac{1}{K+2} + \frac{3K}{6K+1}\right] + X_8$$

$$M_F = \frac{(3K+1)\left[\frac{w(a^2 + ac - 2c^2)}{6}\right] - X_8}{2(6K+1)} - \frac{X_8}{2}\left[\frac{1}{K+2} - \frac{3K}{6K+1}\right]$$

FOR SPECIAL CASE: b=c=o , a=d=h

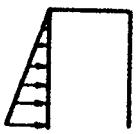

$$V = \frac{wh^2K}{4L(6K+1)} \qquad H_A = \frac{wh}{2} - H_F$$

$$H_F = \frac{wh(3K+4)}{40(K+2)} \qquad M_F = \frac{wh^2}{60}\left[\frac{27K+7}{2(6K+1)} - \frac{1}{K+2}\right]$$

$$M_A = \frac{wh^2}{60}\left[\frac{27K+7}{2(6K+1)} + \frac{3K+7}{K+2}\right]$$

## Table B2.3.1-1 Formulas for Rectangular Bents (Cont)

14. HORIZ. TRIANGULAR RUNNING LOAD

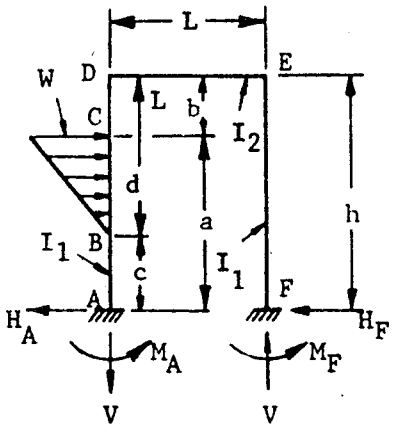


$$V = \frac{w(2a + c)(a - c)}{6L} - \frac{M_A}{L} - \frac{M_F}{L}$$

$$H_A = \frac{w(a - c)}{2} - H_F$$

$$H_F = \frac{w(2a^2-ac-c^2)}{12h} - \frac{X_{11}}{2h} + \frac{X_{12}(K - 1)}{2h(K + 2)}$$

where:

$$X_{11} = \frac{w}{60h^2(d-b)} \left[ 5hd^4-3d^5-20hdb^3-12b^4(d+h) \right]$$

$$X_{12} = \frac{w}{60h^2(a-c)} \left[ 15(h+c)(a^4-c^4) - 12(a^5-c^5) - 20ch(a^3-c^3) \right]$$

$$M_A = \frac{\left[ 3K+1 \right]\left[ \frac{w(2a^2-ac-c^2)}{6} - X_{11} \right]}{2(6K + 1)} + \frac{X_{12}}{2} \left[ \frac{1}{K + 2} + \frac{3K}{6K + 1} \right] + X_{11}$$

$$M_F = \frac{\left[ 3K+1 \right]\left[ \frac{w(2a^2-ac-c^2)}{6} - X_{11} \right]}{2(6K + 1)} - \frac{X_{22}}{2} \left[ \frac{1}{K + 2} - \frac{3K}{6K + 1} \right]$$

FOR SPECIAL CASE: b=c=o, a=d=h

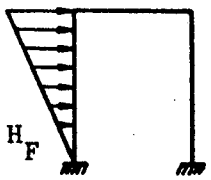

$$V = \frac{3Kwh^2}{4L(6K + 1)} \qquad H_A = \frac{wh}{2} - H_F$$

$$H_F = \frac{wh(7K + 11)}{40(K + 2)} \qquad M_A = \frac{wh^2}{120} \left[ \frac{87K+22}{6K+1} + \frac{3}{K+2} \right]$$

$$M_F = \frac{wh^2}{40} \left[ \frac{21K + 6}{6K + 1} - \frac{1}{K + 2} \right]$$

## Table B2.3.1-1 Formulas for Rectangular Bents (Cont)

| | |
|---|---|
| 15. MOMENT ON HORIZ. SPAN 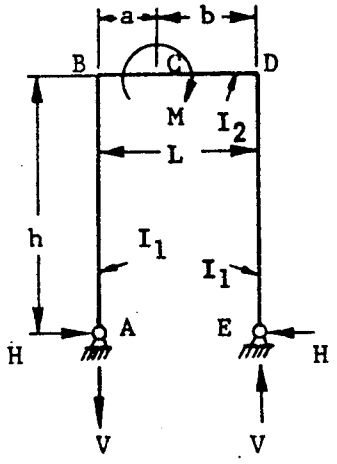  | $V = \frac{M}{L}$<br>$H = \frac{3(b - L/2)M}{Lh(2K + 3)}$<br>FOR SPECIAL CASE: a=o, b=L<br>$V = \frac{M}{L}$<br>$H = \frac{3M}{2h(2K + 3)}$<br> 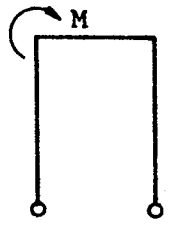  |
| 16. MOMENT ON HORIZ. SPAN 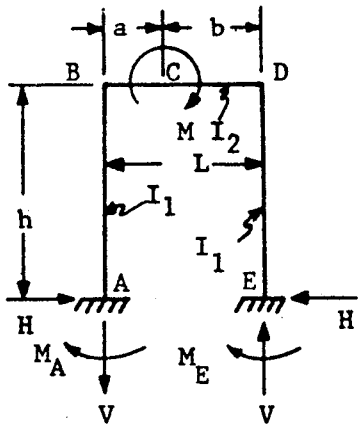  | $V = \frac{6(ab + L^2K)M}{L^3(6K + 1)}$<br>$H = \frac{3(b - a)M}{2Lh(K + 2)}$<br>$M_A = M\left[\frac{6ab(K+2) - L[a(7K+3) - b(5K-1)]}{2L^2(K+2)(6K+1)}\right]$<br>$M_E = VL - M - M_A$<br>FOR SPECIAL CASE: a=o, b=L<br>$V = \frac{6KM}{L(1 + 6K)}$<br>$H = \frac{3M}{2h(K + 2)}$<br>$M_A = \frac{(5K - 1)M}{2(K + 2)(6K + 1)}$<br> 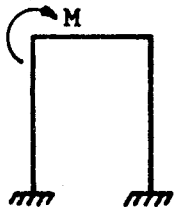  |

## Table B2.3.1-1 Formulas for Rectangular Bents (Cont)

### 17. MOMENT ON SIDE SPAN

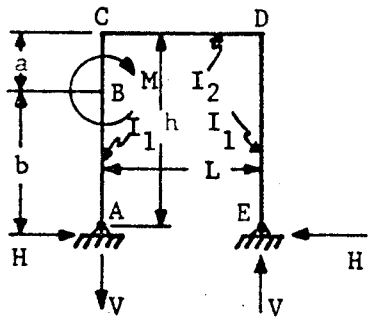


$$V = \frac{M}{L} \qquad H = \frac{3\left[K(2ab+a^2) + h^2\right]M}{2h^3(2K+3)}$$

FOR SPECIAL CASE: a=o, b=h

$$V = \frac{M}{L}$$

$$H = \frac{3M}{2h(2K+3)}$$

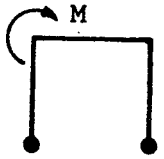


### 18. MOMENT ON SIDE SPAN

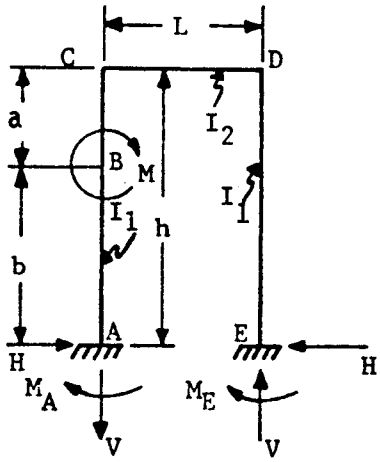


$$V = \frac{6bKM}{hL(6K+1)} \qquad H = \frac{3bM\left[2a(K+1) + b\right]}{2h^3(K+2)}$$

$$M_A = \frac{-M}{2h^2(K+2)(6K+1)}\left[4a^2+2ab+b^2+K(26a^2-5b^2) + 6aK^2(2a-b)\right]$$

$$M_E = VL - M - M_A$$

FOR SPECIAL CASE: a=o; b=h

$$V = \frac{6KM}{L(6K+1)}$$

$$H = \frac{3M}{2h(K+2)}$$

$$M_A = \frac{M(5K-1)}{2(K+2)(6K+1)}$$

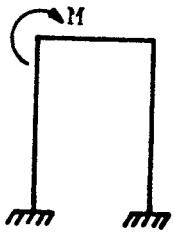

## B2.3.2 Triangular Bents

In Table B2.3.2-1 formulas are given for triangular bents with various types of loading. In all cases, constraining moments, reactions, and applied loads are positive when acting as shown. The value of K should be computed by the equation

$$K = \frac{I_1 S_2}{I_2 S_1} \qquad \text{(B2-5)}$$

## Table B2.3.2-1 Formulas for Triangular Bents

| | |
|---|---|
| 1. VERT. CONCENTRATED LOAD 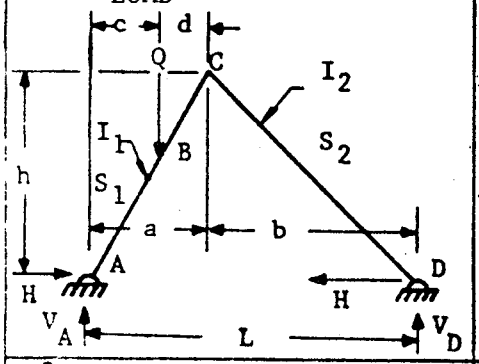  | $V_A = Q - V_D$<br>$V_D = \frac{Qc}{L}$<br>$H = \frac{Qc}{h}\left[\frac{b}{L} + \frac{d(a+c)}{2a^2(K+1)}\right]$ |
| 2. VERT. CONCENTRATED LOAD 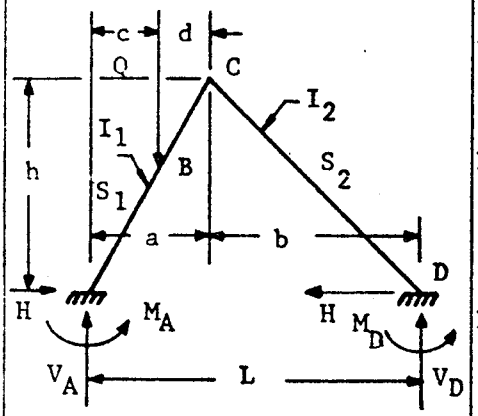  | $V_A = Q - V_D$<br>$V_D = \frac{Qc}{L}\left[1 - \frac{d(a+d)}{2a^2}\right]$<br>$H = \frac{Qcb}{Lh} + \frac{Qcd}{6La^2h(K+1)}\left\{\left[-b(3K+4) - 2L\right](a+d) + 2(2L+b)(a+c) + 3ac\right\}$<br>$M_A = \frac{Qcd}{6a^2(K+1)}\left[(a+d)(3K+4) - 2(a+c)\right]$<br>$M_D = \frac{Qc^2d}{2a^2(K+1)}$ |
| 3. HORIZ. CONCENTRATED LOAD 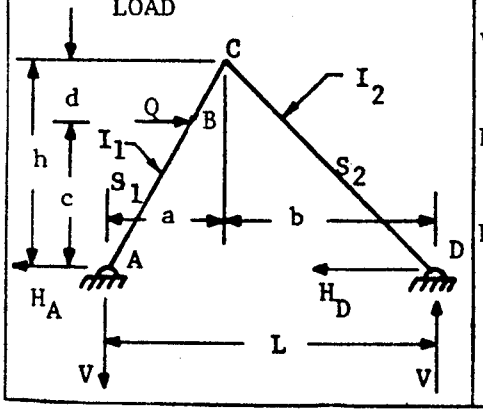  | $V = \frac{Qc}{L}$<br>$H_A = Q - H_D$<br>$H_D = \frac{Qc}{h}\left[\frac{b}{L} + \frac{d(h+c)}{2h^2(K+1)}\right]$ |

## Table B2.3.2-1 Formulas for Triangular Bents (Cont)

| | |
|---|---|
| 4. HORIZ. CONCENTRATED LOAD 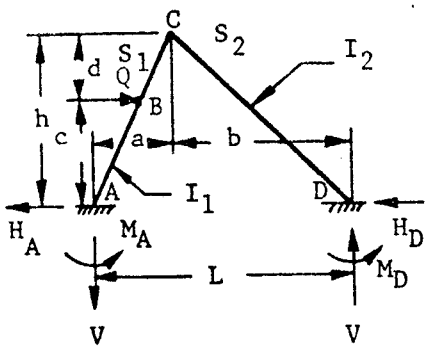  | $V = \frac{Qc}{L}\left[1 - \frac{d(h+d)}{2h^2}\right]$; $H_A = Q - H_D$<br>$H_D = \frac{Qc}{Lh}\left\{b + \frac{d}{6h^2(K+1)}\left[(h+d)(-b[3K+4] - 2L) + 2(2L+b)(h+e) + 3ac\right]\right\}$<br>$M_A = \frac{Qcd}{6h^2(K+1)}\left[(h+d)(3K+4) - 2(h+c)\right]$<br>$M_D = \frac{Qcd}{6h^2(K+1)}(h + 2c + d)$ |
| 5. VERTICAL UNIFORM RUNNING LOAD 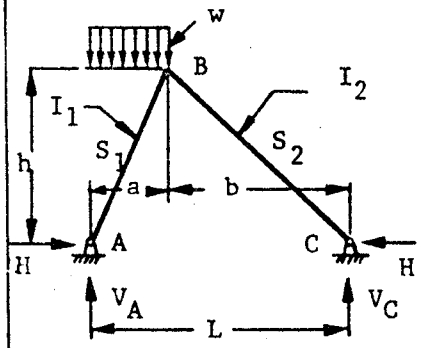  | $V_A = wa\left[1 - \frac{a}{2L}\right]$<br>$V_C = \frac{wa^2}{2L}$<br>$H = \frac{wa^2}{8h}\left[\frac{4b}{L} + \frac{1}{1+K}\right]$ |
| 6. VERTICAL UNIFORM RUNNING LOAD 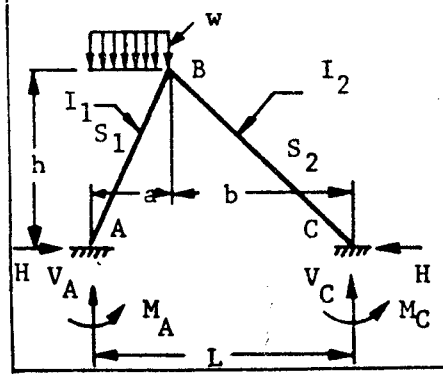  | $V_A = wa\left[1 - \frac{3a}{8L}\right]$ : $V_C = \frac{3wa^2}{8L}$<br>$H = \frac{wa^2}{24Lh(K+1)}\left[b(10 + 9K) + 2L + a\right]$<br>$M_A = \frac{wa^2(3K+2)}{24(K+1)}$<br>$M_c = \frac{wa^2}{24(K+1)}$ |

## Table B2.3.2-1 Formulas for Triangular Bents (Cont)

| | |
|---|---|
| 7. HORIZ. UNIFORM RUNNING LOAD 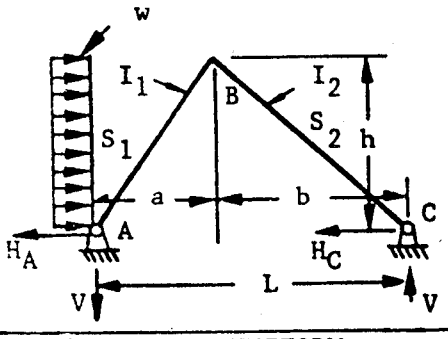  | $V = \frac{wh^2}{2L}$ <br> $H_A = wh - H_C$ <br> $H_C = \frac{wh}{8}\left[\frac{4b}{L} + \frac{1}{K+1}\right]$ |
| 8. HORIZ. UNIFORM RUNNING LOAD 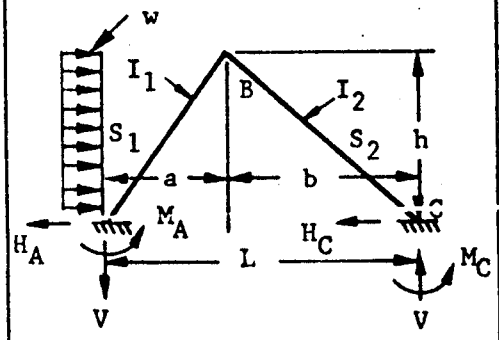  | $V = \frac{3wh^2}{8L}$ <br> $M_A = wh - M_C$ <br> $M_C = \frac{wh}{8L(K+1)}\left[b(3K+4) + a\right]$ <br> $M_A = \frac{wh^2(3K+2)}{24(K+1)}$ $\qquad M_C = \frac{wh^2}{24(K+1)}$ |
| 9. APPLIED MOMENT AT APEX 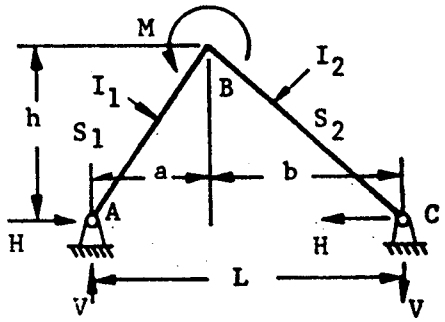  | $V = \frac{M}{L}$ <br> $H = \frac{M}{hL}\left[\frac{a - bK}{K+1}\right]$ |

# PLATES

B

## Table B2.3.2-1 Formulas for Triangular Bents (Cont)

| | |
|---|---|
| 10. APPLIED MOMENT AT APEX 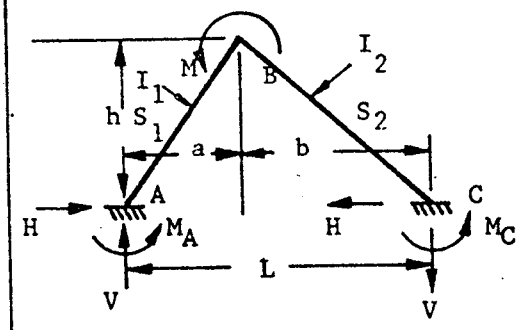  | $V = \frac{3M}{2L}$<br>$H = \frac{3M(a - bK)}{2hL(K + 1)}$<br>$M_A = \frac{KM}{2(K + 1)}$<br>$M_C = \frac{M}{2(K + 1)}$ |

## References

B2-1 Duberg, J. E. and Kemper, "Stress Analysis by Recurrence Formula of Reinforced Circular Cylinders Under Lateral Loads," NACA TN1219, March 1947

B2-2 "Structures Handbook", MAC Report No. 339, McDonnell Aircraft Corporation, 16 March 1960

B2-3 "Structural Analysis Bulletins", MAC Report No. 338, McDonnell Aircraft Corporation, 1 March 1960

## B3.0.0 Plates

### B3.1.0 General Data

#### B3.1.1 Unstiffened Flat Plates Loaded Normal to the Surfaces

A plate is a member whose thickness is small compared to its other dimensions. The surface may be of any shape, but circular and rectangular areas are the most common.

Classification of Plates According to Thickness:

A. Thin plates with small deflection, $< 1/2t$, and the average thickness is $< 1/4$ the width, breadth or diameter. Bending is the main action resisting the normal loads.

B. Thin plates with large deflection $> 1/2t$ but $< 5t$. Reaction to normal loads is by both bending and direct tension.

C. Membranes depend entirely on tension and stretching of the middle plane. The effects of bending can be neglected.

D. Thick plates are those in which the thickness is $> 1/4$ the width or breadth, and shearing stresses are important, corresponding to short deep beams. Such plates are not common.

The plate is supported or clamped continuously along inner or outer edges, or along closed lines on the surface. A plate differs from the beam in that it bends in all planes normal to its surface, whereas the beam bends in only a longitudinal plane.

#### B3.1.2 Edge Restraint (Fixity)

The degree of support provided to the plate element at its edges by adjoining structural elements has a marked effect on buckling and bending stresses. The degree of edge restraint may be approximated from the following idealized edge conditions:

A. Elastically Restrained Edge -- This is an edge about which the plate is elastically restrained from rotating freely. The deflection in the transverse direction is zero. The degree of restraint is defined by the rotational restraint coefficient, $\epsilon$, which is proportional to the ratio of the stiffness of restraining member to that of the plate.

B. Fixed or Built-in Edge ($\epsilon = \infty$) - This is an edge about which the plate cannot rotate. The deflection in the transverse direction along the edge is zero. The tangent plane to the deflected surface along this edge coincides with the initial position of the plate.

C. Simply Supported Edges ( $\varepsilon \neq 0$) - This is an edge condition where the plate is free to rotate about the centerline of the edge (no restraining bending moments about the edge). The deflection in the transverse direction along the edge is zero.

D. Free Edge ( $\varepsilon = 0$) - This is an edge that is entirely free to rotate and to deflect transversely.

In general, torsionally weak edge members will act almost as simple supports, while torsionally stiff edge members will provide almost clamped or fixed edges.

B3.1.3 Symbols

The following notation is used in the analyses of flat plates:

$a$ = Length of plate, inches

$b$ = Width of plate, inches

$t$ = Thickness of plate, inches

$w$ = Normal distributed loading, PSI

$E$ = Modulus of elasticity, PSI

$f_b$ = Maximum bending stress, PSI = $\sigma_b$

$f_r$ = Maximum radial stress, PSI = $\sigma_r$

$f_t$ = Maximum tension stress, PSI = $\sigma_t$

$f_{tan}$ = Maximum tangential stress, PSI = $\sigma_{tan}$

$y$ = Maximum deflection of plate due to normal loading, inches

$\mu$ = Poisson's Ratio

$m$ = Reciprocal of Poisson's Ratio

$K$ = Loading, support, and edge force factor for deflection

$K_1$ = Loading, support, and corner force factor for stress

$K_2$ = Loading and support factor for slope

$L$ = Length, in (dimension to be used in formulas, Ref. Table B3.2.0-1.

$M$ = End moment, in-lb (per in.)

$R$ = Corner force, lb.

$F_E$ = Edge force, lb.

$r_0$ = Radius of a circular area on which load is acting (for solid plates or plates with concentric trunnions), in.

$r$ = Radius

$V_X$ = Edge force distributed along X axis, lb.

TABLE OF CONTENTS

$V_Y$ = Edge force distributed along Y axis, lb.

P = Total applied load - lbs.

$\theta$ = Slope of plate measured from horizontal, radians

$F_1$ = Circular plate force factor - Simply supported

$F_2$ = Circular plate force factor - Fixed edges (R/X>0.6)

$F_3$ = Circular plate force factor - Fixed edges (R/X>0.6)

NOTE: K factors are based on Poisson's ratio of 0.3. There will be little error for other values.

Stress is assumed less than elastic limit. Stress concentrations must be accounted for.

Dimensions "a" and "b" are interchanged with "L" in calculations for stress and deflection. Refer to tables for usage criteria.

Throughout this section it is assumed that the structural components undergoing the action of external forces conform to the following criteria:

A. Material is perfectly elastic; i.e., within the elastic limit.

B. Material is homogeneous - exhibits same physical properties throughout.

C. Isotropic - elastic properties are same in all directions.

D. Constant thickness.

## B3.2.0 Thin Flat Plates with Small Deflection

Formulas for stress and deflection are based on very closely approximate mathematical analyses, and may be accepted as sufficiently accurate when previously stated material assumptions and thickness and deflection criteria hold true. Data are from Reference B3-1.

Formulas for stress and deflection of thin plates:

NOTE: Dimensions 'a' and 'b' are interchanged with 'L' in calculations for stress and deflection. Refer to tables for usage criteria.

a.) Rectangular, Square, Triangular, and Elliptical Shapes

$$f_{MAX} = \frac{K_1 w L^2}{t^2} \qquad y_{MAX} = \frac{K w L^4}{E t^3}$$

Obtain $K_1$ and K from Table B3.2.0-1 or the referenced Figures B3.2.0-1 through B3.2.0-10.

b.) Circular Plate Formulas

1.) Uniform load - Simply supported edges:

$$f_b = \frac{-3P}{8\pi m\, t^2}(3m+1) \qquad y = -\frac{3P\,(m-1)(5m+1)\,a^2}{16\pi E m^2\, t^3}$$

2.) Uniform load - Fixed edges:

$$f_b = \frac{3P}{4\pi t^2} \qquad y = \frac{3P\,(m^2-1)\,a^2}{16\,E\pi m^2\, t^3}$$

3.) Eccentrically Applied Spot Load

Obtain F values from Table B3.2.0-2 and apply the following equations for appropriate boundary condition:

Simply Supported Edges:

$$f_b = -F_1\left(\frac{P}{t^2}\right)$$

Fixed Edges $(r/X < 0.6)$:

$$f_b = -F_2\left(\frac{P}{t^2}\right)$$

Fixed Edges $(r/X > 0.6)$:

$$f_b = -F_3\left(\frac{P}{t^2}\right)$$

c.) Partially Loaded Rectangular Plate - All Edges Supported:

Obtain $K_1$ and K from Table B3.2.0-3 and apply the following equations

$$f = \frac{K_1 P}{t^2} \qquad y = \frac{K w L^2}{E t^3}$$

Corner and Edge Forces - Simply Supported Rectangular Plates:

$$R = K_1 wab \qquad F_E = K w L$$

Obtain $K_1$ and K from Table B3.2.0-1 or the appropriate referenced Figure B3.2.0-1 through -10.

## Table B3.2.0-1 Rectangular, Square, Triangular, and Elliptical Plates

| | a/b MANNER OF LOADING AND CASE NUMBER | L | LOCATIONS OF STRESS AND DEFLECTION | Figure No. |
|---|---|---|---|---|
| 1 | ALL EDGES SUPPORTED UNIFORM LOAD OVER ENTIRE SURFACE | b | S MAX. AT CENTER<br>Y MAX. AT CENTER | B3.2.0-1 |
| 2 | ALL EDGES FIXED UNIFORM LOAD OVER ENTIRE SURFACE | b | S MAX. AT CENTER OF LONG EDGES<br>Y MAX. AT CENTER | B3.2.0-1 |
| 3 | 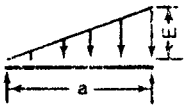 ALL EDGES SUPPORTED DISTRIBUTED LOAD VARYING LINEARLY ALONG LENGTH | b | | B3.2.0-2 |
| 4 | 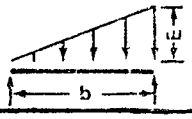 ALL EDGES SUPPORTED DISTRIBUTED LOAD VARYING LINEARLY ALONG BREADTH | b | | B3.2.0-2 |
| 5 | 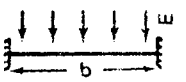 LONG EDGES FIXED, SHORT EDGES SUPPORTED UNIFORM LOAD OVER ENTIRE SURFACE | b | S MAX. AT CENTER OF FIXED EDGES<br>Y MAX. AT CENTER | B3.2.0-3 |
| 6 | 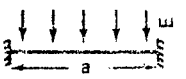 SHORT EDGES FIXED, LONG EDGES SUPPORTED UNIFORM LOAD OVER ENTIRE SURFACE | b | S MAX. AT CENTER OF FIXED EDGES<br>Y MAX. AT CENTER | B3.2.0-3 |
| 7 | ONE LONG EDGE CLAMPED, OTHER THREE EDGES SUPPORTED UNIFORM LOAD OVER ENTIRE SURFACE | b | S MAX. AT CENTER OF FIXED EDGE<br>Y MAX. AT CENTER | B3.2.0-4 |
| 8 | ONE SHORT EDGE CLAMPED, OTHER THREE EDGES SUPPORTED UNIFORM LOAD OVER ENTIRE SURFACE | b | S MAX. AT CENTER OF FIXED EDGE<br>Y MAX. AT CENTER | B3.2.0-4 |
| 9 | ONE SHORT EDGE FREE, OTHER THREE EDGES SUPPORTED UNIFORM LOAD OVER ENTIRE SURFACE | b | S MAX. AT CENTER OF FREE EDGE<br>Y MAX. AT CENTER | B3.2.0-5 |
| 10 | 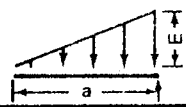 ONE SHORT EDGE FREE, OTHER THREE EDGES SUPPORTED DISTRIBUTED LOAD VARYING LINEARLY ALONG LENGTH | b | S MAX. AT CENTER OF FREE EDGE<br>Y MAX. AT CENTER | B3.2.0-5 |
| 11 | 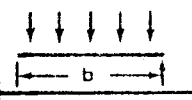 ONE LONG EDGE FREE, OTHER THREE EDGES SUPPORTED UNIFORM LOAD OVER ENTIRE SURFACE | a | S MAX. AT CENTER OF FREE EDGE<br>Y MAX. AT CENTER | B3.2.0-6 |
| 12 | 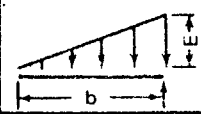 ONE LONG EDGE FREE, OTHER THREE EDGES SUPPORTED DISTRIBUTED LOAD VARYING LINEARLY ALONG LENGTH | a | S MAX. AT CENTER OF FREE EDGE<br>Y MAX. AT CENTER | B3.2.0-6 |
| 13 | 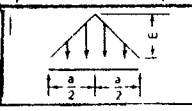 ALL EDGES SUPPORTED DISTRIBUTED LOAD IN FORM OF A TRIANGULAR PRISM | b | S MAX. AT CENTER<br>Y MAX. AT CENTER | B3.2.0-7 |

## Table B3.2.0-1 Rectangular, Square, Triangular, and Elliptical Plates (Cont'd)

| b/a | MANNER OF LOADING AND CASE NUMBER | CASE | LOCATIONS OF STRESS AND DEFLECTION | L |
|---|---|---|---|---|
| Fig. B3.2.0-8 | ALL EDGES FIXED, DISTRIBUTED LOAD VARYING LINEARLY ALONG LENGTH | 14 | MAX. $S_b$ IS AT $x = \pm 1/2\ b;\ y = 0.55a$ | a |
| | | 15 | FOR $S_b$ AT $x = \pm 0;\ y = 0.6a$ | a |
| | | 16 | MAX. $S_a$ IS AT $x = 0;\ y = a$ | a |
| | | 17 | FOR $S_a$ AT $x = 0;\ y = 0$ | a |
| | | 18 | FOR $S_a$ AT $x = 0;\ y = 0.6a$ | a |

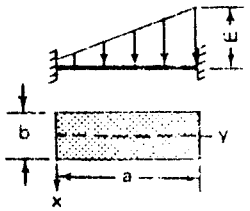

RECTANGULAR SOLID

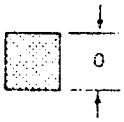

SQUARE, SOLID (L = a)

| CASE | MANNER OF LOADING AND CASE NUMBER | K | $K_1$ | LOCATIONS OF STRESS AND DEFLECTION |
|---|---|---|---|---|
| 19 | EDGES SUPPORTED ABOVE AND BELOW (CORNERS HELD DOWN) UNIFORM LOAD OVER ENTIRE SURFACE | 0.043 | 0.29 | S MAXIMUM AT CENTER<br>Y MAXIMUM AT CENTER |
| 20 | EDGES SUPPORTED BELOW ONLY (CORNERS FREE TO RISE) UNIFORM LOAD OVER ENTIRE SURFACE | 0.044 | 0.28 | S MAX. AT CORNERS ON DIAGONAL SECTION<br>Y MAXIMUM AT CENTER |
| 21 | ALL EDGES FIXED UNIFORM LOAD OVER ENTIRE SURFACE | 0.014 | 0.31 | S MAXIMUM AT CENTER OF EACH EDGE<br>Y MAXIMUM AT CENTER |

ELLIPTICAL, SOLID

| a/b | CASE | MANNER OF LOADING AND CASE NUMBER | L | LOCATIONS OF STRESS AND DEFLECTION | |
|---|---|---|---|---|---|
| 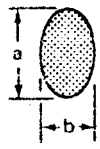  | 22 | EDGE SUPPORTED UNIFORM LOAD OVER ENTIRE SURFACE | b | S MAXIMUM AT CENTER<br>Y MAXIMUM AT CENTER | Fig. B3.2.0-9 |
| | 23 | EDGE FIXED UNIFORM LOAD OVER ENTIRE SURFACE | b | S MAXIMUM AT END OF SHORTER PRINCIPAL AXIS<br>Y MAXIMUM AT CENTER | Fig. B3.2.0-10 |

## Table B3.2.0-1 Rectangular, Square, Triangular, and Elliptical Plates (Cont'd)

| | MANNER OF LOADING AND CASE NUMBER | | K | $K_1$ | LOCATION OF STRESS AND DEFLECTION | L |
|---|---|---|---|---|---|---|
| 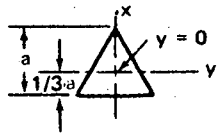 EQUILATERAL TRIANGLE, SOLID | EDGES SUPPORTED DISTRIBUTED LOAD OVER ENTIRE SURFACE | 24 | 0.01 | 0.149 | S MAXIMUM AT y = 0, x = -0.062a<br>Y MAXIMUM AT CENTER | a |
| | | 25 | 0.01 | 0.155 | S MAXIMUM AT y = 0, x = 0.129a<br>Y MAXIMUM AT CENTER | a |

| | MANNER OF LOADING AND CASE NUMBER | | K | $K_1$ | LOCATION OF STRESS AND DEFLECTION | L |
|---|---|---|---|---|---|---|
| 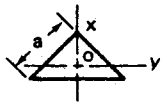 RIGHT ANGLE ISOSCELES TRIANGLE, SOLID | EDGES SUPPORTED DISTRIBUTED LOAD OVER ENTIRE SURFACE | 26 | 0.0095 | 0.13 | S MAXIMUM AT CENTER<br>Y MAXIMUM AT CENTER | a |

| | θ | | 45° | | 60° | | 90° | | 180° | | |
|---|---|---|---|---|---|---|---|---|---|---|---|
| | CASE | MANNER OF LOADING AND CASE NUMBER | K | $K_1$ | K | $K_1$ | K | $K_1$ | K | $K_1$ | L |
| 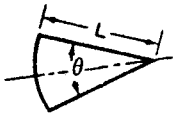 CIRCULAR SECTOR, SOLID | 27 | EDGES SUPPORTED DISTRIBUTED LOAD OVER ENTIRE SURFACE | 0.0054 | 0.11 | 0.01 | 0.15 | 0.025 | 0.22 | 0.087 | 0.31 | a |
| | 28 | | 0.0054 | 0.10 | 0.01 | 0.15 | 0.025 | 0.24 | 0.087 | 0.52 | a |

| | θ | | 0° | | 30° | | 45° | | 60° | | 75° | | |
|---|---|---|---|---|---|---|---|---|---|---|---|---|---|
| | CASE | MANNER OF LOADING AND CASE NUMBER | K | $K_1$ | K | $K_1$ | K | $K_1$ | K | $K_1$ | K | $K_1$ | L |
| 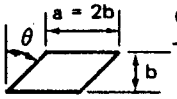 PARALLELOPIPED (SKEW SLAB) | 29 | ALL EDGES SUPPORTED DISTRIBUTED LOAD OVER ENTIRE SURFACE | – | 0.50 | – | 0.50 | – | 0.45 | – | 0.40 | – | 0.16 | b |
| | 30 | EDGES b SUPPORTED EDGES a FREE DISTRIBUTED LOAD OVER ENTIRE SURFACE | – | 0.76 | – | 0.61 | – | 0.44 | – | 0.25 | – | – | a |

**LOCATIONS OF STRESS AND DEFLECTION**

| | | | |
|---|---|---|---|
| 27 | S MAXIMUM (TANGENTIAL) AT MIDPOINT OF CIRCULAR EDGE<br>Y MAXIMUM AT MIDPOINT OF CIRCULAR EDGE | 29 | S MAXIMUM AT CENTER<br>NO DATA AVAILABLE FOR DEFLECTION |
| 28 | S MAXIMUM (RADIAL) ON LINE TO MIDPOINT OF CIRCULAR EDGE<br>Y MAXIMUM AT MIDPOINT OF CIRCULAR EDGE | 30 | S MAXIMUM AT CENTER<br>NO DATA AVAILABLE FOR DEFLECTION |

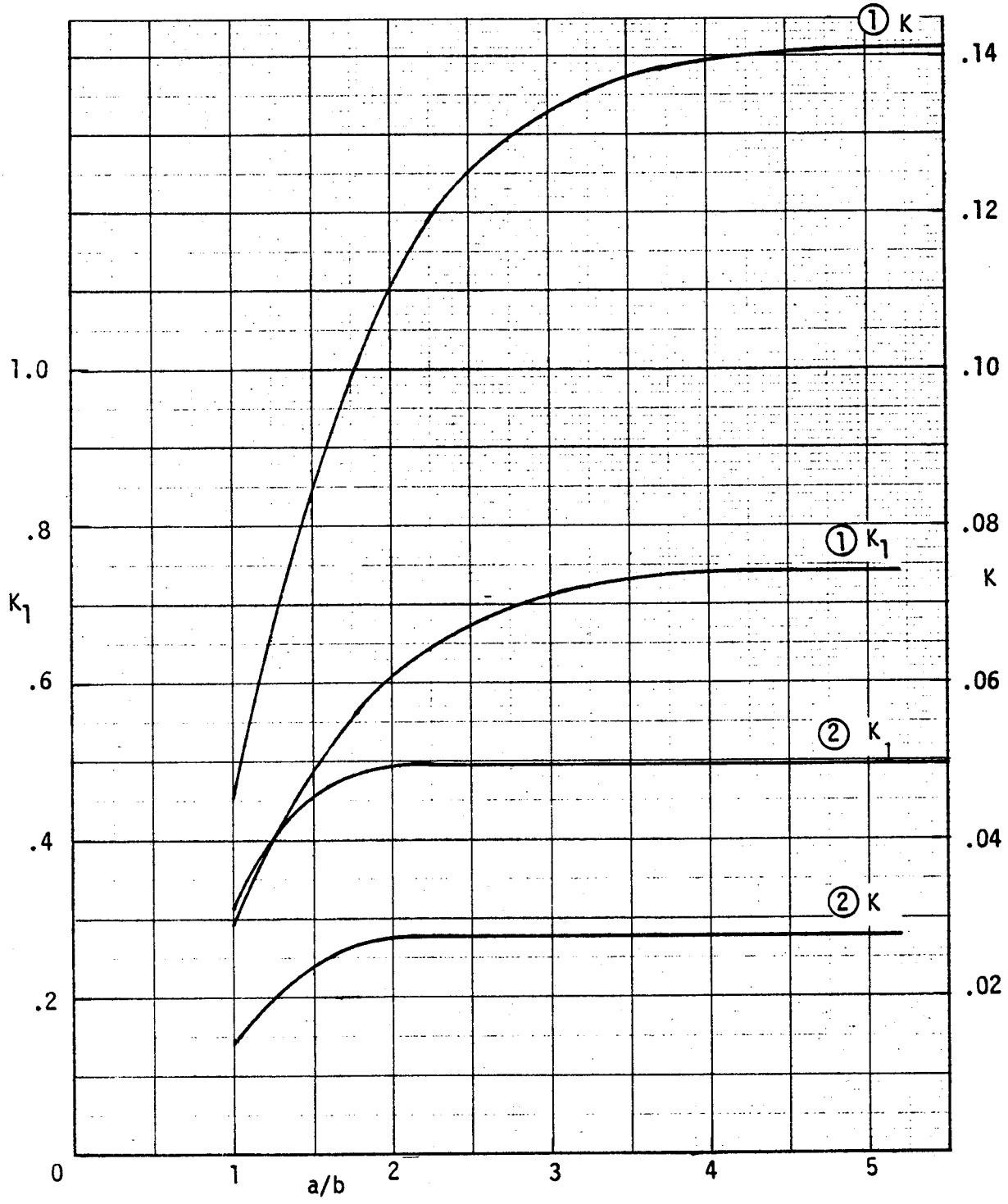


Figure B3.2.0-1 Constants for Determining Stress and Deflection (Cases 1 & 2)

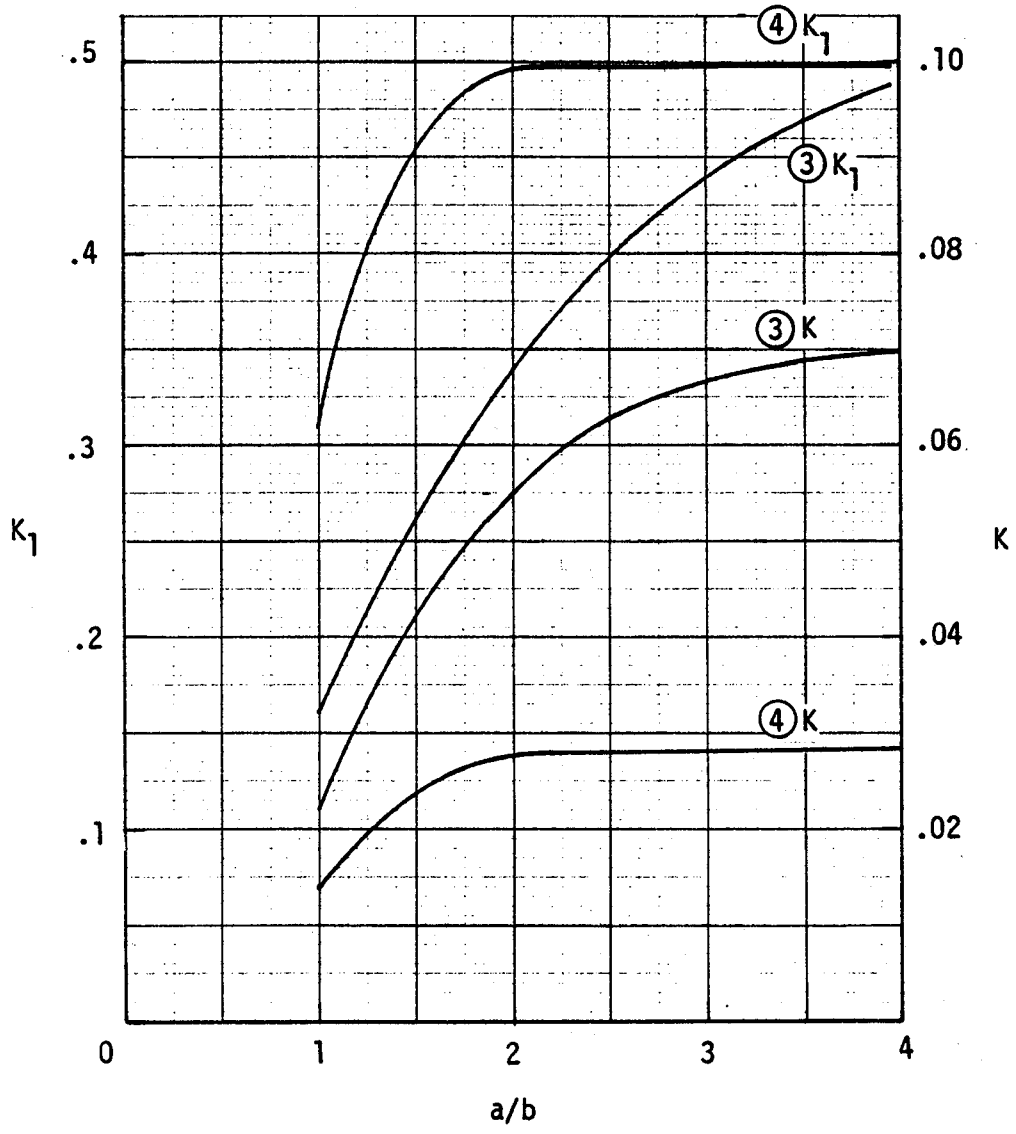


Figure B3.2.0-2 Constants for Determining Stress and Deflection (Cases 3 & 4)

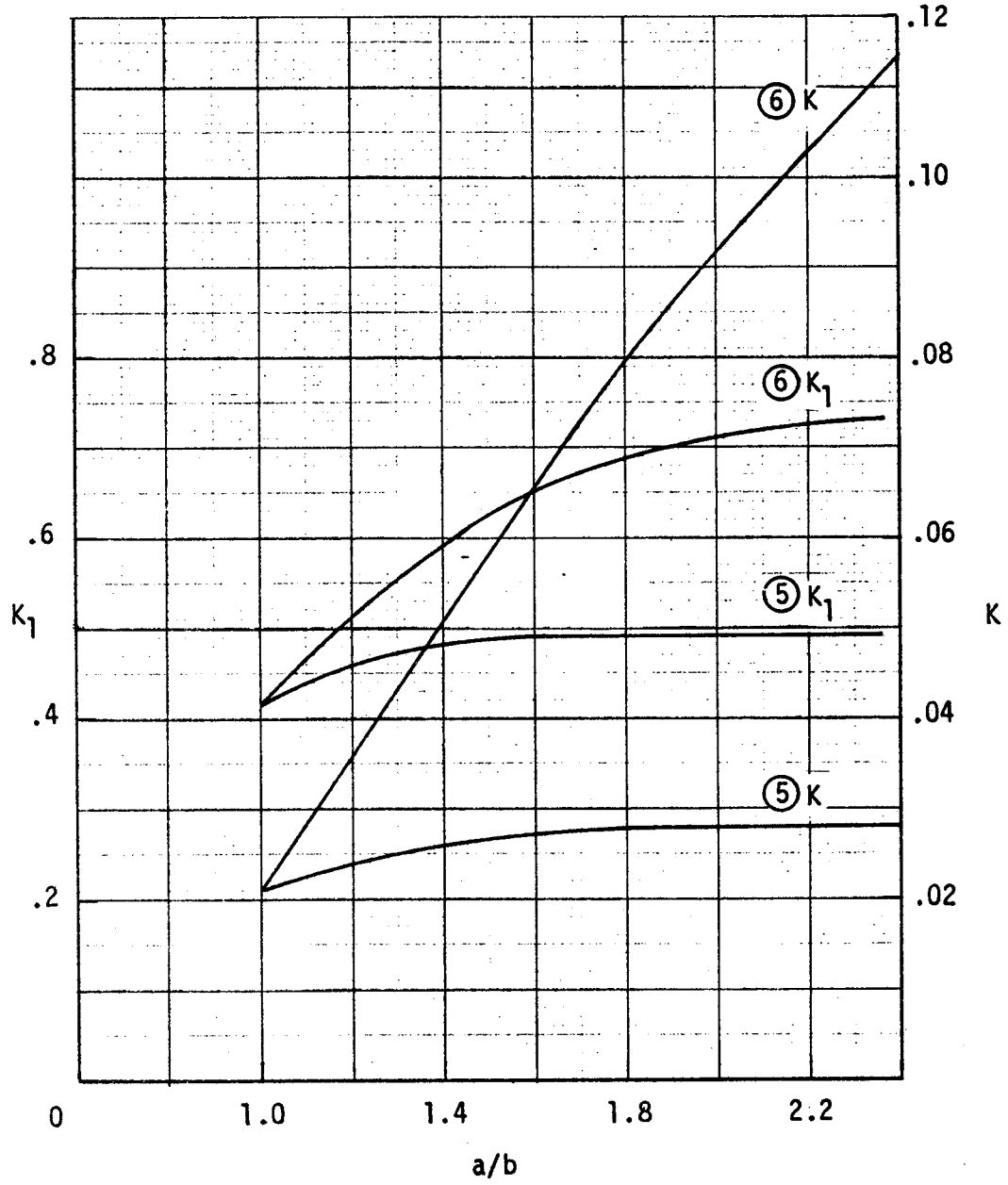


Figure B3.2.0-3 Constants for Determining Stress and Deflection (Cases 5 & 6)

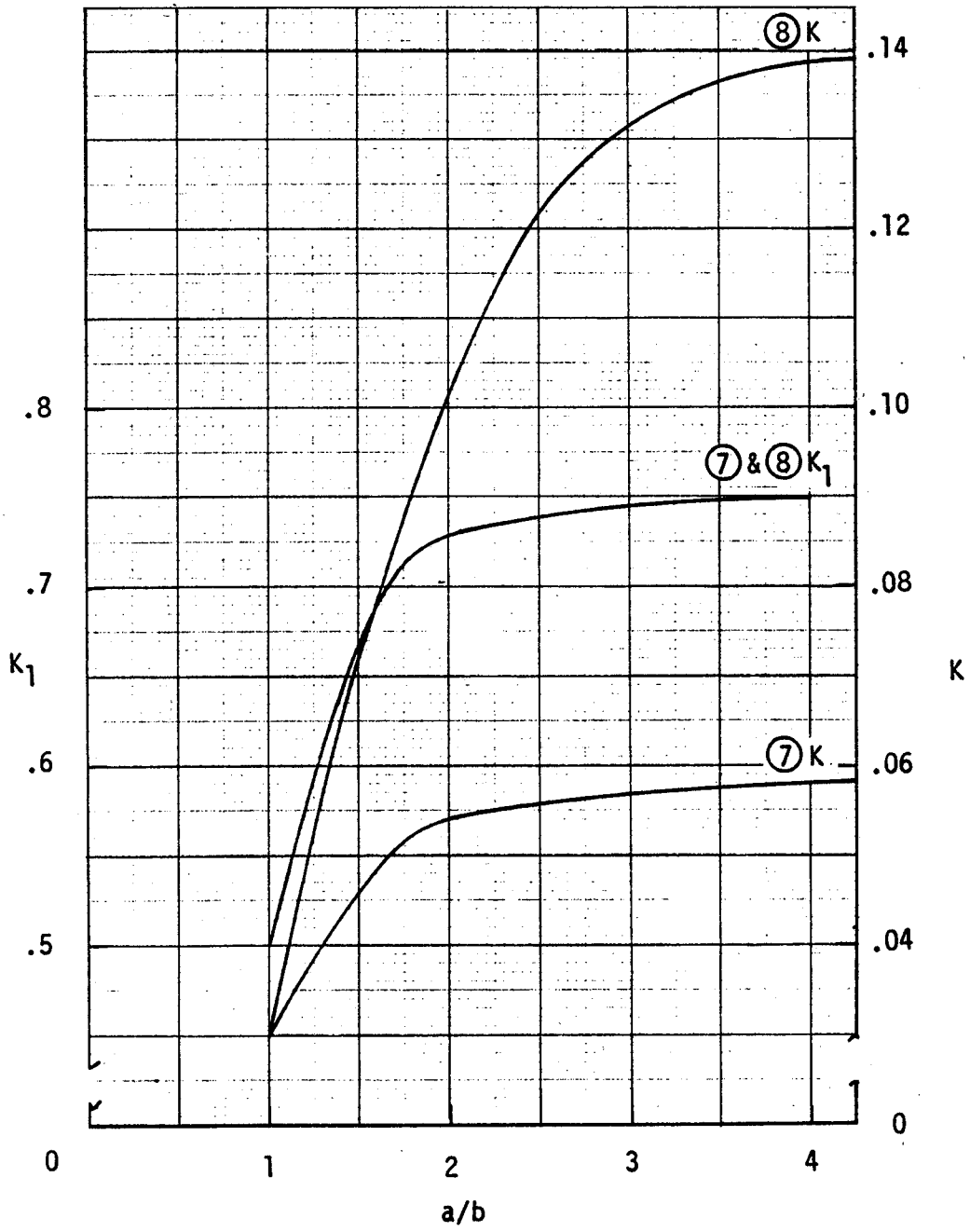


Figure B3.2.0-4 Constants for Determining Stress and Deflection (Cases 7 & 8)

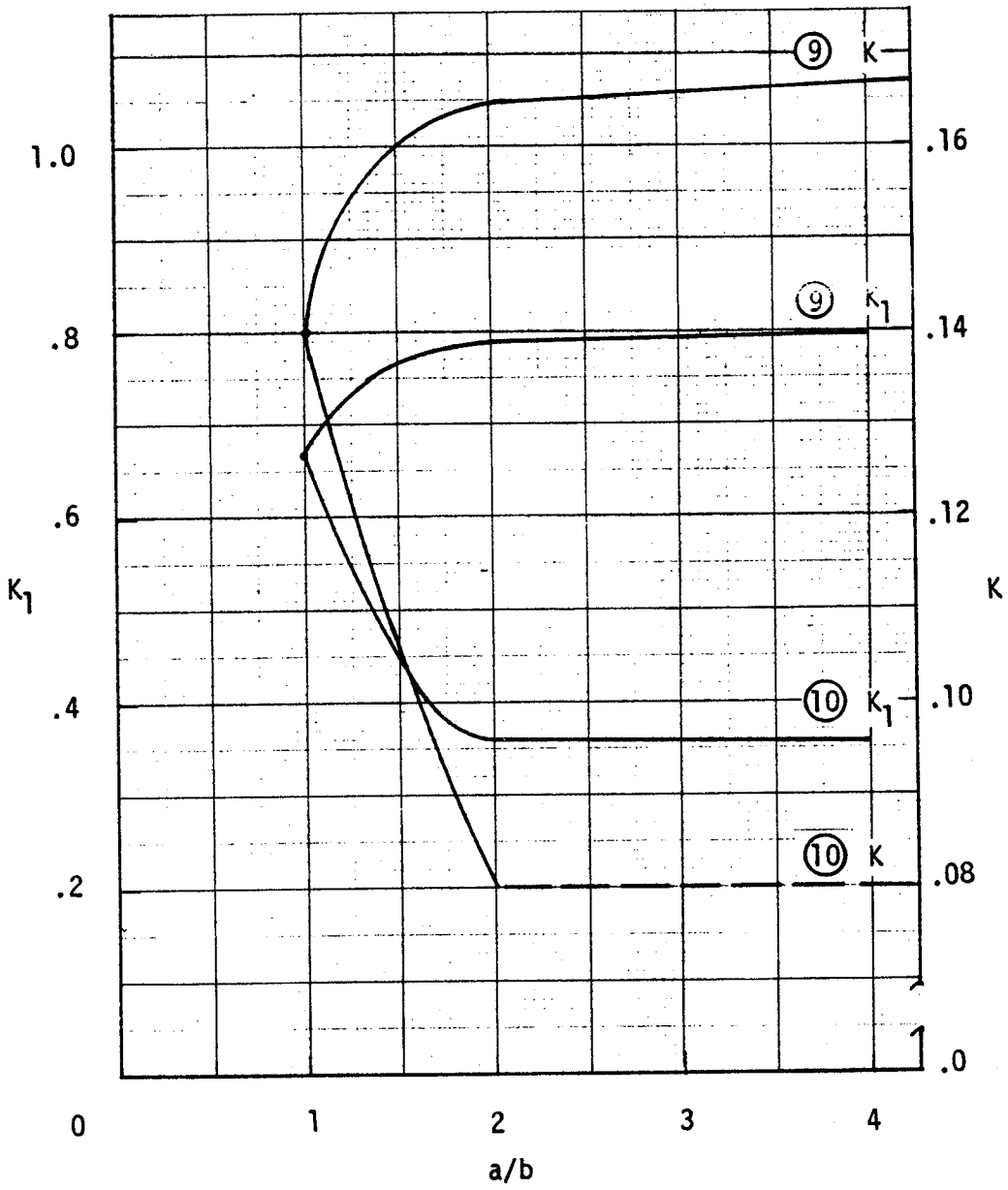


Figure B3.2.0-5 Constants for Determining Stress and Deflection (Cases 9 & 10)

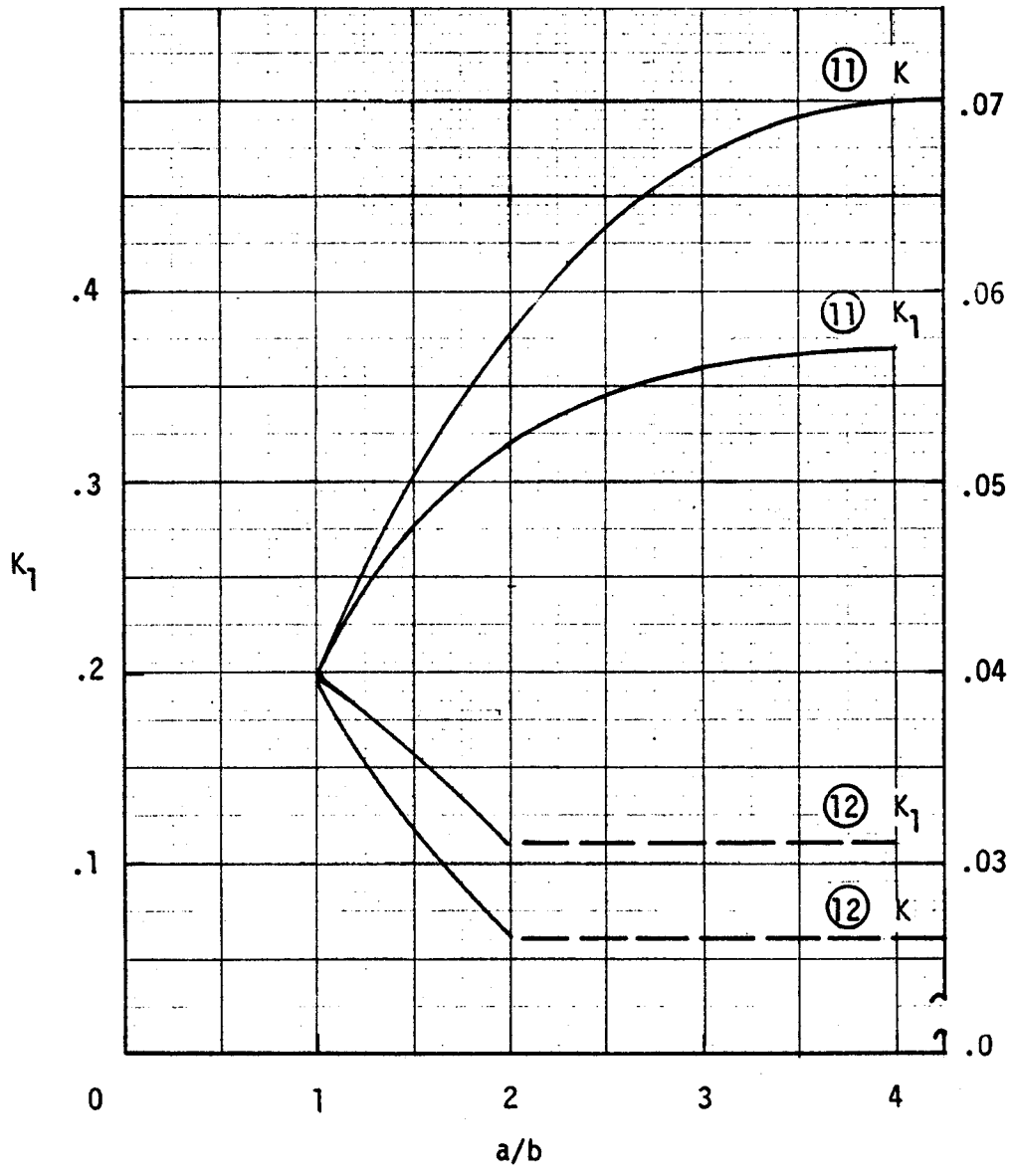


Figure B3.2.0-6 Constants for Determining Stress and Deflection (Case 11 & 12)

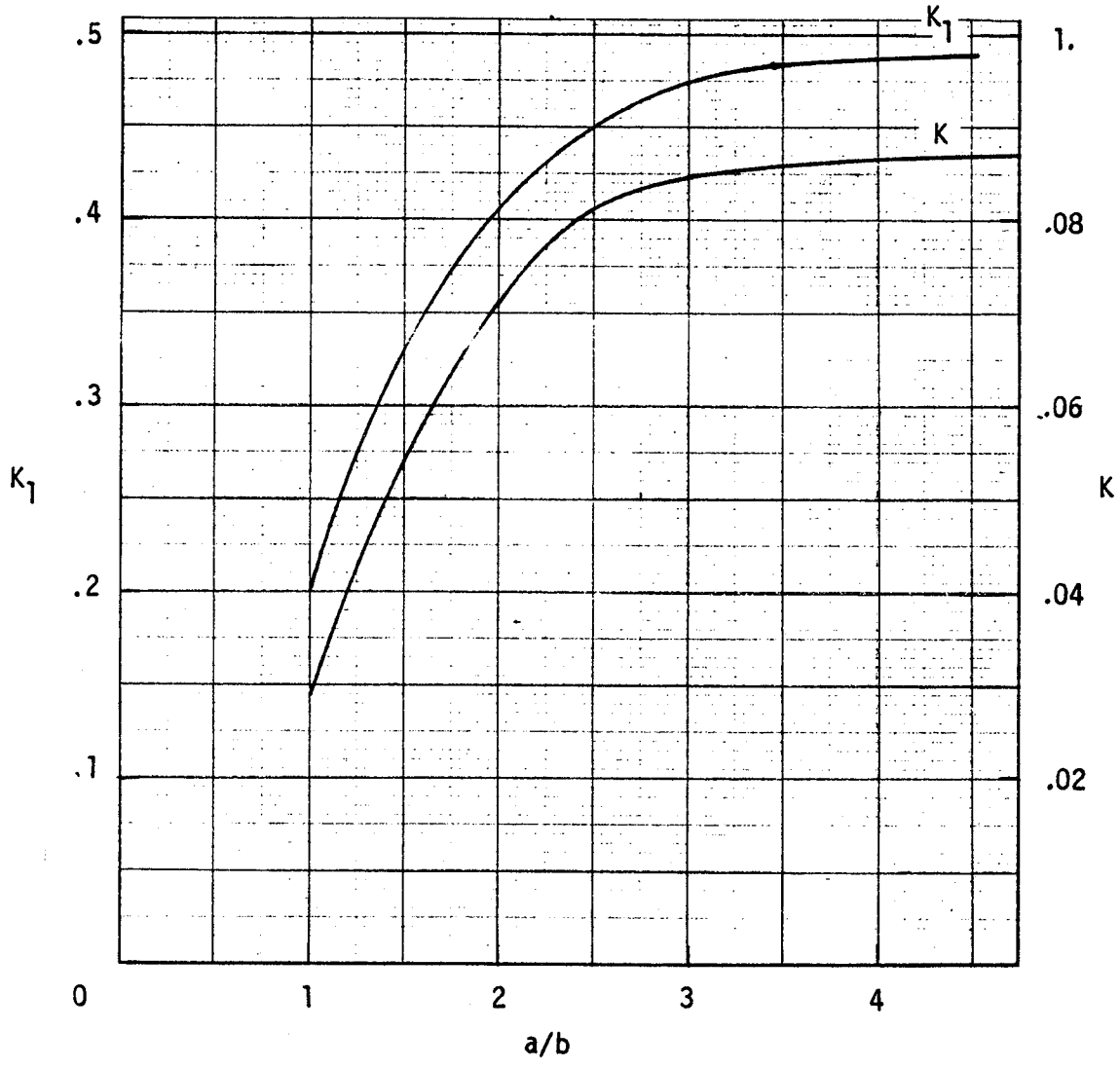


Figure B3.2.0-7 Constants for Determining Stress and Deflection (Case 13)

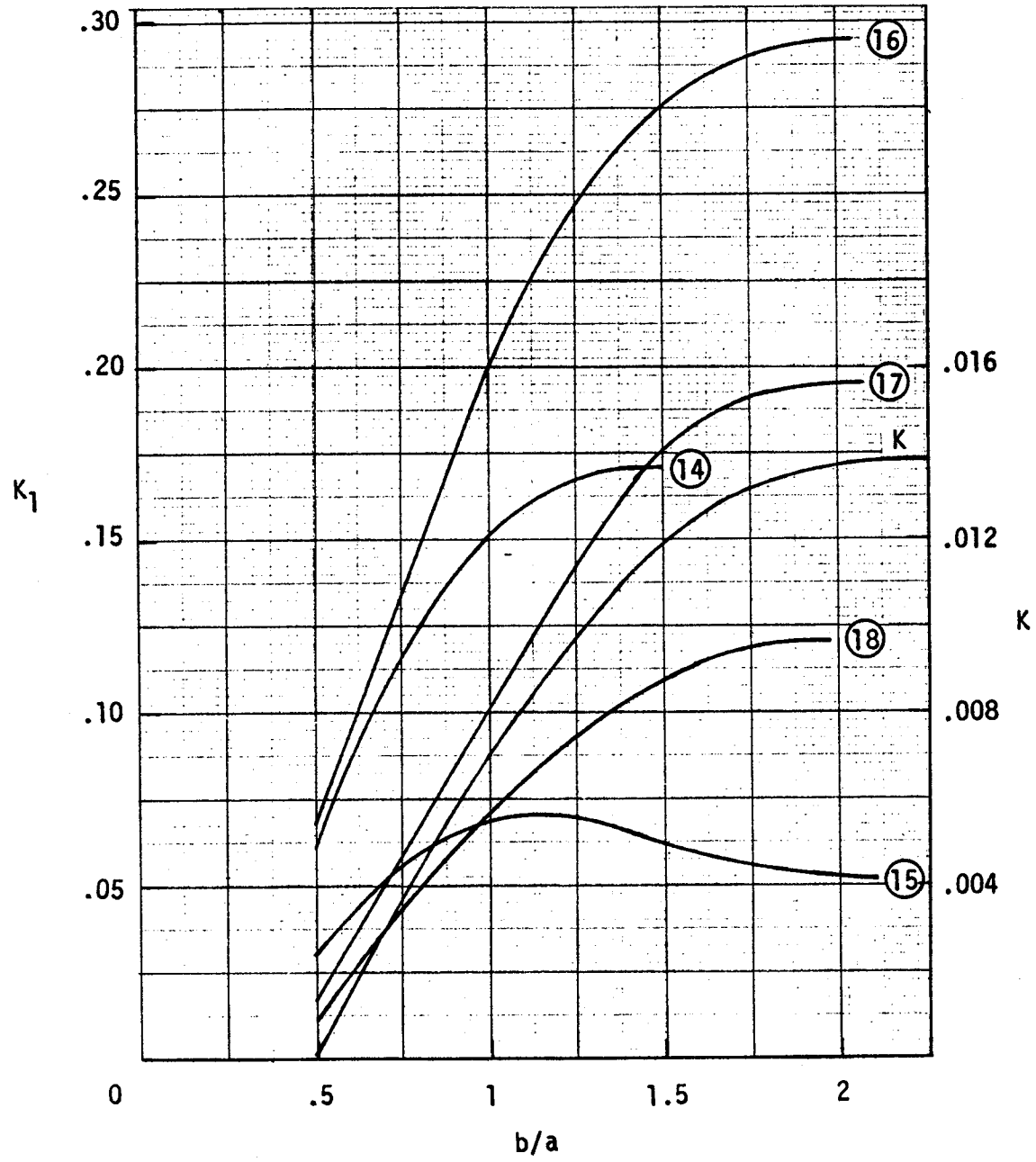


Figure B3.2.0-8 Constants for Determining Stress and Deflection (Cases 14-18)

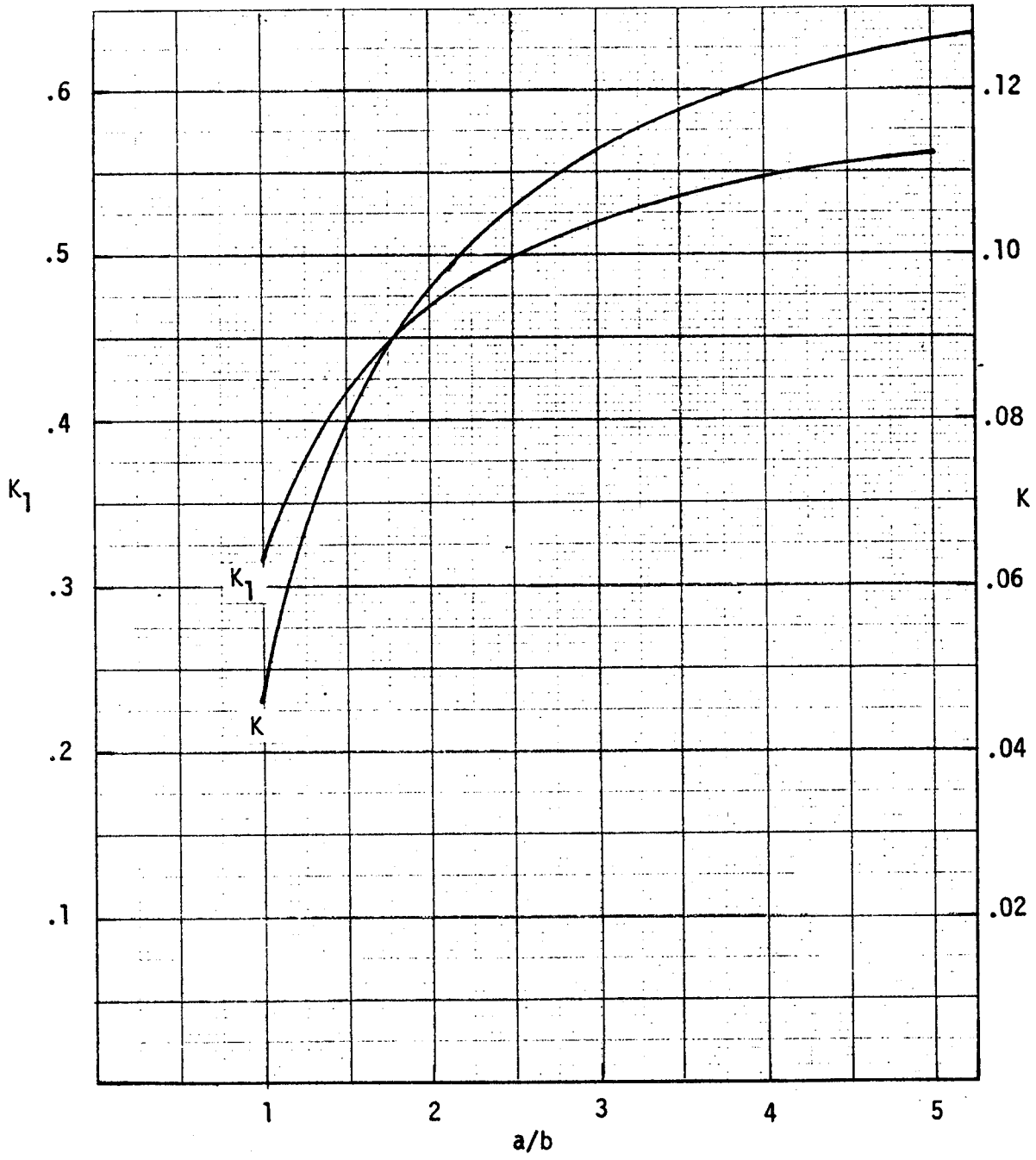


Figure B3.2.0-9 Constants for Determining Stress and Deflection (Case 22)

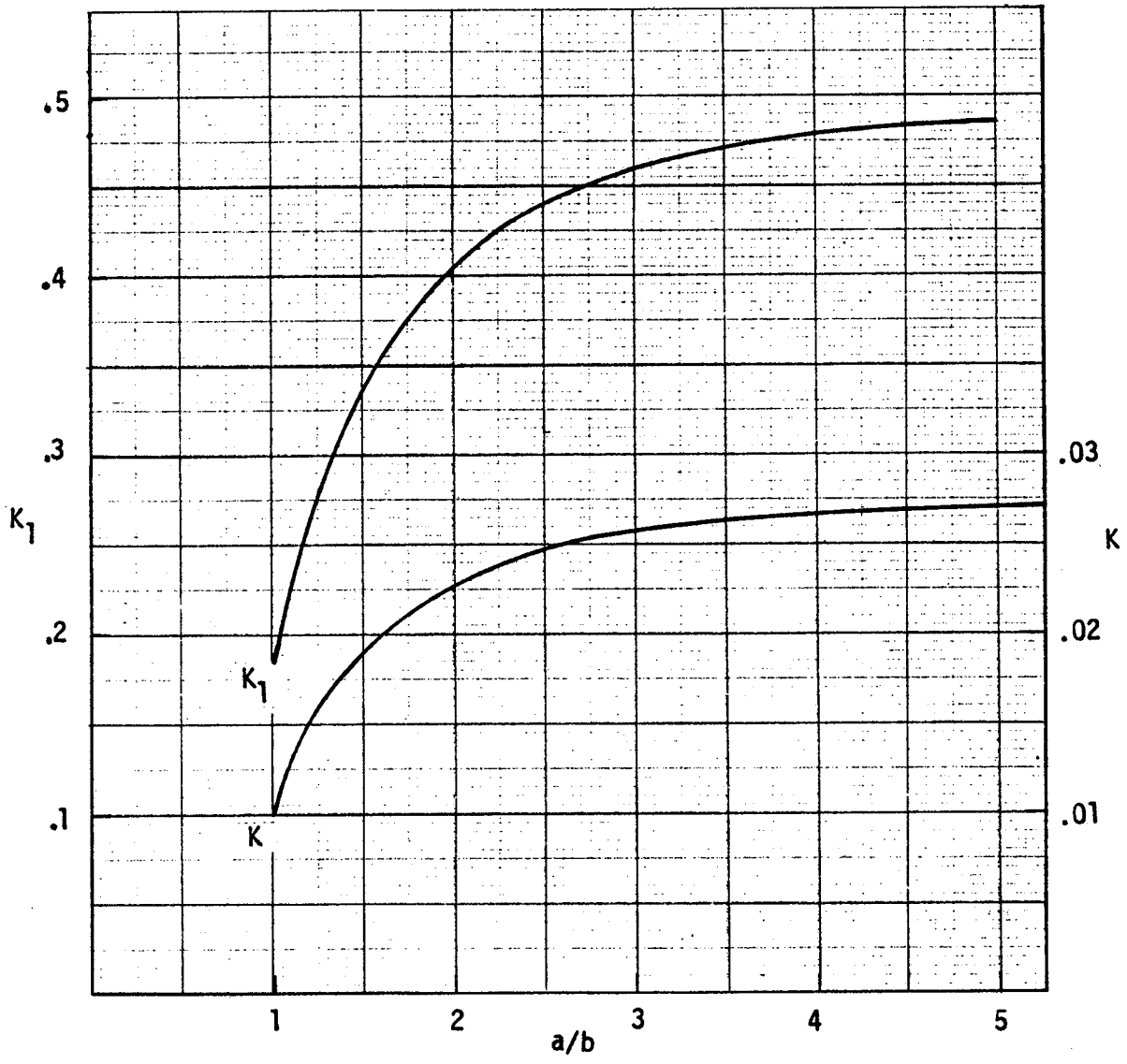


Figure B3.2.0-10 Constants for Determining Stress and Deflection (Case 23)

## Table B3.2.0-2 F Factors for Circular Plate Stresses

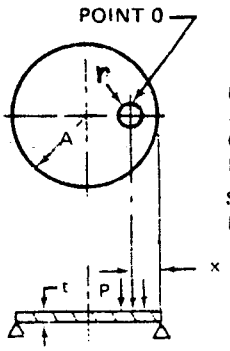


P IS TOTAL LOAD DISTRIBUTED OVER CIRCLE WITH RADIUS R.

SIMPLY SUPPORTED EDGES

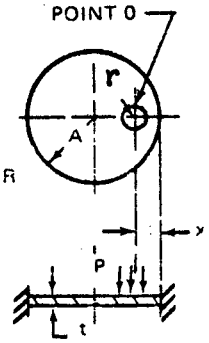


P IS TOTAL LOAD DISTRIBUTED OVER CIRCLE WITH RADIUS R.

FIXED EDGES

### Simply Supported Edges- $F_1$

| X/A | R/A | | | | | | | | | |
|---|---|---|---|---|---|---|---|---|---|---|
| | 0.1 | 0.2 | 0.3 | 0.4 | 0.5 | 0.6 | 0.7 | 0.8 | 0.9 | 1.0 |
| 0.1 | 0.3939 | | | | | | | | | |
| 0.2 | 0.8868 | 0.3939 | | | | | | | | |
| 0.3 | 1.1501 | 0.6920 | 0.3939 | | | | | | | |
| 0.4 | 1.3327 | 0.8868 | 0.6090 | 0.3939 | | | | | | |
| 0.5 | 1.4731 | 1.0328 | 0.7645 | 0.5625 | 0.3939 | | | | | |
| 0.6 | 1.5873 | 1.1501 | 0.8368 | 0.6920 | 0.5326 | 0.3939 | | | | |
| 0.7 | 1.6836 | 1.2482 | 0.9880 | 0.7975 | 0.6437 | 0.5118 | 0.3939 | | | |
| 0.8 | 1.7669 | 1.3327 | 1.0745 | 0.8868 | 0.7366 | 0.6090 | 0.4964 | 0.3939 | | |
| 0.9 | 1.8403 | 1.4069 | 1.1501 | 0.9643 | 0.8165 | 0.6920 | 0.5829 | 0.4846 | 0.3939 | |
| 1.0 | 1.9059 | 1.4731 | 1.2173 | 1.0328 | 0.8868 | 0.7645 | 0.6579 | 0.5625 | 0.4752 | 0.3939 |

### Fixed Edges ($r/x < 0.6$) - $F_2$

| X/A | R/A | | | | | | | | | |
|---|---|---|---|---|---|---|---|---|---|---|
| | 0.1 | 0.2 | 0.3 | 0.4 | 0.5 | 0.6 | 0.7 | 0.8 | 0.9 | 1.0 |
| 0.1 | 0.1552 | | | | | | | | | |
| 0.2 | 0.4690 | 0.1552 | | | | | | | | |
| 0.3 | 0.6992 | 0.3206 | 0.1522 | | | | | | | |
| 0.4 | 0.8702 | 0.4690 | 0.2659 | 0.1552 | | | | | | |
| 0.5 | 1.0052 | 0.5936 | 0.3729 | 0.2378 | 0.1552 | | | | | |
| 0.6 | 1.1165 | 0.6992 | 0.4690 | 0.3206 | 0.2209 | 0.1552 | | | | |
| 0.7 | 1.2110 | 0.7902 | 0.5544 | 0.3930 | 0.2680 | 0.2097 | 0.1552 | | | |
| 0.8 | 1.2931 | 0.8702 | 0.6306 | 0.4690 | 0.3523 | 0.2659 | 0.2017 | 0.1552 | | |
| 0.9 | 1.3657 | 0.9412 | 0.6992 | 0.5340 | 0.4127 | 0.3206 | 0.2499 | 0.1957 | 0.1552 | |
| 1.0 | 1.4308 | 1.0052 | 0.7613 | 0.5936 | 0.4690 | 0.3729 | 0.2974 | 0.2378 | 0.1911 | 0.1552 |

### Fixed Edges ($r/x > 0.6$) - $F_3$

| X/A | R/A | | | | | | | | | |
|---|---|---|---|---|---|---|---|---|---|---|
| | 0.1 | 0.2 | 0.3 | 0.4 | 0.5 | 0.6 | 0.7 | 0.8 | 0.9 | 1.0 |
| 0.1 | 0.2387 | | | | | | | | | |
| 0.2 | 0.4178 | 0.2387 | | | | | | | | |
| 0.3 | 0.4509 | 0.3714 | 0.2387 | | | | | | | |
| 0.4 | 0.4625 | 0.4178 | 0.3432 | 0.2387 | | | | | | |
| 0.5 | 0.4679 | 0.4393 | 0.3915 | 0.3247 | 0.2387 | | | | | |
| 0.6 | 0.4708 | 0.4509 | 0.4178 | 0.3714 | 0.3117 | 0.2387 | | | | |
| 0.7 | 0.4726 | 0.4580 | 0.4336 | 0.3995 | 0.3557 | 0.3021 | 0.2387 | | | |
| 0.8 | 0.4737 | 0.4625 | 0.4439 | 0.4178 | 0.3842 | 0.3432 | 0.2947 | 0.2387 | | |
| 0.9 | 0.4745 | 0.4657 | 0.4509 | 0.4303 | 0.4038 | 0.3714 | 0.3330 | 0.2888 | 0.2387 | |
| 1.0 | 0.4751 | 0.4679 | 0.4560 | 0.4393 | 0.4178 | 0.3915 | 0.3605 | 0.3247 | 0.2841 | 0.2387 |

## Table B3.2.0-3 Simply Supported Rectangular Plate Under Hydrostatic Pressure

a < b

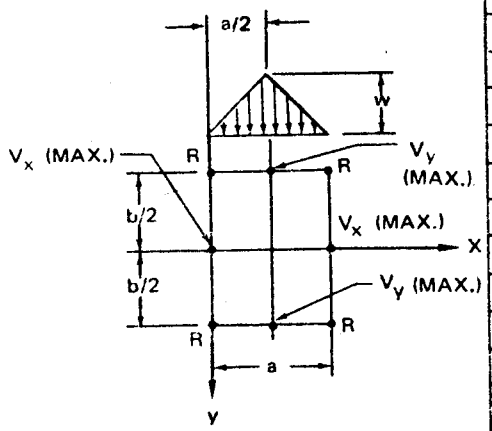


| | K | | $K_1$ | |
|---|---|---|---|---|
| b/a | $V_x$ (MAX.) | $V_y$ (MAX.) | R | REMARKS |
| 1.0 | 0.147 | 0.250 | 0.038 | USE L = a FOR $V_x$ |
| 1.1 | 0.161 | 0.232 | 0.038 | USE L = b FOR $V_y$ |
| 1.2 | 0.173 | 0.216 | 0.037 | |
| 1.3 | 0.184 | 0.202 | 0.036 | |
| 1.4 | 0.193 | 0.189 | 0.035 | |
| 1.5 | 0.202 | 0.178 | 0.034 | |
| 1.6 | 0.208 | 0.108 | 0.033 | |
| 1.7 | 0.214 | 0.158 | 0.031 | |
| 1.8 | 0.220 | 0.150 | 0.030 | |
| 1.9 | 0.224 | 0.142 | 0.029 | |
| 2.0 | 0.228 | 0.135 | 0.028 | |
| 3.0 | 0.245 | 0.090 | 0.019 | |
| ∞ | 0.250 | – | – | |

CORNER AND EDGE FORCES FOR SIMPLY SUPPORTED RECTANGULAR PLATES UNDER A LOAD IN THE FORM OF A TRIANGULAR PRISM

a > b

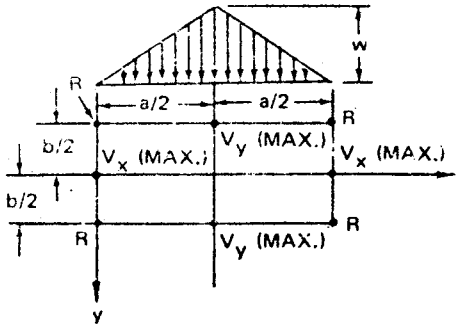


| | K | | $K_1$ | |
|---|---|---|---|---|
| a/b | $V_x$ (MAX.) | $V_y$ (MAX.) | R | REMARKS |
| ∞ | – | 0.50 | – | USE L = a FOR $V_x$ |
| 3.0 | 0.027 | 0.410 | 0.010 | USE L = b FOR V |
| 2.0 | 0.057 | 0.365 | 0.023 | |
| 1.9 | 0.062 | 0.358 | 0.024 | |
| 1.8 | 0.098 | 0.350 | 0.026 | |
| 1.7 | 0.074 | 0.342 | 0.028 | |
| 1.6 | 0.081 | 0.332 | 0.029 | |
| 1.5 | 0.090 | 0.322 | 0.031 | |
| 1.4 | 0.099 | 0.311 | 0.033 | |
| 1.3 | 0.109 | 0.298 | 0.035 | |
| 1.2 | 0.120 | 0.284 | 0.036 | |
| 1.1 | 0.133 | 0.268 | 0.037 | |
| 1.0 | 0.147 | 0.250 | 0.038 | |

CORNER AND EDGE FORCES FOR SIMPLY SUPPORTED RECTANGULAR PLATES UNDER A LOAD IN THE FORM OF A TRIANGULAR PRISM

## Table B3.2.0-3 Simply Supported Rectangular Plate Under Hydrostatic Pressure (Cont'd)

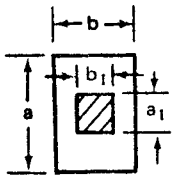


ALL EDGES SUPPORTED.
UNIFORM LOAD OVER
CENTRAL RECTANGULAR
AREA SHOWN SHADED.

| FACTOR FOR MAXIMUM STRESS AT CENTER ($S = S_b$) | | | | | | | | | | | | | | | | | |
|---|---|---|---|---|---|---|---|---|---|---|---|---|---|---|---|---|---|
| $a_1/b$ | a/b = 1 | | | | | | a/b = 1.4 | | | | | | a/b = 2 | | | | | |
| $b_1/b$ | 0 | 0.2 | 0.4 | 0.6 | 0.8 | 1.0 | 0 | 0.2 | 0.4 | 0.8 | 1.2 | 1.4 | 0 | 0.4 | 0.8 | 1.2 | 1.6 | 2.0 |
| 0 | — | 1.82 | 1.38 | 1.12 | 0.93 | 0.76 | — | 2.0 | 1.55 | 1.12 | 0.84 | 0.75 | — | 1.64 | 1.20 | 0.97 | 0.78 | 0.64 |
| 0.2 | 1.82 | 1.28 | 1.08 | 0.90 | 0.76 | 0.63 | 1.78 | 1.43 | 1.23 | 0.95 | 0.74 | 0.64 | 1.73 | 1.31 | 1.03 | 0.84 | 0.68 | 0.57 |
| 0.4 | 1.39 | 1.07 | 0.84 | 0.72 | 0.62 | 0.52 | 1.39 | 1.13 | 1.00 | 0.80 | 0.62 | 0.55 | 1.32 | 1.08 | 0.88 | 8.74 | 0.60 | 0.50 |
| 0.6 | 1.12 | 0.90 | 0.72 | 0.60 | 0.52 | 0.43 | 1.10 | 0.91 | 0.82 | 0.68 | 0.53 | 0.47 | 1.04 | 0.90 | 0.76 | 0.64 | 0.54 | 0.44 |
| 0.8 | 0.92 | 0.76 | 0.62 | 0.51 | 0.42 | 0.36 | 0.90 | 0.76 | 0.68 | 0.57 | 0.45 | 0.40 | 0.87 | 0.76 | 0.63 | 0.54 | 0.44 | 0.38 |
| 1.0 | 0.76 | 0.63 | 0.52 | 0.42 | 0.35 | 0.30 | 0.75 | 0.62 | 0.57 | 0.47 | 0.33 | 0.33 | 0.71 | 0.61 | 0.53 | 0.45 | 0.38 | 0.30 |

NOTE: TOTAL LOAD $W = wa_1b_1$

ALL EDGES SUPPORTED PARTIALLY LOADED RECTANGULAR PLATES

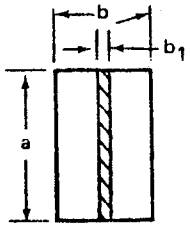


ALL EDGES SUPPORTED.
UNIFORM LOAD ALONG
THE AXIS OF SYMMETRY
PARALLEL TO THE DIMENSION A
($b_1$ VERY SMALL)

| K FACTOR FOR MAXIMUM DEFLECTION | | | | | | | | |
|---|---|---|---|---|---|---|---|---|
| b > a | b/a | 2 | 1.5 | 1.4 | 1.3 | 1.2 | 1.1 | 1.0 |
| L = a | K | 0.108 | 0.099 | 0.096 | 0.092 | 0.087 | 0.081 | 0.074 |
| b < a | a > b | 1.1 | 1.2 | 1.3 | 1.4 | 1.5 | 2.0 | ∞ |
| L = b | K | 0.088 | 0.101 | 0.114 | 0.126 | 0.137 | 0.178 | 0.227 |

NOTE: USE UNIT APPLIED LOAD W IN THIS CASE

ALL EDGES SUPPORTED, PARTIALLY LOADED RECTANGULAR PLATES

Table B3.2.0-3 Simply Supported Rectangular Plate Under Hydrostatic Pressure (Cont'd)

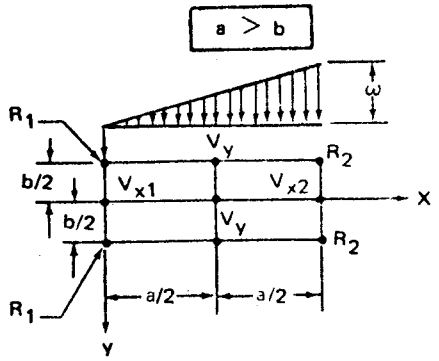


| | K | | | $K_1$ | | |
|---|---|---|---|---|---|---|
| a/b | $V_{x1}$ | $V_{x2}$ | $V_y$ | $R_1$ | $R_2$ | REMARKS |
| ∞ | — | — | 0.250 | — | — | USE L = a FOR $V_{x1}$ $V_{x2}$ USE L = b FOR $V_y$ |
| 5.0 | 0.008 | 0.092 | 0.250 | 0.002 | 0.017 | |
| 4.0 | 0.013 | 0.112 | 0.251 | 0.004 | 0.020 | |
| 3.0 | 0.023 | 0.143 | 0.252 | 0.006 | 0.025 | |
| 2.0 | 0.050 | 0.197 | 0.251 | 0.013 | 0.033 | |
| 1.9 | 0.055 | 0.205 | 0.251 | 0.014 | 0.034 | |
| 1.8 | 0.060 | 0.213 | 0.249 | 0.016 | 0.035 | |
| 1.7 | 0.066 | 0.221 | 0.248 | 0.017 | 0.036 | |
| 1.6 | 0.073 | 0.230 | 0.245 | 0.018 | 0.037 | |
| 1.5 | 0.080 | 0.240 | 0.243 | 0.020 | 0.037 | |
| 1.4 | 0.088 | 0.250 | 0.239 | 0.021 | 0.038 | |
| 1.3 | 0.097 | 0.260 | 0.234 | 0.023 | 0.039 | |
| 1.2 | 0.106 | 0.271 | 0.227 | 0.024 | 0.039 | |
| 1.1 | 0.116 | 0.282 | 0.220 | 0.025 | 0.039 | |
| 1.0 | 0.126 | 0.294 | 0.210 | 0.026 | 0.039 | |

CORNER AND EDGE FORCES FOR SIMPLY SUPPORTED RECTANGULAR PLATES UNDER HYDROSTATIC PRESSURE

## B3.3.0 Thin Flat Plates with Large Deflection

### B3.3.1 Rectangular Plates

Reaction to normal loading is by both bending and direct axial tension which accompanies stretching of the sheet middle plane. Such plates are stiffer, stresses for a given load are less, and stresses for a given deflection are greater than the ordinary theory indicates.

Two support conditions are considered:

A. Simply Supported Plates - Maximum moments and therefore maximum combined stresses and deflections occur at strip midpoints. Maximum plate deflection occurs at plate center. Due to the in-plane tension forces, bending moments are less than for an equivalent plate without lateral restraint.

B. Plates with Fixed Edges - Maximum deflection occurs at strip midpoints and plate center, but maximum stresses occur at the edges where bending moments are greatest. The maximum combined stress occurs at the midpoint of the long side.

Owing to the clamping of the edges, the direct tensile stress decreases considerably, whereas the maximum bending stress increases several times so that finally the maximum total stress becomes larger than in the case of simple support.

Thin plates in aerospace vehicle structures usually fall in between these two cases, and it is recommended that in most solutions an average of the two be taken. Figures B3.3.1-1 through B3.3.1-8 provide stress and deflection data for the two end conditions which are approximately correct for $a>3b$. For $a<3b$ the results are conservative.

Example: An .080 7075-T6 bulkhead web measuring 10 in x 32 in, and is subjected to a pressure of 14 psi. Assume edges are simply supported. Elastic Modulus is $10.3 \times 10^6$ psi.

Find $\frac{1000t}{b} = \frac{1000 \times .080}{10} = 8$

Calculate $\frac{10^7 w}{E} = \frac{14 \times 10^7}{10.3 \times 10^6} = 13.59$

To find direct tension stress, $f_t$, for the simply supported condition, enter Figure B3.3.1-1 with $\frac{10^7 w}{E} = 13.59$. Read up to $\frac{1000t}{b} = 8$. Then across to find $\frac{10^4 f_t}{E} = 10.5$. The direct tension stress is $f_t = \frac{10.5\ E}{10^4} = \frac{10.5 \times 10.3 \times 10^6}{10^4} = 10815$ psi

Repeat this procedure for $f_b$, $f_{max}$, and $Y_{max}$.

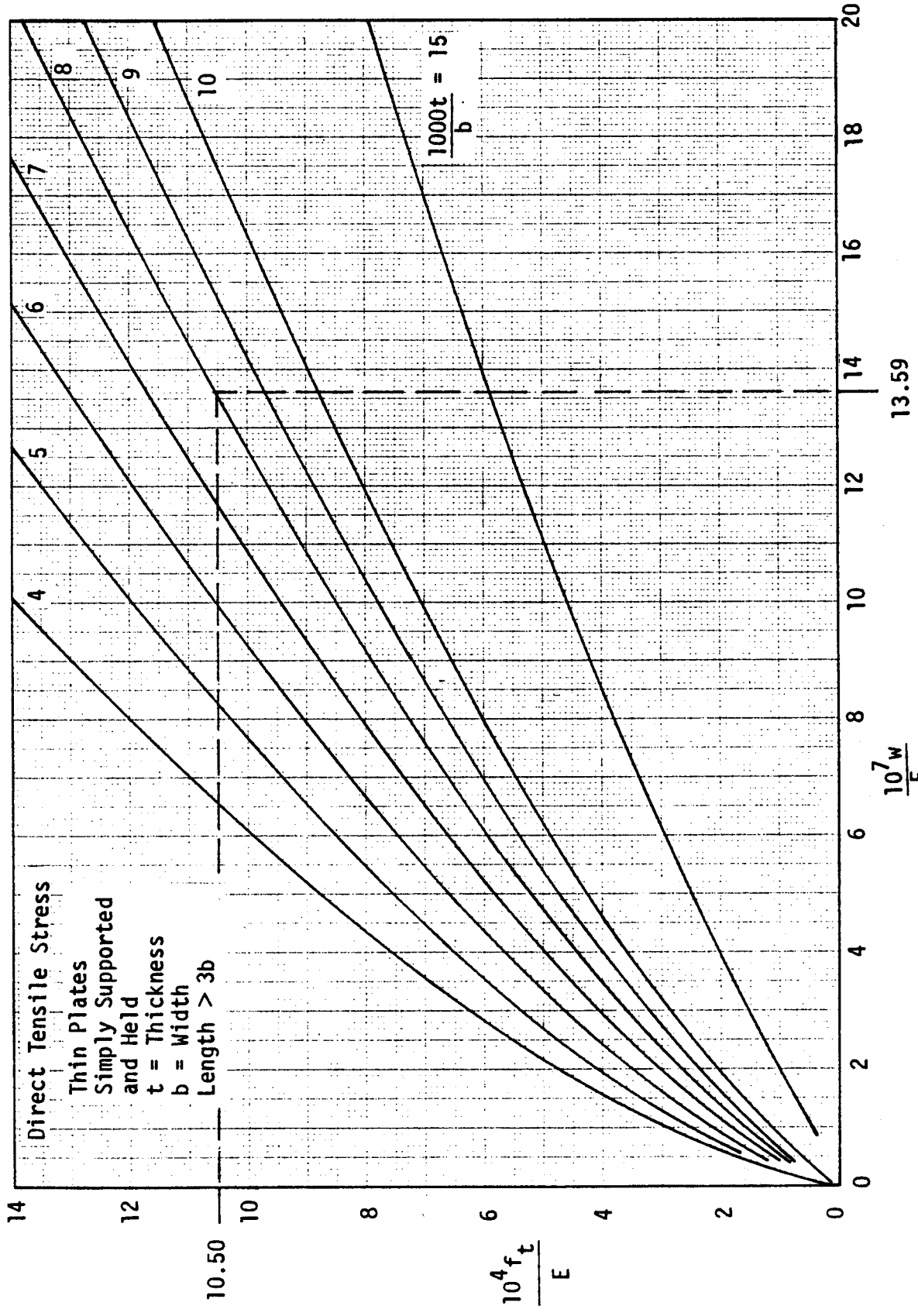


Figure B3.3.1-1 Direct Tension Stress for Thin Simply Supported Plate

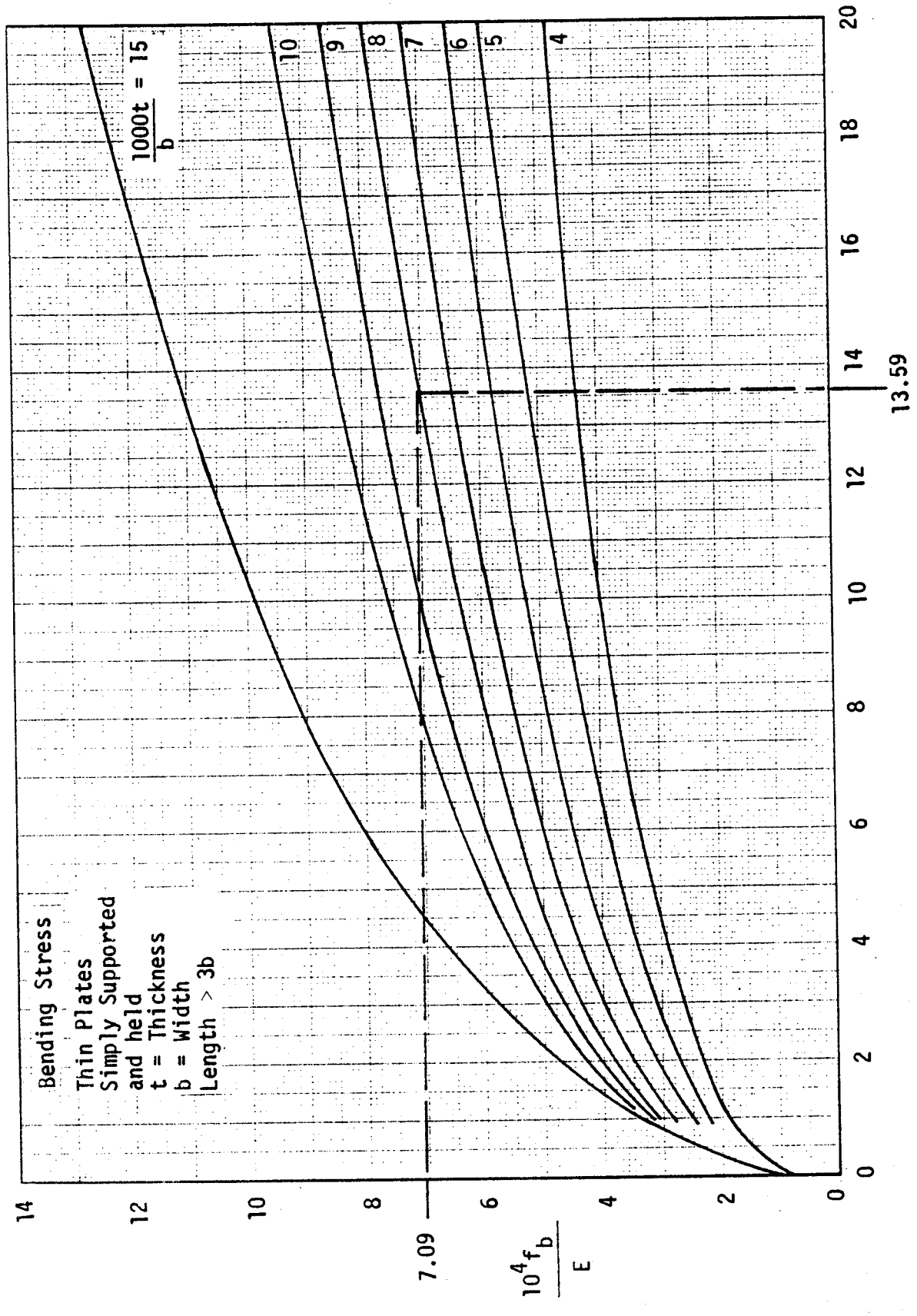


Figure B3.3.1-2 Bending Stress for Thin Simply Supported Plate

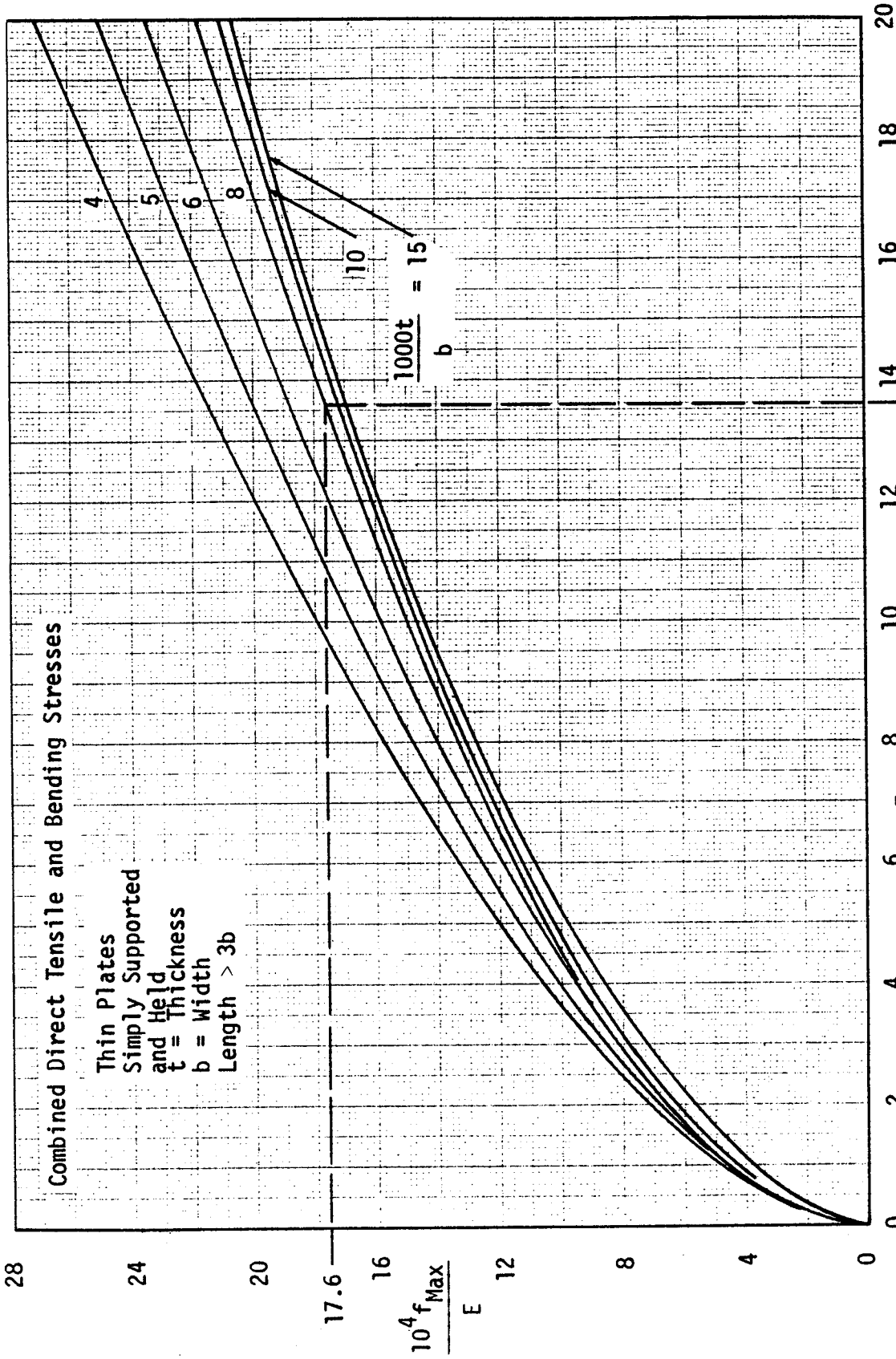


Figure B3.3.1-3 Combined Stress for Thin Simply Supported Plate

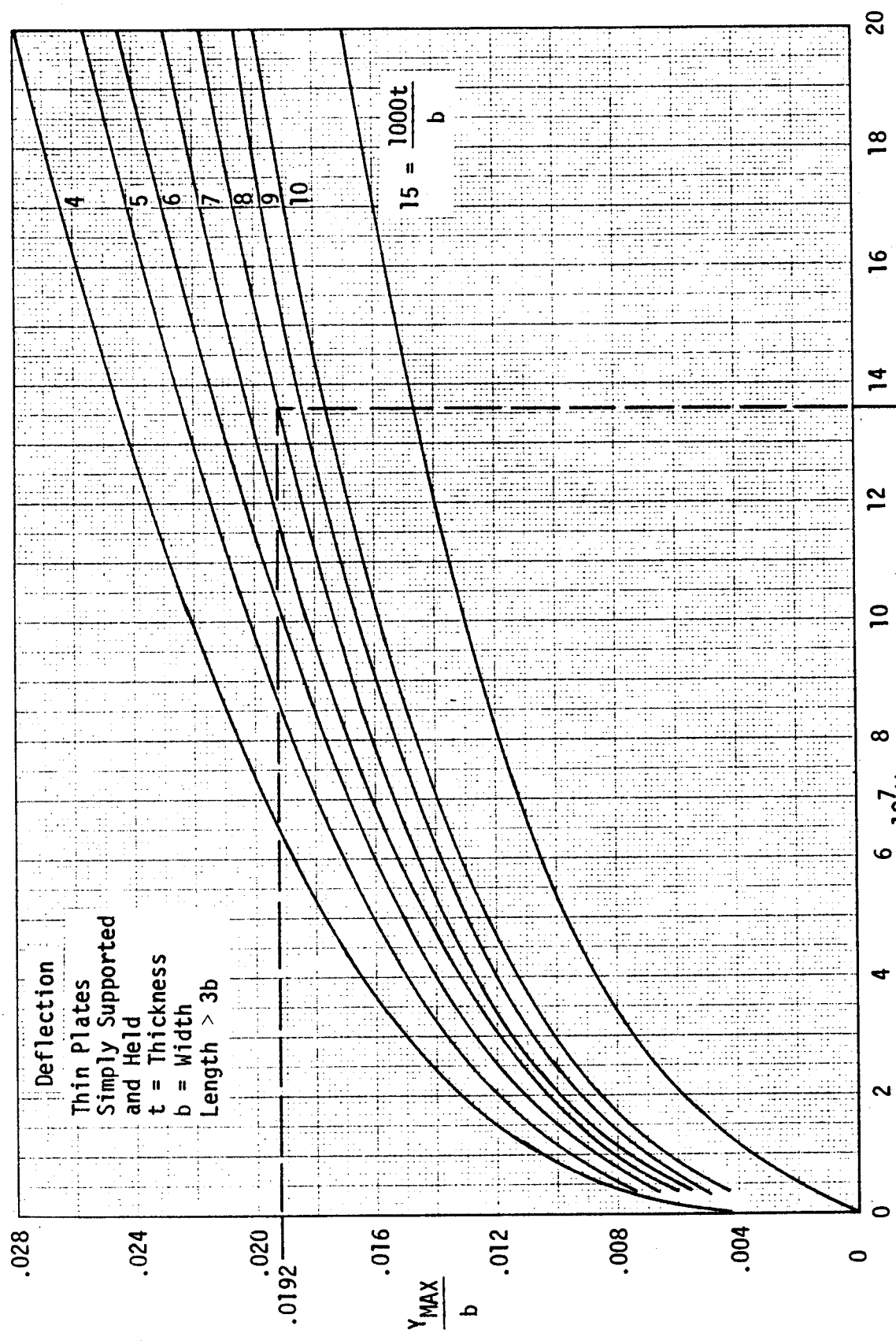


Figure B3.3.1-4 Deflection for Thin Simply Supported Plate

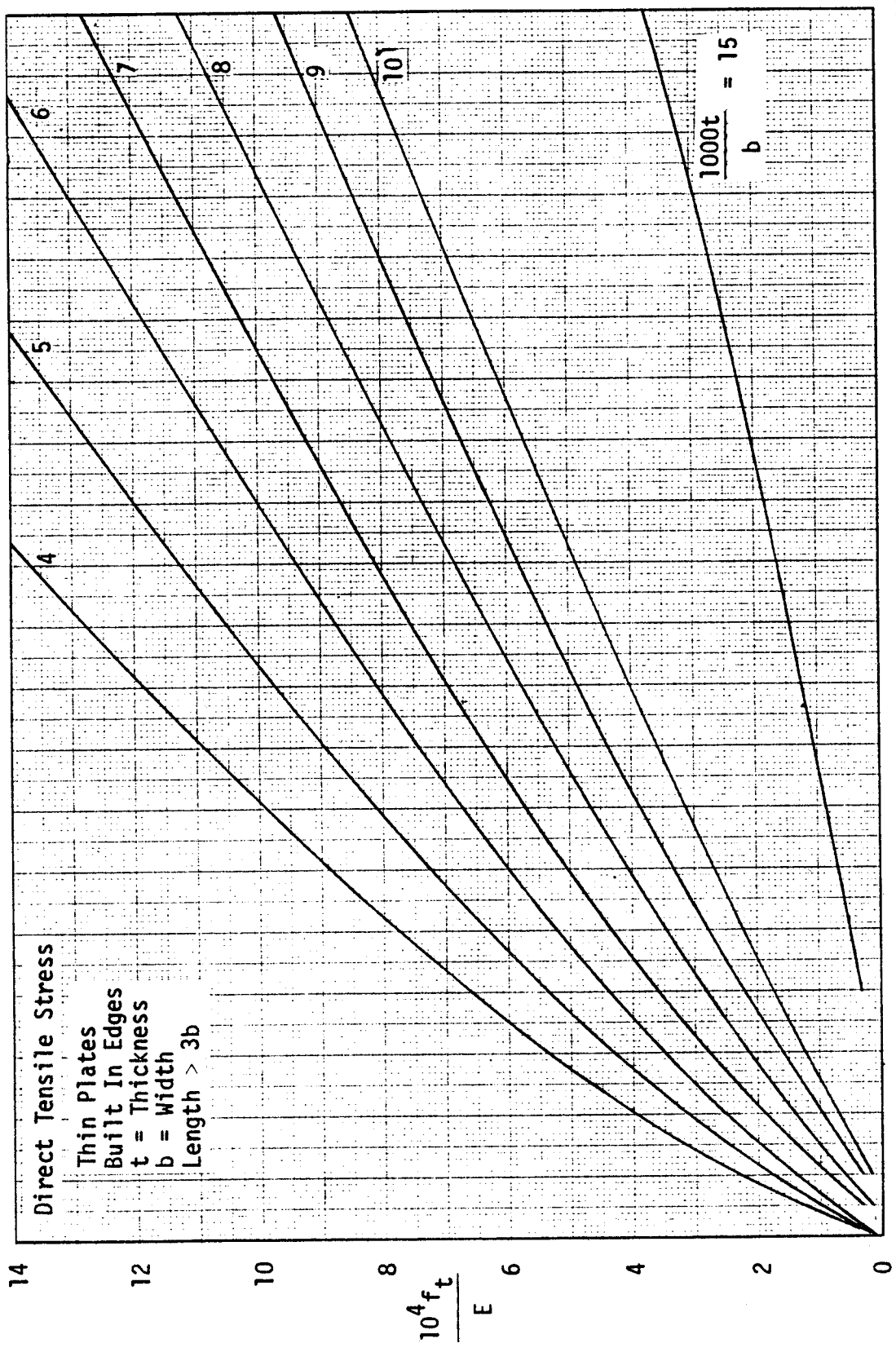


Figure B3.3.1-5 Direct Tension Stress for Thin Fixed Edge Plate

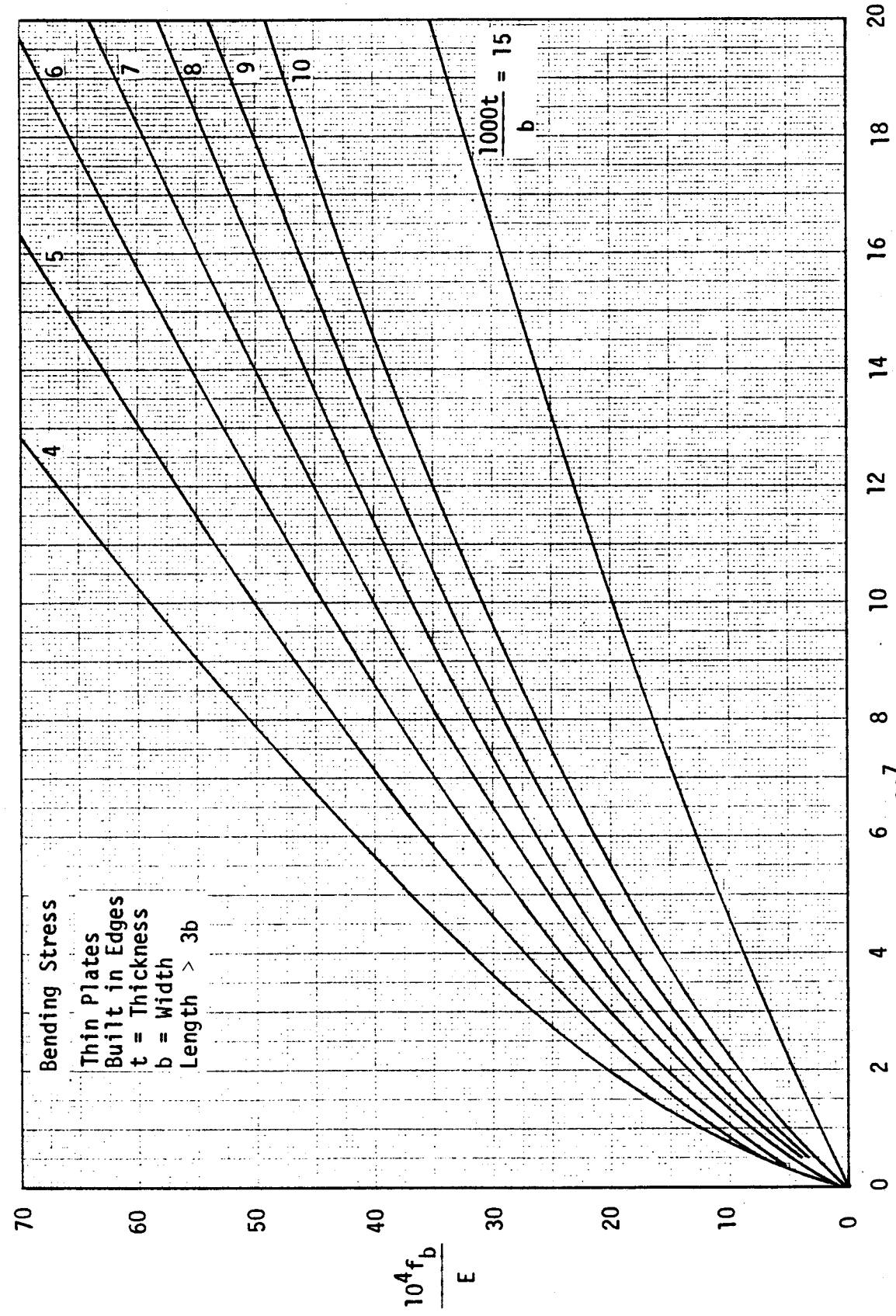


Figure B3.3.1-6 Bending Stress for Thin Fixed Edge Plate

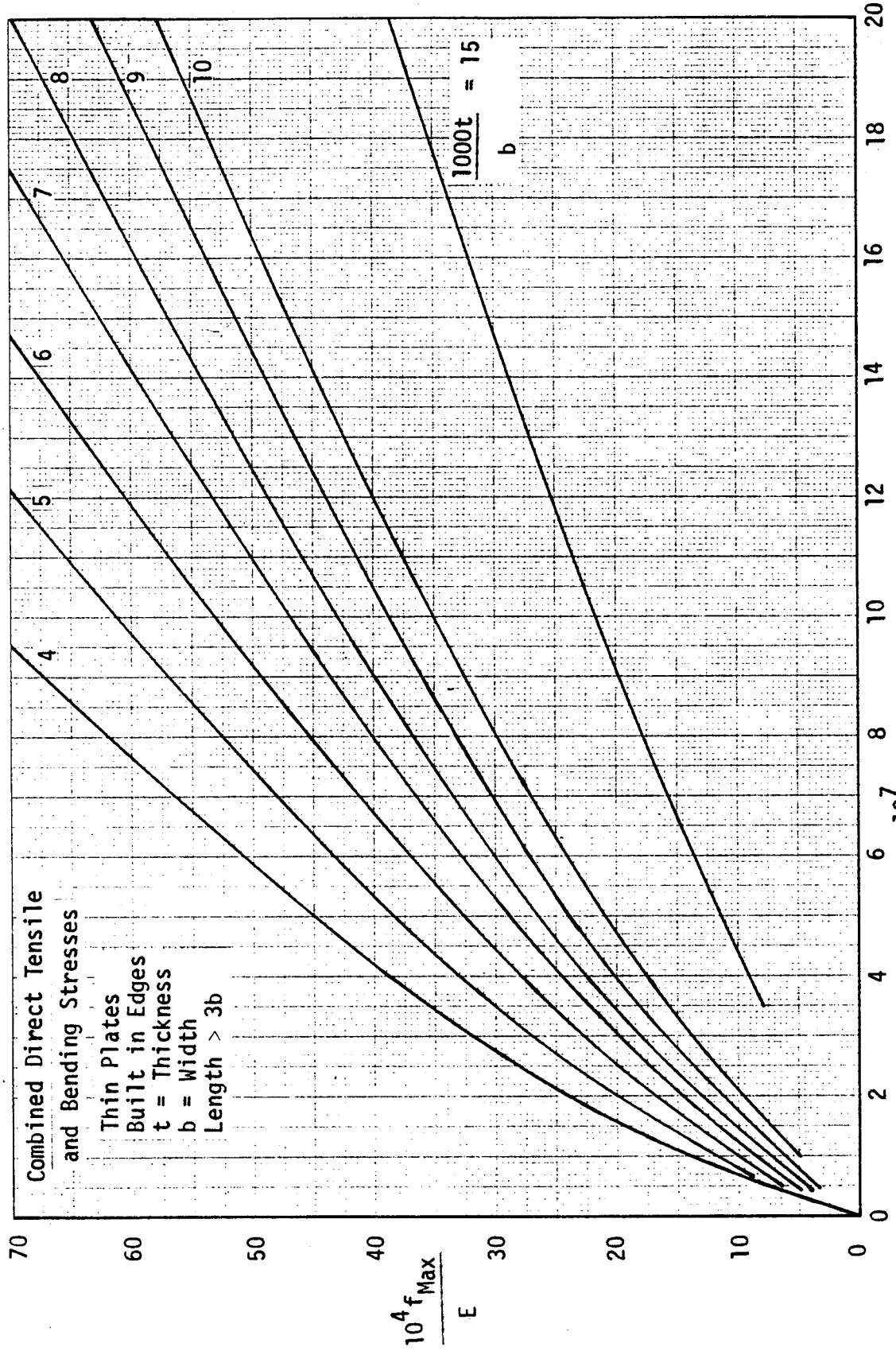


Figure B3.3.1-7 Combined Stress for Thin Fixed Edge Plate

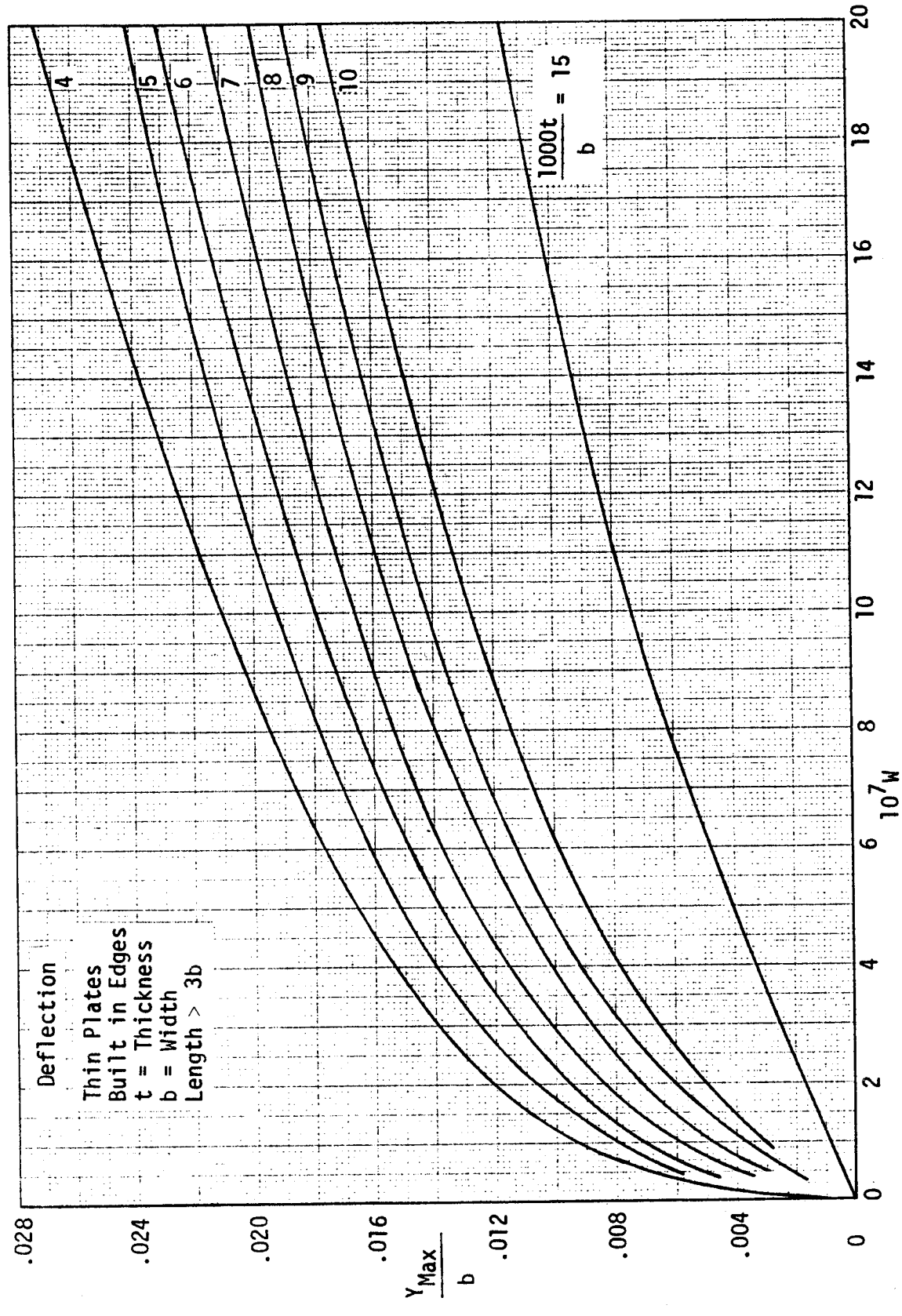


Figure B3.3.1-8 Deflection for Thin Fixed Edge Plate

## B3.3.2 Circular Plates with Large Deflections Under Uniform Loading

Figure B3.3.2-1 shows a circular plate with a clamped edge condition that prevents edge rotation and edge radial displacement. This latter condition requires a radial tensile force at the edge that causes radial membrane stresses.

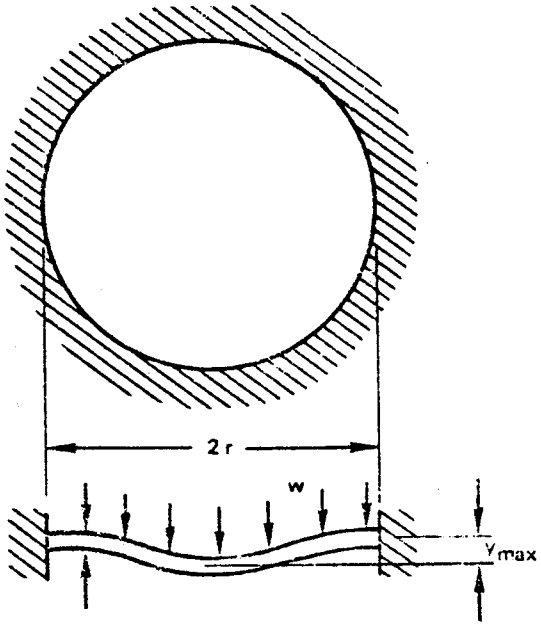


Figure B3.3.2-1 Clamped Circular Plate Geometry and Loading

Plate deflection is not a linear function of the load. It may be determined from Figure B3.3.2-2 for given geometry and load condition.

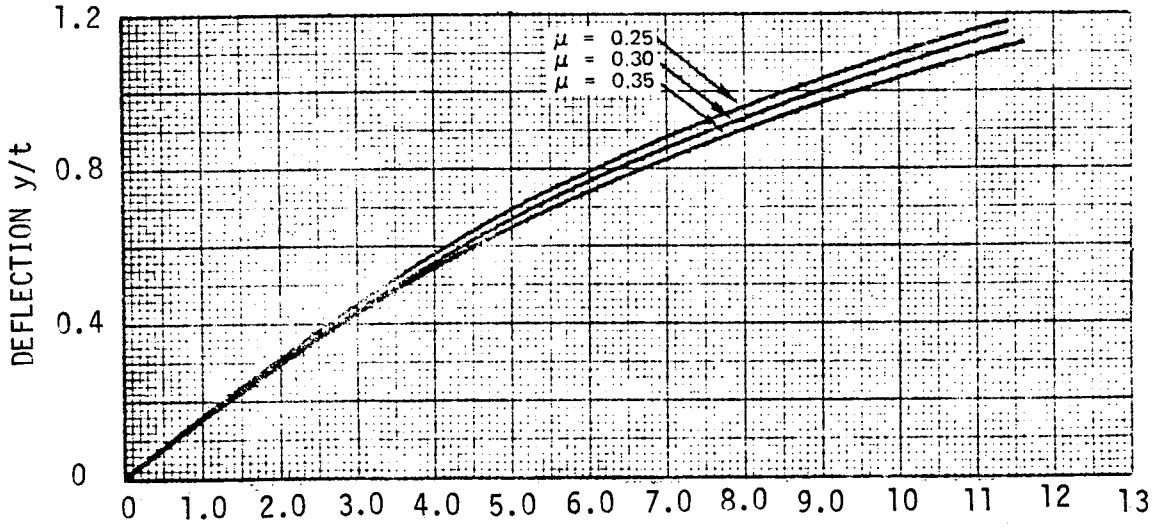


Figure B3.3.2-2 Large Deflections of Clamped Circular Plate Under Uniform Load

Bending stress and membrane stresses at the edge and center of the plate may be determined from Figure B3.3.2-3 based on the ratio of deflection-to-plate thickness as determined from Figure B3.3.2-2.

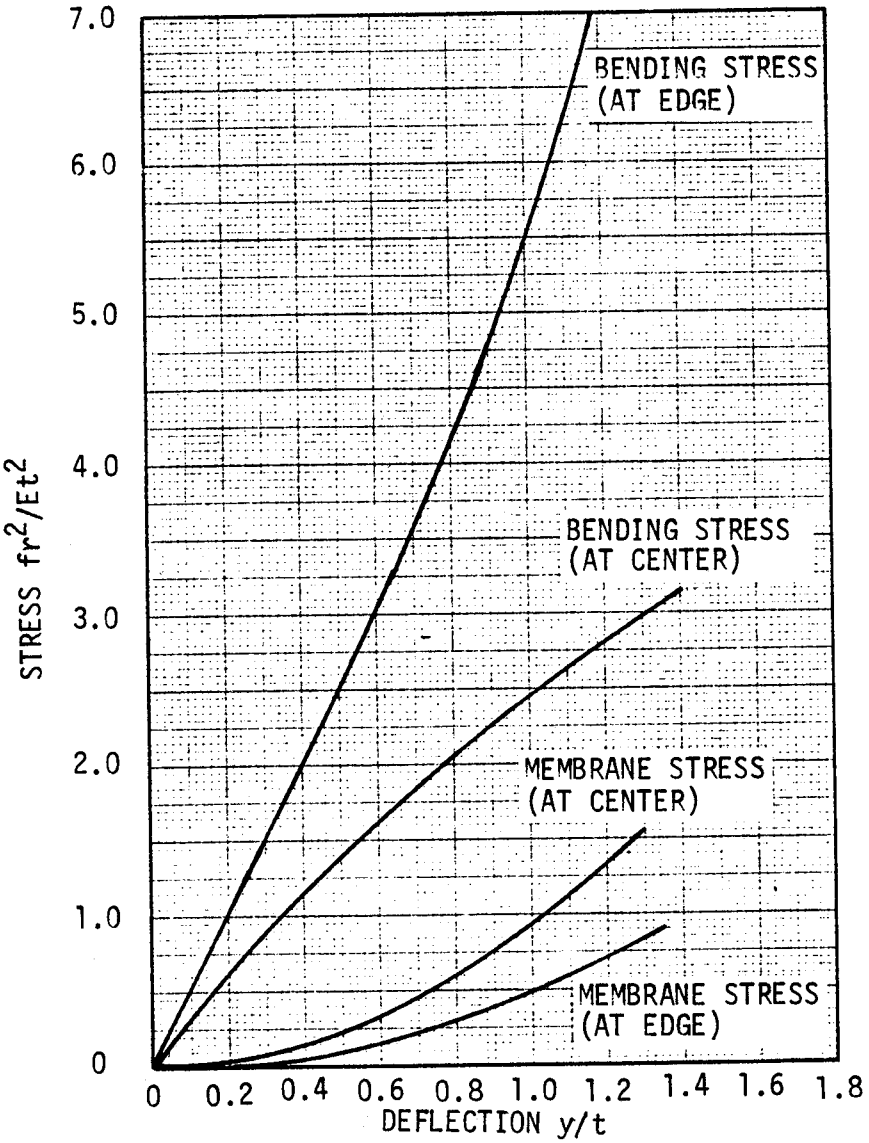


Figure B3.3.2-3 Bending and Membrane Stresses in Clamped Circular Plate Under Uniform Load

Example:

A clamped circular plate with a radius = 4.5

$t = .080$, $w = 12$ PSI, $E = 10.3 \times 10^6$, $\mu = .3$

From Figure B3.3.2-2, $wr^4/E\,t^4 = 12 \times 4.5^4/10.3 \times 10^6 \times .080^4 = 11.664$, $\frac{y}{t} = 1.16$ and $y = .093$.

From Figure B3.3.2-3: (Using $\frac{y}{t} = 1.16$)

Membrane stress @ edge: $fr^2/Et^2 = .725$, $f = 2360$ PSI

Membrane stress @ center: $fr^2/Et^2 = 1.25$, $f = 4069$ PSI

Bending stress @ edge: $f_{b_E} r^2/Et^2 = 6.75$, $f_{b_E} = 21973$ PSI

Bending stress @ center: $f_{b_c} r^2/Et^2 = 2.70$, $f_{b_c} = 8789$ PSI

Max stress @ edge = $f_b + f_t = 24333$ PSI

## B3.4.0 Very Thin Plates - Without Flexural Stiffness

### B3.4.1 Circular Thin Plates - Diaphragms

In the case of very thin plates, the deflection, 'y', may become very large in comparison to 't'. In such cases the resistance of the plate to bending can be neglected, and it can be treated as a flexible membrane.

Formulas for membrane plates:

At center: $(r = 0)$ $f_t = 0.423 \sqrt[3]{\frac{Ew^2r^2}{t^2}}$

At edge: $f_t = 0.328 \sqrt[3]{\frac{Ew^2r^2}{t^2}}$

Max Defl.: $y = 0.662r \sqrt[3]{\frac{wr}{Et}}$

### B3.4.2 Rectangular Thin Plates - Diaphragms

The tension stress in a long membrane of width b and thickness t subjected to uniform loading w and held along the long sides is:

$$f_t = \left[\frac{w^2 E B^2}{24(1-\mu^2)t^2}\right]^{1/3} = 7700 \left[\frac{\left(\sqrt{\frac{10E}{10^4}}\right)w}{\frac{1000t}{b}}\right]^{2/3}$$

The maximum deflection (at the center) is

$$\frac{y}{b} = \frac{wb}{8f_t t} = 1/8\left[\frac{24(1-\nu^2)wb}{E\,t}\right]^{1/3} = .0162\left[\frac{\left(\frac{10^7}{E}\right)w}{\frac{1000t}{b}}\right]^{1/3}$$

Graphs of $f_t$ versus $(\sqrt{10E}\,/\,10^4)\,w$ and $y_{MAX/b}$ versus $10^7 w\,/\,E$ for various values of the parameter 1000t/b are presented in Figures B3.4.2-1 and B 3.4.2-2.

Results are approximately correct for plates held on all four sides if $a > 5b$.

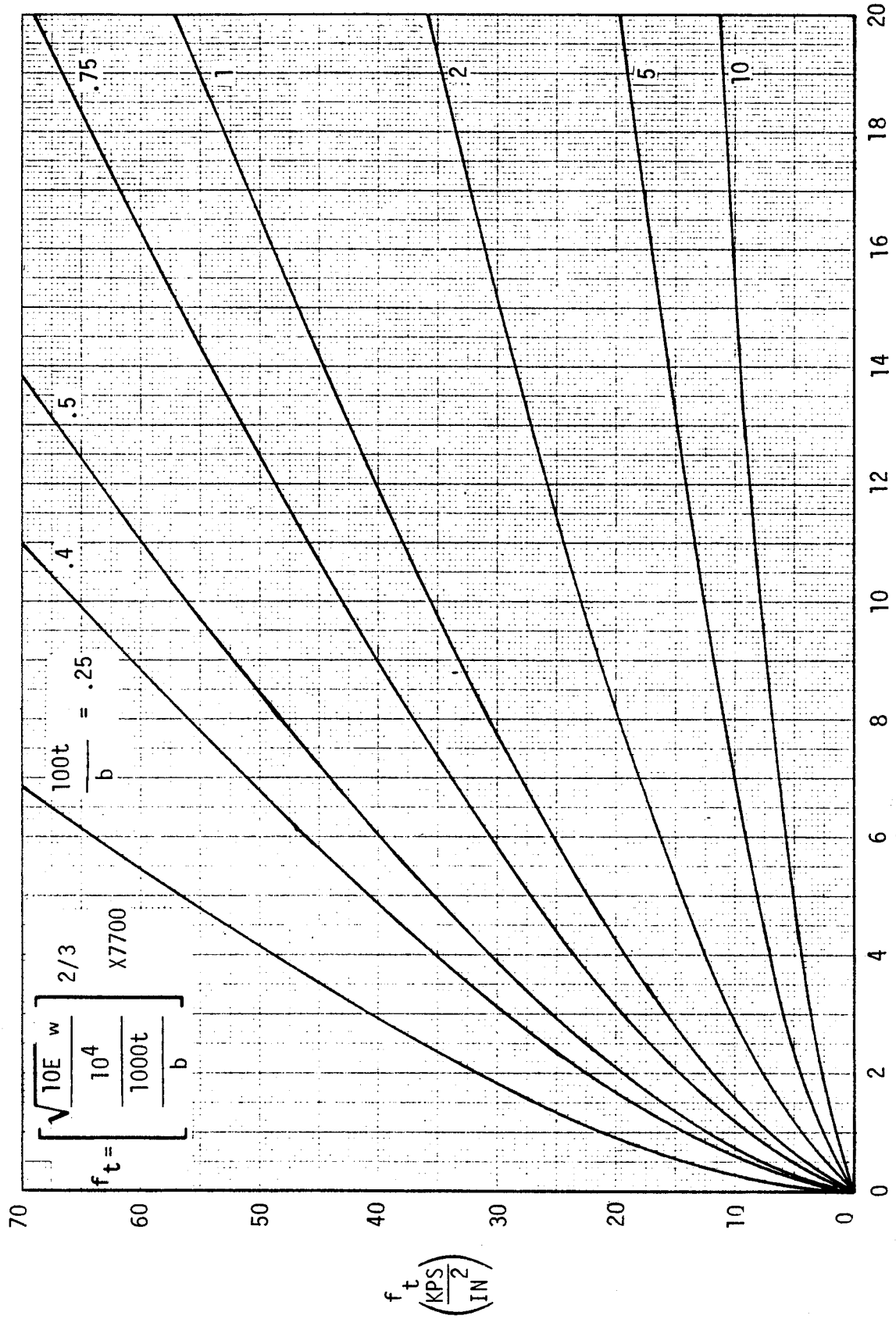


Figure B3.4.2-1 Stress in Membrane Plates Under Uniform Load

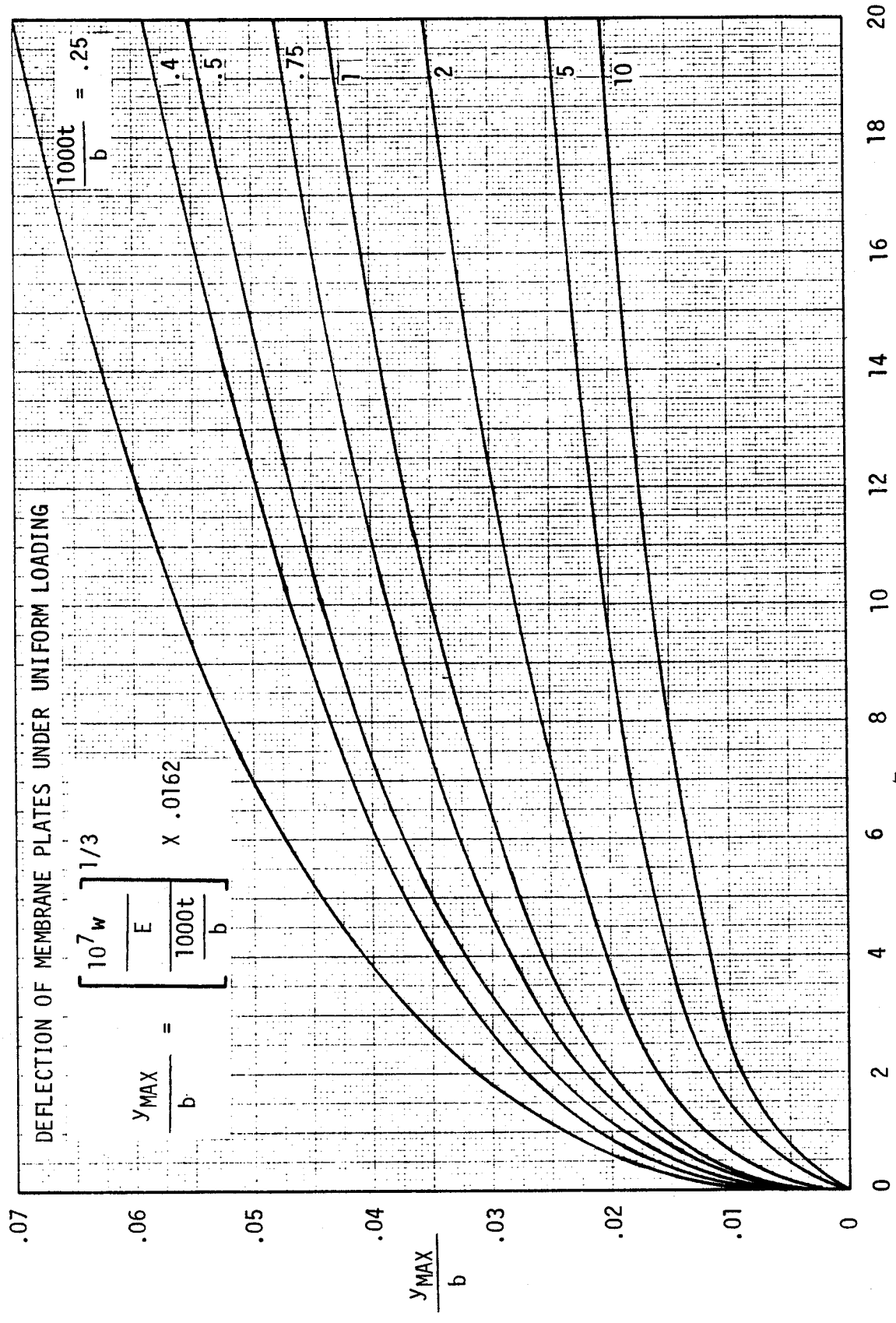


Figure B3.4.2-2 Deflection of Membrane Plates Under Uniform Load

## B3.5.0 Thick Rectangular Plates

For simply supported long plates of width b and thickness t subjected to uniform loading w, the maximum bending stress at the center is:

$$f_b = \frac{3\,w\,b^2}{4t^2} = \frac{750000\,w}{\left(\frac{1000t}{b}\right)^3}$$

and the maximum deflection y (at the center) is:

$$\frac{y}{b} = \frac{5(1-\mu^2)\,w\,b^3}{32\,E\,t^3} = \frac{14.2\,\frac{10^7\,w}{E}}{\left(\frac{1000t}{b}\right)^3}$$

Graphs of $f_b$ versus w, and $y_{MAX}$ / b versus $10^7$ w / E are presented in Figures B3.5.0-1 and B3.5.0-2 respectively.

For plates with built-in edges use the following percentages of stress values obtained for the plate when simply-supported: 2/3 of $f_b$ (Maximum at edge of plate), and 1/5 of y.

Results are approximately correct for plates supported on all four sides if a>3b. For a<3b the results are conservative.

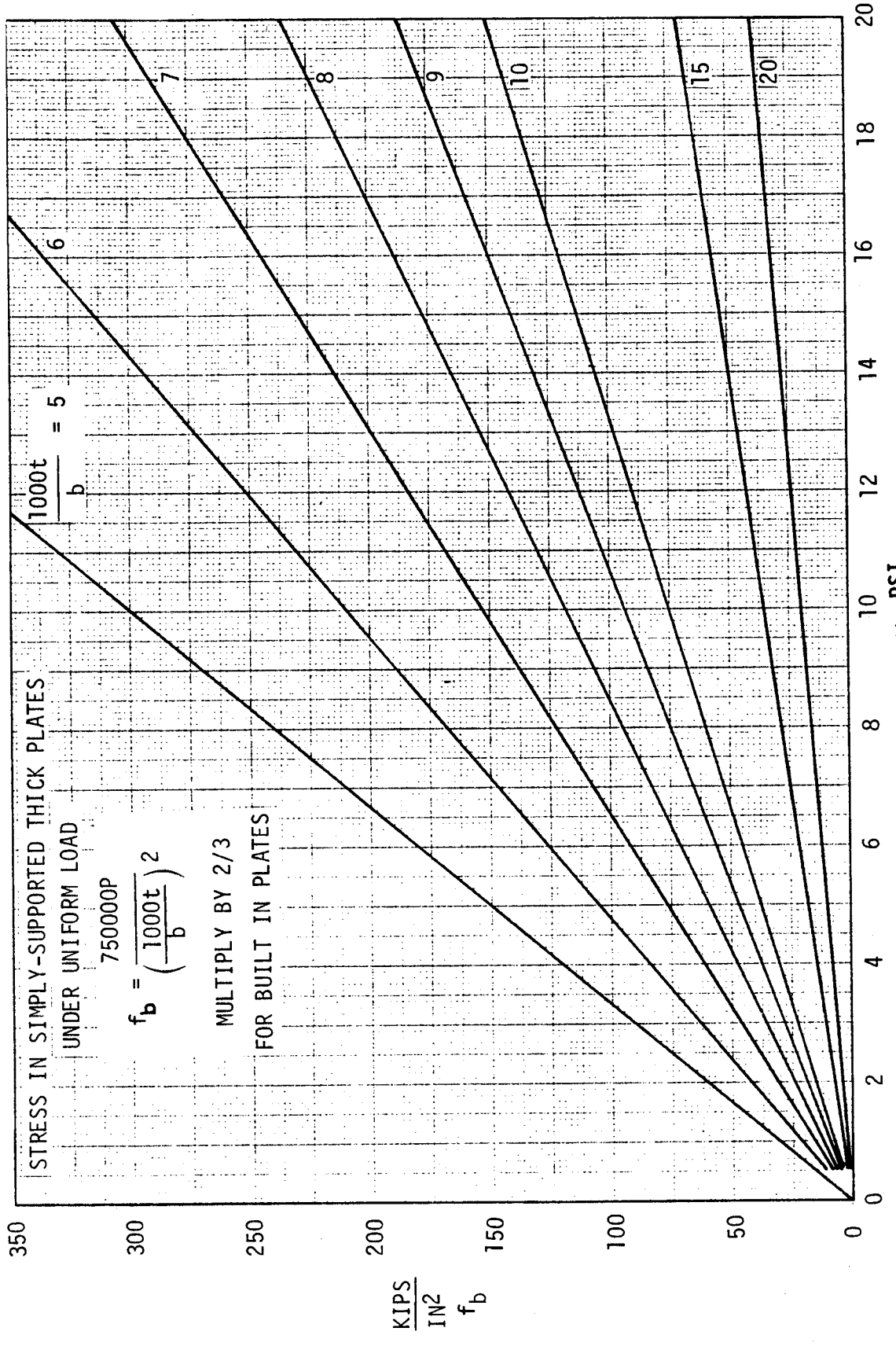


B3.5.0-1 Stress in Simply Supported Thick Plates Under Uniform Load

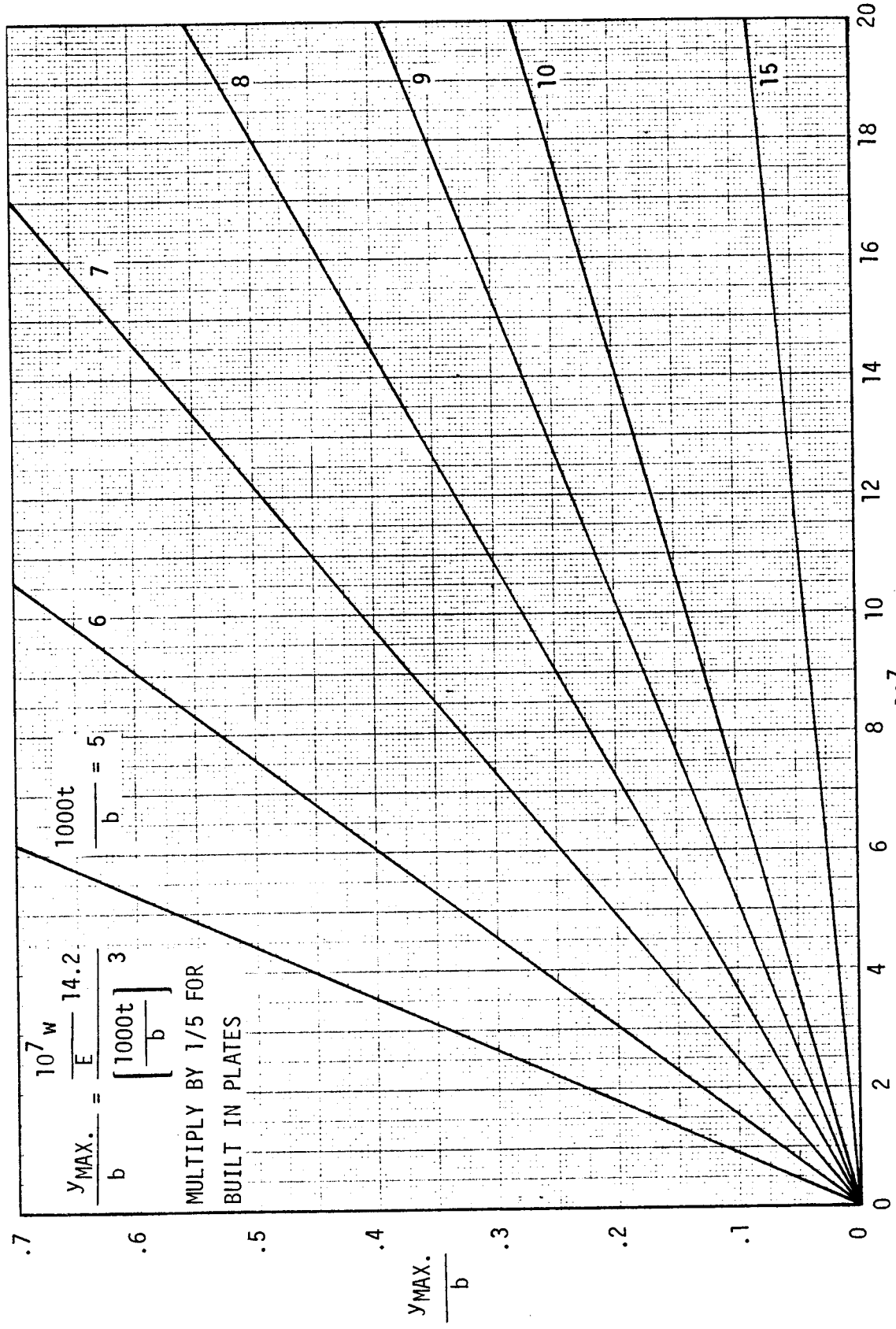


Figure B3.5.0-2 Deflection of Simply Supported Thick Plates Under Uniform Load

## B3.6.0 Stiffened Flat Plates Loaded Normal to the Surfaces

The commonest element of structure is the rectangular stiffened plate. Rectangles of plating are more frequently stiffened in only one direction, the direction being determined by the proportions of the rectangle, the available landing for stiffener ends, or by the direction of the load. When the rectangle of plating has to resist a uniform bending load instead of, or in addition to a plane load, cross-stiffening may give the most efficient design.

Cross stiffening is a system composed of two sets of stiffeners, each set being parallel to one pair of sides of the rectangle, and intersecting each other at right angles. Each set is a repeating system; i.e., the stiffeners in one set are all alike, but may differ from the other set. Also, the spacing of the two sets may be different.

Cross stiffening, by changing the panels of plating encompassed by the stiffeners from very long rectangles to square, or nearly square, panels permits the optimization of the panel thickness and gives lightest design.

The following are various types of stiffening

A. Cross-stiffening. The middle stiffener of either or both sets may be stiffer than the other stiffeners of the set.

B. One set of repeating stiffeners, and a single central stiffener in the other direction. The middle stiffener of the repeating set may be stiffer than the others as in A above.

C. One set of repeating stiffeners only.

D. Plating without any stiffeners.

Fixity and support is defined as follows

(1) All four edges supported.

(2) Short edges fixed, long edges supported.

(3) Short edges supported, long edges fixed.

(4) All four edges fixed.

B3.6.1 Nomenclature

p = uniform distributed load, PSI

a = length of panel, in.

b = width of panel, in.

$S_a(S_b)$ = spacing of long (short) stiffeners

$I_{na}(I_{mb})$ = moment of inertia, including effective width of plating of long (short) repeating stiffeners (as distinguished from central stiffener, which may be different).

$I_{pa}(I_{pb})$ = moment of inertia of effective width of plating only, working with long (short) repeating stiffeners.

$I_a(I_b)$ = moment of inertia, including effective width of plating, of central long (short) stiffener

$A_a(A_b)$ = web area of central long (short) stiffener

$r_a(r_b)$ = distance to centroid of central long (short) stiffener including effective width of skin. (NOTE: $V_a(V_b)$ may be from either skin or free flange.)

$i_a(i_b)$ = unit stiffness; i.e., the moment of inertia of the stiffening per unit width.

$\eta$ = torsion coefficient

$\rho$ = virtual side ratio

B3.6.2 Formulas for cross-stiffened plates

$$i_a = \frac{I_{na}}{S_a} + 2\left(\frac{I_a - I_{na}}{b}\right) \text{ or } i_b = \frac{I_{nb}}{S_b} + 2\left(\frac{I_b - I_{nb}}{a}\right)$$

if the central stiffener is identical to the repeating stiffeners, then:

$i_a = \frac{I_{na}}{S_a}$ or $i_b = \frac{I_{nb}}{S_b}$, and if there are no repeating stiffeners, then: $i_a = 2\frac{I_a}{b}$ or $i_b = 2\frac{I_b}{a}$

$$\eta = .124\sqrt{\frac{I_{pb}^2\, b}{I_a\, I_{nb}\, S_b}} \qquad \rho = \frac{a}{b}\sqrt[4]{\frac{i_b}{i_a}}$$

B3.6.3 Design Curves

Figure B3.6.3-1: "Deflection at Center". The deflection at the center of the rectangle may be treated as maximum.

Figures B3.6.3-2, and B3.6.3-3: "Field Bending Stress in Plating in Long (Short) Direction". The curves refer to the center of the plate as the location of maximum field bending stress.

Figures B3.6.3-4, and B3.6.3-5: "Field Bending Stress in Free Flanges in Long (Short) Direction". Since bending stress in a free flange of a stiffener is mono-axial, while bending stress in the plating is bi-axial, the bending stress for the two cases differ. Above comment applicable to Figure B3.6.3-6.

Figure B3.6.3-7: "Support Bending Stress in Plating". These curves give the bending stress at the centers of edges where fixity exists. For practical purposes the stress at the center of such an edge may be treated as the maximum along that edge.

Figures B3.6.3-8, and B3.6.3-9: "Shear Stress in Long (Short) Webs". The curves give the average vertical shear stress in the web of the long (short) central stiffener at its ends. This is the practical maximum, unless the central stiffener has a much heavier web than the others. In this case, the total shear load in the central web should be obtained from the curves by omitting to divide by the web area. The shear load in the adjacent web can be obtained by assuming a sine distribution along the edge. Dividing this by the web area of the repeating stiffener may give a higher stress than that obtained for the central web.

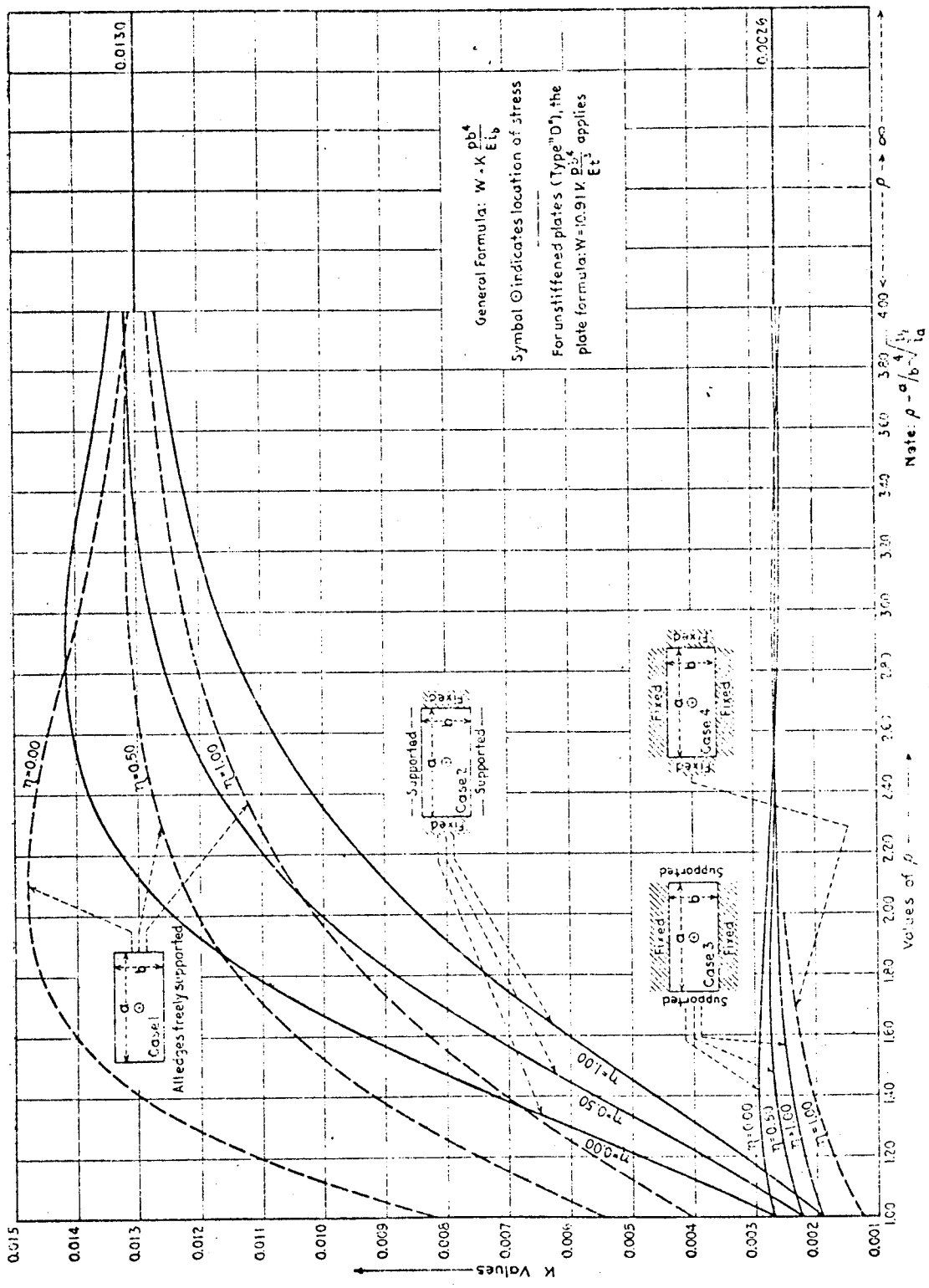


B3.6.3-1 Deflection at Center

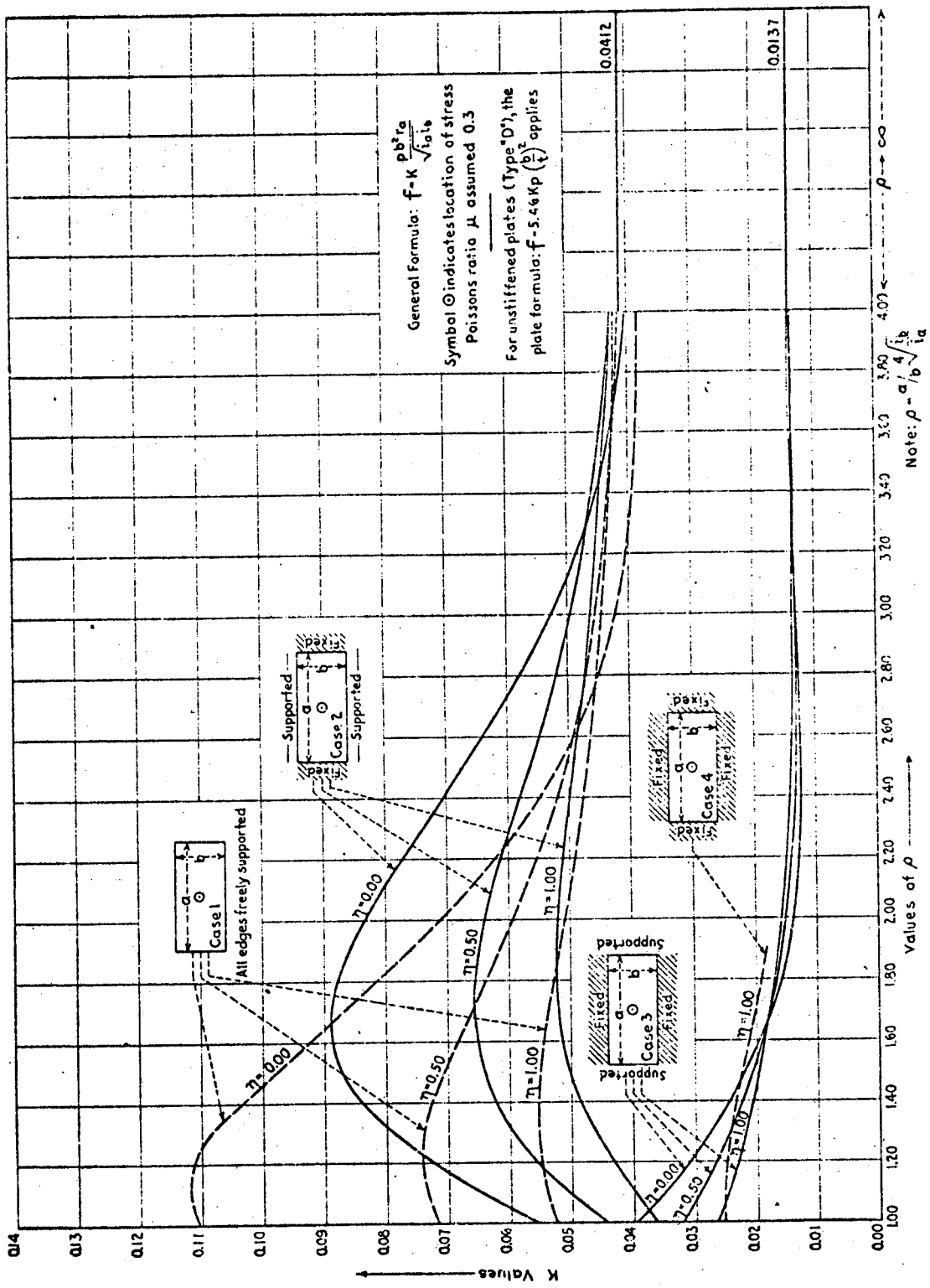


Figure B3.6.3-2 Field Bending Stress in Plating in Long Direction

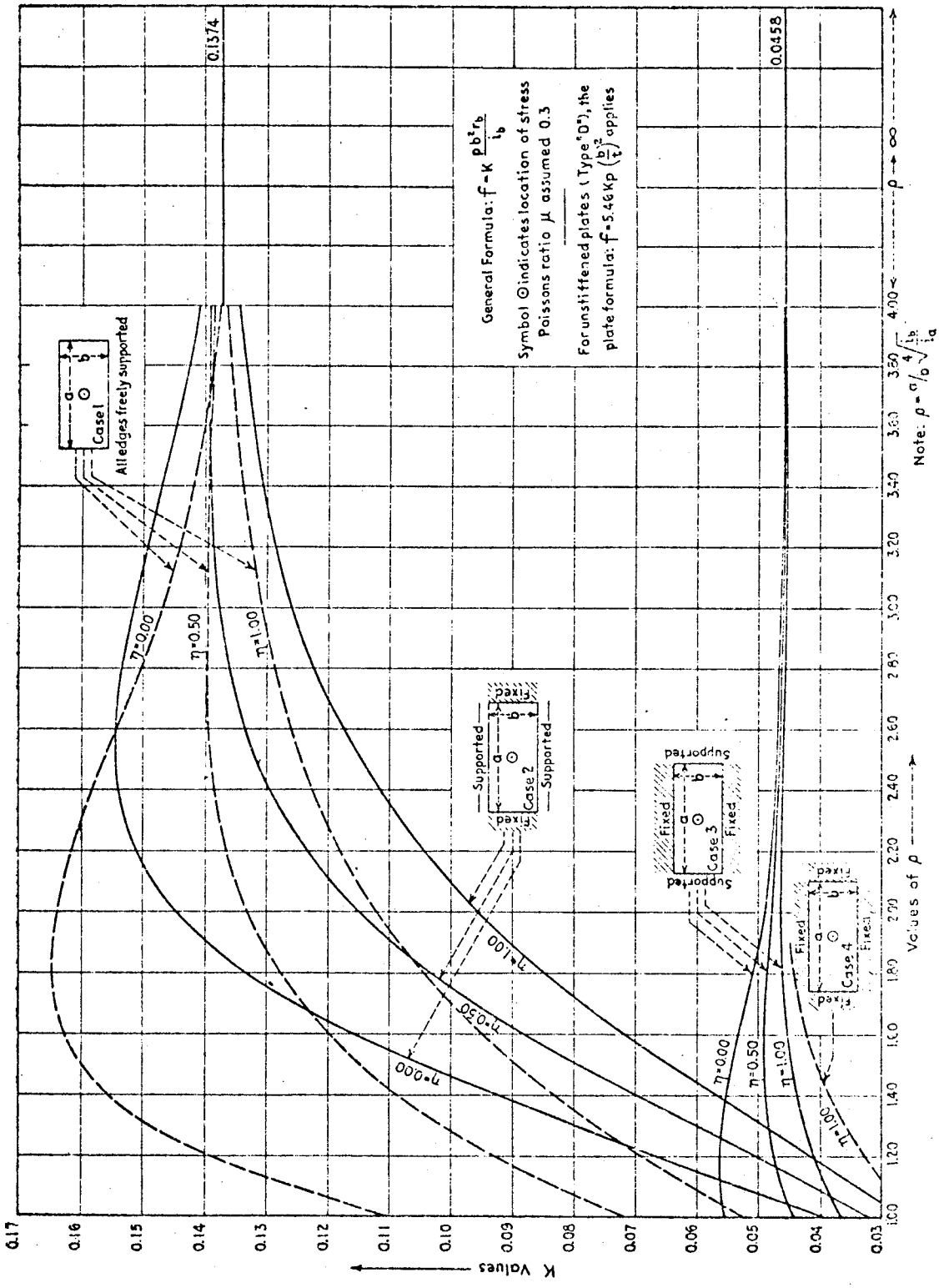


Figure B3.6.3-3 Field Bending Stress in Plating in Short Direction

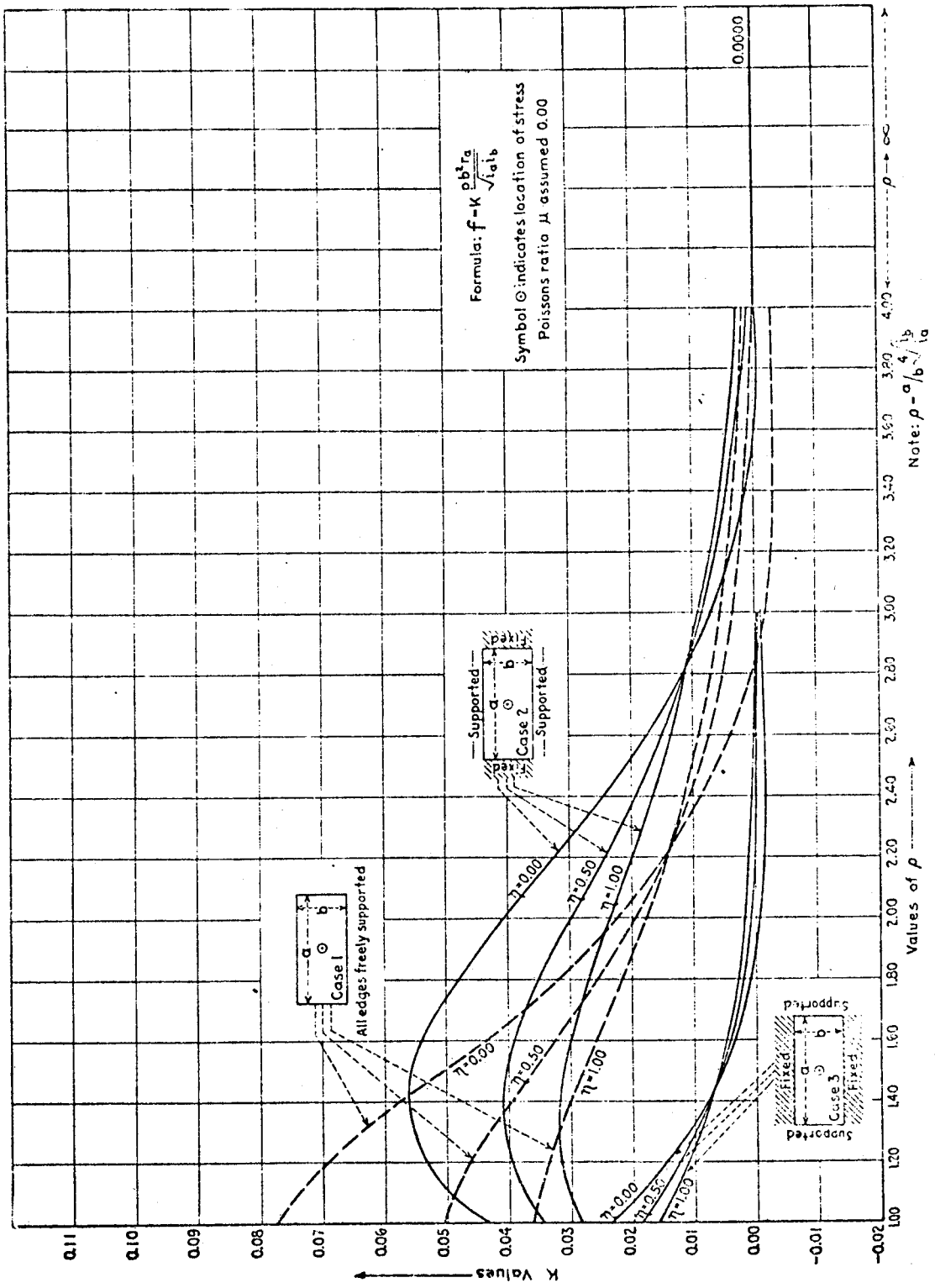


Figure B3.6.3-4 Field Bending Stress in Free Flanges in Long Direction

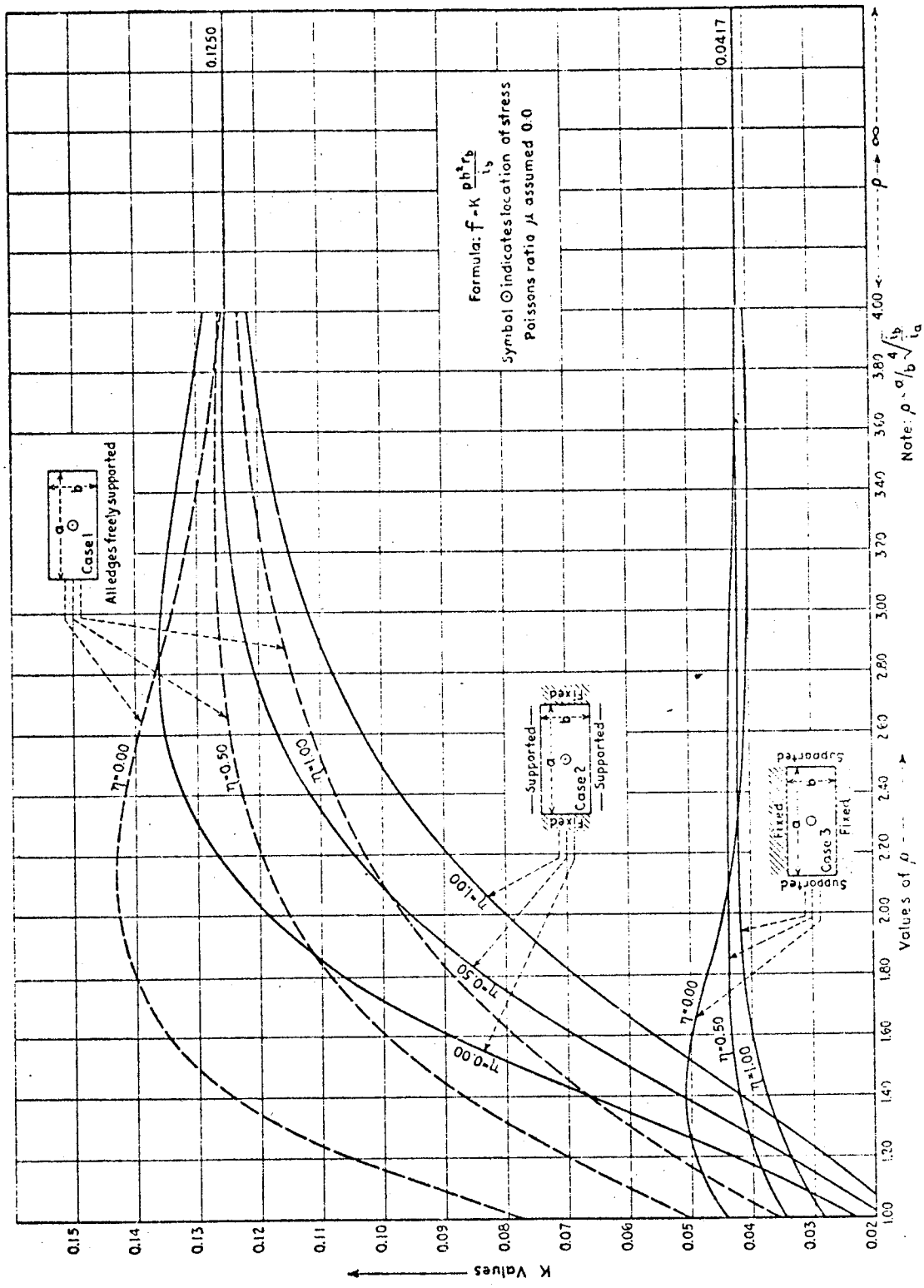


Figure B3.6.3-5 Field Bending Stress in Free Flanges in Short Direction

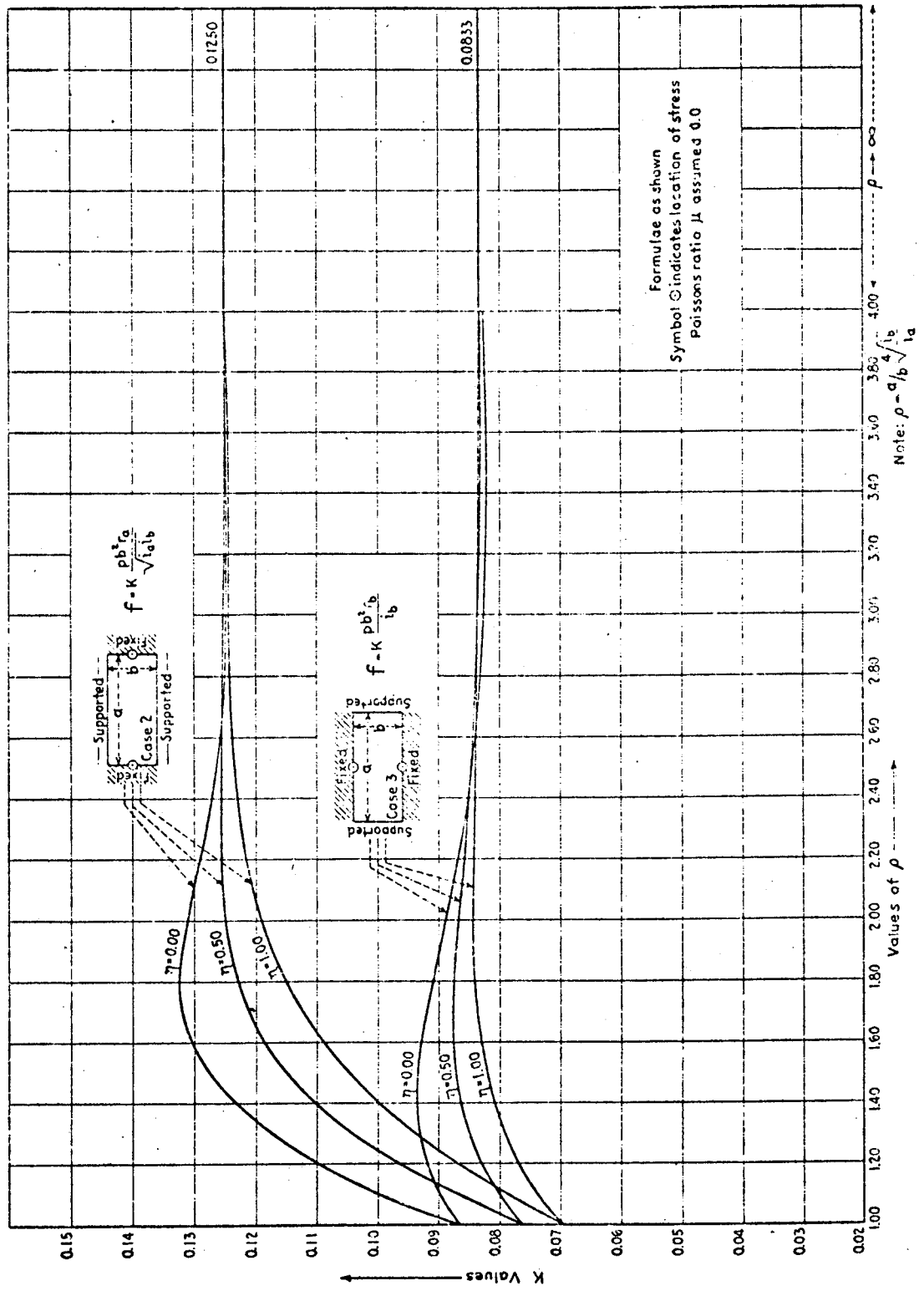


Figure B3.6.3-6 Support Bending Stress in Free Flanges

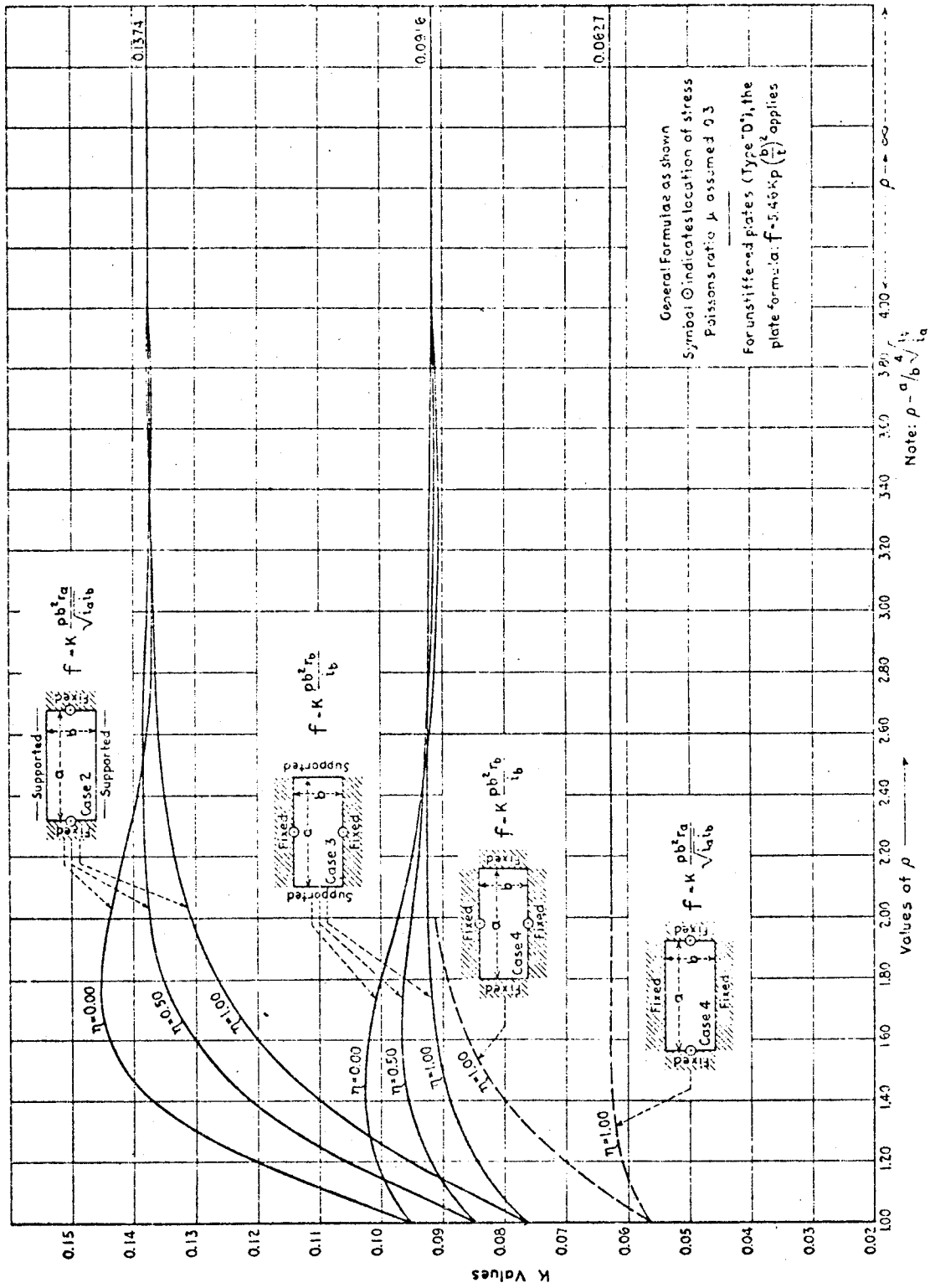


Figure B3.6.3-7 Support Bending Stress in Plating

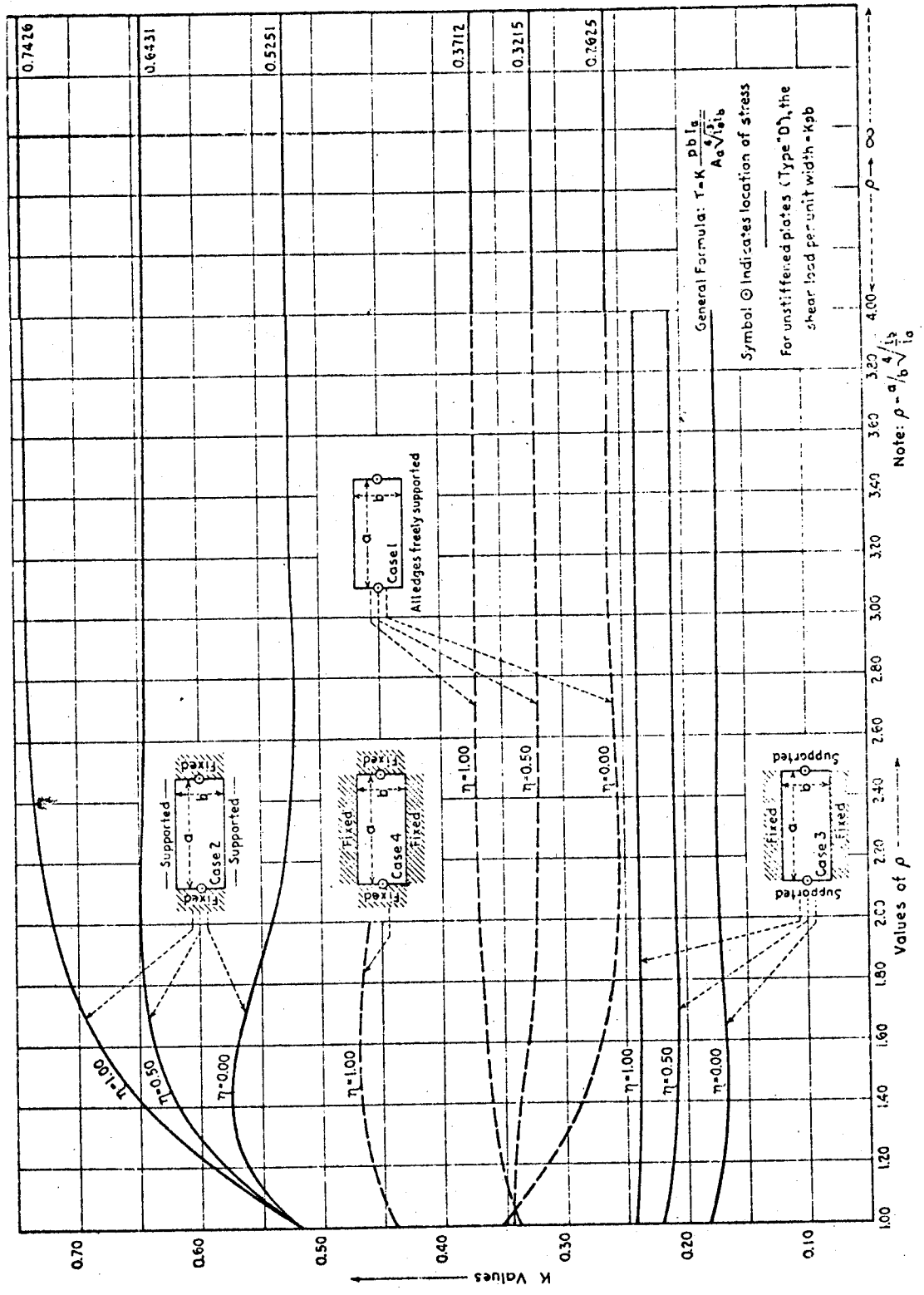


Figure B3.6.3-8 Shear Stress in Long Webs

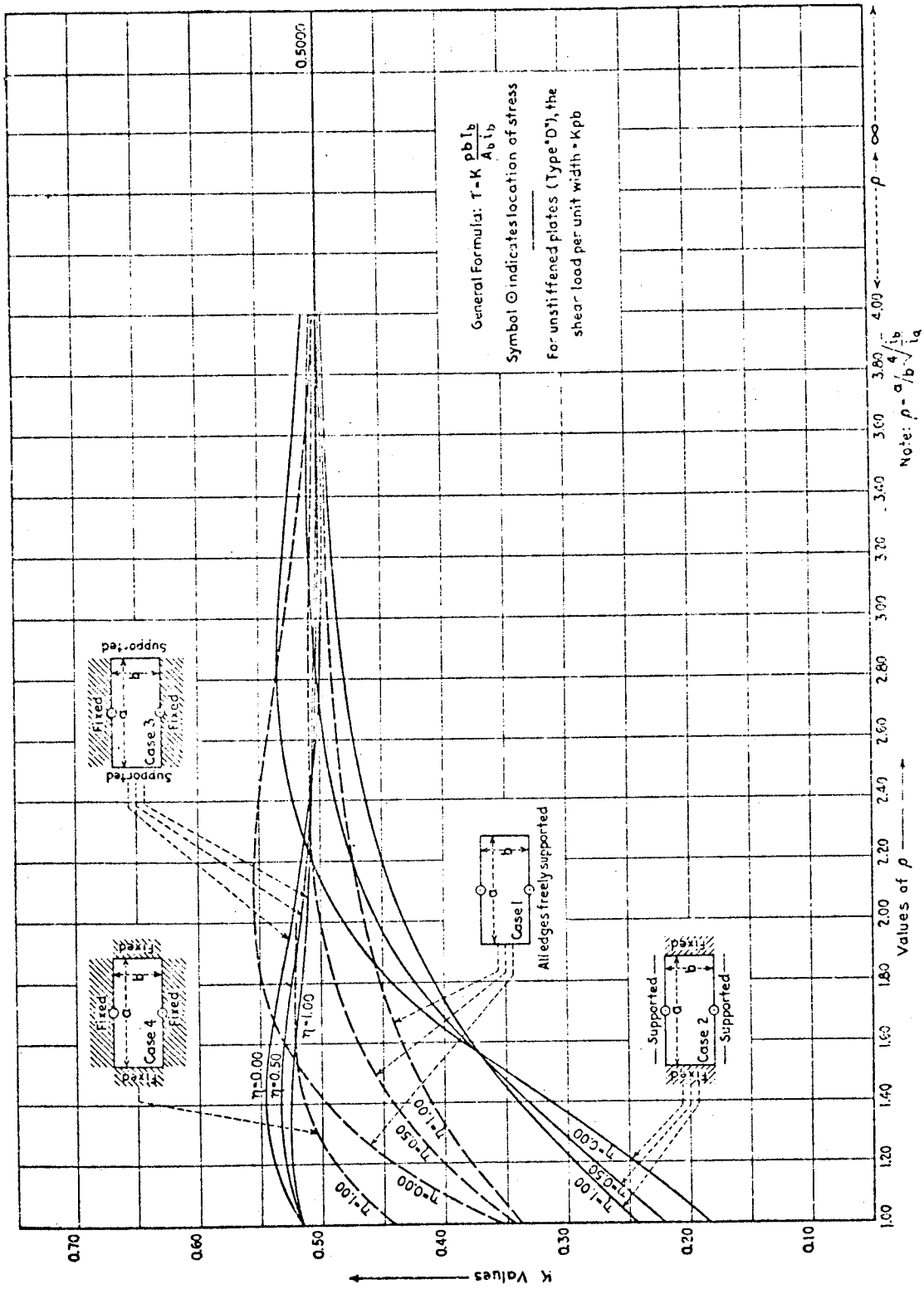


Figure B3.6.3-9 Shear Stress in Short Webs

## REFERENCES

B3-1 Structural Analysis Manual, Development Engineering, McDonnell Douglas Astronautics Company - West, M8.070-ACD dated July 1970.

B3-2 Formulas for Stress and Strain, Raymond J. Roark, 4th Edition, 1965, McGraw-Hill, Inc.

B3-3 Theory of Plates and Shells, Timoshenko and Woinowsky-Krieger, 2nd Edition, 1959 McGraw-Hill, Inc.

B3-4 Design Curves for Cross-Stiffened Plating Under Uniform Bending Load, Lt. Cmdr H. A. Schade, USN, Transactions - Society of Naval Architects and Marine Engineers, Vol. 49, 1941.

# SHEAR WEBS

# TABLE OF CONTENTS

B5.0.0 Shear Webs

B5.1.0 Shear Web Beam Design

B5.1.1 Introduction to Shear Web Beam Design

The shear resistant beam represents one limiting case of beam design. The other limiting case is that of the completely developed diagonal tension field beam. Once the theory for the two limiting cases is understood the intermediate case of the "semi-tension field beam" easily follows. The three possible cases of beam design are illustrated in Figure B5.1.1-1

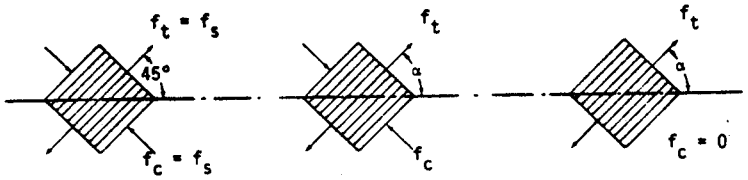


(a) shear resistant, (b) semi-tension field (c) complete tension field

Figure B5.1.1-1 Types of Shear Web Beams

The shear force acting on an element in pure shear can be resolved into an orthogonal tension and compression force system acting at 45 degrees with the direction of the shear force. A very simplified picture of the shear web design can be seen if it is assumed that the tension and compression components are represented by the diagonal members of the pin-jointed truss, shown in Figure B5.1.1-2.

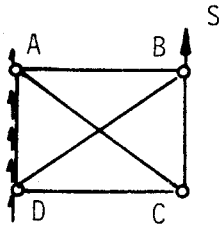


Figure B5.1.1-2 Pin-Jointed Truss

As an external loads is applied, member BD is loaded in tension and member AC in compression. As long as AC remains unbuckled, the web is shear resistant. When the applied load is high enough, member AC will buckle as a column and carry no additional load even though it continues to deform. Thus, member BD carries all of the additional load in tension. This corresponds to the web in the semi-tension field

beam. Since the truss shown is redundant, member AC can be removed and all the load will be carried by member BD. This corresponds to the case of a complete diagonal tension field web since the shear load is now carried solely by a diagonal tension element BD.

The three cases 1) shear resistant, 2) semi-tension field and 3) complete tension field shear web design are discussed in the following sections. In addition, design information is provided for curved semi-tension field beams.

For determining which type of beam design, shear resistant or semi-tension field, is most efficient, the following criteria from Reference B5-1 are given in terms of q, the shear flow in pounds per inch and $h_e$, the web depth in inches.

$q/h_e < 49$ Use semi-tension field design (B5-1)

$q/h_e > 121$ Use shear resistant design (B5-2)

For $q/h_e$ between 49 and 121 it makes little difference which type of beam design is used from an efficiency point of view.

Note: Other specific design requirements may override these general choices.

B5.1.1.1 Symbols

The following list of symbols are commonly used throughout this shear web beam design section. The symbols are listed in alphabetical order. Greek symbols follow the Roman symbol list.

$A$ = Ratio of compression-to-shear critical stress

$A_F$ = Area of the cap, in.$^2$

$A_{RG}$ = Area of the ring, in.$^2$

$A_{ST}$ = Area of the stringer (longeron)

$A_u$ = Area of the stiffener, in.$^2$

$A_{u_e}$ = Effective area of the stiffener, in.$^2$

$A_w$ = Area of the web, in.$^2$

$b$ = Stiffener web or stiffener cap length, in.

$b_o$ = Distance between attachment line and stiffener web centroid

$b_w$ = Height of stiffener web between cap centroids

$B$ = Ratio of applied compression-to-shear stress

$c$ = Distance from section neutral axis to the outer fiber, in.

$C_1$ = Correction factor for web shear stress

$C_2$ = Concentration factor for web shear stress

$C_3$ = Correction factor for cap bending stress

$d$ = Distance between stiffeners or rings, in.

$d_A$ = Attachment spacing, in.

$D$ = Rivet diameter, in.

DT = Diagonal tension

$e$ = Distance from center of web to the centroid of the stiffener, in.

$E$ = Elastic modulus, tension or compression, psi

$E_s$ = Secant modulus, psi

$E_t$ = Tangent modulus, psi

$E_u$ = Elastic modulus for stiffeners, psi

$E_w$ = Elastic modulus for the web, psi

$f$ = Total shear stress in web, psi

$f_b$ = Cap stress caused by external moment, psi

$f_c$ = Compression stress, psi

$f_{DT}$ = Web stress from diagonal tension effects, psi

$f_F$ = Cap stress from diagonal tension effects, psi

$f_{RG}$ = Ring stress from diagonal tension effects, psi

$f_s$ = Web shear stress (average), psi

$f_{s_{max}}$ = Maximum web shear stress, psi

$f_{ST}$ = Stringer stress from diagonal tension effects, psi

$f_t$ = Tension stress, psi

$f_u$ = Stiffener stress from diagonal tension effects, psi

$f_{u_{gross}}$ = Gross area stiffener stress for diagonal tension effects, psi

$f_{u_{max}}$ = Maximum stiffener stress from diagonal tension effects, psi

$f_{sb}$ = Secondary cap bending stress from diagonal tension effects, psi

$F$ = General term for allowable stress, psi

$F_c$ = Column allowable stress for stringer or stiffener, psi

$F_{BM}$ = Modulus of rupture for a cap section, psi

$F_{cc}$ = Column allowable crippling stress for stringer or stiffener, psi

$F_{cy}$ = Compression yield stress, psi

$F_o$ = Stiffener or stringer allowable forced crippling stress, psi

$F_{RG}$ = Ring forced crippling allowable stress, psi

$F_s$ = Web allowable stress, psi

$F_{s_{cr}}$ = Web critical buckling stress, psi

$F_{su}$ = Shear ultimate stress, psi

$F_{sy}$ = Shear yield stress, psi

$F_{tu}$ = Tension ultimate stress, psi

$G$ = Shear elastic modulus, psi

$G_s$ = Secant shear modulus, psi

$G_t$ = Tangent shear modulus, psi

$h$ = Depth of beam or arc distance between stringers, in.

$h_1$ = Web depth for an I-beam, in.

$h_A$ = Depth of beam between web-to-cap attachment pattern centroids, in.

$h_e$ = Depth of beam between cap centroids, in.

$I$ = Moment of inertia in general, $in.^4$

$I_C$ = Compression cap moment of inertia, $in.^4$

$I_F$ = Cap centroidal moment of inertia, in.$^4$

$I_T$ = Tension cap moment of inertia, in.$^4$

$I_u$ = Stiffener centroidal moment of inertia, in.$^4$

$I_{u_{corr}}$ = Corrected stiffener moment of inertia, in.$^4$

$k$ = Diagonal tension factor

$k_c$ = Buckling coefficient for compression stress

$k_{max}$ = Maximum diagonal tension factor

$k_s$ = Buckling coefficient for shear stress

$k_{s_\infty}$ = Buckling coefficient in shear for a long simply supported web

$K_c$ = Modified compression buckling coeffient = $\frac{k_c \pi^2}{12(1-\mu^2)}$

$K_s$ = Modified shear buckling coefficient = $\frac{k_s \pi^2}{12(1-\mu^2)}$

$L'$ = Effective column length, in.

$M$ = External bending moment, in.-lbs.

$M_{sb}$ = Secondary cap bending moment from diagonal tension effects, in.-lbs.

$n$ = Material stress-strain shape factor

PDT = Pure diagonal tension

$P_F$ = Load in cap from diagonal tension effects, lbs.

PS = Pure shear

$P_u$ = Load in stiffener from diagonal tension effects, lbs.

$P_w$ = Load in web from diagonal tension effects, lbs.

$q$ = Web shear flow, lbs./in.

$q_A$ = Attachment shear load (web-to-cap), lbs./in.

$Q_F$ = Static moment of the beam cap above the beam neutral axis, in.$^3$

$Q_w$ = Static moment of the web above the beam neutral axis, $in.^3$

$R$ = Radius of curvature, in.

$R_A$ = Attachment shear load at edge of curved panel, lbs./in.

$R_c$ = Curved panel interaction factor between shear and compression

$R_t$ = Curved panel interaction factor between shear and tension

$R_R$ = Attachment tension load (web-to-stiffener), lbs.

$S$ = Transverse shear load, lbs.

$t$ = Web thickness, in.

$t_u$ = Stiffener thickness against web, in.

$t_w$ = Stiffener web thickness, in.

$w$ = Uniform load intensity on beam end bay from diagonal tension effects, lbs./in.

$\alpha$ = Diagonal tension angle, degrees

$\Delta$ = Empirical correction factor for curved web allowable stress

$\varepsilon$ = Long edge rotational restraint

$\varepsilon_F$ = Cap strain from diagonal tension effects, in./in.

$\varepsilon_{RG}$ = Ring strain from diagonal tension effects, in./in.

$\varepsilon_{ST}$ = Stringer strain from diagonal tension effects, in./in.

$\varepsilon_u$ = Stiffener strain from diagonal tension effects, in./in.

$\varepsilon_w$ = Web strain from diagonal tension effects, in./in.

$\rho$ = Radius of gyration about the stiffener or stringer centroidal axis, parallel to the web, in.

$\eta_p$ = Plasticity factor for plate compression buckling

$\eta_s$ = Plasticity factor for shear buckling

$\mu$ = Poisson's ratio

$\omega d$ = Cap flexibility factor = $.7d \sqrt[4]{\dfrac{t}{(I_C + I_T)h_e}}$

## B5.1.2 Flat Shear Resistant Beam Design

### B5.1.2.1 Introduction to Shear Resistant Beam Design

A beam capable of carrying a design load without buckling of the web is "shear resistant." The web thickness can always be increased to avoid buckling, but such a design is usually not weight efficient. Generally, the lightest way to make a shear resistant beam is to use the thinnest web possible to meet strength requirements with stiffeners spaced to increase the web stability at or above the strength requirements. The weight of these stiffeners will usually be much smaller than the additional weight introduced by increasing the web thickness.

In this section, requirements are given for (1) web strength, (2) web stability, (3) stiffener properties (stiffness, area, and thickness) and (4) attachments. The basic design approach is discussed and a sample problem is given. Common symbols referred to in this section are shown in Figure B5.1.2.1-1.

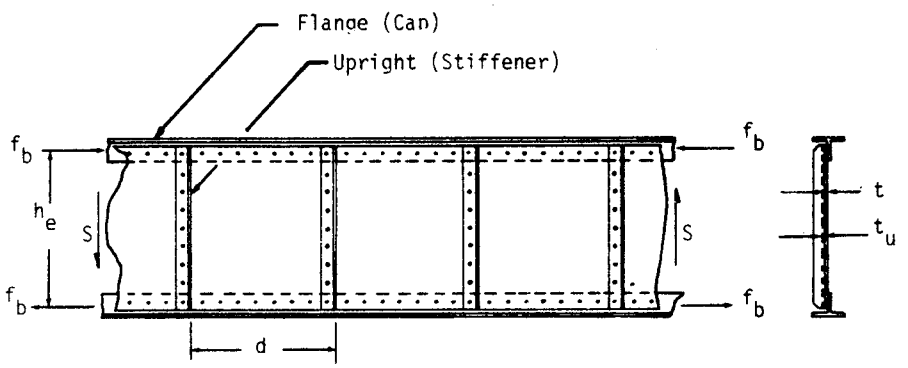


Figure B5.1.2.1-1 Shear Resistant Beam

### B5.1.2.2 Web Strength

The average shear stress in the web of a built up beam is given by the equation:

$$f_{s_{av}} = \frac{SQ_F}{It}\left(1 + \frac{2}{3}\frac{Q_w}{Q_F}\right) \qquad \text{(B5-3)}$$

where $Q_F$ is the static moment of the beam cap and $Q_w$ is the static moment of the beam web, taken from the beam neutral axis.

Often for design, Equation B5-3 is simplified to:

$$f_s = \frac{S}{h_e t} \qquad \text{(B5-4)}$$

The ratio between Equation B5-3 and B5-4 is plotted in Figure B5.1.2.2-1 for an I beam as a function of the web area-to-cap area ratio ($A_w/A_F$) for constant inner cap-to-average cap depth ratios ($h_1/h_e$) of 0.8 and 1.0 which represent the practical design limits. From this figure, values of $A_w/A_F$ greater than 1.0 lead to conservative estimates (over 10%) of the web shear stress based on the simplified Equation B5-4. This fact should be kept in mind when designing shear resistant and semi-tension field beams.

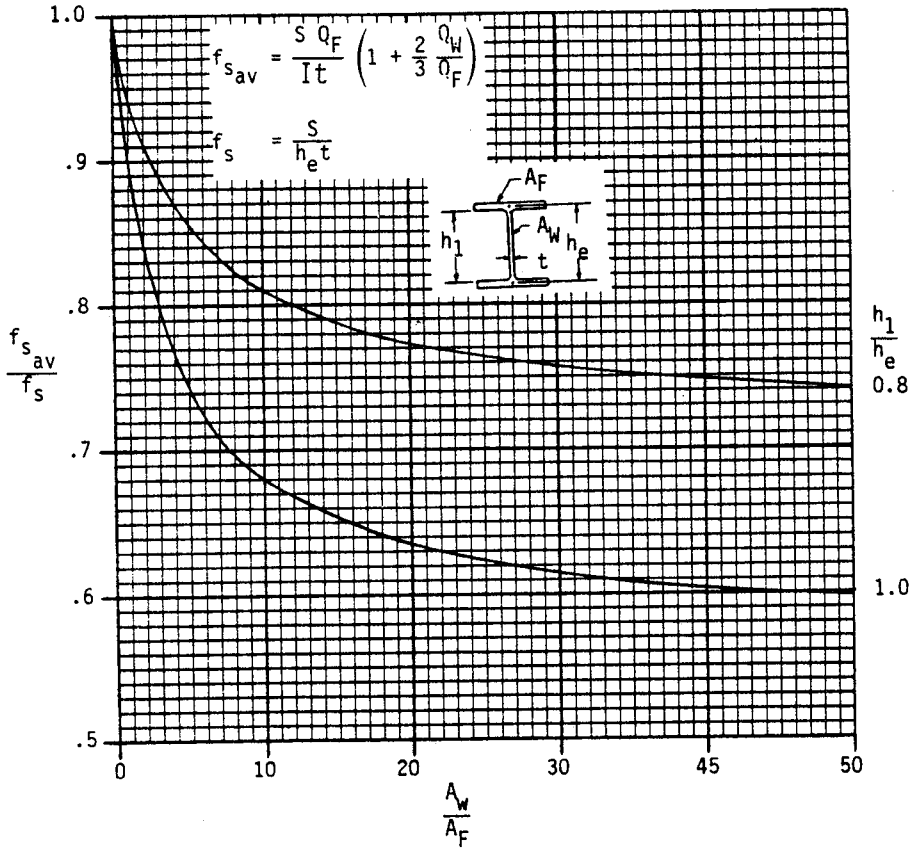


Figure B5.1.2.2-1 Ratio of Exact Average Shear Stress to Approximate Average Shear Stress

B5.1.2.3 Web Stability

The critical (allowable) buckling stress, $F_{s_{cr}}$, of a flat web of depth $h_e$, width d, and thickness t is

$$f_{s_{cr}} = K_s \eta_s E (t/d)^2 \qquad \text{(B5-5)}$$

where $K_s$ is the modified shear buckling coefficient and $\eta_s$ is a factor accounting for stress above the material proportional limit.

$K_s$ is a function of the ratio $d/h_e$ and the edge restraint ($\varepsilon$) provided by the stiffeners and caps. In practice, this edge restraint is difficult to determine. For a web with $d/h_e = 0$, the buckling coefficient, $k_{s\infty}$ ranges between 5.35 if the long edges are simply supported to 8.98 if the long edges are clamped, as shown in Figure B5.1.2.3-1. Figure B5.1.2.3-2 shows the variation of buckling coefficient as a function of $d/h_e$ for both simply supported and clamped long webs. Note that $K_s$ obtained from these figures must be multiplied by $\frac{\pi^2}{12(1-\mu^2)}$ to use with Equation B5-5.

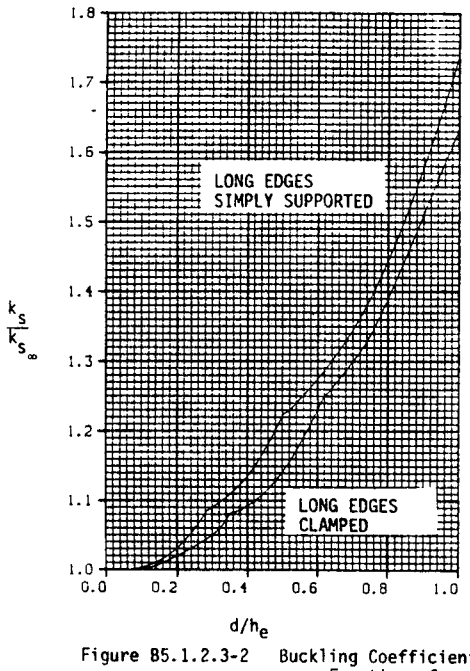


Figure B5.1.2.3-2 Buckling Coefficient as a Function of $\frac{d}{h_e}$ (Ref. B5-2)

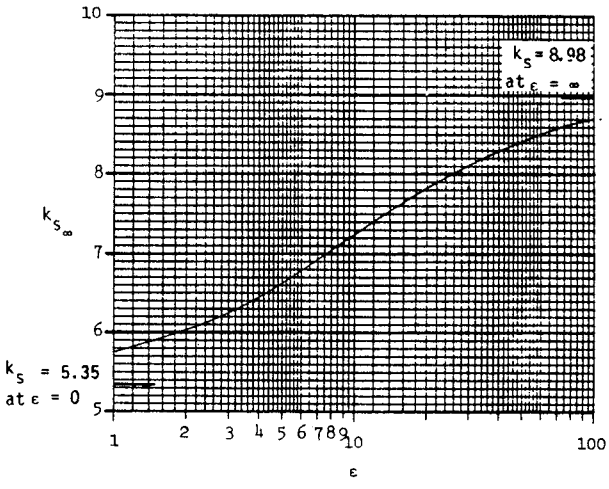


Figure B5.1.2.3-1 Buckling Coefficient for a Plate with $\frac{d}{h_e} = 0$ as Function of Edge Rotational Restraint $\varepsilon$ (Ref. B5-2)

The plasticity factor to be used in Equation B5-5 for plates in shear is inferred in Reference B5-1 as $\eta_s = G_s/G$. This plasticity factor represents a good average for test data, but can lead to unconservative results. For this reason a more conservative plasticity factor is adopted here.

$$\eta_s = (G_t/G)^{1/2} \qquad \text{(B5-6)}$$

Where $G_t$ = Tangent shear modulus, psi and

$G$ = Elastic shear modulus, psi.

These moduli can be obtained directly from material shear stress-strain curves. However, shear stress-strain curves are generally not available. Compression stress-strain curves are readily available, and it is common to establish the values of $G_t/G$ by reducing $E_t/E$ data from compression stress-strain curves. The following method can be used.

A. Assume that $F_{sy} = .55\ F_{cy}$ were $F_{cy}$ is the minimum guaranteed compressive yield stress for the given material from Reference B5-2. (Factor 0.55 is also taken from this reference. It represents the proportional limit in shear and is also very near the ratio of $F_{su}$ to $F_{tu}$ which is usually about 0.60.)

B. From stress-strain curves in Reference B5-2 determine the appropriate material shape factor n. If not available, a value of n = 20 is a good approximation for most materials.

C. Assume values of $F_{s_{cr}}$ and calculate $G_t/G$ from the equation

$$\eta_s = (G_t/G)^{1/2} = \left[\frac{1}{1 + \frac{.002Gn}{F_{sy}}\left(\frac{F_{s_{cr}}}{F_{sy}}\right)^{n-1}}\right]^{1/2} \qquad \text{(B5-7)}$$

with $G = \dfrac{E}{2(1+\mu)}$

D. Plot $F_{s_{cr}}$ vs $F_{s_{cr}}/\eta_s$

Figures B5.1.2.3-3 through B5.1.2.3-5 have been plotted for the more common materials used in design based on Equation B5-7.

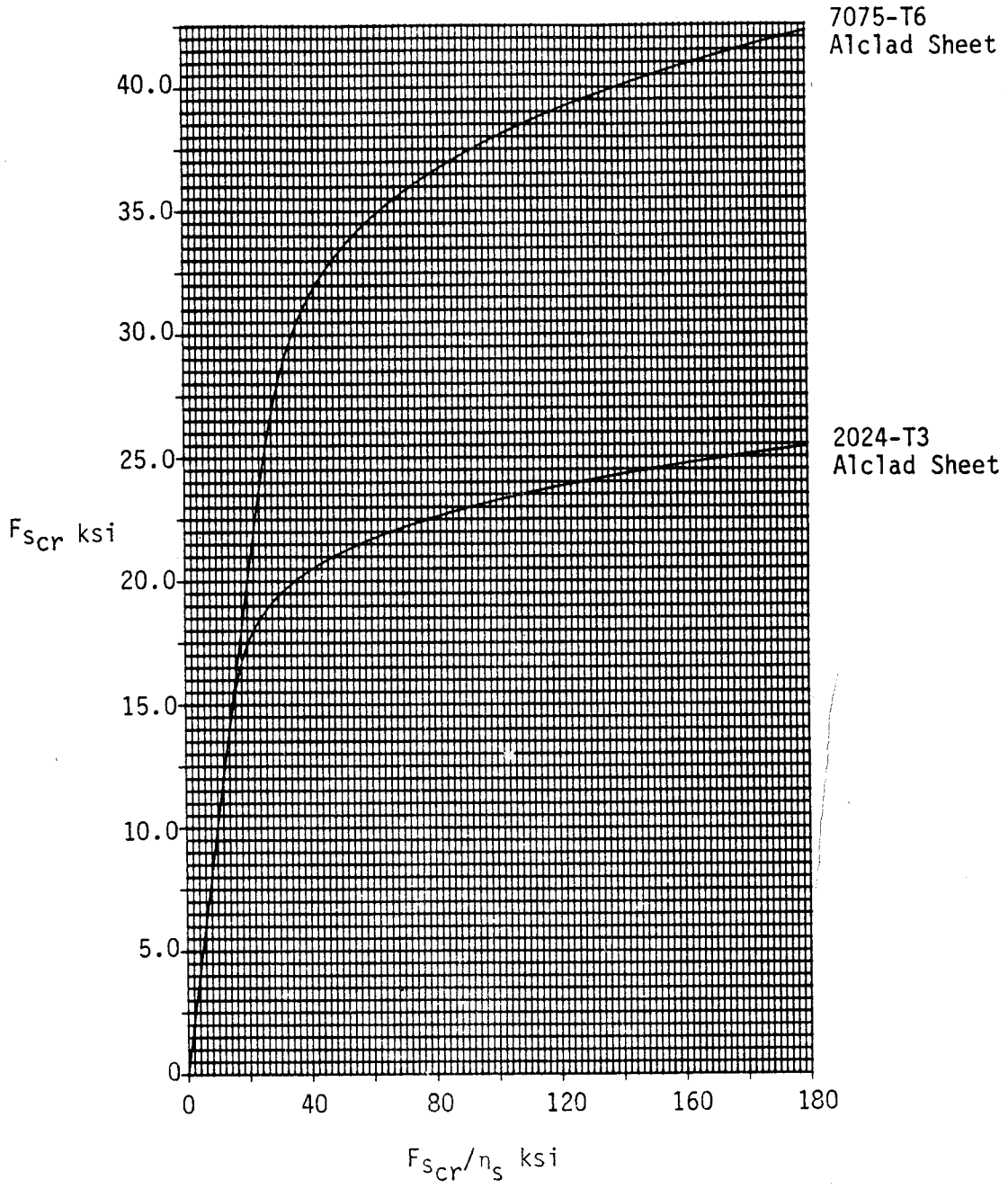


Figure B5.1.2.3-3 Plasticity Correction Curves for Shear Buckling of Alclad Aluminum Sheet

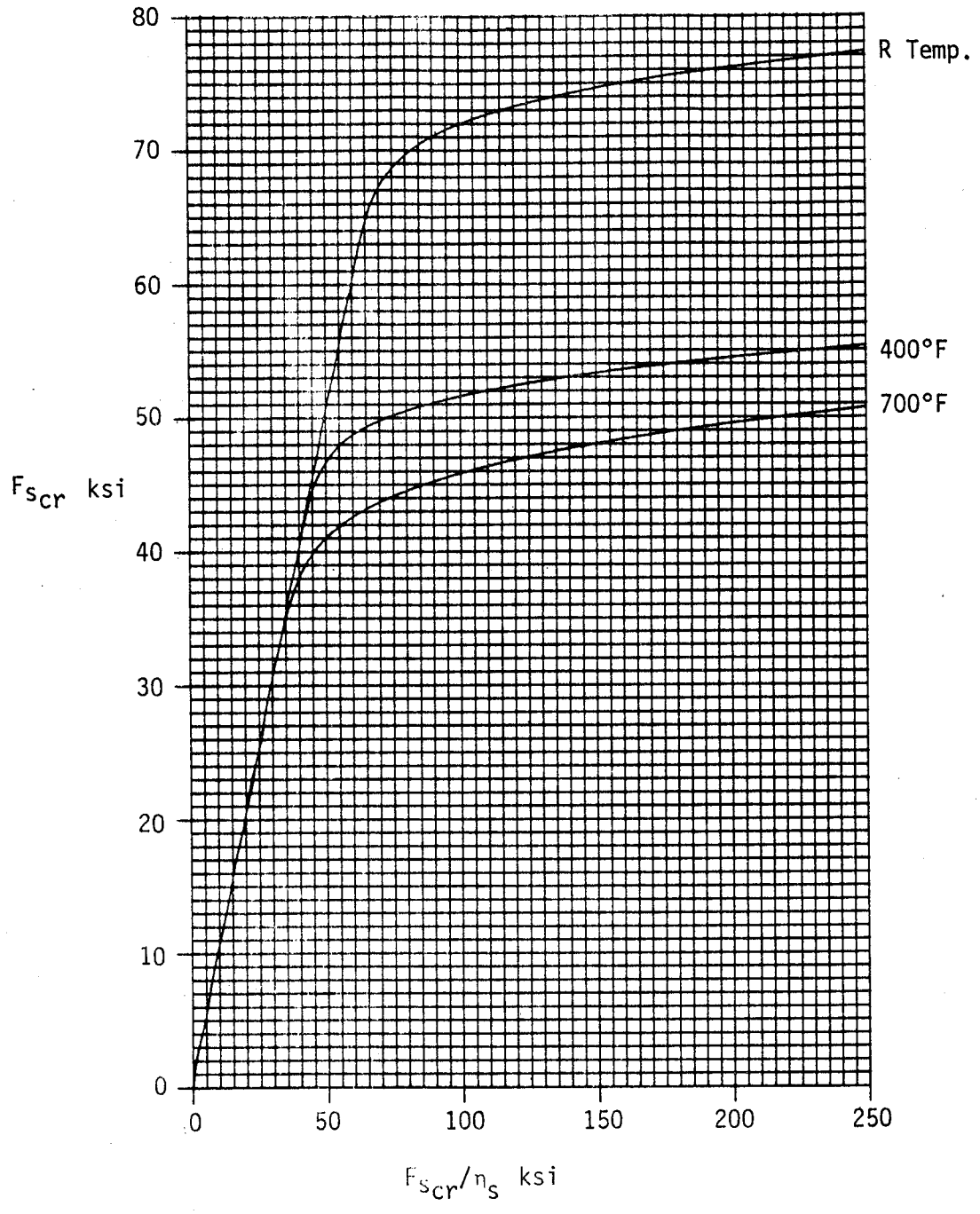


Figure B5.1.2.3-4 Plasticity Correction Curves for Shear Buckling of 6Al-4V Titanium Sheet at Selected Temperatures

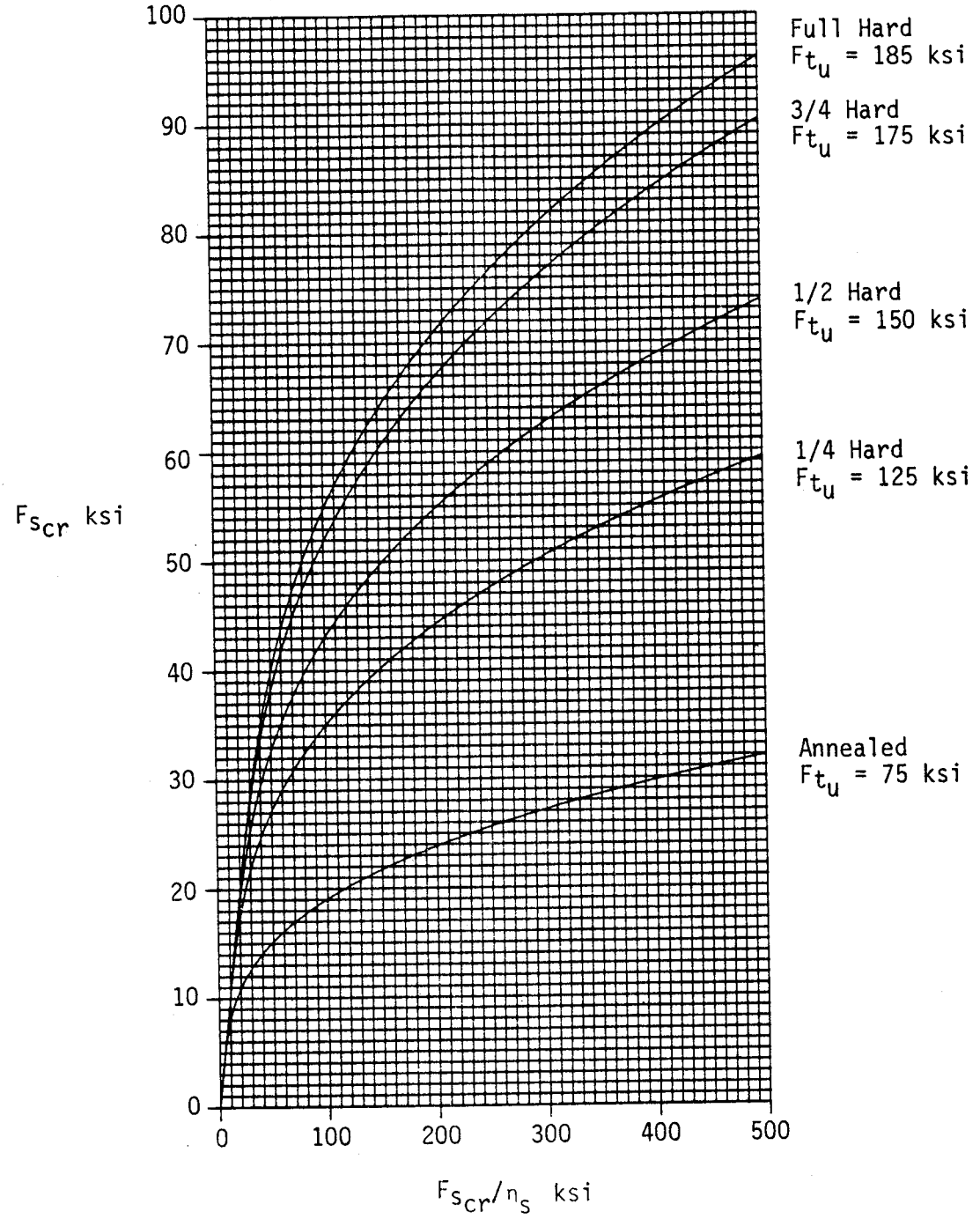


Figure B5.1.2.3-5 Plasticity Correction Curves for Shear Buckling of AISI 301 Stainless Steel Sheet

5.1.2.4 Stiffener Stiffness (single stiffener only)

When web thickness is set by equation B5-4 for strength, then the required stiffener spacing (d) can be calculated from equation B5-5 such that $F_{s_{cr}}$ is equal to or greater than $f_s$. At this calculated stiffener spacing, the stiffener must have a minimum moment of inertia

$$I_u = \frac{0.0217\ dt^3}{\left(\frac{d}{h_e\sqrt{K_s}}\right)^{8/3}} \qquad \text{(B5-8)}$$

in order to prevent the web from buckling across the stiffeners. Note in equation B5-8 that $I_u$ is about the centroidal axis of the stiffener and includes no web material. Also, if stiffeners are spaced closer than given in equation B5-5, then $I_u$ does not apply.

Equation B5-8 is shown graphically in Figure B5.1.2.4-1. If the stiffener is a different material than the web, then $I_u$ should be corrected by the equation

$$(I_u)_{corr} = \left(\frac{E_w}{E_u}\right) I_u \qquad \text{(B5-9)}$$

where $E_w$ and $E_u$ are the elastic moduli of the web and stiffener respectively.

The stiffener, in addition to meeting stiffness requirements of equation B5-8, should always have a cross sectional area ($A_u$) greater than 30 percent of the web area, dt. Stiffener flange thickness ($t_u$) against the web should always have a thickness greater than 60 percent of the web thickness (t). Thus

$$A_u > 0.30\ dt \qquad \text{(B5-10)}$$

$$t_u > 0.60\ t \qquad \text{(B5-11)}$$

Specific $t_u$ requirements for web gauges less than 0.156 inches are given on Table B5.1.2.4-1.

Table B5.1.2.4-1 Minimum Stiffener $t_u$ Requirements

| Web Gauge, t | .025 | .032 | .040 | .051 | .064 | .072 | .081 | .091 | .102 | .125 | .156 | >.156 |
|---|---|---|---|---|---|---|---|---|---|---|---|---|
| Min. Stiff. Gauge, $t_u$ | .025 | .032 | .040 | .051 | .051 | .064 | .064 | .072 | .081 | .081 | .091 | .6t |

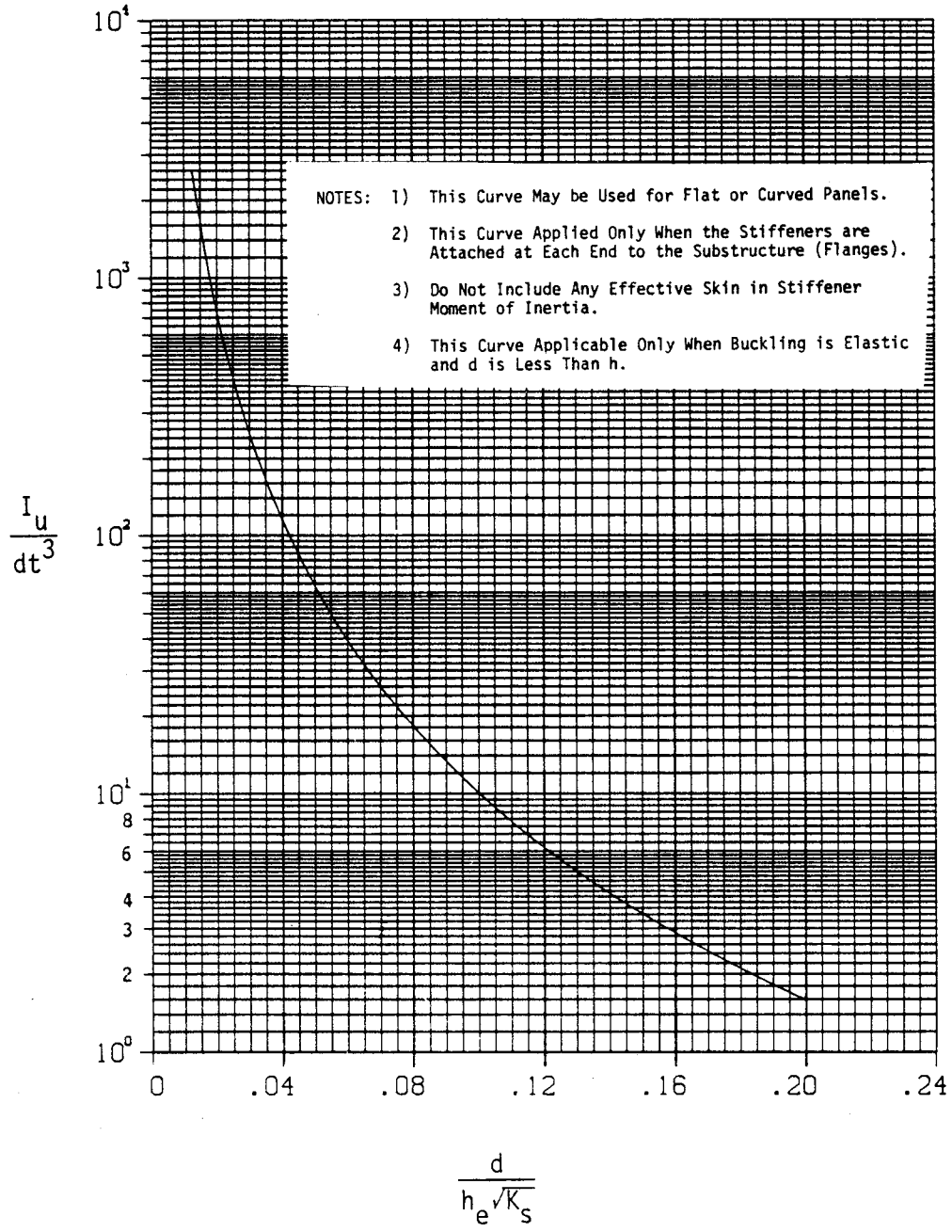


Figure B5.1.2.4-1 Stiffener Moment of Inertia Requirement for Shear Resistant Beam

B5.1.2.5 Attachments

A. Web-to-Cap - Based on the web shear flow, Equation B5-4, the attachment size is determined by q x $d_A$ (load per attachment) where $d_A$ is the attachment spacing. Allowable fastener loads are given in Section C1.

B. Web-to-Stiffener - Theoretically, there is no load transfer between the web and the stiffeners for a shear resistant beam unless the shear flow changes between bays; then fasteners must resist this change in shear. In general, fastener diameter should be near the web thickness, .125 diameter mininum, and pitch should be 4-6D.

C. Stiffeners-to-Cap - It is recommended that these attachments be stronger than the web-to-stiffener attachments. If rivets are used for the web-to-stiffener attachments, then the stiffener-to-cap attachments should have: (1) lockbolts the same diameter , (2) rivets the next larger diameter, or (3) two rivets the same diameter.

B5.1.2.6 Design Approach

The design of stiffened shear resistant beams is a trial and error procedure. In design, the applied shear flow (q) and beam depth ($h_e$) are generally known. The designer must determine web thickness (t), stiffener spacing (d), and stiffener moment of inertia ($I_u$) consistent with minimum weight, minimum cost, or practical spacing and thickness constraints.

From a minimum weight point of view, the goal is to design to the highest possible allowable stress. The maximum possible stress is the ultimate shear strength of the material, if shear is the only applied load. At this maximum stress, based on typical applied shear flows for aircraft, the stiffener spacing is generally too close for practical considerations as determined from the shear buckling Equation B5-5. Therefore, the applied stress must be lowered to produce practical structure. This is accomplished by increasing the web thickness (t). Most practical aircraft designs fall between a ratio $d/h_e$ = 0.20 and 1.0. The designer must weigh his constraints to determine the best $d/h_e$ value. Thus, if minimum weight is the most important constraint, $d/h_e$ should be as small as is practical; however, cost will increase because of the increased number of stiffeners.

The buckling coefficients given in Figure B5.1.2.3-1 and B5.1.2.3-2 cover the range from long edges simply supported to long edges clamped. For design, the simply supported edge conditions should be used, unless sufficient test data is available to justify higher edge restraint buckling coefficients.

An equation useful for preliminary design can be obtained by setting the applied stress Equation B5-4 equal to the allowable buckling stress Equation B5-5. Then web thickness is

$$t = \left( \frac{qd^2}{K_s n_s E} \right)^{1/3} \qquad \text{(B5-12)}$$

NOTE: $f_s = F_{s_{cr}}$ with this equation.

B5.1.2.7 Sample Problem (Shear Resistant Beam)

Given: $q$ = 2000#/in (No other applied loads),
$h_e$ = 10 inches,
Web Material is 7075-T6 Alclad,
Stiffener is 7075-T651 extruded Zee section,
Poisson's Ratio $\mu$ = 0.30,
Constraint: Minimum weight is required and
$d$ = 6.0 inches (minimum stiffener spacing).

A. Check to see if a shear resistant beam is the appropriate design from Equation B5-1 and B5-2.

$q/h_e = 2000/10 = 200 > 121$

Thus, the shear resistant beam is best approach.

B. Find the buckling coefficient, $K_s$, using Figures B5.1.2.3-1 and -2.

From Figure B5.1.2.3-1 for infinitely long simply supported edges, $\varepsilon = 0$, $k_{s_\infty} = 5.35$.

From Figure B5.1.2.3-2 for $d/h_e = 6/10 = 0.60$, $k_s/k_{s_\infty} = 1.27$. Then $k_s = (k_s/k_{s_\infty})\, k_{s_\infty} = 1.27(5.35) = 6.79$ and the modified buckling coefficient is

$$K_s = k_s \left(\frac{\pi^2}{12\ (1-\mu^2)}\right) = 6.79 \left(\frac{\pi^2}{12\ (1-0.3^2)}\right) = 6.14$$

C. Find the web thickness.

Assume $\eta_s = 1.0$, then, from Equation B5-12

$$t = \left(\frac{qd^2}{K_s \eta_s E}\right)^{1/3} = \left(\frac{2000(6.0)^2}{6.14(1.0)(10.5 \times 10^6)}\right)^{1/3} = 0.104 \text{ in.}*$$

*If using sheet material use next standard gauge, t = .125 inch. This sample would be machined plate.

D. Check assumption $\eta_s = 1.0$.

From Equation B5-4

$$f_s = q/t = 2000/(0.104) = 19{,}231 \text{ psi}$$

From Figure B5.1.2.3-3 or Equation B5-7 with

$$f_s = F_{s_{cr}} = 19{,}231 \text{ psi}$$

$$F_{s_{cr}}/\eta_s = 19{,}231$$

$$\eta_s = F_{s_{cr}}/19{,}231 = 19{,}231/19{,}231 = 1.0.$$

Thus the assumption ($\eta_s = 1.0$) is correct. If it were not, Steps C to D would be iterated with the calculated $\eta_s$ until $\eta_s$ assumed in Step C agrees with the calculated $\eta_s$ in Step D.

E. Find $I_u$ required for the stiffener from Equation B5-8 or Figure B5.1.2.4-1.

$$I_u = \frac{0.0217\ dt^3}{\left(\frac{d}{h_e\sqrt{K_s}}\right)^{8/3}} = \frac{0.0217(6)(0.104)^3}{\left(\frac{6}{10\sqrt{6.14}}\right)^{8/3}} = 0.0064 \text{ in.}^4$$

F. Determine $A_u$ for the stiffener such that the $t_u$ and $I_u$ requirements are satisfied. From Equation B5-10, $A_u = 0.3dt = 0.3(6.0)(0.104) = 0.187$ in.$^2$ for minimum weight.

From the table on Figure B.5.1.2.4-1 for t = 0.104 inch, required $t_u$ = 0.081 inch and from Step E, required $I_u$ = 0.0064 $in^4$.

From the Standards Manual, Vol. I, page 607.122, configuration B meets the area requirement, exceeds the $I_u$ requirement, and is close to the $t_u$ requirement. Thus the following shape is chosen

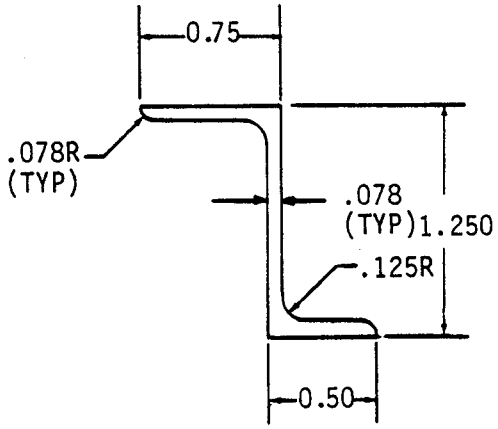


G. Based on section B5.1.2.5, 3/16 D rivets will be sufficient for the shear loads.

## B5.1.3 Flat Semi-Tension Field Beam Design

### B5.1.3.1 Introduction to Semi-Tension Field Beam Design

For ratio's of applied shear flow to beam depth less than 49 as defined by Equation B5-1, a beam should be designed as a semi-tension field type. When the web is allowed to buckle under load, additional forces are generated within the beam which must be resisted by the stiffeners, caps, and attachments as shown in Figure B5.1.3.1-1.

The NACA carried on a comprehensive study and testing program to develop a better understanding of semi-tension field beam action. The results of this program, reported in NACA TN 2661 (Reference B5-1), are presented in this section. These results are subject to the following limitations:

1. Stiffener thickness to web thickness ratio shall be per Figure B5.1.2.4-1, but in no case less than 0.6.

2. Stiffener spacing (d) should not be too much outside the range $0.2 < d/h_e < 1.0$.

3. Tests by the NACA cover the range $200 < h_e/t_u < 1500$. Unconservative results may exist outside this range.

4. Stiffener area should be in the range $0.3 < A_u/A_W < 0.5$. This limitation is primarily for minimum weight; $A_u/A_W$ can certainly be greater than 0.5 for strength requirements.

### B5.1.3.2 Web Analysis

If the applied shear load is less than the allowable buckling load for the web, then the web is in a state of pure shear at the neutral axis as indicated in Figure B5.1.3.2-1a. If the normal stresses due to bending over the depth of the web are neglected, this shear stress arrangement can be assumed constant over the full depth of the web.

If the web is thin, then it will buckle under a certain critical load and if the load is increased beyond this critical buckling value, the buckle pattern will approach a pure tension field as indicated in Figure B5.1.3.2-1b.

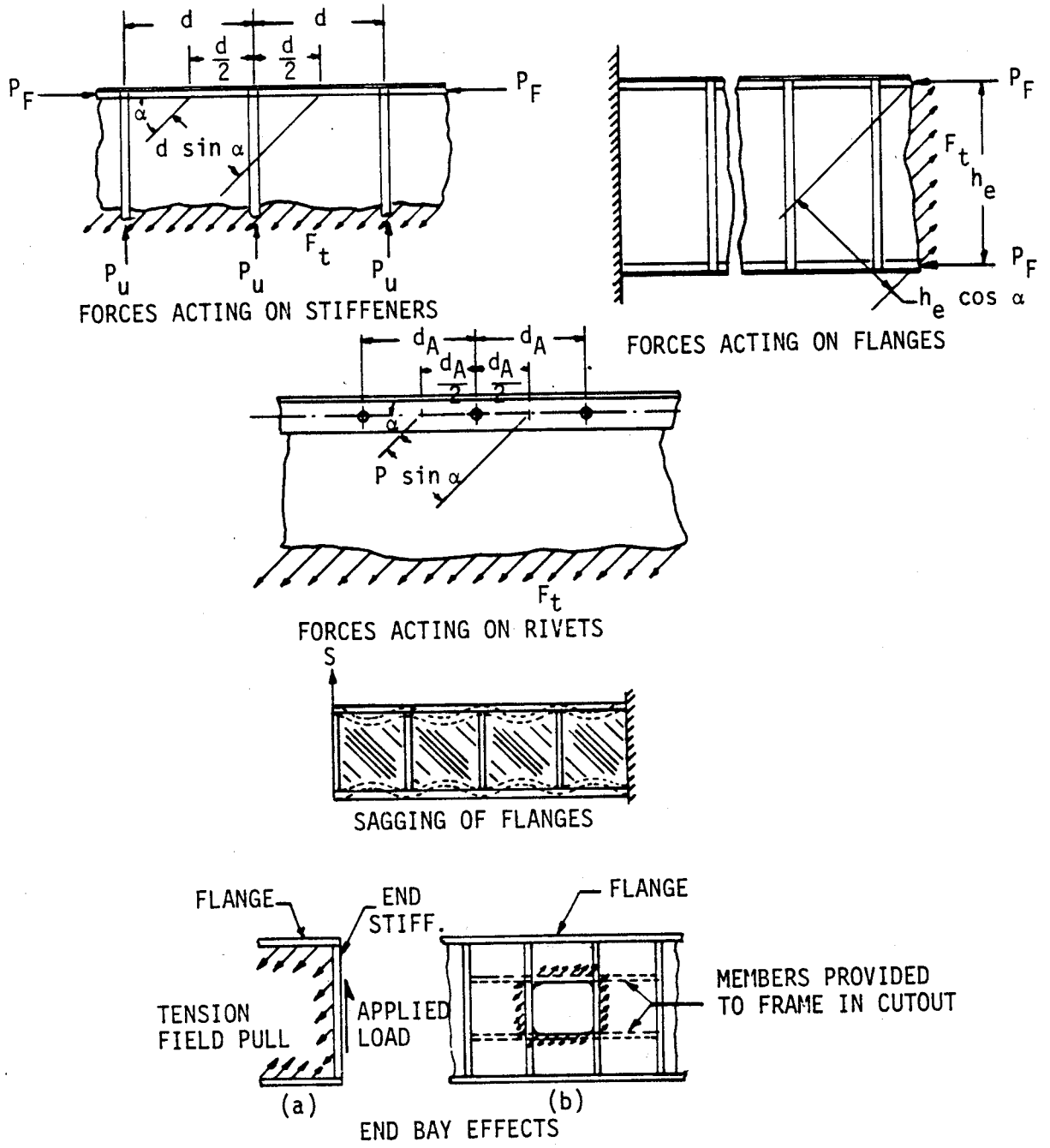


Figure B5.1.3.1-1 Diagonal Tension Forces Affecting Beam Design

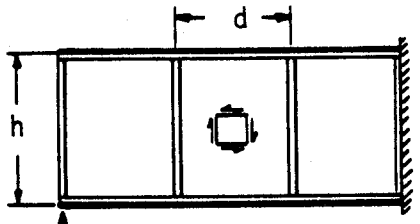


(a) Nonbuckled (Shear-Resistant) Web

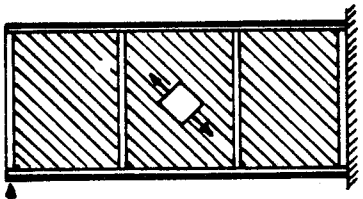

(b) Pure Diagonal-Tension Web

Figure B5.1.3.2-1 State of Stress in a Beam Web

In the usual practical thin web beam in aircraft construction, the state of stress in the web is intermediate between pure shear and pure diagonal tension. The engineering theory as developed by the NACA assumes that this intermediate state of incomplete diagonal tension can be divided into two parts; a part $f_s$ carried by pure shear and a part $f_{DT}$ carried by pure diagonal tension. Under this assumption one can write the total stress as

$$f = f_s + f_{DT},$$

where

$f_s$ and $f_{DT}$ can be written

$$f_{DT} = kf$$

$$f_s = (1-k)f$$

where k is the "diagonal-tension factor" which expresses the degree to which the diagonal tension is developed by a given load. Thus, the state of pure shear is measured by k = 0 and the state of pure diagonal tension by k = 1. Figure B5.1.3.2-2 illustrates the stress condition for the limiting cases of k = 0 and k = 1 and also for the intermediate case. The letters PS, DT and PDT as labeled on the figure mean pure shear, diagonal tension, and pure diagonal tension respectively relative to web stress conditions.

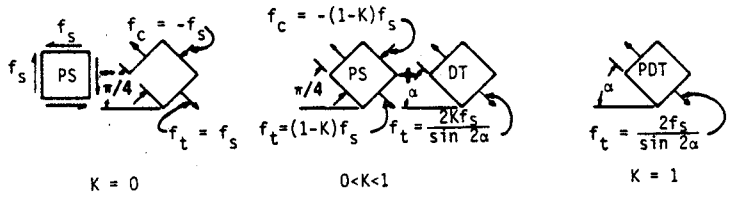


Figure B5.1.3.2-2 Resolution of Web Stresses at Different Stages of Diagonal Tension

A. Web Shear Stress ($f_s$) - The shear flow can be closely approximated for deep beams by $q = S/h_e$. From this it follows that the nominal web shear stress is

$$f_s = q/t \qquad \text{(B5-13)}$$

B. Initial Web Buckling Stress ($F_{s_{cr}}$) - This stress as given by Equation B5-5 is

$$F_{s_{cr}} = K_s \eta_s E (t/d)^2$$

If the critical stress is above the material proportional limit, then the plasticity correction factors given in Section B5.1.2.3 for shear resistant beams should be applied. Values for $K_s$ can be obtained from Figure B5.1.2.3-1 and B5.1.2.3-2.

In determining $F_{s_{cr}}$, it is recommended for design to assume simply supported long edges when determining $k_s$ and correct this for the effect of $d/h_e$ as discussed in Section B5.1.2.3. The effect of more exact values on the diagonal tension factor (k) is small.

C. Diagonal Tension Factor (k) - Having determined the loading ratio $f_s/F_{s_{cr}}$ from steps A and B, the diagonal tension factor k can be read from Figure B5.1.3.2-3 or the equation

$$k = \tanh\left[\left(0.5 + \frac{300td}{Rh}\right)\left(\log_{10}\frac{f_s}{F_{s_{cr}}}\right)\right] \qquad \text{(B5-14)}$$

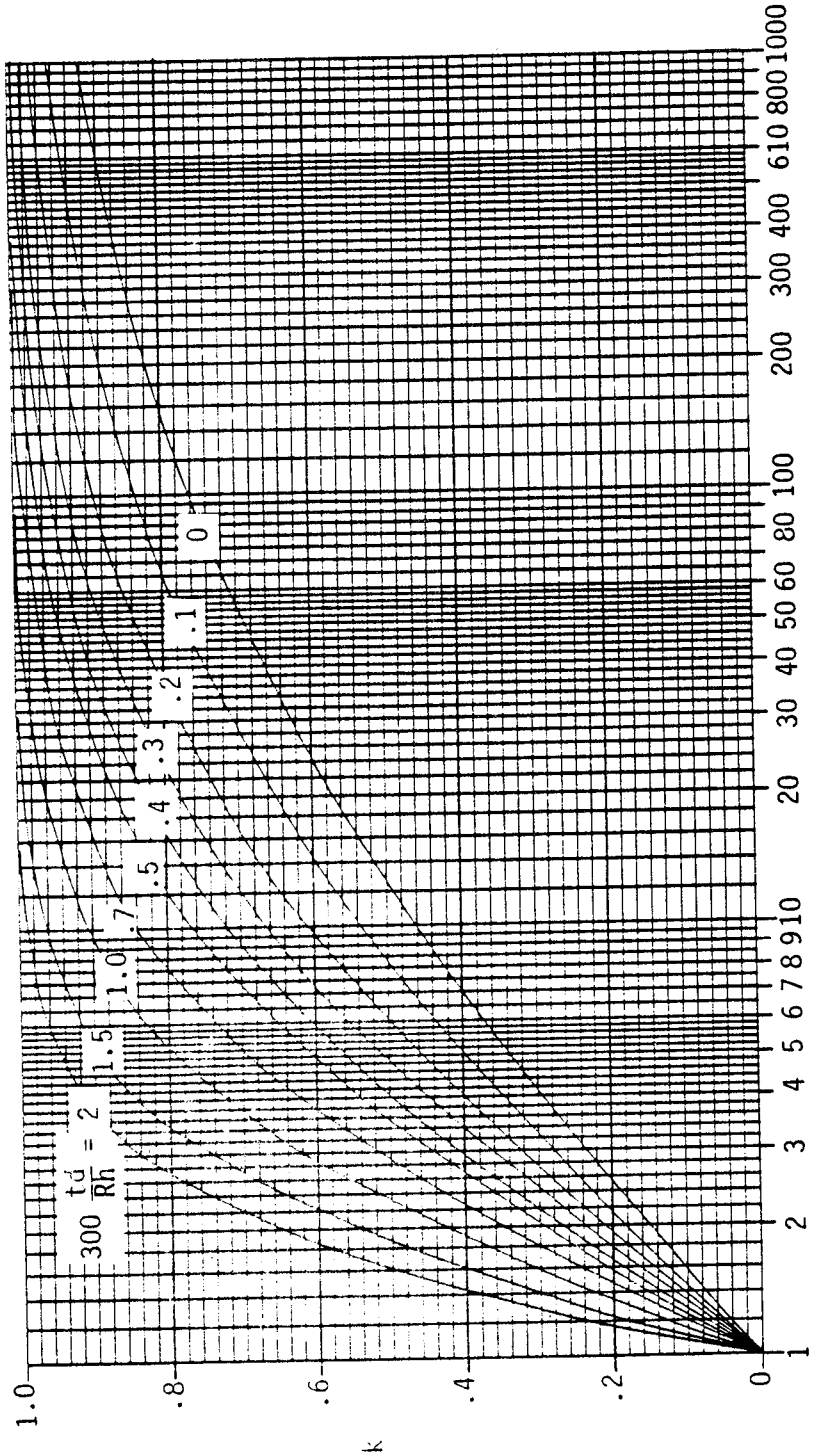


$\frac{f_s}{F_{scr}}$

NOTE: 1. If h>d replace $\frac{td}{Rh}$ by $\frac{th}{Rd}$

2. If $\frac{d}{h}$ (or $\frac{h}{d}$)> 2, use 2.

3. For flat webs use zero curve

Figure B5.1.3.2-3 Diagonal Tension Factor k

where R = ∞ for flat panels. (The valve d/h used later for curved panels should be greater than 1.0, but not larger than 2.0. If less than 1.0 use h/d.)

It is recommended that the diagonal tension factor at ultimate load be limited to a maximum value,

$$k_{max} = 0.78 - (t - 0.012)^{1/2} \qquad \text{(B5-15)}$$

in order to avoid excessive wrinkling and permanent set at limit load; thereby inviting fatigue failure. A tabular solution of this criterion is given below:

| (t) in. | .020 | .025 | .032 | .040 | .051 | .064 | .072 | .081 | .091 | .102 | .125 | .156 | .188 | .250 |
|---|---|---|---|---|---|---|---|---|---|---|---|---|---|---|
| $k_{MAX}$ | .69 | .67 | .64 | .61 | .58 | .55 | .53 | .52 | .50 | .48 | .44 | .40 | .36 | .29 |

D. Maximum Applied Web Shear Stress ($f_{s_{max}}$) - Once the web has buckled, the maximum stress in the web becomes a function of the diagonal tension factor (k), the angle of tension wrinkle ($\alpha$), and the stiffness of the upper and lower beam caps ($I_F$). This relationship is defined by the empirical equation

$$f_{s_{max}} = (1 + k^2 C_1)(1 + kC_2)\, f_s \qquad \text{(B5-16)}$$

where the constants $C_1$ and $C_2$ (defined in Figures B5.1.3.2-4a, b) represent the effects of the tension wrinkle and the sagging of the caps, respectively.

E. Allowable Web Shear Stress ($F_s$) - This stress is determined by tests and depends on the value of diagonal tension factor k as well as on the details of the web-to-cap and web-to-stiffener fastening. Figure B5.1.3.2-5 gives conservative values (as much as 10 percent) for the allowable web shear stress as a function of k and the tension ultimate strength of the material. Use data from this figure unless test data is available; see Section E6. The allowable web shear stress should not be less than the maximum applied shear stress as defined by the equation

$$M.S. = \frac{F_s}{f_{s_{max}}} - 1 \qquad \text{(B5-17)}$$

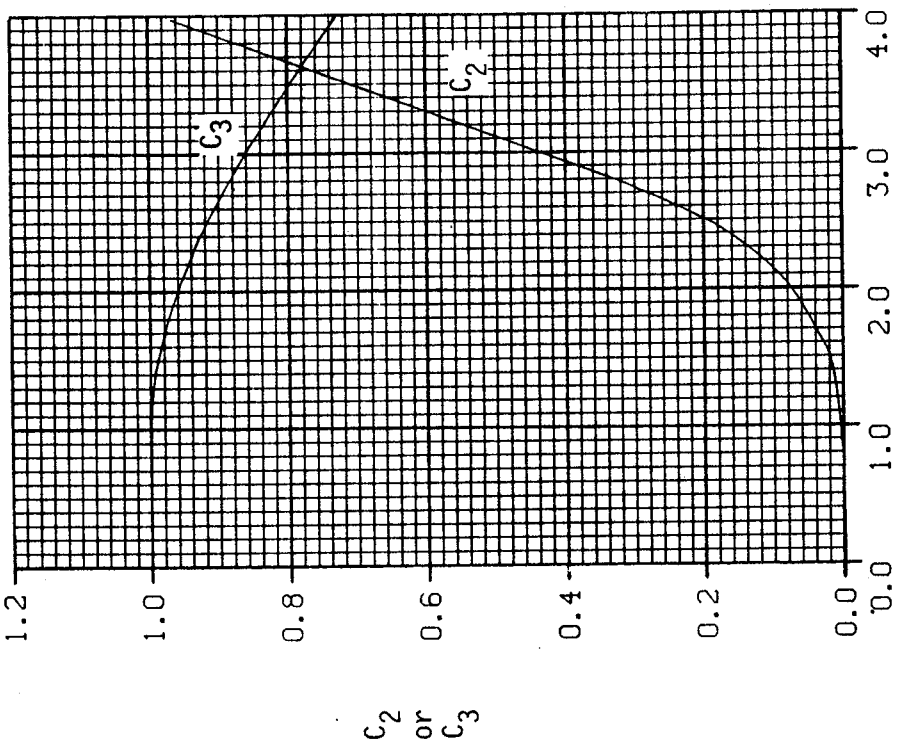


Figure B5.1.3.2-4.b Stress Concentration Factors $C_2$ and $C_3$

$$\left(\omega d = .7d \sqrt[4]{\frac{t}{(Ic + I_T)h_e}}\right)$$

(Ref. B5-1)

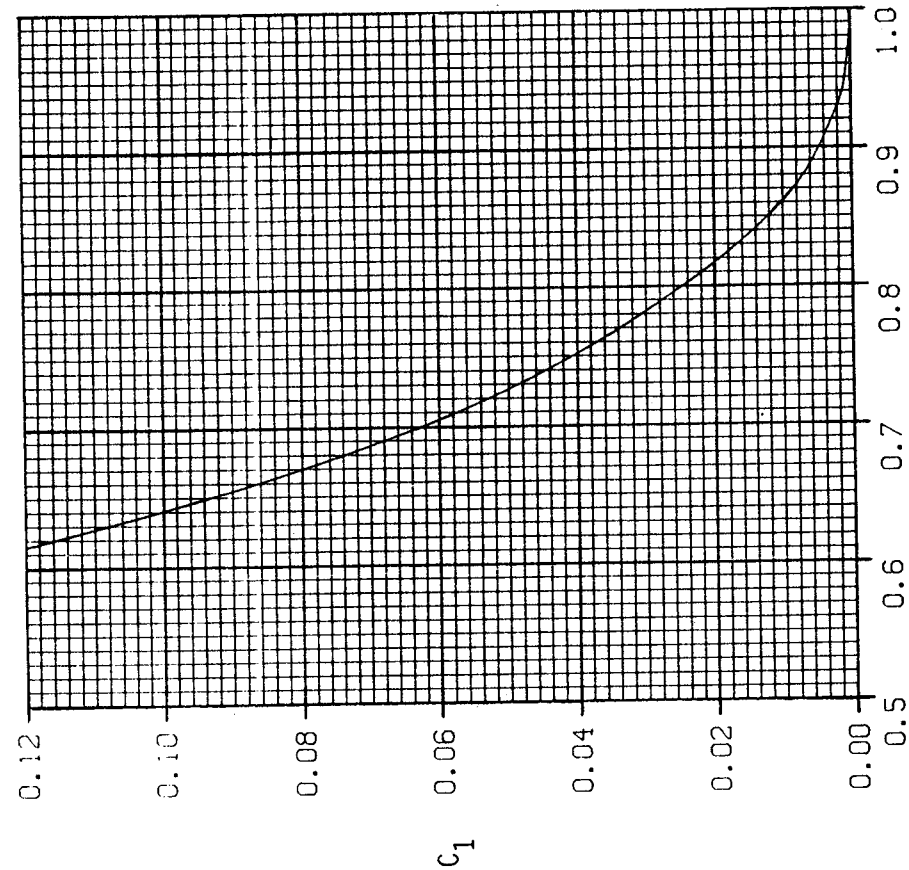


Figure B5.1.3.2-4a Correction Factor $C_1$ for Diagonal Tension

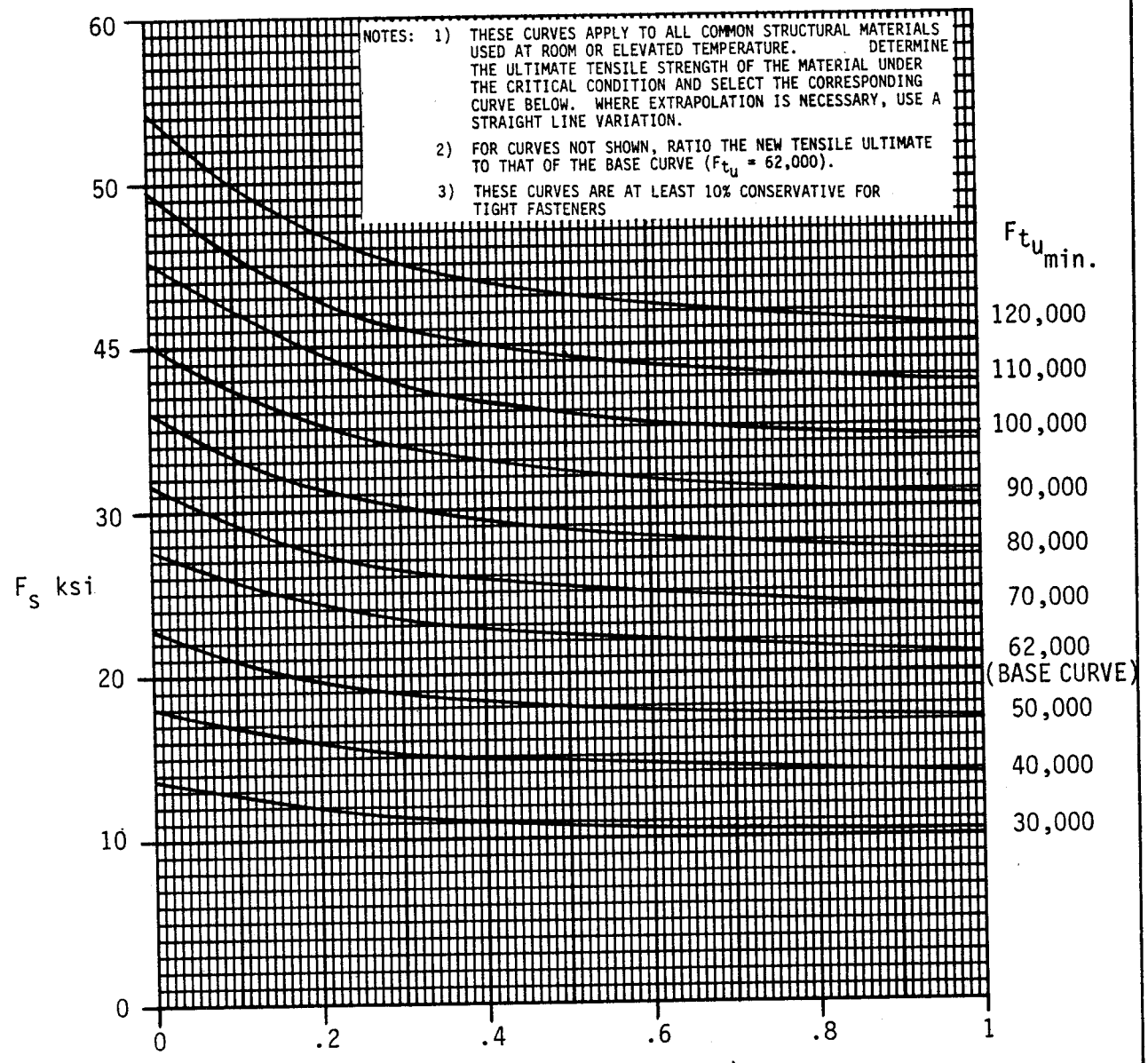


NOTE:

| MATERIAL | $F_{tu_{min.}}$ |
|---|---|
| 2024-T4 | 62,000 |
| 7075-T6 | 73,000 |

Figure B5.1.3.2-5 Allowable Gross Area Web Stress ($\alpha$ = 45°)

B5.1.3.3 Stiffener Analysis

Stiffeners for a diagonal tension beam are governed by the same stiffness criteria as for a shear resistant beam up to the onset of initial buckling. The required moment of inertia ($I_u$) to meet stiffness requirements is given by Equation B5-8. Once initial buckling occurs, axial stresses are introduced on the stiffener which set additional requirements for the stiffener moment of inertia and also set requirements for the stiffener area ($A_u$).

A. Average Stiffener Applied Stress ($f_u$) - When the web buckles, additional compression stresses are introduced into the stiffener ($f_u$) and also the cap ($f_F$) as defined by the equations

$$f_u = \frac{-k\, f_s \tan\alpha}{\frac{A_{u_e}}{dt} + .5\,(1-k)} \qquad \text{(B5-18)}$$

$$f_F = \frac{-k\, f_s}{\left[\frac{2A_F}{h_e t} + .5\,(1-k)\right] \tan\alpha} \qquad \text{(B5-19)}$$

The angle $\alpha$ in these equations is defined by the equations

$$\tan^2\alpha = \frac{\varepsilon_w - \varepsilon_F}{\varepsilon_w - \varepsilon_u} \qquad \text{(B5-20a)}$$

$$\varepsilon_u = \frac{f_u}{E_u} \qquad \text{(B5-20b)}$$

$$\varepsilon_F = \frac{f_F}{E_F} \qquad \text{(B5-20c)}$$

$$\varepsilon_w = \frac{f_s}{E_w}\left[\frac{2k}{\sin 2\alpha} + (1-k)(1+\mu)\sin 2\alpha\right] \qquad \text{(B5-20d)}$$

The stiffener effective area ($A_{u_e}$) is given by the equations

$$A_{u_e} = A_u \text{ for back-to-back stiffeners} \qquad \text{(B5-21a)}$$

$$A_{u_e} = \frac{A_u}{1 + \left(\frac{e}{\rho}\right)^2} \quad \text{for single stiffeners} \qquad \text{(B5-21b)}$$

Note: $A_u$ does not include web area.

If the stiffeners have a very deep web, such as a bulkhead between spars which is flanged over and attached to the spar web, then assume that

$$A_{u_e} = 12\ t_u^2 \qquad \text{(B5-21c)}$$

Based on Equations B5-18 through B5-21, stiffener stress ($f_u$) must be found by successive approximations. Thus, assume $\alpha$; solve for $f_u$ and $f_F$; solve for $\varepsilon_u$, $\varepsilon_F$, and $\varepsilon_w$. Then solve for $\alpha$ from Equation B5-20a. (Note that the strains $\varepsilon_u$ and $\varepsilon_F$ are negative.) If the calculated $\alpha$ does not agree with assumed $\alpha$, then use it as the next approximation. Three iterations are usually enough to get agreement. Then $f_u$ and $f_F$ may be determined from Equation B5-18 and -19.

For most practical designs the sine $2\alpha$ is near 1.0 because $\alpha$ lies between $38^0$ and $45^0$. Also, $\varepsilon_F$ is usually negligible with respect to $\varepsilon_w$. Figure B5.1.3.3-1 is plotted from Equation B5-18, based on these assumptions, as a function of $A_{u_e}/dt$ and k. The value used for tan $\alpha$ is defined in Figure B5.1.3.3-2. From Figure B5.1.3.3-1, $f_u$ is determined as

$$f_u = f_s \left(f_u/f_s\right) \qquad \text{(B5-22a)}$$

This value, $f_u$, is based on an effective area . Gross area stiffener stress should be determined from the ratio of $A_{u_e}/A_u$ as

$$f_{u_{gross}} = f_u \left(A_{u_e}/A_u\right) \qquad \text{(B5-22b)}$$

$$\frac{f_u}{f_s} = \frac{k \tan \alpha}{\frac{A_{ue}}{dt} + 0.50\ (1-k)}$$

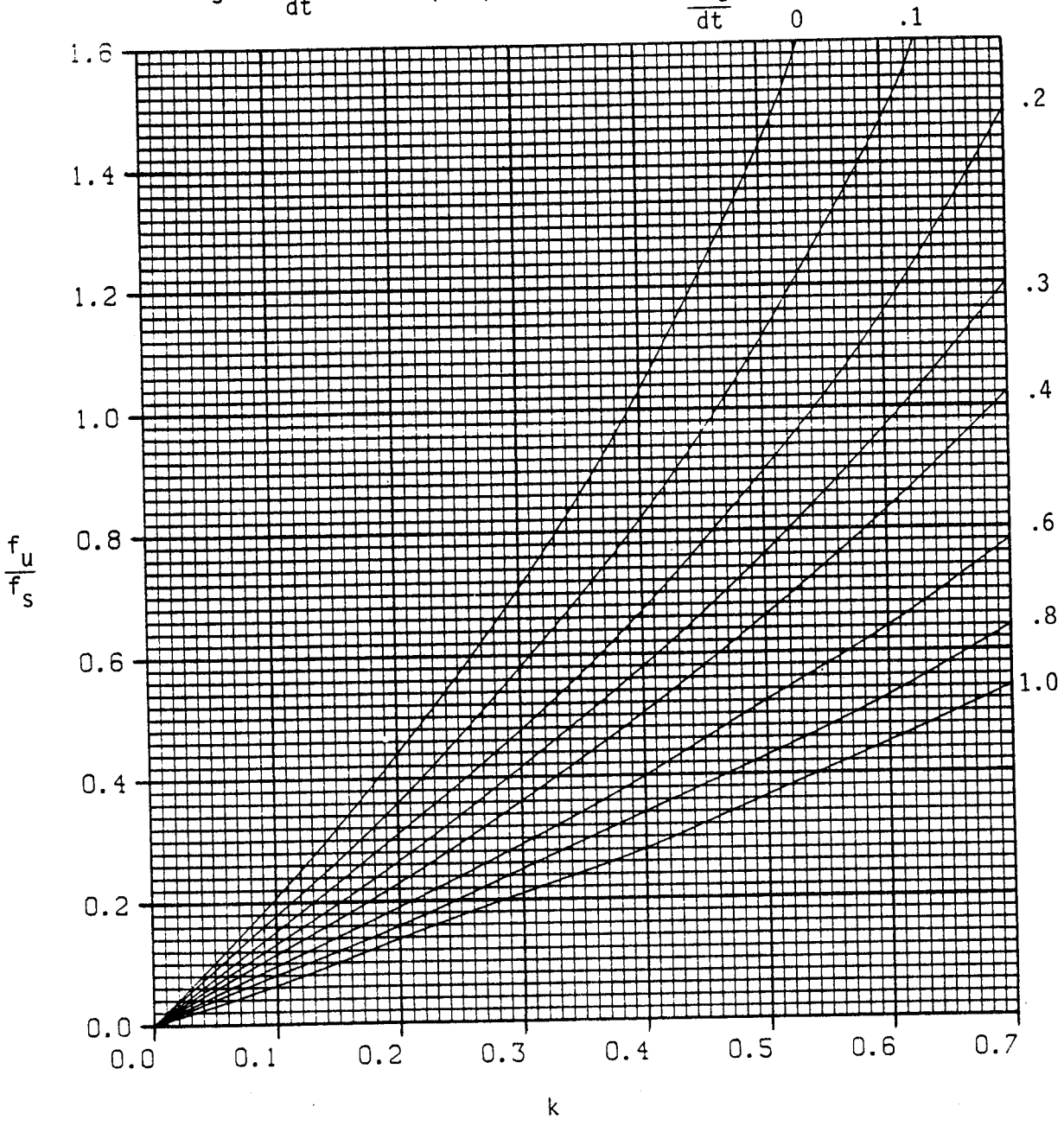


Figure B5.1.3.3-1 Stiffener Stress Ratio

Ref. B5-1

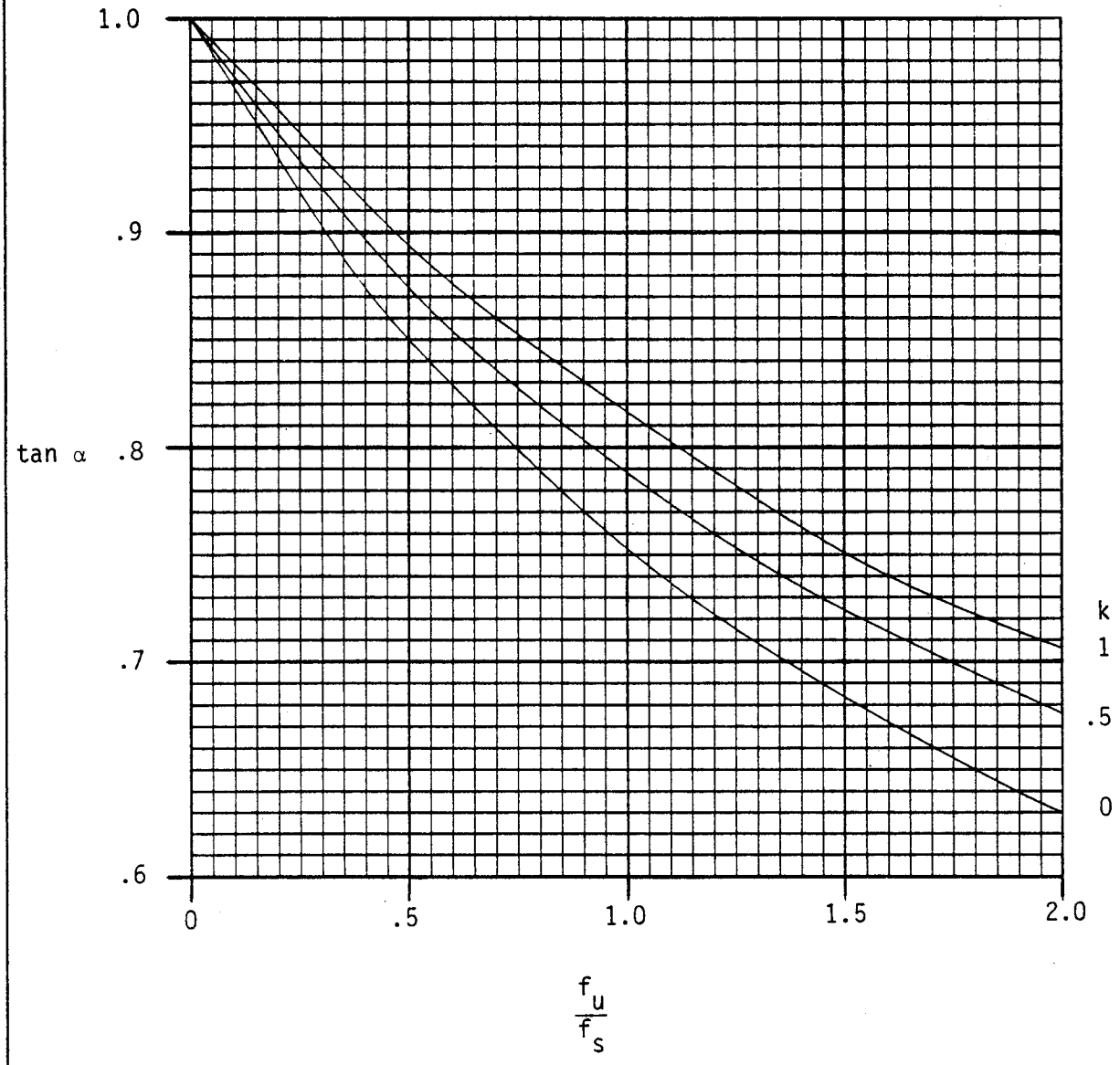


Figure B5.1.3.3-2 Values for tan α Used With Figure B5.1.3.3-1

Ref. B5-1

B. Maximum Stiffener Applied Stress ($f_{u_{max}}$) - Under a condition of pure diagonal tension (and constant shear load along the depth of the beam) the stiffener stress would be constant along its length. Because this ideal condition is never attained, the stiffener stress actually has a maximum value at the middle of the stiffener and a lesser value towards the ends, a fact referred to as "gusset effect."

Figure B5.1.3.3-3 gives an empirical relationship for the ratio of maximum stress-to-average stress ($f_{u_{max}}/f_u$) as a function of k and $d/h_e$. $f_{u_{max}}$ is then determined as

$$f_{u_{max}} = f_u \left( \frac{f_{u_{max}}}{f_u} \right) \qquad \text{(B5-23)}$$

C. Allowable Stress in Stiffener - Possible stiffener failure modes are forced crippling and column failure. Both modes are difficult to analyze and empirical results are required.

1. Forced Crippling ($F_o$) - The shear buckle which forms in the web tends to force a buckle in the stiffener leg attached to the web. The stiffener thus weakened will in turn induce buckling in the outstanding leg which leads to stiffener failure. This effect is most pronounced in stiffeners where $t_u$ is less than t. Since this type of crippling is of a local nature, it is assumed to depend upon the maximum stiffener stress, $f_{u_{max}}$.

The allowable stress for forced crippling ($F_o$) has been determined based on tests for panels with angle and Z-stiffeners as a function of the diagonal tension factor k and the ratio $t_u/t$ for 2024 and 7075 aluminum. It is defined conservatively (possibly as much as 25 percent) by the following equations: (Note: If test results are available, they should override these equations.)

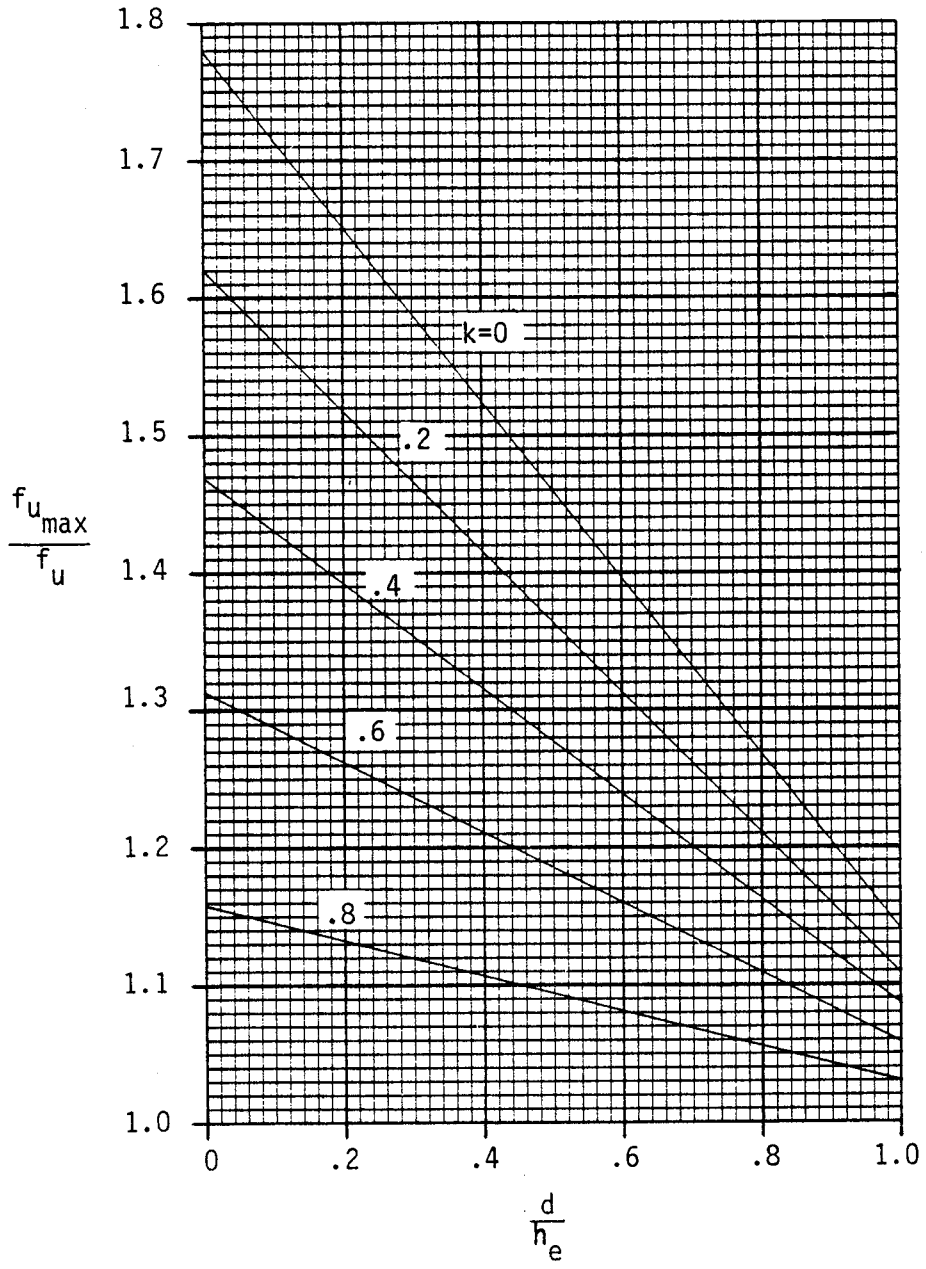


NOTE: On curved webs; for rings, read abscissa as $\frac{d}{h}$; for stringers, read abscissa as $\frac{h}{d}$

Figure B5.1.3.3-3 Ratio of Maximum Stress to Average Stress in Web Stiffener

Ref. B5-1

For 2024-T3 Aluminum Alloy

$$F_o/\eta_p = 26{,}000\ k^{2/3}\ [t_u/t]^{1/3} \qquad \text{(B5-24a)}$$

Single Stiffener

$$F_o/\eta_p = 20{,}982\ k^{2/3}\ [t_u/t]^{1/3} \qquad \text{(B5-24b)}$$

Back-to-Back Stiffener

For 7075-T6 Aluminum Alloy

$$F_o/\eta_p = 32{,}500\ k^{2/3}\ [t_u/t]^{1/3} \qquad \text{(B5-25a)}$$

Single Stiffener

$$F_o/\eta_p = 26{,}227\ k^{2/3}\ [t_u/t]^{1/3} \qquad \text{(B5-25b)}$$

Back-to-Back Stiffener

Equations B5-24a through B5-25b are plotted in Figures B5.1.3.3-4 for $F_o/\eta_p$ as a function of k and $t_u/t$.

For hat section stiffeners, no empirical data is available. Since the hat is supported on two edges, unlike an angle or a Z-shape, replace $t_u/t$ with $3t_u/t$ (the ratio of the square root of the buckling coefficients for two edges supported and one edge supported, the other free) in Equations B5-24 and 25.

When using Equations B5-24 and -25 for integral stiffeners, use $1.5t_w/t$ in place of $t_u/t$ where the the stiffener has an outstanding flange; use $t_w/t$ for stiffeners without an outstanding flange. ($t_w$ is the web thickness of the integral stiffener).

For stresses above the proportional limit, reduced stresses are obtained from a plot of $F_o$ vs $F_o/\eta_p$ where a conservative plasticity factor is used.

$$\eta_p = (E_T/E)^{1/2} \qquad \text{(B5-26)}$$

When this type data is not available, it may be generated from Equation B5-7 with E and $F_{cy}$ substituted for G and $F_{sy}$ respectively. Figure B5-1.3.3-5 through B5.1.3.3-7 are plotted for the more common materials used in design.

$$F_o/n_p = 26{,}000\ k^{2/3}\ (\frac{t_u}{t})^{1/3}$$

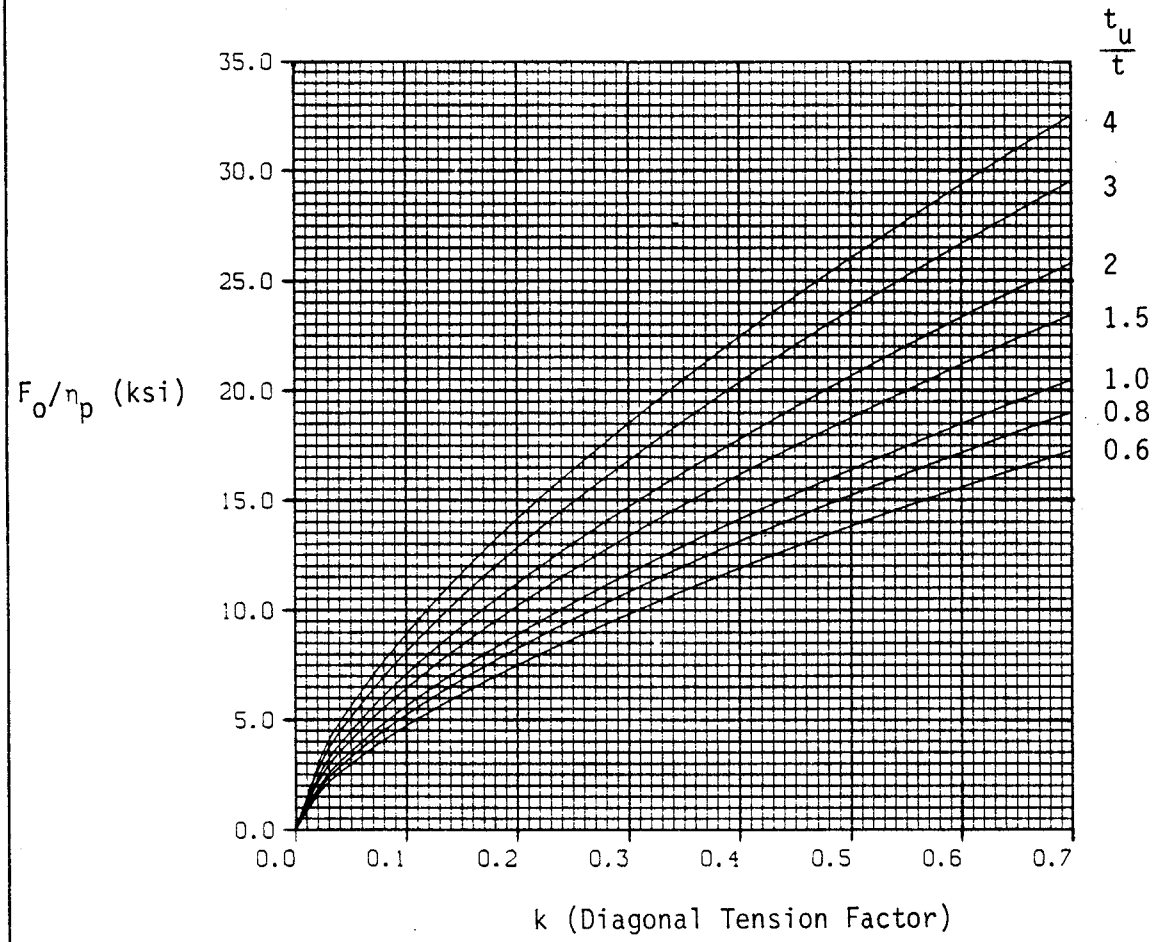


| Material | Single Stiff. Multiply $F_o$ by | Double Stiff. Multiply $F_o$ by |
|---|---|---|
| 2024-T3 | 1 | 0.807 |
| 7075-T6 | 1.25 | 1 |

B5.1.3.3-4 Forced Crippling - Single Stiffener 2024-T3

Ref. B5-1

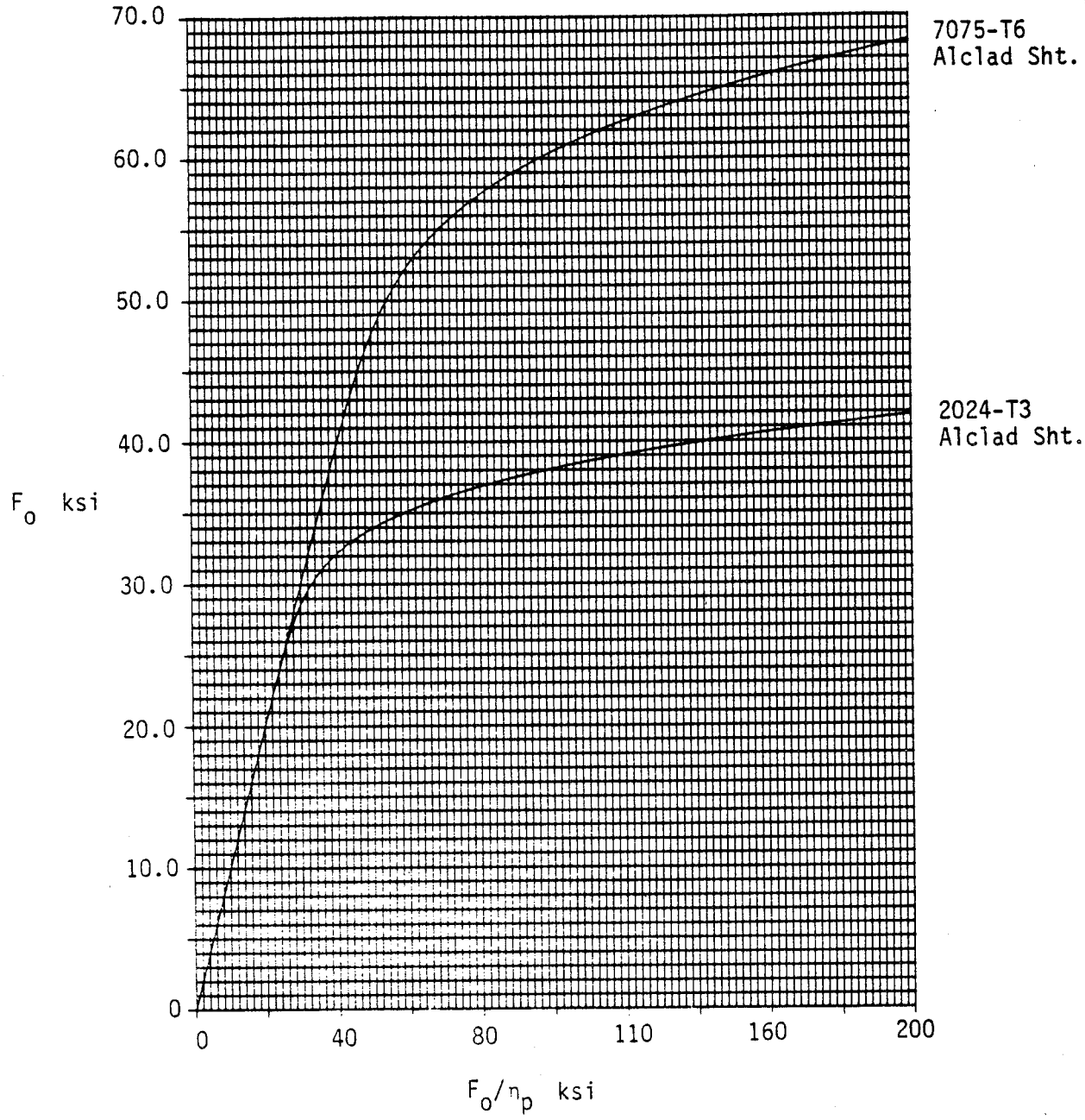


Figure B5.1.3.3-5 Plasticity Correction Curves for Forced Crippling of Alclad Aluminum Sheet

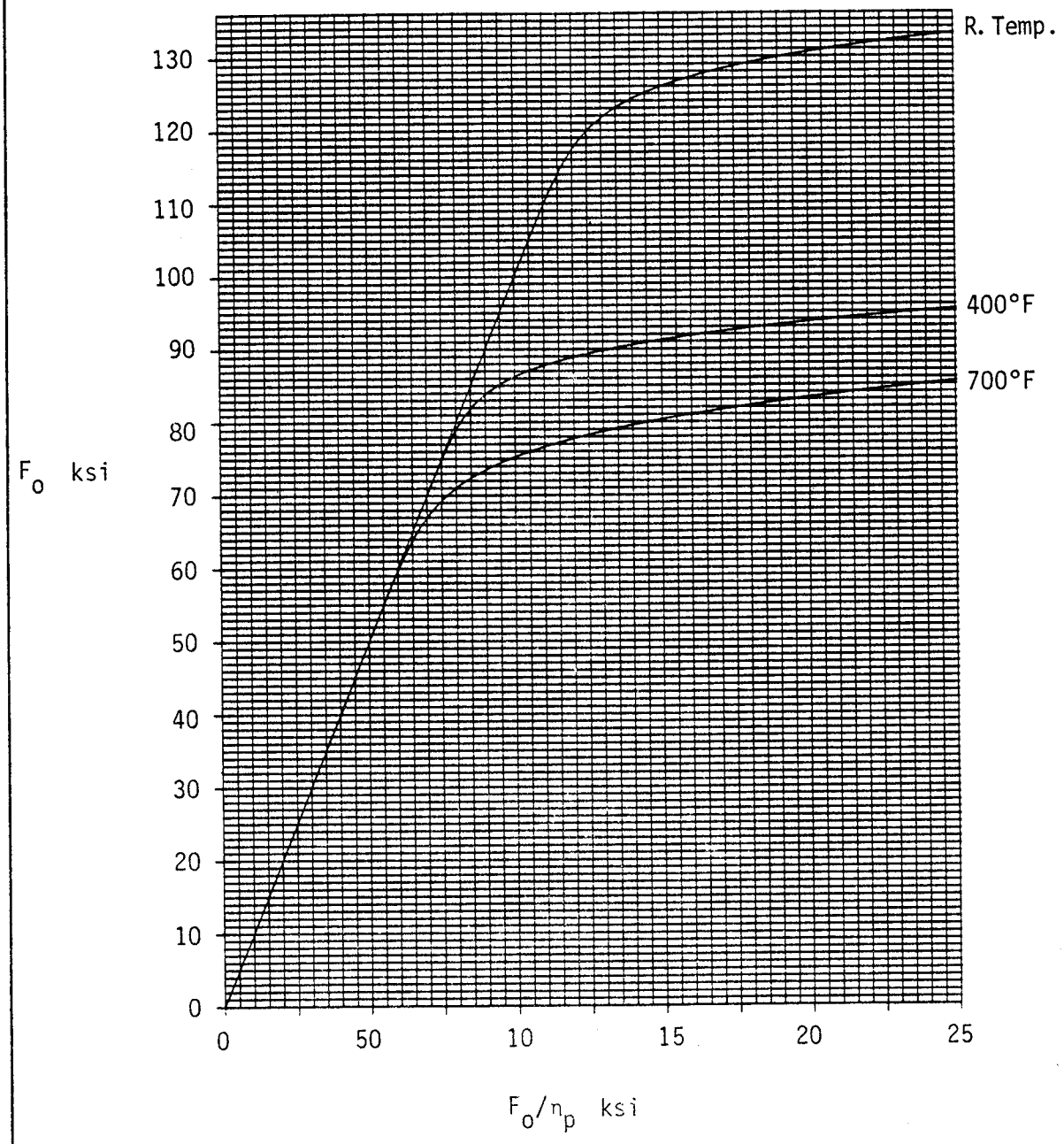


Figure B5.1.3.3-6 Plasticity Correction Curves for Forced Crippling of 6Al-4V Titanium Sheet at Selected Temperature

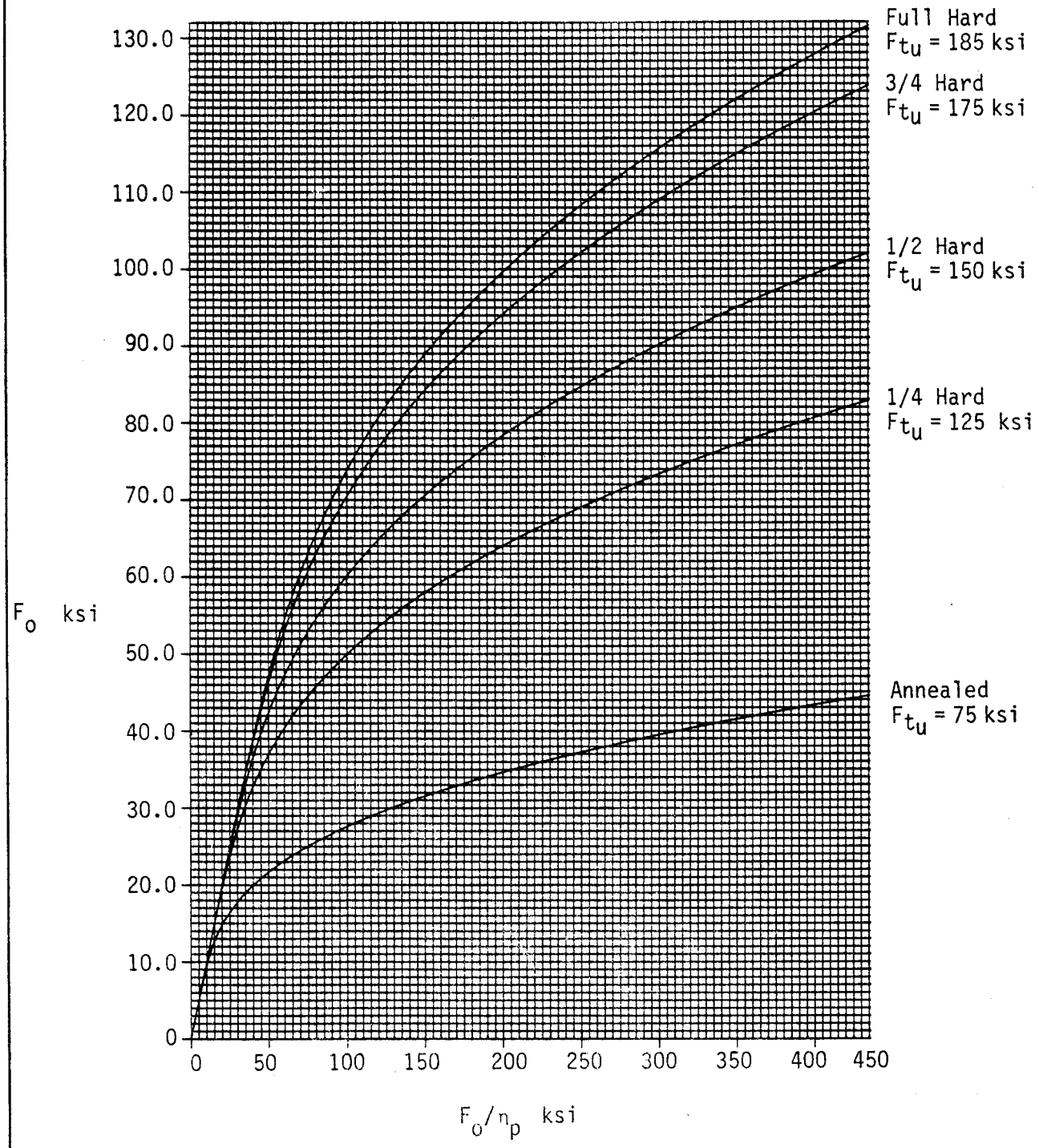


Figure B5.1.3.3-7 Plasticity Correction Curves for Forced Crippling of AISI 301 Stainless Steel Sheet

$F_o$ should be compared with $f_{u_{max}}$ for determining margins of safety,

$$M.S. = \frac{F_o}{f_{u_{max}}} - 1 \qquad \text{(B5-27)}$$

2. Column Failure ($F_c$) - The buckling strength of diagonal tension beam stiffeners cannot be handled by simple column theory because the web restrains the stiffener against buckling. As soon as the stiffener begins to buckle out of the plane of the web, the tension diagonals at the stiffener become kinked which introduce a restraining kick force distributed along the stiffener length that is proportional to the deflection. This type of column action is handled by effective column length equations based on test data. For back-to-back stiffeners

$$L' = \frac{h_e}{\sqrt{1 + k^2(3-2d/h_e)}} \quad \text{for } d < 1.5\ h_e \qquad \text{(B5-28)}$$

$$L' = h_e \text{ for } d > 1.5\ h_e$$

For single uprights

$$L' = h_e/2 \qquad \text{(B5-29)}$$

Based on these effective column lengths, column allowable strength ($F_c$) may be determined by either the Euler-Engesser equation or Johnson's parabola as discussed in Section B6. Test curves of $F_c$ vs $L'/\rho$ may also be used as given in Section E6. The resulting value of $F_c$ should be compared with $f_{u_{gross}}$, Equation B5-22b. Thus

$$M.S. = \frac{F_c}{f_{u_{gross}}} - 1 \qquad \text{(B5-30a)}$$

For single stiffeners, the applied stress $f_u$ (Equation B5-22a) should not exceed the crippling strength of the stiffener ($F_{cc}$) as determined in Section B6. Thus

$$M.S. = \frac{F_{cc}}{f_u} - 1 \qquad \text{(B5-30b)}$$

B5.1.3.4 Cap Analysis

The cap axial component of the diagonal tension stress ($f_F$), defined by Equation B5-19, increases the cap primary stress on the compression side and decreases the cap primary stress on the tension side. Primary stress ($f_b$) is determined by simple Mc/I or $M/(h_e A_F)$ analysis.

A bending moment is created in the cap between the stiffeners due to the vertical component of the diagonal tension stress $f_u$, defined by Equation B5-18. This moment creates a sagging effect on the cap between the stiffeners. The maximum moment over the stiffeners is given by the equation

$$M_{sb} = \frac{1}{12} k f_s t d^2 \tan\alpha \, C_3 \qquad \text{(B5-31)}$$

where $C_3$ is given in Figure B5.1.3.2-4b. Refer to Section B5.1.3.3A for computation of $\tan\alpha$, or use Figure B5.1.3.3-2 if simplifying assumptions were used.

Cap bending stress $f_{sb}$ is determined from the simple beam equation $M_{sb}c/I_F$ where c is the distance from the cap neutral axis to the extreme outer fiber. Effective web should be included in determining c and $I_F$, but is usually neglected because of its small contribution. For calculating bending stress, use c as defined in Figure B5.1.3.4-1 for the tension and compression cap, respectively.

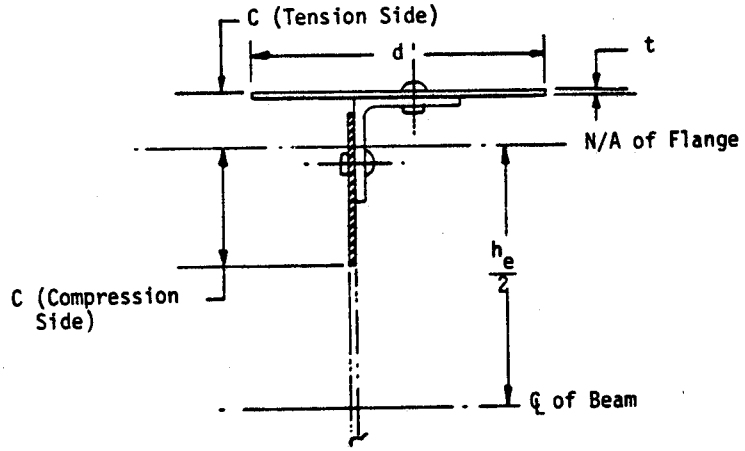


Figure B5.1.3.4-1 Definition of c for Tension and Compression Cap

The cap margin of safety is then determined from the equation

$$M.S. = \frac{1}{\frac{f_b + f_F}{F} + \frac{f_{sb}}{F_{BM}}} - 1 \qquad \text{(B5-32)}$$

F is the appropriate material allowable stress, tension ultimate or compression yield, and $F_{BM}$ is the modulus of rupture for the cap section.

B5.1.3.5 Attachments

A. Web-to-Cap Attachments - These attachments carry a running load per inch ($q_A$) equal to

$$q_A = \frac{S}{h_A}(1 + 0.414\ k) \qquad \text{(B5-33)}$$

where $h_A$ is the distance between the centroids of the attachment patterns for the top and bottom caps (in general $h_A \neq h_e$). Based on Equation B5-33, the load per attachment can be calculated based on the spacing. This value must be greater than the attachment allowable strength as given in Section C1. Values for $q_A$ from Equation B5-33 are plotted in Figure B5.1.3.5-1 as a function of $S/h_A$ and k.

B. Web-to-Stiffener Attachments - These attachments must have a shear strength to transfer differences in shear load between adjacent web bays to the stiffener. In addition, they must have a tension strength to prevent the wrinkled web from pulling away from the stiffener. The tension load developed for this type of action is defined for compression panels stiffened with single Z-type stiffeners in Section B6.3.5.

For single stiffeners, determine the attachment load $R_R$ from Equation B6-29 and the experimental data of Figure B6.3.5-2 in Section B6. The attachment tension load is determined from Equation B6-29:

$$R_R = \frac{E}{1-\mu^2}\frac{1}{(f/t_w)^3}\left[\frac{(3)(f/t_w) + b_w/t_w}{(3)(f/t_w) + (4)(b_w/t_w)}\right]\frac{t_s}{5}\,p \qquad \text{(B5-34a)}$$

where $f/t_w$ is an empirical term determined from Figure B6.3.5-2 based on the values of $b_o/t_u$ and p/D.

(Note: p is attachment pitch and D is attachment diameter.)

$$q_A = q\ (1 + 0.414\ k)$$

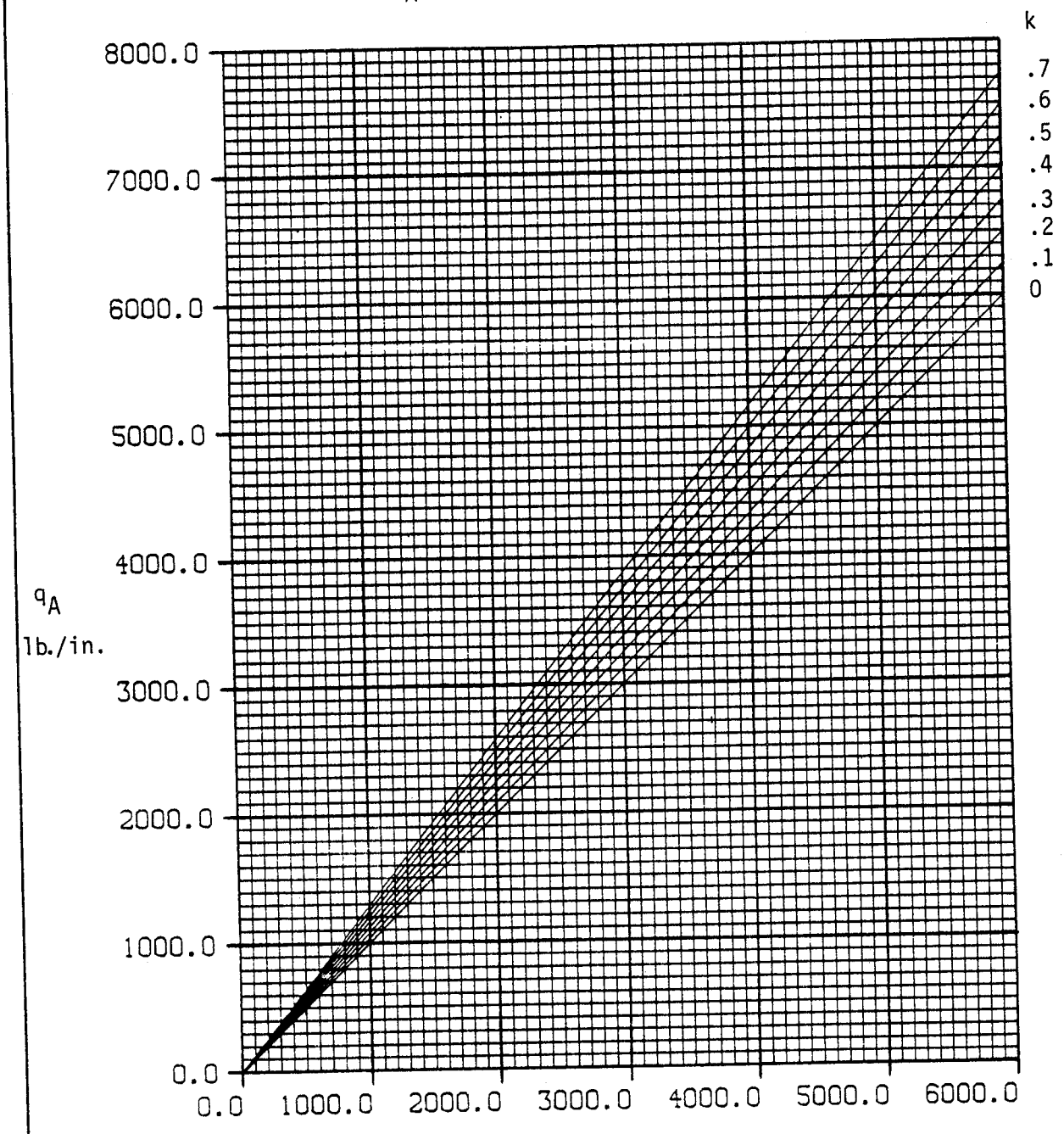


$$q = \frac{S}{h_A}\ \text{lb./in.}$$

Figure B5.1.3.5-1 Rivet Loads, Web-to-Flange

$t_s$ is the beam web thickness, bw and tw are the stiffener web length and thickness, respectively.

For back-to-back stiffeners, the requirements are not as clear. Reference B5-1 gives a tentative criteria that attachments have a tension capability greater than:

$(0.15)(F_{tu})(t)$ for back-to-back stiffeners

$(0.22)(F_{tu})(t)$ for single stiffeners

This criteria has been shown to be too conservative. However, the ratio 0.15/0.22 = 0.68 is valid for use. Therefore, for back-to-back stiffeners calculate tension load in the attachment as:

$$R_{R_{BB}} = 0.68\, R_{R_S} \qquad \text{(B5-34b)}$$

The allowable attachment tension strength is given in Section $C_1$ for protruding head and flush rivets.

Web-to-stiffener attachments should be spaced 4 to 5D apart to prevent permanent buckles from forming between attachments.

C. Stiffener-to-Cap Attachments - These end attachments must transfer the stiffener end load to the cap. This end load is defined as

$$P_u = f_u A_{u_e} \qquad \text{(B5-35)}$$

This equation neglects the gusset effect (decrease in $f_u$ toward the end of the stiffener) and is conservative. However, web-to-cap shear forces are neglected which make Equations B5-35 a close approximation of the load.

The guidelines of Section B5.1.2.5C should also be followed for stiffener-to-cap attachments. Thus, these end attachments should be higher strength than the basic stiffener-to-web attachments.

B5.1.3.6 Beam End Bay Reinforcement

Just as diagonal tension forces produce vertical forces which cause sagging of the caps and are reacted by the beam stiffeners; they also produce horizontal forces which must also be reacted to avoid end sagging. Generally, this is done on either end of the beam with horizontal stiffeners (and/or closer spaced vertical stiffeners) and web doublers as shown in Figure B5.1.3.6-1.

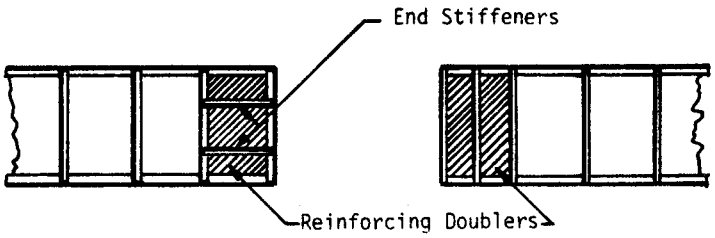


Figure B5.1.3.6-1 End Bay Reinforcement

End reinforcing should be designed to resist a uniformly distributed end load due to diagonal tension horizontal forces as given by the Equation

$$w = \frac{k\ t\ f_s}{\tan \alpha} \qquad \text{(B5-36)}$$

The value for $\tan \alpha$ should be the same as determined in Section B5.1.3.3A.

B5.1.3.7 Design Approach

Semi-tension field beam design is similar to shear resistant beam design. Thus, the procedure is basically one of trial and error with q and $h_e$ as the given parameters. Lightest weight design is obtained for the smallest possible web thickness (t) to carry the shear load. Web thickness required is a function of the diagonal tension factor (k) and is limited by the allowable shear strength for the web material as defined in Figure B5.1.3.2-5.

Once web thickness is determined, stiffener area ($A_u$) should be set as small as possible consistent with the stiffener loads introduced by diagonal tension or other outside loading such as pressure.

Cap area ($A_F$) should be sized to meet the primary bending stresses on the beam as well as the additional stresses caused by diagonal tension forces, both axial and bending.

The primary difference between semi-tension field beam design and shear resistant beam design is that the former requires the evaluation of many more equations in arriving at the final design solution. A computer program is available to aid in the design selection process. This program is described in Section E7.

Some simple observations can be made to aid the designer in preliminary sizing of semi-tension field beams, regarding web, stiffener, and cap dimensions.

A. Web - For the web, maximum stress is a function of the applied stress $f_s$, the diagonal tension factor k, and a constants $C_1$ and $C_2$. For $\tan\alpha = 1.0$, $C_1 = 0$. $C_2$ varies as a function of cap moment of inertia and the ratio $h_e/t$. This latter value should be between 200 and 1500. For minimum weight, the highest value is appropriate. Also, for most beams, the moment of inertia of the caps seldom exceeds 1.0. Based on these assumptions, the term $\omega d$ for determining $C_2$ will rarely exceed 2.0 for reasonable stiffener spacings; say 6 to 12 inches. Therefore, a reasonable maximum value for $C_2$ is 0.10. Also based on Equation B5-15 the maximum value for the diagonal tension factor k to avoid excessive deformations at ultimate load is 0.78. With these limitations, the maximum value to be expected for $f_{s_{max}}$ from Equation B5-16 is $f_{s_{max}} = 1.08$ fs from which it follows that a good approximation for web thickness based on Equation B5-4 and B5-17 is

$$t = \frac{1.08q}{F_s} \qquad \text{(B5-37)}$$

where $F_s$ should be taken from Figure B5.1.3.2-5 for the appropriate material with k = 0.78.

B. Single Stiffeners - For single stiffeners, the NACA gives the following guidelines for determining effective stiffener area.

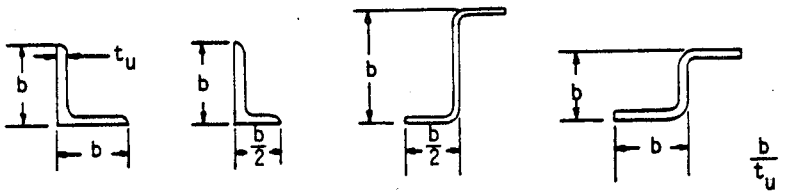


| $\frac{A_{ue}}{A_u}$ | | | | |
|---|---|---|---|---|
| .51 | .41 | .40 | .44 | 8 |
| .57 | .46 | .40 | .44 | 16 |

B5.1.3.7-1 Ratio of Effective to Actual Area of Uprights

Follow these guidelines as an aid in establishing the effective stiffener area for single stiffeners.

C. Caps - For caps, the stress from Equation B5-19 is

$$f_F = - \frac{k\, f_s}{\tan \alpha \left[ \frac{2A_F}{h_e t} + .5\,(1-k) \right]}$$

Most aircraft shear panels have ratios $2A_F/h_e t$ less than 2.0 and as previously noted k should be about 0.78 maximum for minimum weight. With these assumptions, the cap stress due to semi-tension field should be about

$$f_F \simeq 0.40\, f_s \qquad \text{(B5-38)}$$

This stress must be added to the basic compression stress as determined by $M/h_e$ relationships.

The cap bending stresses are given by Equation B5-31

$$M_{sb} = \frac{1}{12} k f_s t d \tan \alpha\, C_3$$

As with the stiffeners, $\omega d$ rarely exceeds 2. Therefore, $C_3$ can be taken as 1.0 and k can be assumed to be 0.78 as a first approximation. With $\alpha = 45^o$, the cap bending stress can be determined for compression as

$$f_{sb} \simeq 2qd \qquad \text{(B5-39)}$$

where c/I has been assumed equal 30 which is representative of most aircraft cap members. Tension bending stress will rarely be a problem since the distance from the neutral axis to the outer fiber is so small. These relationships, Equation B5-38 and B5-39 combined with the interaction equation B5-32 give the following approximate relationship for the compression cap area.

$$A_F \simeq \frac{M/h_e}{\left(1 - \frac{2qd^2}{F_{BM}}\right) F_{cy} - 0.4\, f_s} \qquad \text{(B5-40)}$$

B5.1.3.8 Sample Problem (Semi-Tension Field Beam)

Given: $q$ = 500 lb/in (ultimate)

$M$ = 400,000 in lb (constant - ultimate)

$h$ = 20 inch

Web Material = 7075-T6 Alclad

$F_{tu}$ = 73,000 psi
$E$ = 10.3 x $10^6$ psi } (Ref. B5-2)
$\mu$ = 0.30

Stiffener and Cap Material = 7075-T6 Ext.

$F_{tu}$ = 82,000 psi
$F_{cy}$ = 74,000 psi } (Ref. B5-2)
$E_c$ = 10.7 x $10^6$

Assume Stiffener is a Z-Section and the Cap is a Tee Section

Constraints: Minimum Weight is Required
$d$ = 6.0 inch (minimum)
$t$ = 0.010 inch (minimum)

Step 1. First check to see if a semi-tension field beam is the most efficient design from Equation B5-1. Assume $h_e$ = h-0.5 = 20 - .5 = 19.5, then

$$q/h_e = 500/19.5 = 25.6 < 49$$

Thus, a semi-tension field beam is efficient.

Step 2. Find the web thickness and $f_s$

From Equation B5-37 with $F_s$ = 25,000 psi from Figure B5.1.3.2-5 for k = .78 and $F_{t_u}$ = 73,000 psi

$$t = \frac{1.08q}{F_s} = \frac{1.08(500)}{25,000} = 0.022 \text{ inch}$$

Use closest, lower standard gauge, t = 0.020 since Equation B5-37 should be conservative; then

$$f_s = \frac{500}{0.020} = 25,000 \text{ psi}$$

Step 3. Find the initial buckling stress ($F_{s_{cr}}$) (assume $\eta_s = 1.0$)

First calculate the buckling coefficient based on $d/h_e$ = 6.0/19.5 = 0.310 from Figure B5.1.2.3-2. As already noted, simply supported edge conditions should be used unless supporting test data is available.

Thus $k_{s_\infty}$ = 5.35 (simple support)

$k_s/k_{s_\infty}$ = 1.09 from Figure B5.1.2.3-2 and

the modified buckling coefficient is

$$K_s = 1.09\ (5.35)\ \frac{\pi^2}{12\left(1-0.3^2\right)} = 5.27$$

The critical stress is then determined from equation B5-5 as

$$F_{s_{cr}} = K_s \eta_s E \left[\frac{t}{d}\right]^2 = 5.27\ (1.0)(10.3\text{x}10^6)\left[\frac{0.020}{6}\right]^2 = 603 \text{ psi}$$

Step 4. Find the diagonal tension factor k for

$$\frac{f_s}{F_{s_{cr}}} = \frac{25,000}{603} = 41.5$$

Then from Figure B5.1.3.2-3 or Equation B5-14

$$k = \tanh [.5 \log_{10}(f_s/F_{s_{cr}})] = \tanh (.5 \log_{10} 41.5) = 0.67$$

This value is checked with Equation B5-15 to assure excessive wrinkling will not occur. Thus

$$k_{max} = 0.78-(t-.012)^{1/2} = 0.78-(0.020-.012)^{1/2} = 0.69$$

Excessive wrinkling is no problem.

Step 5. Find the stiffener area.

For minimum weight, $A_u$ should be about 30 percent of dt. Thus

$$A_u = 0.30(6)(0.020) = 0.036 \text{ in.}$$

However, based on Figure B5.1.3.7-1 for Z sections, the actual area must be greater than

$$A_u = \frac{A_{u_e}}{0.40} = \frac{0.036}{0.40} = 0.090 \text{ in.}^2$$

which accounts for single-sided stiffeners.

From the Standards Manual, page 607.125, S1647068 meets this area requirement reasonably closely.

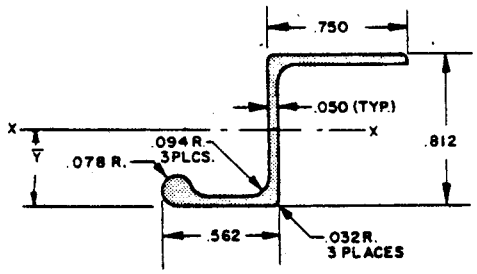


$A_u = 0.112 \text{ in.}^2$, $I_{xx} = 0.0118 \text{ in.}^4$, $\bar{y} = .400 \text{ in.}$

Equation B5-21b is used as a further check. Thus,

$$A_{u_e} = \frac{A_u}{1 + \left(\frac{e}{\rho}\right)^2} = \frac{0.112}{1 + \left(\frac{.412 + .010}{.325}\right)^2} = 0.042$$

which is close to the minimum stiffener area requirement of 0.036.

The ratio $f_u/f_s$, found from Figure B5.1.3.3-1 with $k = 0.67$ and $A_{u_e}/dt = 0.35$, is 1.05. $f_u$ is found from Equation B5-22a, $f_u = (f_u/f_s)\, f_s = (1.05)(25{,}000) = 26{,}250$ psi.

Gross stiffener stress is given by Equation B5-22b as

$$f_{u_{gross}} = f_u\left(\frac{A_{u_e}}{A_u}\right) = 26{,}250\left(\frac{.042}{0.112}\right) = 9844 \text{ psi}$$

Maximum stiffener stress is determined from Figure B5.1.3.3-2 for $k = 0.67$ and $d/h_e = 0.31$, and from Equation B5-23

$$f_{u_{max}} = f_u\left(\frac{f_{u_{max}}}{f_u}\right) = 26{,}250\ (1.2) = 31{,}500 \text{ psi}$$

These applied stresses must be compared to the allowable stresses for forced crippling and column buckling.

Forced crippling stress is obtained from Equation B5-25a where $\eta_p$ is taken as 1.0 as a first approximation

$$F_o/\eta_p = 32{,}500\ (k)^{2/3}\left(\frac{t_u}{t}\right)^{1/3}$$

$$= 32{,}500\ (0.67)^{2/3}\left(\frac{0.050}{.020}\right)^{1/3} = 33{,}759 \text{ psi}$$

From Equation B5-27

$$M.S. = \frac{F_o}{f_{u_{max}}} - 1 = \frac{33{,}759}{31{,}500} - 1 = +0.07$$

Column allowable stress can either be determined from the Euler Engesser equation or Johnson's Parabola, but since the section b/t's are so high, the latter method will be used. The crippling stress determined for this method is also useful for comparing with the average upright effective area stress. Crippling stress is best handled by tabular form.

Based on data in Section B6, $F_{cc}$ is determined thus

| Element | b | t | A | b/t | $\sqrt{F_c/E(b/t)}$ | $F_{cc}/F_{cy}$ | $F_{cc}$ | $F_{cc}A$ |
|---|---|---|---|---|---|---|---|---|
| 1 | .725 | .05 | .036 | 14.5 | 1.217 | .5 | 37,000 | 1332 |
| 2 | .762 | .05 | .038 | 15.24 | 1.279 | 1.0 | 74,000 | 2812 |
| 3 | .459 | .05 | .023 | 9.18 | .763 | .7 | 51,800 | 1191 |
| 4 | - | - | .010 | | - | - | 74,000 | 740 |
| | | | .107 | | | | | 6075 |

$$F_{cc} = \frac{6075}{0.107} = 56{,}776 \text{ psi}$$

Then from Johnson's Parabola, the column allowable stress is

$$F_c = F_{cc} - \frac{F_{cc}^2}{4\pi^2 E}(L'/\rho)^2 \text{ where } L' = \frac{19.5}{2} = 9.75 \text{ for}$$

for single sided stiffeners.

$$F_c = 56{,}776 - \frac{56{,}776^2}{4\pi^2\,(10.7 \times 10^6)}\left(\frac{9.75}{0.325}\right)^2 = 49{,}907 \text{ psi}$$

These stresses ($F_{cc}$ and $F_c$) are used in Equations B5-30 a and b to give the following margins of safety

$$\text{M.S.} = \frac{F_c}{f_{u_{gross}}} - 1 = \frac{49{,}907}{9{,}844} - 1 = +4.07$$

$$\text{M.S.} = \frac{F_{cc}}{f_u} - 1 = \frac{56{,}776}{26{,}250} - 1 = +1.16$$

Step 6. Find cap area. From Section B1, page B1-43 the bulk modulus stress for a 7075-T6 extrusion with a section modulus of 1.5 is 118,000 psi. Then from Equation B5-40

$$A_F = \frac{M/h_e}{\left[1 - \frac{2qd^2}{F_{BM}}\right] F_{cy} - .4\, f_s} =$$

$$\frac{400{,}000/19.40}{\left(1 - \frac{2(500)6^2}{118{,}000}\right) 74{,}000 - .4\,(25{,}000)} = 0.50 \text{ in.}^2$$

From the Standards Manual, page 603.132, cross section D nearly meets the requirements.

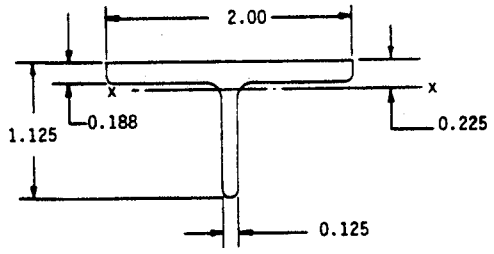


$A = 0.498 \text{ in.}^2$, $I_{xx} = 0.371 \text{ in.}^2$, $\bar{y} = 0.225$ in.

Based on these section properties, the exact value of $h_e$ is determined as $h_e = h - (2)(\bar{y}) = 20 - 2\,(.225) =$ 19.55 in. Note: $h_e = 19.50$ was assumed to start the design. The crippling allowable for the T section is calculated as $F_{cc} = 69{,}278$ psi from data in Section B6.

The cap axial stress components are calculated from $M/h_e$ analyses and Equation B5-19, where tan $\alpha$ is obtained from Figure B5.1.3.3-2 as 0.78. Due to the external moment

$$f_b = \frac{M}{h_e A_F} = \frac{400{,}000}{19.55(.498)} = 41{,}085 \text{ psi}$$

Due to diagonal tension

$$f_F = \frac{k\, f_s}{\tan\alpha \left[\frac{2A_F}{h_e t} + .5\,(1-k)\right]} =$$

$$\frac{0.67\,(25{,}000)}{0.78\left[\frac{2(.498)}{19.55(0.020)} + .5\,(1-0.67)\right]} = 7917 \text{ psi}$$

The axial stress for the compression side is

$$f_c = 41{,}085 + 7{,}917 = 49{,}002 \text{ psi}$$

Bending stress for the compression cap is calculated from Equation B5-31 and Mc/I. Thus

$$M_{sb} = \frac{1}{12} k\, f_s\, td^2 \tan\alpha\, C_3$$

where $C_3$ equals 1.0 from Figure B5.1.3.2-4b based on

$$\omega d = .7 \sqrt[4]{\frac{t}{(I_C+I_T)h_e}} =$$

$$.7(6) \sqrt[4]{\frac{.020}{(.0371 + .0371)\ 19.55}} = 1.44$$

Therefore,

$$M_{sb} = \frac{1}{12}(0.67)(25{,}000)(0.020)(6)^2(0.78)(1) = 784 \text{ in.-lb.}$$

and $$f_{sb} = \frac{Mc}{I_F} = \frac{784\,(.900)}{.0371} = 19{,}019 \text{ psi}$$

The margin of safety for the cap is calculated from Equation B5-32 as

$$M.S. = \frac{1}{\frac{f_c}{F_{cc}} + \frac{f_{s_b}}{F_{BM}}} - 1 = \frac{1}{\frac{49{,}002}{69{,}278} + \frac{19{,}019}{118{,}000}} - 1 = +.15$$

Step 7. Check margin of safety for web from Equation B5-17. Values for $f_{s_{max}}$ and $F_s$ are required. $f_{s_{max}}$ is defined by Equation B5-16. $C_1$ is obtained from Figure B5.1.3.2a. For $\tan \alpha = 0.78$, $C_1 = .03$. The constant $C_2$ is found from Figure B5.1.3.2b (where $\omega d = 1.44$) to be 0.02.

Note: The assumption of $C_2 = .1$ was made in preliminary calculation of t from Equation B5-37. From Equation B5-16

$$f_{s_{max}} = [(1 + k^2 C_1)(1 + k\, C_2)]\, f_s =$$

$$[1 + (.67^2)(.03)][1 + (.67)(.02)]\, 25{,}000 = 25{,}676 \text{ psi}$$

$F_s$ obtained from Figure B5.1.3.2-5 with $k = .67$ and $F_{t_u} =$ 73,000 psi is 25,805 psi.

The margin of safety from Equation B5-17 is

$$M.S. = \frac{F_s}{f_{s_{max}}} - 1 = \frac{25{,}805}{25{,}626} - 1 = +.007$$

Step 8. Check Attachments

The web-to-cap attachments are determined based on the applied load as given by Equation B5-33.

$$q_A = S/h_A\,(1 + 0.414k) =$$

$$10{,}000/18.87\,[1 + 0.414\,(0.67)] = 677 \text{ lbs./in.}$$

1/4 inch diameter rivets are adequate for this shear load at 1.0 inch spacing, based on fastener allowables in Section C1. Bearing is critical. The allowable is $139{,}000\,(.020)(.250)/1 = 695$ lbs./in.

For single stiffeners, the web-to-stiffener tension load requirement given by Equation B5-34 (for $b_o/t_u =$ $.285/.05 = 5.7$, $b_w/t_w = .762/.05 = 15.25$ and $p/d = 5$

with the assumption that 3/16 inch diameter rivets will be used) is

$$R_R = \frac{E}{1-\mu^2} \frac{1}{(f/t_w)^3} \left[\frac{3f/t_w + b_w/t_w}{3f/t_w + 4b_w/t_w}\right] \frac{t_s}{5} p =$$

$$\frac{10.7 \times 10^6}{1-.3^2} \frac{1}{(5.5)^3} \left[\frac{3(5.5) + 15.25}{3(5.5) + 4(15.25)}\right] \frac{.020}{5} (.94)$$

$$= 109 \text{ lbs.}$$

From attachment tension curves in Section C1, 3/16 inch diameter fasteners at 1.0 inch spacing are adequate for this load. The allowable is extrapolated as 225 lbs./in. for protruding head rivets in 0.020 inch thick web.

The stiffener-to-cap load is given by Equation B5-35 as

$$P_u = f_u A_{u_e} = 26{,}250\ (0.042) = 1102 \text{ lbs./in.}$$

Two (2) 1/4 inch diameter titanium lockbolts are adequate for this load, based on allowables in Sectin C1. Thus, for bearing critical structure, the allowable strength is

$$2\ (139{,}000)(0.020)(0.250) = 1390 \text{ lbs.}$$

Step 9. End Bay Effects

From Equation B5-36, the distributed load on the beam end is

$$w = \frac{k\ t\ f_s}{\tan \alpha} = \frac{0.67\ (0.020)(25{,}000)}{0.78} = 429 \text{ lbs./in.}$$

The bending moment on a simple supported beam is

$$M = \frac{wh_e^2}{8} = \frac{429\ (19.55^2)}{8} = 20{,}519 \text{ in.-lbs.}$$

This moment must be resisted by the end two stiffeners which are 6 inches apart. Based on simple $Ad^2$ analysis, the moment of inertia for these stiffeners is

$$I = A_u d^2/2 = (0.112)(6)^2/2.0 = 2.02 \text{ in.}^4$$

Thus, the bending stress is low.

$$\sigma = \frac{Mc}{I} = \frac{20,519(3)}{2.02} = 30,474 \text{ psi}$$

However, horizontal stiffeners must be inserted in this last bay to allow it to work as a beam since the web is so thin (.020 inches). Two or three horizontal stiffeners should be more than sufficient. Web doublers are also required for the increased shear load. An .020 inch thick doubler should be sufficient.

Step 10. Check the simple hand solution with the computer solution and reiterate as required to obtain a minimum weight solution. The following table shows a comparison between the hand solution (based on the preliminary calculations in this section) and the computer solution as described in section E7. Further iterations are left to the Designer.

Table B5.1.3.8-1 Comparison of Hand Solution With Computer Solution in Section E7

| ITEM | HAND SOLUTION | COMPUTER SOLUTION |
|---|---|---|
| Applied Stress, $f_s$, psi | 25,000 | 25,000 |
| Initial Buckling Stress, $F_{scr}$, psi | 603 | 625 |
| Diagonal Tension Angle, $\alpha$, degrees | 38.0 | 38.5 |
| Diagonal Tension Factor, k | .67 | .66 |
| Web Data | | |
| Applied Max Stress, $fs_{max}$, psi | 25,676 | 25,247 |
| Allowable Stress, $F_s$, psi | 25,805 | 27,491 |
| M.S. for Web Failure | +.007 | +.009 |
| Stiffener Data | | |
| Forced Crippling | | |
| Max Stiffener Stress, $f_{umax}$, psi | 31,500 | 30,628 |
| Forced Crippling Allowable Stress, $F_o$, psi | 33,759 | 33,591 |
| M.S. for Forced Crippling Failure | +.07 | +.097 |
| Column Failure | | |
| Stiffener Gross Area Stress, $f_{ugross}$, psi | 9,844 | 9,535 |
| Column Allowable Stress, $F_c$, psi | 49,907 | 50,224 |
| M.S. for Column Failure | 4.07 | 4.27 |
| Stiffener Yield | | |
| Stiffener Applied Stress, $f_u$, psi | 26,250 | 25,700 |
| Stiffener Crippling Stress, $F_{cc}$, psi | 56,776 | 56,776 |
| M.S. for Yield Failure | +1.16 | +1.21 |
| Flange Data | | |
| Flange Stress from Applied Moment, $f_b$, psi | 41,085 | 41,085 |
| Flange Stress from Diagonal Tension, $f_F$, psi | 7,917 | 7,676 |
| Total Axial Stress in Flange, $f_D$, psi | 49,002 | 48,761 |
| Bending Stress in flange from Sagging, $f_{sb}$, psi | 19,019 | 19,036 |
| Flange Allowable stress from Direct Stress, $F_{cc}$,psi | 69,278 | - |
| Flange Modulus of Rupture Stress, $F_{BM}$, psi | 118,000 | - |
| M.S. for Flange Failure | +.15 | - |
| Attachment Data | | |
| Web-to-Flange | | |
| Applied Shear, $q_A$, lbs./in. | 677 | 638 |
| Allowable Shear, lb./in. | 695 | 695 |
| M.S. for Attachment | +.03 | +.09 |
| Web-to-Stiffener | | |
| Applied Shear, $R_R$, lbs. | 109 | 321 |
| Allowable Shear, lbs. | 225 | 362 |
| M.S. for Attachments | +1.06 | +.13 |
| Stiffener-to-Flange M.S. | | |
| Applied Shear, $P_u$, lbs. | 1,102 | 1,529 |
| Allowable Shear, lbs. | 1,390 | 1,068 |
| M.S. for attachments | +.26 | +.43 |

## B5.1.4 Curved Web Semi-Tension Field Beams

### B5.1.4.1 Introduction to Curved Web Semi-Tension Field Beam Design

The analysis of curved web semi-tension field beams follows very closely the methods developed for flat web semi-tension field beams. In the case of curved web systems, the stringers (longerons) are analogous to the caps of a flat web system, whereas the rings (frames) are analogous to the stiffeners in the flat web system. Figure B5.1.4.1-1 shows a typical curved web system and defines the various terms which will be used in this section.

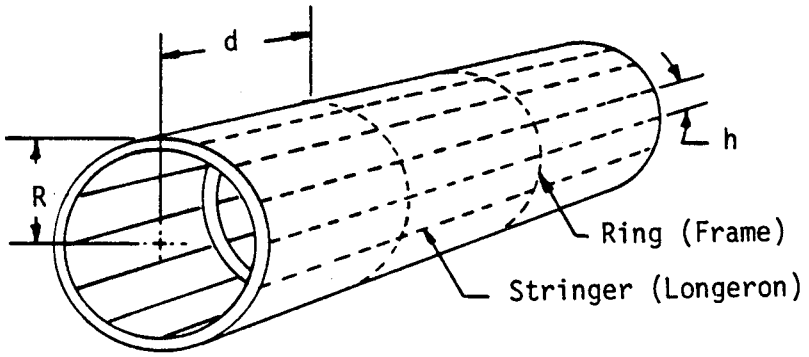


Figure B5.1.4.1-1 Typical Terminology for a Curved Web System

### B5.1.4.1 Web Analysis

A. Web Shear Stress ($f_s$) - The determination of applied shear stresses in a fuselage shell or a curved beam is generally more complicated than for a flat web system. The curved structure is subject to applied torque and bending moments due to flight and ground conditions. In addition, pressurized cabins in modern aircraft introduce further complicatons. For these reasons, applied shear flows are generally determined based on finite element modeling techniques where the shear stresses ($f_s$) at any particular location in the curved shell can be determined from the output of the finite element along with the tension and compression stresses ($f_t$ and $f_c$).

B. Actual Initial Buckling Stress ($F_{s_{cra}}$) - Because curved shell structure carries bending loads which produce axial compression and tension stresses in the stringers, as well as shear stresses in the skin, the onset of initial buckling for shear is not as straight forward as for a flat web system. Thus, it is influenced by the compression and tension stresses.

When a curved panel is subject to shear stress ($f_s$) and compression stress ($f_c$), the panel buckles according to the interaction equation

$$\frac{f_c}{f_{c_{cr}}} + \left(\frac{f_s}{F_{s_{cr}}}\right)^2 = 1.0 \qquad \text{(B5-41)}$$

Where $f_c$ and $f_s$ are the applied compression and shear stresses determined from the finite element model. $F_{c_{cr}}$ and $F_{s_{cr}}$ are the initial buckling stresses for a curved panel loaded by pure compression and shear, respectively. $F_{c_{cr}}$ and $F_{s_{cr}}$ are defined as

$$F_{c_{cr}} = K_c \eta_p E \left(\frac{t}{b}\right)^2 \qquad \text{(B5-42a)}$$

$$F_{s_{cr}} = K_s \eta_s E \left(\frac{t}{b}\right)^2 \qquad \text{(B5-42b)}$$

where the buckling coefficients can be found in Figures B5.1.4.2-1 through -3 for simply supported curved panels. The plasticity factors $\eta_s$ and $\eta_p$ are defined in Section B5.1.2.3 and B5.1.3.3. The value for b is always the smaller of d or h.

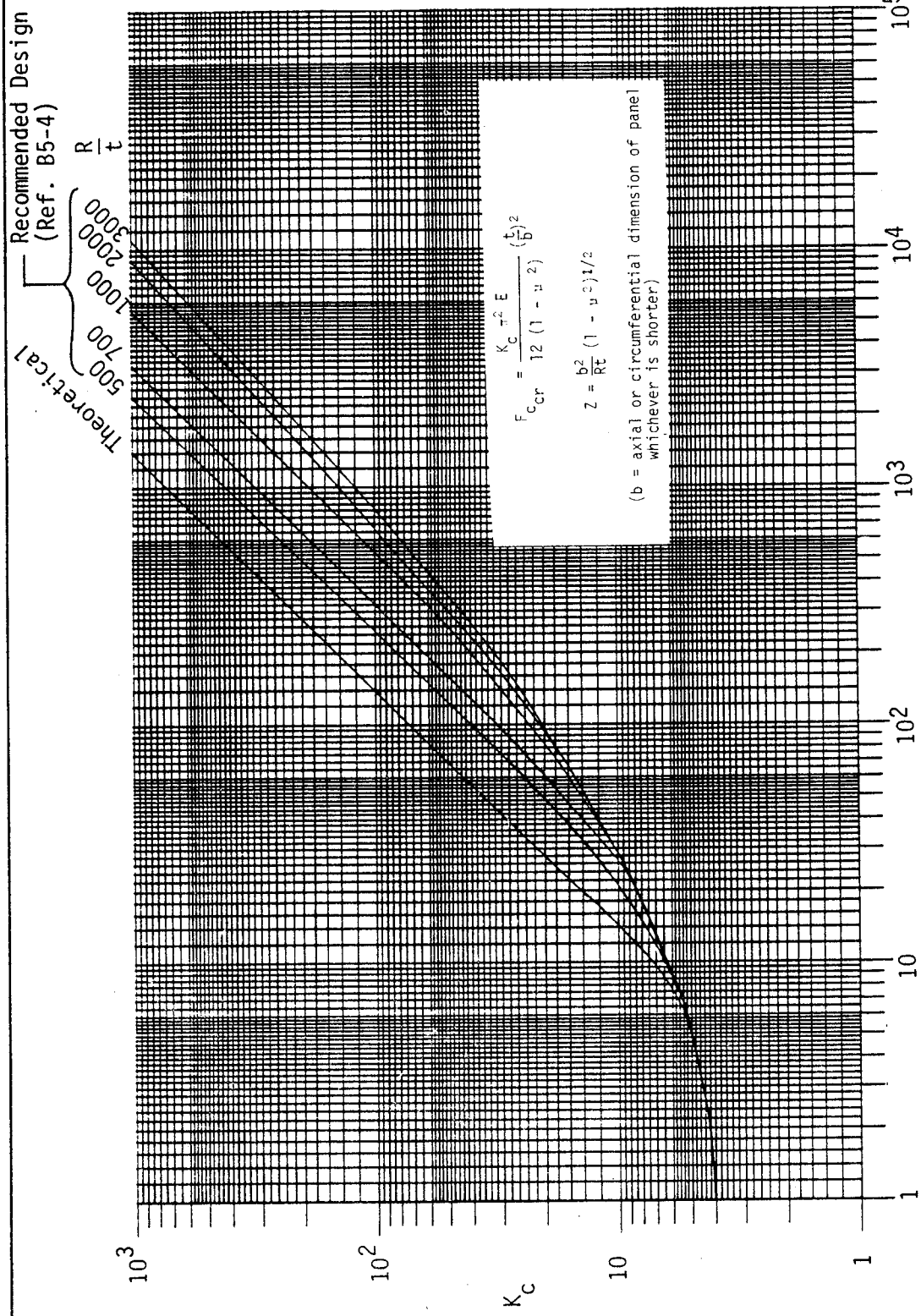


Figure B5.1.4.2-1 Axial Compressive Buckling Coefficients for Long Curved Simply Supported Plate

Ref. B5-4

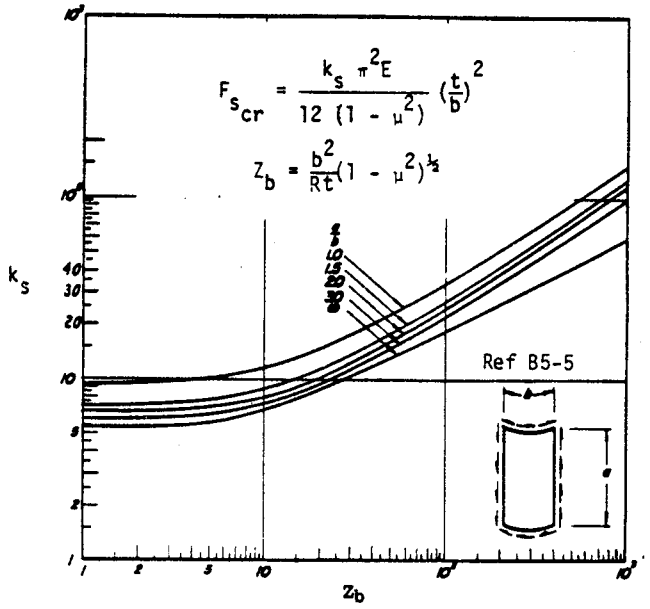


Figure B5.1.4.2-2 Shear Buckling Coefficients for Long Simply Supported Curved Plates

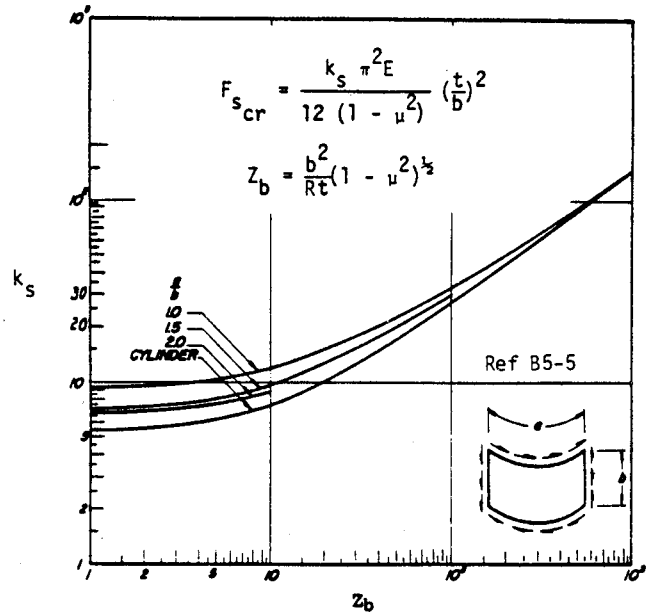


Figure B5.1.4.2-3 Shear Buckling Coefficients for Wide Simply Supported Curved Plates

Based on Equations B5-41, B5-42a, and B5-42b, the actual shear stress at which initial buckling starts can be found from the equation

$$F_{s_{cr_a}} = F_{s_{cr}} R_c \qquad \text{B5-43a)}$$

where

$$R_c = \frac{-B/A + \sqrt{(B/A)^2 + 4}}{2} \qquad \text{(B5-43b)}$$

$$A = F_{c_{cr}} / F_{s_{cr}} \qquad \text{(B5-43c)}$$

$$B = f_c / f_s \qquad \text{(B5-43d)}$$

If the curved panel is subject to shear stress ($f_s$) and tension stress ($f_t$), it will buckle according to the relationship.

$$\frac{f_s}{F_{s_{cr}}} - \frac{1}{2}\frac{f_t}{F_{c_{cr}}} = 1 \qquad \text{(B5-44)}$$

where $F_{s_{cr}}$ and $F_{c_{cr}}$ are as previously defined.

The actual initial shear buckling stress can then be determined as

$$F_{s_{cr_a}} = F_{s_{cr}} R_t \qquad \text{(B5-45a)}$$

where

$$R_t = 1 + \frac{f_t}{2F_{c_{cr}}} \qquad \text{(B5-45b)}$$

C. Diagonal Tension Factor (k) - Equation B5-14 or Figure B5.1.3.2-3 can be used for determining k based on the ratio $f_s/F_{s_{cr_a}}$ as defined in sections A and B.

D. Maximum Applied Web Stress ($f_{s_{max}}$) - For flat web systems, this maximum stress was given by Equation B5-16; $f_{s_{max}} = f_s (1 + k^2C_1)(1 + kC_2)$. For curved web systems, no corresponding theory has been developed. The factors $C_1$ and $C_2$ are assumed as zero. Therefore $f_{s_{max}} = f_s$. In order to compensate for the error introduced by this assumption, the allowable stress determined for flat panels must be multiplied by an empirical factor for curved panels which depends on the properties of the stringers and rings.

E. Allowable Web Shear Stress ($F_{s_{all}}$) - The allowable ultimate shear stress in a curved panel is given by the empirical expression

$$F_{s_{all}} = F_s (0.65 + \Delta) \qquad \text{B5-46a)}$$

where

$$\Delta = 0.3 \tanh \frac{A_{RG}}{dt} + 0.10 \tanh \frac{A_{ST}}{ht} \qquad \text{(B5-46b)}$$

Figure B5.1.4.2-3 is a plot of Equation B5-46b. The value for $F_s$ in Equation B5-46a should be obtained from the allowable $F_s$ in Figure B5.1.3.2-5. The allowable stress as determined from equation B5-46a should be greater than the applied shear stress as given by the equation

$$\text{M.S.} = \frac{F_{s_{all}}}{f_s} - 1 \qquad \text{(B5-47)}$$

B5.1.4.3 Stringer Analysis

Geometrically, the stringers of a cylinder correspond to the caps of a flat web beam and the rings correspond to the stiffeners of a flat web beam. Functionally, however, the stringers, as well as the rings of a cylinder under torque load, act like stiffeners of a beam. The strength analysis of the stringers, therefore, involves the same considerations as the strength of the stiffeners, except that bending stresses ($f_b$) may be present in addition to diagonal tension stresses.

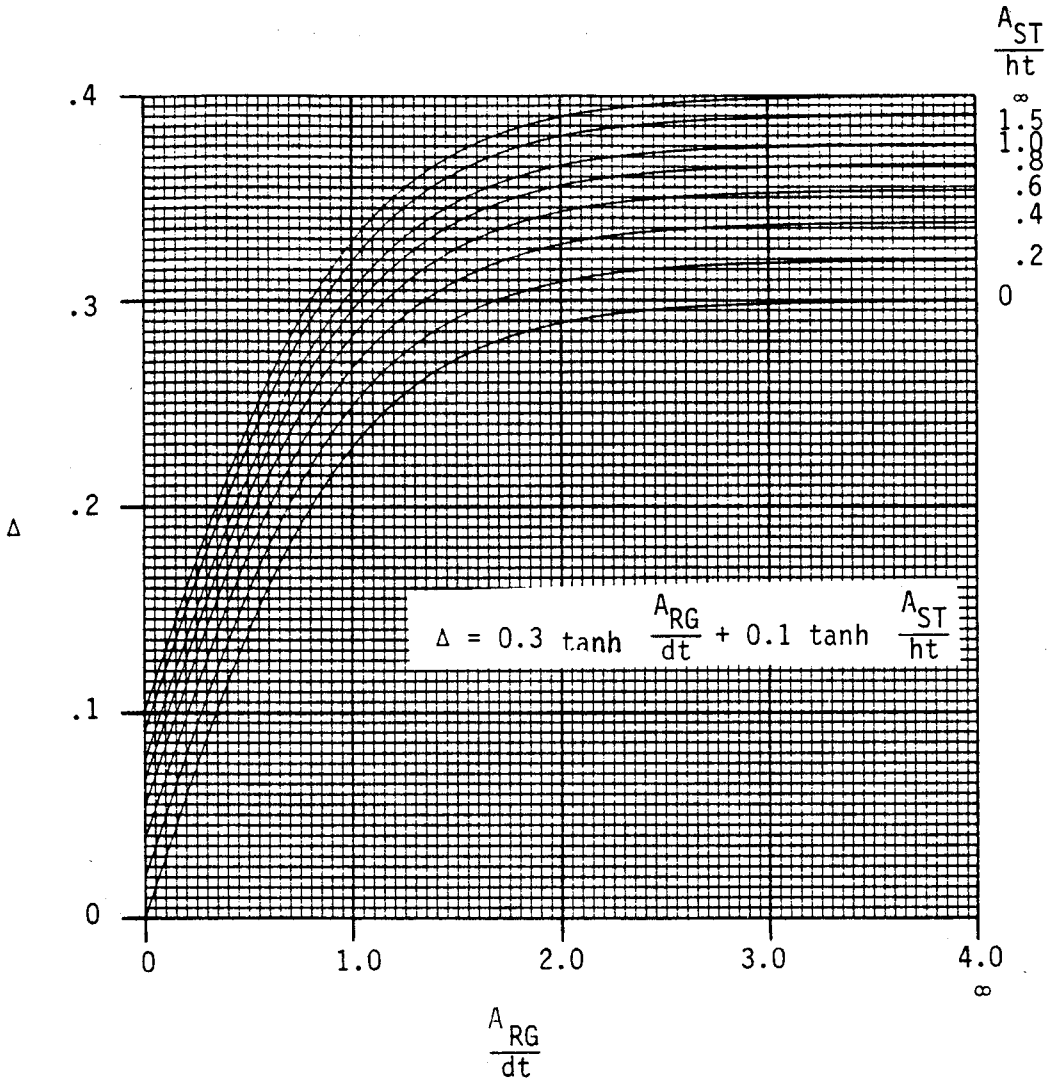


Figure B5.1.4.2-3 Correction for Allowable Ultimate Shear Stress in Curved Webs

A. Average Stringer Applied Stress ($f_{st}$) - When the web buckles, additional compression stresses are introduced into the stringer ($f_{ST}$) and the rings ($f_{RG}$) just as for flat web systems. These stresses are

$$f_{ST} = \frac{-k\, f_s}{\tan\alpha \left[\frac{A_{ST}}{ht} + .5\,(1-k)\, R_c,t^*\right]} \qquad \text{(B5-48)}$$

$$f_{RG} = \frac{-k\, f_s \tan\alpha}{\left[\frac{A_{RG}}{dt} + .5\,(1-k)\right]} \qquad \text{(B5-49)}$$

*$R_c$, t (use $R_c$ or $R_t$ depending on load).

If the rings are floating (not attached to the skin, but only the stringer) then the factor .5 (1-k) should be neglected in Equation B5-49.

The angle $\alpha$ required for solving Equations B5-48 and 49 is defined by the equation

$$\tan^2\alpha = \frac{\varepsilon_w - \varepsilon_{ST}}{\varepsilon_w - \varepsilon_{RG} + \frac{1}{24}\left(\frac{h}{R}\right)^2} \quad \text{for } d > h \qquad \text{(B5-50)}$$

$$\tan^2\alpha = \frac{\varepsilon_w - \varepsilon_{ST}}{\varepsilon_w - \varepsilon_{RG} + \frac{1}{8}\left(\frac{d}{R}\right)^2 \tan^2\alpha} \quad \text{for } h > d \qquad \text{(B5-51)}$$

The values $\varepsilon_w$, $\varepsilon_{ST}$, and $\varepsilon_{RG}$ are

$$\varepsilon_w = \frac{f_s}{E_w}\left[\frac{2k}{\sin 2\alpha} + \sin 2\alpha\,(1-k)(1+\mu)\right] \qquad \text{(B5-52a)}$$

$$\varepsilon_{ST} = f_{ST}/E_{ST} \qquad \text{(B5-52b)}$$

$$\varepsilon_{RG} = f_{RG}/E_{RG} \qquad \text{(B5-52c)}$$

Just as in Section B5.1.3.3, these equations are solved by the method of successive approximations. Thus, assume $\alpha$, solve for $f_{ST}$ and $f_{RG}$, solve for $\varepsilon_w$, $\varepsilon_{ST}$, and $\varepsilon_{RG}$. Then solve for $\alpha$ from either Equation B5-50 or B5-51. Three iterations are generally enough to get agreement between $\alpha$.

For curved panels, the angle $\alpha$ is dependent on the ratio h/R or d/R. For large values of R (typical of commercial jets) these ratios have little effect on the angle $\alpha$ and $45^o$ is a reasonable assumption. For small values of R, $\alpha$ can be in the range of 20 to 30 degrees.

B. Maximum Stringer Applied Stress ($f_{ST_{max}}$) - The gusset effect for flat web stiffeners applies equally as well for curved web systems. Therefore, Figure B5.1.3.3-3 gives the ratio ($f_{ST_{max}}/f_{ST}$) as a function of k and $h_e/d$ (in this case h/d). $f_{ST_{max}}$ is defined as:

$$f_{ST_{max}} = f_{ST}\left(\frac{f_{ST_{max}}}{f_{ST}}\right) \qquad \text{(B5-53)}$$

C. Bending Stress in Stringer ($M_{ST}$) - In addition to the axial stress in the stringer, there is also a secondary bending stress which tends to bow the stringer inward between rings. The secondary bending moment is given as

$$M_{ST} = \frac{f_s h\, td^2\, k \tan\alpha}{24R} \qquad \text{(B5-54)}$$

This is an empirical expression and should be considered acting at the rings (skin in tension) and also halfway between the rings (skin in compression).

D. Allowable Stringer Stress - Possible stringer failure modes are forced crippling and column failure. Both modes of failure are caused by compression loads and are difficult to analyze. The following equations should be used.

1. Force Crippling - For a flat web system, only diagonal tension forces act on the stiffeners. For a curved panel, bending stresses may also be present. This type of interaction should be handled by the following equation.

$$M.S. = \frac{1}{\frac{f_c + f_{sb}}{F_{cc}} + \frac{f_{ST_{max}}}{F_o}} - 1 \qquad \text{(B5-55)}$$

where $f_c$ is the compression stress caused by shell bending and $f_{sb}$ is the compression stress caused by stringer bending between the rings as defined by the bending moment, Equation B5-54. An effective width of skin equal to 30t should be included with the stringer for calculating $f_c$ and $f_{sb}$.

$f_{ST_{max}}$ is defined by Equation B5-53 with data from Figure B5.1.3.3-3.

$F_{cc}$ is the allowable crippling stress for the stringer as determined in Section B6, or from data in Section E6.

$F_o$ should be taken from Equations B5-24 and -25 in Section B5.1.3.3C for the appropriate material, 2024 or 7075.

2. Column Failure - The stringers should be checked for column failure based on the following equations:

$$M.S. = \frac{1}{\frac{f_c + f_{sb}}{F_c}} - 1 \text{ between rings} \qquad \text{(B5-56a)}$$

$$M.S. = \frac{1}{\frac{f_c + f_{sb}}{F_{cr}}} - 1 \text{ at rings} \qquad \text{(B5-56b)}$$

where $f_c$ is the applied stringer stress which includes diagonal tension stress ($f_{ST}$) from Equation B5-48.

$f_{sb}$ is the stringer bending stress calculated based on the the bending moment Equation B5-54 for the skin in Equation B5-56a and the cap of the stringer in Equation B5-56b.

$F_c$ is the column allowable for the stringer and effective skin (30t) with c = 4.0 as defined by the Euler Engesser Equation, Johnson's Parabola, or test data.

$F_{cr}$ is the cripping allowable for the stringer cap away from the skin.

B5.1.4.4 Ring Analysis

The stress in the ring due to diagonal tension is hoop compression as given by Equation B5-49.

When floating rings are used (not usually the case for aircraft fuselage structure) the maximum bending moment present in the ring at the junction with the stringers is

$$M_{RG} = \frac{k\, f_s\, t\, h^2\, d \tan\alpha}{12R} \qquad \text{(B5-57)}$$

An additional secondary bending moment exists in the ring mid-bay between the stringers that is half the value given by Equation B5-57.

Nonfloating rings must satisfy the stress ratio criteria between stringers,

$$M_{RG} = \frac{1}{\frac{f}{F_{cc}} + \frac{f_{RG_{max}}}{F_{RG}}} - 1 \qquad \text{(B5-58)}$$

Where f is the stress due to the ring carrying loads other than the tension field ones (as a bulkhead analysis would show).

$f_{RG_{max}}$ is defined similar to Equation B5-23 based on data from Figure B5.1.3.3-2.

$F_{cc}$ is the section crippling strength as determined in Section B6 or from data in Section E6.

$F_{RG}$ is the allowable force crippling stress for the ring based on Figure B5.1.3.3-3 or the appropriate Equation B5-24 or -25.

Floating rings must satisfy the criteria at the stringer junctions and between stringers of

$$M.S. = \frac{1}{\frac{f_{RG} + f_b}{F_{cc}}} - 1 \qquad \text{(B5-59)}$$

Where $f_{RG}$ is the ring compression stress due to diagonal tension (Equation B5-49). It does not peak between stringer junctions as was the case for nonfloating rings.

$f_b$ is the ring bending stress determined from the bending moment Equation B5-57 and the ring section properties.

$F_{cc}$ is the ring crippling allowable determined as in Section B6 or from test data in Section E6.

B5.1.4.5 Attachment Loads

For the edge of a curved panel attached to a stringer, the required attachment shear strength per inch is

$$R_A = q\left[1 + k\left(\frac{1}{\cos\alpha}\right) - 1\right] \qquad \text{(B5-60)}$$

For an edge attached to a ring, replace the $\cos\alpha$ with $\sin\alpha$.

If the sheet is continuous across a stringer (typical of fuselage shells), but the shear flow changes at the stringer, then the attachments must carry the difference in shear flow between the bays. In such cases, neither the factor k nor the angle $\alpha$ is needed.

Attachments should fulfill the requirements for tension strength as given in Section B5.1.3.5 for flat web systems. Since curved surfaces are encountered mostly on the outer surface of the airframe where flush attachments are required for aerodynamic reasons,

attachment tension strength is a very important item because flush fastener strength is less than protruding head fastener strength. Refer to Section C1 for attachment allowable strength data for flush attachments.

B5.1.4.6 Design Approach

Curved web systems in modern aircraft are generally not sized by diagonal tension considerations as is the case for flat web systems. Usually, compression and tension combined with shear, due to fuselage bending, are overriding conditions. Fuselage pressurization requirements set the skin gauges and often dictate the frame sizes. Therefore, the primary purpose for presenting diagonal tension analysis methods for curved panels is to assure that the Designer is aware these additional forces caused by diagonal tension can influence his final design configuration, although his basic sizing information was obtained from finite element modeling which only considered the effects of shell bending, torque, and pressure. The forced crippling mode is generally the problem area, especially if Z-type stringers are used for stiffening the shell.

B5.1.4.7 Sample Problem

For flat web systems, a sample problem was provided to provide insight on how shear resistant and semi-tension field analysis influenced the sizing of a flat web system. For curved web systems, the approach is taken that the panel has already been sized. This sized panel will then be examined to observe the effect of diagonal tension forces on it. A typical DC-9 fuselage constant section skin stringer element is used for the sample problem. The margin of safety from the stress report, based on interaction between compression and shear, is +.07. Pertinent dimensions and geometry are shown in Figure B5.1.4.7-1.

Step 1. Determine the critical buckling stresses for pure compression and pure shear from Equations B5-42a and B5-42b based on the buckling coefficients from Figure B5.1.4.2-1 and -2.

Calculate

$$Z_b = \frac{h^2}{Rt}\left(1-\mu^2\right)^{1/2} = \frac{7.1^2}{61.4(.050)}\left(1-.33^2\right)^{1/2} = 15.50$$

$$R/t = 61.4/.050 = 1228$$

$$d/h = 19/7.1 = 2.68$$

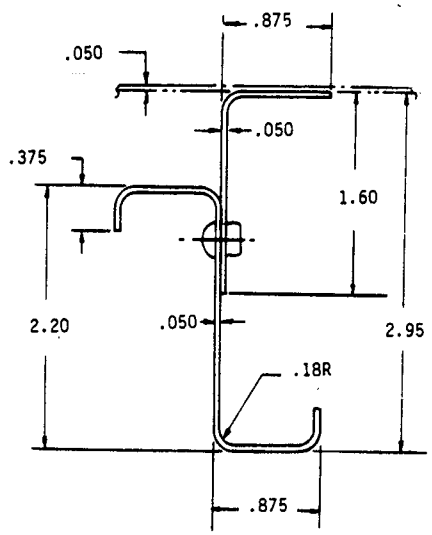


A = .329 in.$^2$, $I_{RG}$ = .308, $\bar{y}$ = 1.391

h = 7.1 in.

d = 19.0 in.

R = 61.4 in.

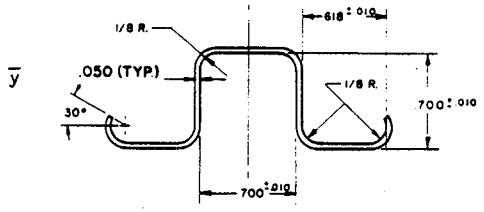


A = .178 in.$^2$, $I_{xx}$ = .013 in.$^4$, $\bar{y}$ = .300 in.

A = .253 in.$^2$, $I_{xx}$ = .025 in.$^4$, $\bar{y}$ = .441 in.

(with 30t skin)

Stringer and Ring Material

7075-T6 Alclad

$F_{cy}$ = 65,000 psi

$E_c$ = 10.5 x $10^6$ psi

$\mu$ = 0.33

Skin Material

2024-T3 Alclad

$F_{tu}$ = 61,000 psi

$F_{cy}$ = 37,000 psi

$E_c$ = 10.7 x $10^6$ psi

$\mu$ = 0.33

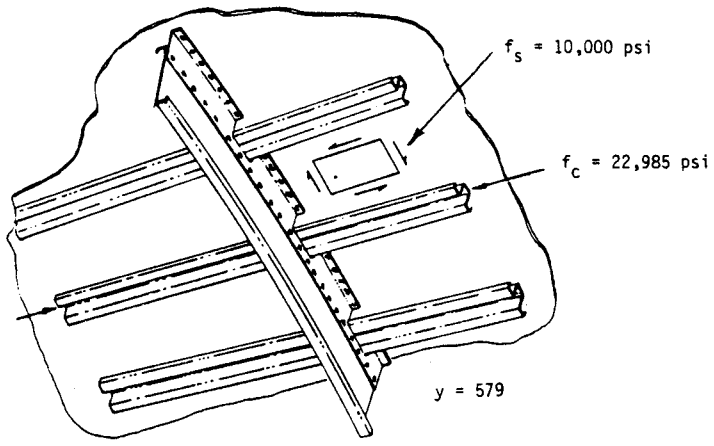


Figure B5.1.4.7-1 Geometry and Data for Sample Problem

From Figures B5.1.4.2-1 and -2

$k_c = 7.5$

$k_s = 8.5$

The modified buckling coefficients are calculated as

$$K_c = k_c \frac{\pi^2}{12(1-\mu^2)} = 7.5\left[\frac{\pi^2}{12(1-.33^2)}\right] = 6.92$$

$$K_s = k_s \frac{\pi^2}{12(1-\mu^2)} = 8.5\left[\frac{\pi^2}{12(1-.33^2)}\right] = 7.85$$

and from Equations B5-42a and b with $\eta_p$ and $\eta_s$ = 1.0.

$$F_{cr} = K_c \eta_p E\left(\frac{t}{h}\right)^2 = 6.92\ (1.0)(10.7 \times 10^6)\left(\frac{.05}{7.1}\right)^2 = 3672 \text{ psi}$$

$$Fs_{cr} = K_s \eta_s E\left(\frac{t}{h}\right)^2 = 7.85\ (1.0)(10.7 \times 10^6)\left(\frac{.05}{7.1}\right)^2 = 4166 \text{ psi}$$

Note: These stresses are below the proportional limit for the material. Otherwise, Figures B5.1.2.3 and B5.1.3.3 should be used to account for plastic effects.

Step 2. Determine the actual shear buckling stress ($F_{s_{cr_a}}$).

Use Equation B5-43a since the applied stresses are compression and shear. Equations B5-43b, c, and d must first be evaluated.

$$A = F_{c_{cr}}/F_{s_{cr}} = 3672/4166 = .88$$

$$B = f_c/f_s = 22{,}984/10{,}000 = 2.30$$

$$R_c = \frac{-B/A + \sqrt{(B/A)^2 + 4}}{2} =$$

$$\frac{-2.3/0.88 + \sqrt{(2.3/0.088)^2 + 4}}{2} = .34$$

Then, from Equation B5-43a

$$F_{s_{cr_a}} = F_{s_{cr}} (R_c) = 4166\ (.34) = 1416 \text{ psi}$$

Step 3. Determine the diagonal tension factor k, from Figure B5.1.3.2-3 or Equation B5-14.

Note: d/h = 19/7.1 = 2.68 which is greater than 2.0; thus, use 2.0.

$$k = \tanh \left[ \left(.5 + 300 \frac{td}{Rh}\right) \log_{10}(f_s/F_{s_{cr_a}}) \right] =$$

$$\tanh \left[ \left(.5 + 300 \left(\frac{(.05)(2.0)}{61.4}\right) \log_{10}(10{,}000/1416) \right] = .685$$

Step 4. Determine the web margin of safety. Use Equation B5-47 which requires the determination of the web allowable strength from Figure B5.1.3.2-5 for $F_{t_u}$ = 62,000 psi and k = .685 with $\Delta$ from Equation B5-46b. Assume $\alpha = 45^o$. From Figure B5.1.3.2-5, $F_s$ = 22,000 psi.

From Equation B5-46b

$$\Delta = .3 \tanh \left(\frac{A_{RG}}{dt}\right) + .1 \tanh \left(\frac{A_{ST}}{ht}\right) =$$

$$.3 \tanh \left(\frac{.329}{19(.05)}\right) + .1 \tanh \left(\frac{.178}{7.1(.05)}\right) = .146$$

Then from Equation B5-46a

$$F_{s_{all}} = F_s\ (.65+\Delta) = 22{,}000\ (.65+.146) = 17{,}512 \text{ psi}$$

and the margin of safety is obtained from Equation B5-46 as

$$M.S. = \frac{F_{s_{all}}}{f_s} - 1 = \frac{17{,}512}{10{,}000} - 1 = + .75$$

Step 5. Determine the stringer stress and check assumption of $\alpha = 45^o$. Equations B5-48 through B5-52 are required for this check.

From Equation B5-48

$$f_{ST} = \frac{-k\ f_s}{\tan\alpha \left[\frac{A_{ST}}{ht} + .5\ (1-k)\ R_c\right]} =$$

$$\frac{-.685\ (10{,}000)}{(1.0)\ \left[\frac{.178}{7.1(.05)} + .5\ (1-.685)\ .34\right]} = -12{,}343 \text{ psi}$$

From Equation B5-49

$$f_{RG} = \frac{-k\ f_s \tan\alpha}{\frac{A_{RG}}{dt} + .5\ (1-k)} = \frac{-.685\ (10{,}000)(1.0)}{\frac{.329}{19\ (.05)} + (1-.685)} = -13{,}596 \text{ psi}$$

Then the strains are determined from Equation B5-52 as

$$\varepsilon_w = \frac{f_s}{E_w}\left[\frac{2k}{\sin 2\alpha} + \sin 2\alpha\ (1-k)(1+\mu)\right] =$$

$$+ \frac{10{,}000}{10.7 \times 10^6}\left[\frac{2(.685)}{1.0} + (1)(1-.685)(1+.33)\right] =$$

$$+ .00167$$

$$\varepsilon_{ST} = f_{ST}/E_{ST} = -12{,}343/10.5 \times 10^6 = -.00118$$

$$\varepsilon_{RG} = f_{RG}/E_{ST} = -13{,}596/10.5 \times 10^6 = -.00129$$

The diagonal tension angle is checked from Equation B5-50 as

$$\tan^2\alpha = \frac{\varepsilon_w - \varepsilon_{ST}}{\varepsilon_w - \varepsilon_{RG} + \frac{1}{24}\left(\frac{h}{R}\right)^2} =$$

$$\frac{.00167 + .00118}{.00167 + .00129 + \frac{1}{24}\left(\frac{7.1}{61.4}\right)^2} = .810$$

and $\alpha = 42.0$ degrees.

Thus, our initial assumption of 45° is probably within the accuracy of the theory.

Step 6. Determine the maximum stringer stress. From Figure B5.1.3.3-3 for k = .685 and h/d = .374, $f_{ST_{max}}/f_{ST}$ = 1.18. The maximum stringer stress is then determined from Equation B5-53 as

$$f_{ST_{max}} = f_{ST}\left(\frac{f_{ST_{max}}}{f_{ST}}\right) = -12{,}343\ (1.18) = -14.565\ \text{psi}$$

Step 7. Determine the stringer bending moment. Use Equation B5-54.

$$M_{ST} = \frac{f_s\ h\ t\ d^2\ k \tan\alpha}{24R} =$$

$$\frac{10{,}000\ (7.1)(.05)(19)^2(.685)}{24(61.4)} = 596\ \text{in.-lbs.}$$

Step 8. Determine stringer allowable stresses, $F_{cc}$, $F_o$, $F_{cr}$, and $F_c$. $F_{cc}$, the stringer crippling stress, is determined from charts in Section E6. From these charts the crippling stress is determined as

$$F_{cc} = \frac{\Sigma F_{cr_i} A_i}{\Sigma A_i} = 60{,}667\ \text{psi}$$

The forced crippling allowable stress ($F_o$) is determined from Equation B5-25a where $t_u$ is being replaced by $3t_u$ for a hat section.

1/3

$$F_o/\eta_p = 32{,}500\ k^{2/3}\ (3t_u/t)^{1/3} =$$

$$32{,}500\ (.685)^{2/3}\ (3 \times .05/.05)^{1/3} = 36{,}406\ \text{psi}$$

This value is entered into Figure B5.1.3.3-4 for 7075-T6 aluminum and found to require no plasticity correction. Therefore, $F_o$ = 36,406 psi.

$F_{cr}$, the stringer outer cap crippling stress, is

determined from the same chart in Section E6 for rolled section hats supported on both edges that was used for $F_{cc}$. From this chart, $F_{cr}$ = 61,500 psi.

$F_c$ is determined from Johnson Parabola with L' = $L/\sqrt{4.0}$ using properties of the hat section with 30t skin.

Thus

$$F_c = F_{cc} - \frac{F_{cc}^2}{4\pi^2 E}\left(\frac{L'}{\rho}\right)^2 = 60{,}667 -$$

$$\frac{60{,}667^2}{4\pi^2 \quad (10.5 \times 10^6)}\left[\frac{19/2}{\sqrt{.025/.253}}\right]^2 = 52{,}558 \text{ psi}$$

Step 9. Determine the stringer margins of safety for forced crippling from Equation B5-55 using data already calculated in Steps 6, 7, and 8.

The applied stress includes the primary stress $f_c$ = 22,984 psi, plus the stringer bending stress $f_{sb}$ with 30t skin which is

$$f_{sb}\frac{Mc}{I} = +596\left[\frac{.359}{.025}\right] = 8{,}558 \text{ psi}$$

The combination of these stresses is 31,542 psi. With this applied stress and the appropriate stresses from Steps 6, 7, and 8, the forced crippling margin of safety is

$$M.S. = \frac{1}{\frac{f_c + f_{sb}}{F_{cc}} + \frac{f_{ST_{max}}}{F_o}} - 1 =$$

$$\frac{1}{\frac{31{,}542}{60{,}667} + \frac{14{,}565}{36{,}406}} - 1 = +.09$$

Note: This margin is greater than, but close to, the margin determined based on interaction between shear and compression of +.07.

Step 10. Determine the stringer margins of safety for column loads at the center of the stringer and over the rings from Equations B5-56a and b, using data already calculated in Steps 6, 7, and 8. In these equations, the applied axial stress $f_c$ includes the diagonal tension stress as defined in Step 5.

$$f_c = 22,984 + 12,343 = 35,327 \text{ psi}$$

The bending stress for the skin mid-bay from Step 9 is

$$f_{sb} = 8558 \text{ psi}$$

For the outstanding flange over the frame, the bending stress is

$$f_{sb} = 596 \left[\frac{.441}{.025}\right] = 10,518 \text{ psi}$$

These values of applied stress, along with the appropriate allowables are substituted into Equations B5-56a and b to give a center bay margin of safety.

$$M.S. = \frac{1}{\frac{f_c + f_{sb}}{F_c}} - 1 = \frac{1}{\frac{35,327 + 8558}{52,558}} - 1 = +.20$$

and an end-bay margin of safety

$$M.S. = \frac{1}{\frac{f_c + f_{sb}}{F_{cc}}} - 1 = \frac{1}{\frac{35,327 + 10,518}{61,500}} - = +.34$$

Step 11. Check frame strength based on Equation B5-58. Values required are $f_{RG_{max}}$, f, $F_{RG}$, and $F_{cc}$. Based on the design loads, f is tension; therefore, it can be neglected in the interaction.

$f_{RG_{max}}$ is determined from Figure B5.1.3.3-3 with $k = .685$ and $h/d = .374$. This figure gives $f_{RG_{max}}/f_{R_G} = 1.18$ and from Equation B5-53 with $f_{RG}$ from Step 5

$$f_{RG_{max}} = f_{RG}\left[\frac{f_{RG_{max}}}{f_{RG}}\right] = -13,596\ (1.18) = -16,043 \text{ psi}$$

$F_{RG}/n_p$ is determined from Figure B5.1.3.3-4 or Equation B5-25a as

$$F_{RG}/n_p = 32,500\ (k)^{2/3}\ (t_u/t)^{1/3} =$$

$$32,500\ (.685)^{2/3}\ (.05/.05)^{1/3} = 25,252 \text{ psi}$$

for which $F_{RG} = 25,252$ in Figure B5.1.3.3-3. The margin of safety is calculated from Equation B5-58 as

$$M.S. = \frac{1}{\frac{f}{F_{cc}} + \frac{f_{RG_{max}}}{F_{RG}}} - 1 = \frac{1}{0 + \frac{16.043}{25,252}} - 1 + 0.57$$

Step 12. Check attachments. Flush 3/16 inch diameter attachment rivets are used to tie the longerons to the skin, for which the allowable tension stress is given in Section C1 as 249 lbs.

There is little change in shear between longerons from the shell analysis. The fasteners are good for shear by inspection.

The tension applied load is found from Equation B6-29 and Figure B6.3.5-2 in Section B6 for $b_o/t_u = 0.375/0.05 = 7.5$, $b_w/t_w = 0.70/0.05 = 14.0$, and $p/D = 1.25/0.288 = 6.65$ as

$$R_R = \frac{E}{1-\mu^2}\frac{1}{(f/t_w)^3}\left[\frac{3f/t_w + b_w/t_w}{3f/t_w + 4b_w/t_w}\right]\frac{t_s}{5}P =$$

$$\frac{10.5 \times 10^6}{1-.3^2}\frac{1}{(7.0)^2}\left[\frac{3(7) + 14}{3(7) + 4(14)}\right]\frac{.05}{5}\ 1.25 = 191 \text{ lbs.}$$

Thus, the fasteners are good in tension.

## B5.2.0 Cutouts in Shear Web Beams

Cutouts in shear web beams are a necessary design consideration for practical aircraft structural design. These cutouts will range from small circular holes for hydraulic or electrical systems to large or irregular holes which require nearly complete removal of the web for equipment installation or access.

The cutout sizes are separated into three general groups: small, moderate, and large. Small cutouts are less than 2.5 inches in diameter and less than 40 percent of the beam depth. Moderate cutouts are greater than 2.0 inches in diameter and between 40 and 75 percent of the beam depth. Large cutouts are greater than 70 percent of the beam depth and/or are more complex than a round hole. Each of these size cutouts is covered in the sections that follow.

All beams covered in B5.2.1 through B5.2.4 are shear resistant.

## B5.2.1 Small Cutouts

Small cutouts should be round holes reinforced by circular doublers as shown in Figure B5.2.1-1.

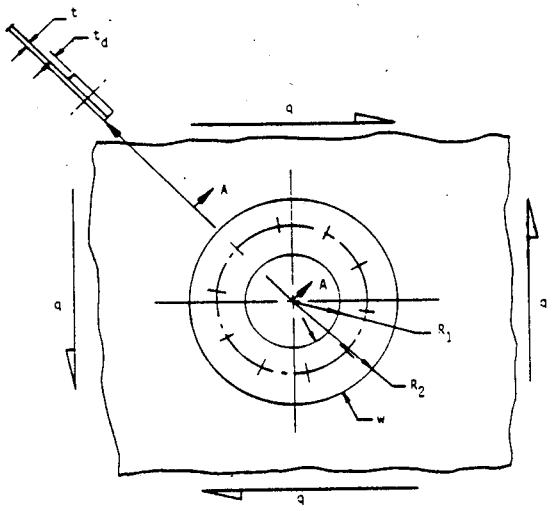


$R_1$ = Hole Radius

$R_2$ = Doubler Outer Radius

w = Width of Doubler

t = Web Thickness

$A_{w_c}$ = Area of the Web Cutout

$t_d$ = Doubler Thickness

$A_d$ = Area of the Doubler

Figure B5.2.1-1 Shear Web Reinforcement for Small Round Holes

The following guidelines should be followed for small hole reinforcements:

A. As a rule of thumb $t_d$ = 2 gages more than t.

B. Area of the doubler ($A_d$) = 1.50 times the area of the web cutout (through Section A-A), $A_{w_c}$.

C. Sufficient fasteners must be installed to carry the shear load around the hole.

As an example of reinforcement around a small round hole, assume:

2024-T3 Clad Sheet

t = .050 in.

R = .750 in.

q = 300 lbs./in.

Determine the doubler size and fastener requirements:

$$A_{W_c} = .050\ (.750) = .0375\ \text{in.}^2$$

$$t_d = 2 \text{ gages more than } t = .072 \text{ in.}$$

$$A_d = 1.5\ A_{W_c} = 1.5\ (.0375) = .0562\ \text{in.}^2$$

$$w = \frac{A_d}{t_d} = \frac{.0562}{.072} = .781 \text{ in.}$$

From Section A5.1.0, 1/8 inch diameter rivets are minimum structural fasteners without design supervision approval. From section C1.0.0, 10 AD4 (1/8D) rivets at 0.712 spacing are good for 545 lbs./in. (page C1-6).

This is more than adequate for the applied shear of 300 lbs/in. and will provide a good tie between the doubler and the web. Edge distance requirements of 2D + 1/16 inch are exceeded with the chosen arrangement. Doubler thickness could be made greater and w reduced to meet minimum edge distance requirements.

Reference B5-6 has shown that a plate with this proportion of doubler is about 10 to 20 percent better in buckling than a flat plate with no hole. Thus, as a conservative estimate, use flat plate buckling charts, Figures B5.1.2.3-1 and -2 to determine if the plate is shear resistant. If the panel is not shear resistant, assume the shear is 2q and put sufficient fasteners in for this shear.

If the plate is machined, the doubler can possibly be integral, depending on the plate stock. In this case, the doubler proportions can range from the dimensions previously given to those defined as follows:

$$A_d = 1.25\ A_{w_c}$$
$$t_d/w = 6$$

Then, $t_d = 2.74\sqrt{R_1 t}$ and $w = t_d/6$.

For the example problem:

$$t_d = 2.74\sqrt{(.75)(.05)} = .53 \text{ in.}$$
$$w = t_d/6 = .53/6 = .09 \text{ in.}$$

These dimensions are preferred, but a compromise must be made to keep the plate stock (i.e., chip loss) to a minimum.

B5.2.2 Moderate Cutouts

Moderate cutouts, greater than 2.0 inch diameter and between 40 and 75 percent of beam depth, are normally reinforced by return-lip lightening holes formed into the web. The cutout should, if possible, be round.

Two standard lightening holes designs are used: S4931552 and S2241840. The S2241840 hole is limited in use to very small holes, diameters of 2.00 to 3.00 inches. Holes may be irregular, but the minimum radius limitations must be met.

The S4931552 hole is preferred. The deep flange provides the best hole reinforcement, thereby, delaying web buckling at the hole. Again, the hole may be irregular, but minimum radius requirements must be met.

The NACA developed (from extensive testing) an empirical formula to determine the allowable shear flow for beam webs of this type (see Figure B5.2.2-1).

$$q_{all} = K\,t\left[f_{sh}\left(1-\left(\frac{D}{h}\right)^2\right) + f_{sc}\left(\frac{D}{h}\right)^{1/2}\right]\frac{c'}{b} \qquad \text{(B5-61)}$$

Where:

$$K = 0.85 - .0006\,\frac{h}{t} \qquad \text{(B5-62)}$$

$f_{sh}$ = shear buckling stress of a long plate of width h and thickness t (obtain from Figure B5.2.2-2), psi

$f_{sc}$ = shear buckling stress of a long plate of width c and thickness t (obtain from Figure B5.2.2-2), psi

b = center-to-center hole spacing, in

D = hole clear diameter, in.

h = height of beam (flange rivet line to flange rivet line), in.

c = space between holes (b-D), in.

c' = "flat" web between holes (from design data for lightening hole), in.

Note: Net section (i.e., c' x t and (h-D) x t) shear stress should be nearly equal to the web yield stress ($f_{sy}$).

The following example illustrates usage of the NACA method:

Assume: Material 2024-T42 Clad
t = .050 in., D = 2.500 in., b = 5.00 in., c = 2.500 in.
h = 5.00 in., c' (from S2241840-3) = 1.55 in.

From Equation B5-61:

$$q_{all} = \left[0.85-(.0006)\left(\frac{5}{.05}\right)\right](.05)\left[(11.700)\left[1-\left(\frac{2.5}{5}\right)^2\right]+ (22{,}750)\left(\frac{2.5}{5}\right)^{1/2}\right]\frac{1.55}{5} = 304.43 \text{ lbs./in.}$$

If the web is machined, the flange around the holes should be near the preferred dimensions given. Equations B5-61 and B5-62 still apply.

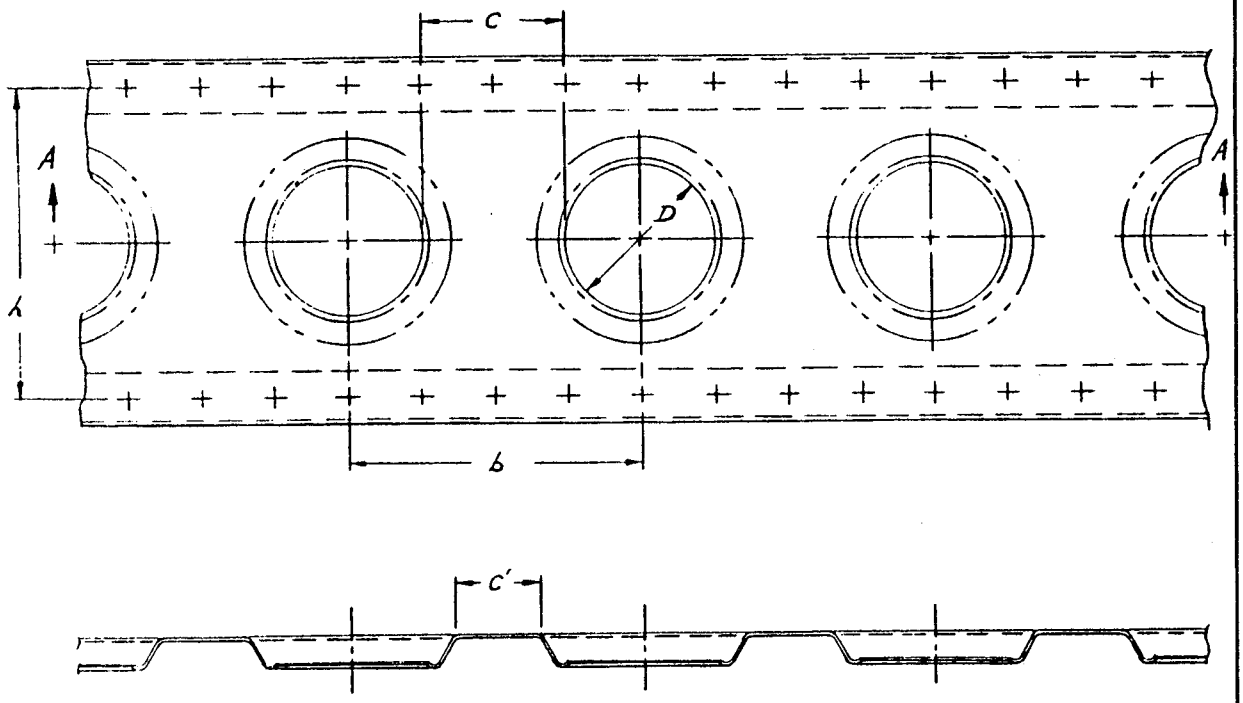


SECTION A-A

Figure B5.2.2-1 Moderate Cutout in Beam

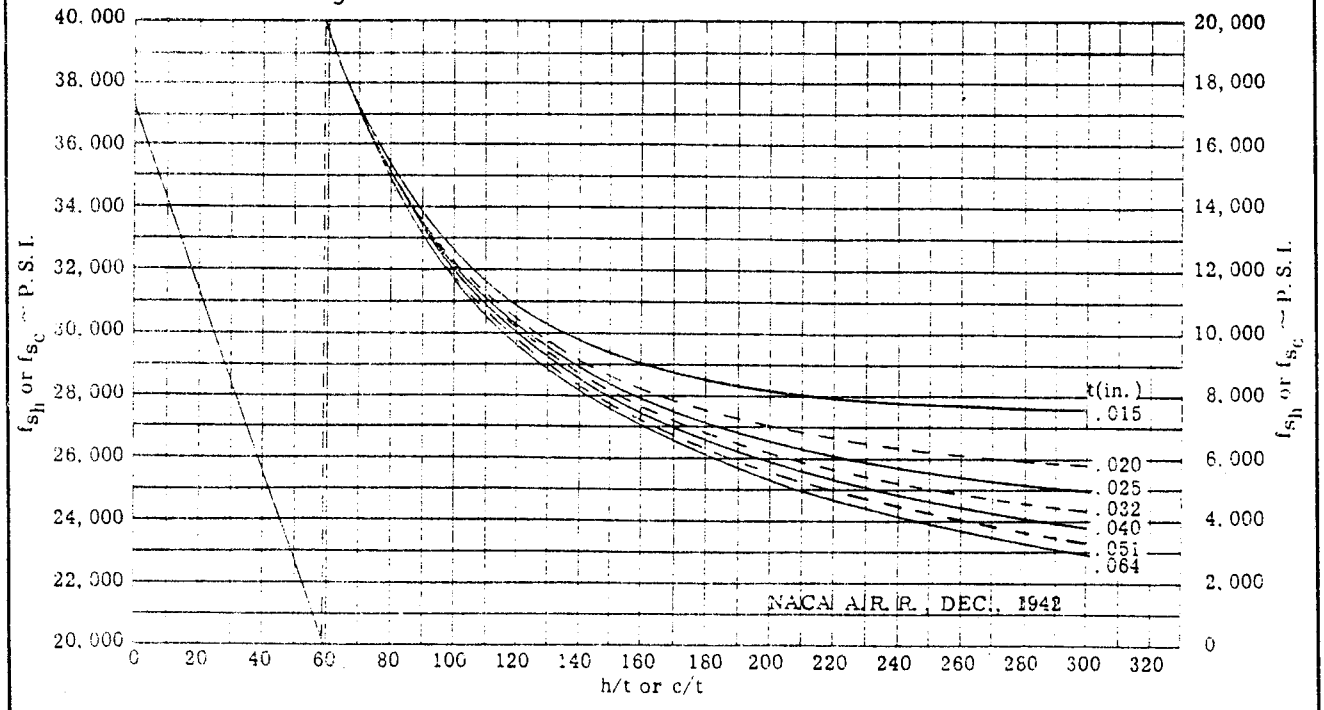


Figure B5.2.2-2 Buckling Shear Stresses, $f_{sh}$ or $f_{sc}$, for Solid Webs of 2024-T42 Aluminum Alloy

B5.2.3 Large Cutouts

Large cutouts, which are greater than approximately 70% of the beam depth and/or are rectangular, are generally reinforced with flat doublers and "framing" members. A special case is the airload wing rib which has an extremely large cutout, lightening hole-type reinforced in heavy gage material. These cases both are discussed in this section.

A. Framing Cutouts with Flat Doublers As an example assume that a beam web requires a cutout as shown in Figure B5.2.3-1.

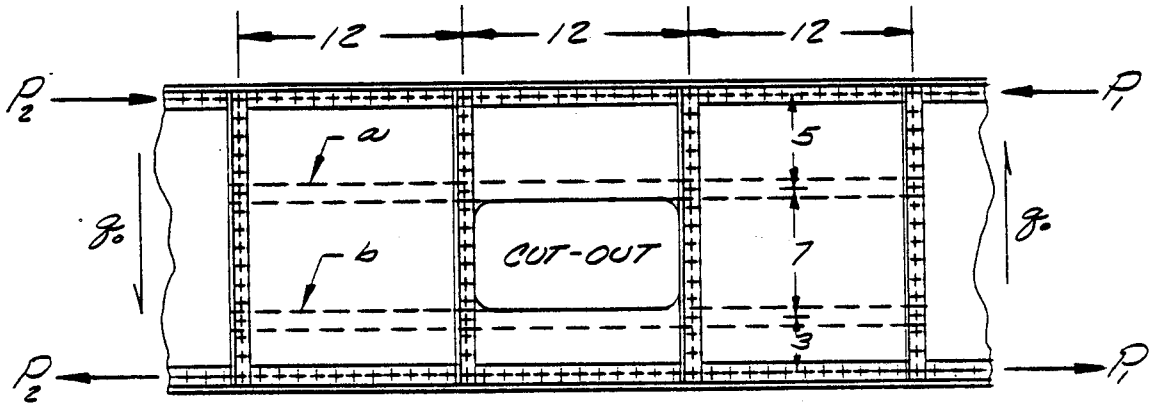


Figure B5.2.3-1 Typical Large Cutout in a Beam

Before the cutout is made, the members shown by solid lines (flanges, stiffeners, webs) are present. The members "a" and "b" are added to frame the cutout as shown by the broken lines.

In order to determine the loads around the cutout assume a shear flow equal and opposite to that present with no cutout ($q_o$ in Figure B5.2.3-1) acting at the cutout. Determine the corresponding balancing loads in the framed area due to this shear flow. Add the resulting shear flow system to the original loads to get the final loads.

In Figure B5.2.3-2 (A), all shear flows are shown as they act on the edge members (on the flanges and stiffeners).

If there were no cutout there would be a constant shear flow, $q_o$, in all of the panels. A shear flow equal and opposite to that in the center panel (cutout) of Figure B5.2.3-2 (A) is applied to the center panel in Figure B5.2.3-2 (B). Since this represents a self-balancing load system, no external reactions outside of the framing areas are required. The loads in the framed areas due to $q_o$ in Figure B5.2.3-2 (B) are next determined. To eliminate redundancies, it is usually assumed that the same shear flow exists in the panels above and below the cutout. It is also assumed that shear flows are the same in the panels to the left and right of the cutout.

The shear flow in the panels above and below the center panel must statically balance the force due to $q_o$. From equilibrium,

$$\Sigma F_V = 0, \text{ and } q_o\ (7) = q\ (5 + 3)$$

$$q = 7/8\ q_o$$

The shear flows in the panels to the left and right of the center panel must also statically balance the force due to qo. Thus,

$$\Sigma F_H = 0, \text{ and } q_o\ (12) = q\ (12 + 12)$$

$$q = 1/2\ q_o$$

The shear flows in the corner panels must also balance the force due to the shear flow in the panel between them. For the panels in the right hand bay

$$\Sigma F_V = 0, \text{ and } 1/2\ q_o\ (7) = q\ (5 + 3)$$

$$q = \frac{1/2\ q_o\ (7)}{8} = 7/16\ q_o$$

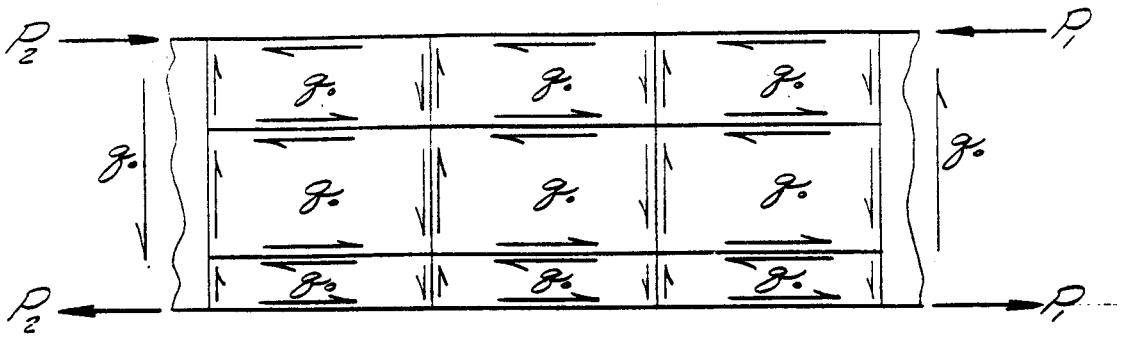


Figure B5.2.3-2 (A) Shear Flow with No Cutout

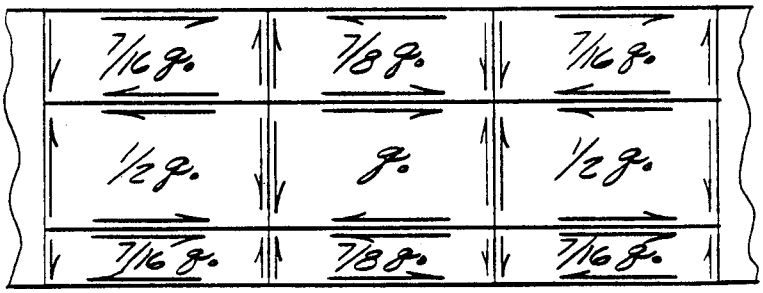


Figure B5.2.3-2(B) Self-balancing Loads

The final shear flows Figure B5.2.3-2 (C) are calculated by adding the values in Figure B5.2.3-2 (A) and (B) algebraically. Note that:

1. The shear flow in the center panel (the cutout) is $q = q_o - q_o = 0$, as it should be.

2. The shear flows above and below and to the left and right of the cutout add, giving a number greater than the original value of $q_o$.

3. The shear flows in the corner panels are smaller than the original value of $q_o$.

This is the way the changes occur in the area framed about a cutout. The pattern is commonly referred to as a "Tic-Tac-Toe" effect.

From equilibrium, axial loads are developed in all of the framing members due to the cutout. These will add or subtract (depending upon their directions) to any loads present before the cutout was made (as in the case of the beam flanges). The axial loads due to the cutout can be calculated from Figure B5.2.3-2 (B) or the total axial loads in all of the members can be calculated from Figure B5.2.3-2 (C). These are illustrated in Figures B5.2.3-2 (D), (E), and (F).

Once the internal loads are known, the members can be checked for strength using standard methods of stress analysis.

The cutout could have been framed without extending the framing members into the bay on the right of the cutout. This case is illustrated in Figure B5.2.3-3 (A), (B), and (C).

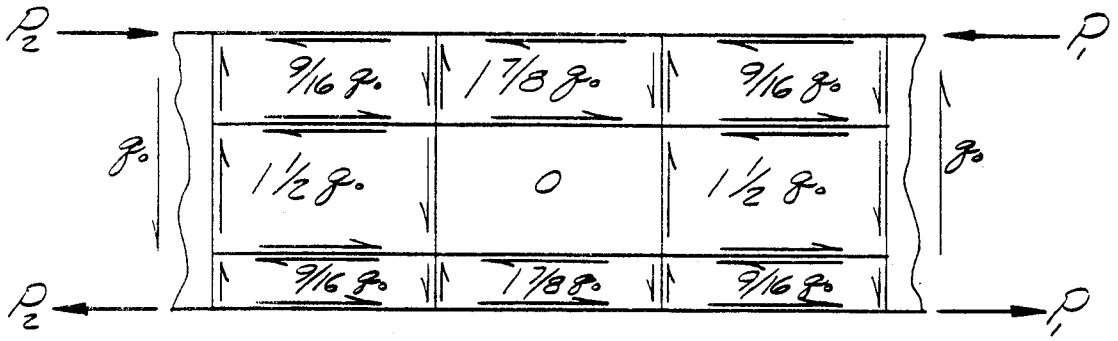


Figure B5.2.3-2 (C) Final Shear Flow

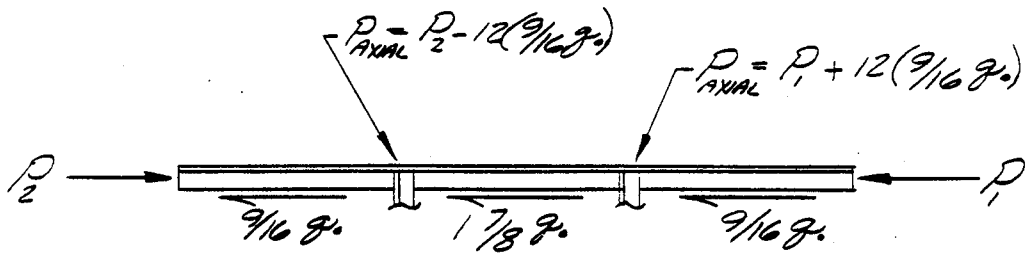


Figure B5.2.3-2 (D) Axial Load Distribution in Upper Flange

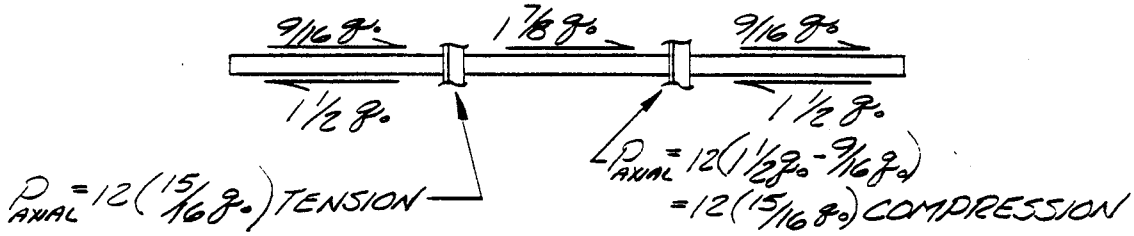


Figure B5.2.3-2 (E) Axial Load Distribution in Framing Member Above Cutout

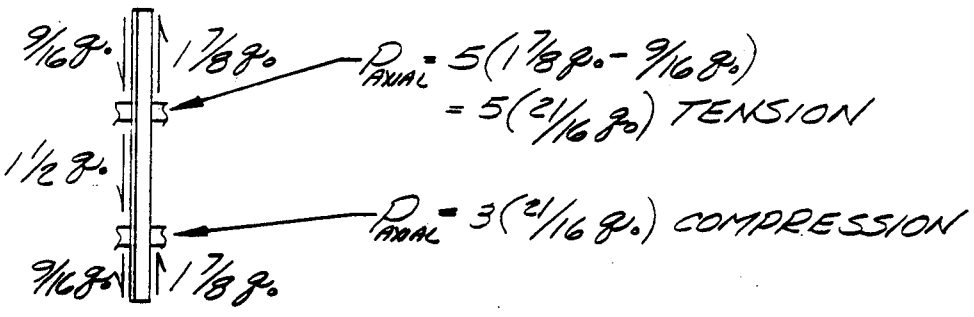


Figure B5.2.3-2 (F) Axial Load Distribution in Stiffener Bordering Cutout on Left Side

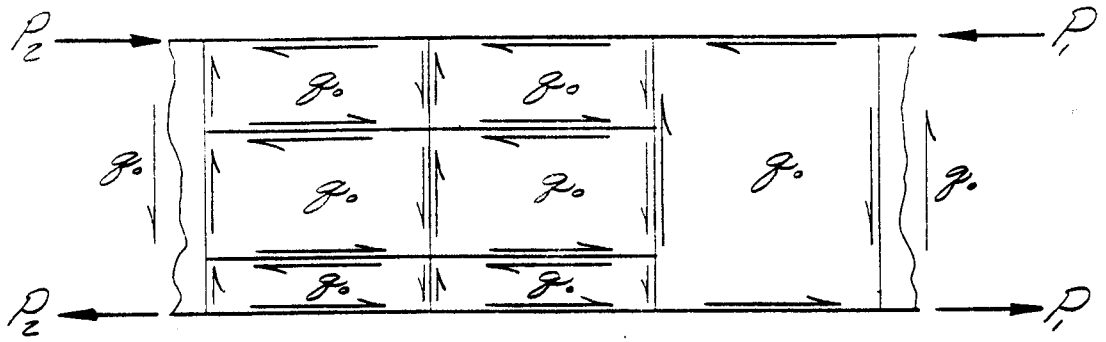


Figure B5.2.3-3 (A) Before Cutout

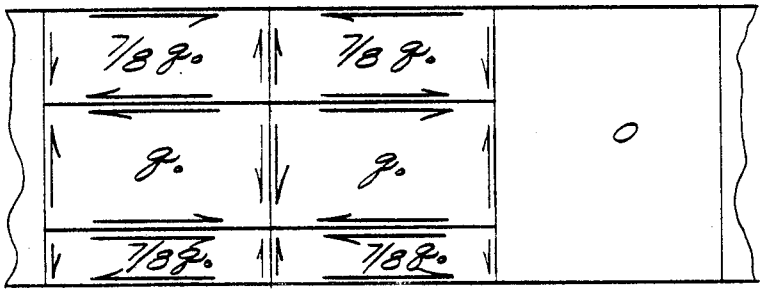


Figure B5.2.3-3 (B) Self-Balancing Internal Loads

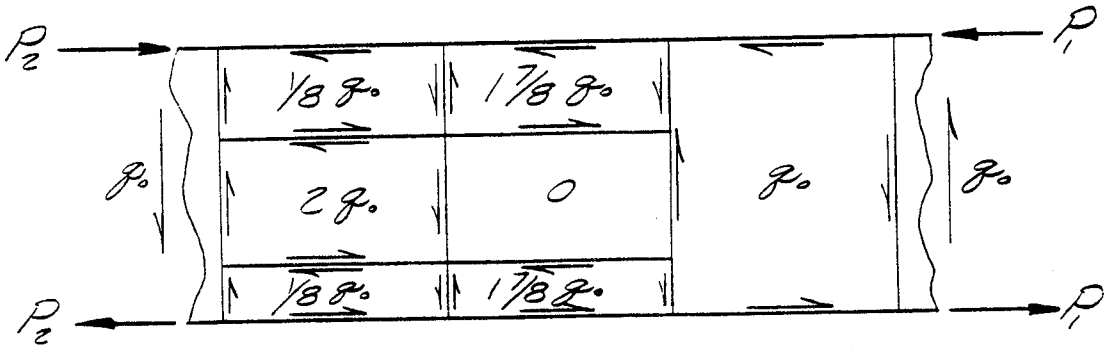


Figure B5.2.3-3 (C) Final Shear Flow Distribution

Had the 7-inch wide cutout been required at the bottom of the beam, the framing could have been done with only one member as illustrated in Figures B5.2.3-4 (A), (B), and (C). This represents the minimum of adequate framing for any cutout. That is, there must be a minimum of one redistribution bay on one side of the cutout, at least two redistribtion bays on the other side, and there must be framing members defining the bays. These framing members will always be loaded axially.

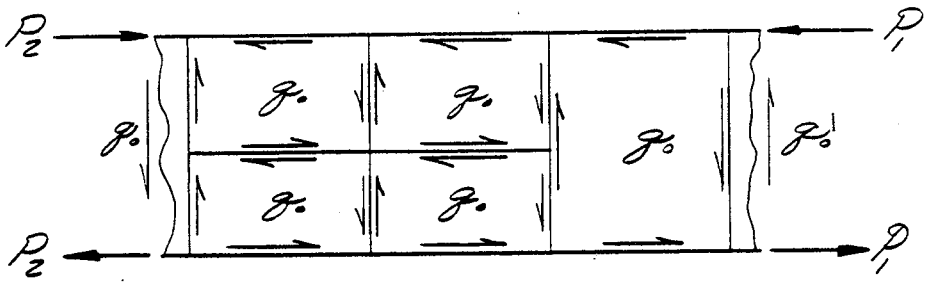


Figure B5.2.3-4 (A) Before Cutout

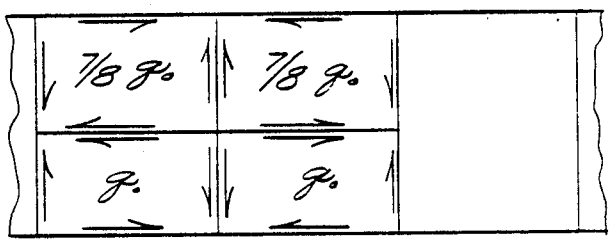


Figure B5.2.3-4 (B) Self-Balancing Internal Loads

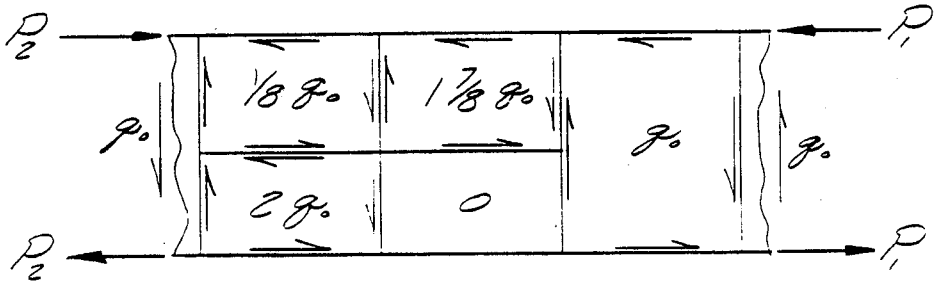


Figure B5.2.3-4 (C) Final Shear Flow Distribution

Note that in the previous examples (Figures B5.2.3-2, -3, and -4 the sum of the loads on all edge members (framing members) is zero. No external loads are needed for equilibrium. This is always the case when a set of self-balancing shear flows are applied to a flat panel structure or to a 3-dimensional box structure with a cutout on any side. Although the method is shown only for a flat beam it is also applicable to any structure with a cutout on any side.

Figures B5.2.3-5 (A), (B), and (C) show the doubler installations required to strengthen the panels with increased shear flows due to the cutout. Figures B5.2.3-5 (A), (B), and (C) correspond to the cutout arrangements shown in Figures B5.2.3-2 (C), B5.2.3-3 (C), and B5.2.3-4 (C), respectively.

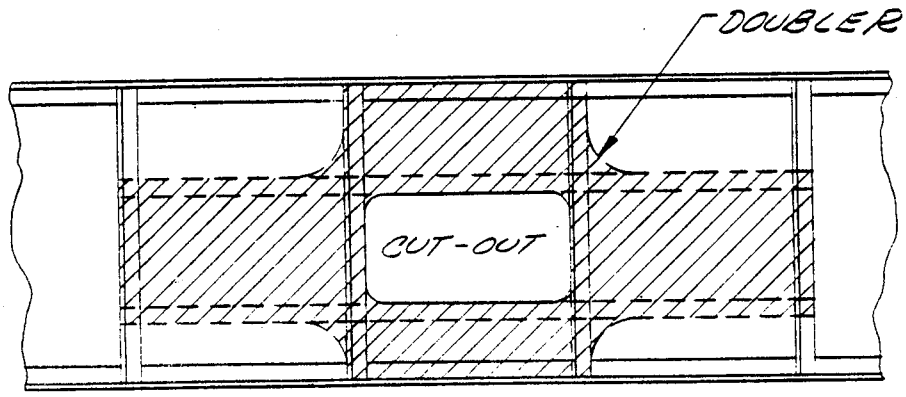


Figure B5.2.3-5 (A)

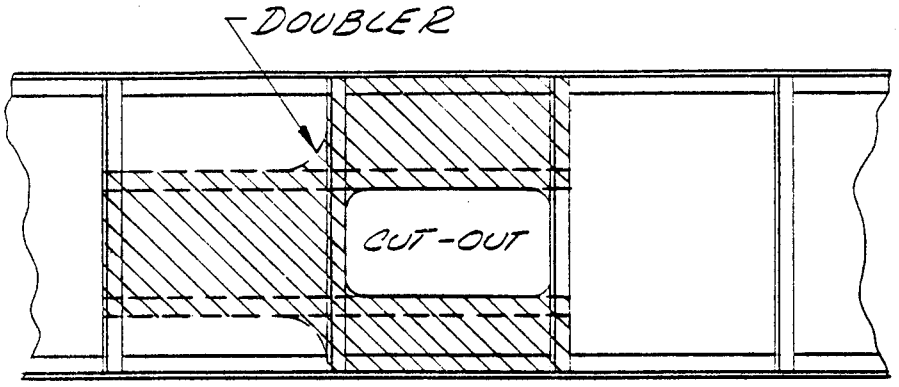


Figure B5.2.3-5 (B)

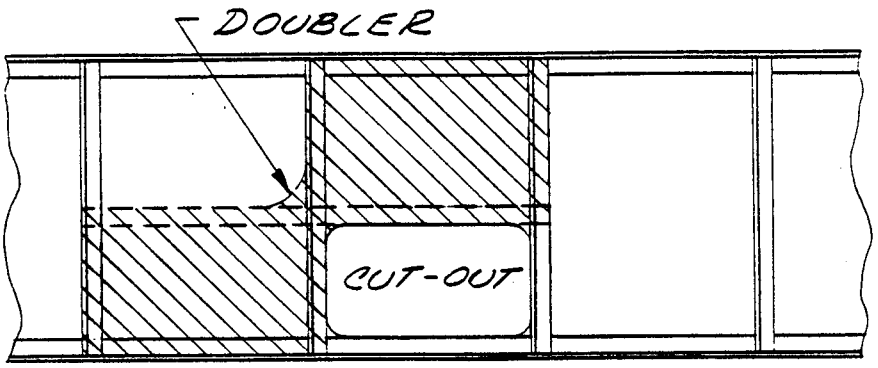


Figure B5.2.3-5 (C)

B. Framing Cutouts with Heavy Doublers or Bents Frequently a cutout in the web of a beam must be so deep that it removes nearly all of the web. (This is the case for fail-safe analysis of a wing spar with a cracked web also.) In this case, the method previously described cannot be used. Instead the "brute force" approach is necessary and a heavy doubler, or bent, is provided around the cutout to carry the shear. This is illustrated in Figure B5.2.3.6. (In the case of a failed web, the spar cap carries the load.)

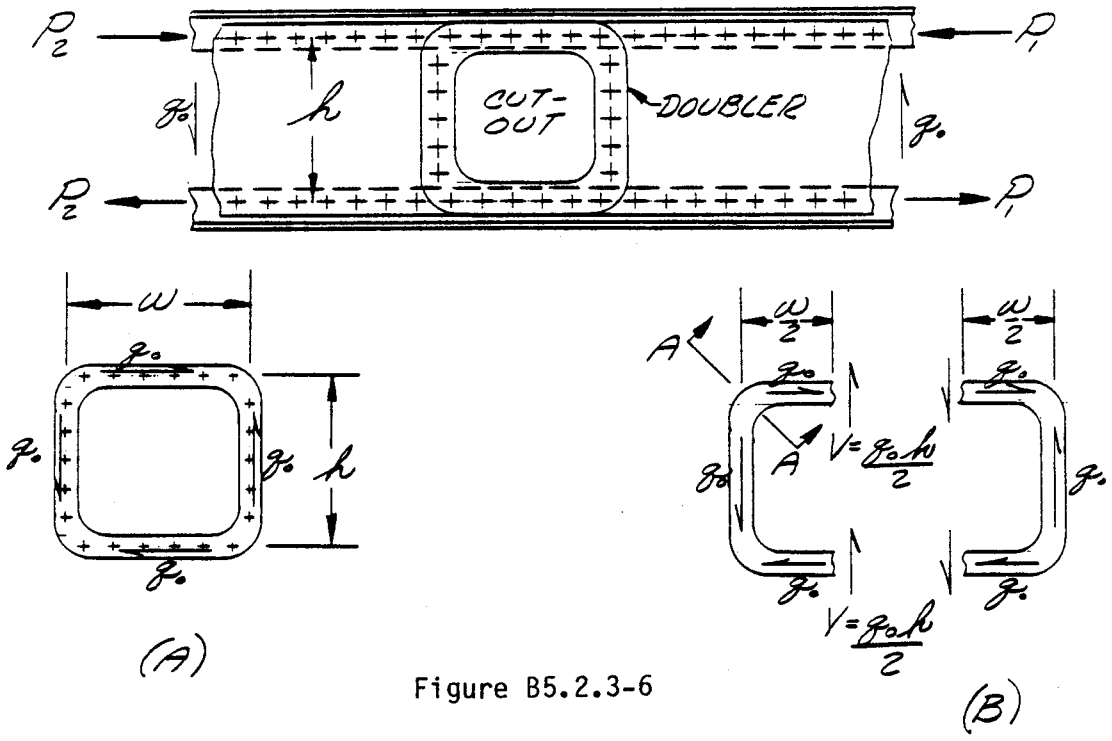


Figure B5.2.3-6

As shown in Figure B5.2.3-6 the doubler whose thickness is yet to be determined is made to fit around the cutout as shown. Generous internal radii are designed into the web and doubler at the corners to keep stress levels low in the high stress concentration area. Attachments are provided as shown to pickup the basic shear flow in the web.

The loading imposed on the doubler is shown in detail (A), namely, the shear flow $q_o$. Strictly speaking the doubler should be analyzed as a frame. With reasonable symmetry the loading in detail (B) can be assumed at the center of the frame. That is, one half of the total shear, $q_o\ (\frac{h}{2})$ is resisted in the top of the frame, one half in the bottom and a pin joint (no bending moment) exists at the cut. The bending moment, axial loads and shears at any section of the frame follow as a matter of statics.

At Section A-A

$$M = V\ w/2 = \frac{q_o hw}{4} \qquad \text{(B5-63)}$$

(There may also be a little relieving moment due to $q_o$.)

$$F_V = V = \frac{q_o h}{2} \qquad \text{(B5-64)}$$

$$F_H = q_o\ w/2 \qquad \text{(B5-65)}$$

The thickness of doubler required to take the loads can thus be determined using standard methods of stress analysis. The doubler should have sufficient out-of-plane stiffness to provide simple support for the beam web. This will normally be provided by the thickness required for strength purposes.

Sometimes the location of the cutout is such that the doubler can be deeper at the top (or bottom). In such a case, the deeper part can be assumed to carry a greater portion of the total shear, V, and the lower part a smaller portion. This is illustrated in Figure B5.2.3-7. The cutout does not extend to the upper flange. The upper part is assumed to carry 4/5 of the total shear and the lower part only 1/5.

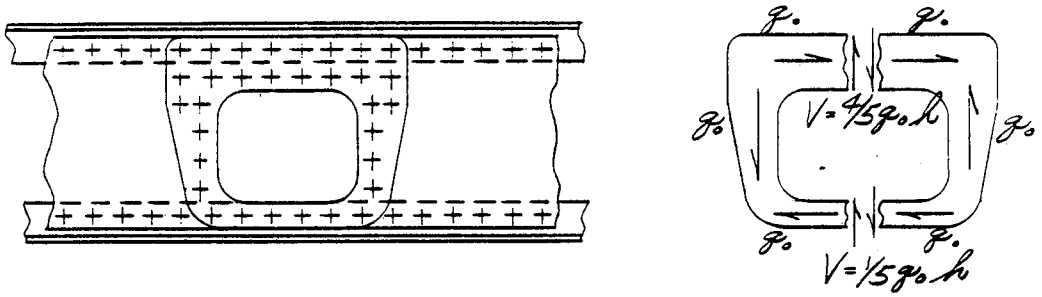


Figure B5.2.3-7

The cases illustrated are for shear resistant webs. If a semi-tension field is present, the diagonal tension effect results in a transverse pull on the stiffeners framing the sides of a cutout.

Actually an end bay effect exists wherever a buckled panel ends and the structural member along the edge of the panel must carry the bending due to the diagonal tension load as well as the usual axial load.

## B5.2.4 Large Cutouts - Special

Large cutouts occur in webs of structure such as airload ribs in a wing, horizontal stabilizer or vertical stabilizer or in floor beams in the fuselage. These beam/rib structures are depicted in Figures B5.2.4-1 through -3.

In each case, the beam is designed to be shear resistant in the flat web area. The flanges of the holes (in the sheet metal design) are formed per S4931552-3 or -4. The beam caps are designed for both primary and secondary bending. The primary bending and basic shear web design procedures are provided in previous portions of this chapter.

A simplified method of determining the secondary bending effects on the beam are presented here. The beams of Figures B5.2.4-1 through -3 can all be idealized as shown in Figure B5.2.4-4. In each quadrant of the panel is a critical section (A, B, C, D) where buckling will begin.

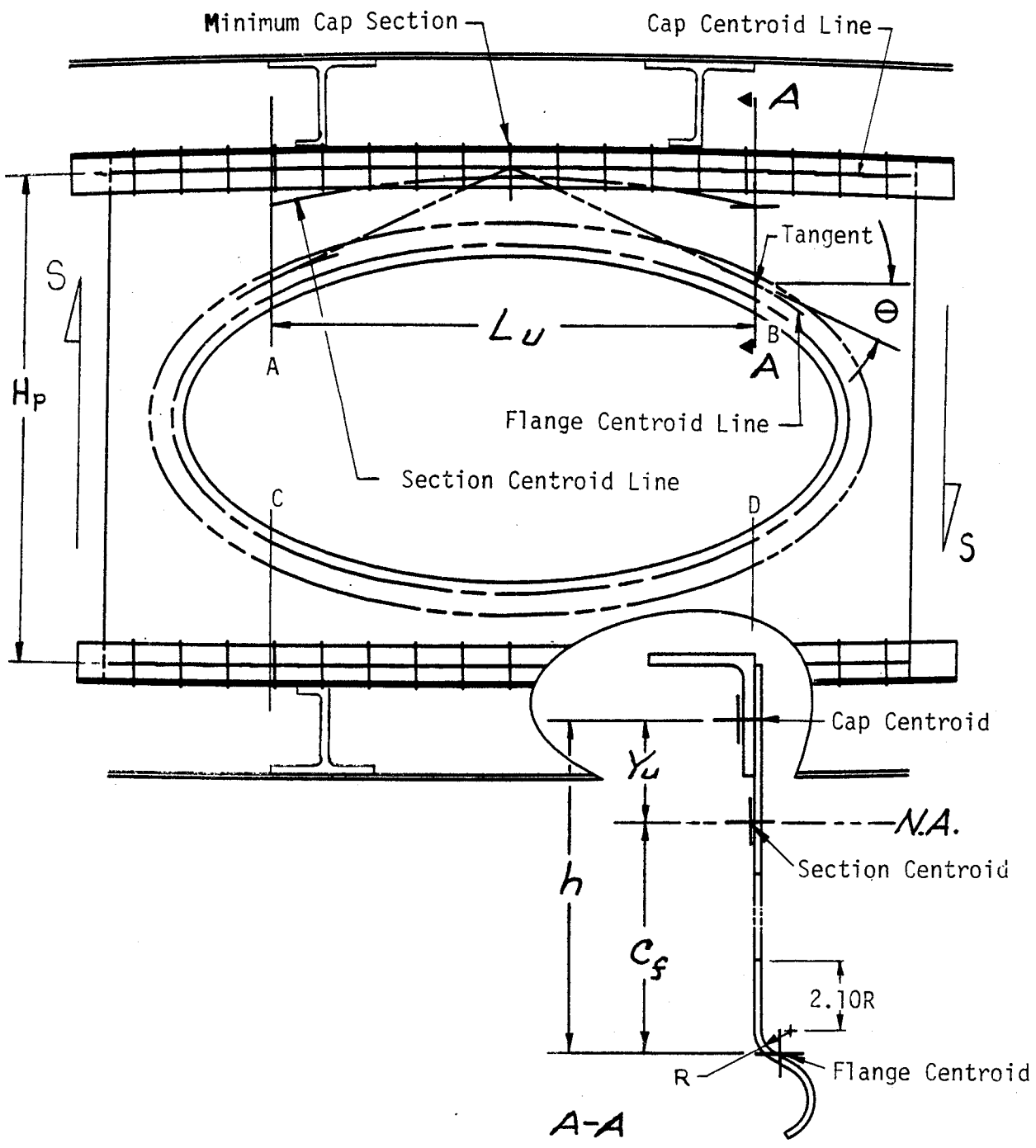


Figure B5.2.4-1 Wing Airload Rib Cutout

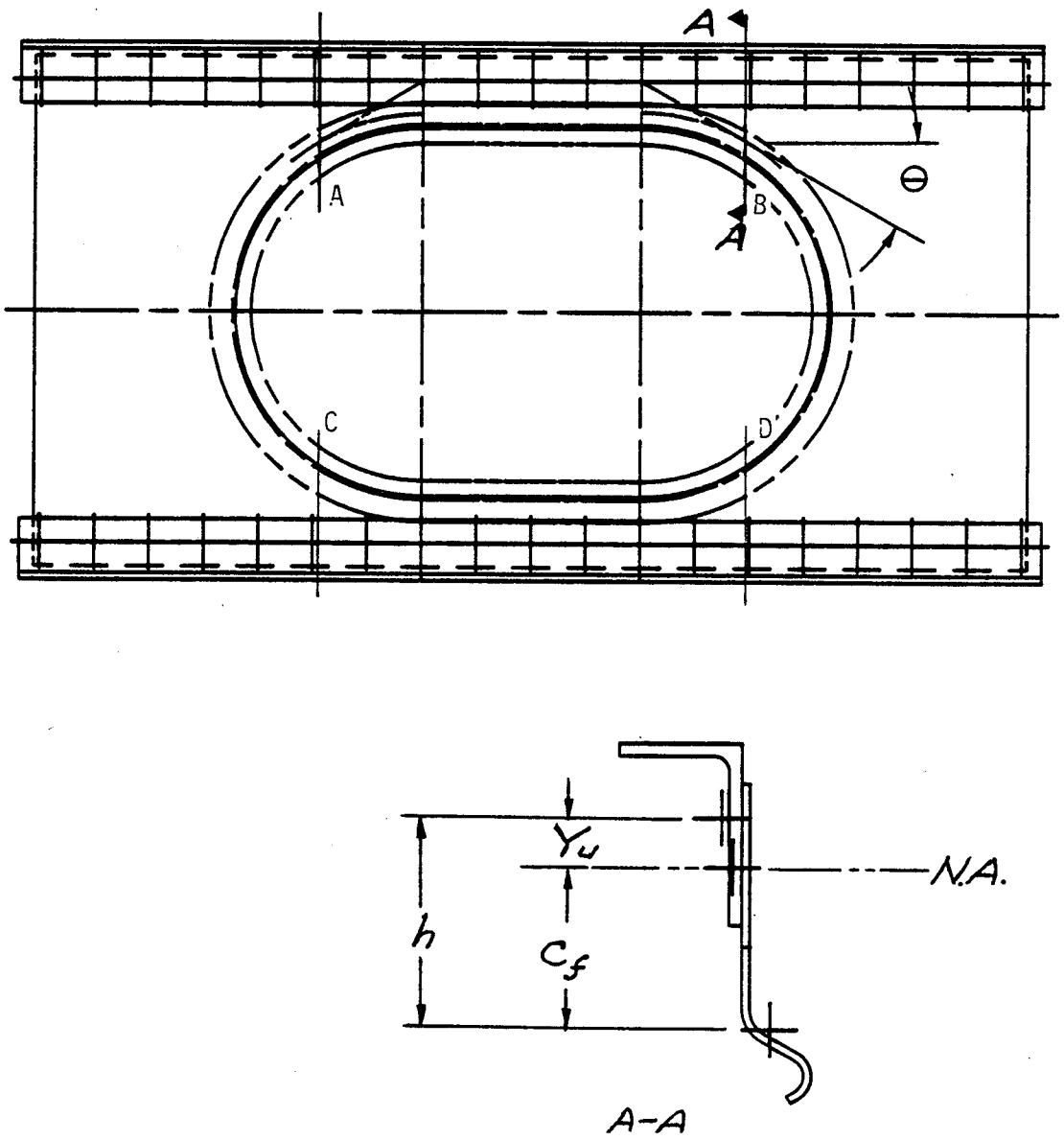


Figure B5.2.4-2 Floor Beam Cutout - Sheet Metal

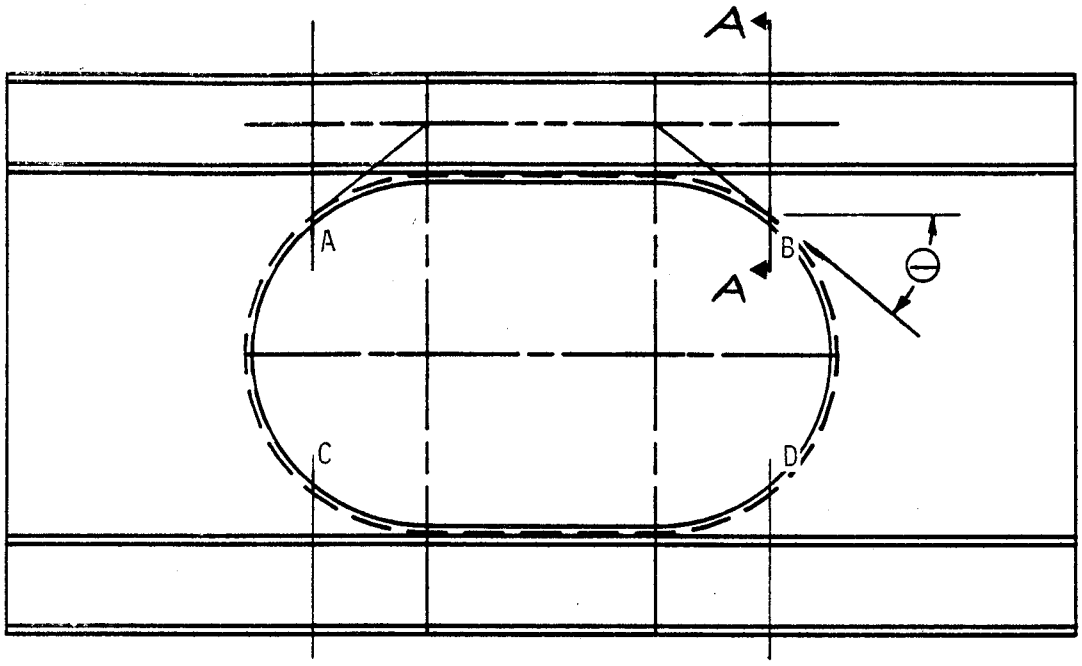


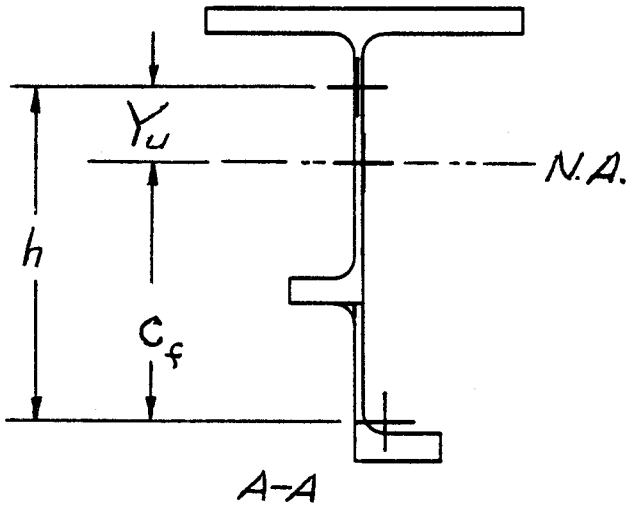


Figure B5.2.4-3 Floor Beam Cutout-Machined

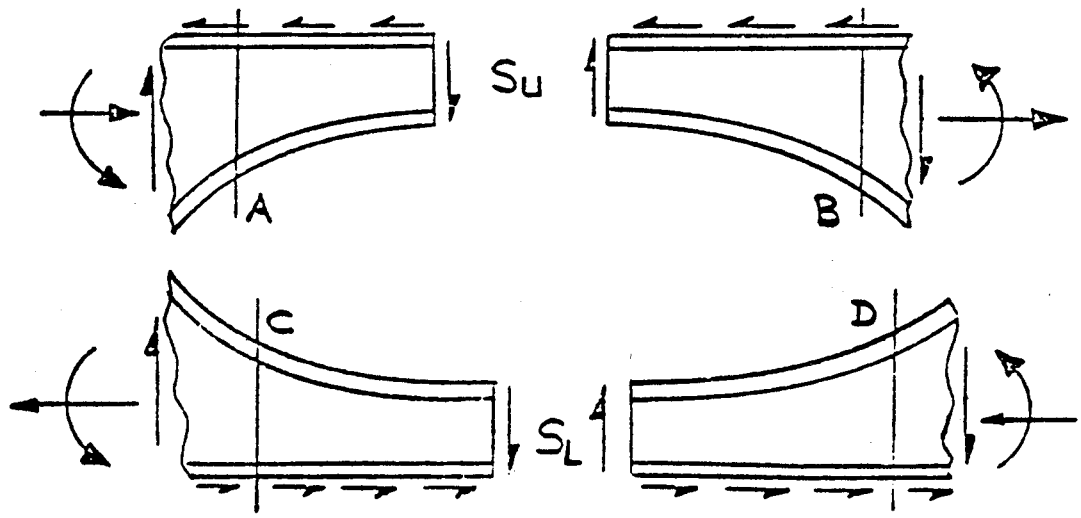


Figure B5.2.4-4 Rib Cutout Idealization

This critical section location is found by extending a tangent from the beam cap centroid at the beam material minimum section to the centroid of the hole reinforcing flange. Beam properties for each of the sections are determined. The values of $S_U$ and $S_L$ are directly proportional to the beam stiffness between the critical sections (A-B vs. C-D).

Between A and B and C and D the shear loads $S_U$ and $S_L$ are carried by beam cap bending - the beam consisting of the cap and hole flange (with unbuckled web between them). See Figure B5.2.4-5.

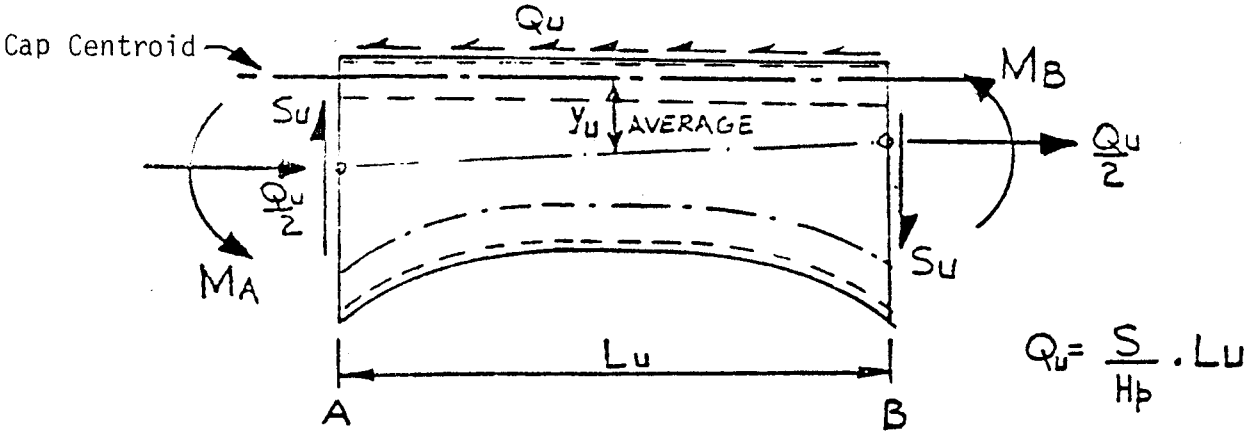


Figure B5.2.4-5

Calculate the allowable shear load as follows:

Sum moments and note that $S_U = S - S_L$

Upper half, $$M_A + M_B = S_U L_U - S \frac{L_U}{H_p} Y_U$$

Lower half, $$M_C + M_D = S_L L_L - S \frac{L_L}{H_p} Y_L$$

This leads to

$$S_{ALL} = \left[ \frac{M_A + M_B}{L_U} + \frac{M_C + M_D}{L_L} \right] \left[ \frac{H_p}{H_p - Y_U - Y_L} \right] \qquad \text{(B5-66)}$$

where $M_A$, etc., are allowable bending moments of the respective critical sections.

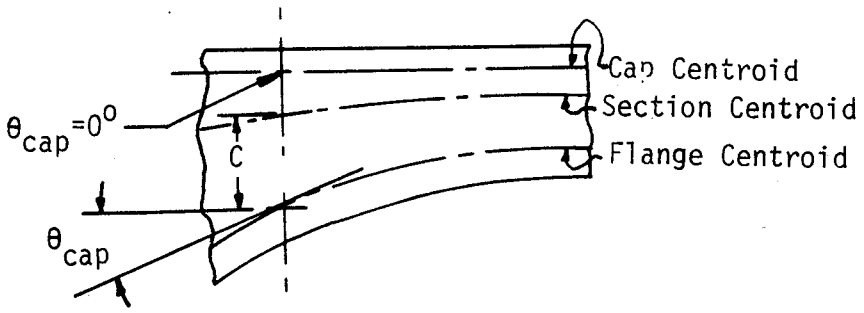


The allowable bending moment is given by

$$M_{ALL} = \frac{F_{ALL\ I}}{C} \cos^2 \theta_{cap} \qquad \text{(B5-67)}$$

from which $M_A$, $M_B$, $M_C$, and $M_D$ are determined. As most of the cutout panels are critical at the formed flange, C is the distance to the formed cap and $\theta$ the angle to its tangent.

If the web at any section begins to buckle under combined shear force and bending moment, computed using the usual interaction equation

$$R_s^2 + R_b^2 = 1$$

and assuming the point of inflection at the minimum section, then the allowable bending moment is calculated in two steps:

1. Calculated $M_{WB}$, the bending moment at which the web buckles and $F_{WB}$ the critical cap stress at web buckling.

2. Calculate $\Delta M$, the bending moment required to increase the critical cap stress from $F_{WB}$ to $F_{ALL}$ with the web assumed to carry no additonal bending stress, Thus

$$\Delta M = (F_{ALL} - F_{WB})\ A_{cap}\ h \cos \theta_{cap} \qquad \text{(B5-68)}$$

where Acap is the cap area normal to the cutout tangent and h is the distance between cap centroids. The section allowable ending moment for web buckling is

$$M_{ALL} = M_{WB} + \Delta M \qquad \text{(B5-69)}$$

When calculating $F_{ALL}$ for compression of the web cutout formed flanges, which typically form the perimeter of the cutouts, effective flange width of b = 2.10R is used. 'R' is the flange lip bend radius. $F_{cc}$ is then determined per Section B6.5.0.

The following example illustrates the usage of equation B5-66. For the wing air load rib cutout shown in Figure B5.2.4-1, assume q=242 lbs/in. The web is shear resistant. The following geometric and allowable properties are obtained for the section at points A,B,C,D.

| Sect | h | $F_{all}$ | $\theta_{cap}$ | I | $C_f$ | $M_{all}^{***}$ | $H_p$ | $L_U, L_L$ | $Y_U, Y_L$ |
|---|---|---|---|---|---|---|---|---|---|
| | in | ksi | Deg | $in^4$ | in | in kips | in | in | in |
| A | 6.88 | 60.4* | 36 | 3.969 | 3.832 | 40.95 | 19 | 17.4 | 2.39 |
| B | 6.66 | 80.0** | 36 | 3.817 | 3.627 | 49.54 | 19 | 17.4 | 2.39 |
| C | 6.22 | 80.0** | 35 | 2.953 | 3.420 | 46.35 | 19 | 17.4 | 2.09 |
| D | 6.0 | 60.4* | 37 | 2.688 | 3.270 | 31.67 | 19 | 17.4 | 2.09 |

* Allowable crippling stress of flange
** Tension ultimate stress of flange
*** From equation B5-67

From equation B5-66

$$S_{all} = \left[\frac{40.95+49.54}{17.4} + \frac{46.35+31.67}{17.4}\right]\left[\frac{19}{19-2.39-2.09}\right] = 12.67 \text{ kips}$$

and $q_{all}$=12,670/19=667 lbs/in.

The margin of safety is

$$M.S. = \frac{667}{242} - 1 = 1.76$$

A similar, more conservative result which neglects the relieving moment due to $q_o$ could be obtained from equation B5-63. Thus

$$M = \frac{q_o hw}{4} = \frac{242(19)17.4}{4} = 20{,}001 \text{ in. lbs.}$$

The average allowable bending moment for the four corners is

$$M_{all} = \frac{40{,}950+49{,}540+46{,}350+31{,}670}{4} = 42{,}130 \text{ in. lbs.}$$

and

$$M.S. = \frac{42130}{20001} - 1 = 1.11$$

## REFERENCES

B5-1 Kuhn, P., Peterson, J. P., and Levin, R. L., "A Summary of Diagonal Tension, Part I - Methods of Analysis", NACA TN 2661, May 1959.

B5-2 Gerard G. and Becker, H., Handbook of Structural Stability, Part I = "Buckling of Flat Plate", NACA TN 3781, July 1957.

B5-3 Military Standardization Handbook, "Metallic Materials and Elements for Aerospace Vehicle Structure", MIL HDBK-5C, 15 September 1976.

B5-4 Schilderout and Stein, "Critical Combinations of Shear and Direct Axial Stress for Curved Rectangular Panels", NACA TN 1928.

B5-5 Gerard and Becker, Handbook of Structural Stability, Part III, "Buckling of Curved Plates and Shells", NACA TN 3883.

B5-6 Kroll, W., Instability in Shear of Simply Supported Square Plates with Reinforced Hole; Research Paper RP 2037, National Bureau of Sandards, Nov. 1949.

B5-7 Bruhn, E., Analysis and Design of Flight Vehicle Structures, 1975.

# COLUMN BUCKLING

TABLE OF CONTENTS

## B6.0.0 Column Buckling

### B6.1.0 Introduction

Column failures are classified under the two general headings of primary instability and secondary instability. Primary instability occurs when the column bends, twists, or bends and twists along its longitudinal axis. The column cross section is translated, rotated, or translated and rotated, but not distorted. Secondary instability occurs when the column cross-sectional elements distort, but the longitudinal edges where two adjacent elements intersect remain straight. Primary and secondary instability failures are illustrated in Figure B6.1.0-1.

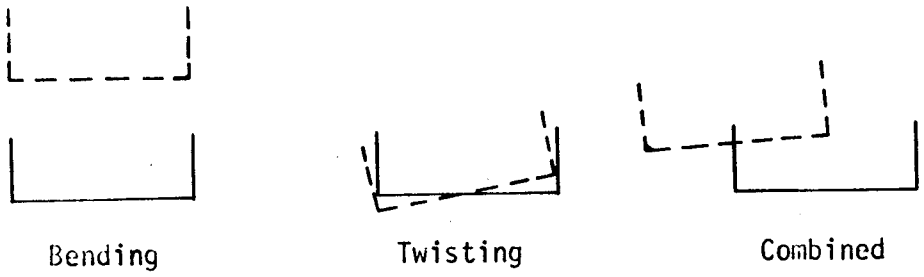


a. Primary Instability

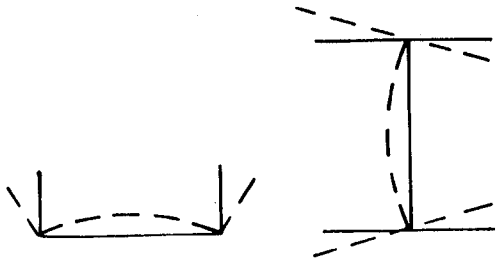

b. Secondary Instability

Figure B6.1.0-1 Primary and Secondary Instability of a Column

Primary instability of a column is considered in this section. Secondary instability is covered in Section B7.0.0. Section B6.2.0 presents equations and design charts relative to the types of columns frequently encountered in aircraft design. Supplementary information such as inelastic effects, end fixity, and attachment criteria are given in Section B6.3.0. Section B6.4.0 presents preliminary design information. Section B6.5.0 presents the design approach to be used for compression panels in production design.

B6.1.1 Symbols

| | |
|---|---|
| A | Column or panel cross-sectional area, in.$^2$ |
| $A_1$ | Area of compression panel skin, $b_s t_s$, in.$^2$ |
| $A_2$ | Area of compression panel stringer, in.$^2$ |
| b | Element or panel width, in. |
| $b_a$ | Width of stringer flange against skin, in. |
| $b_e$ | Effective skin width, in. |
| $b_f$ | Width of stringer flange away from skin, in. |
| $b_o$ | Distance between centerline of stringer web and attachment, in. |
| $b_w$ | Width of stringer web, in. |
| c | End fixity or subscript denoting compression |
| $c_e$ | Effective end fixity |
| $c_{end}$ | Fixity at the ends of a beam column or continuous support |
| C | Centroid of cross section |
| $C_p$ | Coupling parameter, $x_o/I_p$ |
| $C_w$ | Warping constant (see Section E1.0.0) |
| $C_1$, $C_2$ | Arbitrary constants |
| D | Attachment diameter, in. |
| e | Eccentricity, in., subscript denoting edge or effective |
| E | Modulus of elasticity, psi |
| $E_s$ | Secant modulus, psi |
| $E_t$ | Tangent modulus, psi |
| f | Function; distance between centerline of stringer web and a line along which attachments effectively clamp flange to skin; general term for applied stress, psi |
| $f_1$ | Applied skin stress, psi |
| $f_2$ | Applied stringer stress, psi |
| $f_b$ | Applied bending stress, psi |

| | |
|---|---|
| $F$ | Allowable stress in general or with subscripts, psi |
| $F_B$ | Allowable axial stress for bending instability, psi |
| $F_c$ | Allowable compression stress, psi |
| $F_{cc}$ | Allowable crippling stress, psi |
| $F_{cr}$ | Allowable critical buckling stress, psi |
| $F_T$ | Allowable axial stress for twisting instability, psi |
| $F_x$ | Allowable axial stress for bending instability about x axis, psi |
| $F_y$ | Allowable axial stress for bending instability about y axis, psi |
| $G$ | Modulus of rigidity, psi |
| $h_y$ | Distance in y direction between centroid and skin centerline, in. |
| $I$ | Moment of inertia, in.$^4$ (Subscripts denote bending axis, xx and yy) |
| $I_c$ | Polar moment of inertia about centroid, in.$^4$ |
| $I_o$ | Polar moment of inertia about shear center, in.$^4$ |
| $j$ | Constant, $\sqrt{EI/P}$ |
| $J$ | Torsion constant (see Section E1.0.0) |
| $k_f$ | Resistance of skin to antisymmetrical bending |
| $k_m$ | Buckling coefficient for skin |
| $k_p$ | Twisting resistance of skin to instability |
| $k_s$ | Twisting resistance of stiffener to instability |
| $k_\phi$ | Combined resistance of cross section to twisting instability |
| $\ell, L$ | Column or panel length, in. |
| $L'$ | Effective column or panel length, $L/\sqrt{c}$, in. |
| $M$ | Bending moment, in.-lbs. |
| $M_c$ | Bending moment at center of beam column, in.-lbs. |
| $M_e$ | Bending moment at ends of beam column, in.-lbs. |
| $M_o$ | Bending moment on beam when axial load is zero, in.-lbs. |
| $O$ | Shear center |
| $p$ | Constant for torsion-bending interaction or attachment pitch, in. |

| | |
|---|---|
| $P$ | Axial load on column, lbs. |
| $P_{cr}$ | Critical column buckling load, $\pi^2\left(\frac{EI}{L^2}\right)$, lbs. |
| $P_e$ | Euler buckling load, lbs. ($P_e = P_{cr}$) |
| $q$ | Constant for torsion-bending interaction or distributed load on column, lbs./in. |
| $r$ | Constant for torsion-bending interaction |
| $R$ | Cylinder radius, in., or stress ratio |
| $R_c$ | Stress ratio for compression load |
| $R_R$ | Attachment tension load, lbs. |
| $t$ | Element or panel thickness, in. |
| $t_a$ | Thickness of stringer flange against skin, in. |
| $t_f$ | Thickness of stringer flange away from skin, in. |
| $t_w$ | Thickness of stringer web, in. |
| $t_s$ | Thickness of skin, in. |
| $V$ | Shear, lbs. |
| $V_o$ | Shear on beam when axial load is zero, lbs. |
| $w$ | Normal load on beam, lbs./in. |
| $x$ | Distance along beam |
| $x_o$ | Distance in x direction between centroid and shear center, in. |
| $y$ | Beam deflection |
| $y_o$ | Distance in y direction between centroid and shear center, in. |
| $\alpha$ | Rotational spring constant |
| $\delta$ | Deflection, in. |
| $\epsilon$ | Strain, in./in. |
| $\eta_B$ | Plasticity factor for bending instability, $E_t/E$ |
| $\eta_p$ | Plasticity factor for plate instability, $(E_t/E)^{1/2}$ |
| $\eta_T$ | Plasticity factor for twisting instability |
| $\theta$ | Slope of beam |

$\lambda$ Half wave length or $1./j = \sqrt{P/EI}$

$\mu$ Poisson's ratio

$\rho$ Radius of gyration, $\sqrt{I/A}$, in. (Subscripts denote bending axis)

## B6.2.0 Types of Columns

### B6.2.1 Uniformly Loaded Column

Columns are used as aircraft structure to transmit a load from A to B. The distance transversed and the load applied are generally known factors. The designer must devise the most efficient cross-sectional shape to transfer the load. From a minimum weight point of view, this generally implies column design with the minimum cross-sectional area and subsequently the highest possible stress. Maximum stress is limited by column cross section geometry, length, and material as specified by bending and twisting instability equations.

The axial stress which will cause bending instability of a column is defined by the Euler-Engesser equation.

$$F_B = \frac{\pi^2 \eta_B E}{(L'/\rho)^2} \qquad \text{(B6-1)}$$

Twisting instability is defined by the equation

$$F_T = \eta_T \left[ \frac{GJ + EC_w \left(\frac{\pi}{L'}\right)^2}{I_o} \right] \qquad \text{(B6-2)}$$

Interaction between these equations depends on the cross-sectional shape and the restraint applied to the column. When no restraint exists, column cross-sectional shape determines the interaction. In general, the cross section may be unsymmetrical or have one or two axes of symmetry. Detailed discussion of what follows can be found in Reference B6-1.

B6.2.1.1 Unsymmetrical Section

Figure B6.2.1.1-1 shows the most general case for a column cross section.

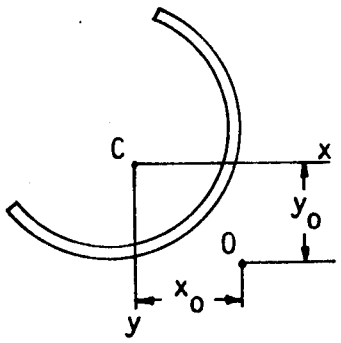


Figure B6.2.1.1-1 General Column Cross Section

Bending and twisting instability stress interact as defined by the cubic equation.

$$F^3 + p\,F^2 + qF + r = 0 \qquad \text{(B6-3)}$$

$$p = \frac{I_o}{I_c}\left[\frac{A}{I_o}\left(F_x y_o^2 + F_y x_o^2\right) - \left(F_x + F_y + F_T\right)\right]$$

$$q = \frac{I_o}{I_c}\left[F_x F_y + F_x F_T + F_y F_T\right]$$

$$r = \frac{I_o}{I_c}\left[F_x F_y F_T\right]$$

In these equations, bending instability stresses ($F_x$ and $F_y$) are based on the principal axis of the section. Twisting instability stress (Equation B6-2) is computed based on a warping constant and polar moment of inertia relative to the section shear center. When stresses are above the proportional limit, plasticity corrections should be made to the combined stress, F, and not $F_x$, $F_y$, or $F_T$.

Equation B6-3 has three positive roots. The smallest root is always less than $F_x$, $F_y$, and $F_T$. For this reason, unsymmetrical sections are not desirable as columns.

B6.2.1.2 Section Symmetrical About One Axis

A channel cross section shown in Figure B6.2.1.2-1 has one axis of symmetry. The y-axis bending instability stress is not coupled with the twisting instability stress. Equation B6-1 applies for y-axis bending. The x-axis bending instability stress interacts with the twisting instability stress based on the quadratic equation:

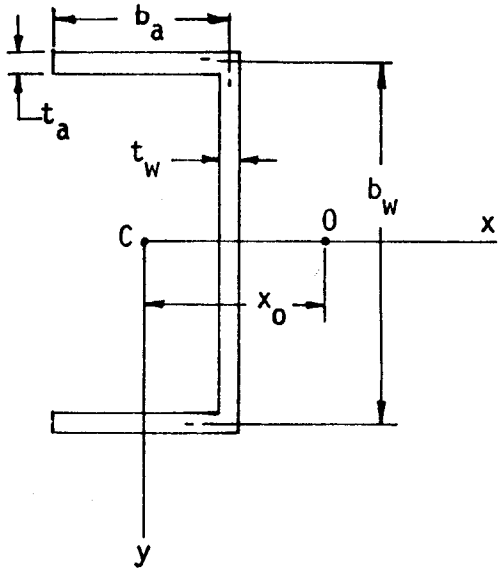


Figure B6.2.1.2-1 Section Symmetrical About One Axis

$$F^2 + qF + r = 0 \qquad \text{(B6-4)}$$

$$q = -\frac{I_o}{I_c}\left[F_x + F_T\right]$$

$$r = \frac{I_o}{I_c}\left[F_x F_T\right]$$

When evaluating the torsional instability stress, warping constant and polar moment of inertia are computed about the section shear center. Plasticity corrections should be made to the combined stress, F and not $F_x$, $F_y$, or $F_T$.

Equation B6-4 has two positive roots. The lowest root is always less than either $F_x$ or $F_T$. Interaction is shown in Figure B6.2.1.2-2 for ratios of $I_o/I_c$.

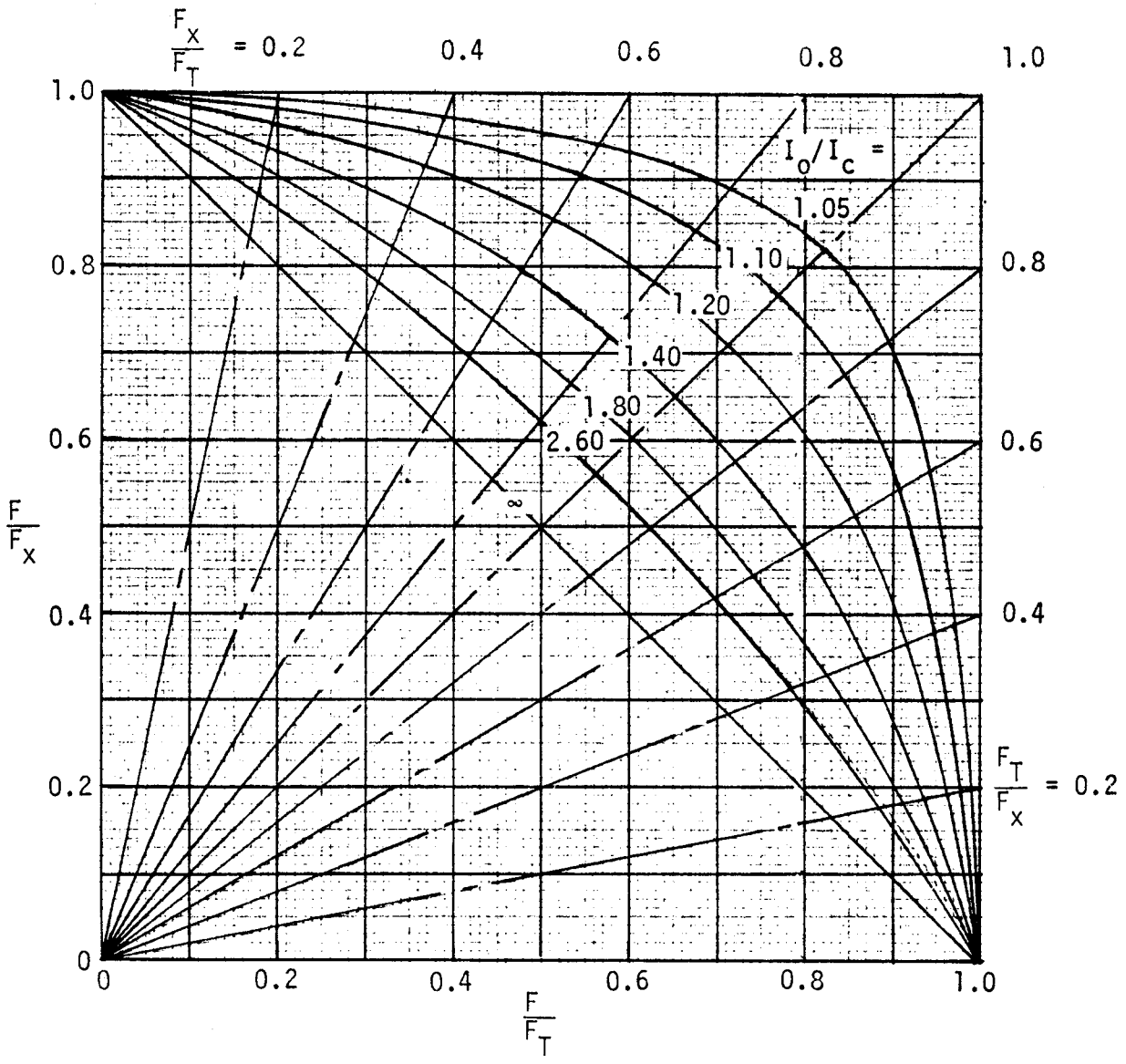


Figure B6.2.1.2-2 Interaction Between Bending and Twisting for a Section with One Axis of Symmetry

For a channel with constant wall thickness, the ratio of flange length-to-channel depth ($b_a/b_w$) is equal to 0.327 if secondary stresses for the elements are equal. With this constraint, $I_o/I_c$ is 1.95. The ratio $F_T/F_x$ is about 0.05, so from Figure B6.2.1.2-2, the failing stress is 3.0 percent less than the torsional instability stress. Torsional instability stress is 50 percent less than y-axis bending instability stress.

B6.2.1.3 Section Symmetrical About Two Axes

There is no interaction between bending and twisting instability stresses in this case. Equations B6-1 and B6-2 must be satisfied independently. An I section having equal moment of inertia about both the x and y axis is an efficient section. A tube is even more efficient. The tube, being a closed section, will not be subject to torsional instability stress. An I section, which is sized by equating the Euler-Engesser, and secondary stresses will always have the torsional instability stress as a higher mode of failure. Design charts and weight comparisons are given for both I sections and tubes in Section B6.4.0.

B6.2.1.4 Compression Panels (Refer to Section B6.5.0 for design approach)

A compression panel can be classified as a column if the panel width b is considerably greater than the thickness (or radius of gyration in more general terms) and is a fixed parameter. In this case, the support along the unloaded edges is ignored and the panel is assumed to behave as a column.

Like columns, the compression panel (wide column) can have cross sections that are unsymmetrical, have one axis of symmetry, or have two axes of symmetry. The same type of interaction formulas apply. However, modification must be made to the various constants. Also, rotational and bending restraints must be applied.

Most large transport wing and horizontal stabilizer primary structure fall into a wide column classification. Fuselage skin and stringer panel strength can be conservatively approximated by wide column analysis when the frame spacing-to-radius ratio is small.

For wide column analysis, both the Euler-Engesser Equation (B6-1) and the twisting instability Equation (B6-2) apply. Instability can be either symmetrical or antisymmetrical as shown in Figure B6.2..4-1, depending on the spring restraint offered by the skin and stringers.

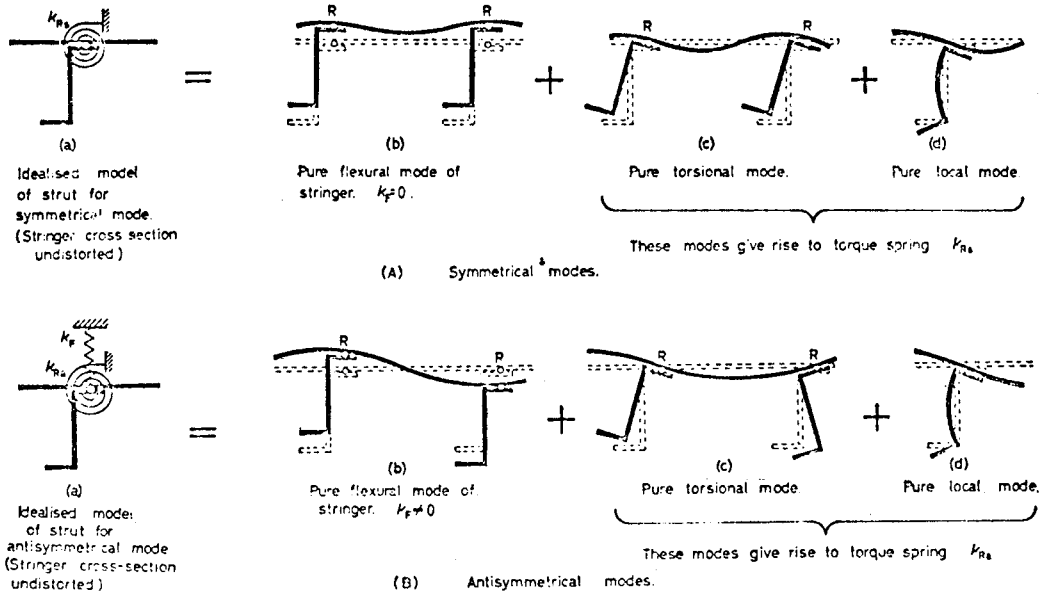


Figure B6.2.1.4-1 Deformations at Instability for Stiffened Panels

Equations B6-1 and B6-2 are modified to account for spring restraints as follows:

$$F_B = \eta_B \left[ \frac{\pi^2 E}{(\lambda/\rho)^2} + \frac{k_f}{A} \left( \frac{\lambda}{\pi} \right)^2 \right] \qquad \text{(B6-5)}$$

$$F_T = \eta_T \left[ \frac{GJ + EC_W \left( \frac{\pi}{\lambda} \right)^2 + K_\phi \left( \frac{\lambda}{\pi} \right)^2}{I_o} \right] \qquad \text{(B6-6)}$$

where

$$k_\phi = \frac{k_p \, k_s}{k_p + k_s}$$

$k_p$ and $k_s$ are the rotational restraints offered by the skin and stringer respectively. Approximate expressions for these spring restraints $k_f$, $k_p$, and $k_s$ are given in Table B6.2.1.4-1, based on derivations given in Reference B6-2.

Table B6.2.1.4-1 Approximate Values for Skin and Stringer Spring Restraints

| Mode | $k_f$ | $k_p$ | $k_s$ |
|---|---|---|---|
| Symmetrical | 0 | $\frac{E}{1-\mu^2}\left(\frac{t_s}{b_s}\right)^3$ | $\frac{E}{4(1-\mu^2)}\left[\frac{1}{\frac{b_w}{t_w^3}+3\frac{b_o}{t_a^3}}\right]$ |
| Antisymmetrical | $\frac{4E}{1-\mu^2}\left(\frac{t_s}{b_s}\right)^3$ | $\frac{E}{3(1-\mu^2)}\frac{t_s^3}{b_s}\left(1+.7\frac{f_e-F_i}{f_e}\right)$ | |
| Symmetrical Curved Panel of Radius R (Failure Outward) | $E\frac{b_s t_s}{R^2}$ | Note: $f_e$ = applied edge stress<br>$F_i$ = initial buckling stress | |

These expressions neglect the effect of compression stress and wave length, but are generally accurate enough for preliminary design. More accurate theoretical expressions that consider compression stress and wave length are given in Reference B6-2. Test data are not available.

The constants for twisting instability, $C_w$ and $I_o$, in Equation B6-6 must be computed about a restrained shear center which lies in the plane of the skin at a distance $x_E$ from the web of the stringer as shown in Figure B6.2.1.4-2. Values for $C_w$, $I_o$, and $x_E$ are given in Section E1.0.0 on section properties.

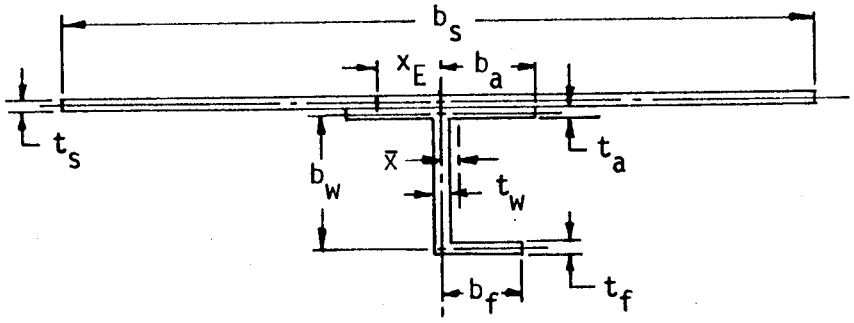


Figure B6.2.1.4-2 Geometry Definition for Stiffened Panel

Interaction between Equations B6-5 and B6-6 is determined from the quadratic equation

$$F^2 - \frac{1}{1-C_p^2}(F_x + F_T)\,F + \frac{1}{1-C_p^2}F_x F_T = 0 \qquad \text{(B6-7)}$$

as given in Reference B6-2, and plotted in Figure B6.2.1.4-3. The coupling parameter $C_p$ is defined as

$$C_p = \frac{e}{(I_o/A)^{1/2}} \qquad \text{(B6-8)}$$

where

$$e = x_E - \bar{x} \qquad \text{(B6-9)}$$

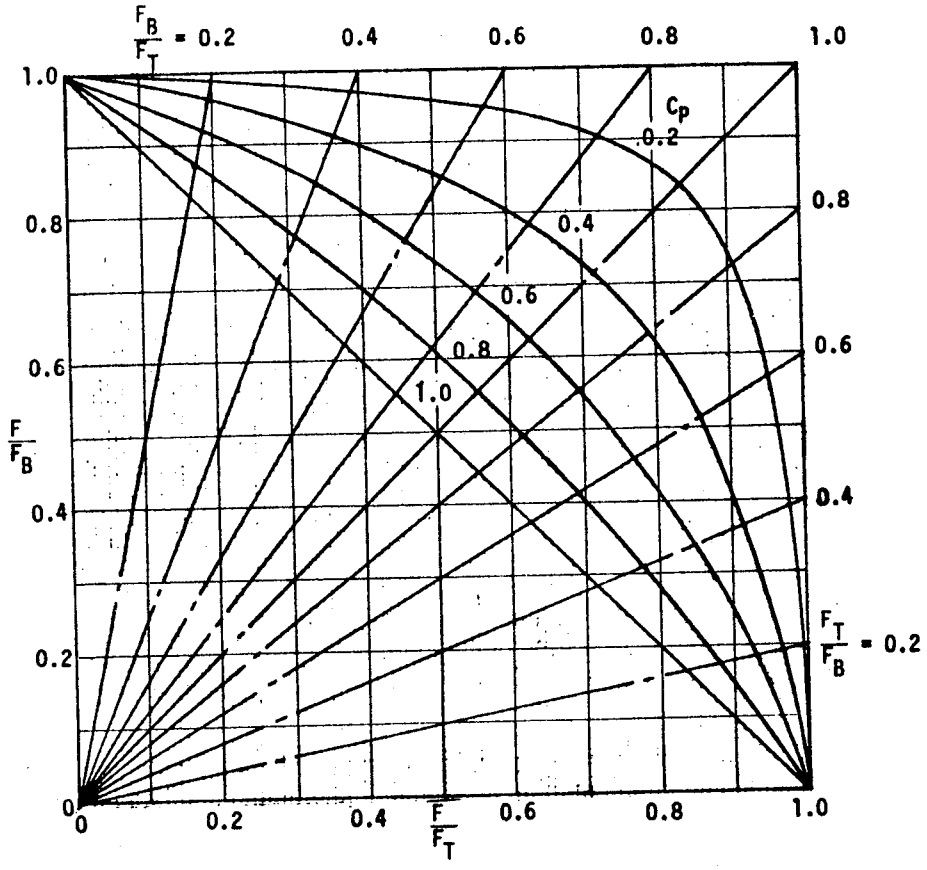


Figure B6.2.1.4-3 Interaction Between Bending and Twisting for a Stiffened Panel

The value for stress in Equation B6-5 and B6-6 has a minimum value depending on the half-wavelength, $\lambda = L'/n$, except for the case of symmetrical bending where $k_f = 0$. In this case, Equation B6-5 is simply the Euler-Engesser equation for $n = 1$. However, when $k_f \neq 0$ and $k_\phi \neq 0$, then a minimum stress is obtained at a prescribed half-wavelength for both Equation B6-5 and B6-6. These values are given in Table B6.2.1.4-2 for the case when skin is unbuckled and $k_\phi$ is assumed indepenent of end load. These equations are particularly important when the coupling parameter, $C_p = 0$. Then bending and twisting are independent of each other. For a given column length, L', minimum stress may occur for values of $n \neq 1$. For coupled failure, $C_p \neq 0$, the value of effective column length may be substituted for $\lambda$.

Table B6.2.1.4-2 Minimum Stress and Corresponding Half Wave length for Bending and Twisting Instability

| Mode | Half-Wavelength, $\lambda$ | $F_{min}$ |
|---|---|---|
| Antisymmetrical Bending | $\left[\frac{E I_{xx}}{k_f}\right]^{1/4}$ | $\frac{2\sqrt{E I_{xx} k_f}}{A}$ |
| Symmetrical or Antisymmetrical Twisting | $\left[\frac{E C_w}{k_\phi}\right]^{1/4}$ | $\frac{GJ+2\sqrt{E C_w k_\phi}}{I_o}$ |

B6.2.2 Beam Columns

The beam column is a structural member which functions both as a beam subjected to transverse bending loads and simultaneously as a column subjected to axial end loads. End loads may be either tension or compression. Axial tension tends to straighten the beam and thus reduce the bending moments produced by transverse loads. Axial compression has the opposite effect and may greatly increase the maximum bending moment and deflection. In either case, the solution cannot be obtained by simple superposition, but must be arrived at by methods that take into account the change in deflection produced by the axial load.

### B6.2.2.1 Beam Columns with Axial Compressive Loads

The total moment at any point on a single span is

$$M = C_1 \sin \frac{x}{j} + C_2 \cos \frac{x}{j} + f(w) \qquad \text{(B6-10)}$$

$$j = \sqrt{\frac{EI}{P}}$$

The shear at any point on the beam is

$$V = \frac{C_1}{j} \cos \frac{x}{j} - \frac{C_2}{j} \sin \frac{x}{j} + f(w) \qquad \text{(B6-11)}$$

Deflection and beam slope can be computed from the equations

$$y = \frac{M_o - M}{P} \qquad \text{(B6-12)}$$

$$\Theta = \frac{V_o - V}{P} \qquad \text{(B6-13)}$$

where $M_o$ and $V_o$ are the moments and shears at a given point when the axial load is zero.

The constants, $C_1$, $C_2$, and f(w) are given in Table B6.2.2-1 for beam columns with various end supports and transverse loads. When maximum moment is not given, it may be obtained by plotting several values of moment along the beam and constructing a smooth curve through the points.

# Table B6.2.2-1 Single Span Beam Columns with Axial Compression Loads

| Loading | $C_1$ | $C_2$ | f(w) | Eq. for Point of Max Bending Moment | Eq. for Max. Span Bending Moment |
|---|---|---|---|---|---|
| Equal End Moments. No Side Load 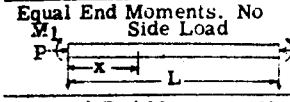  | $M_1 \tan \frac{L}{2j}$ | $M_1$ | o | $x = \frac{L}{2}$ | $M_{max} = \frac{M_1}{\cos \frac{L}{2j}}$ |
| Unequal End Moments. No Side Load 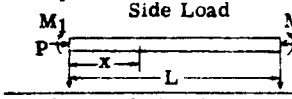  | $\frac{M_2 - M_1 \cos \frac{L}{j}}{\sin \frac{L}{j}}$ | $M_1$ | o | $\tan \frac{x}{j} = \frac{M_2 - M_1 \cos \frac{L}{j}}{M_1 \sin \frac{L}{j}}$ | $M_{max} = \frac{M_1}{\cos \frac{x}{j}}$ |
| Uniform Side Load. No End Moments 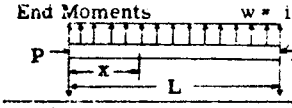  | $\frac{wj^2 (\cos \frac{L}{j} - 1)}{\sin \frac{L}{j}}$ | $-wj^2$ | $wj^2$ | $x = .5\ L$ | $M_{max} = wj^2 (1 - \sec \frac{L}{2j})$ |
| Uniform Side Load Plus End Moments 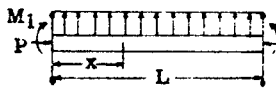  | $\frac{D_2 - D_1 \cos L/j}{\sin L/j}$ where $D_1 = M_1 - wj^2$ $D_2 = M_2 - wj^2$ | $D_1$ | $wj^2$ | $\tan \frac{x}{j} = \frac{D_2 - D_1 \cos \frac{L}{j}}{D_1 \sin \frac{L}{j}}$ | $M_{max} = \frac{D_1}{\cos \frac{x}{j}} + wj^2$ |
| Concentrated Side Load. No End Moments 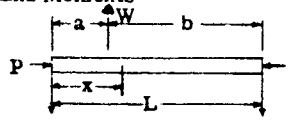  | $x < a$, $-W \sin \frac{b}{j} \Big/ \sin \frac{L}{j}$ <br> $x > a$, $+W \sin \frac{a}{j} \Big/ \tan \frac{L}{j}$ | o <br> $-W \sin \frac{a}{j}$ | o <br> o | $\tan x/j = \frac{C_1}{C_2}$ | $M_{max} = \left(C_1^2 + C_2^2\right)^{\frac{1}{2}}$ |
| Triangular Loading. No End Moments 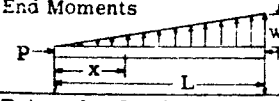  | $\frac{-wj^2}{\sin \frac{L}{j}}$ | o | $\frac{wj^2 x}{L}$ | | |
| Triangular Loading. No End Moments 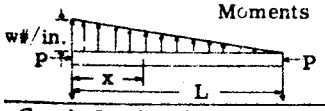  | $\frac{wj^2}{\tan \frac{L}{j}}$ | $-wj^2$ | $\frac{wj^2 (1-x)}{L}$ | | |
| Couple Loading (Clockwise) 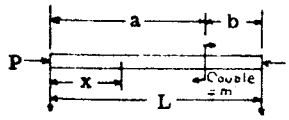  | $x < a$, $-m \cos \frac{b}{j} \Big/ \sin \frac{L}{j}$ <br> $x > a$, $-m \cos \frac{a}{j} \Big/ \tan \frac{L}{j}$ | o <br> $m \cos \frac{a}{j}$ | o <br> o | | |

w or W is positive when upward.
M is positive when it tends to cause compression on the upper fibers of the beam at the section being considered.

B6.2.2.2 Beam Columns with Axial Tension Loads

A conservative approach for evaluating moments is to neglect the axial loads and compute moments based solely on the transverse loads. If more accurate results are desired, they can be obtained by using Equation B6-10 to B6-13 where the constants, $C_1$, $C_2$, and f(w) are obtained from Table B6.2.2-2. In this case, the value for E used when computing j, should be based on the secant modulus that corresponds with the applied axial stress rather than tangent modulus. The results from Table B6.2.2-2 become inaccurate for ratios $M/M_o$ greater than 0.90. Calculation should be carried to four significant figures.

Note:

1. W or w is positive when upward.
2. M is positive when producing compression in upper fibers.
3. $j = \sqrt{EI/P}$ with a dimension of length.
4. $D_1 = M_1 - wj^2$; $D_2 = M_2 - wj^2$
5. All angles for trigonometric functions are in radians.
6. When the formula for the maximum moment is not provided in the table, methods of differential calculus may be employed, if applicable, to find the location of maximum moment; or moments at several points in a span may be computed and a smooth curve then drawn through the plotted results. The same principle applies in the case of a complicated combination of loadings.
7. All points where concentrated loads or moments are acting should also be checked for maximum possible bending moments.
8. Before the total stress can reach the yield point a compression beam column may fail due to buckling. This instability failure is independent of lateral loads. The maximum P that the structure can sustain may be computed pertaining to the boundary condition without regard to lateral loads. A check using ultimate loads should always be made to insure that P is not beyond the critical value.
9. It is recommended that all calculations should be carried to at least four significant figures.

## Table B6.2.2-2 Single Span Beam Columns with Axial Tension loads

| CASE NO. | LOADING | $C_1$ | $C_2$ | f (w) | MAX. MOMENT |
|---|---|---|---|---|---|
| 1 | UNEQUAL END MOMENTS 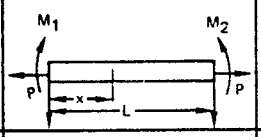 | $\frac{M_2 - M_1(\text{Cosh } L/j)}{\text{Sinh } L/j}$ | $M_1$ | 0 | $M_{max} = \frac{M_1}{\text{Cosh } x/2j}$ WHERE $\text{Tanh } x/j = \frac{M_2 - M_1(\text{Cosh } L/j)}{-M_1(\text{Sinh } L/j)}$ |
| 2 | EQUAL END MOMENTS 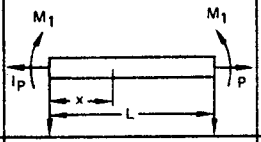 | $-M_1(\text{Tanh } L/2j)$ | $M_1$ | 0 | $M_{max} = \frac{M_1}{\text{Cosh } L/2j}$ |
| 3 | UNIFORM LOAD 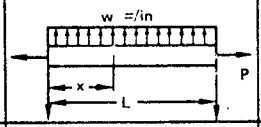 | $\frac{wj^2(1 - \text{Cosh } L/j)}{\text{Sinh } L/j}$ | $wj^2$ | $-wj^2$ | $M_{MAX} = wj^2(\text{Sech } L/2j) - 1)$ |
| 4 | UNIFORM LOAD PLUS END MOMENTS 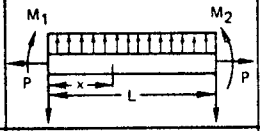 | $\frac{D_2 - D_1(\text{Cosh } L/j)}{\text{Sinh } L/j}$ SEE NOTE 4 | $D_1$ SEE NOTE 4 | $-wj^2$ | $M_{MAX} = \frac{D_1}{\text{Cosh } x/j} - wj^2$ WHERE $\text{Tanh } x/j = \frac{-D_2 - D_1(\text{Cosh } L/j)}{D_1(\text{Sinh } L/j)}$ SEE NOTE 4 |
| 5 | CONCENTRATED LOAD 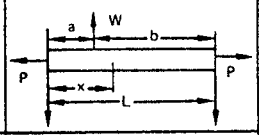 | $x < a$: $\frac{-Wj(\text{Sinh } b/j)}{\text{Sinh } L/j}$ <br> $x > a$: $\frac{Wj(\text{Sinh } a/j)}{\text{Tanh } L/j}$ | 0 <br> $-Wj(\text{Sinh } a/j)$ | 0 <br> 0 | $M_{max} = \frac{-C_2^2 - C_1^2(\text{Cosh } x/j)}{C_2}$ WHERE $\text{Tanh } x/j = -\frac{C_1}{C_2}$ |
| 6 | UNIFORMLY INCREASING LOAD 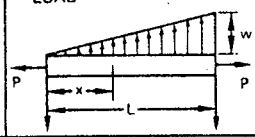 | $\frac{wj^2}{\text{Sinh } L/j}$ | 0 | $-\frac{wj^2 x}{L}$ | OCCURS AT $\text{Cosh } x/j = +j/L(\text{Sinh } L/j)$ SOLVE FOR x/j AND x, SUBSTITUTE INTO EQUATION B6-10 |
| 7 | UNIFORMLY DECREASING LOAD 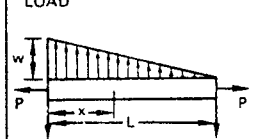 | $\frac{-wj^2}{\text{Tanh } L/j}$ | $wj^2$ | $-wj^2(1-x/L)$ | OCCURS AT $\text{Cos}\frac{L-x}{j} = j/L(\text{Sinh } L/j)$ SOLVE FOR x/j AND x, AND SUBSTITUTE INTO EQUATION B6-10 |
| 8 | SYMMETRICAL TRIANGLE LOAD 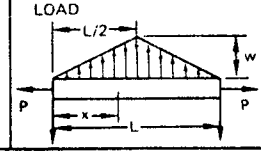 | $x < L/2$: $\frac{2wj^3}{L(\text{Cosh } L/2j)}$ <br> $x > L/2$: $\frac{-2wj^3(\text{Cosh } L/j)}{L(\text{Cosh } L/2j)}$ | 0 <br> $\frac{4wj^3}{L}\text{Sinh } L/2j$ | $\frac{-2wj^2 x}{L}$ <br> $-2wj^2(1 - x/L)$ | $M_{MAX} = \frac{2wj^3}{L}(\text{Tanh } L/2j) - wj^2$ |

## Table B6.2.2-2 Single Span Beam Columns with Axial Tension Loads (continued)

| CASE NO. | LOADING | $C_1$ | $C_2$ | f (w) | MAX. MOMENT |
|---|---|---|---|---|---|
| 9 | PARTIAL UNIFORMLY DISTRIBUTED LOAD 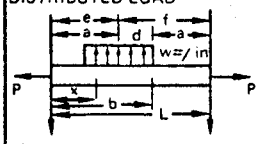 | $x < a$ : $\frac{-2wj^2(\text{Sinh } d/2j)\text{Sinh } f/j}{\text{Sinh } L/j}$<br>$a < x < b$:<br>$\frac{2wj^2(\text{Sinh } d/2j)(\text{Sinh } e/j) - wj^2(\text{Sinh } b/j)}{\text{Tanh } L/j}$<br>$b < x < L$: $\frac{2wj^2(\text{Sinh } d/2j)\text{Sinh } e/f}{\text{Tanh } L/j}$ | 0<br>$wj^2(\text{Cosh } a/j)$<br>$-2wj^2(\text{Sinh } d/j)\text{Sinh } e/f$ | 0<br>$-wj^2$<br>0 | SEE NOTE (6) |
| 10 | SYMMETRICAL PARTIAL UNIFORM DISTRIBUTED LOAD 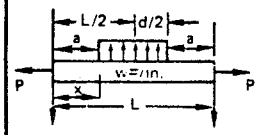 | $x < a$: $-\frac{wj^2(\text{Sinh } d/2j)}{\text{Cosh } L/2j}$<br>$a < x < L-a$: $-wj^2(\text{Cosh } a/j)\text{Tanh } L/2j$<br>$L-a < x < L$ : $\frac{wj^2(\text{Sinh } d/2j)\text{Cosh } L/j}{\text{Cosh } L/2j}$ | 0<br>$-wj(\text{Sinh } a/j)$<br>$-2wj^2(\text{Sinh } d/2j)\text{Sinh } L/2j$ | 0<br>$-wj^2$<br>0 | $wj^2\left[\frac{\text{Cosh } a/j}{\text{Cosh } L/2j} - 1\right]$<br>AT MIDSPAN |
| 11 | TWO SYMMETRICAL CONCENTRATED LOADS  | $x < a$: $-\frac{Wj(\text{Cosh } b/2j)}{\text{Cosh } L/2j}$<br>$a < x < L-a$: $Wj(\text{Sinh } a/j)\text{Tanh } L/2j$<br>$L-a < x < L$: $\frac{Wj(\text{Cosh } L/j)\text{Cosh } b/2j}{\text{Cosh } L/2j}$ | 0<br>$-wj(\text{Sinh } a/j)$<br>$\frac{-Wj(\text{Sinh } L/j)\text{Cosh } b/2j}{\text{Cosh } L/2j}$ | 0<br>0<br>0 | $-Wj\frac{\text{Sinh } a/j}{\text{Cosh } L/2j}$<br>AT MIDSPAN |
| 12 | CONCENTRATED MOMENT 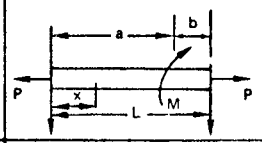 | $x < a$: $-\frac{m(\text{Cosh } b/j)}{\text{Sinh } L/j}$<br>$x > a$.: $-\frac{M(\text{Cosh } a/j)}{\text{Tanh } L/j}$ | 0<br>$M(\text{Cosh } a/j)$ | 0<br>0 | SEE NOTE (6) |
| 13 | FIXED END BEAM - UNIFORM LOAD 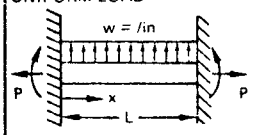 | $\frac{-wLj}{2}$ | $\frac{wLj}{2(\text{Tanh } L/2j)}$ | $-wj^2$ | AT $x = 0$<br>$M_{max} = wj^2\left[\frac{L/2j}{\text{Tanh } L/2j} - 1\right]$ |
| 14 | FIXED END BEAM-CONCENTRATED LOAD AT CENTER 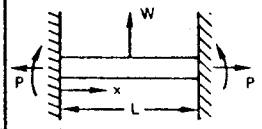 | $x < L/2$ : $-Wj/2$<br>$x > L/2$ : $\frac{Wj}{2}\left[2(\text{Cosh } L/2j) - 1\right]$ | $\frac{Wj}{2}\left[\frac{(\text{Cosh } L/2j) - 1}{\text{Sinh } L/2j}\right]$<br>$\frac{Wj}{2}\left[\frac{(\text{Cosh } L/2j) - \text{Cosh } L/j}{\text{Sinh } L/2j}\right]$ | 0<br>0 | $M_{max} = Wj/2\left[\frac{1-(\text{Cosh } L/2j)}{\text{Sinh } L/2j}\right]$<br>At $x = L/2$ |
| 15 | CANTILEVER-CONCENTRATED END LOAD 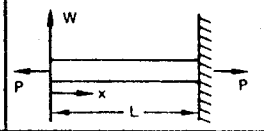 | | | | $M_{max} = Wj(\text{Tanh } L/j)$<br>At $x = L$ |
| 16 | CANTILEVER-UNIFORM LOAD 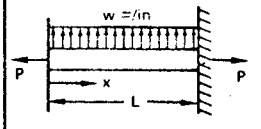 | | | | $M_{max} = wj[L(\text{Tanh } L/j) - j(1\text{-Sec } L/j)]$<br>At $x = L$ |
| 17 | FIXED END BEAM – LATERAL DISPLACEMENT  | | | | $M_{max} = \frac{a\,P(\text{Tanh } L/2j)}{2\,[L/2j - (\text{Tanh } L/2j)]}$<br>at $x = 0$, and<br>$-M_{max}$ at $x = L$ |

B6.2.2.3 Beam Columns on Continuous Supports

A large percentage of aircraft primary structure fall under this classifiction. Airloads, fuel loads, and fuselage pressurization loads supply the transverse loads. Ribs and frames provide the continuous support for the primary structure. The three moment equation can be adapted to handle this type of problem if terms are added to account for axial load. However, in aircraft applications, the number of supports is usually large and hand solution becomes tedious. Computer programs are available to handle detailed solutions. For preliminary analyses, Figure B6.2.2.3-1 shows the solution for the center bay of a beam column on equally spaced continuous supports having three, five, and seven bays. Transverse load, I, and E are assumed constant over the beam. End restraint is varied for $c_e$ = 1, 2, and 3. For known values of $P/P_{cr}$, the rotational restraint, $\alpha\ell/EI$, and fixity c, of the center bay can be determined. Moment at the ends and midpoint of the center bay can then be found from Figures B6.2.2.3-2 and -3. The value $P_{cr}$ is the Euler load.

$$P_{cr} = \frac{\pi^2 E I}{L^2} \qquad \text{(B6-14)}$$

where the value of E corresponds to the tangent modulus for the material at the applied stress level, P/A.

In general, Figure B6.2.2.3-1 shows that center bay fixity:

1. Decreases as the ratio $P/P_{cr}$ approaches 1.0.
2. Increases as the number of supports increases.
3. Increases as the fixity of the end bay increases.

Another factor of importance not shown on the figure is that the center bay fixity decreases as the supports are displaced, which can occur due to overall bending of a box structure with rib supports.

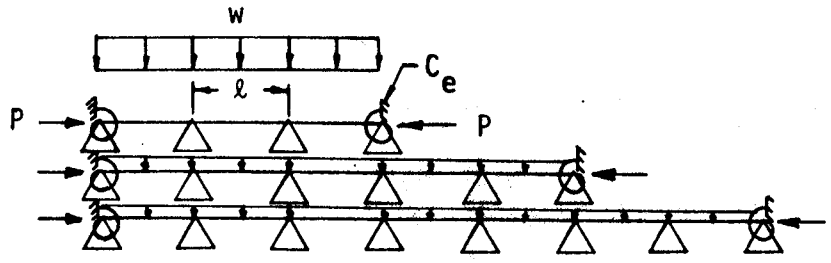


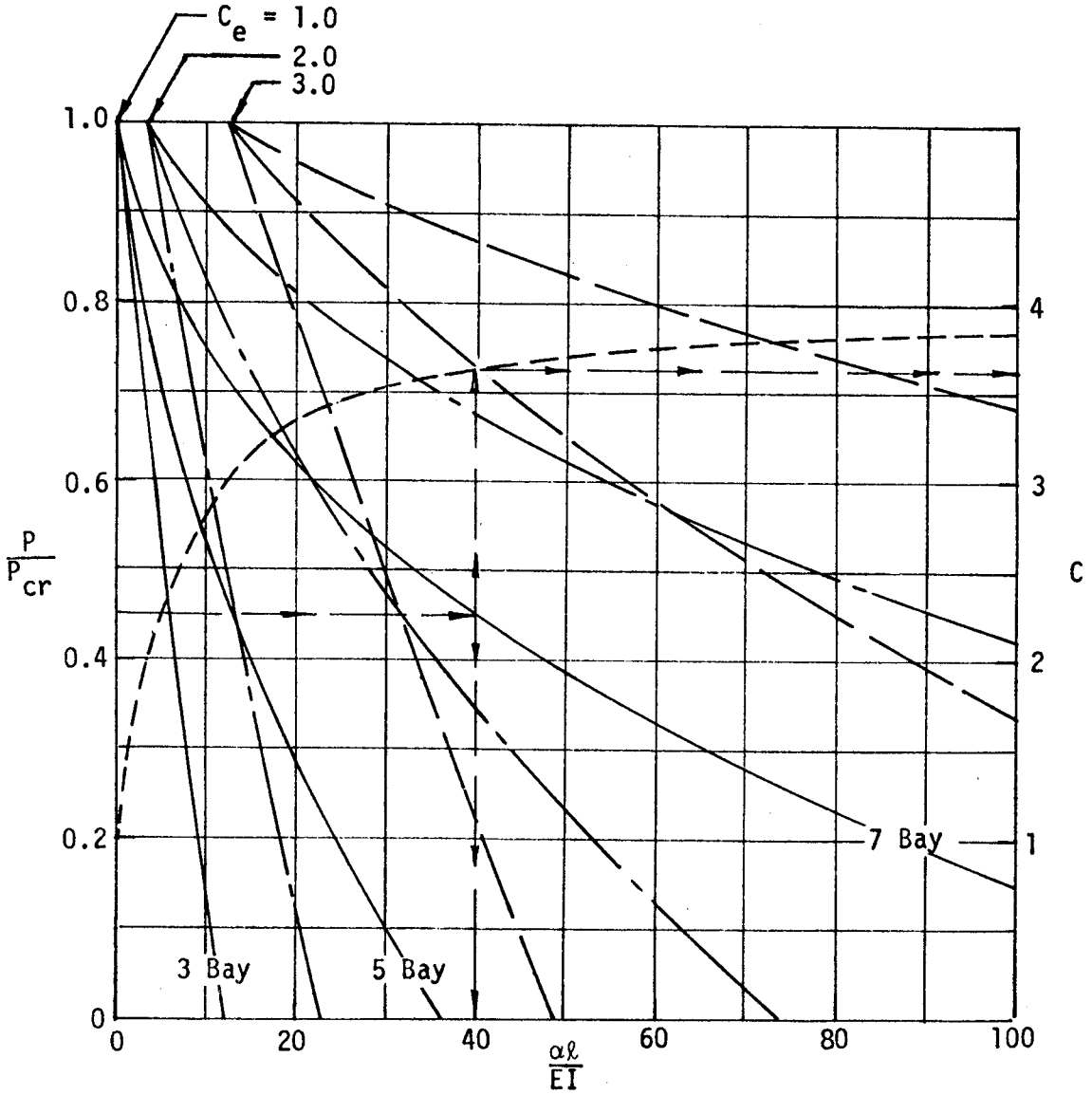


Figure B6.2.2.3-1 Center Bay Fixity for a Beam Column or Continuous Supports

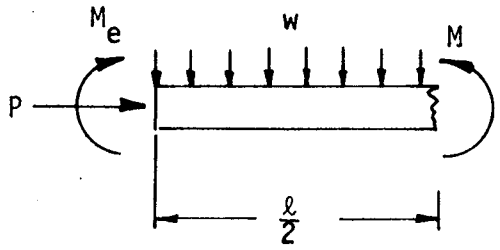


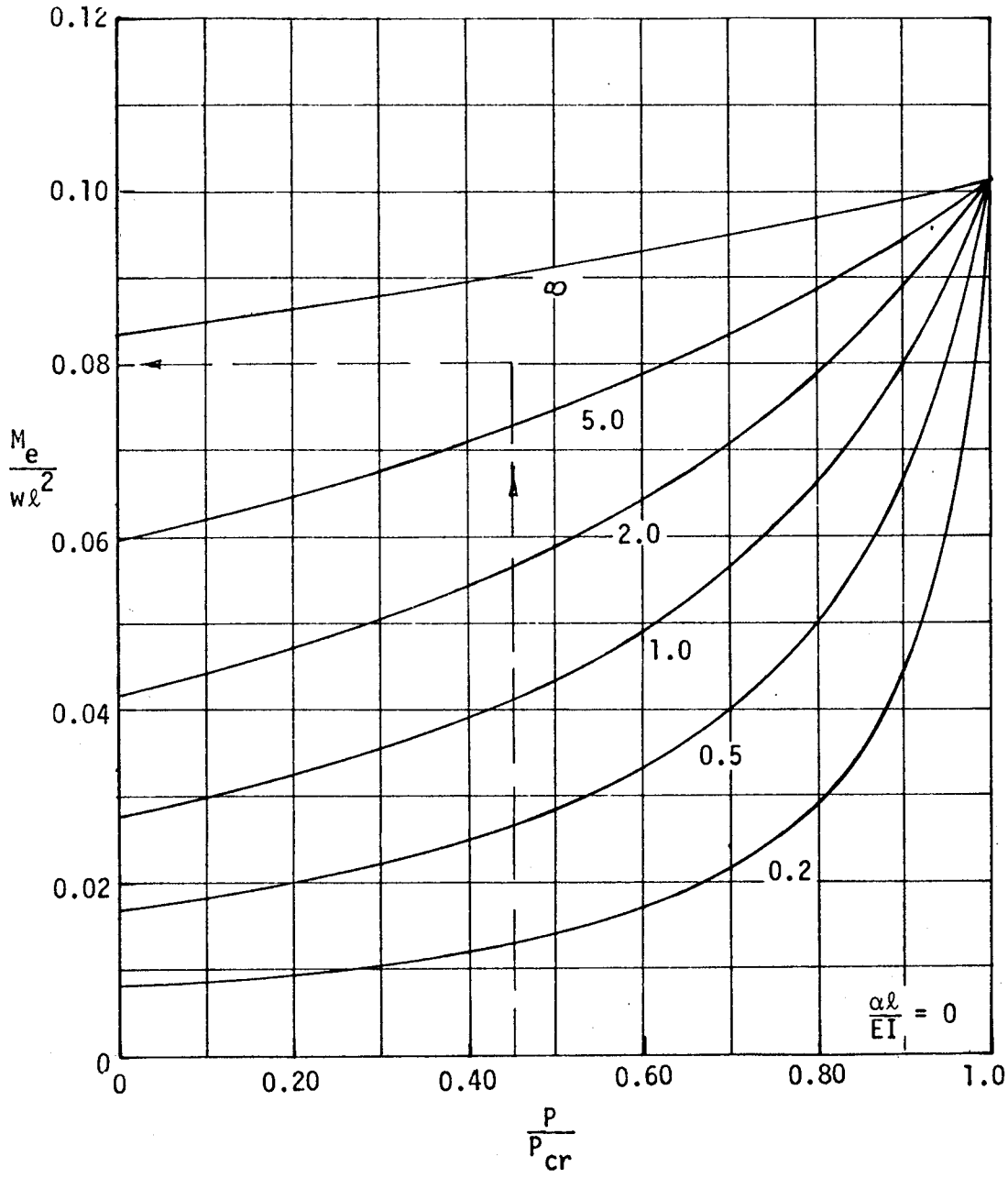


Figure B6.2.2.3-2 End Moment for a Beam Column

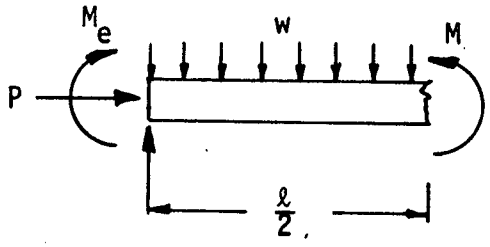


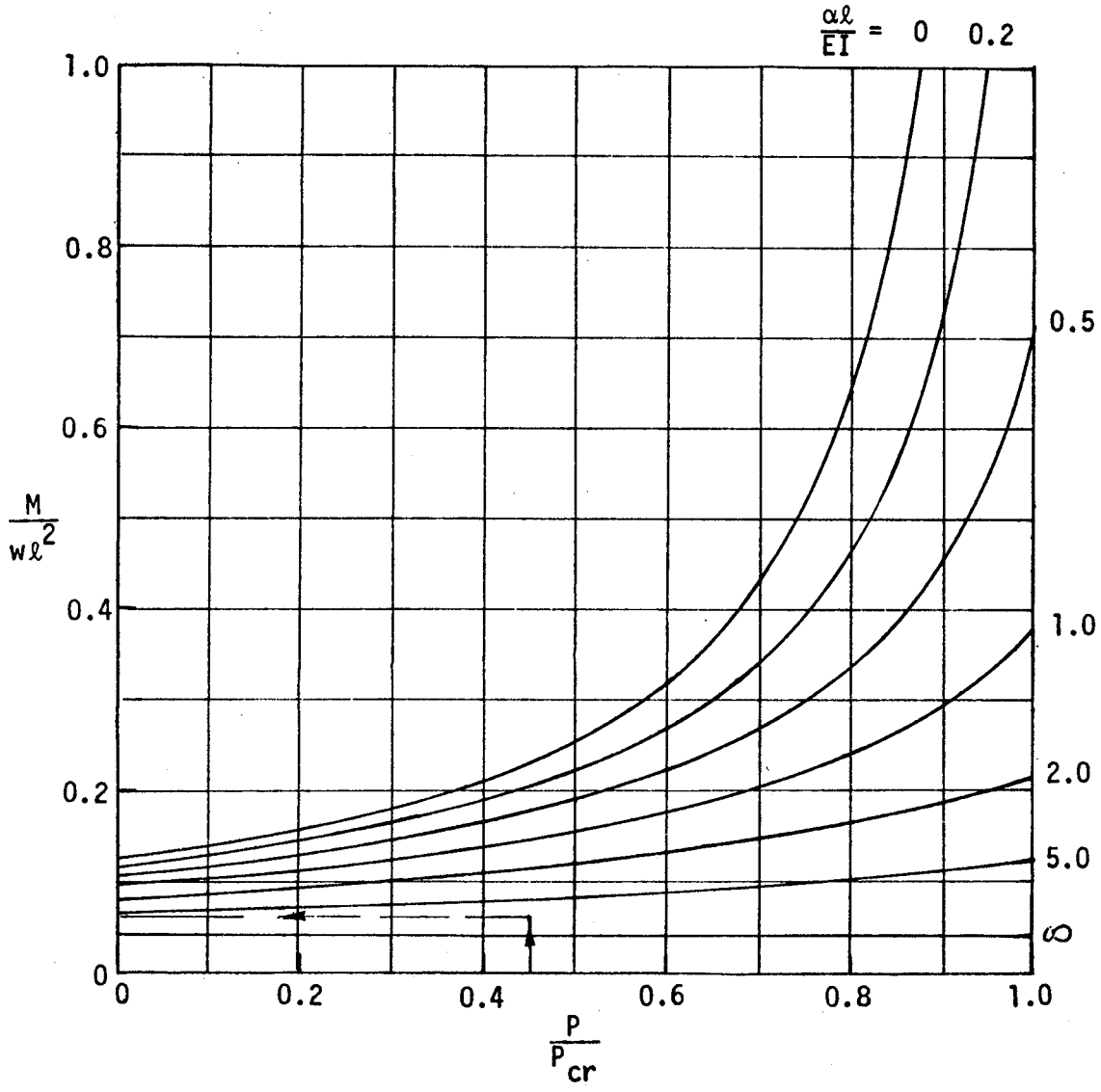


Figure B6.2.2.3-3 Mid-Bay Moment for a Beam Column

The following example illustrates the usage of Figures B6.2.2.3-1 to -3. A seven-bay continuous beam is loaded with a transverse load of w = 138 lbs./in. and an applied axial load of P = 200,000 lbs. The beam is 7075-T6 aluminum with constant I of 5 in.$^4$ and A of 5 in.$^2$; L = 34 in. Material properties for this material are taken from Figure B6.3.1-1.

Applied stress level is

$$f = P/A = 200,000/5 = 40,000 \text{ psi}$$

for which

$$E_t = E = 10.4 \times 10^6 \text{ psi.}$$

The value $P_{cr}$ is computed as

$$P_{cr} = \frac{\pi^2(10.4 \times 10^6)5}{34^2} = 443,961 \text{ lbs.}$$

and the ratio

$$\frac{P}{P_{cr}} = \frac{200,000}{443,961} = 0.450$$

The rotational fixity for the end bays is taken conservatively as 1.0. Then from Figure B6.2.2.3-1

$$\frac{\alpha \ell}{EI} = 40.0$$

and

$$c = 3.62 \text{ for the center bay.}$$

From Figure B6.2.2.3-2 and -3

$$M_e \simeq 0.08(138)(34^2) = 13,000 \text{ in.-lbs.}$$

$$M \simeq 0.06(138)(34^2) = 9,600 \text{ in.-lbs.}$$

The stresses produced by these moments must be interacted with the applied axial stress to determine if the design is good. Refer to Section B6.3.3 for appropriate interaction equations.

## B6.2.2.4 Eccentric Columns

This type of column is similar to the beam column because a transverse bending moment is introduced, in this case by the eccentric load. The transverse bending moment is magnified by the axial column load. Outer fiber stress for the cross section will be the limiting factor. Table B6.2.2.4-1 gives various cases for a column loaded by eccentric load. The maximum moment for these columns is dependent on the ratio of applied load to Euler load. Figures B6.2.2.4-1 and -2 give the moment for the seven cases shown in Table B6.2.2.4-1. The Euler load is computed from Equation B6-14.

Table B6.2.2.4-1 Eccentrically Loaded Columns

| | | | |
|---|---|---|---|
| 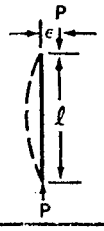 | CASE 1 – PINNED-PINNED (SINGLE ECCENTRICITY)<br>M AT $y = \frac{\pi}{2\lambda}$ |  | CASE 5 – FREE-FIXED (SINGLE ECCENTRICITY)<br>M AT $y = 0$ |
| 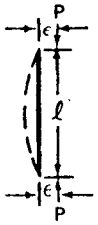 | CASE 2 – PINNED-PINNED (DOUBLE ECCENTRICITY)<br>M AT $y = \frac{\ell}{2}$ | 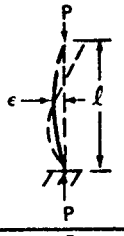 | CASE 6 – FREE-FIXED (INITIAL CURVATURE) |
|  | CASE 3 – PINNED-PINNED (COMPOUND ECCENTRICITY) | 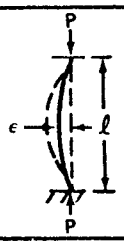 | CASE 7 – FIXED-FIXED (INITIAL CURVATURE)<br>M AT $y = 0, \ell$ |
| 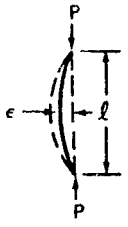 | CASE 4 – PINNED-PINNED (INITIAL CURVATURE)<br>M AT $y = \frac{\ell}{2}$ | | |

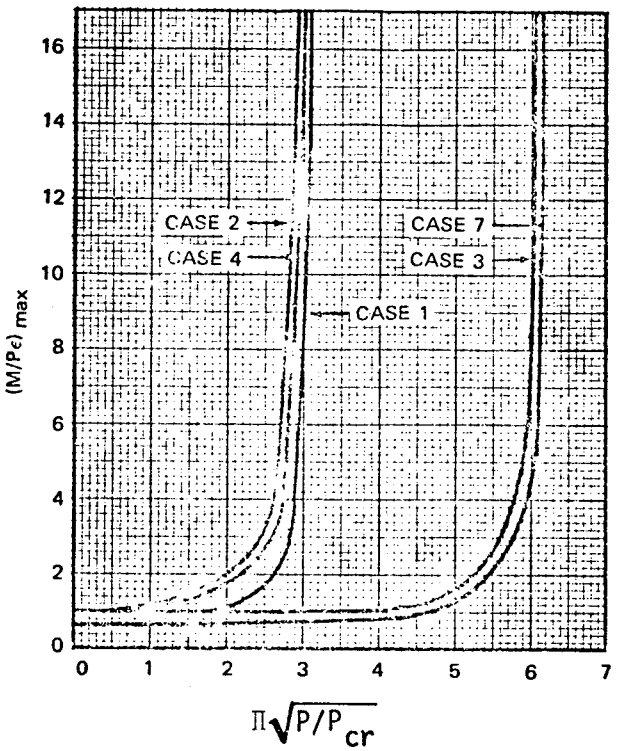


Figure B6.2.2.4-1 Maximum Moment for Eccentrically Loaded Column (Cases 1-4 and 7)

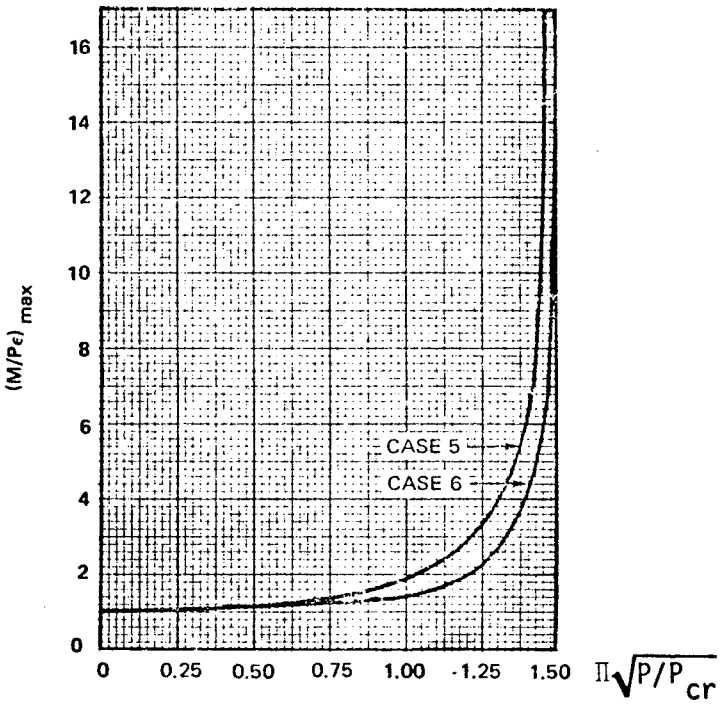


Figure B6.2.2.4-1 Maximum Moment for Eccentrically Loaded Column (Cases 5 and 6)

## B6.2.3 Columns with Distributed Axial Loads

Table B6.2.3-1 shows four different cases of columns with axial distributed load. Both the distributed load and the end load may be compressive, or either one may be a tensile load while the other is compressive. However, in all cases it is the critical combination of the two loads that represents the conditions for elastic buckling. Values of the buckling loads are presented in graphical form in Figure B6.2.3-1. The results are exact within the limitations of the ordinary elastic theory of column buckling.

For the four different end conditions shown, the loading consists of a uniformly distributed axial force q per unit length of the column and a concentrated force P at the upper end of the column. Both end loads are shown as compressive (positive). Either one may become tensile (negative). The columns are assumed to have constant flexural rigidity EI in the plane of buckling, and the loads are assumed to remain vertical during buckling.

Two special cases are noted from Figure B6.2.3-1: (1) if $q = 0$ the column buckles at a load $P_{cr} = P_e$ where $P_e$ is the buckling load, and (2) if $P = 0$, then buckling occurs because of the distributed axial force only, its value being given by $q\,\ell_{cr}$. If $q\,\ell$ is larger than this critical value, the axial force, P, is then negative (tension). If $q\,\ell$ is negative, then P exceeds the Euler load. Values for $P_e$ and the ratio of $(q\,\ell)_{cr}/P_e$ are given in Table B6.2.3-1.

Table B6.2.3-1 Column End Conditions

| | CASE 1 | CASE 2 | CASE 3 | CASE 4 |
|---|---|---|---|---|
| | 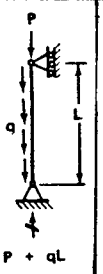  |   |   |   |
| $P_e$ | $\frac{\pi^2 EI}{L^2}$ | $\frac{\pi^2 EI}{4L^2}$ | $\frac{20.191\ EI}{L^2}$ | $\frac{4\pi^2 EI}{L^2}$ |
| $\frac{P_e}{EI/L^2}$ | 9.8696 | 2.4674 | 20.191 | 39.478 |
| $\frac{(qL)_{cr}}{P_e}$ for P = 0 | 1.881 | 3.176 | 2.600 | 1.890 |

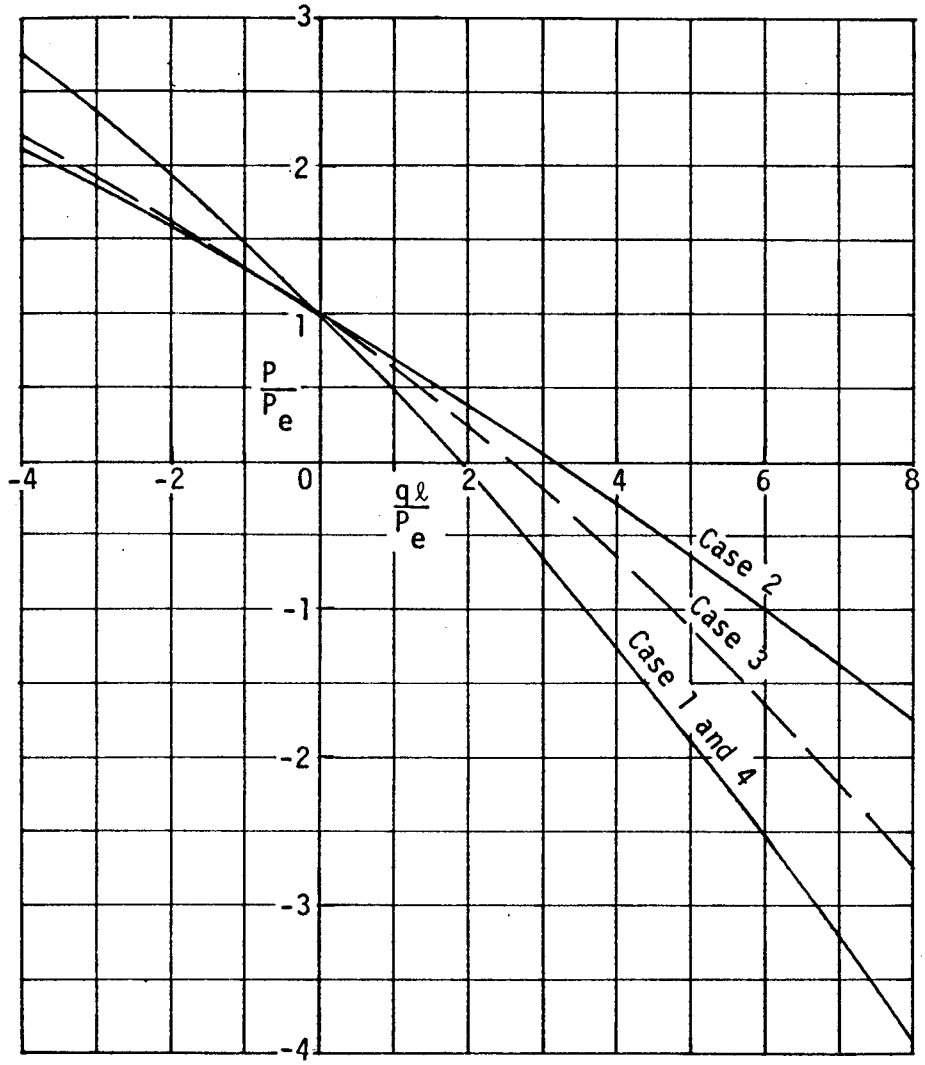


Figure B6.2.3-1 Critical Buckling Loads

With the data presented in Figure B6.2.3-1 and Table B6.2.3-1, the critical combinations of concentrated force P and distributed axial load q can be found. As an example:

Given a hinged-hinged column (Table B6.2.3-1, Case #1) where E = $10 \times 10^6$ psi, I = 4.0 $in.^4$ and L = 34 inches. A uniform distributed load is applied of q = 5000 pounds per inch along the column length.

Find the maximum load P that can be carried at the top of the column before buckling occurs.

From Table B6.2.3-1

$$P_e = \frac{\pi^2 E I}{\ell^2} = \frac{\pi^2 (10 \times 10^6) 4}{34^2} = 341{,}509 \text{ lbs.}$$

The ratio

$$\frac{q \ell}{P_e} = \frac{5{,}000(34)}{341{,}509} = 0.498$$

Figure B6.2.3-1 is entered with this value and ratio of axial force to critical load is determined as

$$\frac{P}{P_e} = 0.75$$

Thus, the column can carry an axial load of P = 0.75 (341,509) = 256,132 lbs., in addition to the uniformly distributed load q.

If the applied axial stress, P/A, is above the material proportional limit, the calculation should be rerun using the tangent modulus that corresponds to the applied stress for determining the critical load, $P_e$. The procedure is then iterative.

## B6.3.0 Supplementary Information

### B6.3.1 Inelastic Effects

The equations for bending instability and twisting instability are applicable for the elastic range. If stress is above the material proportional limit, then modulus of elasticity used in the equations must be reduced by a plasticity factor. For bending instability, tangent modulus is generally accepted as a conservative approximation to inelastic behavior. The plasticity factor is

$$\eta_B = E_t/E \qquad \text{(B6-15)}$$

The appropriate plasticity factor for torsional instability is not so well defined. Tests on cruciform sections suggest that the ratio of secant modulus-to-elastic modulus may be appropriate. However, if a spring restraint is applied, the modulus may take on a different value. A conservative plasticity factor used for plate type problems is

$$\eta_T = (E_t/E)^{1/2} \qquad \text{(B6-16)}$$

This factor should be used for preliminary torsional instability calculations unless test data can substantiate the usage of a less conservative plasticity factor.

When using the interaction formulas for bending and twisting, plasticity corrections should be made on the combined stress and not on the individual stresses. The exact plasticity factor is not known for the combined case. Tangent modulus gives conservative results and for this reason should be used for preliminary sizing.

A conventional method for handling plastic corrections is by use of the "A" scale. Any instability equation can be separated into two portions. One involves material properties and the other involves geometry. For example the Euler-Engesser equation (B6-1) can be written as

$$\text{"A" Scale} = \frac{F_B}{E_T} = \frac{\pi^2}{(L'/\rho)^2} \qquad \text{(B6-17)}$$

In a similar manner, for the twisting instability equation, B6-2, "A" scale = $F_T/(E\ E_T)^{1/2}$. These material properties can be obtained directly from stress-strain-modulus curves, given in Mil-Hnbk-5C. Figures B6.3.1-1 and -2 show typical stress-strain-modulus curves for 7075-T6 plate and 7075-T6 extrusion.

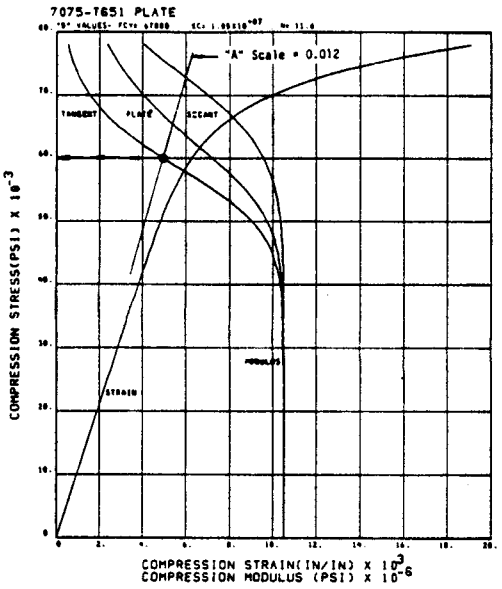


Figure B6.3.1-1 Minimum Guaranteed Compression Stress-Strain-Modulus Curve for 7075-T651 Plate (RT)

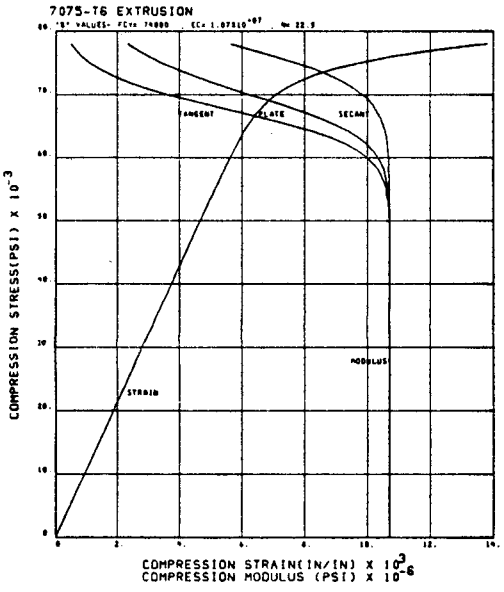


Figure B6.3.1-2 Minimum Guaranteed Compression Stress-Strain Curve for 7075-T6 Extrusion (RT)

The following example illustrates usage of Figure B6.3.1-1:

For a column, $L'/\rho = 28.7$, bending instability is critical; therefore, from Equation B6-17

$$\text{"A" Scale} = \frac{\pi^2}{(28.7)^2} = 0.012$$

This slope is laid off on Figure B6.3.1-1 and the stress is determined from the tangent modulus line as F = 60,000 psi.

B6.3.2 End Fixity

The column instability equations are based on the assumption that the column is pinned on both ends, as shown in Figure B6.3.2-1, so that its ends can rotate freely. Generally, aircraft compression members are supported in such a way that the ends are partially restrained. If a compression member is restrained against rotation at both ends, the deflection curve will have the shape as shown in Figure B6.3.2-1b. Points of reverse curvature exist along the column. At these points there is zero bending moment. The length of the column between points of zero bending moment may therefore be treated as a pin-ended column by substitution of this "effective" length into the column equations. In the case of a column rigidly fixed at both ends, Figure B6.3.2-1c, the points of reverse curvature occur at a distance from the ends equal to one quarter of the column length. The effective length is therefore equal to L/2. By definition, end fixity is

$$c = (L/L')^2 \qquad \text{(B6-18)}$$

In the case of the rigidly fixed column, c = 4.0.

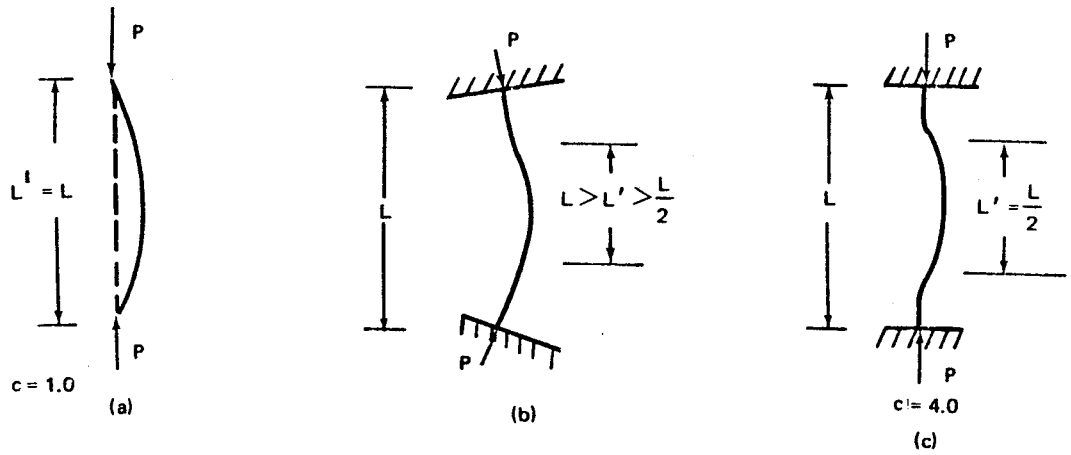


Figure B6.3.2-1 Column End Fixity Conditions

The end fixity for eight special cases of column support are shown in Table B6.3.2-1.

Table B6.3.2-1 End Fixity Coefficients for Columns

| CASE | COLUMN SHAPE AND END CONDITIONS | | END FIXITY COEFFICIENT |
|---|---|---|---|
| 1 | 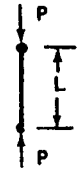 | UNIFORM COLUMN, AXIALLY LOADED, PINNED ENDS. | $c = 1$ $\frac{1}{\sqrt{c}} = 1$ |
| 2 |  | UNIFORM COLUMN, AXIALLY LOADED, FIXED ENDS. | $c = 4$ $\frac{1}{\sqrt{c}} = .5$ |
| 3 | 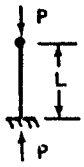 | UNIFORM COLUMN, AXIALLY LOADED, ONE END FIXED, ONE AND PINNED. | $c = 2.05$ $\frac{1}{\sqrt{c}} = .70$ |
| 4 | 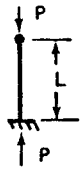 | UNIFORM COLUMN, AXIALLY LOADED, ONE END FIXED, ONE END FREE. | $c = 0.25$ $\frac{1}{\sqrt{c}} = 2.0$ |
| 5 |  | UNIFORM COLUMN, DISTRIBUTED AXIAL LOAD, FIXED ENDS. | $c = .79$ $\frac{1}{\sqrt{c}} = .365$ |
| 6 | 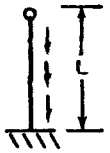 | UNIFORM COLUMN, DISTRIBUTED AXIAL LOAD, ONE END FIXED, ONE END PINNED. | $c = 3.55$ (APPROX) $\frac{1}{\sqrt{c}} = .530$ |
| 7 | 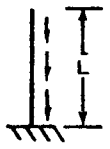 | UNIFORM COLUMN, DISTRIBUTED AXIAL LOAD, ONE END FIXED, ONE END FREE. | $c = .75$ $\frac{1}{\sqrt{c}} = 1.12$ |
| 8 |  | UNIFORM COLUMN, DISTRIBUTED AXIAL LOAD, PINNED ENDS. | $c = 1.67$ $\frac{1}{\sqrt{c}} = .732$ |

Figure B6.3.2-2 gives the end fixity for special cases 2 and 3 and also the more general fixity values for varying degrees of end restraint. In this figure, the value for bending restraint coefficient, is defined as

$$\alpha = - M/\Theta \qquad \text{(B6-19)}$$

where M is the end moment and $\Theta$ is the angle of rotation at the column ends. For the case of rigid restraint at both ends, if $\Theta = 0$, $\alpha$ is infinite and c = 4.0 which corresponds to the fixity given in Table B6.3.2-1, case 2.

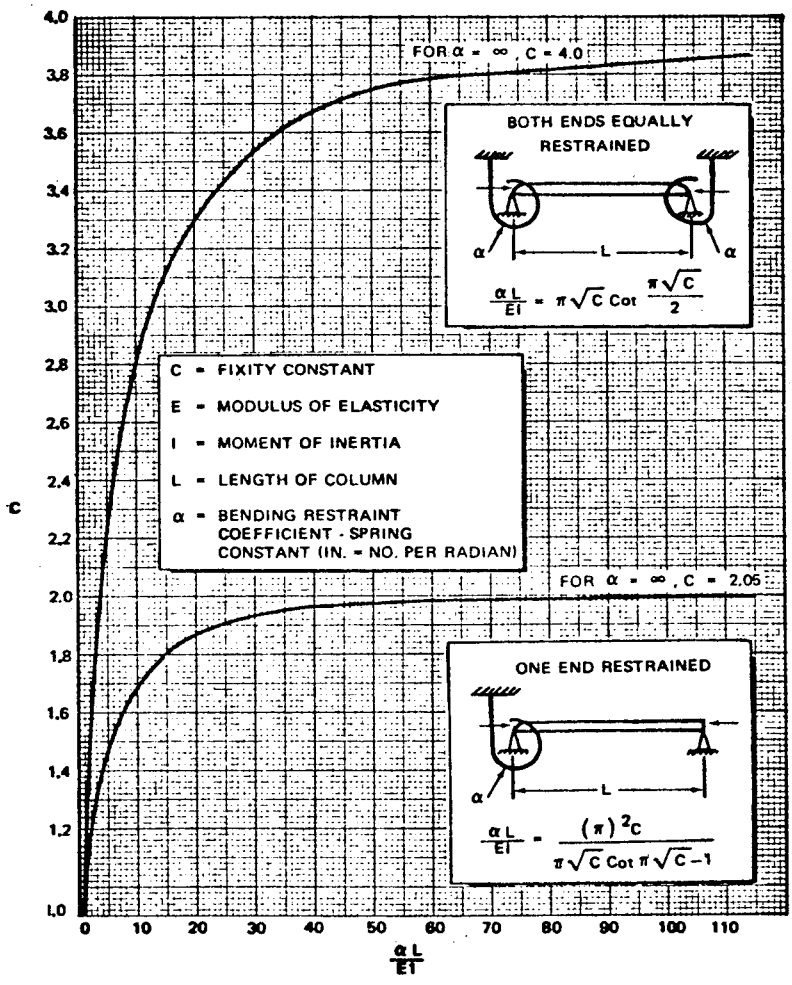


Figure B6.3.2-2 End Fixity Conditions

When the fixity at either end of a column is known, the equivalent fixity for a column may be obtained from Figure B6.3.2-3. The critical load is then computed from the equation

$$P_{cr} = C_e \pi^2 EI/\ell^2 \qquad \text{(B6-20)}$$

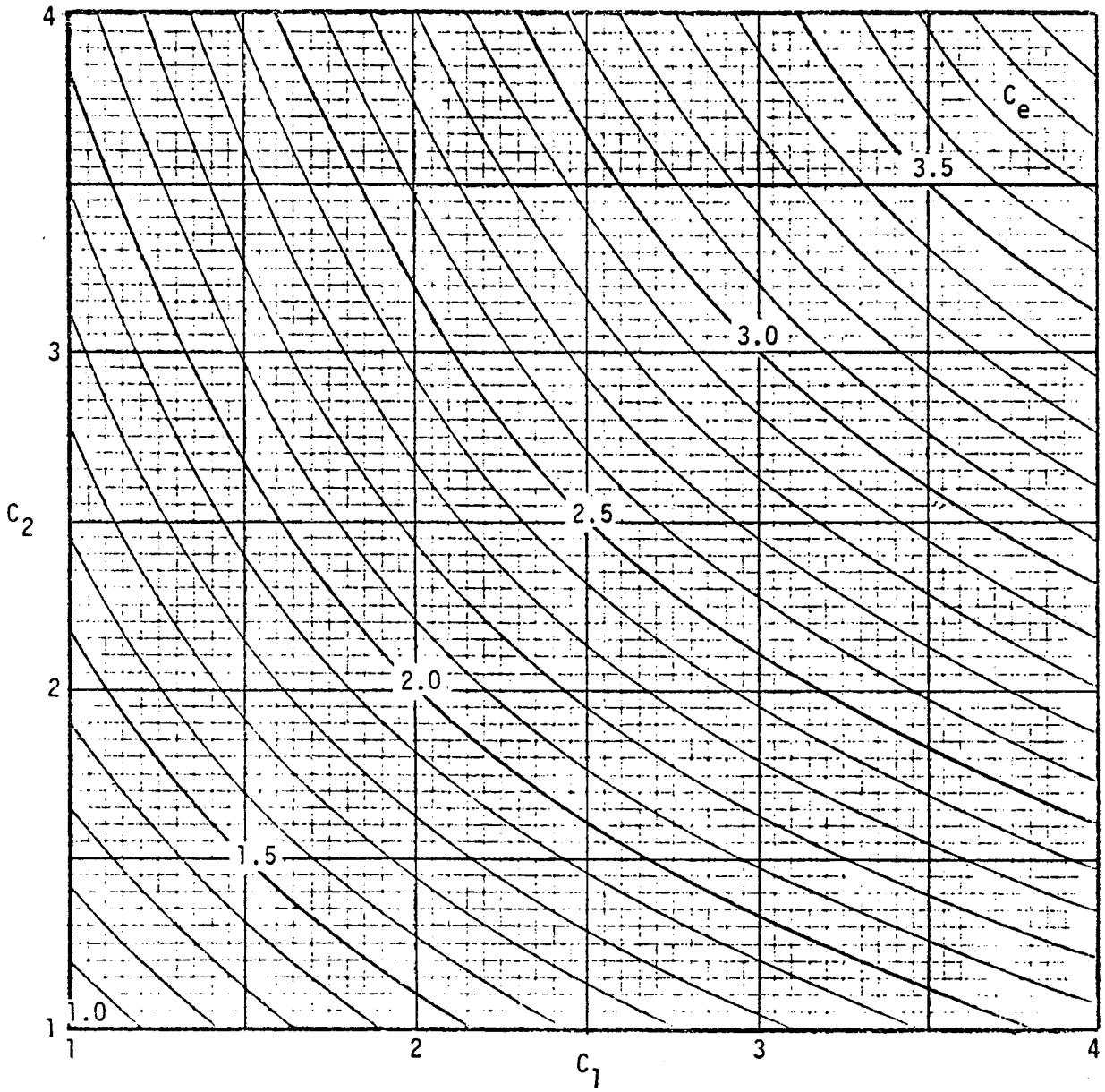


Figure B6.3.2-3 Effective End Fixity for Beam Column Having Unequal End Restraints

When using end fixity to compute column critical loads, it is important to note that the increase in column strength is proportional to end fixity increase only in the elastic region. This fact can be illustrated best by an example. Assume that a 7075-T6 plate has a length, L = 30 in. and a moment of inertia, I = 4.0 in.$^4$ and an area A = 4.0 in.$^2$. The elastic modulus is 10.5 x $10^6$ psi. Compute the critical load for c = 1.0 and 4.0.

Based on elastic analysis,

$$F_{cr} = \frac{c\,\pi^2 E}{(L/\rho)^2} = \frac{1.0\pi^2(10.5 \times 10^6)}{(30/1)^2} = 115{,}145 \text{ psi for } c = 1.0$$

and

$$F_{cr} = 4(115{,}145) = 460{,}582 \text{ psi for } c = 4.0$$

This indicates that a 300 percent increase in strength can be obtained by increasing the end fixity from 1.0 to 4.0. However, the stresses exceed the material proportional limit. Based on the "A" scale approach given in Section B6.3.1, the plastic stresses are obtained from Figure B6.3.1-1 as

$F_{cr}$ = 59,000 psi for c = 1.0

$F_{cr}$ = 67,000 psi for c = 4.0 ($F_{cy}$ cutoff)

Therefore, the actual increase in stress is about 13.6 percent.

B6.3.3 Interaction

Data is given in Section B6.2.2 for determining the bending moment on beam columns that takes into account the deflected shape of the beam. The bending moment produces stresses that interact with the column stresses. When stresses are in the elastic range, bending stresses and column stresses are additive. Thus,

$$f_c + f_b = f \qquad \text{(B6-21)}$$

where

$f_c$ = axial compression stress

$f_b$ = outer fiber bending stress

$f$ = combined stress for outer fiber

Equation B6-21 gives conservative results when stresses are above the material proportional limit. However, it is very useful for design purposes because of its simplicity. It can be put in the form of an interaction equation by dividing both sides by the combined stress to give

$$\frac{f_c + f_b}{F} = R_c = 1.0 \qquad \text{(B6-22)}$$

The combined stress, is the maximum allowable stress which depends on the load condition and type of loading. For tension loads, F can be either tension yield stress or tension ultimate stress. For compression loads, it is usually compression yield stress, column buckling stress, or column crippling stress. In any case, the summation of bending and axial stress cannot exceed the allowable stress. For efficient design, the ratio $R_c$ should equal 1.0, unless shear stresses are applied.

In aircraft structure, compression panels are generally loaded by shear in addition to bending and compression. For wing structure the shear is primarily due to flexure. The interaction equation in this case is

$$R_c^2 + R_s^2 = 1.0 \qquad \text{(B6-23)}$$

For fuselage structure, shear is primarily due to torque. The interaction equation for this case is

$$R_c + R_s^{1.75} = 1.0 \qquad \text{(B6-24)}$$

These interaction equations are plotted in terms of safety margin in Figures B6.3.3-1 and -2. When using Equations B6-22 to B6-24, the allowable compression stress is determined based on: (1) whether bending produces compression in the skin or the stringer outstanding flange, and (2) whether bending moment is at the center or end of the panel. Table B6.3.3-1 shows the appropriate allowable stress.

Table B6.3.3-1 Allowable Compression Stresses for Interaction Equation

| Moment Location | Member in Compression | Equation | Allowable |
|---|---|---|---|
| End | Skin | B6-23 or B6-24 | $F_{cy}$ |
| End | Flange | B6-22 | $F_{cc}$ |
| Center | Skin | B6-23 or B6-24 | $F_c$ |
| Center | Flange | B6-22 | $F_c$ |

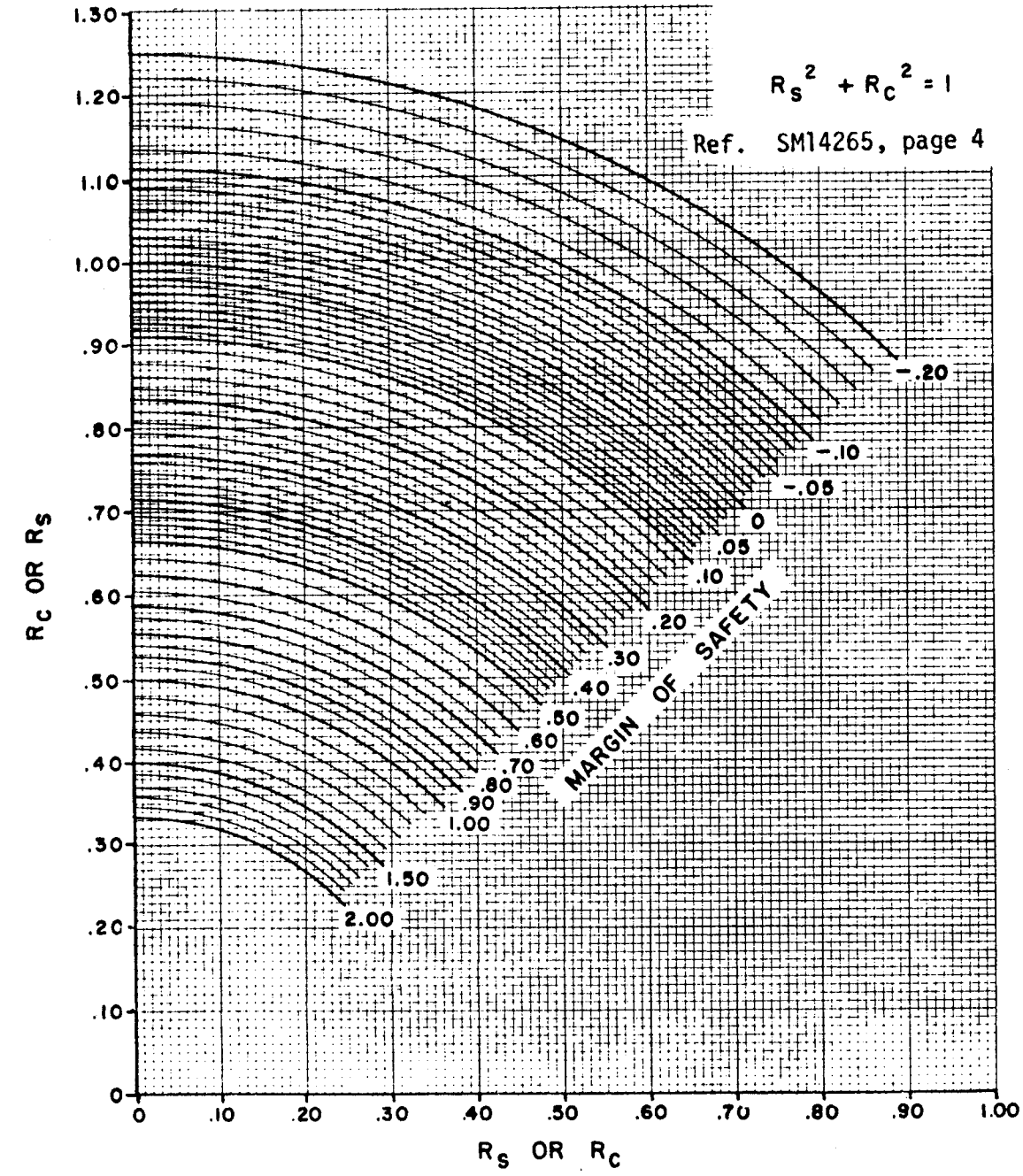


Figure B6.3.3-1 Interaction Curve for Axial Compression and Flexural Shear

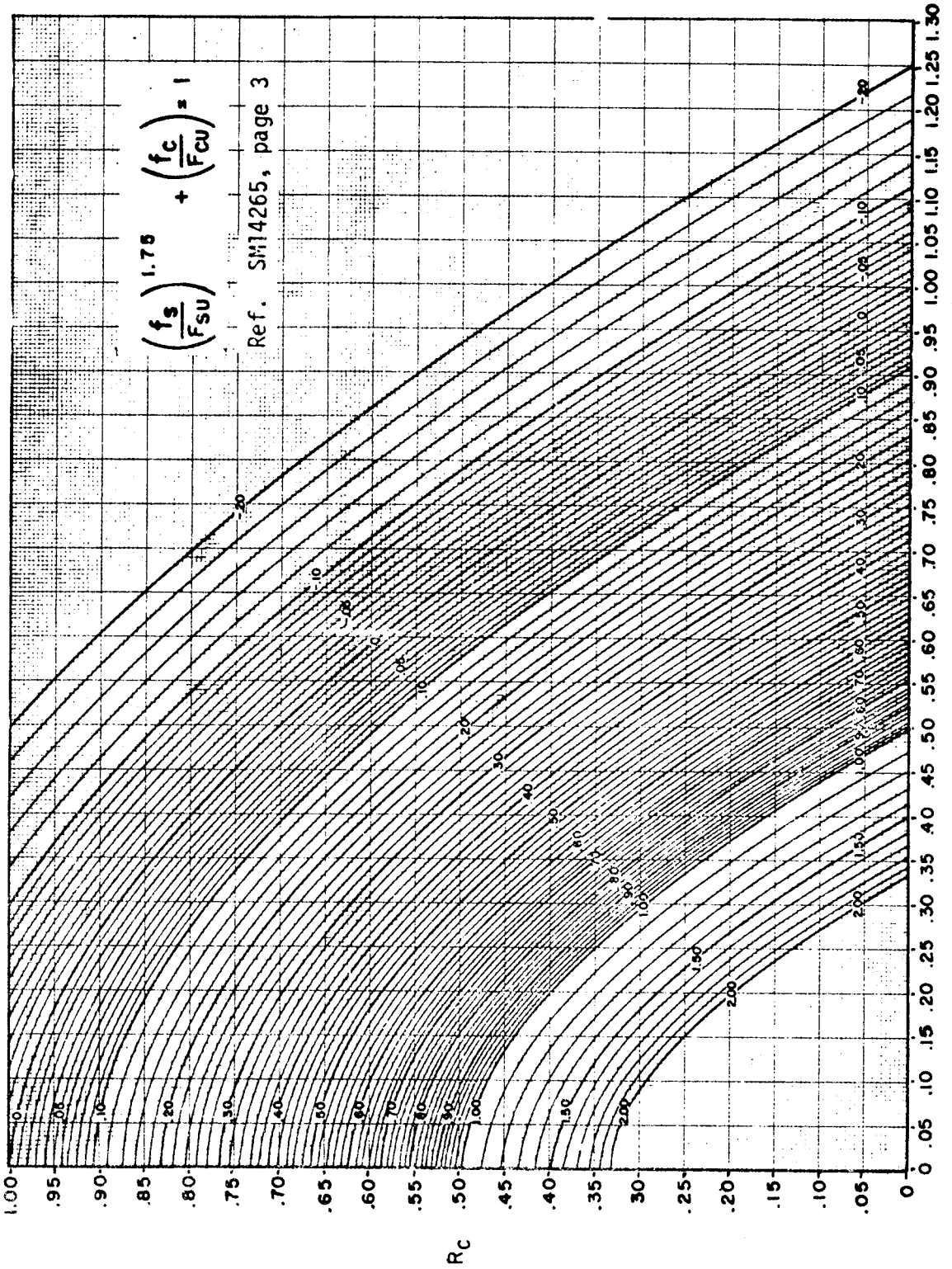


Figure B6.3.3-1 Interaction Curve for Axial Compression and Torque Shear

NOTE: $F_{cy}$ = compression yield, psi
$F_{cc}$ = crippling stress, psi
$F_c$ = column buckling stress, psi (see Section B6.5.2)

B6.3.4 Buckled Skin

Compression panels are often designed so that skin will buckle before maximum load is reached. When this happens, the skin stress is no longer uniformly distributed over the panel width, $b_s$. Total load on the skin-stringer combination is given by the equation

$$P = t_s \int_{-.5b_s}^{.5b_s} f(x)\, dx + f_2 A_2 \qquad \text{(B6-25)}$$

Various theoretical studies have been made to determine the skin stress distribution, f(x), after buckling. They lead to long complicated equations which are dependent on the boundary conditions and difficult to apply. For design purposes, it is common practice to replace the integral term with an effective width of skin, $b_e$, and a uniform stress, $f_1$, which gives the same total skin load as would be obtained if the non-uniform stress distribution were known. This leads to the equation for total load on the skin-stringer combination

$$P = f_1 b_e t_s + f_2 A_2 \qquad \text{(B6-26)}$$

where the stress $f_1$ and $f_2$ are determined based on uniform compression at constant strain, $\varepsilon$.

Various equations have been proposed for determining the skin effective width in Equation B6-26. The Von Karmen effective width equation gives an applied load that correlates well with integral, Z and J stiffened compression panel tests. This equation is

$$b_e = \left[\frac{3.62\eta_p E}{f_1}\right]^{1/2} t_s \qquad \text{(B6-27)}$$

Half of the width should be placed on either side of the stringer web when applying Equation B6-27 to integral, Z, or J stiffened compression panels. A plot of the ratio (b/t) is given in Figure B6.3.4-1 for 2024 and 7075 aluminum sheet.

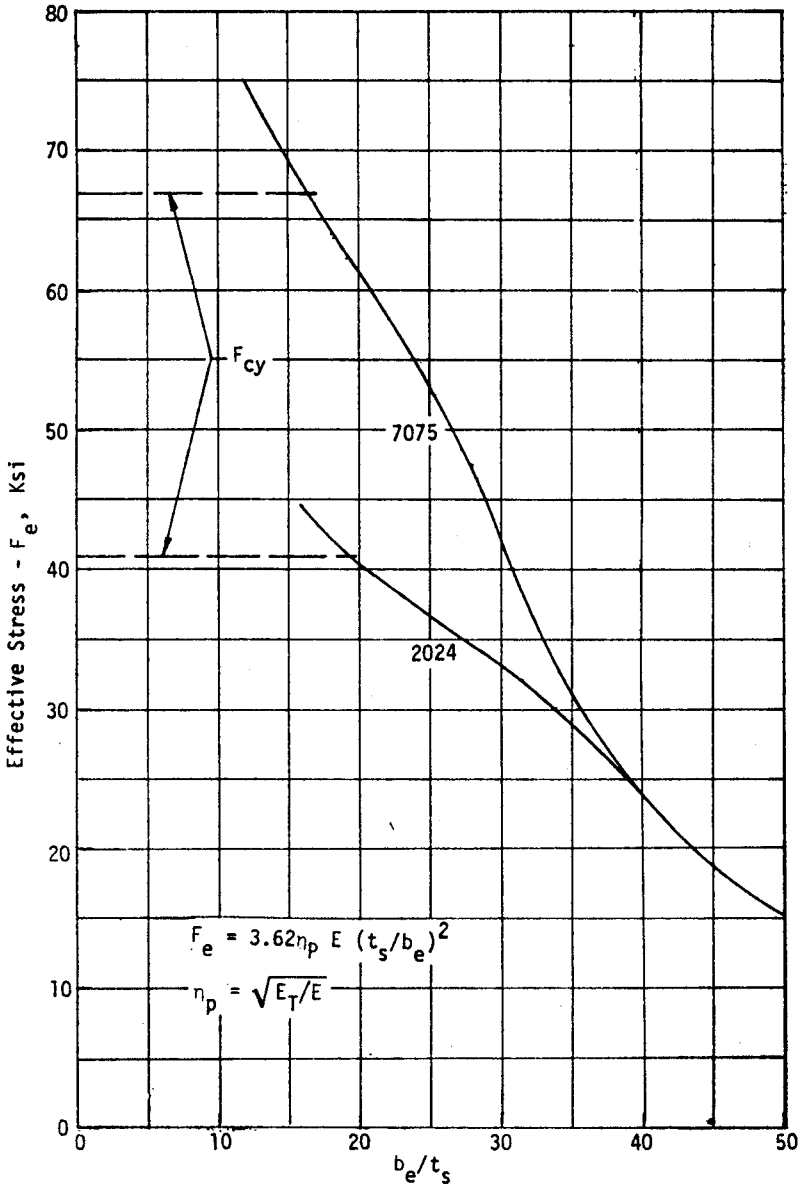


Figure B6.3.4-1 Effective Width for 2024 and 7075 Sheet

Strictly speaking, a reduced effective width should be used for computing panel bending stiffness, but this is not recommended when using the Von Karmen effective width equation. Once the skin is buckled, incremental changes in load that produce incremental changes in strain, also produce incremental changes in effective width because it too is a function of strain. This leads to the equation for reduced effective width

$$b_e' = b_e + \varepsilon \frac{d(b_e)}{d\varepsilon} \qquad \text{(B6-28)}$$

which characterizes the resistance of the skin to bending moment and corresponding bending instability. The Von Karmen effective width equation underestimates the actual effective width. Therefore, further reduction should not be made for computing the cross section moment of inertia.

B6.3.5 Attachment Criteria

For wide column design, the skin is usually attached to the stringer by mechanical methods (rivets or Hucks). If the stringer is stiff enough to enforce a node point, then the skin will buckle about the center of the stiffener web. The resulting skin rotation creates a tension force in the attachment that is resisted by the flange of the stiffener against the skin. An idealized stiffener is shown in Figure B6.3.5-1. The force in the attachment is given in Reference B6-3 as

$$R_R = \frac{E}{1-\mu^2} \frac{1}{(f/t_w)^3} \left[ \frac{3\frac{f}{t_w} + \frac{b_w}{t_w}}{3\frac{f}{t_w} + 4\frac{b_w}{t_w}} \right] \frac{t_s}{5} p \qquad \text{(B6-29)}$$

The value of $f/t_w$ was determined experimentally in Reference B6-3 for Z and channel stringers and full depth webs and is given in Figures B6.3.5-2 for various ratios P/D and $b_o/t_w$. If geometry is known, the required rivet tension load can be determined. Allowable rivet load based on McDonnell Douglas tests is given for rivets installed by the driv-matic method or the Gemcor method and Hucks in Figure B6.3.5-3.

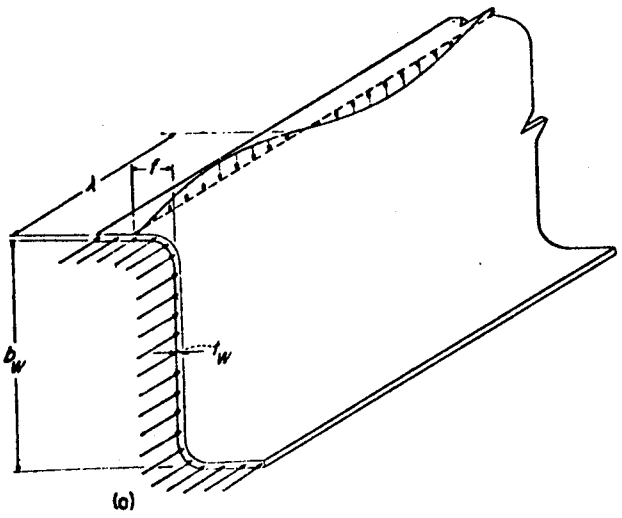


(a) Loads on stringer.

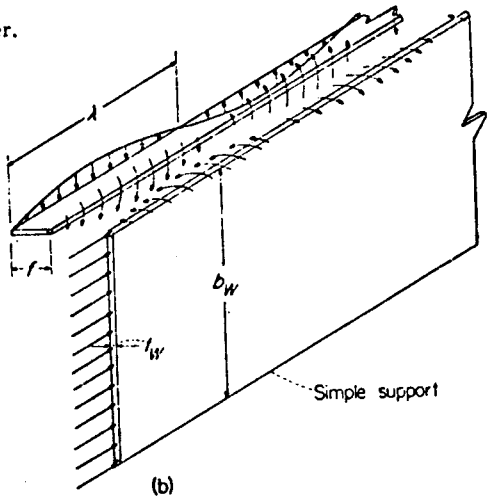


(b) Idealized stringer.

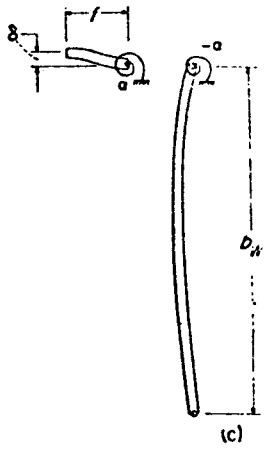


(c) Distortion of idealized stringer.

Figure B6.3.5-1 Loads and Deformations for Calculating Deflectional Stiffness of Short Z-Sections

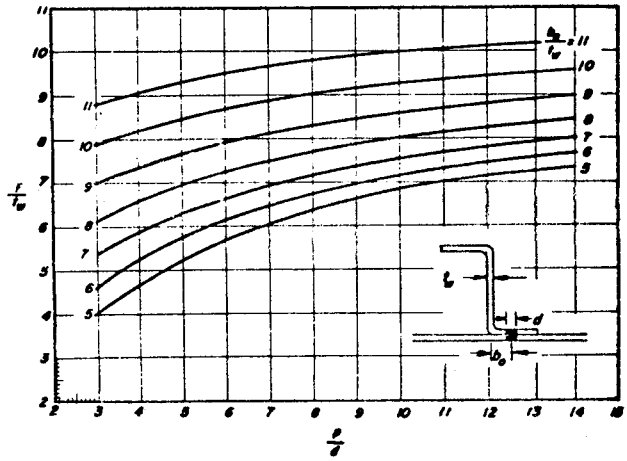

Figure B6.3.5-2 Experimentally Determined Values of Effective Rivet Offset for Z and Channel Stringers and Full-Depth Channel Webs

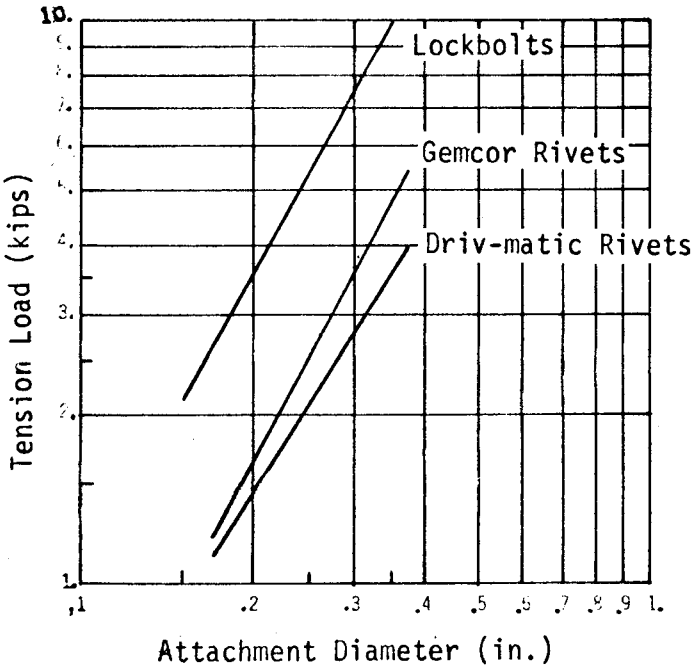


Figure B6.3.5-3 Allowable Tension Load in Attachments

Equation B6-29 shows that for a compression panel of specified material, the load in the attachments is effected by four parameters:

1. $f/t_w$ - ratio of effective attachment offset-to-web thickness.
2. $b_w/t_w$ - ratio of web width-to-web thickness
3. $t_s$ - skin gage
4. $p$ - rivet pitch

Of these four parameters, $f/t_w$ is the most effective in reducing attachment load because it is a cubic factor. Increasing the ratio $b_w/t_w$ can help reduce the load, but this can lead to failure of the web by plate buckling. Caution should be exercised here. Skin gage decrease is important, but this is usually determined by compressive load requirements. Attachment pitch decrease helps. Generally this is set at 4.0 or 5.0 D minimum. The ratio of $b_w/t_w$ is about 18.0. The ratio $b_o/t_w$ should be greater than 4.0. For $b_o/t_w = 5.0$, and $P/D = 5.0$, the ratio $f/t_w = 5.25$ from Figure B6.3.5-2 with $b_w/t_w = 18$ and $\mu = 0.3$, Equation B6-30 becomes

$$R_R = 0.003\ Et_s\ D \qquad \text{(B6-30)}$$

The tension load given by this equation is set equal to the allowable tension load in Figure B6.3.5-3 to obtain the plot of minimum attachment diameter versus skin gage in Figure B6.3.5-4. Superimposed on this plot is a bandwidth that represents the range of practical attachment diameter to be used with various skin thicknesses. The lower bound is the approximate rule that attachment diameter should be equal to skin thickness. The upper bound represents maximum values used on present McDonnell Douglas transports. The values of $b_o/t_w$, pitch, and $b_w/t_w$ should be adjusted to fall within this bandwidth.

Rivet pitch must satisfy the criteria given in Reference B6-3.

$$p/b_s < 0.9\sqrt{2/K_m} \qquad \text{(B6-31)}$$

where values of $K_m$ are given in Figure B6.3.5-5 in terms of the known geometry. When conditions shown in Figure B6.3.5-4 are met, rivet pitch will generally satisfy Equation B6-31.

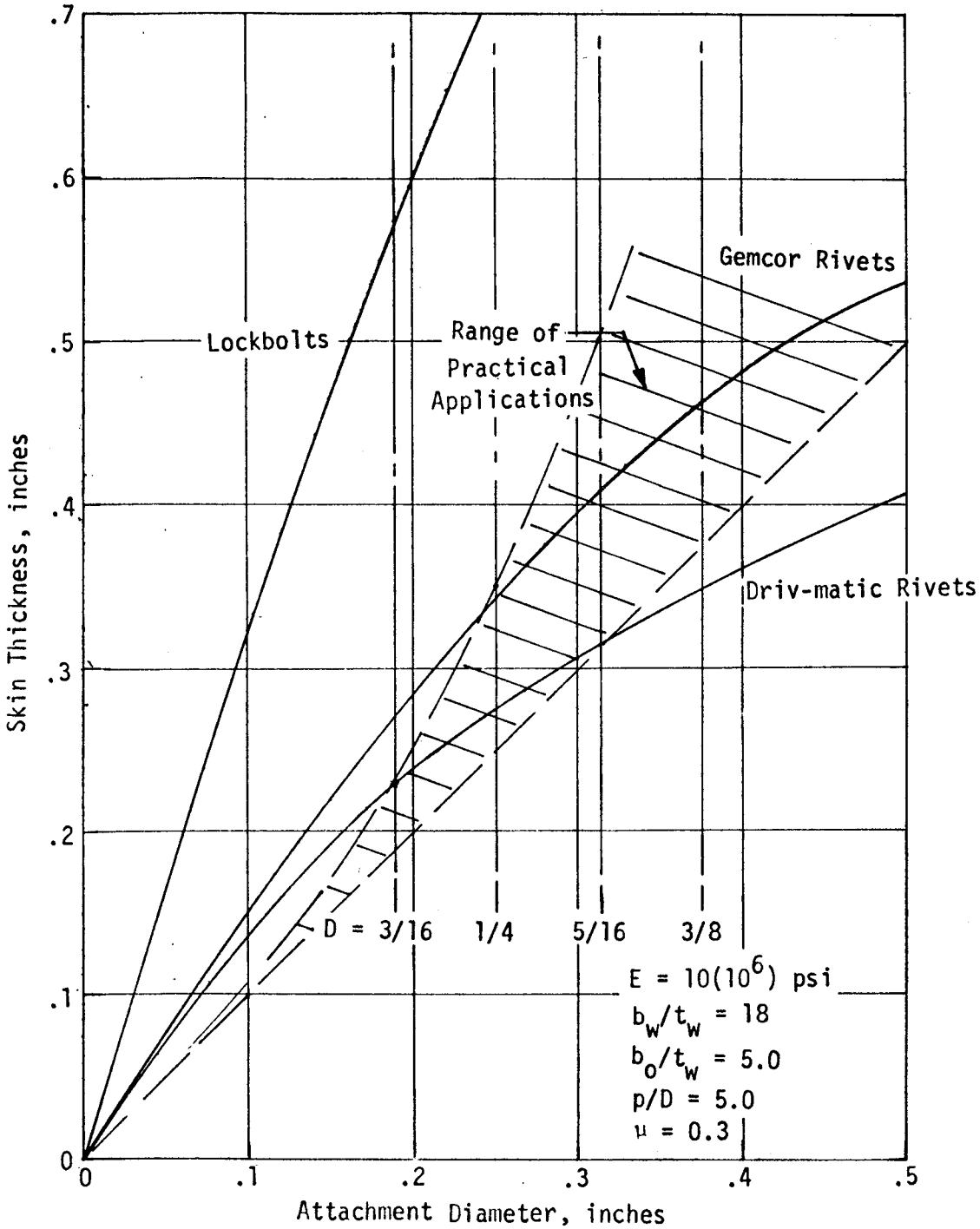


Figure B6.3.5-4 Attachment Diameter Requirements for Compression Panel Applications

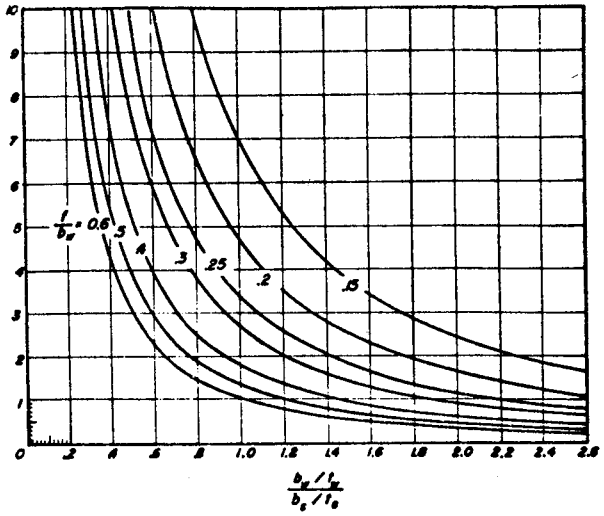


Figure B6.3.5-5 Maximum Stress Coefficients for Skin-Stringer Panels that Fail by Wrinkling

## B6.4.0 Preliminary Design

### B6.4.1 Minimum Weight Columns

Symmetrical columns are the most efficient from a weight point of view because bending and twisting instability do not interact leading to a lower combined stress. As pointed out in Section B6.2.0, I sections and tubes are very efficient. Figure B6.4.1-1 shows a plot of optimum stress-to-density ratio for these sections when made from aluminum, titanium, and steel. The curves are based on the assumption that Euler-Engesser and secondary buckling stresses occur simultaneously at the applied stress level. Highest stress-to-density ratio yields the lightest section. For a given load, P, the lightest section is obtained for the shortest column length, L. This fact is reflected in Figure B6.4.1-1 by the structural index $P/L^2$ on the absicca of the plot. As structural index increases, titanium becomes more efficient than aluminum. Finally, steel becomes more efficient than titanium. This is purely from a weight basis. Cost efficiency must also be evaluated for design. Generally, the tube is more weight efficient than the I section. However, at structural indices greater than 250.0, first, titanium and then steel I sections become more weight efficient than aluminum tubes.

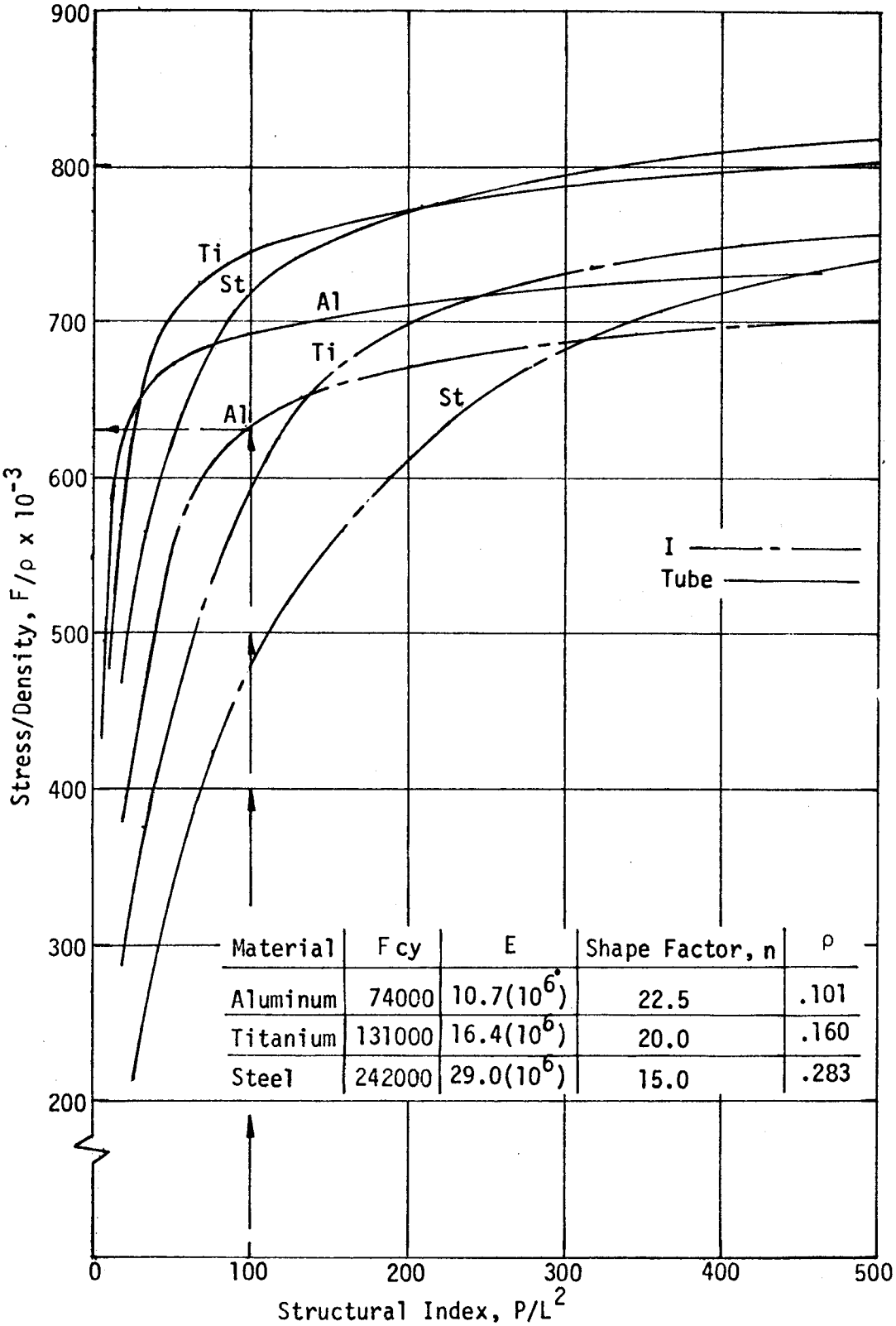


| Material | F cy | E | Shape Factor, n | ρ |
|---|---|---|---|---|
| Aluminum | 74000 | 10.7(10^6) | 22.5 | .101 |
| Titanium | 131000 | 16.4(10^6) | 20.0 | .160 |
| Steel | 242000 | 29.0(10^6) | 15.0 | .283 |

Figure B6.4.1-1 Comparison of Structural Efficiencies for I and Tube Columns

Material selection for I sections and tubes should be made from consideration of cost and weight. Once selection is made, Figures B6.4.1-2 and -3 can be used to size the most weight efficient I section and tube respectively. As an example of design chart usage:

Assume an I section strut is required to span a distance L = 40 inches. The applied axial load P = 160,000 lbs. Structural index is computed as

$$P/L^2 = 160{,}000/40^2 = 100$$

From Figure B6.4.1-1, aluminum is the most efficient material at this structural index. Stress-to-density ratio is 632,000. Stress is computed as

$$F = 632{,}000\ (0.101) = 63{,}200 \text{ psi}$$

From Figure B6.4.1-2, for $P/L^2 = 100$, and aluminum material, optimum $b_w/t_w = 23.0$ and $b_w/L = .0584$. Thus

$$b_w = .0584L = .0584\ (40) = 2.336 \text{ in.}$$

and

$$t_w = b_w/23 = 2.336/23 = 0.102 \text{ in.}$$

Then based on secondary instability considerations

$$b_a = 0.881 b_w = 0.881(2.336) = 2.058 \text{ in.}$$

$$t_a = 2.691 t_w = 2.691(0.102) = .274 \text{ in.}$$

A section sized in this manner will not be critical for twisting instability. The following check illustrates this.

For an I section, warping constant about the shear center is given in Section E1.0.0 as

$$C_w^2 = t_f h^2 b^3/24 = 0.274(2.336)^2\ (2 \times 2.058)^3/24 = 4.34 \text{ in.}^6$$

and the torsion constant is

$$J = (2bt_f^3 + ht_w^3)/3 =$$

$$[2(2 \times 2.058)(0.274)^3 + 2.336(0.102)^3]/3 = 0.057 \text{ in.}$$

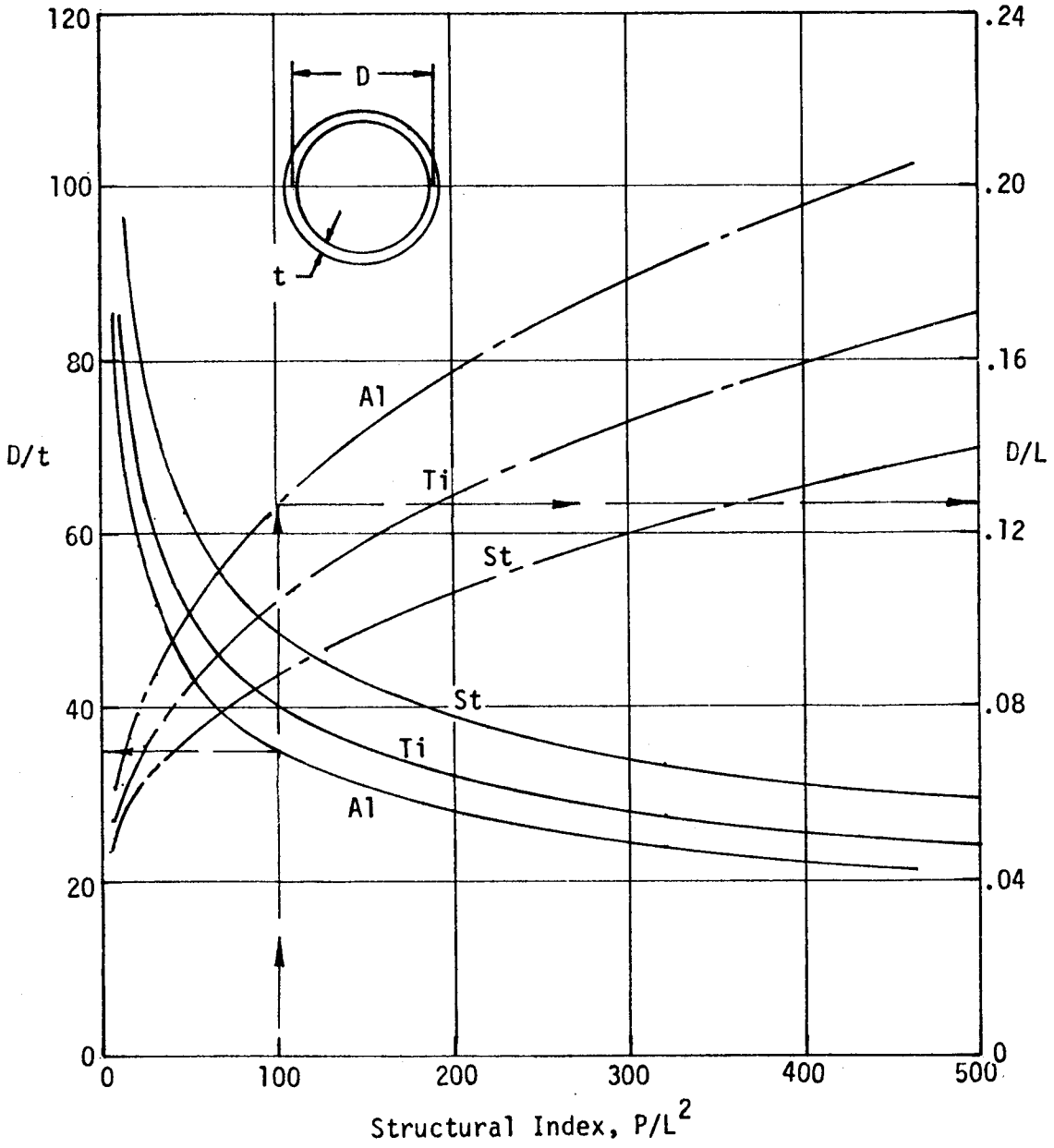


Figure B6.4.1-2 Design Chart for Minimum Weight Tubes

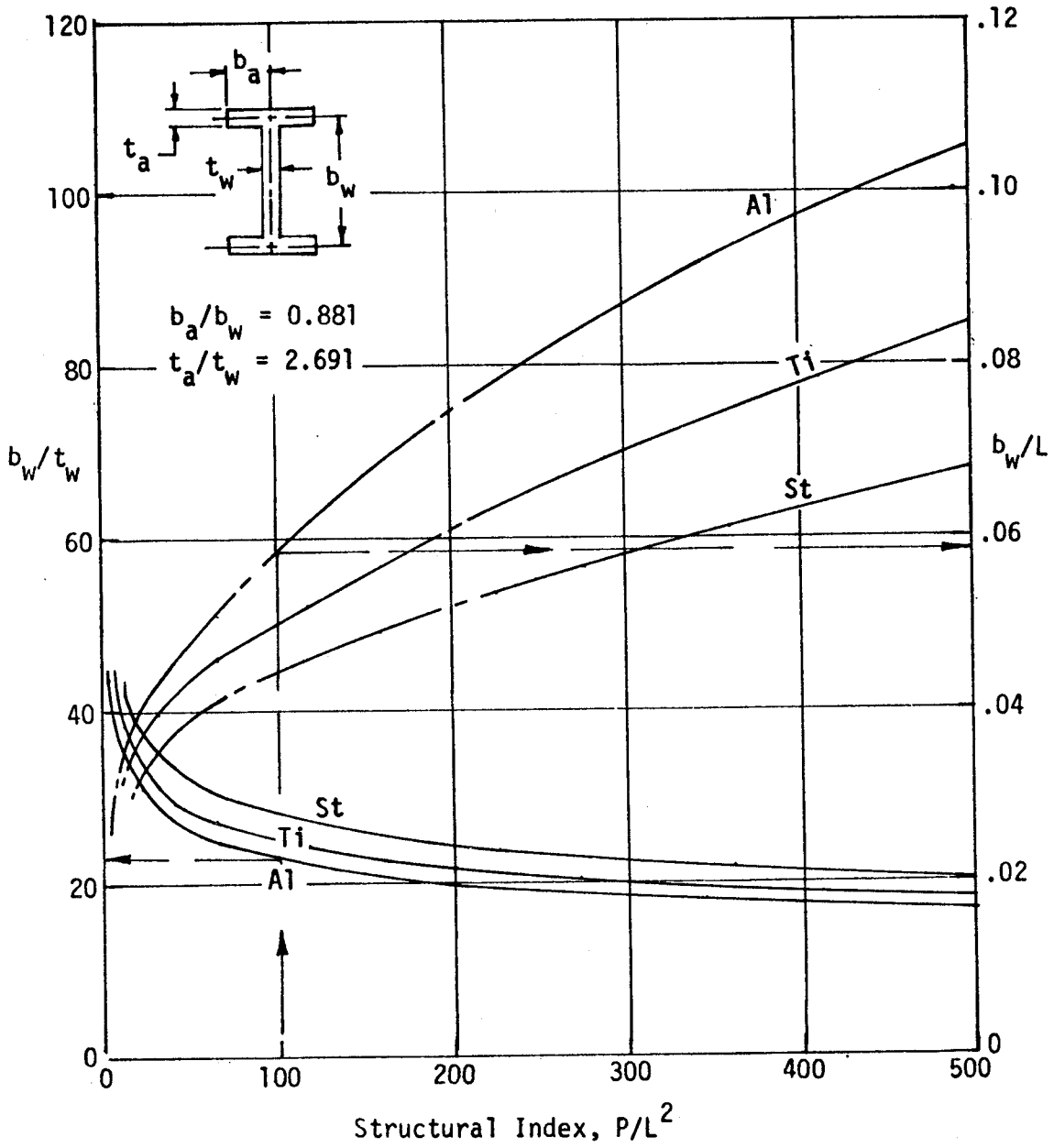


Figure B6.4.1-3 Design Chart for Minimum Weight I Sections

Polar moment of inertia is computed as $I_o = 6.4$ in.$^4$. The torsional instability stress is given by Equation B6-2 as

$$F_T = \eta_p \left[ \frac{GJ + EC_w(\pi/L')^2}{I_o} \right]$$

$$\text{"A"} = [\, 0.385(0.057) + 4.34(\pi/40)^2]/6.4 = 0.00761$$

$$F_T = 66{,}000 \text{ psi}$$

which is greater than the Euler-Engesser stress.

B6.4.2 Minimum Weight Panels

Wide column open-section compression panels are generally sized based on the Euler-Engesser equation and secondary buckling considerations. Twisting instability and its interaction with bending instability is neglected for initial design. This assumption is generally acceptable if the section is near symmetrical. For final design, torsional instability should be investigated to insure that the interaction is minimal. It is a difficult problem to place an absolute value on the amount of interaction because of the approximations required in determining torsional instability stress, such as approximations for spring constants and plasticity factors. If interaction is within ten percent of the Euler-Engesser stress, then conservatism imposed by using the Von Karmen effective skin width equation for determining the bending instability stress will probably compensate for the difference and the interaction can be neglected.

The usual assumption for optimum design of panels is that maximum efficiency will be obtained if the Euler-Engesser and secondary instability stresses are equal to the applied stress. When this is the case, maximum efficiency can be obtained for various cross section shapes. Maximum efficiencies for some of the more common shapes are given in Table B6.4.2-1, based on results from Reference B6-4. The Y stiffened shape is the most efficient shape. However, manufacturing difficulties and corrosion problems in closed sections have led to more common acceptance of Z, J and integral stiffened panels for aircraft application.

Table B6.4.2-1 Compression Efficiencies for Various Shapes

| Panel Type | $A_2/A_1$ | Maximum Efficiency | $A_2/A_1$ | Efficiency |
|---|---|---|---|---|
|  | 2.16 | 1.23 | - | - |
|  | 1.30 | 1.030 | 0.5 | 0.82 |
|  | 1.47 | 0.911 | 0.5 | 0.68 |
|  | 1.28 | 0.793 | 0.5 | 0.58 |
|  | 1.46 | 0.656 | 0.5 | 0.44 |

The maximum efficiencies shown in Table B6.4.2-1 correspond to stiffening ratios which are much higher than can normally be used for high aspect ratio transport structure. This is because wing flutter and fuselage pressurization requirements dictate a skin gage thicker than that dictated by compressive load requirements. A compromise stiffening ratio that meets flutter and pressurization requirements, as well as fail-safe requirements, is about 50 percent. Efficiencies for this stiffening ratio are also shown in Table B6.4.2-1. They are on the order of 20-30 percent less than maximum efficiencies.

Computer programs are available for sizing compression panels based on optimum considerations. Skin and stiffener material may be different. Constraints may be placed on stringer spacing, panel length, and maximum stress. Computer output is a dimensional cross section that will meet axial load requirements. As an aid in ballparking the initial design, Figures B6.4.2-1 through B6.4.2-4 are given. These design charts are for preliminary sizing of 7075-T6 aluminum integral and J stiffened skin panels having stiffening ratios of 0.5 and 1.0. Auxiliary equations required for sizing the panels are given in Table B6.4.2-2 and Figure B6.3.4-1.

In general, the design charts show that the most efficient compression panel design for a constant structural index $P_1/L'$ depends on the ratio of stringer spacing to effective width ($b_s/b_e$). At low values of structural index, it is more efficient to let the skin buckle ($b_s > b_e$). For high values of structural index, best efficiency is obtained when the skin is fully effective ($b_s = b_e$).

The following example illustrates the usage of Figures B6.4.2-1 through B6.4.2-4.

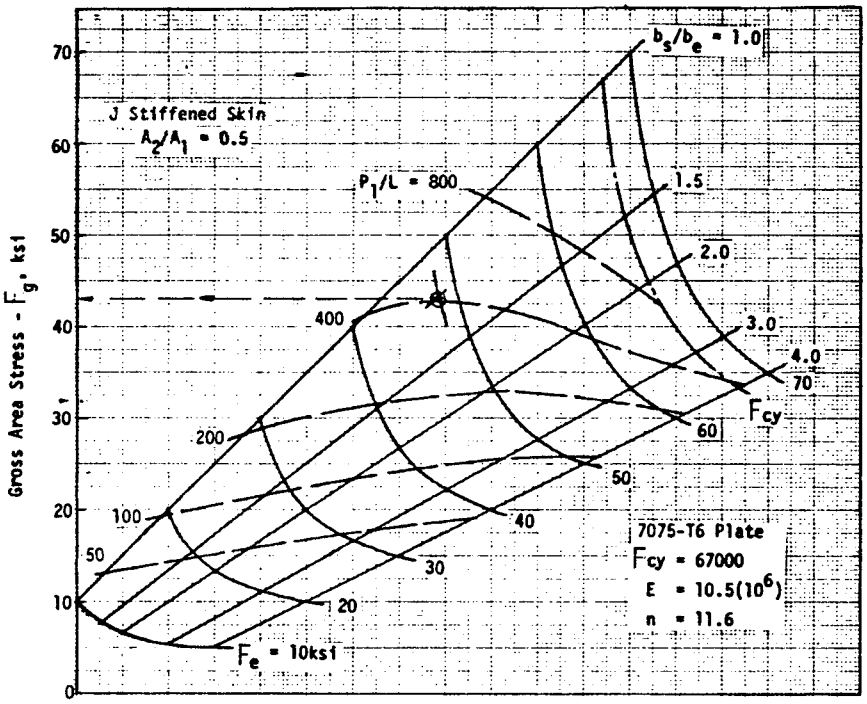


Figure B6.4.2-1 Design Chart for J Stiffened Skin, $A_2/A_1$ = 0.5

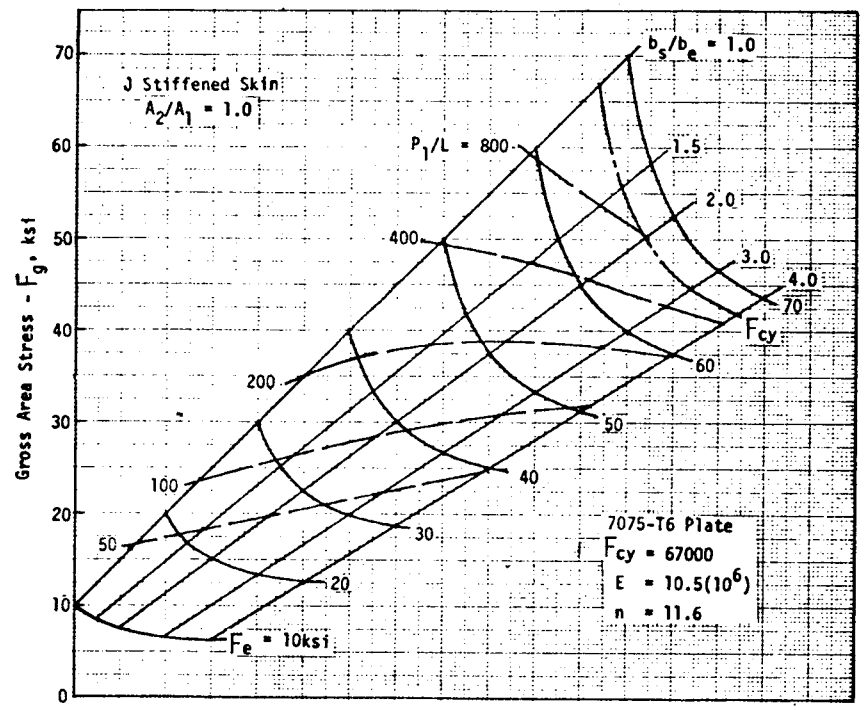


Figure B6.4.2-2 Design Chart for J Stiffened Skin, $A_2/A_1$ = 1.0

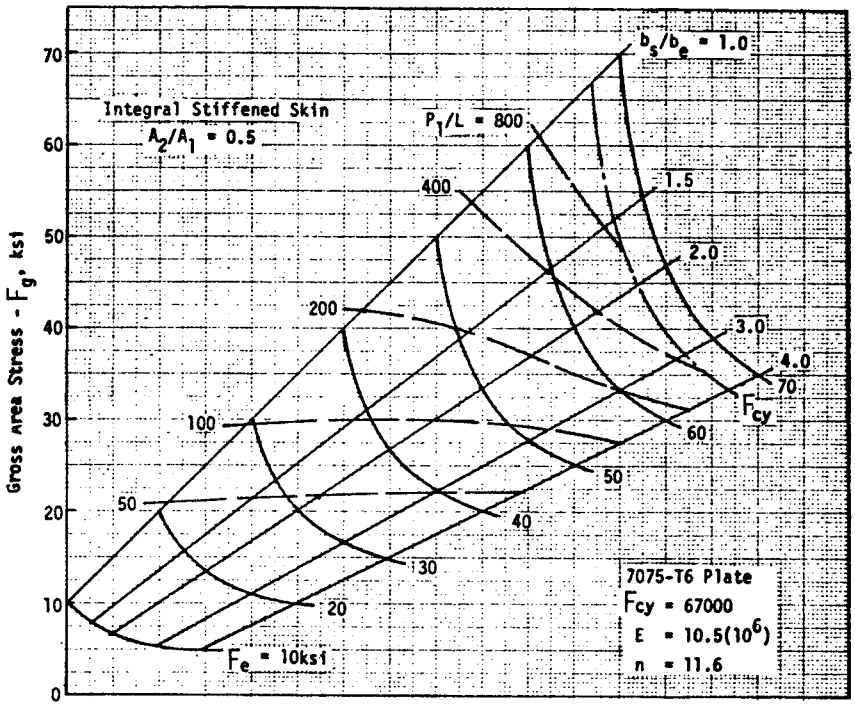


Figure B6.4.2-3 Design Chart for Integral Stiffened Skin, $A_2/A_1$ = 0.5

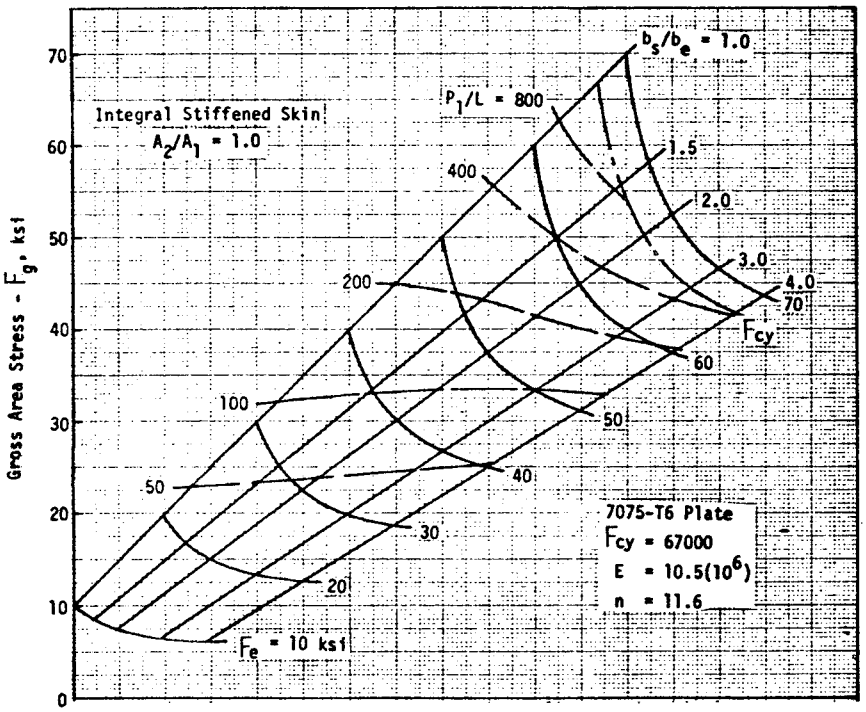


Figure B6.4.2-4 Design Chart for Integral Stiffened Skin, $A_2/A_1$ = 1.0

Table B6.4.2-1 Optimum Element Dimensions

| Element Dimensions | Auxiliary Equation | Remarks |
|---|---|---|
| $t_s$ | $\left(\frac{P_1 \left(b_s/b_e\right)}{\sigma_e\left(1 + \frac{A_2}{A_1}\frac{b_s}{b_e}\right)}\right)$ | |
| $b_e$ | $\left(\frac{b_e}{t_s}\right) t_s$ | $\frac{b_e}{t_s}$ from Figure B6.3.4-1 |
| $b_s$ | $\left(\frac{b_s}{b_e}\right) b_e$ | |
| $b_a$ | $2.08t_s + 0.688 \quad t_s \leq 0.3$<br>$1.312 \quad t_s > 0.3$ | $b_a = 0$ for integral |
| $t_a$ | $0.7\ t_s$ | $t_a = 0$ for integral |
| $A_2$ | $\left(\frac{A_2}{A_1}\right) b_s t_s$ | |
| $b_w$ | $\left[\left(\frac{b_w}{t_w}\right)\left(\frac{A_2 - 2b_a t_a}{1.327}\right)\right]^{1/2}$ | $\frac{b_w}{t_w}$ from Figure B6.3.4-1 |
| $t_w$ | $\frac{b_w}{\left(b_w / t_w\right)}$ | |
| $b_f$ | $0.327\ b_w$ | |
| $t_f$ | $t_w$ | |

A wide column, J stiffened skin panel is to be made from 7075-T6 plate. The following design requirements must be met:

1. $P_1$ = 10,000 lbs./in.
2. $L'$ = 24.5 in.
3. $c$ = 1.0
4. $A_2/A_1$ = 0.50

Find the panel dimensions.

$$P_1/L' = 10{,}000/24.5 = 408$$

From Figure B6.4.2-1, optimum $b_s/b_e$ = 1.20 at an effective area stress level of about 48,500 psi. This corresponds to a gross area stress of 43,000 psi. From Figure B6.3.4-1, the b/t ratio for skin and stiffener web is determined as 27.0 for $F_e$ = 48,500 psi. Then from the auxiliary equation in Table B6.4.2-1, the following panel dimensions are determined.

$$t_s = \frac{10{,}000(1.2)}{48{,}500(1. + 0.5 \times 1.2)} = 0.155 \text{ in.}$$

$$b_e = 27.3(0.155) = 4.23 \text{ in.}$$

$$b_s = 1.2(4.23) = 5.08 \text{ in.}$$

$$t_a = 0.07(0.155) = 0.108 \text{ in.}$$

$$A_2 = 0.50(5.08)(0.155) = 0.394 \text{ in.}^2$$

$$b_w = \left\{27.3\left[\frac{0.394 - 2 \times 1.01 \times 0.108}{1.327}\right]\right\}^{1/2} = 1.90 \text{ in.}$$

$$t_w = 1.90/27.3 = 0.070 \text{ in.}$$

$$b_f = 0.372(1.90) = 0.621 \text{ in.}$$

$$t_f = 0.07 \text{ in.}$$

These dimensions are shown in Figure B6.4.2-5.

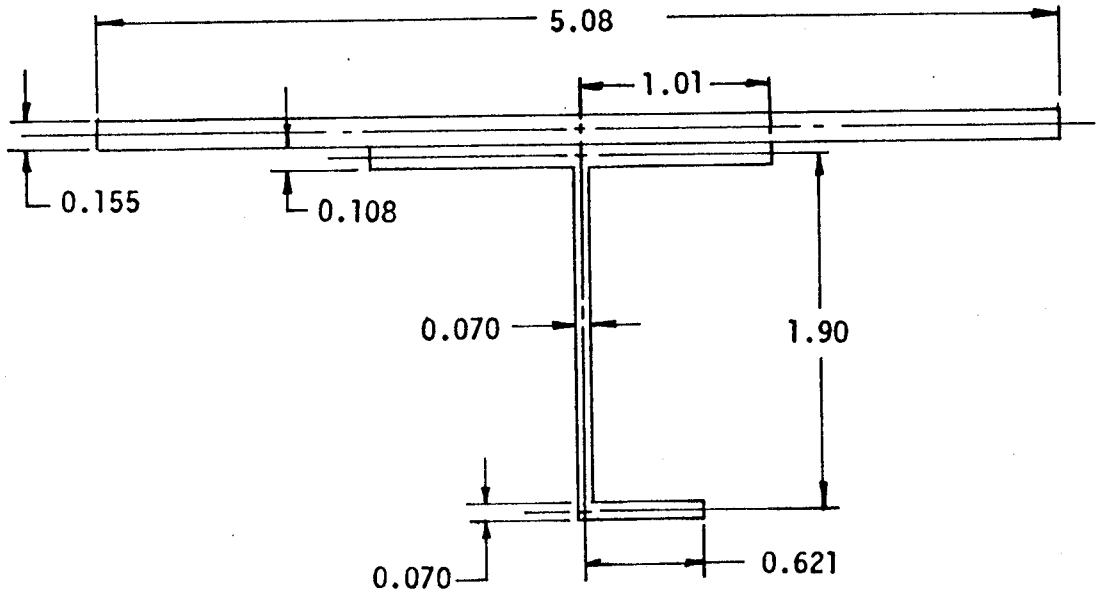


Figure B6.4.2-5 Optimum Geometry for Sample Problem

This section must be investigated for torsional instability.

The section constants required for the analysis are obtained from design charts in Section E1.0.0. These charts are entered with

$$\alpha = \frac{A_2}{b_e t_s} = \frac{0.394}{[4.23(0.155) + 1.01(0.108)]} = 0.515$$

$$\rho = \frac{b_f t_f}{b_w t_w} = \frac{0.621(0.070)}{1.90(0.070)} = 0.327$$

In determining $\alpha$, half of the stringer flange area against the skin was lumped with the skin to give an equivalent Z section. The following section constants are obtained using a stringer depth defined from the centerline of the skin to the centerline of the outstanding flange.

$$I_{xx} = 6.40\left[\frac{2.03^3(0.070)}{12}\right] = 0.312 \text{ in.}^4$$

$$x_E = 0.275(0.621) = 0.171 \text{ in.}$$

$$C_w = 0.20\left[\frac{(0.621)^2(2.03)^3(0.070)}{3}\right] = 0.015 \text{ in.}^6$$

$$I_o = 2.2\left[\frac{(2.03)^3(0.070)}{3}\right] = 0.429 \text{ in.}^4$$

The value for $C_p$ cannot be obtained from the design chart for a J section because the skin is centered over the web. For this case $\bar{x}$ from the stringer web was computed as $\bar{x} = -0.013$, and from Equation B6-8,

$$C_p = \frac{0.171-(-0.013)}{(0.429/1.05)^{1/2}} = 0.288$$

The torsion constant is computed from Equation E1-22 for the stringer as

$$J = 1/3\ [2(1.01)(0.108)^3 + 1.9(0.070)^3 + 0.621(0.070)^3] = 0.0014 \text{ in.}^4$$

Skin and stringer spring restraints are computed from Table B6.2.1.4-1. (Subscripts s and a denote symmetrical and antisymmetrical modes, respectively.)

$$K_{f_s} = 0$$

$$K_{f_a} = \frac{4(10.5)(10^6)}{1-0.3^2}\ \frac{0.155^3}{5.08} = 1311$$

$$K_{p_s} = \frac{10.5(10^6)}{1-0.3^2}\ \frac{0.155^3}{5.08} = 8458$$

In order to compute the antisymmetrical plate spring restraint, initial buckling stress, $F_i$, is approximated using the buckling equation for a plate simply supported on both unloaded edges (tests indicate about 1.5 times this).

$$F_i = 3.62E\left(\frac{t}{b}\right)^2 = 3.62(10.5)(10^6)\left(\frac{0.155}{5.08}\right)^2 = 35{,}400 \text{ psi}$$

Then

$$K_{p_a} = \frac{10.5(10^6)}{3(1-0.3^2)}\left[\frac{0.155^3}{5.08}\right]\left[1 + 0.7\left(\frac{48{,}500-35{,}400}{48{,}500}\right)\right] = 3352$$

Stringer rotational restraint is computed with $b_o = 0$ which is valid for J and integral sections.

$$K_s = \frac{10.5(10^6)}{4(1-0.3^2)}\left[\frac{1}{(1.9/0.07^3)}\right] = 521$$

The combined rotational restraints are obtained as

$$K_{\phi_s} = \frac{8458(521)}{8458+521} = 491$$

$$K_{\phi_a} = \frac{3352(521)}{3352+521} = 451$$

Then from Equations B6-5 and B6-6

$$F_{x_s} = \frac{\pi^2(10.5)(10^6)}{44.92^2} = 51{,}000 \text{ psi}$$

$$F_{T_s} = \frac{3.85(10^6)(0.00114) + 10.5(10^6)(0.015)\left(\frac{\pi}{24.5}\right)^2 + 491\left(\frac{24.5}{\pi}\right)^2}{0.429} =$$

86,000 psi

Similarly,

$$F_{x_a} = 127{,}000 \text{ psi}$$

$$F_{T_a} = 80{,}000 \text{ psi}$$

Both antisymmetrical stresses are greater than either symmetrical stress. Therefore, only the symmetrical mode need be considered. The ratio

$$\left(\frac{F_x}{F_T}\right)_s = \frac{51{,}000}{86{,}000} = 0.593$$

Figure B6.2.1.4-3 is entered with this ratio and the previously computed value for $C_p = 0.288$ to obtain

$$\frac{F}{F_x} \sim 0.90$$

This is within 10 percent and interaction can be neglected.

## B6.5.0 Design Approach for Compression Panels

### B6.5.1 General Guidelines

New compression panel designs should be rough sized for minimum weight as described in Section B6.4.2. This rough sizing will establish optimum stress levels and, subsequently, optimum stringer spacings, stringer depths, and rib or frame spacings. Practical considerations should then be imposed on the optimum values to obtain a general structural arrangement. Specific compression panel elements within this arrangement should be designed to meet the interaction requirements defined in Section B6.3.3. Figure B6.5.2-1 shows typical compression panel dimension nomenclature.

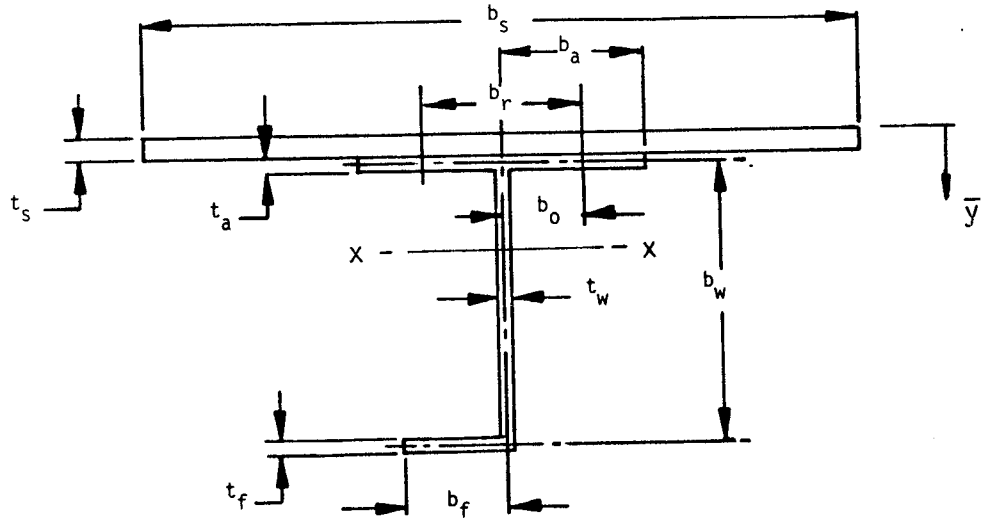


Figure B6.5.2-1 Typical Compression Panel Dimensions

The following guidelines with respect to these panel dimensions will assure a successful design:

A. For wing structure and empennage structure, rough size and detail new compression panel designs based on a stiffening ratio (stringer area-to-skin total area) of $A_2/A_1 = 0.50$, unless flutter information is available to allow higher stiffening ratios and the associated lighter weight design. Stiffening ratios less than 50 percent are not allowed because of damage tolerance considerations.

   For pressurized fuselage structure use $A_2/A_1 = 0.30$. In this case, higher stiffening ratios will not, generally, produce lighter weight structure because pressure load requirements usually set the skin thickness higher than is required for axial compression loads. A minimum stiffening ratio is usually sufficient to transmit compression panel loads between frames. Stringer depth should be kept as small as possible to maximize cargo volume.

B. Set $t_w \simeq t_f$ (optimum design theory indicates $t_w$ slightly greater than $t_f$ gives best panel efficiency).

C. Set stringer b/t ratios such that the sum of element crippling stresses is greater than the compression panel allowable stress. Ratios representative of compression panels already tested at DAC are:

$$b_a/t_a < 10$$

$$b_w/t_w = 18 \text{ to } 22$$

$$b_f/t_f = 6 \text{ to } 8$$

   The empirical Johnson's Parabola (used for column allowable stress in Section B6.5.2.1) requires that the element crippling stresses be greater than the column allowable stress for practical values of $L'/\rho$. Optimum design theory (Section B6.4.2), permits the element initial buckling stress to equal the column allowable stress. This procedure leads to crippling stresses and subsequently column allowable stresses based on Johnson's Parabola that are less than those defined by optimum design theory. Test data are not available to substantiate optimum theory so the designer must assure that the element crippling stresses sum to a value greater than the

column allowable stress. This will amount to about a 6 percent increase in optimum design theory panel weight as shown in the sample problem, Section B6.5.4.

D. Set $t_a \geq 0.7\ t_s$ (to prevent forced crippling).

E. Set $b_f/b_w$ = .40 to .50 (to prevent rolling of the stringer).

Note: A ratio of 0.327 as defined by optimum design theory may be sufficient, but test data is not available to substantiate this low a ratio.

F. Set $b_o$ as small as possible (to prevent face wrinkling). Don't set it so small that there is not enough edge distance on clips that step to the stringer flange against the skin.

G. Set rivet pitch = 4 to 5D [5D preferable] (wing and empennage structure), 6 to 7D (fuselage structure).

H. Size attachments based on tension requirements as defined by equation B6-29.

B6.5.2 Compression Panel Allowable Stress - Axial Load

Compression panels should be designed to satisfy the interaction equations of Section B6.3.3. These interaction equations require definition of the compression panel allowable stress. Test results are preferred for allowable stress, but if they are not available, the analysis methods in this section should be used to obtain allowable stress values prior to test verification.

Calculate allowable stress based on the Johnson's parabola, the Euler-Engesser equation, and the lateral instability equation. Lowest allowable stress obtained from these three methods should be used in the interaction equation. These equations are not theoretically correct, but conservative assumptions are made which provide good correlation with test data. Thus, for Johnson's parabola, only the stringer is considered when calculating the section crippling stress and the flange against the skin is assumed unsupported by the skin. For the Euler-Engesser equation, a conservative effective width is used.The "exact" analysis method shown in Section B6.2.1.4 is not used because it is difficult to evaluate the constants and factors that are required.

B6.5.2.1 Johnson's Parabola

The column allowable stress based on Johnson's parabola is

$$F_c = F_{cc} - \frac{F_{cc}^2}{4\pi^2 E}\left[\frac{L'}{\rho}\right]^2 \qquad \text{(B6-32)}$$

where

$F_{cc}$ = the allowable crippling stress for the stringer only, psi.

$E$ = the stringer elastic modulus, psi

$L'$ = the panel effective length, $L' = L/\sqrt{c}$, in.

$\rho$ = the panel radius of gyration which includes both stringer area and effective skin area ($b_e\, t_s$), $\rho = \sqrt{\frac{I}{A}}$, in.

Figure B6.5.2.1-1 is a plot of Equation B6-32 as a function of $L'/\rho$ for variations in the crippling stress. It is intended to use this figure for 7075-T651 extrusion material, but it can be used for any material with $E = 10.2 \times 10^6$ psi.

Values for $F_{cc}$, $L'$, and $b_e$ should be computed as follows:

A. Allowable Crippling Strength ($F_{cc}$) - This strength is defined as

$$F_{cc} = \frac{\sum_{i=1}^{n} F_{cc_i} A_i}{\sum_{i=1}^{n} A_i} \quad \text{(stringer alone)} \qquad \text{(B6-33)}$$

where $F_{cc_i}$ is the crippling stress for each stringer element of length $b_i$ and thickness $t_i$ which is determined based on test curves or empirical data. For extruded shapes, which are common to aircraft structure, use Figure B6.5.2.1-2. For rolled stiffener shapes, use data in Section E6.

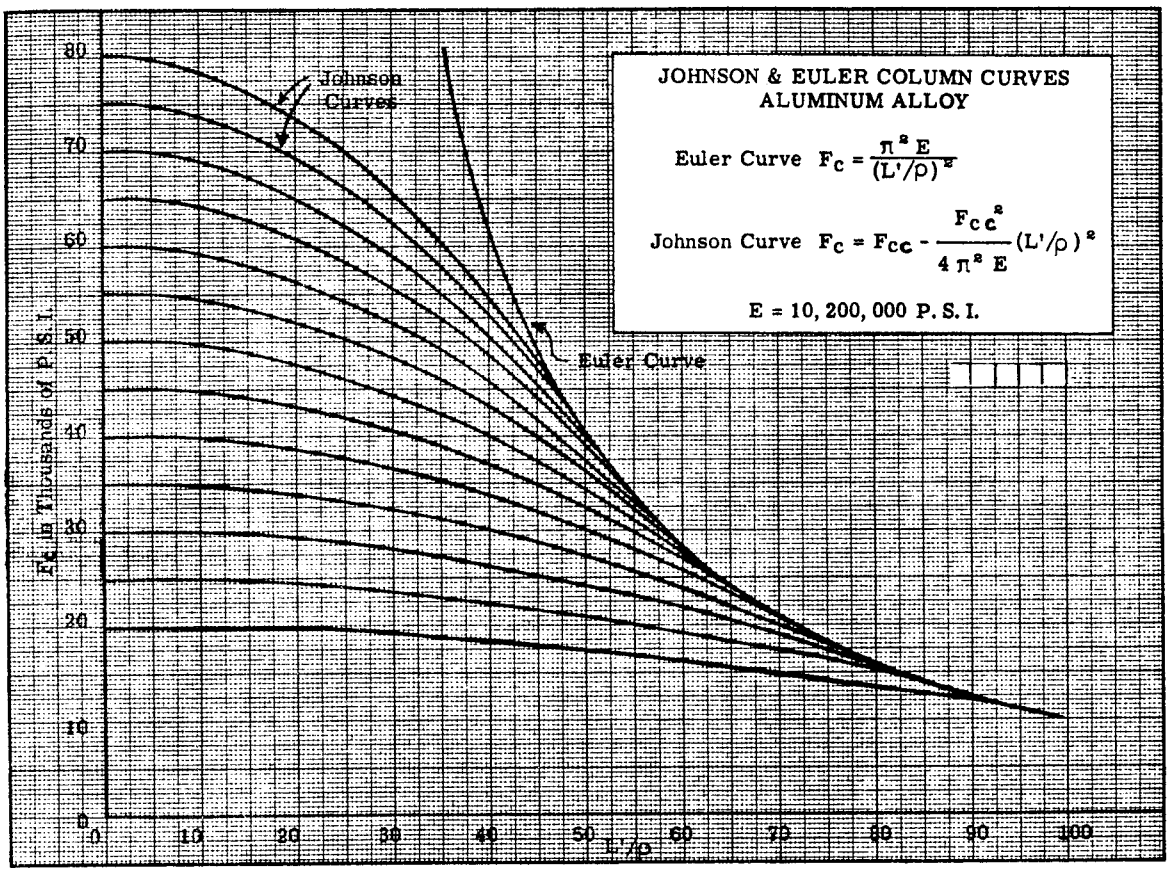


Figure B6.5.2.1-1 Compression Panel Allowable Stress (Johnson's Parabola), E = 10.2 x $10^6$ psi

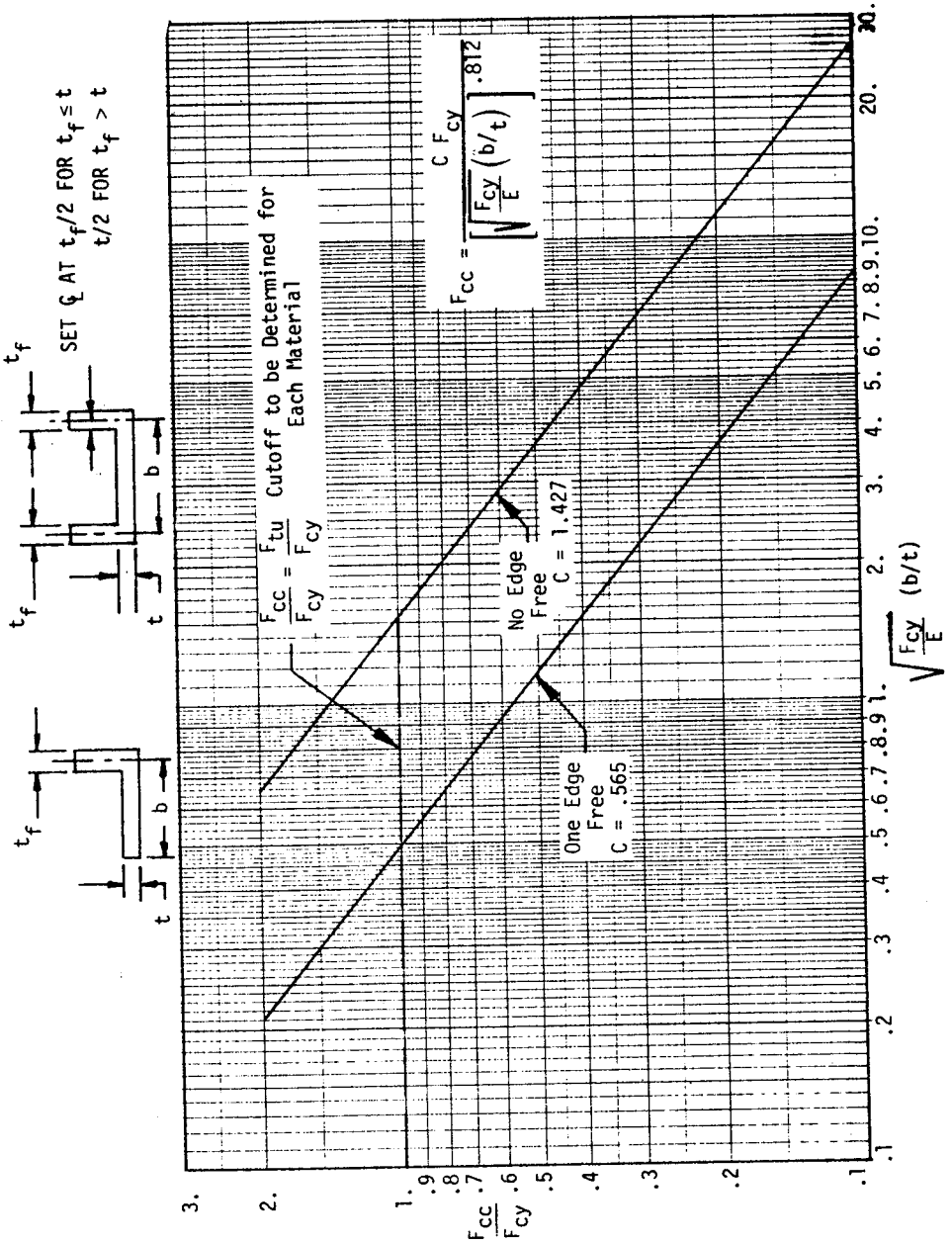


Figure B6.5.2.1-2 Nondimensional Crippling Curve (This curve is applicable to all ductile aircraft materials at both room and elevated temperature)

B. Effective Length L' - The panel effective length is defined as

$$L' = L/\sqrt{c} \qquad \text{(B6-34)}$$

L = Panel length, in.

c = panel end fixity (use c = 1.5 for wing and empennage structure; use c = 2.0 for fuselage structure).

C. Effective Skin Width ($b_e$) - Effective width for the skin is shown in Figure B6.5.2.1-3.

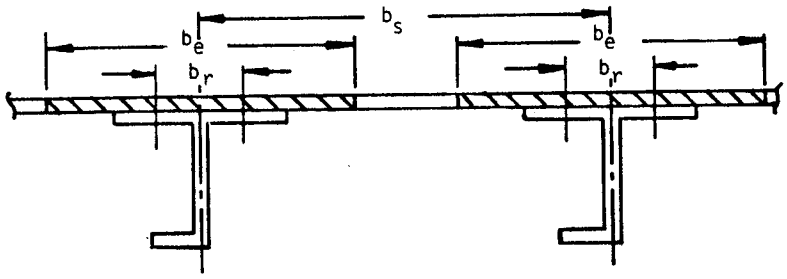


Figure B6.5.2.1-3 Skin Effective Width

It is defined as

$$b_e = b_r + 1.9\, t_s \sqrt{\frac{E}{F_c}} \text{ for } t_s \geq .125 \qquad \text{(B6-35a)}$$

$$b_e = b_r + .2375 \sqrt{\frac{E}{F_c}} \text{ for } t_s = .1 \text{ to } .124 \qquad \text{(B6-35b)}$$

$$b_e = b_r + 2.4\, t_s \sqrt{\frac{E}{F_c}} \text{ for } t_s \leq .099 \qquad \text{(B6-35c)}$$

and is subject to the limitation that $b_e < b_s$.

$F_c$ = the panel allowable stress (can also be applied, beam column, or lateral instability stress), psi.

$b_r$ = the distance between rivets for "J" sections, in.

The procedure for determining $b_e$ is iterative. Thus, (1) calculate $F_{cc}$ for the stiffener; (2) assume $F_c = F_{cc}$; (3) calculate $b_e$; (4) calculate I and A for the combined stringer and effective skin; (5) calculate $L'/\rho$; (6) calculate $F_c$. Iterate steps 3 to 6 until agreement is obtained between the assumed $F_c$ and the calculated $F_c$. Three iterations are usually enough to get agreement.

For design purposes, it is sufficient to assume $b_e = b_r + 30t_s$ for 2024-T3 skin and $b_e = b_r + 25t_s$ for 7075-T6 skin and skip the iteration.

B6.5.2.2 Euler-Engesser Equation

The column allowable stress based on the Euler-Engesser equation is defined in the form of "A" scale by Equation B6-17 as

$$\text{"A" scale} = \frac{F_c}{E_t} = \frac{\pi^2}{(L'/\rho)^2}$$

where

$E_t$ = the weighted tangent modulus between the stringer area and effective skin area, psi.

$L'$ = the effective column length as defined in Section B6.5.2.1B.

$\rho$ = the radius of gyration for the stringer area and effective skin area ($b_e t_s$), $\rho = \sqrt{I/A}$, in.

Values for $E_t$, $L'$, and $b_e$ are defined as follows:

A. Tangent Modulus ($E_t$) - A plot of stress versus tangent modulus is required when using the Euler-Engesser Equation. If the skin and stringer are the same material, the "A" scale method, as defined in Section B6.3.1, is a simple way to obtain the allowable stress. Generally, skin and stringer material are not the same. In this case, a stress-tangent modulus curve is required that is weighted, depending on the stringer area and the skin effective area, as defined by the equations

$$E_{t_{av}} = \frac{E_{t1}\, b_e t_s + E_{t2}\, A_2}{b_e t_s + A_2} \qquad \text{(B6-36a)}$$

$$f_{c_{av}} = \frac{f_1 b_e t_s + f_2 A_2}{b_e t_s + A_2} \qquad \text{(B6-36b)}$$

Values for $E_{t1}$, $f_1$ and $E_{t2}$, $f_2$ are obtained from material stress-strain tangent modulus curves, such as shown in Figure B6.3.1-1 for constant strain. A weighted stress-tangent modulus curve is constructed based on Equations B6-36a and -36b. The construction of this curve is rather tedious by hand, because the effective width is also a variable in Equations B6-36a and -36b. A computer solution is available to simplify the analysis method (see Section E7).

A quick rough estimate of the allowable stress can be obtained by simply superimposing the two stress-tangent modulus curves, constructing an "A" scale line based on section geometry, and proportioning the distance between the two material curves along the constant "A" scale line based on the ratio $A_2/A_1$. Figure B6.5.2.2-1 shows this method for 7075-T651 plate and 7075-T6 extrusion. A, is effective area.

Minimum guaranteed design curves are provided in Figure B6.5.2.2-2 and -3 for common combinations used at DAC. Thus, 2024-T3 or 7075-T6 skin in combination with 7075-T651 extrusion. If stress-tangent modulus curves are not available, they may be constructed based on the equation

$$E_t = \frac{E}{1 + \frac{.002En}{F_{cy}} \left(\frac{f}{F_{cy}}\right)^{n-1}} \qquad \text{(B6-37)}$$

where

$E$ = the material elastic modulus, psi.

$F_{cy}$ = the material minimum guaranteed compression yield strength, psi.

$n$ = A material stress-strain shape factor obtained from MIL-HDBK-5A; use 20 if no value is available.

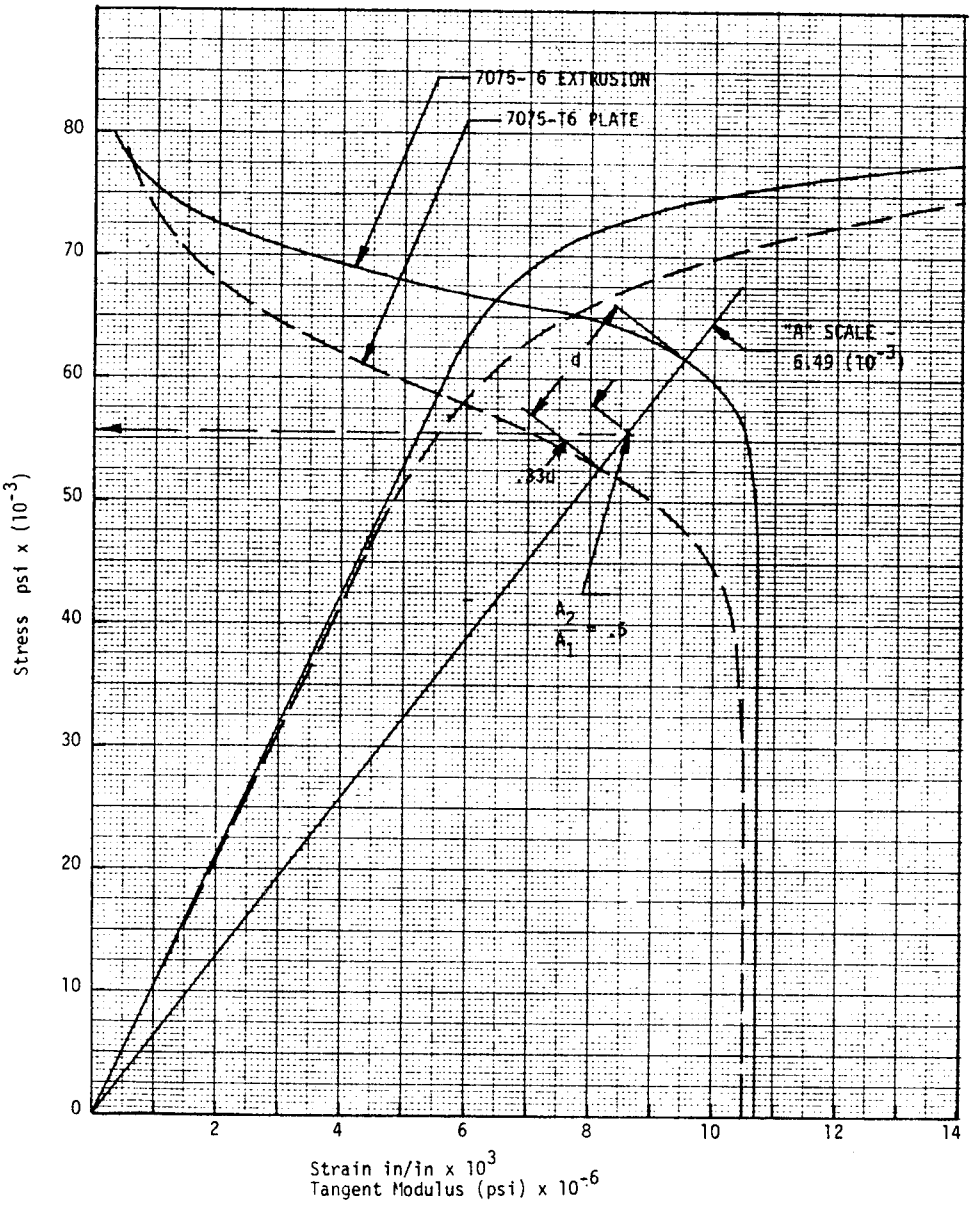


Figure 6.5.2.2-1 Approximate "A" Scale Method for Skin and Stringer of Different Material
Note: This is unconservative at the knee of the curves.

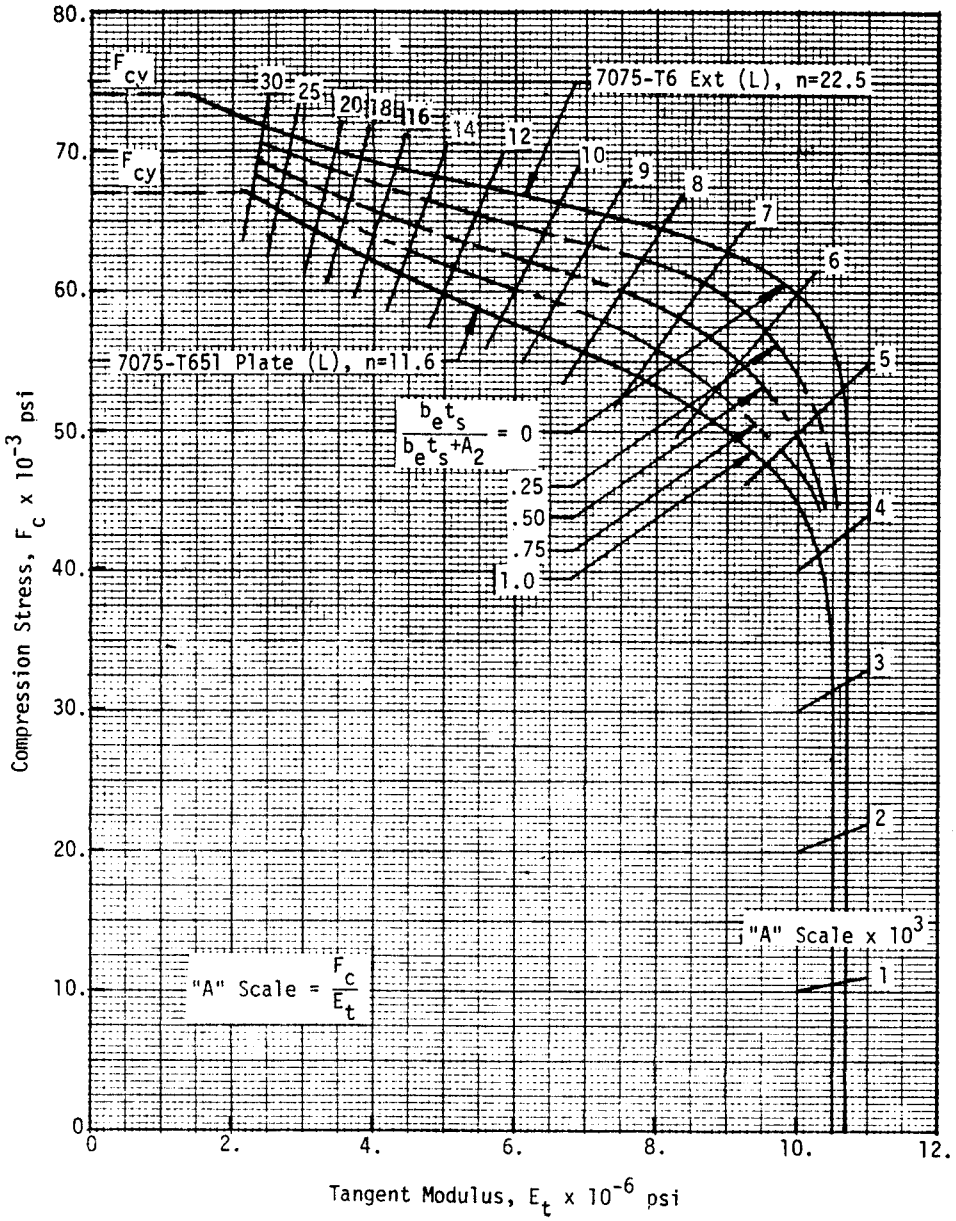


Figure B.6.5.2.2-2 Column Allowables at Room Temperature for 7075-T651 Plate and 7075-T6 Ext.

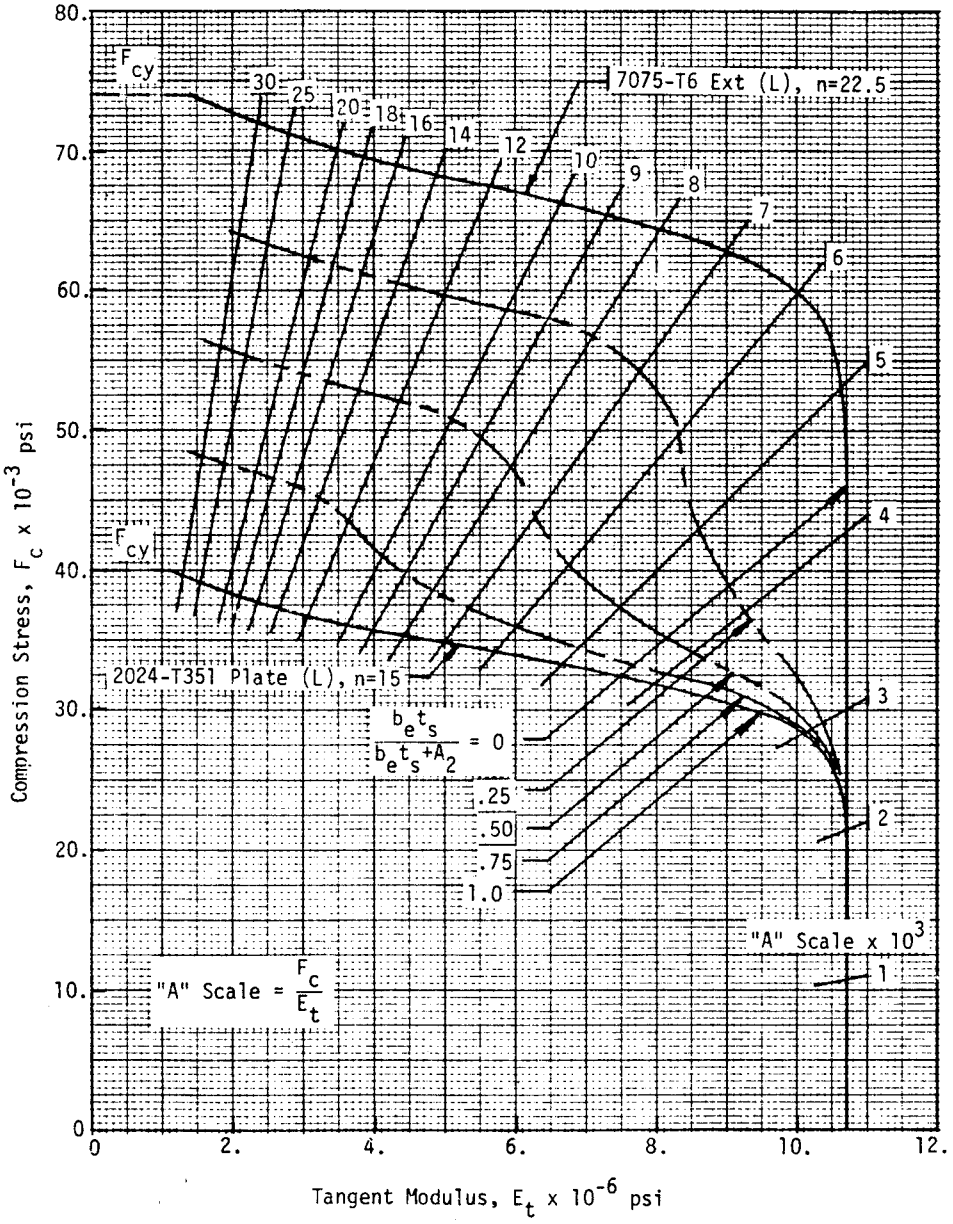


Figure B6.5.2.2-3 Column Allowables at Room Temperature for 2024-T351 Plate and 7075-T6 Ext.

B. Effective Length (L') - Equation B6-34 defines L'. The same fixity value, c, applies as given in Section B6.5.2.1B.

C. Effective Skin Width ($b_e$) - Use the value defined in Section B6.3.4 by Equation B6-27 which can also be expressed as

$$b_e = 1.9\, t_s \sqrt{\frac{\eta_p E}{f_1}} \qquad \text{(B6-38)}$$

This equation is plotted in Figure B6.3.4-1 for 2024-T3 and 7075-T6 material. It is similar to Equation B6-35a, except $b_r$ is taken as zero and E is corrected for plasticity effects by $\eta_p = \sqrt{E_t/E}$ when $f_1$, the skin effective area stress, is above the skin material proportional limit.

Reference B6-10 shows that Equations B6-36 and B6-38, along with the Euler-Engesser equation correlate test loads (not stresses) for "J" and integral stiffened sections within $\pm 9$ percent.

Note: When comparing stress levels between Johnson's parabola and Euler-Engesser equation, use the same effective area. Preferrably the area determined for Johnson's parabola, as this more nearly correlates stress test data.

The procedure for determining the Euler-Engesser allowable stress is as follows:

A. Assume an allowable stress.

B. Obtain the ratio $b_e/t_s$ for this stress from Figure B6.3.4-1 at the assumed stress (or Equation B6-38).

C. Calculate $b_e = (b_e/t_s)\, t_s$.

D. Calculate section properties for the combined stringer area and skin effective area; $A_e$, y, $I_{xx}$, $\rho_{xx}$.

E. Calculate "A" = $\pi^2/(L'/\rho)^2$ based on appropriate end fixity, c.

F. Determine the allowable stress from the appropriate "A" scale chart (Figures B6.5.2.2-2 and -3).

G. Compare allowable stress calculated in (F) with allowable stress assumed in (A).

H. Repeat steps B through G until agreement between assumed and calculated allowable stress is obtained.

For design purposes, it is sufficient to assume $b_e = 30t_s$ for 2024-T3 skin and $b_e = 25t_s$ for 7075-T6 skin and skip the iteration.

B6.5.2.3 Lateral Instability

This failure mode is determined based on theory in Reference B6-1 for the buckling of a bar on elastic supports. Figure B6.5.2.3-1 shows term definition for a typical stringer element.

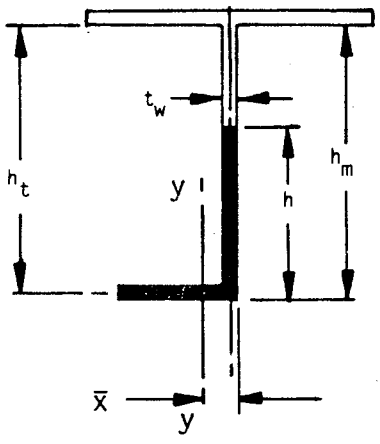


Figure B6.5.2.3-1 Stringer Term Definition for Lateral Instability

The shaded area of this stringer is treated as a beam on elastic support. The effective height, h, is determined from Figure B6.5.2.3-2 based on the actual stringer dimension $h_m$. Lateral

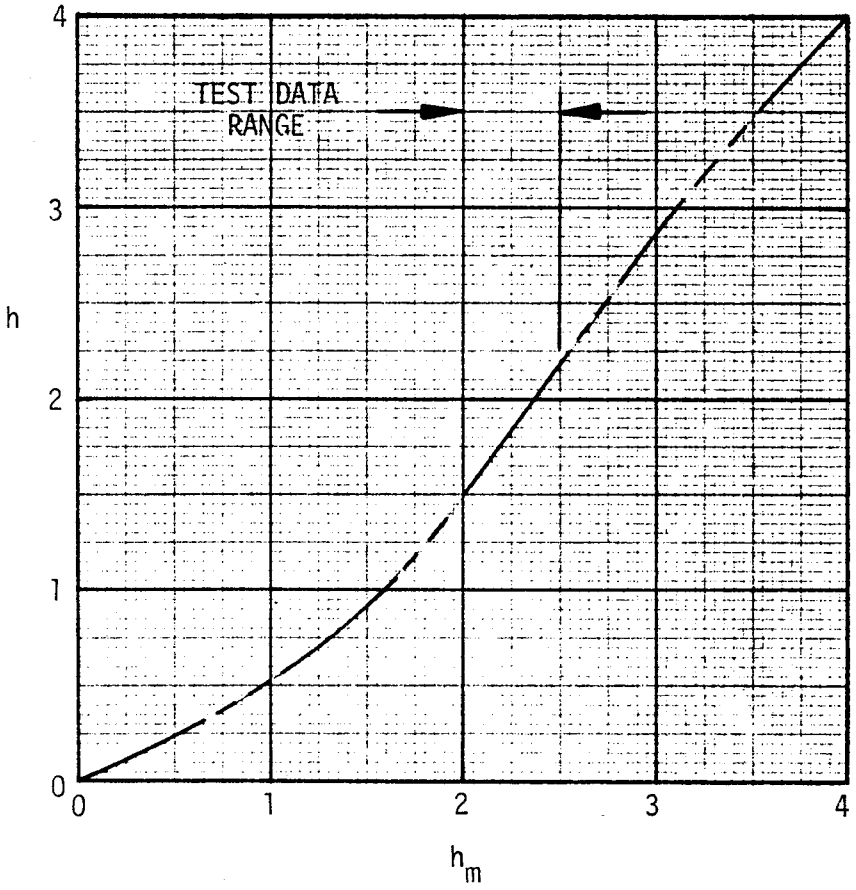


Figure B6.5.2.3-2 Effective Stringer Web Height for Lateral Instability

section properties are then calculated for this effective cross section about the section neutral axis. The Euler-Engesser Equation (B6-17) is used to determine the allowable stress based on an effective column length which accounts for the support against buckling provided by the stringer web. The column effective length (L') is determined from Figure B6.5.2.3-3 based on the rigidity of the elastic support which is defined as

$$\beta = \frac{E\, t_w^3}{4\, h_t^3} \qquad \text{(B6-39)}$$

The lateral buckling stress is calculated as follows:

A. Determine $\beta$ from Equation B6-39 based on the stringer dimensions.

B. Determine the effective web height from Figure B6.5.2.3-2.

C. Calculate the section properties for the effective column; $A_e$, x, $I_{xx}$, and $\rho_{xx}$.

D. Calculate $\frac{\beta L^4}{16EI}$ and enter Figure B6.5.2.3-3 to determine L'/L.

E. Calculate the effective column length as $L' = \frac{L'}{L}\ L$.

F. Calculate "A" scale = $\pi^2/(L'/\rho_{xx})^2$.

G. Read the allowable stress $F_c$ from an appropriate stress-tangent modulus curve for the stringer based on the "A" scale value determined in step F.

H. Determine the lateral buckling load based on the section effective area as $P = F_c A_e$ where the value for effective area includes the stringer area plus effective skin area which is based on the lateral stability allowable stress, $F_c$. Use Equation B6-35a, -35b or 35c for determining the skin effective width. For design it is sufficient to assume $b_e = b_r + 30t_s$ for 2024-T3 skin and $b_e = b_r + 25t_s$ for 7075-T6 skin.

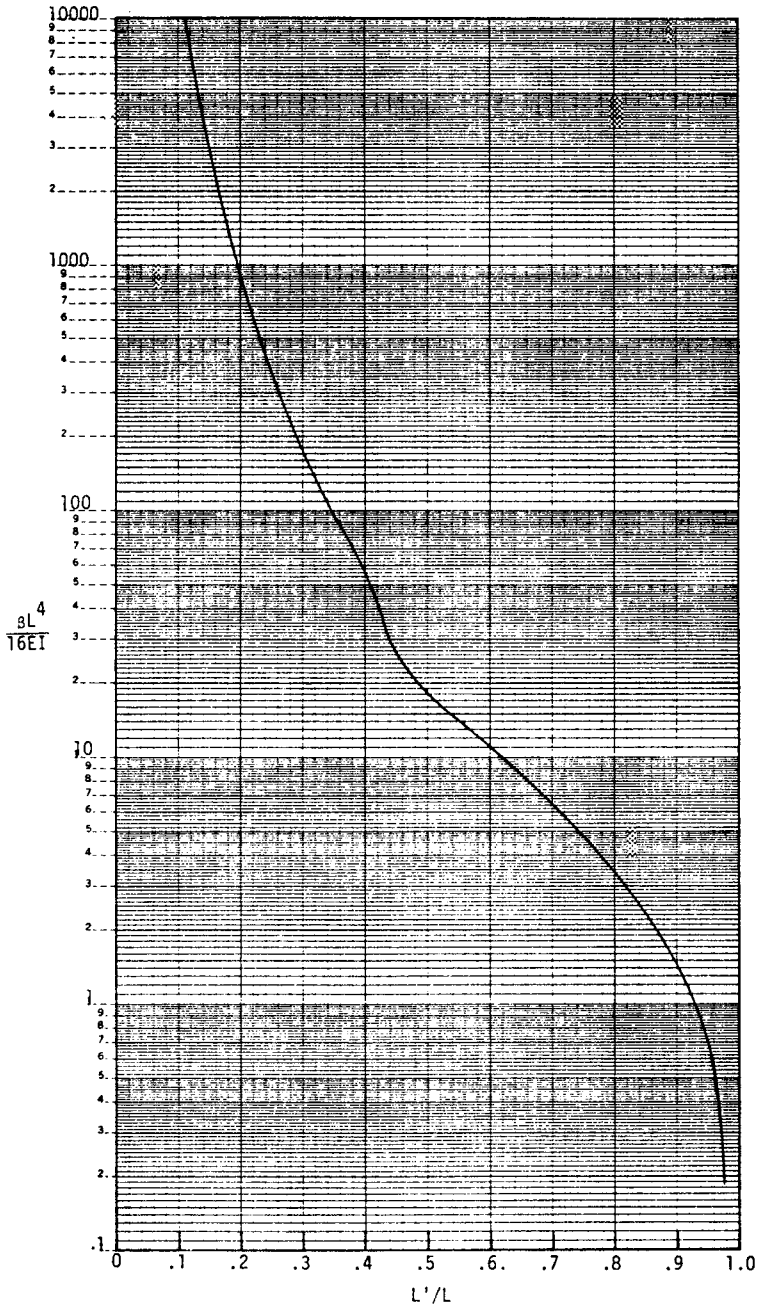


Figure B6.5.2.3-3 Effective Column Length for Lateral Instability

## B6.5.3 Compression Panel Allowable Stress - Beam Column

Typical aircraft compression panels are subjected to normal loads in addition to compression loads. These normal loads produce bending moments over continuous supports which effectively provide a degree of end fixity, c, as can be determined by analysis from the ratio $M/\theta$ where M is the bending moment and $\theta$ is the angle of rotation at the support. Section B6.2.2.3 covers this type of problem and shows that the effective fixity, c, can vary from 1 to 4, depending on (1) the ratio of applied load to Euler load ($P/P_{cr}$), (2) the number of continuous supports, (3) the end restraint provided at the first and last bay, and (4) the rotational restraint provided by a rib or frame at the support.

For design, continuous beam analysis is not clearly defined because of items 2, 3, and 4. Therefore, it is recommended to design for c = 2 when determining the moment between supports and c = 3.5 when determining the moments over supports for beam column designs. Figures B6.5.3-1 through -2 from Reference B6-6 give the bending moments for c = 2 and 3.5 based on the applied axial load P (lbs.) and the beam normal load $w_o$ (lbs./in.).

Note: 1) When using Figures B6.5.3-1 through -2, substitute $E_t$ for E at applied stresses, P/A, above the material proportional limit. Thus, at the applied stress, determine $E_t$ from a stress-tangent modulus curve and use this value when entering the Figures.

2) Geometric properties to be used should include skin effective area as determined by the effective width Equations B6-35a, B6-35b or B6-35c at the applied axial stress level.

The bending stresses produced from the beam column bending moments should be interacted with the axial loads as defined by equations in Section B6.3.3 for determining margins of safety. Table B6.3.3-1 defines the maximum stress which can be attained by the application of axial load and beam column bending moments at both the center and ends of the beam column. At the ends, the maximum stress is rather obvious; thus, it is either skin compression yield or flange crippling stress depending on the direction of applied normal load. At the center of the column, the maximum combined stress is not so obvious. Table B6.3.3-1 defines it as the column allowable stress which is determined in Section B6.5.2 for c = 1.5 for wing or 2.0 for fuselage structure.

Theoretically, the maximum combined stress at the center of the column should be based on the beam column end fixity, but as noted this is a variable which is difficult to determine. For beam column design, the end fixity is assumed (c = 2). If the allowable combined stress was also computed for c = 2 based on the equations in Section B6.5.3, an allowable load could be obtained for the beam column that is greater than the pure axial allowable load. This is not possible. In fact, in this case, if the exact fixity were known it would be less than c = 2.0. To avoid this problem, the allowable combined stress should be taken conservatively as the column allowable stress for pure axial load with c = 1.5 or 2.0 as previously discussed.

The procedure for calculating the beam column stress is as follows:

A. Determine the allowable combined stress from Section B6.5.2 based on Table B6.3.3-1 over the supports and at the center.

B. Assume an applied axial stress, $f_c$. For this stress obtain $E_t$ from a stress-tangent modulus curve, Figure B6.5.2.2-2 or -3.

C. Calculate $b_e$ from Equation B6-35a, B6-35b or B6-35c at the assumed stress.

D. Calculate section properties for the stringer area and skin effective area; $A_e$, $\bar{y}$, $I_{xx}$, $\rho_{xx}$.

E. Calculate the applied load $P = f_c A_e$.

F. Calculate $\mu = \dfrac{PL^2}{E_t I_{xx}}$

G. Enter Figure B6.5.3-1 or -2 and read off $\dfrac{M}{w_o L^2}$

H. Calculate $M = \left(\dfrac{M}{w_o L^2}\right) w_o L^2$

I. Calculate $f_b = \dfrac{Mc}{I_{xx}}$ where c is the appropriate distance from the neutral axis to outer fiber that is in compression.

J. Calculate the combined stress $f_c + f_b$ and compare this stress to the appropriate allowable stress in step A.

K. Repeat steps B through J until agreement is obtained. The resulting stress is defined as the beam column allowable stress, $F_{B.C.}$

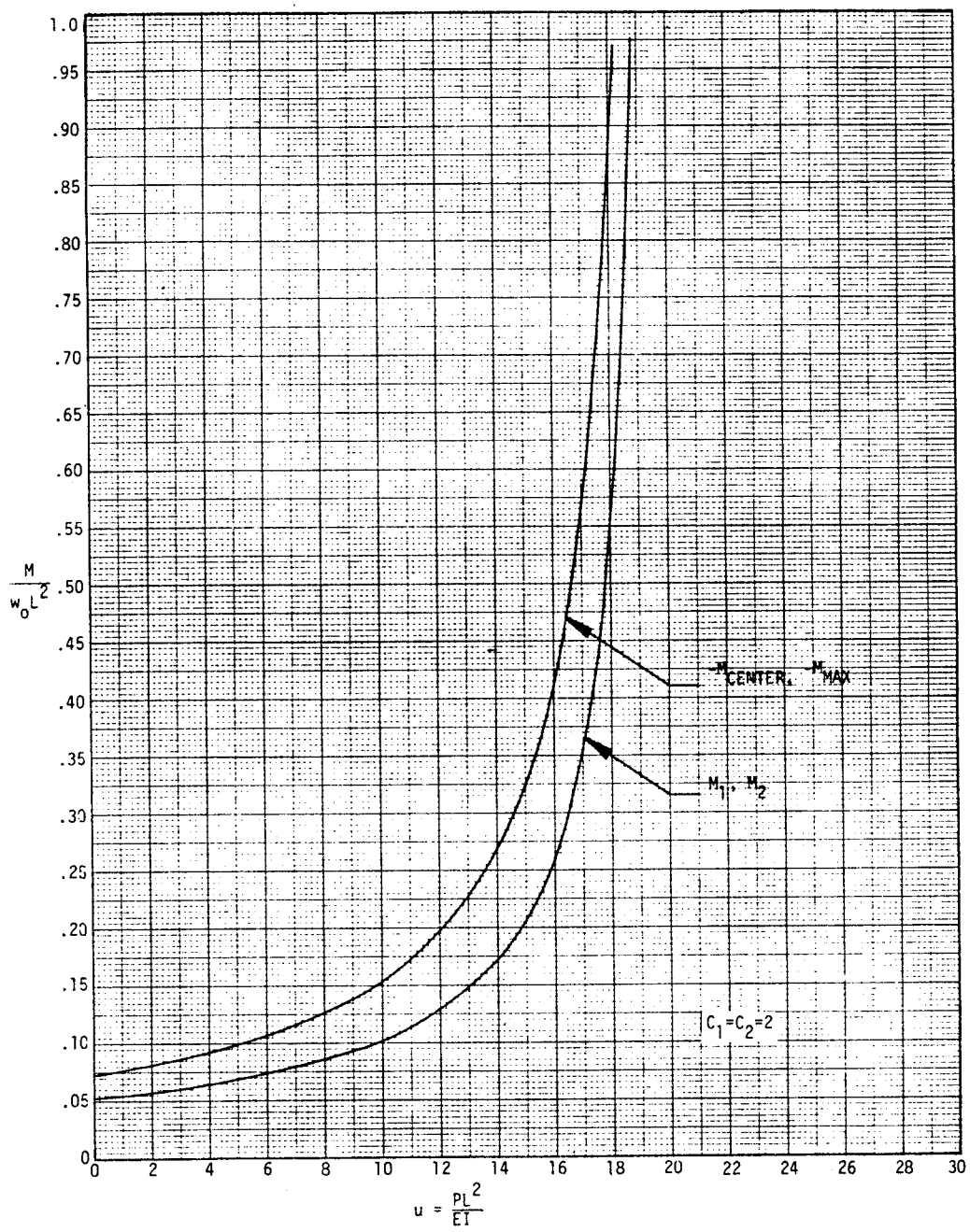


Figure B6.5.3-1 Beam Column Bending Moment, c = 2

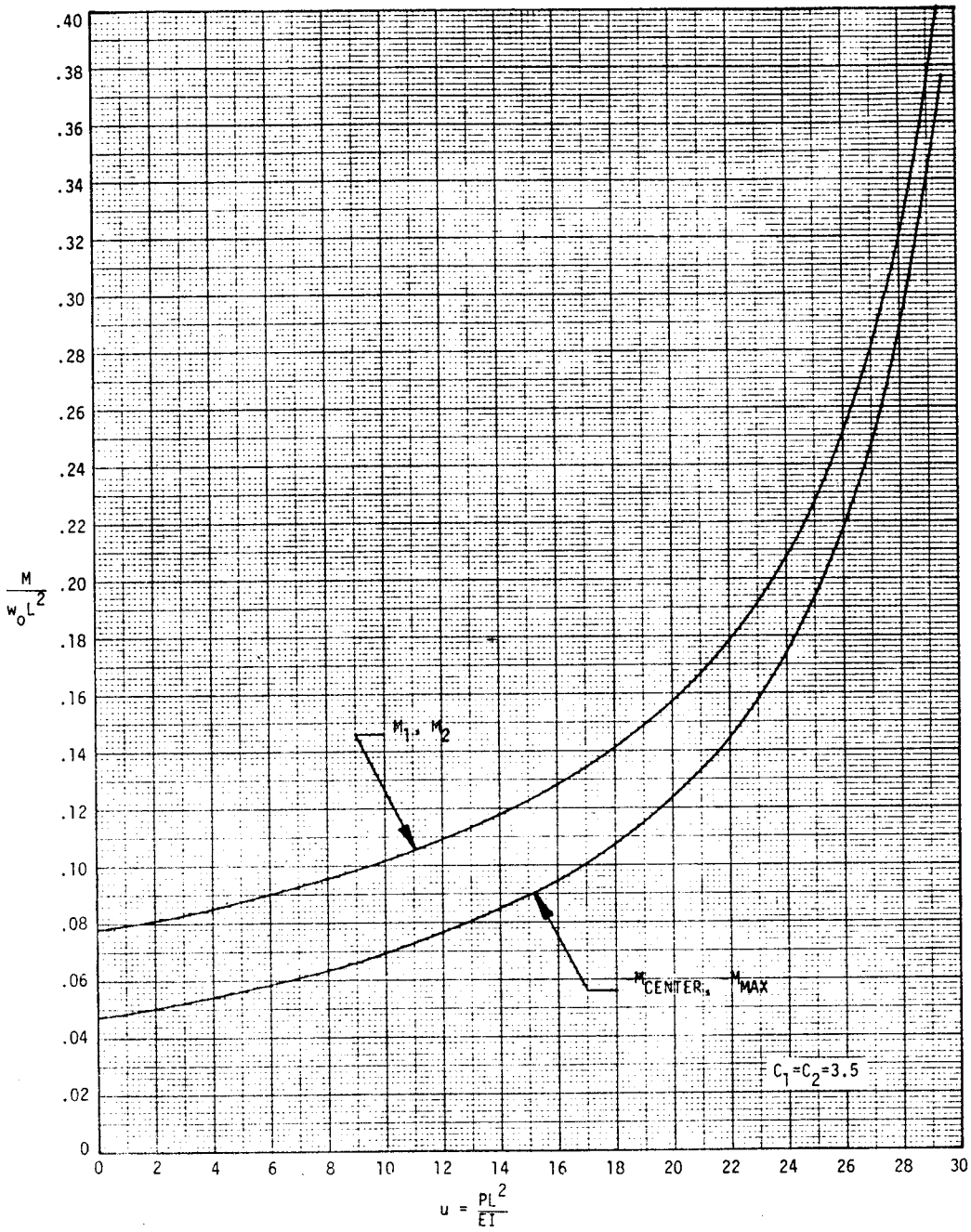


Figure B6.5.3--2 Beam Column Bending Moment, c = 3.5

B6.5.4 Sample Problem

B6.5.4.1 Panel Under Axial Loads

A wing compression panel is required to transfer an axial ultimate load of 10,000 lbs./in. over 30 inches. The skin will be stiffened by a "J" section. Both skin and stringer material will be 7075-T651 plate for which stress-strain data is given in Figure B6.3.1-1. The panel is to be designed for least weight.

In section B6.4.2, an optimum "J" section was sized for $P_1$ = 10,000 lbs./in. and a column length of 24.5 inches, c = 1.0. This corresponds to a 30 inch column with c = 1.5. The optimum panel dimensions are given in Figure B6.4.2-5. These optimum dimensions are first checked against the general guidelines provided in Section B6.5.1.

| Element | Figure B6.4.2-5 Optimum Theory | Guideline Values | Comments |
|---|---|---|---|
| $b_a/t_a$ = 1.01/.108 | 9.35 | 10 or less | Good |
| $b_w/t_w$ = 1.90/.07 | 27.14 | 18-22 | Too High |
| $b_f/t_f$ = .621/.07 | 8.87 | 6-8 | Too High |
| $A_2/A_1$ | .5 | .50 | Good |
| $t_a$ | .108 | .7 $t_s$ = .109 | Good |
| $b_f/b_w$ = .621/1.9 | .327 | .40 | Too Low |

The web and stiffener outstanding flange have b/t ratios which do not meet the guidelines. Also, the ratio $b_f/b_w$ does not meet the guideline. Thicknesses are arbitrarily increased from 0.070 inch to 0.096 inch holding the overall optimum stiffener height (1.99 inch) constant. Flange length $b_f$ is increased to 0.75. The resulting ratios which now meet the guidelines are

$$b_w/t_w = 19.7,$$
$$b_f/t_f = 7.81, \text{ and}$$
$$b_f/b_w = .40.$$

The section, so sized, is shown in Figure B6.5.4-1.

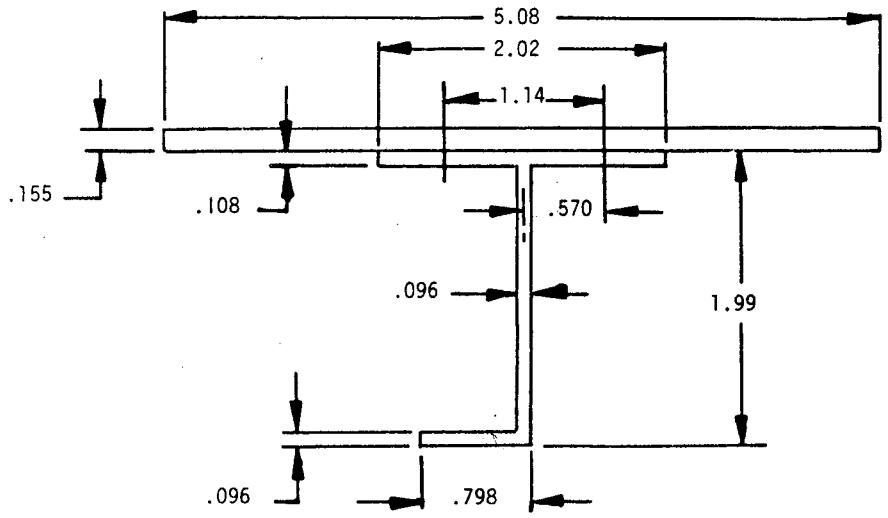


Figure B6.5.4-1 Typical Compression Panel Sized to meet Guidelines

This section is 6 percent heavier than the optimum designed section. It must now be checked against Johnson's parabola, Euler-Engesser, and lateral stability criteria.

Step 1. Determine the crippling allowable stress for the stiffener based on Figure B6.5.3-1. This is best accomplished in tabular form as:

| Element | b | t | b/t | $\sqrt{\frac{F_{cy}}{E}}\frac{b}{t}$ | $F_{cc}/F_{cy}$ | $F_{cc}$ | $A_i$ | $F_{cc}A_i$ |
|---|---|---|---|---|---|---|---|---|
| 2 | 1.01 | .108 | 9.35 | .75 | .72 | 48.240 | .218 | 10,524 |
| 3 | 1.89 | .096 | 19.69 | 1.57 | .98 | 65.660 | .181 | 11,913 |
| 4 | 0.75 | .096 | 7.81 | .62 | .83 | 55,610 | .072 | 4,004 |
| | | | | | | | .471 | 26,441 |

$$F_{cc} = \frac{\Sigma F_{cc}A_i}{\Sigma A_i} = \frac{26,441}{0.471} = 56,138 \text{ psi}$$

Step 2. Determine the effective width of skin from Equation B6-35a. This requires definition of the distance between rivets, $b_r$ which will depend on the rivet tension requirements as defined by Equation (B6-29) and Figure B6.3.5-2.

To obtain $b_r$, assume 3/16 inch Gemcor rivets are good at 5D spacing, p/D = 5.0. The edge distance (2D + 1/16) is 0.44 inch. Therefore:

$$b_o = b_a - .44 = 1.01 - .44 = 0.570 \text{ in.}$$

and $b_o/t_a = 0.570/.108 = 5.29$. Then from Figure B6.3.5-2, $f/t_w = 5.30$ and the attachment tension load from Equation B6-29 is

$$R_R = \frac{E}{1-\mu^2}\,\frac{1}{(f/t_w)^3}\left[\frac{3f/t_w + b_w/t_w}{3f/t_w + 4b_w/t_w}\right]\frac{t_s}{5}\,p =$$

$$\frac{10.5\times10^6}{1-.3^2}\,\frac{1}{(5.30)^3}\left[\frac{3(5.30)+19.19}{3(5.30)+4(19.19)}\right]\frac{.155}{5}\,(.94) = 855 \text{ lbs.}$$

From Figure B6.3.5-3, the allowable strength is seen to be greater than 855 lbs. Therefore, the assumption of 3/16 inch diameter Gemcor rivets is good and

$$b_r = 2b_o = 2\,(.570) = 1.14$$

Edge distance for clips is ignored here for simplicity.

From Equation B6-35a, with $F_c = F_{cc} = 56{,}138$ psi

$$b_e = b_r + 1.9\,t_s\sqrt{\frac{E}{F_c}} =$$

$$1.14 + 1.9\,(.155)\sqrt{\frac{10.5\times10^6}{56{,}138}} = 5.17 \text{ inch}$$

This value is greater than the stringer spacing, so use $b_e = b_s = 5.08$ inch. Note: $F_c$ will be lower than 56,138 psi when Johnson's Parabola is used. An iteration process is often required, which will give higher values for $b_e$. Since the first cut value of $b_e$ is greater than $b_s$ an iteration is not required for this sample problem.

Step 3. Calculate section properties for the stringer and effective skin combination. These values are determined by any accepted method as:

$$A_e = 1.254 \text{ in.}^2, \bar{y} = .371 \text{ in.},$$

$$I_{xx} = .455 \text{ in.}^4, \rho_{xx} = .602 \text{ in.}$$

$$\frac{L}{\sqrt{c}} = \frac{30}{\sqrt{1.5}} = 24.5$$

$$\frac{L'}{\rho} = \frac{24.5}{.602} = 40.70$$

Step 4. Calculate $F_c$ from Johnson's parabola, Equation B6-32 and the allowable load intensity, $P_1$.

$$F_c = F_{cc} - \frac{F_{cc}^2}{4\pi^2 E}\left(\frac{L'}{\rho}\right)^2 = 56{,}138 -$$

$$\frac{56{,}138^2}{4\pi^2(10.5 \times 10^6)}(40.70)^2 = 43{,}544 \text{ psi}$$

$$P_1 = F_c A/b_s = 43{,}544\ (1.254)/5.08 = 10{,}749 \text{ lbs./in.}$$

Note: A is the effective skin and stringer area (the total area for this problem).

Step 5. Calculate $F_c$ from Euler-Engesser equation (B6-17). This will require definition of the skin effective width. The optimum solution gave an effective area stress of 48,500 psi. Use this stress as a first approximation. Enter Figure B6.3.4-1 for 7075 material and determine $b_e/t_s = 27.3$ from which $b_e = 27.3\ (.155) = 4.23$ in. (or use Equation B6-37 and a stress-strain curve).

Calculate section properties for the stringer and effective skin combination as

$$A_e = 1.222 \text{ in.}^2, \bar{y} = .406 \text{ in.},$$

$$I_{xx} = .442 \text{ in.}^4, \rho_{x\bar{x}} = .628 \text{ in.}$$

$$\frac{L'}{\rho} = \frac{24.5}{.628} = 39.01 \text{ in.}$$

Calculate "A" scale, Equation B6-17 as

$$\text{"A"}_{\text{scale}} = \frac{\pi^2}{(L'/\rho)^2} = \frac{\pi^2}{39.01^2} = .00649$$

For this "A" scale, determine $F_c$ from Figure B6.5.2.2-2 as $F_c$ = 53,205 psi. With this stress as the next approximation, find $b_e/t_s$ from Figure B6.3.4-1 as 25.0 and $b_e = (b_e/t_s)\, t_s = 25\ (0.155) = 3.88$ in.

Section properties $L'/\rho$ and "A" scale are calculated as before to give $F_c$ = 53,250 psi. This is close enough.

The allowable load intensity is determined as

$P_1 = F_c A/b_s = 53{,}250\ (1.068)/5.08 = 11{,}195$ lbs./in.

Note: A is the effective skin and stringer area.

Step 6. Calculate the lateral instability stress.

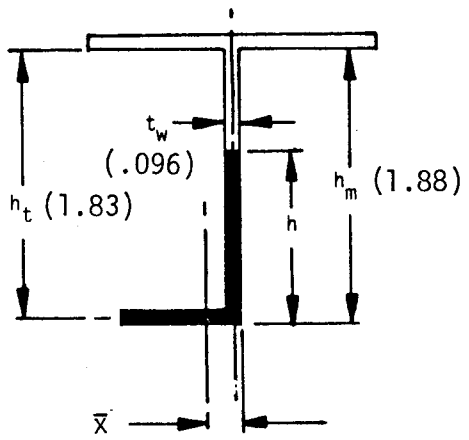


From Figure B6.5.2.3-2 for $h_m$ = 1.88, h is determined as h = 1.33.

Calculate the lateral effective stiffener properties for the shaded section as

$A = .195$ in.$^2$, $\bar{x} = .186$ in.,

$I_{yy} = .0099$ in.$^4$, $\rho_{yy} = .225$ in.

Calculate $\beta$ from Equation B6-37b

$$\beta = \frac{Et_w^3}{4\,h_t^3} = \frac{10.5 \times 10^6\,(.096)^3}{4\,(1.83)^3} = 379$$

Then calculate

$$\frac{\beta L^4}{16\,EI} = \frac{(379)(30^4)}{16\,(10.5\times10^6)(.0099)} = 184.6$$

Use this value on Figure B6.5.2.3-3 to find $L'/L = .295$ from which

$$L' = \left(\frac{L'}{L}\right) L = .295\,(30) = 8.85 \text{ and}$$

$$\frac{L'}{\rho_{yy}} = \frac{8.85}{.225} = 39.33$$

Calculate the "A" scale from Equation B6-17

$$\text{"A" scale} = \frac{\pi^2}{(L'/\rho)^2} = \frac{\pi^2}{(39.33)^2} = .00638$$

$F_c$ can then be determined from Figure B6.3.1-1 as $F_c$ = 51,000 psi.

Calculate the skin effective width

$$b_e = 1.14 + 1.9(.155)\sqrt{\frac{10.5 \times 10^6}{51{,}000}} = 5.37 \text{ in.}$$

Thus, the skin is fully effective.

The load intensity $P_1$ is computed based on the stiffener and stringer effective area (full area in this case) as
$P_1 = F_c\,A_e/b_s = 51{,}000\,(1.254)/5.08 = 12{,}589$ lbs./in.

Step 7. The panel allowable load intensity is taken as the lowest load intensity as determined in Steps 4, 5, and 6. Thus,

$P_1$ = 10,749 lbs./in. (Step 4).

B6.5.4.2 Panel Under Beam Column Loads

For the compression panel in the previous section (B6.5.4.1), determine the maximum axial load intensity which can be applied when a continuous normal load of 50 lbs./in. acts along the panel length which puts the skin in compression at the center of the panel.

The combined compression and bending stress is defined by Equation B6-21 as

$$f = f_c + f_b$$

where the maximum value for f is determined from Table B6.3.3-1 as the flange crippling stress at the supports, $F_{cc_i}$, and the column allowable stress between supports $F_c$. These values were calculated in Section B6.5.4.1, Step 4 as

$$F_{cc_i} = 55{,}610 \text{ psi (flange crippling stress)}$$

$$F_c = 43{,}544 \text{ psi (column allowable, c = 1.5)}$$

Both the center and end must be checked for beam column allowable stress based on a fixity of 2.0 for the center and 3.5 for the ends. The procedure is trial and error. Thus, assume an applied stress $f_c$ and calculate the bending stress $f_b$. Then compare the combined stress to the allowable stress. Zero margin is obtained when they are equal

The allowable beam column stress will be calculated for the center section with gross area properties as defined in Step 3, Section B6.5.4.1

$$A = 1.254 \text{ in.}^2,\ \bar{y} = .371 \text{ in.},\ I_{xx} = .455 \text{ in.}^4$$

Note: If the skin had been buckled at the assumed allowable stress, then the properties should be based on effective area at the assumed stress level, $F_c$ in step 1.

Step 1. Assume arbitrarily that $f_c$ = 40,000 psi for which tangent modulus from Figure B6.5.2.2-2 is $10.3 \times 10^6$

$$P = 40{,}000\ (1.254) = 50{,}160 \text{ lbs.}$$

Step 2. Calculate $\mu = \frac{PL^2}{E_t I} = \frac{50{,}160\ (30)^2}{10.3 \times 10^6 (.455)} = 9.63$

Enter Figure B6.5.3-1 with this value and obtain

$\frac{M}{w_o L^2} = .149$ from $M_{max}$ curve for which

$M = .149\ w_o L^2 = .149\ (50)(30)^2 = 6705$ in.-lbs.

$f_b = \frac{Mc}{I} = \frac{6705\ (.371)}{.455} = 5467$ psi

Step 3. Calculate the maximum applied stress $f_c + f_b =$ 40,000 + 5467 = 45,467 psi which is greater than the allowable stress, $F_c$ = 43,544 psi by 1923 psi.

Step 4. Repeat steps 2 and 3 with $f_c = 40{,}000 - \frac{1923}{2} =$ 39,038 psi. Tangent modulus from Figure B6.5.2.2-2 is $10.35 \times 10^6$ psi and P = 39,038 (1.254) = 48,954 lbs.

Calculate $\mu = \frac{48{,}954(30)^2}{10.35 \times 10^6 (.455)} = 9.364$

Enter Figure B6.5.3-1 with this value and obtain

$\frac{M}{w_o L^2} = .144$ from $M_{max}$ curve for which

$M = .144(50)(30)^2 = 6480$ psi

$f_b = \frac{6480(.371)}{.455} = 5284$ psi

Thus $f_c + f_b = 39{,}038 + 5284 = 44{,}322$ which is greater than the allowable stress by 778 psi. This is reasonably close so the maximum axial stress which can be applied is $F_{B.C.} = 39{,}038 - 778 = 38{,}260$ psi.

The maximum axial load intensity which can be applied is calculated as

$$P_1 = 38{,}260 \frac{1.254}{5.08} = 9444 \text{ lbs./in.}$$

The allowable beam column load intensity must also be checked at the end support.

Step 5. Assume that $f_c$ is equal to the allowable beam column stress between supports, calculated in step 4 (if it turns out greater, no further iteration is required), $f_c$ = 38,260 psi for which tangent modulus from Figure B6.5.2.2-2 is 10.37 x $10^6$ psi. The axial load at this stress is

$$P = 38{,}260\ (1.254) = 47{,}978 \text{ lbs.}$$

Step 6. Determine the bending stress with c = 3.5.

Calculate $\mu = \frac{PL^2}{E_t I} = \frac{47{,}978(30)^2}{10.37 \times 10^6 (.455)} = 9.15$

Enter Figure B6.5.3-2 with this value and obtain

$$\frac{M}{w_o L^2} = .099 \text{ from } M_1 \text{ curve for which}$$

$$M = .099\ w_o L^2 = .099(50)(30)^2 = 4455 \text{ psi and}$$

$$f_b = \frac{Mc}{I} = \frac{4455(1.774)}{.455} = 17{,}370 \text{ psi}$$

Step 7. Calculate the maximum applied stress

$$f_c + f_b = 38{,}260 + 17{,}370 = 55{,}630 \text{ psi.}$$

This stress is higher than the allowable applied stress of 55,610 psi, but close enough. No further iteration is required.

The design section is a balanced section. Thus, the margins are roughly the same at the center and the ends.

Check the beam column fixity to assure that c = 2.0 is a conservative assumption. This check is primarily to illustrate that the fixity is a variable.

Step 8. Determine the bending restraint effect due to normal load.

Calculate the Euler load for the panel from Equation B6-14 with E as the tangent modulus at the beam column allowable stress level as determined in in Step 4.

$$P_{cr} = \frac{\pi^2 EI}{L^2} = \frac{\pi^2(10.35\times10^6)(.455)}{30^2} = 51{,}643 \text{ lbs.}$$

Calculate the ratio $P/P_{cr}$ with P equal to the beam column allowable load as determined in step 4.

$$\frac{P}{P_{cr}} = \frac{38{,}260(1.254)}{51{,}643} = 0.929$$

Enter Figure B6.2.2.3-1 with this value for a simply supported 7 bay continuous beam with end bay fixity, $c_e$ = 1.0 and read off the bending restraint effect due to normal load as $\alpha\ell/EI$ = 2.0. This should provide a conservative estimate because typical wing structure usually has more than 7 continuous bays and because the end bay fixity is usually slightly greater than 1.0.

Step 9. Determine the bending restraint effect due to rotational restraint at the rib. Enter Figure B6.3.2-2 with c = 1.5 (fixity used for the column allowable, which is attributed to rotational restraint) on the curve for a column with both ends equally restrained and read off the bending restraint effect due to rotational restraint at the rib as $\alpha\ell/EI$ = 2.0. The value of c = 1.5 matches test data for typical wing structure. The effect is caused by several factors: 1) some fixity is supplied by the rib tie to the panel; 2) wing structure has contour, but allowables are based on flat panels; 3) crushing loads due to bending causes an effective fixity factor, and acts opposite to fuel pressure and airloads

Step 10. Determine the beam column fixity. Add the two restraint coefficients determined in steps 8 and 9 to obtain

$$\left(\frac{\alpha l}{EI}\right)_T = 2.0 + 2.0 = 4.0$$

Enter Figure B6.3.2-2 with this value for a column with both ends equally restrained and read off c = 2.04. Thus, the assumption c = 2.0 is conservative.

The allowable beam column stress and load intensity as determined in step 4 are

$$F_{B.C.} = 38{,}260 \text{ psi}$$

$$P_1 = 9{,}444 \text{ lbs./in.}$$

These values should be used as the allowables in the interaction Equations B6-23 or -24. If shear was also applied to the compression panel, then the maximum applied stress would have to be less than 38,260 psi.

## REFERENCES

B6-1 Timoshenko, G. P. and Gere, J. M., Theory of Elastic Stability, 2nd Edition, McGraw-Hill, New York, 1961.

B6-2 Argyris, J. H., "Flexure-Torsion Failure of Panels", Aircraft Engineering, Volume XXVI, pages 174-184 and 213-219, 1954.

B6-3 Semonian, J. W. and Peterson, J. P., "An Analysis of the Stability and Ultimate Compressive Strength of Short-Sheet-Panels with Special Reference to the Influence of Riveted Connection Between Sheet and Stringer", NACA Report 1255, 1956.

B6-4 Emero, D. H. and Spunt, L., "Optimization of Multirib and Multiweb Wing Box Structures Under Shear and Moment Loads", AIAA 6th Structures and Materials Conference, Palm Springs, California, April 1965.

B6-5 McGowan, P. R., "Notes on End-Fixity Effects for Beam Columns", McDonnell Douglas Report MDC-J1082.

B6-6 Denke, P. H. and Neuls, G. S., "Beam Column Formulae", Douglas Report SM20024, October 1945.

B6-7 Peery, D. J., Aircraft Structures, McGraw-Hill, New York, 1950.

B6-8 "Structural Principles and Data", Handbook of Aeronautics No. 1, Pitman Publishing Co., New York.

B6-9 Bruhn, E. F., Analysis and Design of Flight Vehicle Structures, Tri-State Offset Co., Ohio, 1965.

B6-10 Schofield, B. E., "A Theoretical Method to Determine Ultimate Strength of Flat Wide Sheet Longitudinally Stiffened by Thin-Walled Open Sections", McDonnell Douglas Report J0946, 1970.

# PLATE BUCKLING

TABLE OF CONTENTS

## B7.0.0 Plate Buckling

### B7.1.0 Introduction

When in-plane loads are applied to the edge of a thin flat sheet, it will buckle at some critical load depending on the ratio of loaded edge length-to-thickness (b/t) and on the degree of support at the edges.

Figure B7.1.0-1 shows the change in buckled shape for a thin flat sheet loaded in compression as the boundary conditions are changed on the unloaded edges from free to restrained.

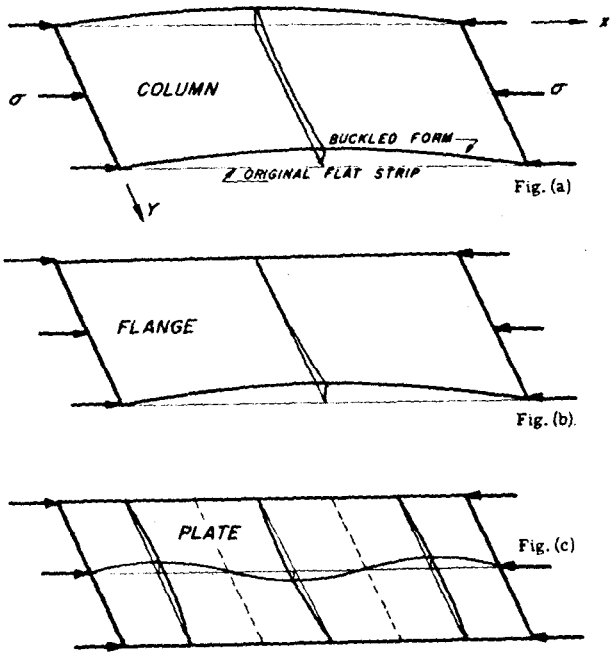


Figure B7.1.0-1 Transition from Column to Plate as Supports are Added Along Unloaded Edges

In Figure B7.1.0-1a, the sides are free and the sheet acts as a column. In Figure B7.1.0-1b, one side is restrained and the other side is free. Such a restrained sheet is referred to as a flange. In Figure B7.1.0-1c, both sides are restrained and this restrained sheet is referred to as a plate.

Design curves are provided in this section for determining the critical (initial) buckling stress for flange and plate elements. The design curves are separated into four distinct sections; Flat Plates (Section B7.2.0), Composite Shapes (Section B7.3.0), Curved Panels (Section B7.4.0), and Flat Orthotropic Plates (Section B7.5.0).

It should be emphasized that the curves in this section are for determining the initial buckling stress. After initial buckling, the straight unloaded edges of a flange or plate will still withstand loads. The strength after initial bucking is referred to as the crippling strength. This topic is discussed under Column Buckling, Section B6.5.0.

Restraint along the unloaded flange and plate element edges can vary from a simple support condition to a clamped support condition. The degree of restraint between these conditions is referred to by a rotational restraint coefficient, $\epsilon$, which is defined as

$$\epsilon = \frac{4S_v b}{\eta D} \qquad \text{(B7-1)}$$

where

$S_v$ = the stiffness per unit length of elastic restraining medium or moment required to rotate a unit length of elastic medium through one-fourth radian.

$D$ = the flexural rigidity of the flange or plate per unit length,

$$\frac{Et^3}{12\,(1-\mu^2)}$$

$\eta$ = a plasticity reduction factor, to allow for decrease in D above the material proportional limit.

In as much as $S_v$ is difficult to determine, this section will look primarily at the following idealized cases of edge restraint.

A. Clamped or Fixed Edges (C) Edges where the plate cannot deflect or rotate.

B. Simply Supported Edges (SS) Edges where the plate cannot deflect, but can freely rotate.

C. Free Edges (F) Edges that are entirely free to deflect and rotate. Thus, no restraint.

The derivation of equations and design charts used in this section are provided in References B7-1 thru B7-3. The assumptions made in the derivations are:

A. The plate is flat and of uniform thickness.

B. The thickness is not more than one-quarter of the least lateral dimension.

C. The maximum deflection is not more than one-half the thickness.

D. Material is perfectly elastic; i.e., within the elastic limit.

E. Material is homogenous. Exhibits the same physical properties throughout (except Section B7.5.0).

F. Material is isotropic. The elastic properties are the same in all directions (except Section B7.5.0).

B7.1.1 Symbols

| | |
|---|---|
| $a$ | Long dimension of a plate, in. |
| $b$ | Short dimension or loaded edge of a plate, in. |
| $E$ | Modulus of Elasticity, Young's Modulus of the plate material in compression, psi |
| $E_s$ | Secant Modulus, psi |
| $E_t$ | Tangent modulus, psi |
| $f$ | Percentage thickness of base material less clad to total plate thickness |
| $F_{cr}$ | Critical buckling stress, psi |
| $F_{cy}$ | Allowable compressive yield stress, psi |
| $F_{s_{cr}}$ | Critical shear buckling stress, psi |
| $G$ | Shear modulus, psi |
| $G_s$ | Secant shear modulus, psi |

$k_b$ Bending buckling coefficient

$k_c$ Compressive buckling coefficient

$k_s$ Shear buckling coefficient

$k_y$ External pressure buckling coefficient

R Ratio of applied stress to allowable stress (subscripts denote compression [c], shear [s], bending [b], and external pressure [p])

t Thickness of the plate, in.

$\epsilon$ Rotational restraint coefficient

$\eta$ Plasticity correction factor (subscript p is compression; s is shear)

$\overline{\eta}$ Cladding reduction factor

$\mu$ Poisson's Ratio, within the elastic range

## B7.2.0 Buckling of Flat Plates Under Various Loads

### B7.2.1 Compression Loads

The initial buckling stress for a flat plate under compression loads is

$$F_{cr} = \frac{\pi^2 \eta_p k_c E}{12\,(1-\mu^2)}\left(\frac{t}{b}\right)^2 \qquad \text{(B7-2)}$$

where $k_c$ is the compression buckling coefficient that depends on the degree of support of the edges and $\eta_p$ is a plasticity factor $(E_t/E)^{1/2}$ for stresses above the material proportional limit.

Figures B7.2.1-1 through B7.2.1-4 give values of $k_c$ for flat plate and flange elements, having various degrees of unloaded edge restraint, as a function of the element aspect ratio (a/b). The first three figures are for constant compressive load. Figure B7.2.1-4 is for linearly varying compressive load. Figure B7.2.1-5 gives the value for $k_c$ as a function of b/t for a long rectangular plate element when the edges are restrained by stiffeners which are torsionally weak (Z) and torsionally strong (hat). Generally for design, b/t ratios for typical skin stiffened compression panels range from 20 to 150 and the stiffeners are torsionally weak. Thus, the buckling coefficient for determining initial skin buckling may vary from a simply supported condition (4.0) to a clamped condition (6.96).

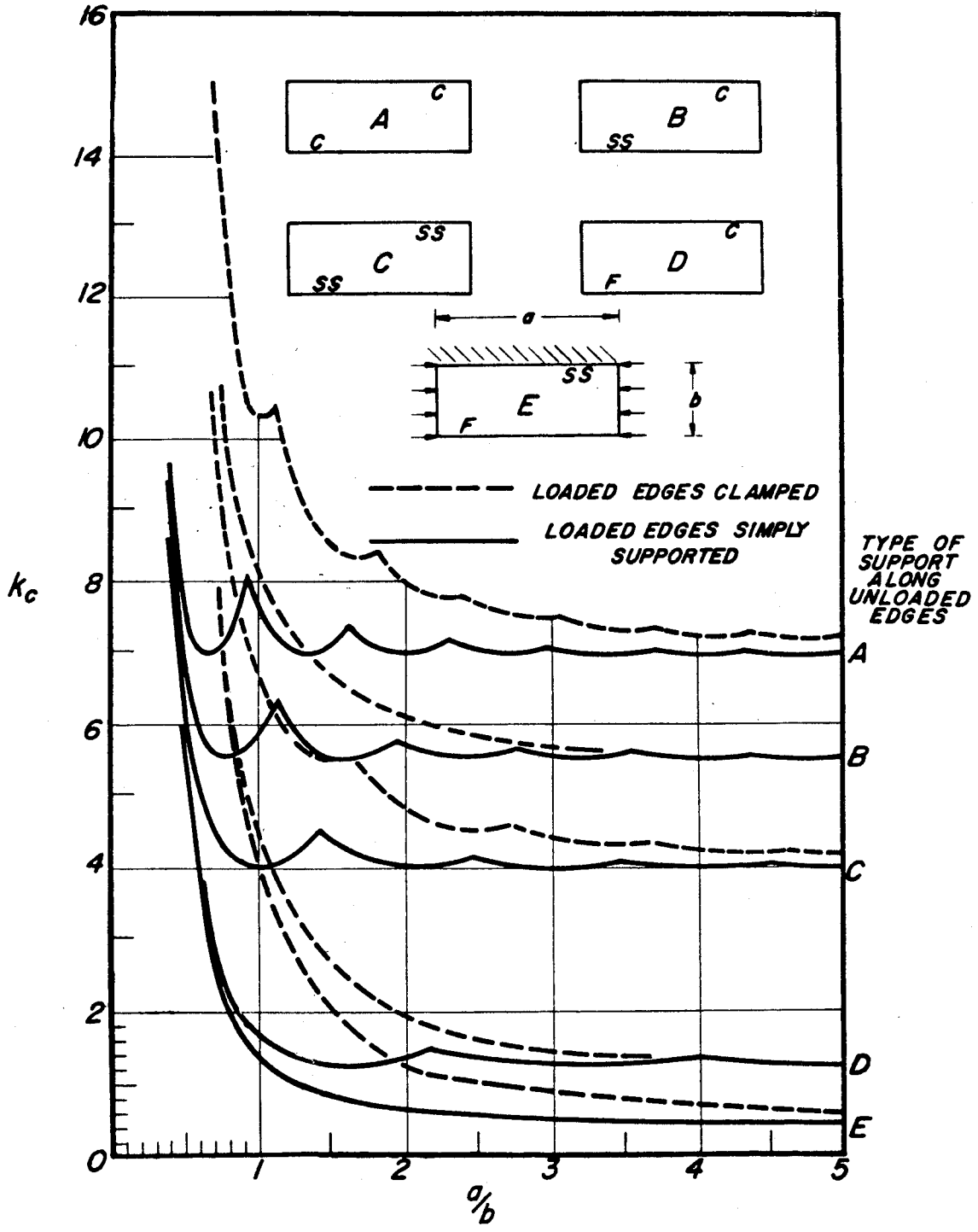


Figure B7.2.1-1 Compressive-Buckling Coefficients for Flat Rectangular Plates (Ref B7-3)

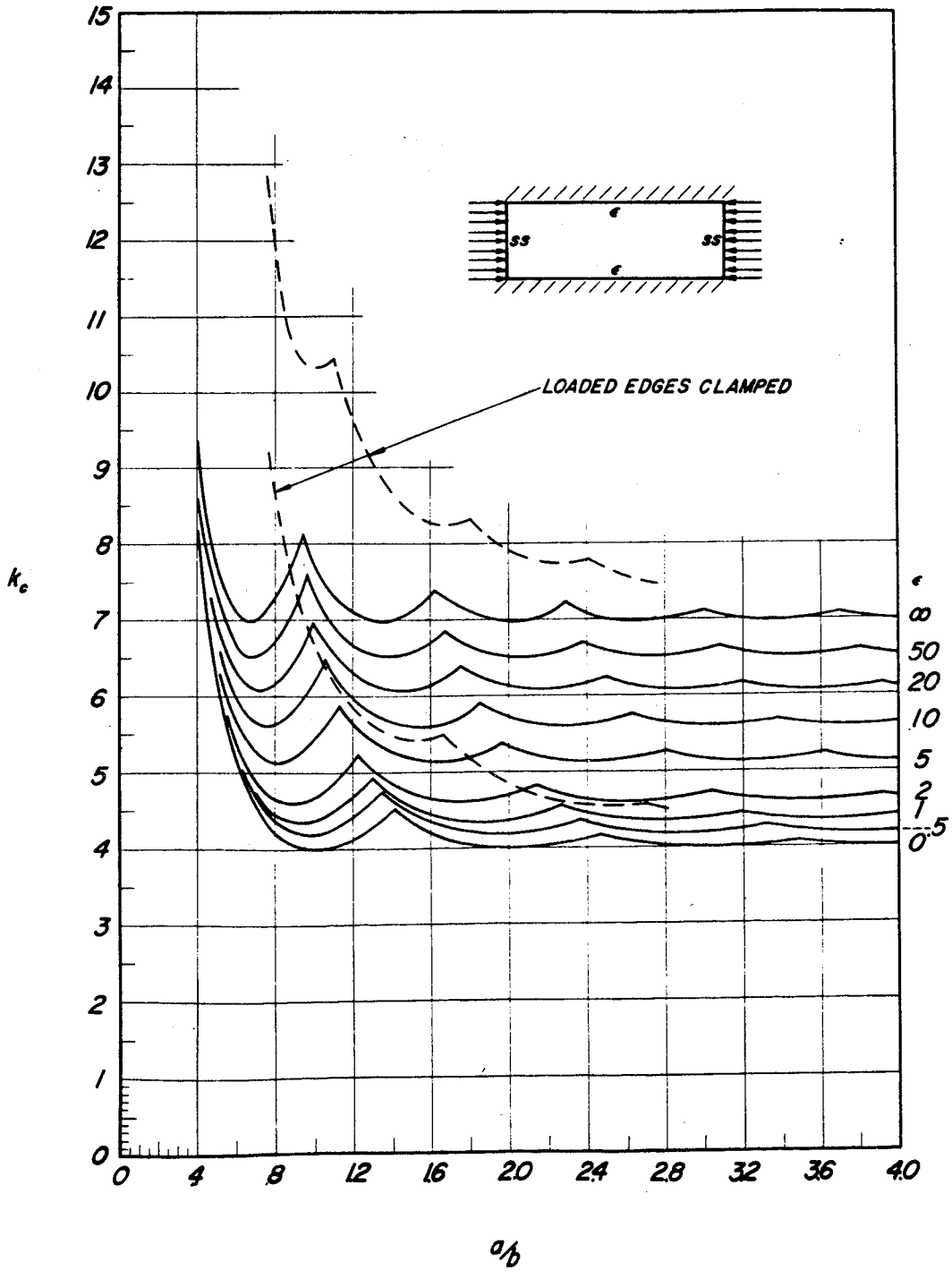


Figure B7.2.1-2 Compressive-Buckling Stress Coefficient of Plates as a Function of a/b for Various Amounts of Edge Rotational Restraint (Ref B7-3)

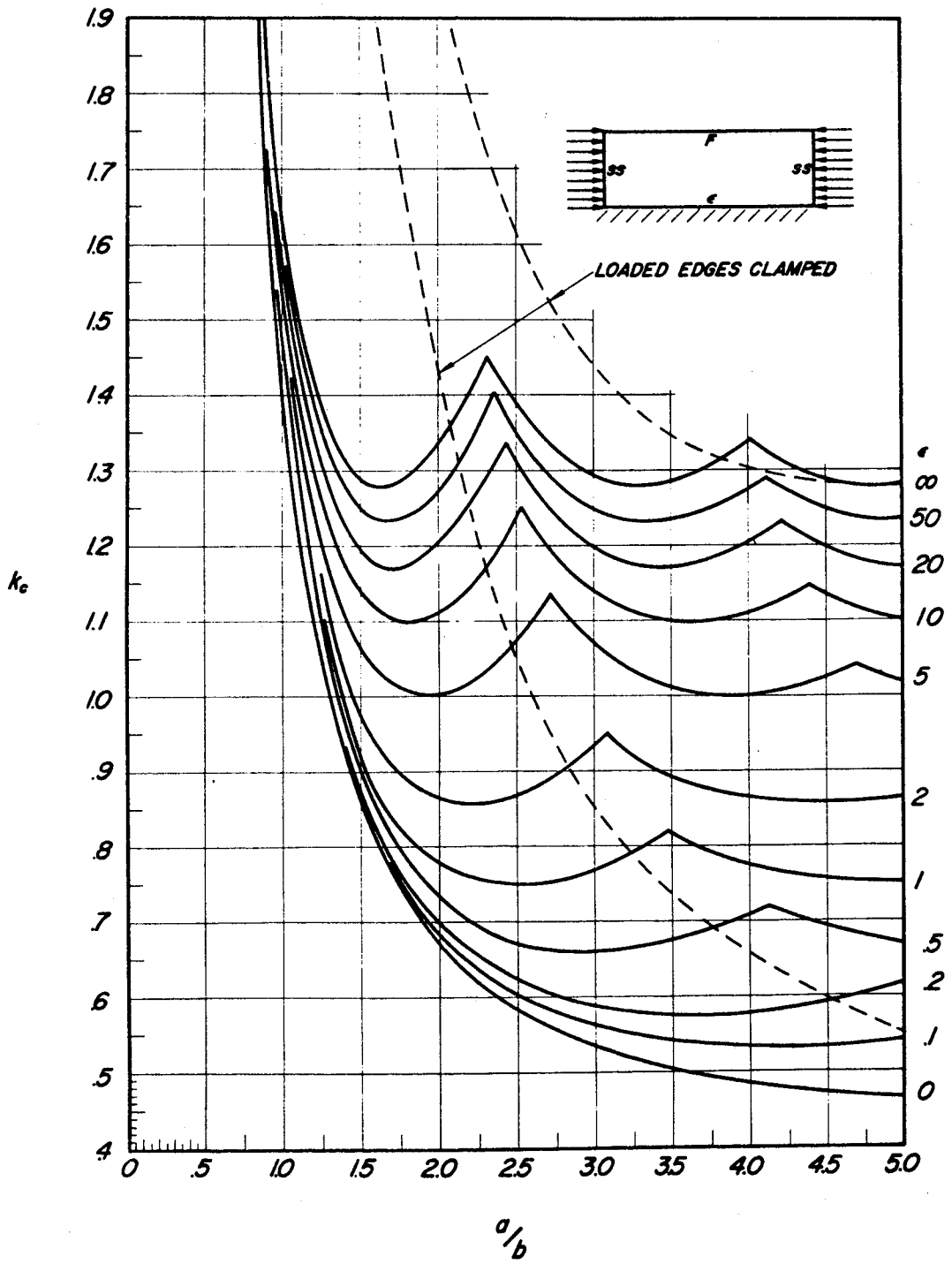


Figure B7.2.1-3 Compressive-Buckling Stress Coefficient of Flanges as a Function of a/b for Various Amounts of Edge Rotational Restraint (Ref B7-3)

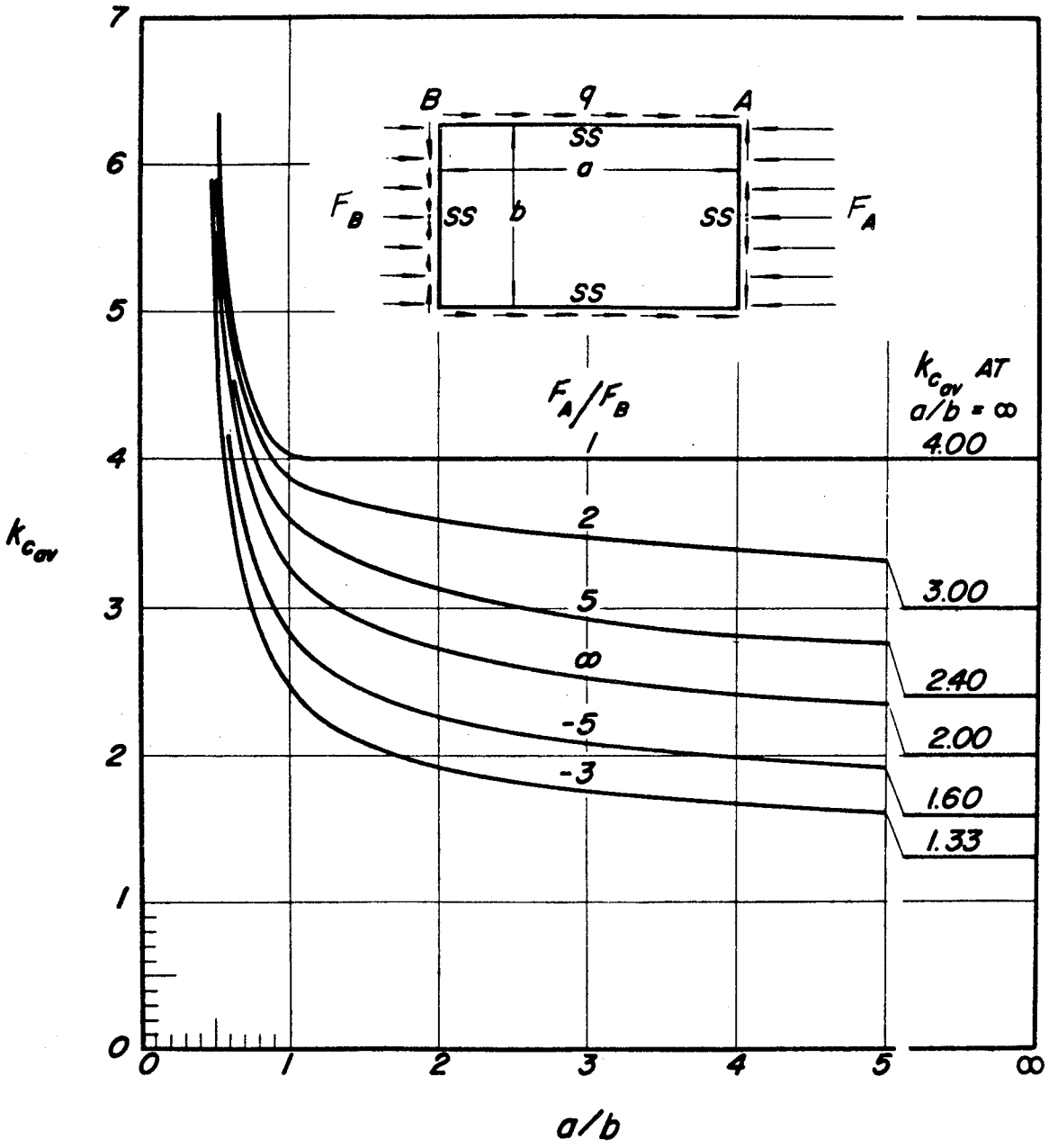


Figure B7.2.1-4 Average Compressive-Buckling Stress Coefficient for Rectangular Flat Plate of Constant Thickness with Linearly Varying Axial Loads (Ref B7-3)

$$F_{av} = \frac{k_{c_{av}} \pi^2 E}{12(1-\mu^2)} \left(\frac{t}{b}\right)^2$$

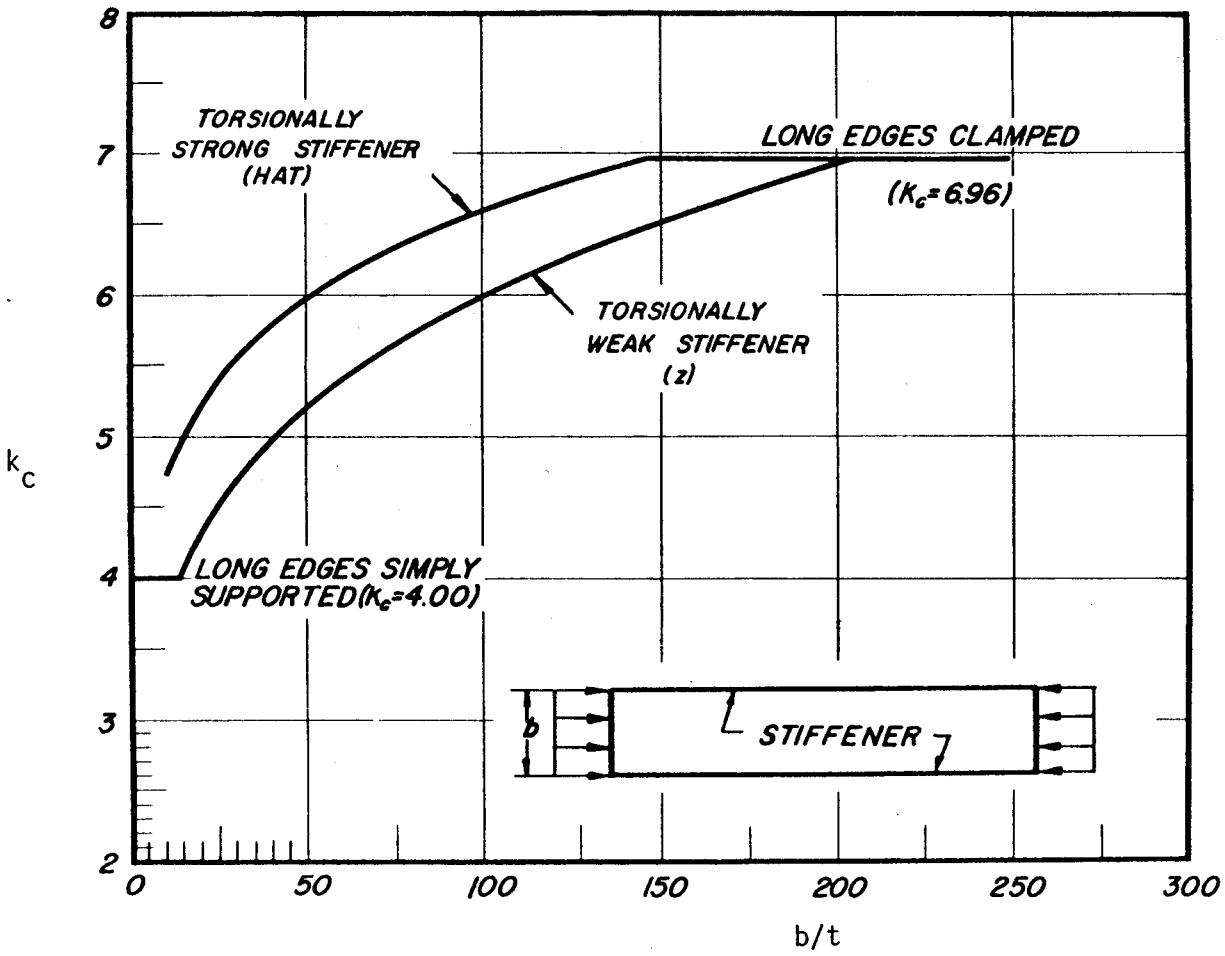


Figure B7.2.1-5 Compressive-Buckling Coefficient for Long Rectangular Stiffened Panels as a Function of b/t and Stiffener Tortional Rigidity (Ref B7-3)

When determining the initial buckling stress for plate elements, it is sometimes necessary to correct stresses for plastic and cladding effects.

A. Plastic Buckling of Flat Plates If the buckling or instability occurs at a stress which is above the material proportional limit, then E and $\mu$ are not constant (or the same) as they were in the elastic range. A plasticity correction factor is required in Equation B7-2 which is defined as

$$\eta_p = (E_t/E)^{1/2} \qquad \text{(B7-3)}$$

A tremendous amount of theoretical and empirical work has been done to obtain values of the plasticity correction factors. They vary, as shown in Table B7.2.1-1, depending on the unloaded edge boundary conditions. Figure B7.2.1-6 is a plot of these plasticity factors as a function of compressive stress. For plate elements, the test data scatters between curves A and D. Equation B7-3 is also shown on this figure. It represents a conservative correction factor which can be used for any plate boundary condition.

A simple method for obtaining stresses above the proportional limit is to plot $F_{cr}$ versus $F_{cr}/\eta_p$. Then, from Equation B7-2, calculate $F_{cr}/\eta_p$ based on elastic properties and plate geometry and read $F_{cr}$ from the plotted curve. Figures B7.2.1-7 through B7.2.1-9 are plotted for the more common materials used in design. If design curves are not available, use the method described in Section B5.1.2.3 and B5.1.3.3C to construct them. Also, ignore the variation of $\mu$ above the proportional limit because Equation B7-3 is already conservative.

B. Effects of Cladding on the Critical Buckling Stress

When clad aluminum alloy is used, further corrections must be made to the critical buckling stress, Equation B2-2. Historically, this has been done with a clad reduction factor $\eta$. A more simple and conservative approach for design is to use bare material properties and reduce the total material thickness by the thickness of the cladding material. Thus, in Equation B2-2 substitute (ft) for t where f is the ratio of base material thickness less clad material to total material thickness. Table B7.2.1-2 gives f for some typical clad aluminum alloys.

Table B7.2.1-1 Inelastic Factors for Plate Buckling (Ref. B7-5)

| Structure (type of buckling | Elastic Factor, $\eta = E_t/E$ | See Curve Figure B7.2.1-6 |
|---|---|---|
| Long flange, one unloaded edge simply supported | $\frac{E_{sec}}{E}$ | A |
| Long flange, one unloaded edge clamped | $\frac{E_{sec}}{E}\left[0.330 + 0.670\left(\frac{1}{4} + \frac{3}{4}\frac{E_{tan}}{E_{sec}}\right)^{1/2}\right]$ | B |
| Long plates, both unloaded edges simply supported | $\frac{E_{sec}}{E}\left[\frac{1}{2} + \frac{1}{2}\left(\frac{1}{4} + \frac{3}{4}\frac{E_{tan}}{E_{sec}}\right)^{1/2}\right]$ | C |
| Long plate, both unloaded edges clamped | $\frac{E_{sec}}{E}\left[0.352 + 0.648\left(\frac{1}{4} + \frac{3}{4}\frac{E_{tan}}{E_{sec}}\right)^{1/2}\right]$ | D |
| Short plate loaded as a column, L/b < 1 | $\frac{1}{4}\frac{E_{sec}}{E} + \frac{3}{4}\frac{E_{tan}}{E}$ | E |
| Square plate loaded as a column, L/b = 1 | $0.114\frac{E_{sec}}{E} + 0.886\frac{E_{tan}}{E}$ | F |
| Long column, L/b > 1 | $\frac{E_{tan}}{E}$ | G |

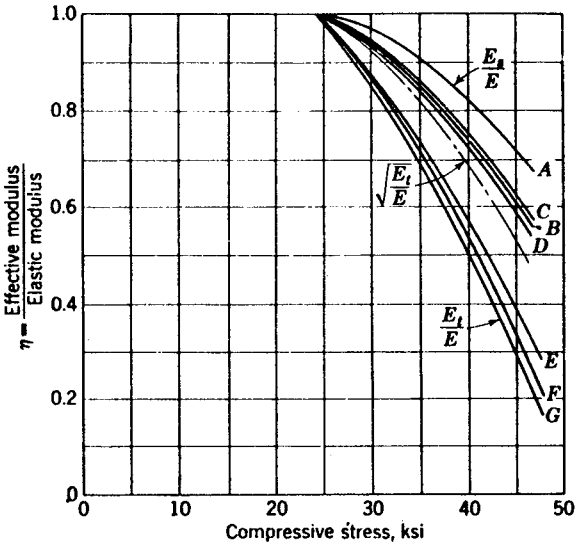


Figure B7.2.1-6 Typical Variation of Inelastic Factors η with Stress (Aluminum Alloy 2024-T3) (Ref B7-5)

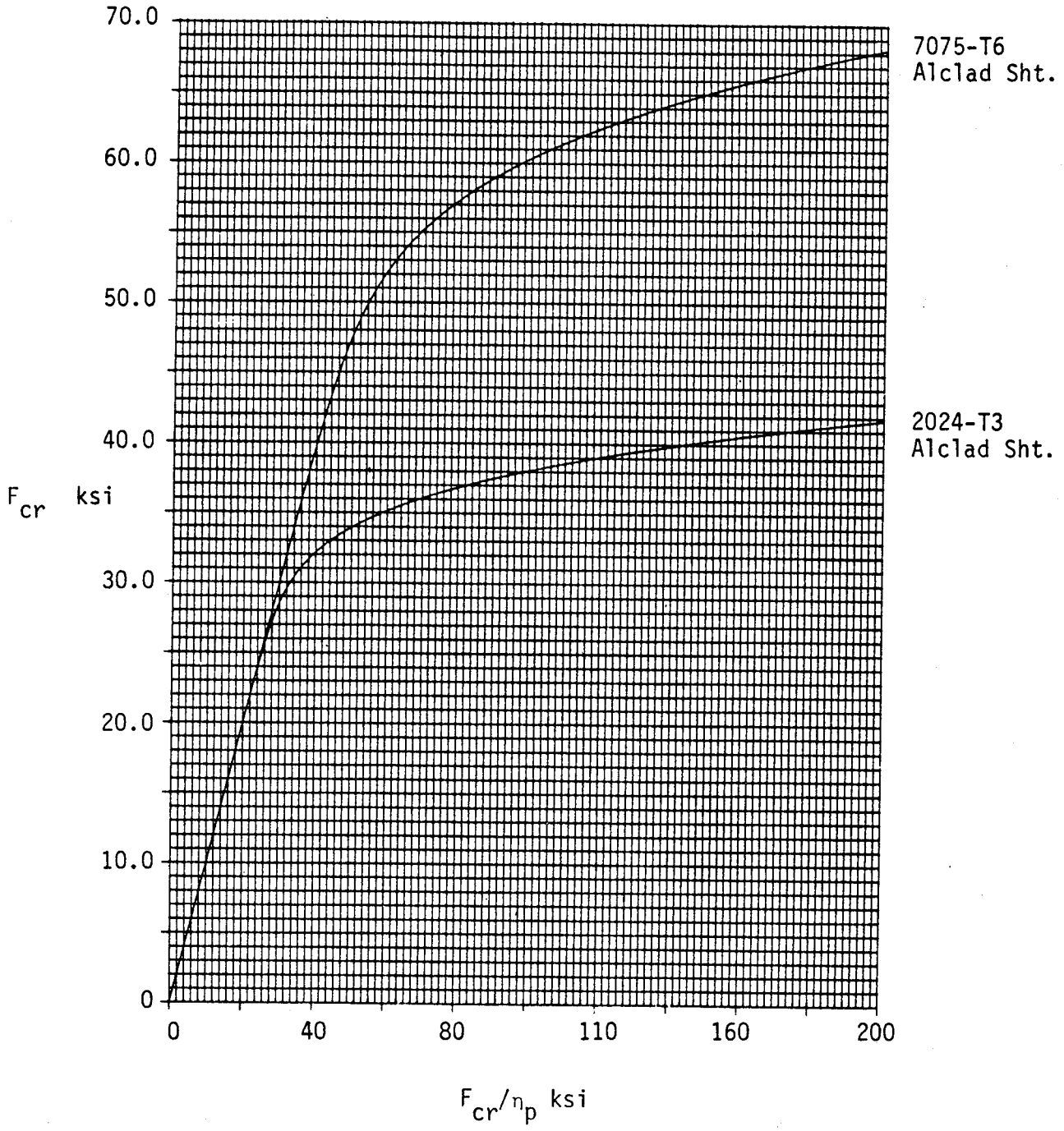


Figure B7.2.1-7 Plasticity Correction Curves for Buckling of Alclad Aluminum Sheet

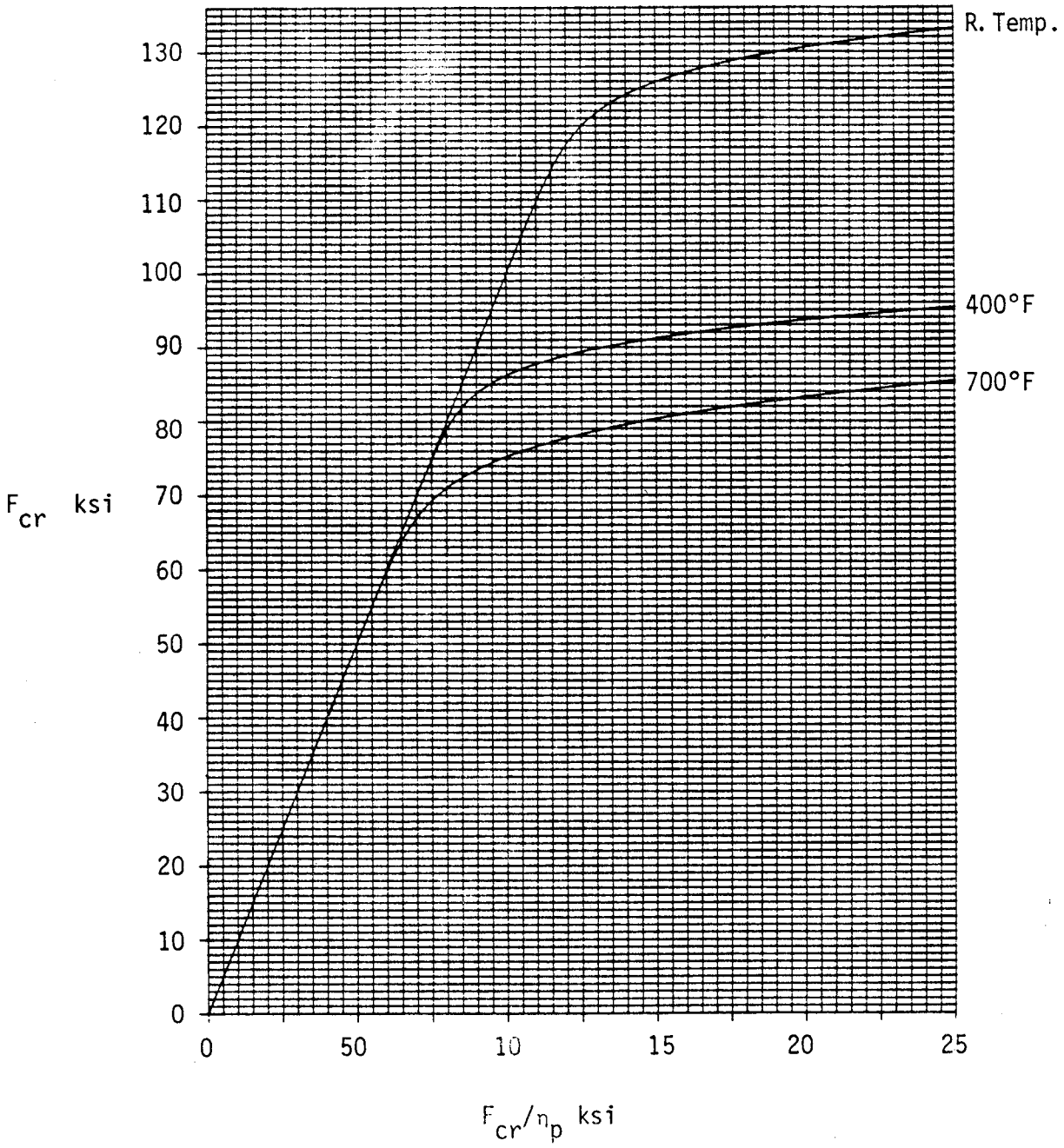


Figure B7.2.1.-8 Plasticity Correction Curves for Buckling of 6Al-4V Titanium Sheet at Selected Temperatures

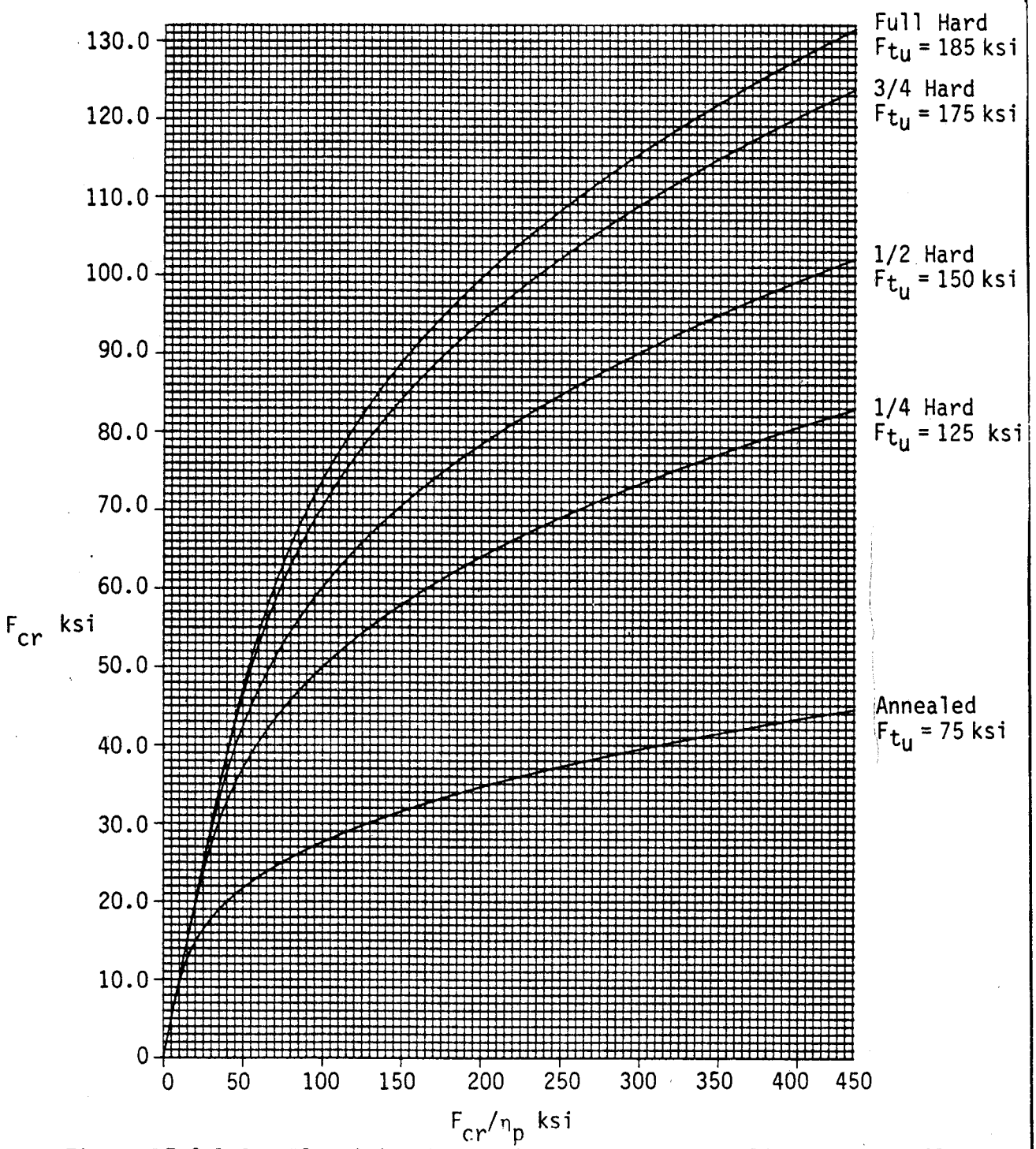


Figure B7.2.1-9 Plasticity Correction Curves for Buckling of AISI 301 Stainless Steel Sheet

Table B7.2.1-1 Cladding Reduction Factors (Ref. B7-3)

| Material Designation | Cladding Material | Total Plate Thickness, in. | Reduction Factor for Clad Material f |
|---|---|---|---|
| Alclad 2014 | 6053 | <0.040 | 0.80 |
| | | >0.040 | 0.90 |
| Alclad 2024 | 1230 | <0.064 | 0.90 |
| | | >0.064 | 0.95 |
| Alclad 7075 | 7072 | All Thickness | 0.92 |

B7.2.2 Shear Loads

The initial buckling stress for a flat plate under shear loading is

$$F_{s_{cr}} = \frac{\pi^2 \eta_s k_s E}{12\,(1-\mu^2)} \left(\frac{t}{b}\right)^2 \qquad \text{(B7-3)}$$

where $k_s$ is the shear buckling coefficient that depends on the degree of support along the edges and $\eta_s$ is a plasticity factor $(G_t/G)^{1/2}$ for stresses above the material proportional limit.

Figure B7.2.2-1 gives the shear buckling coefficient for flat plate elements, having simply supported and clamped edge restraints, as a function of the element aspect ratio (a/b).

Figures B7.2.2-2 through B7.2.2-4 should be used to correct for stresses above the material proportional limit. To construct curves not given here, use the method described in Section B5.1.2.3.

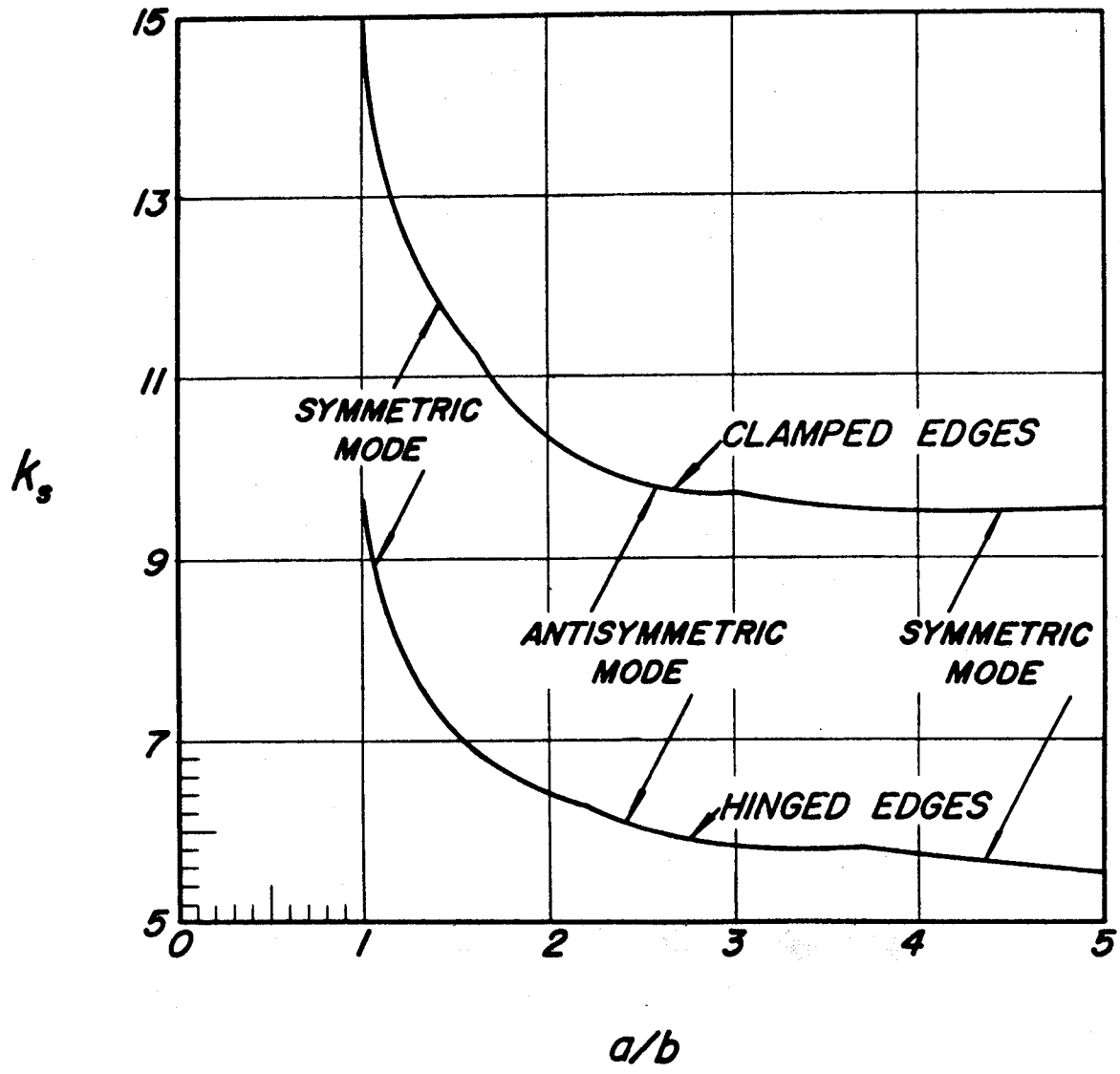


Figure B7.2.2-1 Shear-Buckling Stress Coefficient of Plates as a Function of a/b for Clamped and Hinged Edges (Ref B7-3)

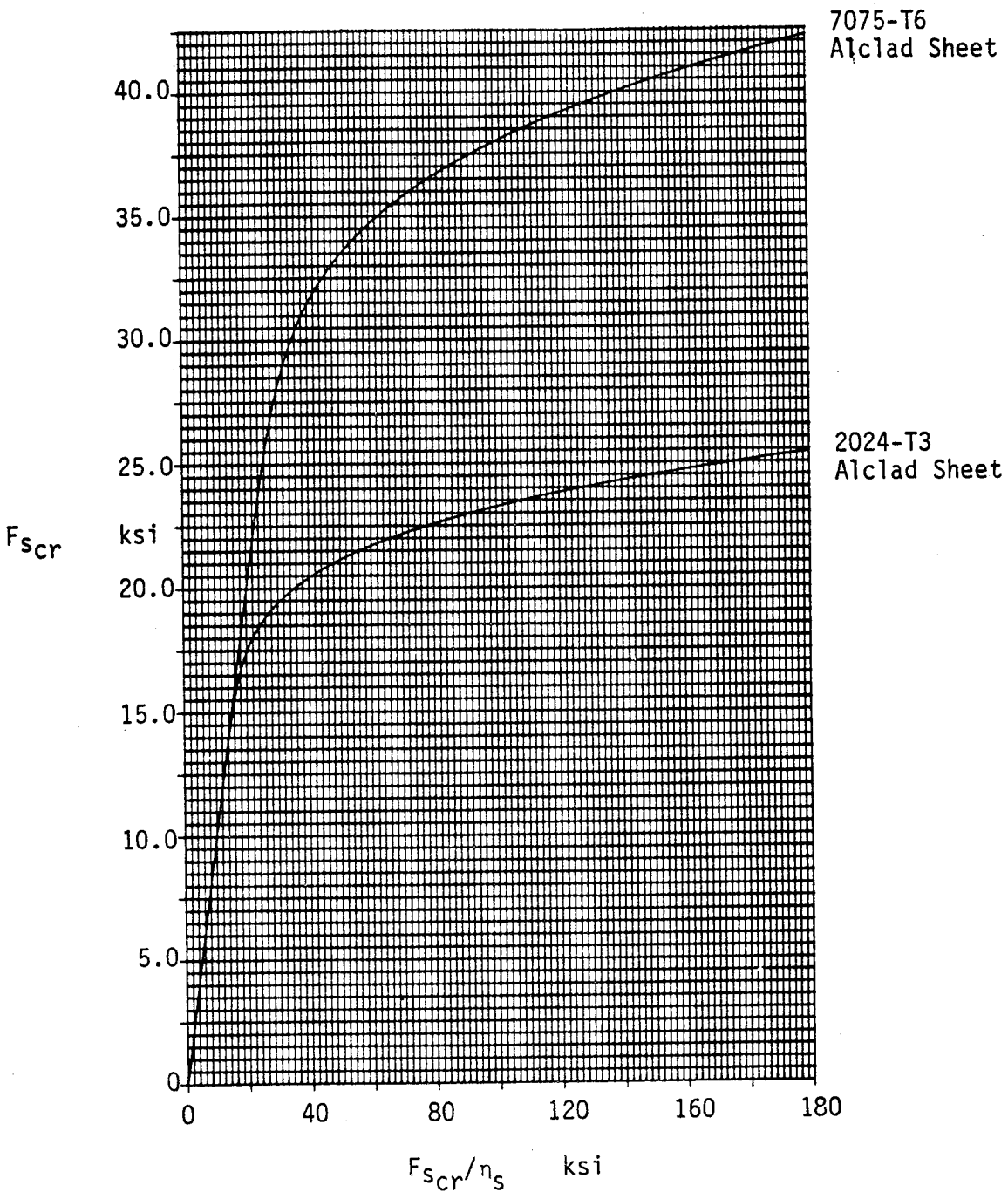


Figure B7.2.2-2 Plasticity Correction Curves for Shear Buckling of Alclad Aluminum Sheet

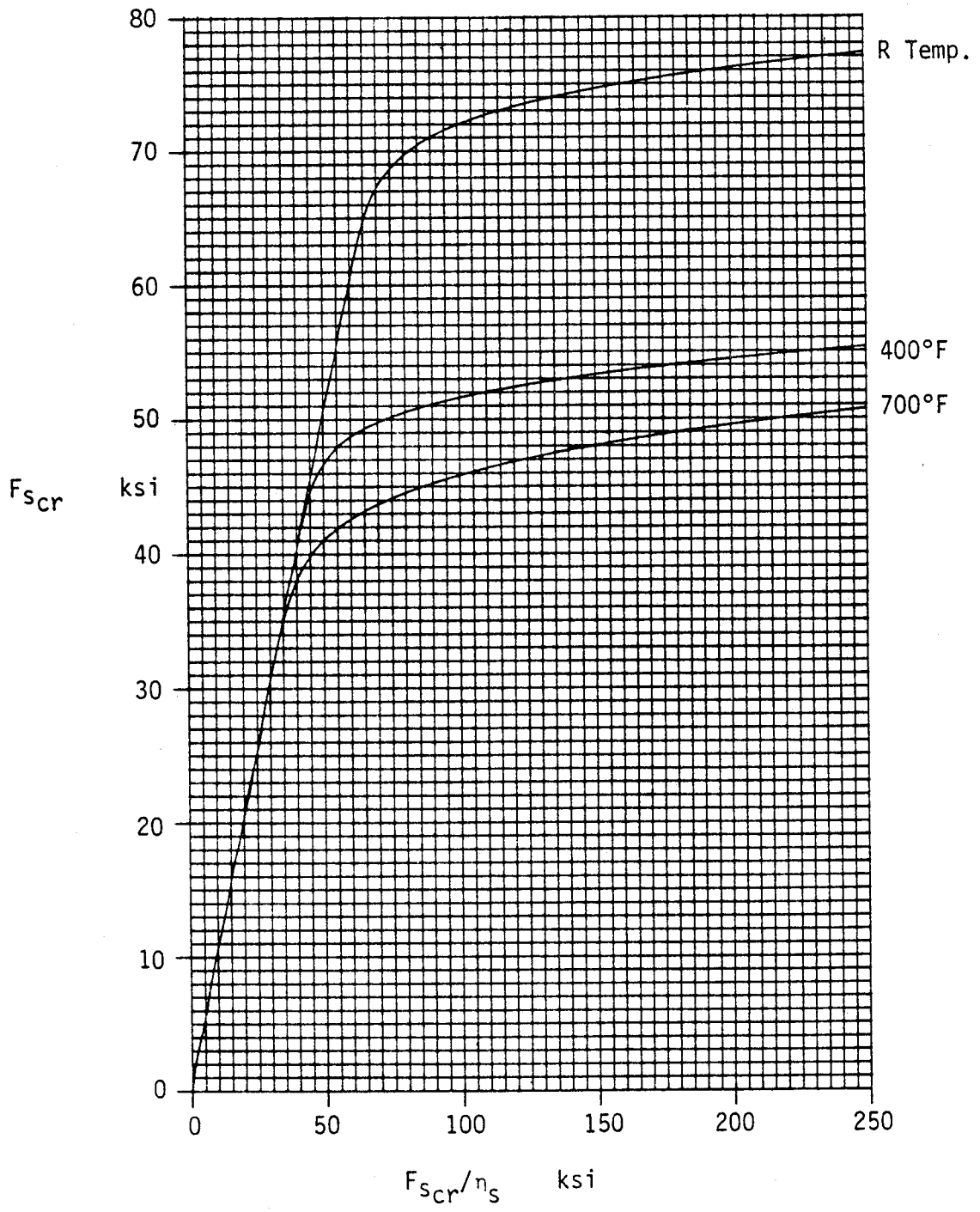


Figure B7.2.2-3 Plasticity Correction Curves for Shear Buckling of 6Al-4V Titanium Sheet at Selected Temperatures

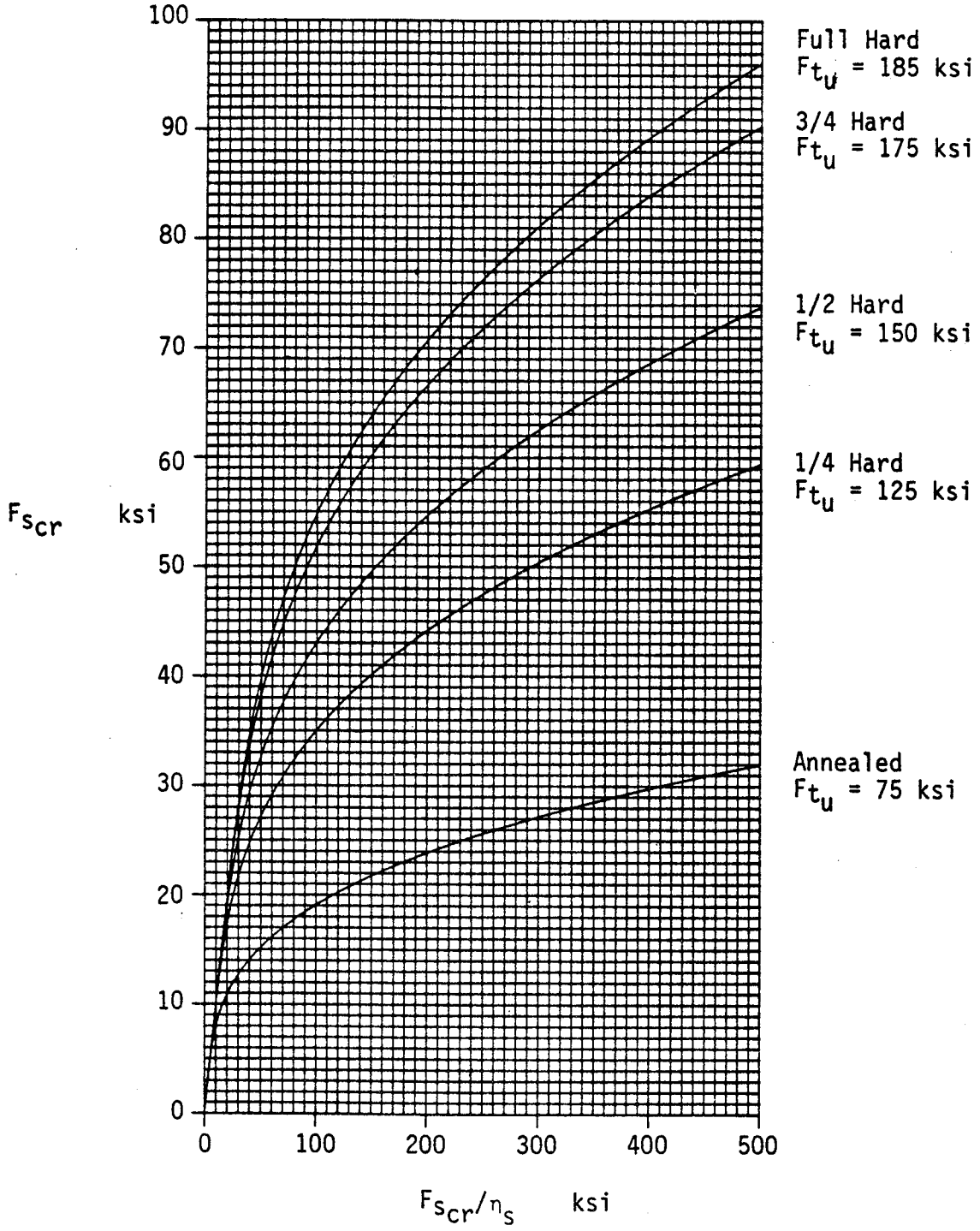


Figure B7.2.2-4 Plasticity Correction Curves for Shear Buckling of AISI 301 Stainless Steel Sheet

B7.2.3 Bending Loads (In-Plane)

The initial buckling stress for flat plate elements under 'in-plane' bending loads is

$$F_{cr} = \frac{\pi^2 k_b \eta_p E}{12\,(1-\mu^2)} \left(\frac{t}{b}\right)^2 \qquad \text{(B7-4a)}$$

where $k_b$ is the bending buckling coefficient that depends on the degree of support along the edges and $\eta_p$ is the same plasticity factor as used for plates under compression loads.

Figure B7.2.3-2 gives values of $k_b$ for a flat plate supported on its edges with varying degrees of rotational restraint as a function of plate aspect ratio (a/b).

When axial loads are applied to the plate in addition to 'in-plane' bending loads, the neutral axis is not coincidental with the centroidal axis as shown in Figure B7.2.3-1. Thus, c is not equal to $\bar{y}$.

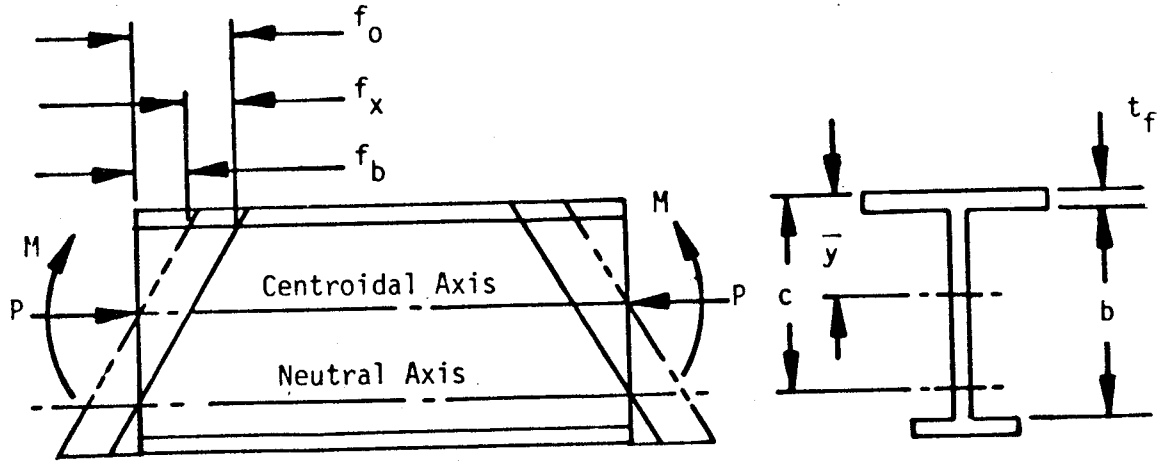


Figure B7.2.3-1 Combined Loading on a Plate Element (Bending and Axial Compression)

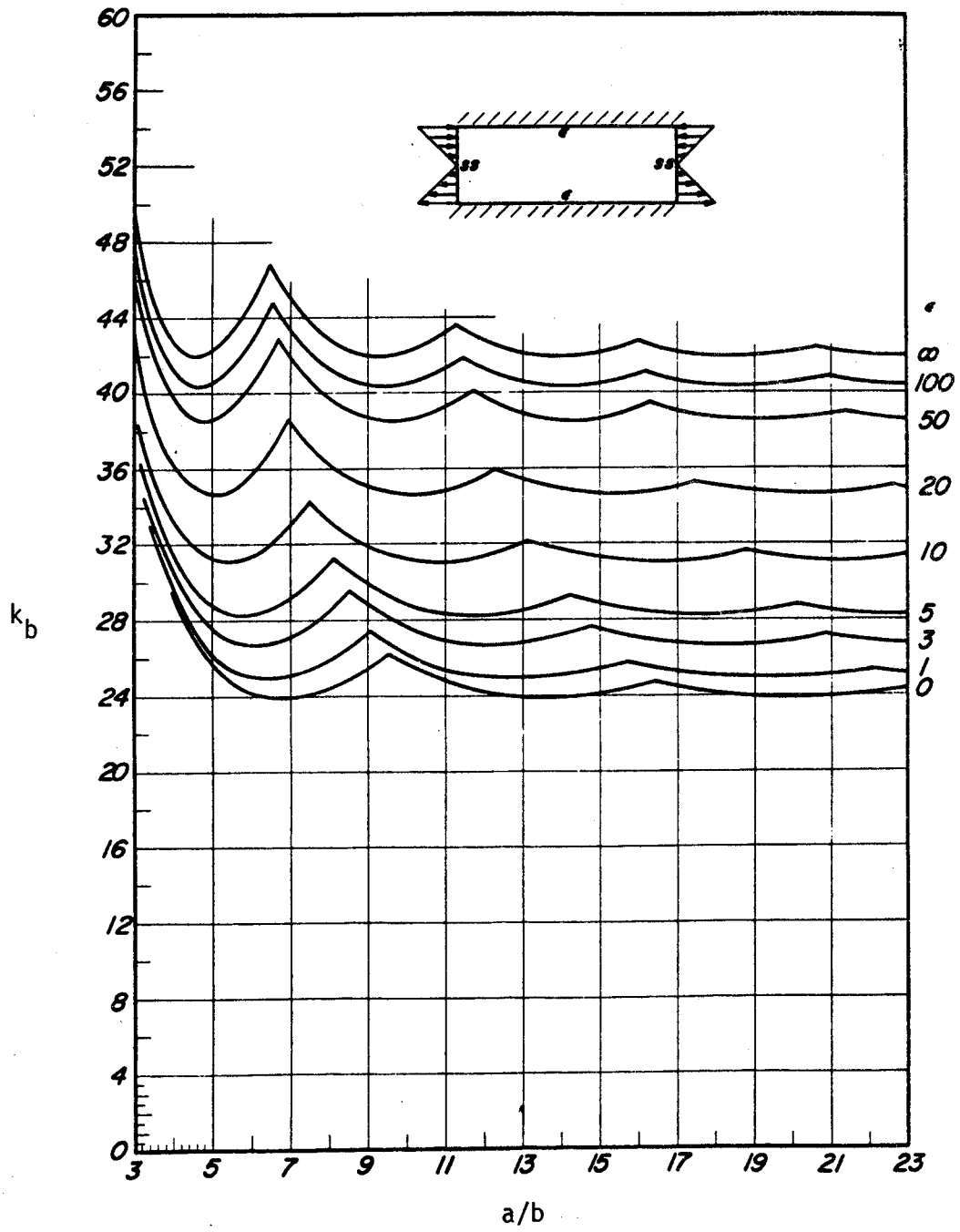


Figure B7.2.3-2 Bending-Buckling Coefficients of Plates as a Function of a/b for Various Amounts of Edge Rotational Restraint (Ref B7-3)

The buckling coefficient for plates loaded in this manner is dependent on the distance from the edge of the plate loaded in compression to the neutral axis (zero stress axis) which is defined as

$$c = \left(1 + \frac{f_x}{f_b}\right)\left(\bar{y}-t_f\right) \qquad \text{(B7-4b)}$$

where

$f_x$ = applied axial stress, P/A, psi

$f_b$ = maximum applied bending stress along the compressed edge of the plate, M $(\bar{y}-t_f)/I$, psi

Figures B7.2.3-3 through B7.2.3-8 give the buckling coefficients ($k_b$) for plates loaded in bending and axial compression as a function of the ratio between c and the plate width b defined as

$$\beta = \frac{b}{c} \qquad \text{(B7-4c)}$$

If the stresses are above the material proportional limit, use the correction curves, Figures B7.2.1-7 through B7.2.1-9 or construct curves as described in Section B7.2.1.

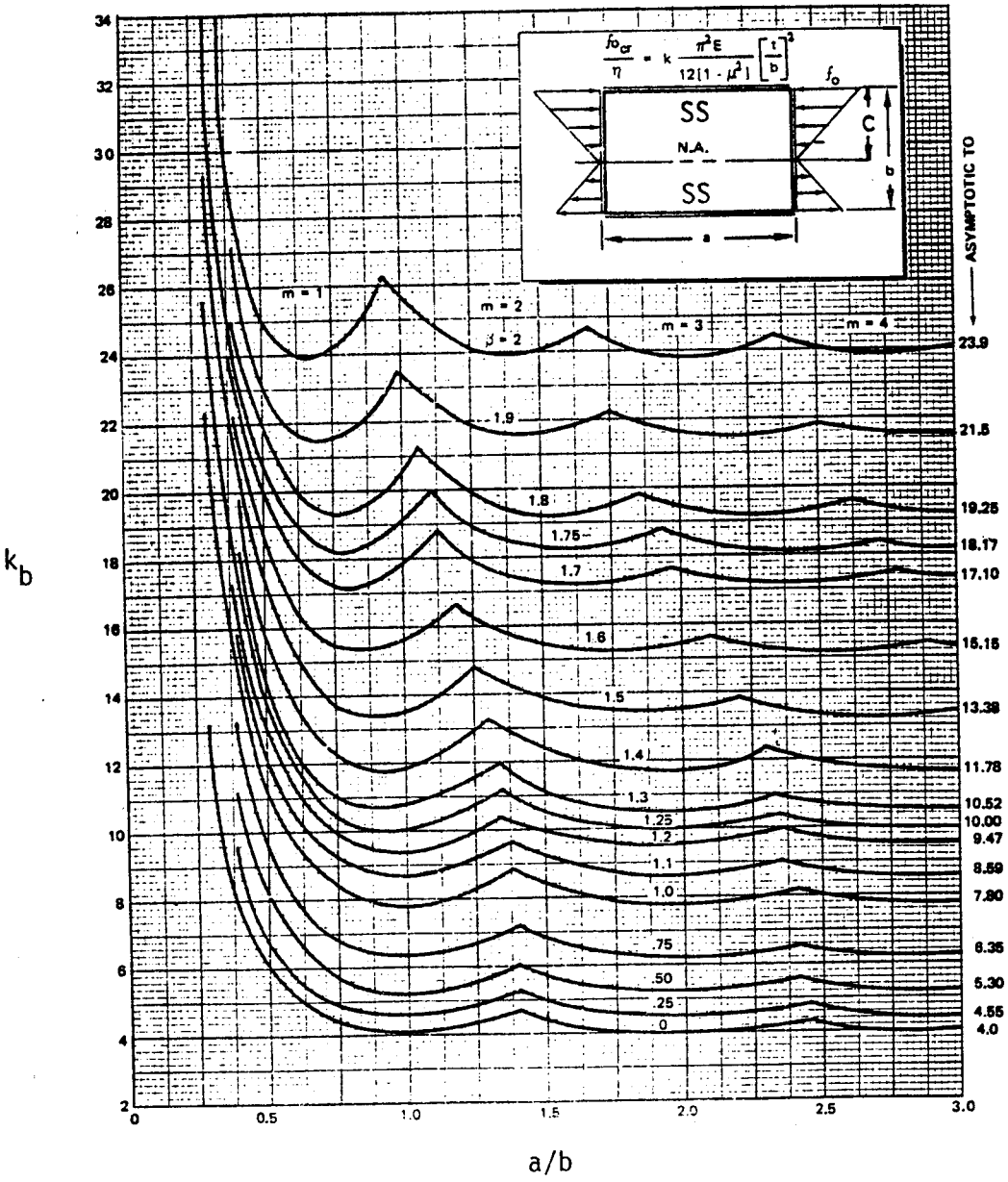


Figure B7.2.3.-3 Buckling Coefficients for a Flat Plate in Bending in the Plane of the Plate, all Edges are Simply-Supported (Ref B7-4)

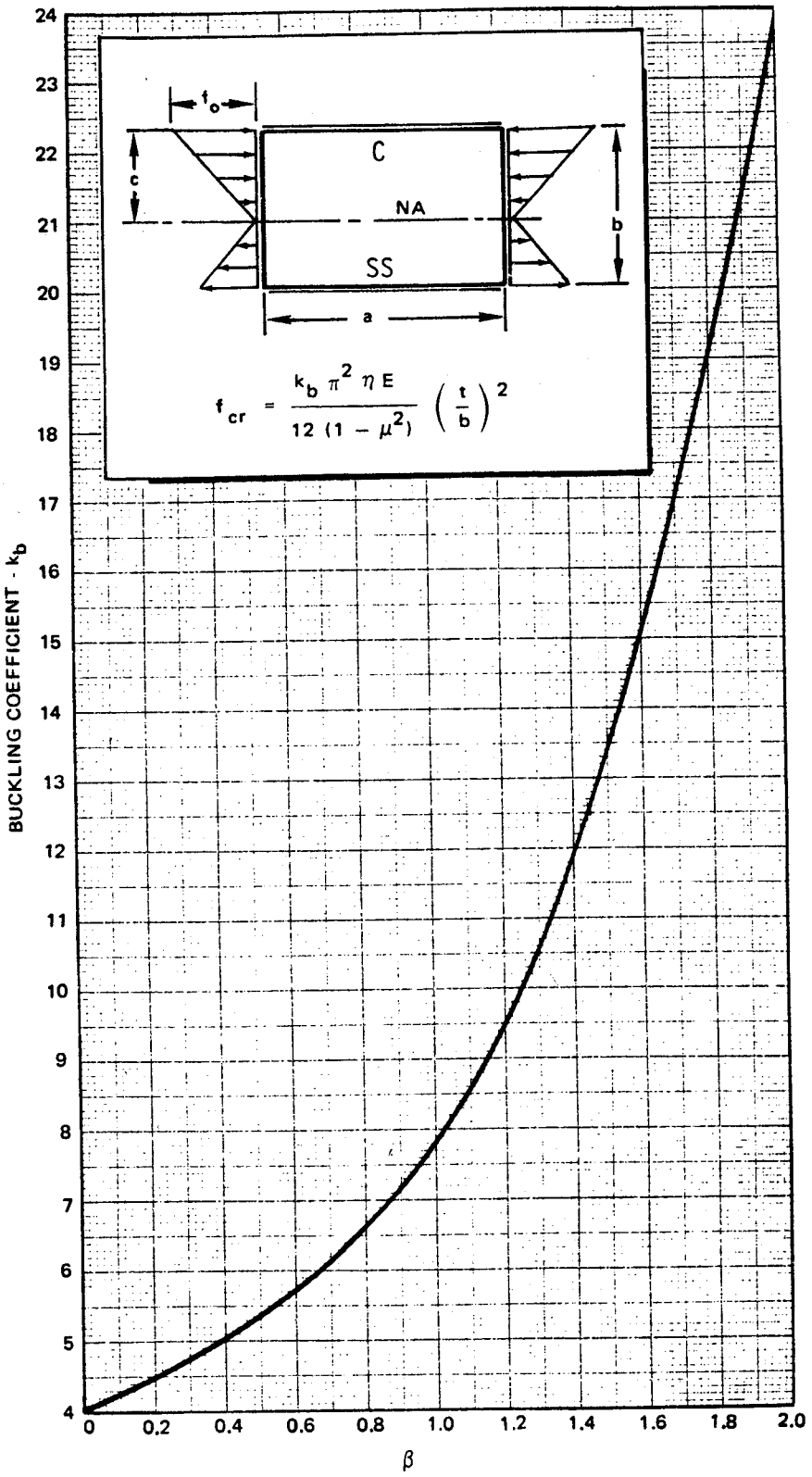


Figure B7.2.3-4 Buckling Coefficients for Bending in Plane of the Plate $a/b \geq 4.0$. Both Sides Simply-Supported (Ref B7-4)

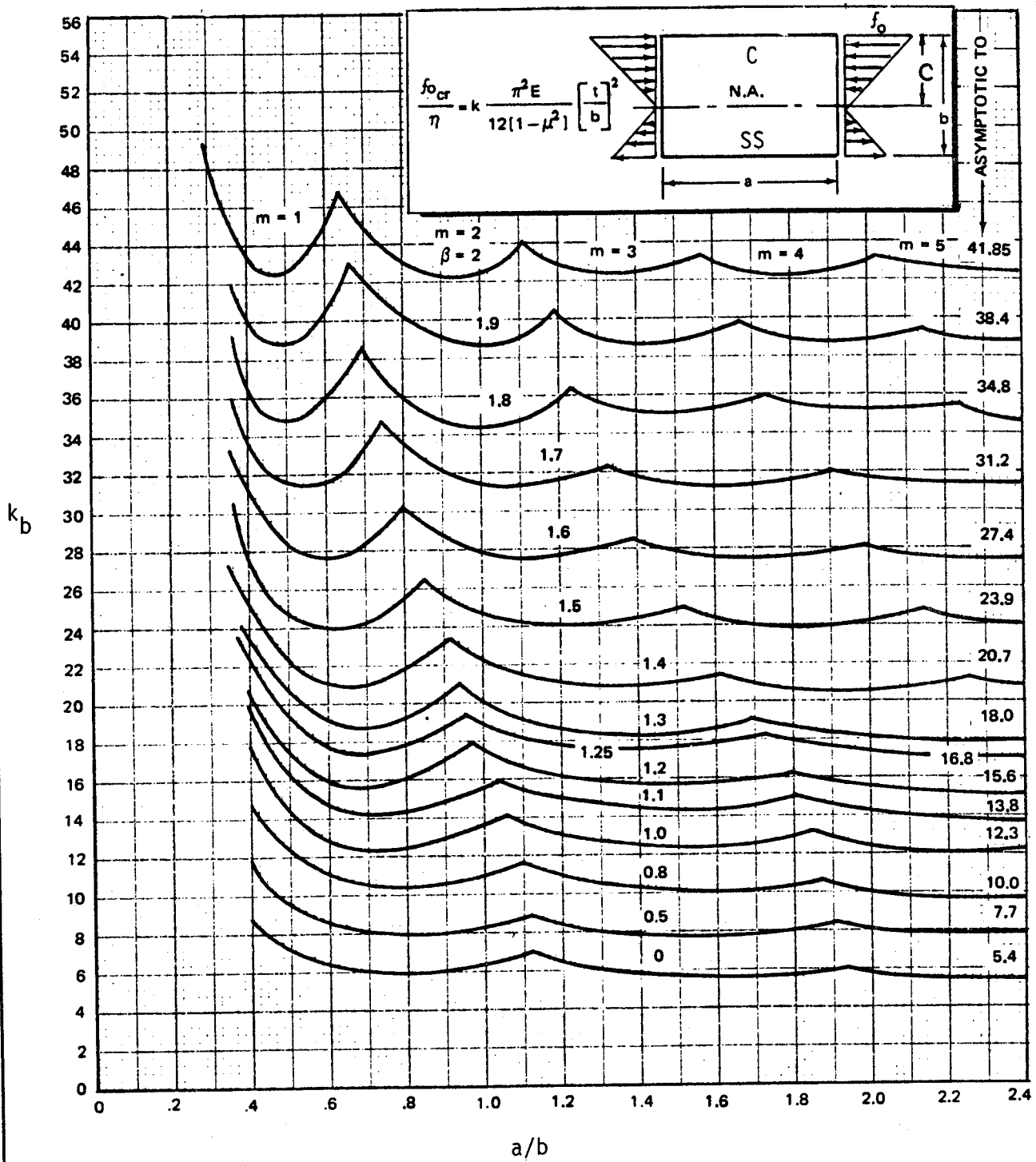


Figure B7.2.3-5 Buckling Coefficients for a Plate in Bending in the Plane of the Plate--Tension Side Simply-Supported and Compression Side Fixed (Ref B7-4)

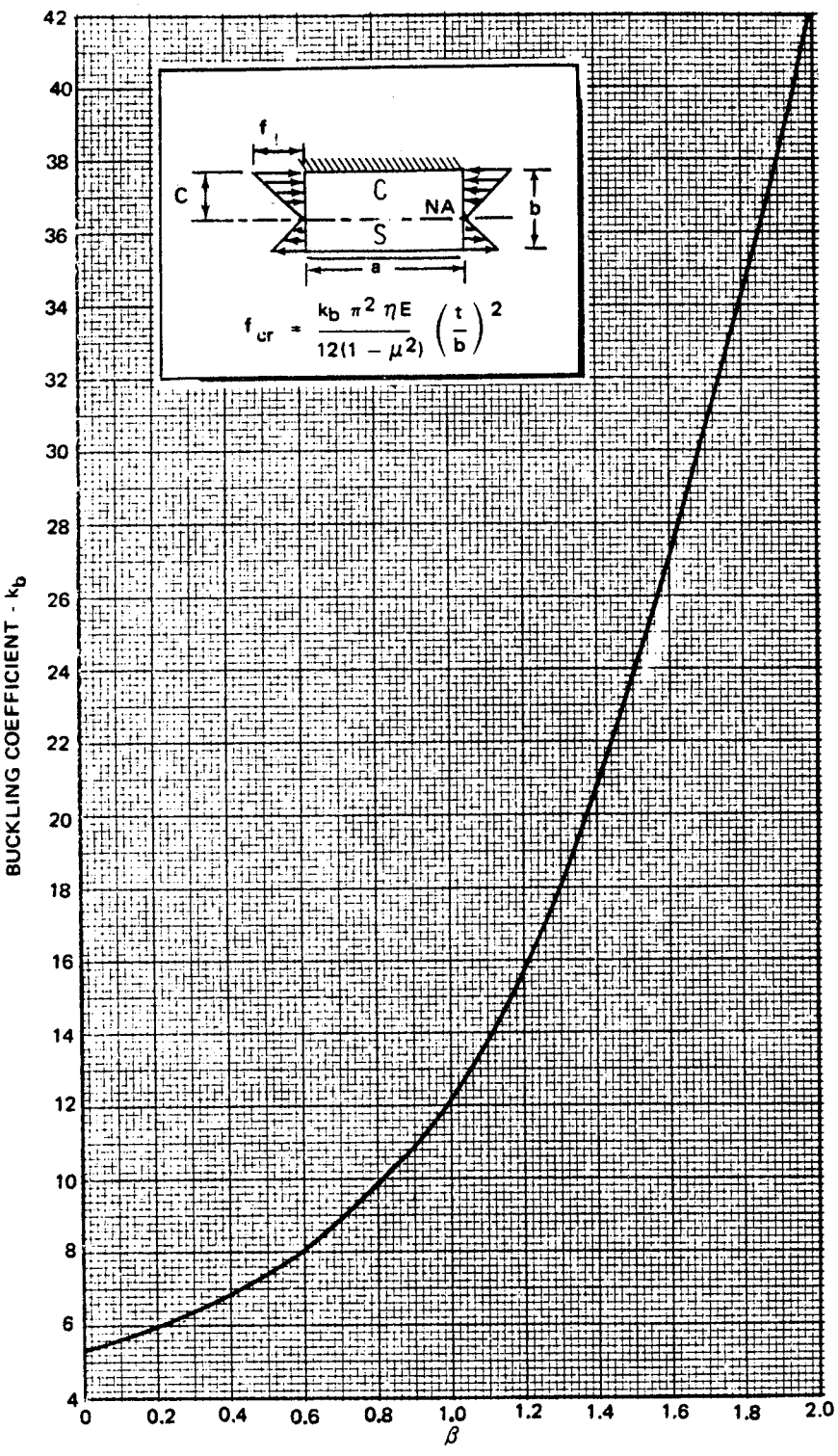


Figure B7.2.3-6 Buckling Coefficients for a Plate in Bending in the Plane of the Plate When a/b≥2.4--Tension Side Simply-Supported and Compression Side Fixed (Ref B7.4)

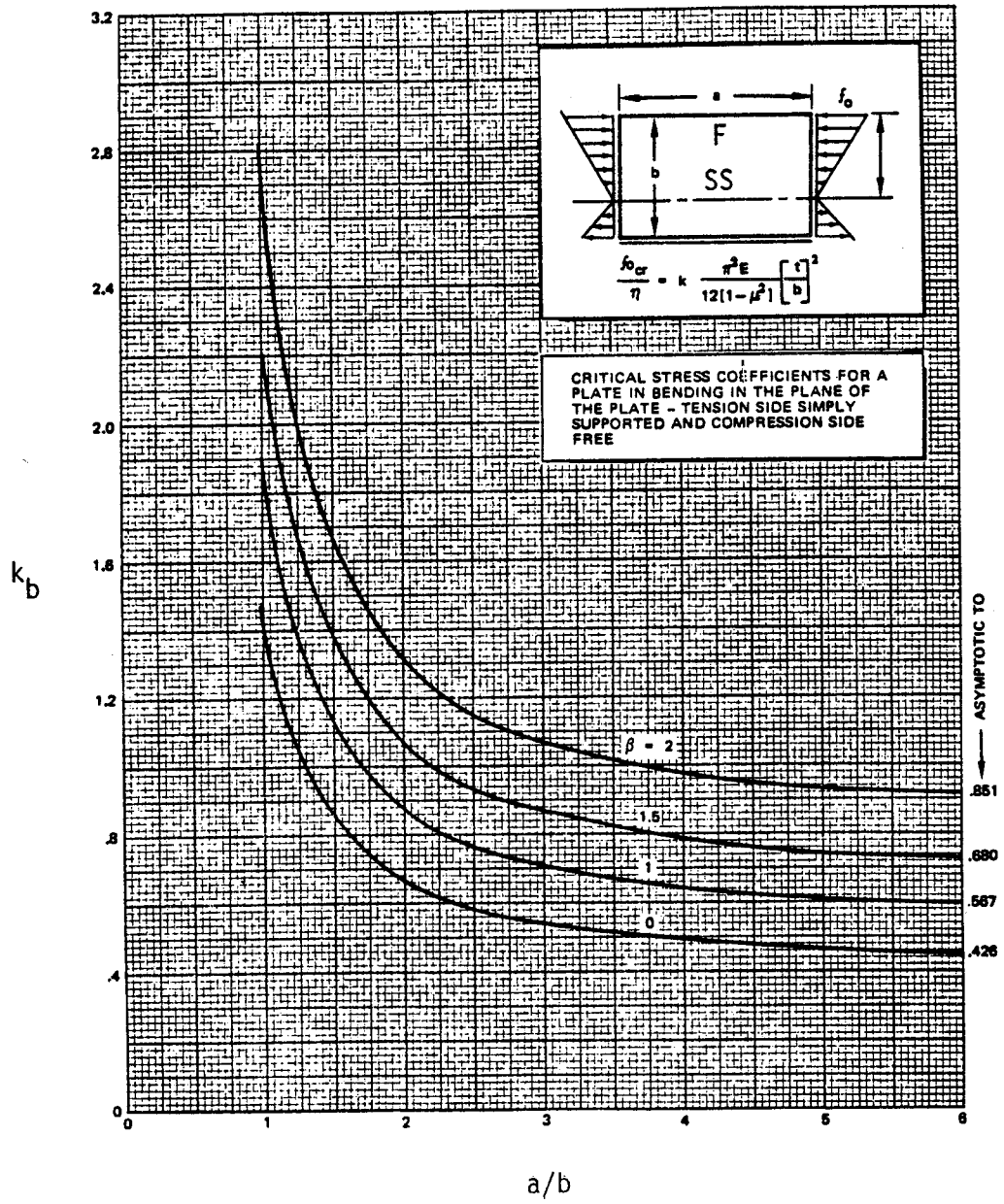


Figure B7.2.3-7 Buckling Coefficients for a Plate in Bending in the Plane of the Plate--Tension Side Simply-Supported and the Compressive Side Free (Ref B7-4)

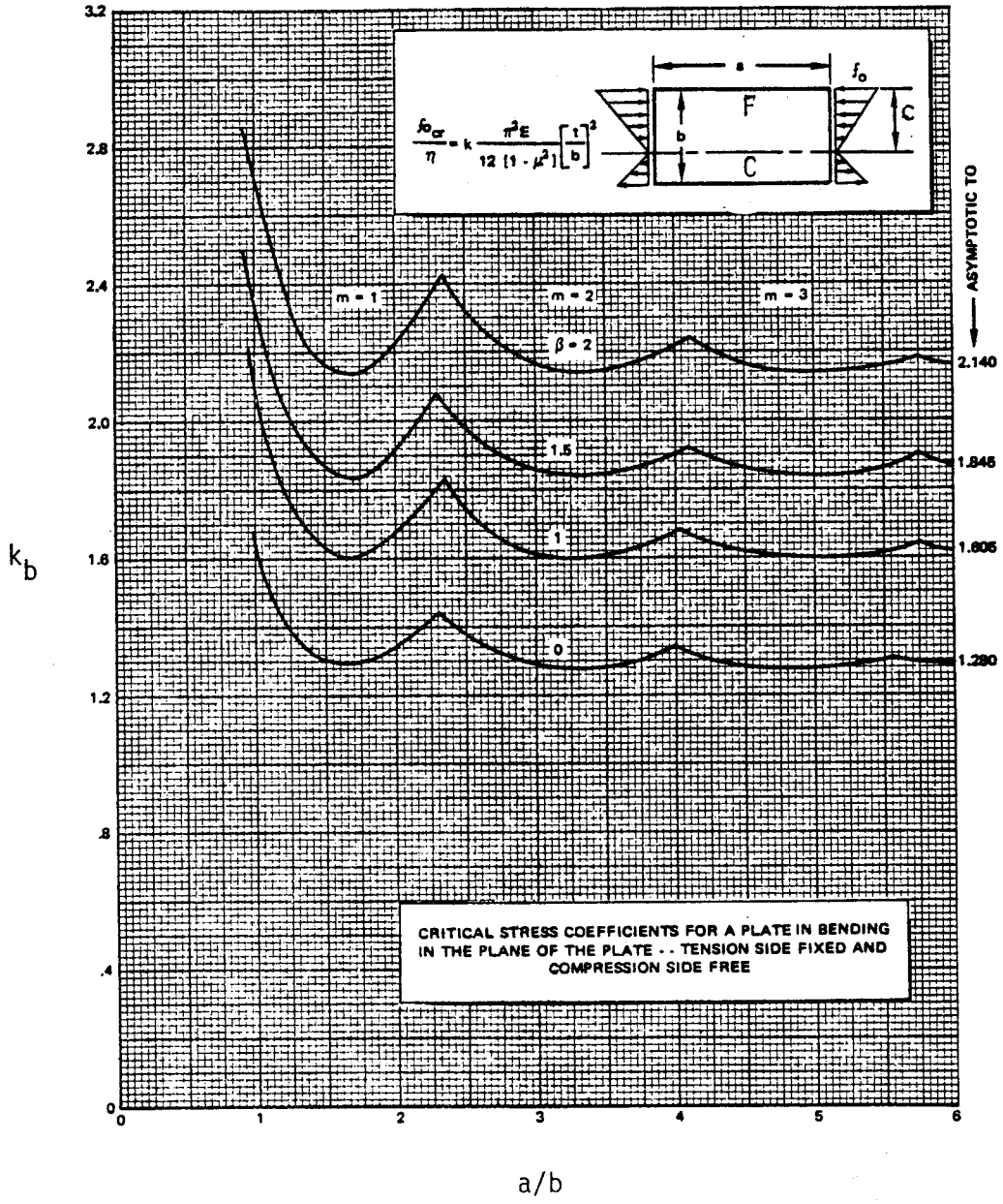


Figure B7.2.3-8 Buckling Coefficient for a Plate in Bending in the Plane of the Plate--Tension Side Fixed and Compression Side Free (Ref B7-4)

### B7.2.4 Combined Loads

When dealing with combined loads, it is customary to form stress ratios R which represent the ratio of the applied stress-to-the allowable stress. The allowable stresses are determined for the specific loading condition based on the buckling coefficients in this section. Applied loads are specified for a given design problem.

#### B7.2.4.1 Bending and Longitudinal Compression

The interaction equation for combined bending and longitudinal compression is

$$R_b^{1.75} + R_c = 1.0 \qquad \text{(B7-5)}$$

Figure B7.2.4-1 is a plot of Equation B7-5. It should be used to determine the margin of safety for the plate.

#### B7.2.4.2 Bending and Shear

The interaction equation for combined bending and shear loading is

$$R_b^2 + R_s^2 = 1 \qquad \text{(B7-6)}$$

The margin of safety can be found by the equation

$$\text{M.S.} = \frac{1}{(R_b^2 + R_s^2)^{1/2}} - 1 \qquad \text{(B7-7)}$$

Figure B7.2.4-2 is a plot of Equation B7-6. Use it or Equation B7-7 to determine the margins of safety for the plate.

#### B7.2.4.3 Compression (Tension) and Shear

The interaction formula is

$$R_c + R_s^2 = 1 \qquad \text{(B7-8)}$$

The margin of safety equation is

$$\text{M.S.} = \frac{2}{(R_c + \sqrt{R_c^2 + 4R_s^2})} - 1 \qquad \text{(B7-9)}$$

Figure B7.2.4-3 is a plot of Equation B7-8. If the direct stress is tension, then use the negative values for $R_c$ based on the compression allowables.

B7.2.4.4 Compression, Bending and Shear

Interaction curves for this system of buckling conditions are given in Figure B7.2.4-4 which give the bending stress ratio $R_b$ as a function of the shear stress ratio $R_s$ for variations in the compression stress ratio $R_c$. To use this interaction curve, calculate $R_b$, $R_s$, and $R_c$. Enter the curve with $R_b$ and $R_s$. The intersection of these values defines the required $R_c$ for zero margin of safety. The calculated value, value, $R_c$, must be equal to or less than the value determined from Figure B7.2.4-4.

If margins of safety are required, use Figure B7.2.4-5. Enter this figure with $R_s$ and $R_b$, point 1 on the figure. Construct a line through the origin and this point to intersect the curves of $R_c/R_s$. Read either $R_{BA}$ or $R_{SA}$. The margin of safety equations are shown on Figure B7.2.4-5. Note: If $R_c$ is less than $R_s$, use the left hand side of the figure.

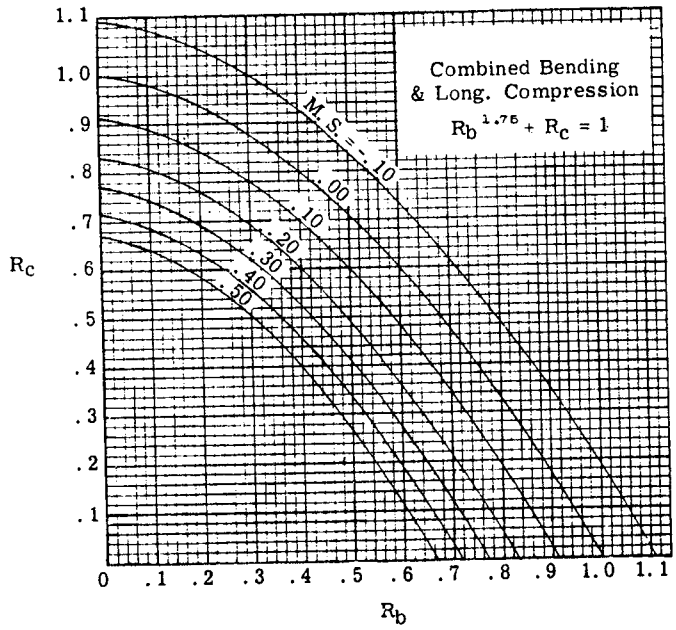


Figure B7.2.4-1 Interaction Curves for Combined Bending and Longitudinal Compression Stress

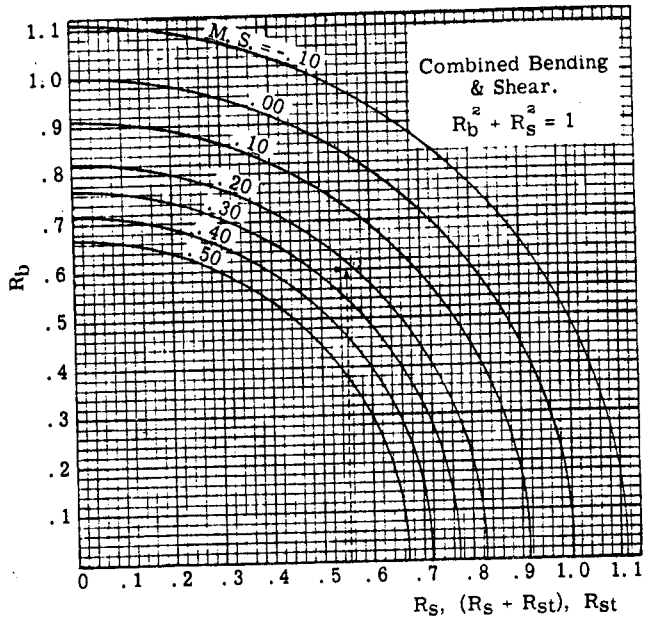


Figure B7.2.4-2 Interaction Curves for Combined Bending and Shear Stress

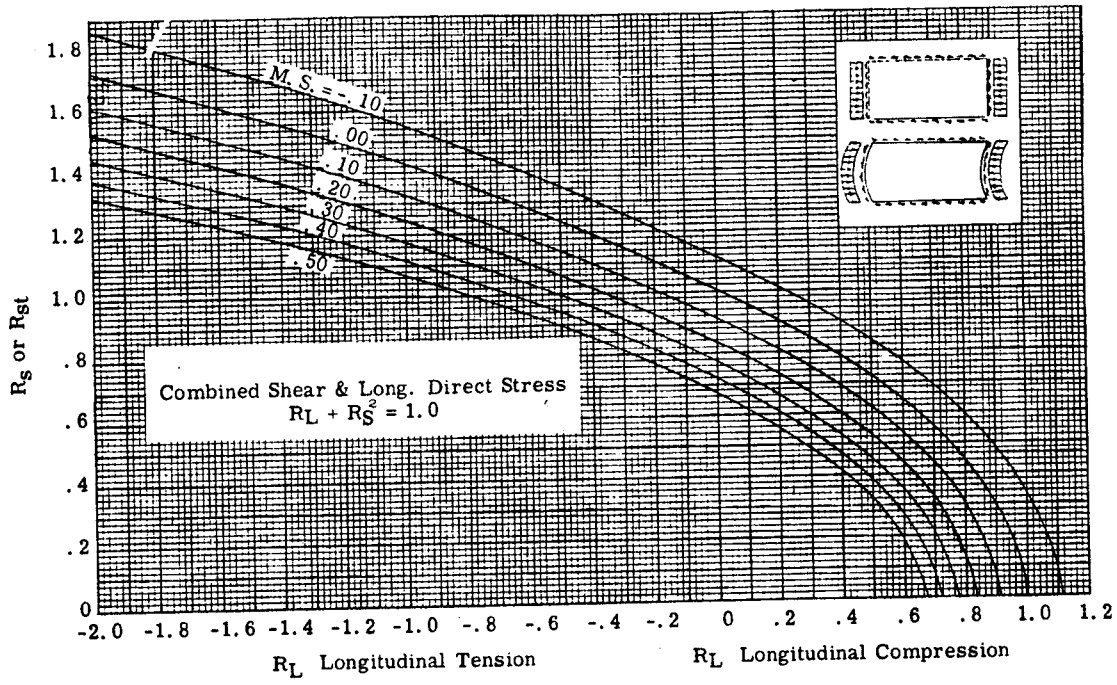


Figure B7.2.4-3 Interaction Curves for Combined Shear and Longitudinal Direct Stress

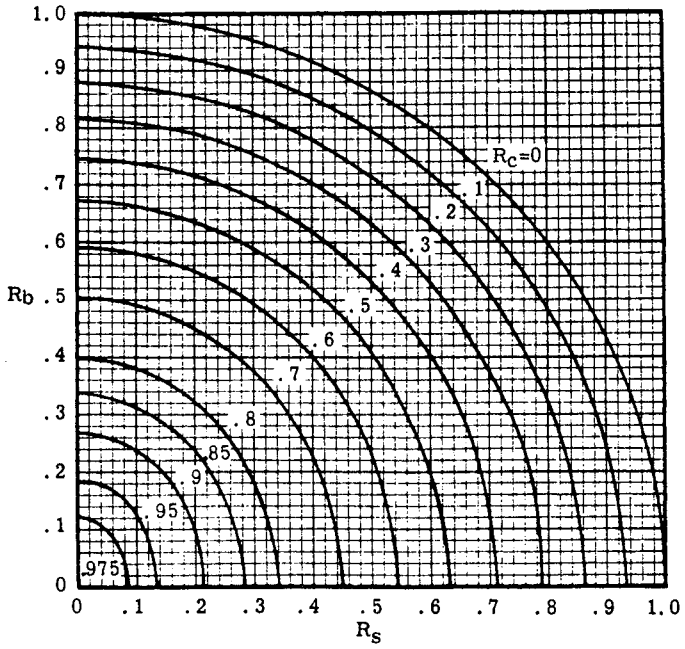


Figure B7.2.4-4 Interaction Curves for Combined Compression, Bending and Shear Stress

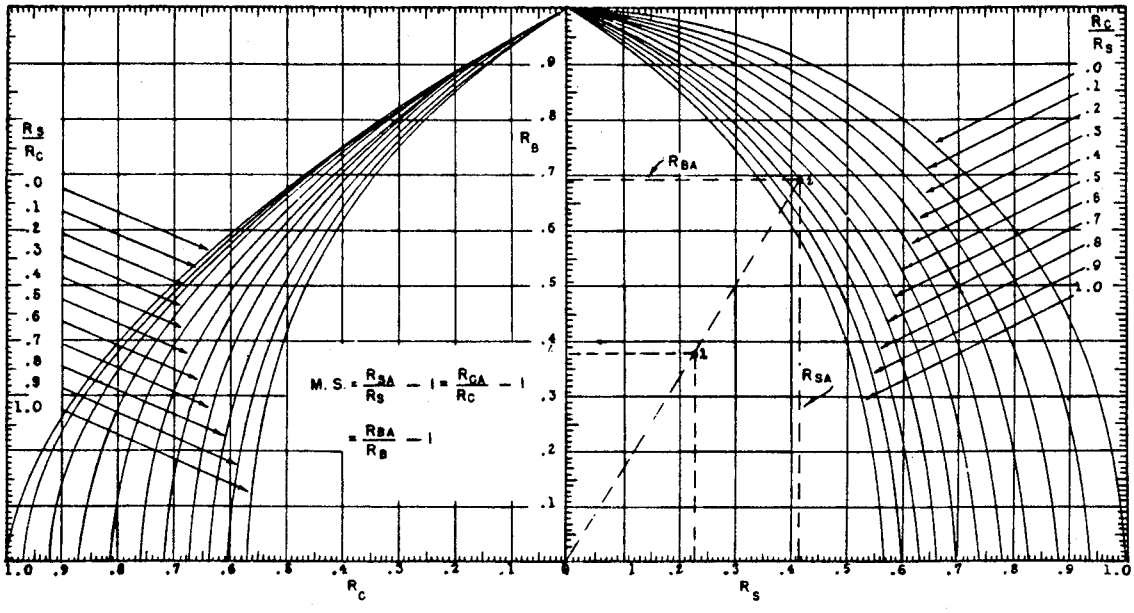


Figure B7.2.4-5 Interaction Curves for Combined Compression, Bending and Shear Stress

## B7.3.0 Buckling of Composite Shapes Under Compression Loads

Figures B7.3.0-1 through B7.3.0-9 give the buckling coefficients for composite shapes under compression loads. These curves reflect the restraining (or detrimental) effect of the adjacent elements on plate buckling.

To find the buckling coefficient for the flange use

$$k_f = k_w \, (b_f/b_w)^2 (t_w/t_f)^2 \qquad \text{(B7-10)}$$

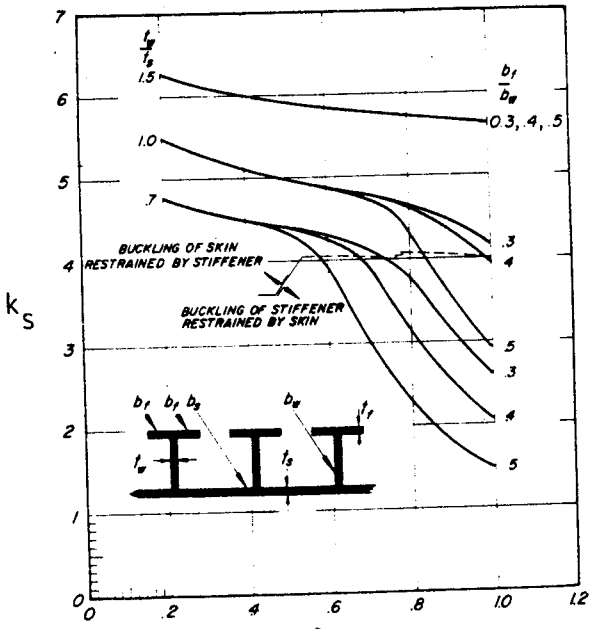


Figure B7.3.0-1 T-Section Stiffeners
$t_w/t_f = 1.0$; $b_f/t_f > 10$; $b_w/b_s > .25$
(Ref B7-9)

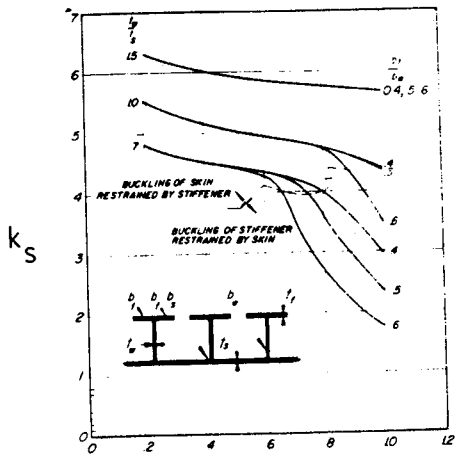


Figure B7.3.0-2 T-Section Stiffeners
$t_w/t_f = .7$; $b_f/t_f > 10$; $b_w/t_s > .25$
(Ref B7-9)

$$F_{cr} = \frac{k_s \pi^2 E}{12(1-\mu^2)} \left(\frac{t_s}{b_s}\right)^2$$

$$F_{cr} = \frac{k_s \pi^2 E}{12(1-\mu^2)} \left(\frac{t_s}{b_s}\right)^2$$

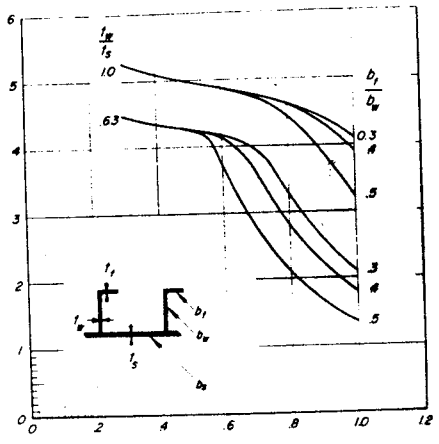


Figure B7.3.0-3 Z-Section Stiffeners, $t_w/t_s$ = .50 and .79 (Ref B7-8)

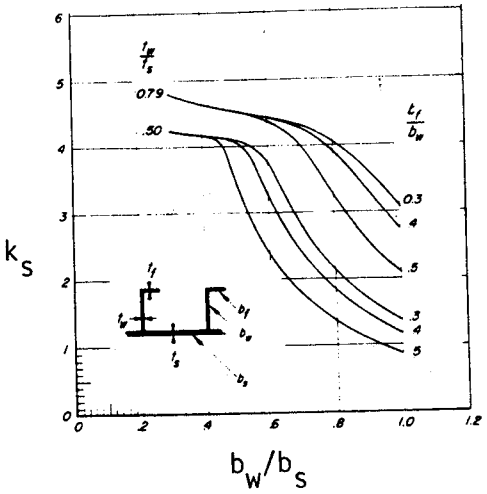


Figure B7.3.0-4 Z-Section Stiffeners, $t_w/t_s$ = .63 and 1.0 (Ref B7-8)

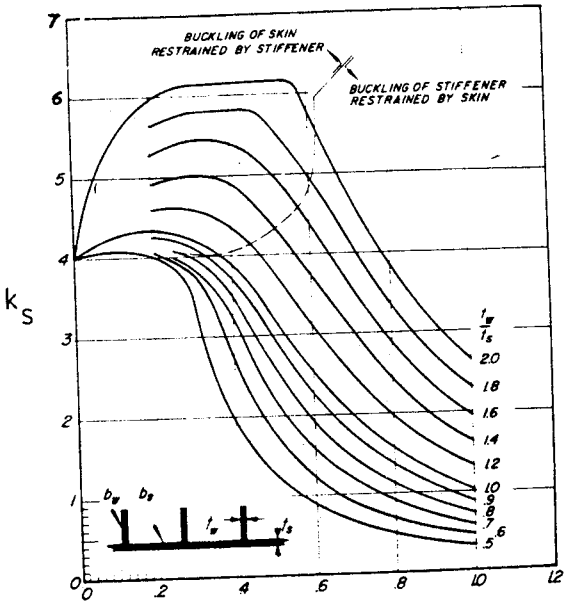


Web Stiffeners. $.5 < t_w/t_s < 2.0$

Figure B7.3.0-5 Compressive Local Buckling Coefficients for Infinitely Wide Idealized Flat Plates (Ref B7-9)

$$F_{cr} = \frac{k_h \pi^2 E}{12(1-\mu^2)} \left(\frac{t_h}{h}\right)^2$$

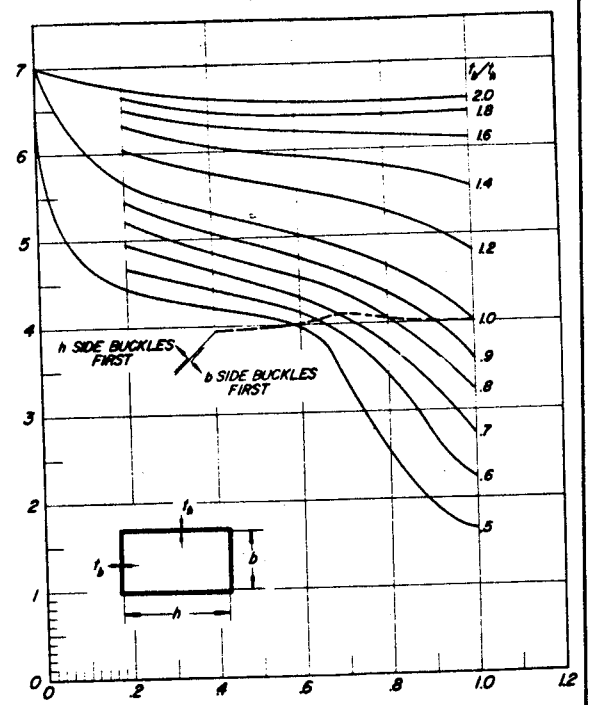


Figure B7.3.0-6 Rectangular Tube Section Stiffeners (Ref B7-10)

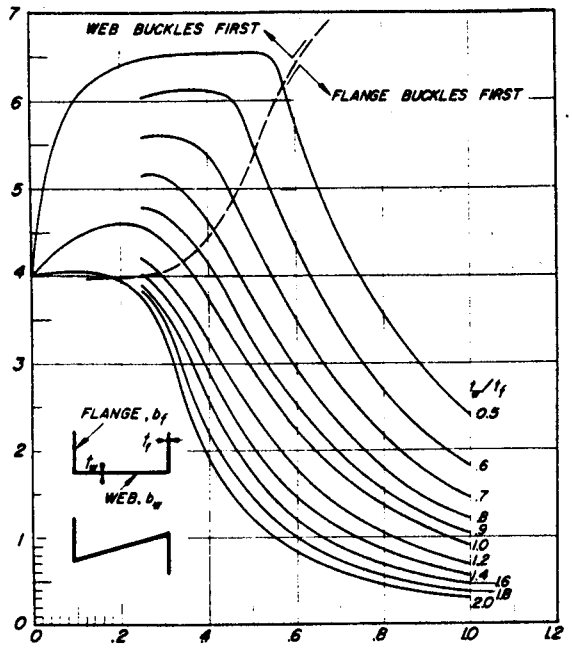


Figure B7.3.0- 7 Channel and Z-Section Stiffeners (Ref B7-10)

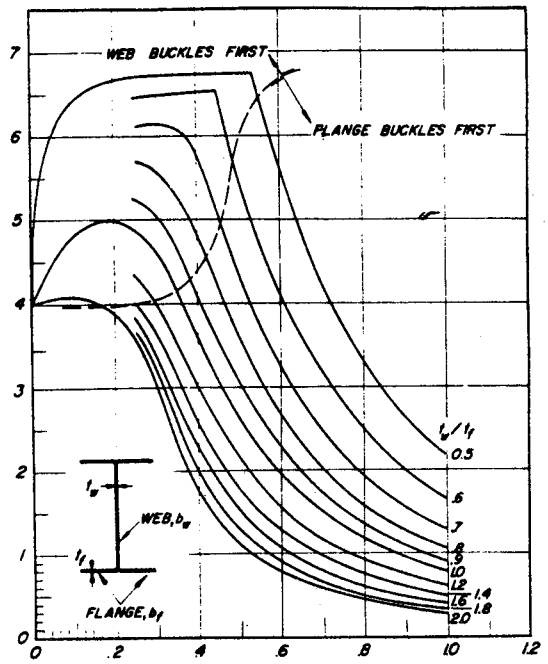


Figure B7.3.0- 8 H-Section Stiffeners (Ref B7-10)

$$F_{cr} = \frac{k_w \pi^2 E}{12(1-\mu^2)} \left(\frac{t_w}{b_w}\right)^2$$

$$F_{cr} = \frac{k_w \pi^2 E}{12(1-\mu^2)} \left(\frac{t_w}{b_w}\right)^2$$

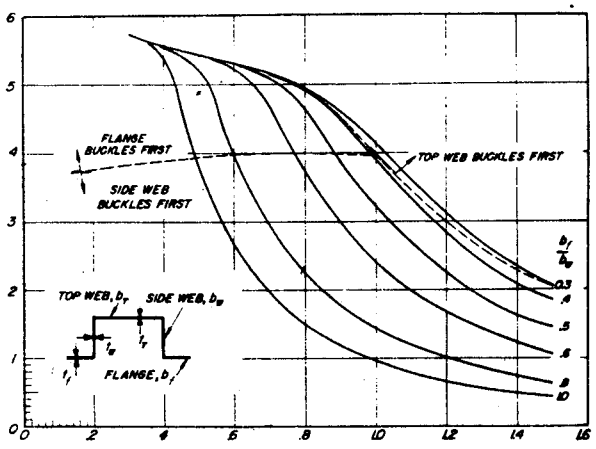


Figure B7.3.0- 9 Buckling Stress for Hat-Section Stiffeners (Ref B7-11)

$$t=t_f=t_w=t_t; F_{cr} = \frac{k_t \pi^2 E}{12(1-\mu^2)} \left(\frac{t_t}{b_t}\right)^2$$

## B7.4.0 Buckling of Curved Plate

### B7.4.1 Compression Loads

The initial buckling stress for a curved plate under axially compression loads is the same as for flat plates

$$F_{cr} = \frac{\pi^2 k_c \eta_p E}{12\,(1-\mu^2)} \left(\frac{t}{b}\right)^2 \qquad \text{(B7-11)}$$

where $k_c$ is the compression buckling coefficient that depends on the radius to thickness ratio of the curved plate and the support along the edges. $\eta_p$ is the same plasticity factor as was used for flat plates. Plasticity correction factors in Figures B7.2.1-7 through B7.2-9 are applicable.

Figures B7.4.1-1 gives the compression buckling coefficients for long curved plates.

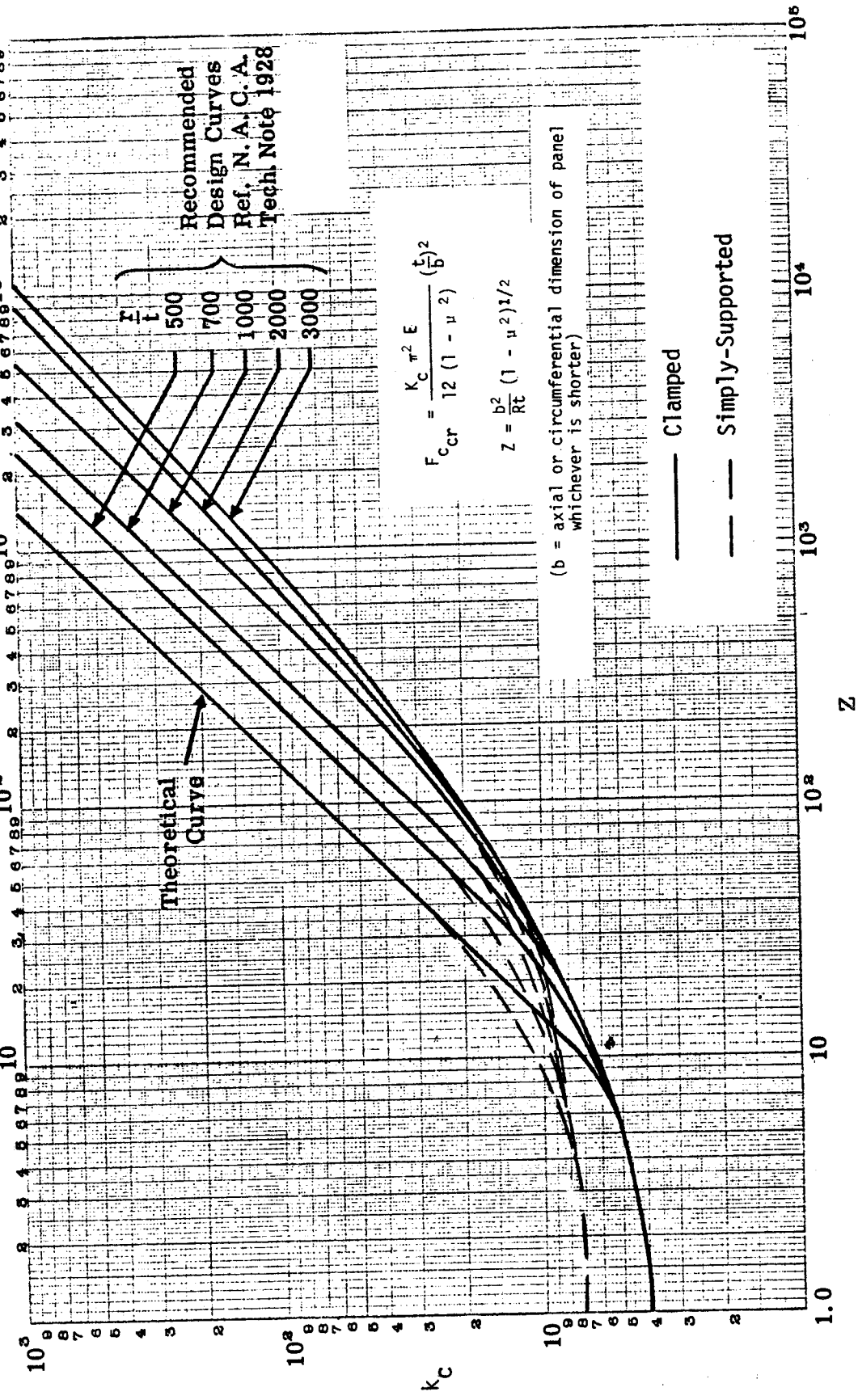


Figure B7.4.1-1 Axial Compressive Buckling Coefficients for Long Curved Plates (Ref B7-12)

B7.4.2 Shear Loads

The initial buckling stress for a curved plate under shear loads is the same as for flat plates

$$F_{cr} = \frac{\pi^2 k_s \eta_s E}{12\,(1-\mu^2)} \left(\frac{t}{b}\right)^2 \qquad \text{(B7-12)}$$

where $k_s$ is the shear buckling coefficient that depends on the radius-to-thickness ratio of the curved plate and the support along the edges. $\eta_s$ is the same plasticity factor used for flat plates. Plasticity correction factors in Figures B7.2.2-2 through B7.2.2-4 are applicable.

Figures B7.4.2-1 through B7.4.2-4 give the shear buckling coefficients for long and wide curved plates having simply-supported and clamped edges.

B7.4.3 External Radial Pressure

The initial buckling stress for a curved plate under external pressure loads is

$$F_{cr} = \frac{\pi^2 k_y \eta_p E}{12\,(1-\mu^2)} \left(\frac{t}{b}\right)^2 \qquad \text{(B7-13)}$$

where $k_y$ is the external pressure buckling coefficient and $\eta_p$ is the same plasticity factor used for flat plates, Figures B7.2.1-7 through B7.2.1-9.

Figure B7.4.3-1 gives the external pressure buckling coefficient as a function of the radius-to-thickness ratio for the curved plate.

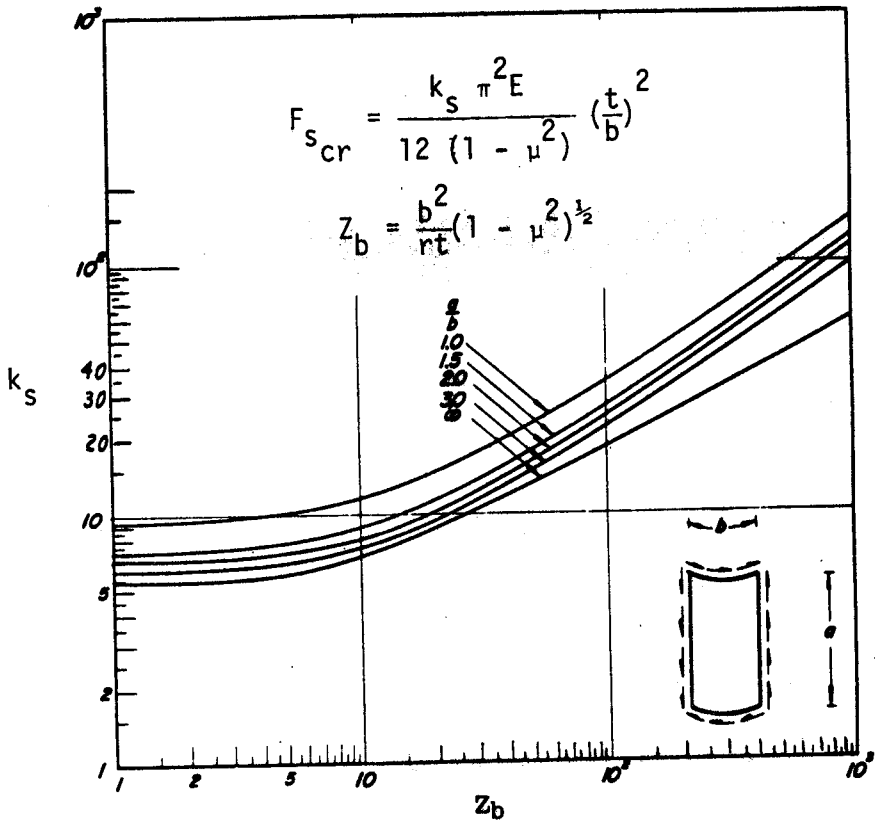


Figure B7.4.2-1 Shear Buckling Coefficients for Long Simply-Supported Curved Plates (Ref B7-13)

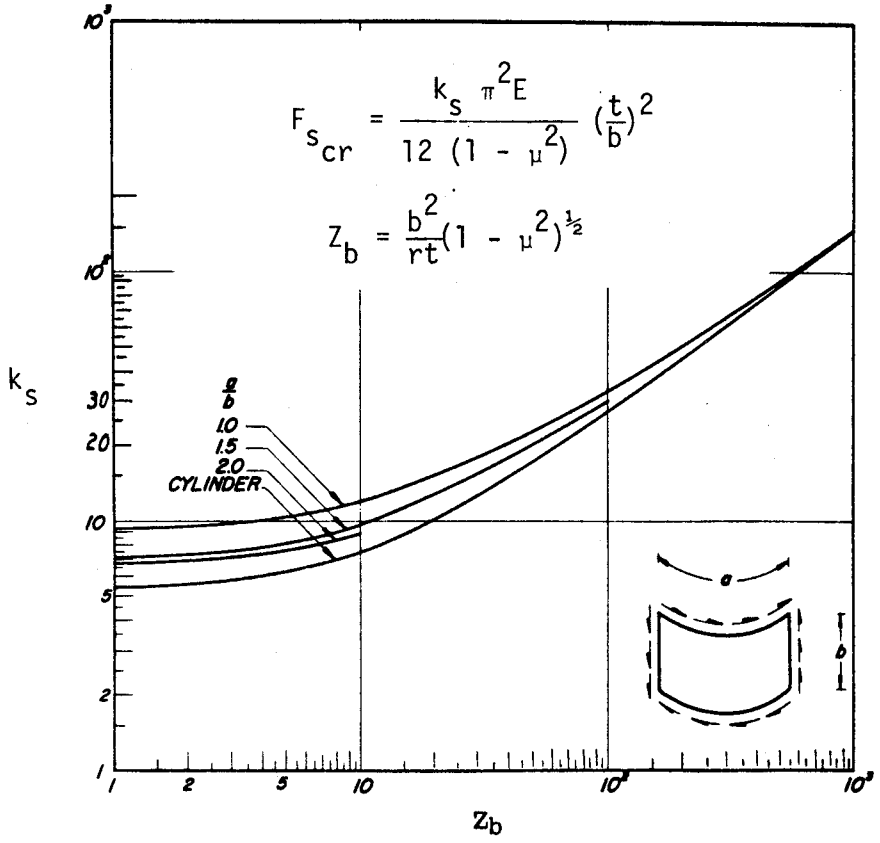


Figure B7.4.2-2 Shear Buckling Coefficient for Wide Simply-Supported Curved Plates (Ref B7-13)

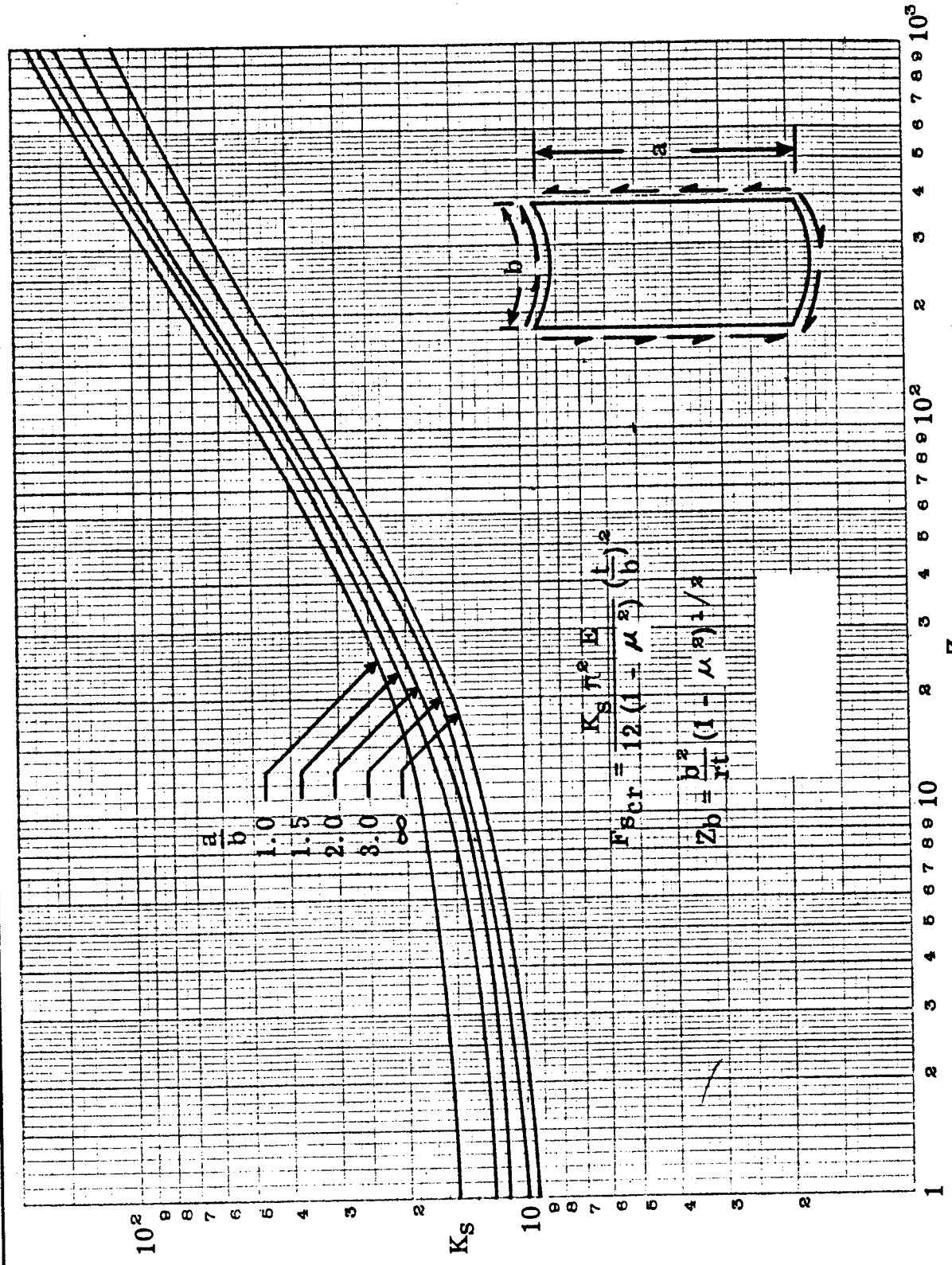


Figure B7.4.2-3 Shear Buckling Coefficients for Long Clamped Curved Plates (Ref B7-12)

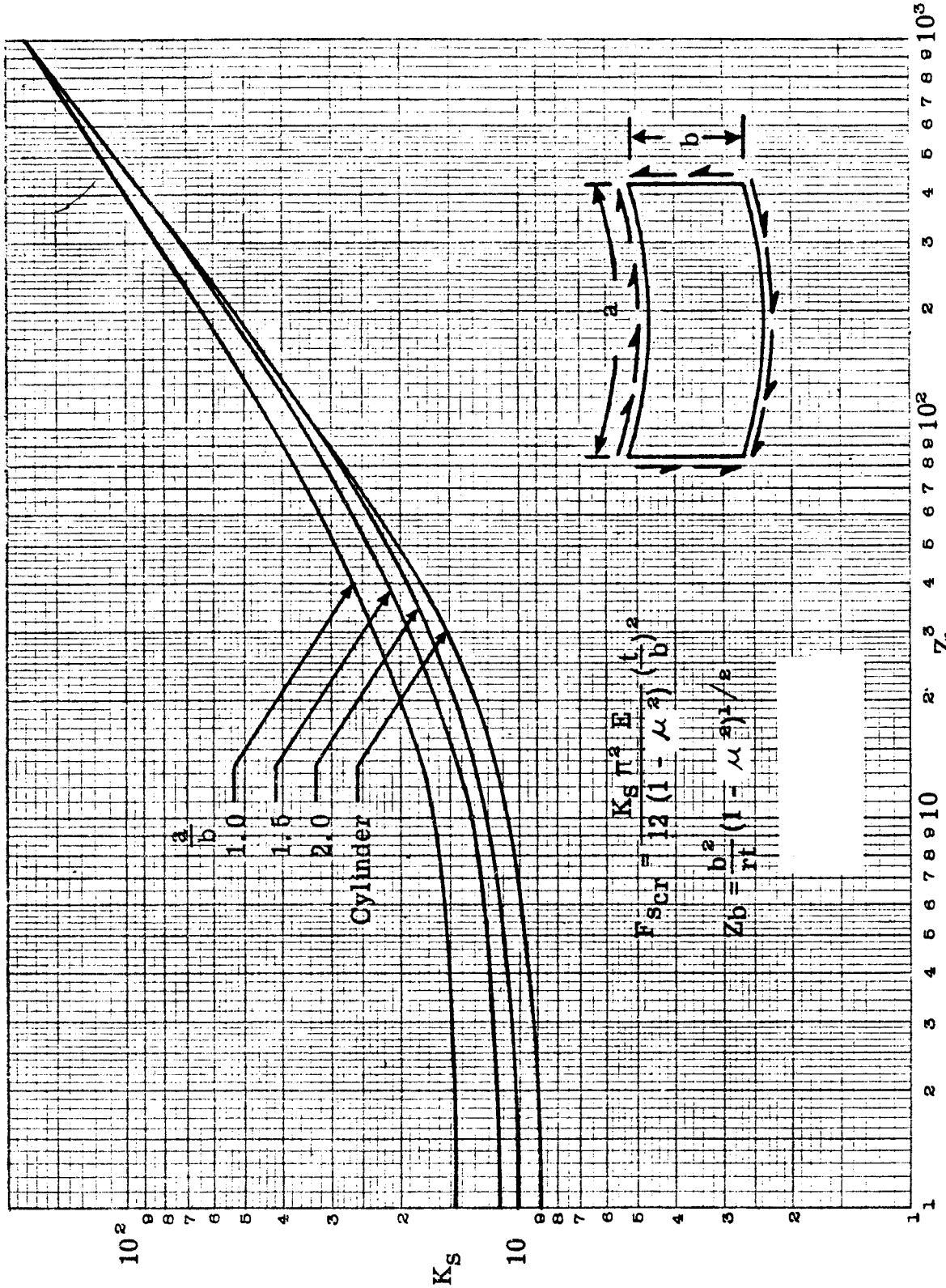


Figure B7.4.2-4 Shear Buckling Coefficients for Wide Clamped Curved Plates (Ref B7-12)

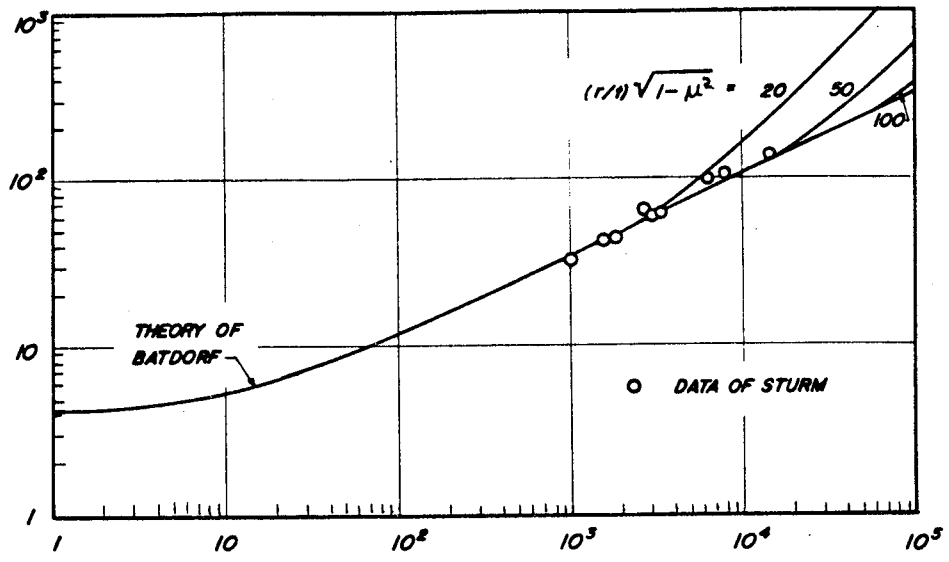


$$Z_L = \frac{L^2}{Rt}(1-\mu^2)$$

Figure B7.4.3-1 Buckling Under External Radial Pressure (Ref B7-1)

B7.4.4 Combined Loads

B7.4.4.1 Shear and Longitudinal Direct Stress

Use the interaction equations for flat plates in Section B7.2.4-3 (Equations B7-8 and B7-9).

B7.4.4.2 Compression and External Pressure

The interaction formula is

$$R_c^2 + R_p = 1 \qquad \text{(B7-14)}$$

Determine allowable stresses from Equations B7-12 and B7-13 for compression and external pressure. Applied stresses are defined for a given problem.

B7.4.4.3 Shear and External Pressure

The interaction formula is

$$R_c^2 + R_p = 1 \qquad \text{(B7-15)}$$

Determine allowable stresses from Equations B7-12 and B7-13 for shear and external pressure. Applied stresses are defined for a given problem.

B7.5.0 Buckling of Flat Orthotropic Plates

Table B7.5.0-1 provides equations for determining the initial buckling loads for orthotropic plates. The plate loads are in plane; compression or shear. In some of the equations, the terms m and/or n appear. These correspond to the number of half-waves in the x and y directions, respectively. The stability equations must be minimized with respect to these values.

All of the equations are in terms of the flexural rigidities $D_{11}$, $D_{12}$, $D_{22}$, and $D_{66}$. These are determined as follows:

$$D_{11} = \frac{E_x t^3}{12(1-\mu_{xy}\mu_{yx})}$$

$$D_{22} = \frac{E_y t^3}{12(1-\mu_{xy}\mu_{yx})}$$

$$D_{66} = \frac{G_{xy} t^3}{12(1-\mu_{xy}\mu_{yx})}$$

For most design problems, the designer should use the computer programs listed in Section E7.

# Table B7.5.0-1 Buckling of Flat Orthotropic Plates ($D_{16} = D_{26} = 0$)

| Loading | Edge Conditions | Buckling Loads | Comments (Assumptions) |
|---|---|---|---|
| Biaxial compression 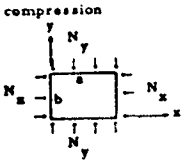 | All sides simply supported | $N_{x,cr} = \frac{\pi^2}{b^2}\left[\frac{D_{11} m^4 (\frac{b}{a})^4 + 2(D_{12} + 2D_{66}) m^2 n^2 (\frac{b}{a})^2 + D_{22} n^4}{m^2 (\frac{b}{a})^2 + \phi n^2}\right]_{min}$ | 1. $\phi = \frac{N_y}{N_x}$<br>2. Equation to be minimized with respect to m, n = 1, 2, .. ∞<br>3. a/b finite |
| Uniaxial compression 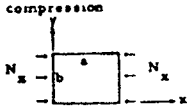 | All sides simply supported | $N_{x,cr} = \frac{\pi^2}{b^2}\left[D_{11} m^2 (\frac{b}{a})^2 + 2(D_{12} + 2D_{66}) n^2 + D_{22} \frac{n^4}{m^2} (\frac{a}{b})^2\right]_{min}$ | 1. Equation to be minimized with respect to m, n = 1, 2, .. ∞<br>2. a/b = finite |
| | All sides simply supported | $N_{x,cr} = 2\frac{\pi^2}{b^2}\left[\sqrt{D_{11} D_{22}} + D_{12} + 2D_{66}\right]$ | 1. a/b = infinite = ∞ |
| | LOADED EDGES S.S. OPPOSITE SIDES FIXED | $N_{x,cr} = \frac{\pi^2}{b^2}\left[D_{11} m^2 (\frac{b}{a})^2 + 2.67 D_{12} + 5.33 \left[D_{22} (\frac{a}{b})^2 \frac{1}{m^2} + D_{66}\right]\right]$ | 1. a/b = finite<br>2. Reference 2.2-21<br>3. Minimized |
| | All sides fixed | $N_{x,cr} = \frac{\pi^2}{b^2}\left[4.6\sqrt{D_{11} D_{22}} + 2.67 D_{12} + 5.33 D_{66}\right]$ | 1. a/b = infinite = ∞ |
| Uniaxial compression 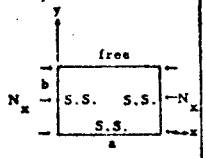  | Three sides simply supported, one side free | $N_{x,cr} = K_s \frac{D_{11}}{b^2}$<br>where $K_s$ is found from the solution of the transcendental equation<br>$\bar{\beta}\left[\bar{\beta}^2 + (\frac{m\pi b}{a})^2 \gamma\right]\left[\bar{\alpha}^2 - (\frac{m\pi b}{a})^2 \nu_{xy}\right]\tanh \bar{\alpha} = \bar{\alpha}\left[\bar{\alpha}^2 - (\frac{m\pi b}{a})^2 \gamma\right]\left[\bar{\beta}^2 + (\frac{m\pi b}{a})^2 \nu_{xy}\right]\tan \bar{\beta}$<br>with<br>$\bar{\beta} = \sqrt{\frac{m\pi b}{a}}\left|\left[(\frac{D_3}{D_{22}})^2 (\frac{m\pi b}{a})^2 - (\frac{D_{11}}{D_{22}})(\frac{m\pi b}{a})^2 + (\frac{N_x b^2}{D_{11}})(\frac{D_{11}}{D_{22}})\right]^{1/2} - (\frac{D_3}{D_{22}})(\frac{m\pi b}{a})\right|^{1/2}$<br>$\bar{\alpha} = \sqrt{\frac{m\pi b}{a}}\left|\left[(\frac{D_3}{D_{22}})^2 (\frac{m\pi b}{a})^2 - (\frac{D_{11}}{D_{22}})(\frac{m\pi b}{a})^2 + (\frac{N_x b^2}{D_{11}})(\frac{D_{11}}{D_{22}})\right]^{1/2} + (\frac{D_3}{D_{22}})(\frac{m\pi b}{a})\right|^{1/2}$<br>$D_3 = D_{12} + 2D_{66}$<br>$\gamma = \frac{4G_{xy}(1 - \nu_{xy}\nu_{yx})}{E_y} + \nu_{xy}$ | 1. a/b = finite<br>2. Minimize $K_s$ with respect to m = 1, 2, .. ∞ |
| | Three sides simply supported, one side free | $N_{x,cr} = h^3\left[\frac{G_{xy}}{b^2} + \frac{m^2\pi^2 E_x}{12 a^2 (1 - \gamma_{xy}\gamma_{yx})}\right]$ | m = 1 is minimum |
| | | $N_{x,cr} = \frac{h^3}{b^2} G_{xy}$ $\qquad \frac{a}{b} = \infty$ | |

## Table B7.5.0-1 Buckling of Flat Orthotropic Plates ($D_{16} = D_{26} = 0$) cont'd.

| Loading | Edge Conditions | Buckling Loads | Comments (Assumptions) |
|---|---|---|---|
| Shear 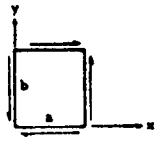  | All sides simply supported | $N_{xy,cr} = \left(\frac{2}{b}\right)^2 (D_{11} D_{22}^3)^{1/4} \left(8.125 + \frac{5.05}{\theta}\right)$<br>where $\theta = \frac{\sqrt{D_{11} D_{22}}}{D_{12} + 2D_{66}} > 1$ | 1. a/b = infinite = ∞ |
| | All sides simply supported | $N_{xy,cr} = \left(\frac{2}{b}\right)^2 \sqrt{D_{22}(D_{12} + 2D_{66})} \left\{11.7 + .5320\theta + .9380\theta^2\right\}$<br>where $\theta = \frac{\sqrt{D_{11} D_{22}}}{D_{12} + 2D_{66}} < 1$ | 1. a/b = infinite = ∞ |
| | All sides fixed | $N_{xy,cr} = \left(\frac{2}{b}\right)^2 (D_{11} D_{22}^3)^{1/4} \left(15.1 + \frac{7.0}{\theta}\right)$<br>where $\theta = \frac{\sqrt{D_{11} D_{22}}}{D_{12} + 2D_{66}} > 1$ | 1. a/b = infinite = ∞ |
| | All sides fixed | $N_{xy,cr} = \left(\frac{2}{b}\right)^2 \sqrt{D_{22}(D_{12} + 2D_{66})} \left\{18.6 + 1.650\theta + 1.900\theta^2\right\}$<br>where $\theta = \frac{\sqrt{D_{11} D_{22}}}{D_{12} + 2D_{66}} < 1$ | 1. a/b = infinite = ∞ |
| | All sides simply supported | $N_{xy,cr} = K \left(\frac{2}{b}\right)^2 (D_{11} D_{22}^3)^{1/4} \quad \theta > 1$<br>where $K = 8.20 + \frac{5}{\theta} + 10^{(A/\beta + B/\beta)}$<br>$A = \frac{.185}{\theta} - .270$<br>$B = .82 + \frac{.46}{\theta} - \frac{.2}{\theta^2}$<br>$\beta = \left(\frac{D_{11}}{D_{22}}\right)^{1/4}$ | 1. a/b = 1.0 |
| | All sides fixed | $N_{xy,cr} = j \left(\frac{2}{b}\right)^2 (D_{11} D_{22}^3)^{1/4} \quad \theta > 1$<br>where $j = j_o + 10^{(A/\beta + B/\beta)}$<br>$j_o = 15 + 7.5/\theta$<br>$A = -.100$ } $\beta \le .6$<br>$B = 1.30 + .2/\theta$<br>$j_o = 19.3 + 8.45/\theta$<br>$A = -.040 + .035/\theta$ } $\beta \ge .6$<br>$B = 1.99 + .38/\theta$<br>$\beta = \left(\frac{D_{11}}{D_{22}}\right)^{1/4}$ | 1. a/b = 1.0 |

Table B7.5.0-1 Buckling of Flat Orthotropic Plates ($D_{16} = D_{26} = 0$) concluded

| Loading | Edge Conditions | Buckling Loads | Comments (Assumptions) |
|---|---|---|---|
| General | General (stiffened plate) | For a stiffened plate, all buckling equations apply with the restriction that $D_{11} = \frac{E^s_x b_s t_s \left\{ -(h_s + t)^2 \Big/ 4\left[ \left(1 + \frac{E^f_x b_s t}{E^s_x b_s t_s}\right)\right] + \frac{h_s^2}{3} + \frac{h_s t}{2} + \frac{t^2}{4} \right\}}{b_s} + \frac{E^f_x t^3}{12(1 - \nu^f_{xy} \nu^f_{yx})}$ $D_{22} = \frac{E^f_y t^3}{12(1 - \nu^f_{xy} \nu^f_{yx})}$ $D_{66} = \frac{G^f_{xy} t^3}{12}$ $D_{12} = \frac{(E^f_y \nu^f_{xy} + E^f_x \nu^f_{yx})}{24(1 - \nu^f_{xy} \nu^f_{yx})} t^3$ 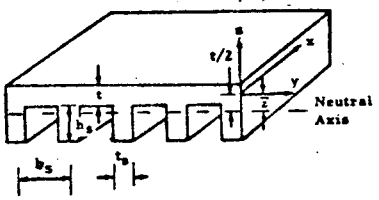  | |

## REFERENCES

B7-1 Bruhn, E. F., Analysis and Design of Flight Vehicle Structures, Tri-State Offset Co., Cincinnati, Ohio, 1965.

B7-2 Lundquist, Eugene E., and Stowell, Elbridge Z., "Critical Compressive Stress for Flat Rectangular Plates Supported Along All Edges and Elastically Restrained Against Rotation Along the Unloaded Edges", NACA Report 733, Washington, 1942.

B7-3 Gerard, George, and Becker, Herbert, "Handbook of Structural Stability, Part I - Buckling of Flat Plates", NACA Report TN3781, Washington, 1957.

B7-4 Anon: Structural Analysis Manual, Development Engineering, McDonnell Douglas Astronautics Company - West, M8.070-ACCD, 1971.

B7-5 Shanley, F. R., Strength of Materials, McGraw-Hill Book Company, Yok, Pa., 1957.

B7-6 Anon: Metallic Materials and Elements for Aerospace Vehicle Structures, MIL-HDBK-5C, 15 September 1976.

B7-7 Anon: Aluminum Standards and Data, The Aluminum Association, 6th ed, March 1979.

B7-8 Gallaher & Broughan: A Method for Calculating the Compressive Strength of Z Stiffened Panels that Develop Local Instability. NACA TN.1482, 1947.

B7-9 Broughan & Baab: Charts for Calculating the Critical Compressive Stress for Local Instability of Idealized T Stiffened Panels, NACA WRL-204, 1944.

B7-10 Kroll, Fisher & Heimerl: Charts for Calculation of the Critical Stress for Local Instability of Columns with I, Z, Channel, Rectangular Tube Sections, NACA WRL-398, 1943.

B7-11 Van Der Maas: Charts for the Calculation of the Critical Compressive Stress for Local Instability of Columns with Hat Sections, Jour. Aero. Sci. Vol. 21, June 1954.

B7-12 Schildsrout and Stein: Critical Combinations of Shear and Direct Axial Stress for Curved Rectangular Panels. NACA T.N. 1928.

B7-13 Gerard and Becker: Handbook of Structural Stability, Part III, Buckling of Curved Plates and Shells, NACA T.N. 3883.

# STIFFNESS

# TABLE OF CONTENTS

# B9.0.0 Stiffness

## B9.1.0 Introduction

In Section B6.0.0, methods are provided to determine compression panel allowable strength for wing, fuselage, and empennage structure. The methods provided are based on the assumption that a simple support condition exists at the ribs (or frames) as a minimum requirement. Thus, there is no deflection (sagging of the ribs) for applied loads less than the compression panel allowable load. Panel failure is confined between ribs as shown in Figure B9.1.0-1. This type of failure is defined as panel instability failure. The rib must have sufficient stiffness to force this mode of failure.


Figure B9.1.0-1 Panel Instability Failure

If the rib does not possess adequate stiffness, then failure will occur with a panel buckle half-wave length that is continuous across the rib. The result is simultaneous failure of both the rib and the compression panel. This type of failure, shown in Figure B9.1.0-2, is called general instability failure.

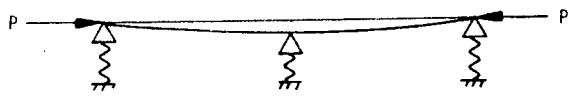


Figure B9.1.0-2 General Instability Failure

The allowable compression panel load defined for panel instability failure is greater than the allowable load defined for general instability failure. Thus, the compression panel can be designed for less weight if panel instability is enforced, which results in overall lightest weight for the structure because compression panel weight fraction is greater than rib weight fraction (about 4 to 1 greater), and, also, because the amount of rib weight required to enforce panel instability is a small fraction of the total rib weight (less than 10 percent). Thus, efficiently designed structure requires panel instability as the failure mode.

In this section, stiffener requirements are provided to force panel instability for simple continuous beams (Section B9.2.0), continuous box structure (Section B9.3.0), and shell structure (Section B9.4.0). Section B9.5.0 gives methods to calculate the actual rib stiffness for solid ribs and ribs with lightening holes. Example problems are provided in Section B9.6.0.

B9.1.1 Symbols

$A$ = Area in general, $in.^2$

$A_c$ = Compression panel skin and stringer area, $in.^2$

$b$ = Length of cutout in rib, in.

$c$ = Subscript for compression and distance from outer fiber to neutral axis, in..

$D$ = Diameter of a shell or fuselage, in.

$e$ = Distance from section neutral axis to the skin centerline, in.

$E$ = Young's Modulus, psi.

$f$ = Applied compression panel stress, psi or subscript for frame

$h$ = Box beam depth between centroids of cover panels, in.

$h_R$ = Rib stiffener depth, in.

$I$ = Moment of inertia, $in.^4$.

$L$ = Panel length between supports, in.

$m$ = Number of spans for a continuous beam

$M$ = Shell or fuselage bending moment, in.-lbs.

$M_A$ = Moments about a point A

$P$ = Applied load, lbs.

$P_{cr}$ = Euler load, lbs. $\frac{\pi^2 EI}{L^2}$

$P_{crush}$ = Crushing load on box beam, lbs.

$P_1$ = Panel load intensity, lbs./in.

$R_F$ = Reduction factor for stiffness depending on the crushing load

$\alpha$ = Rib of frame stiffness required for panel instability failure

$\beta$ = Correction factor for beam stiffness depending on number of stringers

$\gamma$ = Factor for determining $\alpha$, depending on number of spans or stiffness of the box beam

$\delta$ = Deflection of a bar under constant axial applied load, $\delta = \frac{Ph_R}{AE}$, in.

$\theta$ = Small angle made by disturbing a beam from the equilibrium position

B9.1.2 Basic Stiffness Concept

The principal of rib (or frame) stiffness to force panel instability can best be illustrated by a simple model shown in Figure B9.1.2-1.

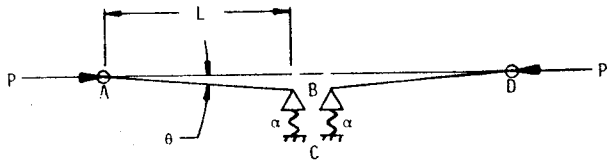


Figure B9.1.2-1 Simple Stiffness Model

In this model, the bar AB is hinged at both ends. It is supported by a spring, BC, which is representative of a rib. The spring has a stiffness, $\alpha$ in lbs./in. A horizontal force P is applied to the bar and at the same time, the bar is slightly disturbed by an amount $\theta L$ which produces a vertical force in the spring, $\alpha\theta L$. By symmetry, the same factors apply to the right half of the problem; i.e., the bar, DB.

By simple statics for the bar from A to B, the summation of moments about point A are

$$\Sigma M_A = P\theta L - \alpha\theta L^2 \qquad \text{(B9-1)}$$

If the moment due to the force in the spring with respect to point A is larger than the moment due to the force P, that is if $\alpha\theta L^2 > P\theta L$, then, stable equilibrium will occur. Thus, the force in the spring will restore the bar to it initial horizontal position and panel instability will occur.

Conversely, if $\alpha\theta L^2 < P\theta L$, then the horizontal position will be unstable and the system will collapse after a slight disturbance which is general instability.

The critical value of P is found from simple equilibrium, $\Sigma M_A = 0$. Thus, $\alpha\theta L^2 = P\theta L$ which gives $P_{cr} = \alpha L$. From symmetry, the total stiffness for the system from A to D is twice $\alpha$. The rib stiffness required for panel instability is therefore

$$\alpha_{req} = \frac{2P_{cr}}{L} \qquad \text{(B9-2)}$$

Any additional stiffness is not required.

## B9.2.0 Simple Continuous Beam Stiffness Requirements

A simple continuous beam having m equal spans of length, L, is shown in Figure B9.2.0-1 for m = 6. The elastic supports have equal spring stiffness $\alpha$.


Figure B9.2.0-1 Simple Continuous Beam, m = 6

To enforce panel instability, the spring stiffness, from Reference B9-1, must be

$$\alpha_{req} = \frac{P_{cr}}{\gamma L} \qquad \text{(B9-3)}$$

where $\gamma$ is a factor defined in Table B9.2.0-1 as a function of the number of equal spans, m.

Table B9.2.0-1 Values $\gamma$ for Continuous Beams

| m | 2 | 3 | 4 | 5 | 6 | 7 | 9 | 11 | ∞ |
|---|---|---|---|---|---|---|---|---|---|
| $\gamma$ | .5 | .333 | .293 | .276 | .268 | .263 | .258 | .255 | .250 |

For the case of m = 2, $\gamma$ = .5, and $\alpha = 2P_{cr}/L$ which is identical to equation B9-2 derived for the simple model.

## B9.3.0 Box Structure Stiffness Requirements

A box structure, such as a wing box, is subjected to bending moments which produce crushing loads in the ribs. The crushing load, shown in Figure B9.3.0-1, is defined for equal tension and compression areas by the equation

$$P_{crush} = \frac{2f^2 A_c L}{Eh} \qquad \text{(B9-4)}$$

where

$A_c$ = the compression panel area, $in.^2$

E = the elastic modulus, psi

f = the applied compression panel stress, psi

h = the box depth between centroids of cover panels, in.

L = the panel length, in.

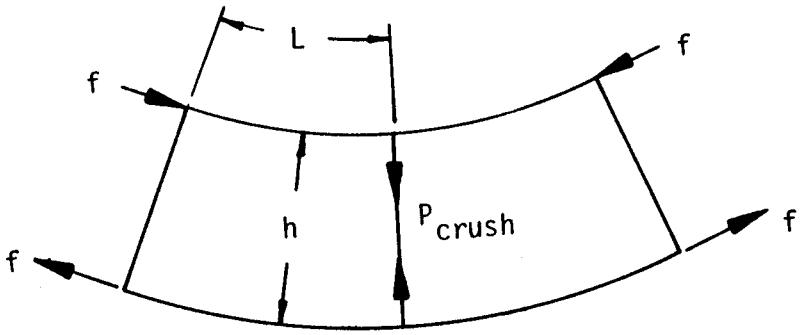


Figure B9.3.0-1 Crushing Loads on a Box Structure

The ribs must be strong enough and stable enough to resist this load, which is a strength requirement.

In addition to the strength requirement, the ribs must be stiff enough to force panel instability as defined by Equation B9-3. This stiffness requirement was defined for box beams with varying number of spans and box stiffness in Reference B9-2 by design charts. Data from these charts have been converted to $\gamma$ values which are given in Table B9.3.0-1 for use with Equation B9-3.

Table B9.3.0-1 Values $\gamma$ for Box Beams

| | $(EI)_t/(EI)_c$ | | | |
|---|---|---|---|---|
| m | .5 | 1 | 2 | ∞ |
| 2 | .113 | .158 | .220 | .500 |
| 3 | .112 | .152 | .198 | .333 |
| 4 | .111 | .149 | .191 | .293 |
| ∞ | .110 | .144 | .179 | .250 |

Note in this table for infinite box stiffness, $(EI)_t/(EI)_c = \infty$, that the values of $\gamma$ are identical to those defined in Table B9.2.0-1 for a continuous beam. This is because an infinitely stiff box beam will not deflect under bending loads. Therefore, no crushing loads are introduced. The effect of crushing loads on the box beam is to increase the stiffness requirement over that for a simple, continuous beam. This increase is defined in Equation B9-3 by a decrease in $\gamma$ as defined in Table B9.3.0-1.

## B9.4.0 Shell Stiffness Requirement

A shell (fuselage) can fail by panel or general instablity, as shown in Figure B9.4.0-1, just as can a continuous beam or box structure. In this case, the frame must provide the stiffness to enforce panel instability.

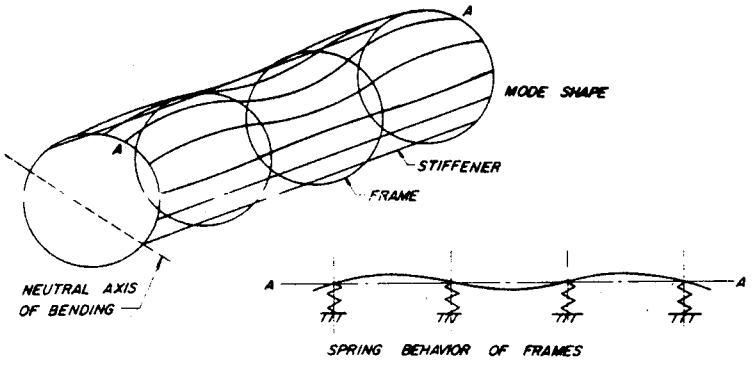


(a) Panel instability.

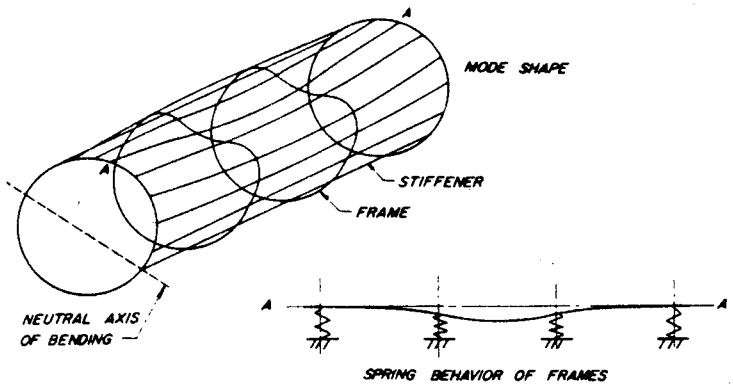


(b) General instability.

Figure B9.4.0-1 Shell Instability Modes

In Reference B9-3, the required frame stiffness for a stiffened shell in pure bending is given by the expression

$$(EI)_f = \frac{MD^2}{16{,}000L} \qquad \text{(B9-5)}$$

where

D = the diameter of the shell, in.

E = the elastic modulus, psi

I = the frame moment of inertia, in.

L = the frame spacing, in.

M = the shell bending moment, in.-lbs.

The factor 1/16,000 was determined by test in Reference B9-3 for small shell diameters (less than 3 feet). Limited test data on the DC-10 has shown that the stiffness requirement applies equally as well for large diameter shells.

Generally, the frame will have adequate stiffness based on other requirements. However, equation B9-5 should always be checked for new fuselage frame designs.

## B9.5.0 Rib Stiffness Calculations

For the simple continuous beam problem, stiffness is usually given by the simple relationship $\frac{P}{\delta} = \frac{AE}{h_R}$. Box beam compression panel structure is generally stiffened by ribs which are either: 1) solid and stiffened on one side, or 2) have lightening holes. In the first case, the rib is eccentrically loaded so that stiffness is a function of $\frac{EI}{h_R}$, as well as $\frac{AE}{h_R}$. In the second case, the stiffness is a function of the rib cap EI and length of cutout in the rib b.

A. Solid Rib Stiffened on One Side of rib is given by the equation The stiffness for this type

$$\alpha_{actual} = \frac{P}{\delta} = \frac{E}{h_R}\left[\frac{1}{\frac{1}{A} + \frac{1}{2}\frac{P}{E}\left(\frac{e}{I}\right)^2 R_F}\right] \qquad \text{(B9-6)}$$

where

A = rib skin and stiffner area, $in.^2$ (use 30t skin)

e = distance from section neutral axis to the skin centerline, in.

E = elastic modulus, psi

I = rib skin and stiffener moment of inertia, $in.^4$

$h_R$ = rib depth, in.

$R_F$ = Reduction factor depending on the crushing load

The value $R_F$ should be obtained from Figure B9.5.0-1 for the ratio of crushing load-to-Euler load for the combined rib web and stiffener section. For applied stress above the material proportional limit, use $E_t$ at the applied stress in determining $P_{cr}$.

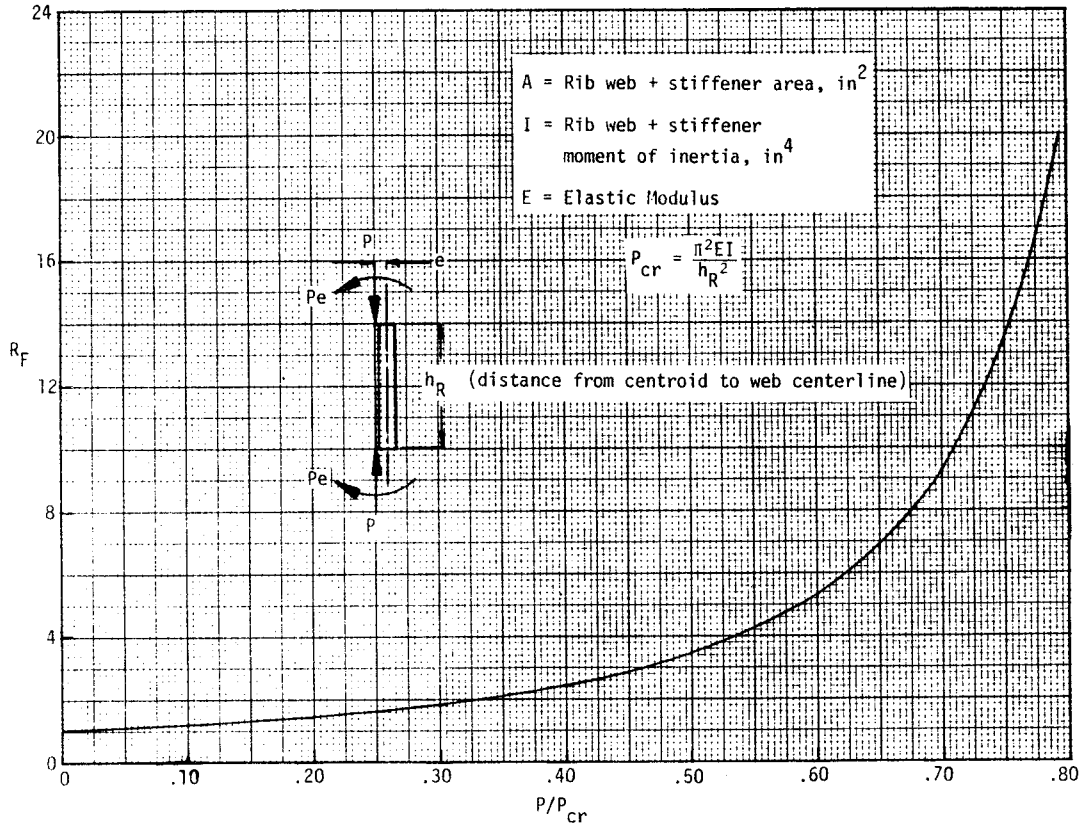


Figure B9.5.0-1 Reduction Factor for Rib Stiffness Due to Eccentric Loading

To evaluate rib stiffness, obtain the required $\alpha$ from Equation B9-3 with $\gamma$ from Table B9.3.0-1. Compute the actual rib stiffness based on the rib crushing load, Figure B9.5.0-1, and Equation B9-6. This value must be greater than the required rib stiffness as defined by Equation B9-3.

B. Rib With a Lightening Hole For this type of rib, stiffness is enforced by a beam which spans a defined width of compression panel as shown in Figure B9.5.0-2.

For the type of cutout shown in Figure B9.5.0-2, the beam span is defined based on a line drawn from the centroid of the minimum effective cap area (use 15t web width on either side of the rivet; rivet edge distance on one side, if less) tangent to the curve which is the locus of points defined by the centroid of the effective lightening hole flange around the hole. Flange length is assumed to be 10t from the tangent line of the radius as shown in Figure B9.5.0-2.

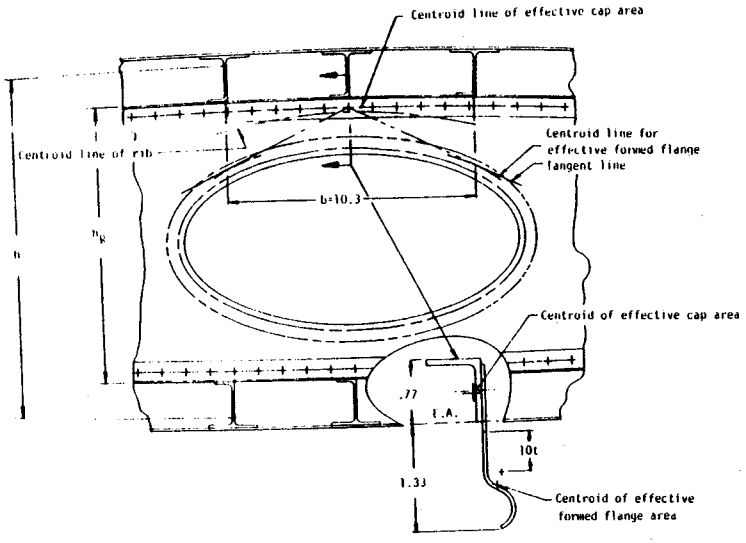


Figure B9.5.0-2 Rib With Lightening Hole

With the beam span, so defined, the rib stiffness required for a simply supported beam is

$$(EI)_{req} = \frac{P_1 b^4}{\gamma \pi^4 L \beta} \qquad \text{(B9-7)}$$

where

b = Beam span, in.

E = Elastic modulus, psi

I = Rib moment of inertia, $in.^4$ (use I for the minimum section

L = Length between ribs, in.

$P_1$ = The compression panel load intensity, lbs./in.

$\beta$ = Factor depending on the number of compression panel stiffeners across the span (see Table B9.5.0-1)

$\gamma$ = Factor depending on the number of equal spans (see Tables B9.2.0-1 or Table B9.3.0-1)

Table B9.5.0-1 Values for $\beta$ as a Function of the Number of Stringers (r) Over the Beam Span, b (Ref. B9-4)

| r | 1 | 2 | 3 | 4 | 5 | 7 | 11 | 19 | 35 | $\infty$ |
|---|---|---|---|---|---|---|---|---|---|---|
| $\beta$ | .493 | .662 | .750 | .800 | .833 | .875 | .917 | .950 | .972 | 1.0 |

For a clamped beam, the required stiffness, equation B9-7, should be divided by 5.12. Judgment is required as to the degree of fixity. The simple support condition should be used for initial design.

## B9.6.0 Example Problem

### B9.6.1 Box Structure

In Section B6.5.4, an aluminum compression panel skin and stringer section ($E = 10.5 \times 10^6$) was sized (Figure B6.5.4-1) for a compression load intensity of 10,000 lbs./in. ($P_{cr} = 50,800$). Properties were

$A_e = 1.222\ in.^2$

$\bar{y} = .406$ in.

$I_{xx} = .422\ in.^4$

$\rho_{xx} = .628$ in.

L = 30 in.

This compression panel is to be supported by aluminum ribs ($E = 10.5 \times 10^6$) without and with cutouts as shown in Figures B9.6.1-1 and -2. Determine if the ribs are stiff enough to support the compression panel at an applied stress equal to the column allowable stress of 48,500 psi.

A. Rib Without Holes For this case, the rib web (30t) and stiffener combined properties are:

$A_e = .194 \text{ in.}^2$

$\bar{y} = .292 \text{ in.}$

$I_{xx} = .0219 \text{ in.}^4$

$\rho_{xx} = .338 \text{ in.}$

$h = 19 \text{ in. and } h_R = 15 \text{ in.}$

1. The crushing load is first computed from Equation B9-4 as

$$P_{crush} = \frac{2f^2 A_c L}{E\,h} = \frac{2(48{,}500)^2(1.222)(30)}{(10.5 \times 10^6)\,19} = 864.5 \text{ lbs.}$$

This assumes $(EI)_t/(EI)_c = 1.0$.

2. Rib strength is checked. Based on the applied crushing load, stress level is determined as

$$f = \frac{P}{A} = \frac{864.5}{.194} = 4456 \text{ psi}$$

which is low and below the material proportional limit. Rib stability is checked from the Euler Equation as

$$P_{cr} = \frac{\pi^2 EI}{h_R^2} = \frac{\pi^2(10.5 \times 10^6)(.0219)}{15^2} = 10{,}087 \text{ lbs.}$$

Thus, the rib is good for strength based on eccentric column data in Section B6.2.2.4.

3. Stiffness requirement is determined from Table B9.3.0-1 for $(EI)_t/(EI)_c = 1$. Here $\gamma = .144$ and the required $\alpha$ is obtained from Equation B9-3.

$$\alpha_{req} = \frac{P_{cr}}{\gamma L} = \frac{50{,}800}{.144\ (30)} = 11{,}678 \text{ lbs./in.}$$

4. Actual rib stiffness is determined from Figure B9.5.0-1 and Equation B9-6. From the Figure for $P/P_{cr}$ = 864.5/10,087 = .086, the reduction factor is determined as $R_F$ = 1.2. Then from equation B9-6

$$\alpha_{actual} = \frac{E}{h_R}\left[\frac{1}{\frac{1}{A} + \frac{e^2}{I} R_F}\right] =$$

$$\frac{10.5 \times 10^6}{15}\left[\frac{1}{\frac{1}{.194} + \frac{.267^2}{.0219}(1.2)}\right] = 72{,}255 \text{ in.-lbs.}$$

which is greater than the required stiffness. Thus, the rib is adequate to support the compression panel.

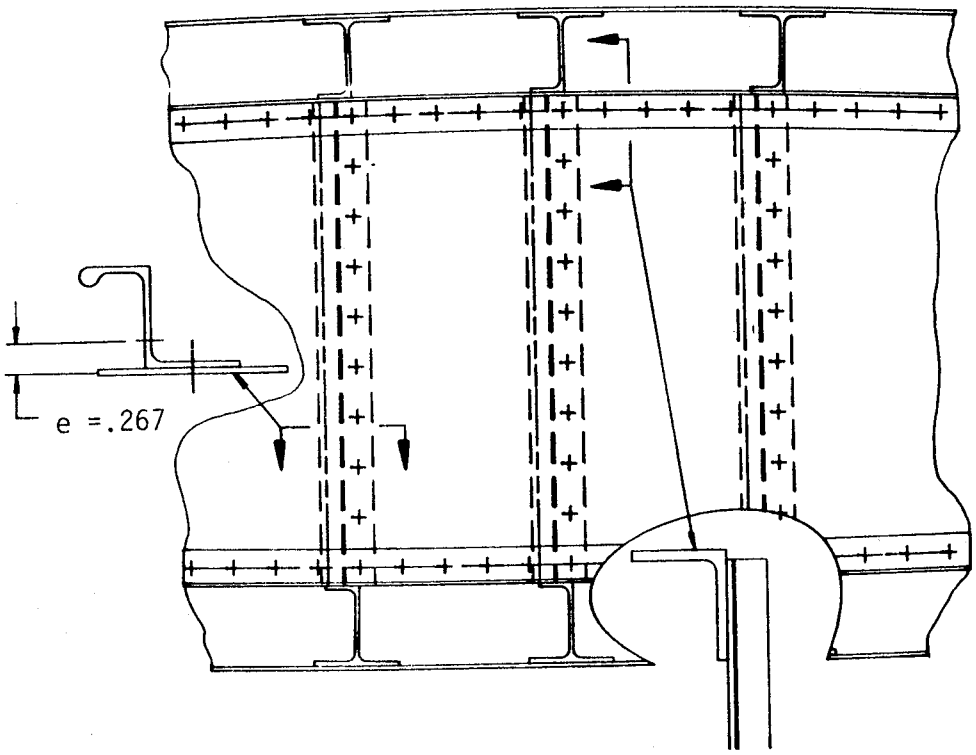


Figure B9.6.1-1 Rib Without Cutout

B. Rib With Cutout For this case, the required rib cap beam dimensions are given in Figure B9.6.1-2. Rib beam minimum I is I = .130 in.$^4$.

The beam span 10.3 inches was determined as described in B9.5.0B. One compression panel skin and stiffener section spans this distance:

1. Rib strength is checked. Based on the applied crushing load determined in A, the maximum moment over the beam span is

$$M = 5.15\ (864.5/2) = 2226 \text{ in.-lbs.}$$

This is a simple support condition which is conservative.

The maximum compression stress in the beam due to bending is

$$f = \frac{Mc}{I} = \frac{2226(.77)}{.130} = 13{,}185 \text{ psi}$$

The maximum tension stress due to bending is

$$f = \frac{Mc}{I} = \frac{2226(1.33)}{.130} = 22{,}774 \text{ psi}$$

These stresses are low and present no problem.

2. Rib stiffness requirement is determined based on Table B9.3.0-1, Table B9.5.0-1, and Equation B9-7. From Table B9.5.0-1, for r = 1, $\beta$ = .493. From Table B9.3.0-1 for m = $\infty$ and $(EI)_t/(EI)_c$ = 1.0, $\gamma$ = .144. Then from Equation B9-7

$$(EI)_{req} = \frac{P_1 b^4}{\gamma \pi^4 L \beta} = \frac{10{,}000\ (10.3)^4}{.144\ \pi^4 (30)(.493)} = 542{,}524 \text{ lb.-in.}^2$$

3. Actual rib stiffness is

$$(EI)_{actual} = (10.5 \times 10^6)(.13) = 1{,}365{,}000 \text{ lbs.-in.}^2$$

Thus, the rib is adequate to support the compression panel.

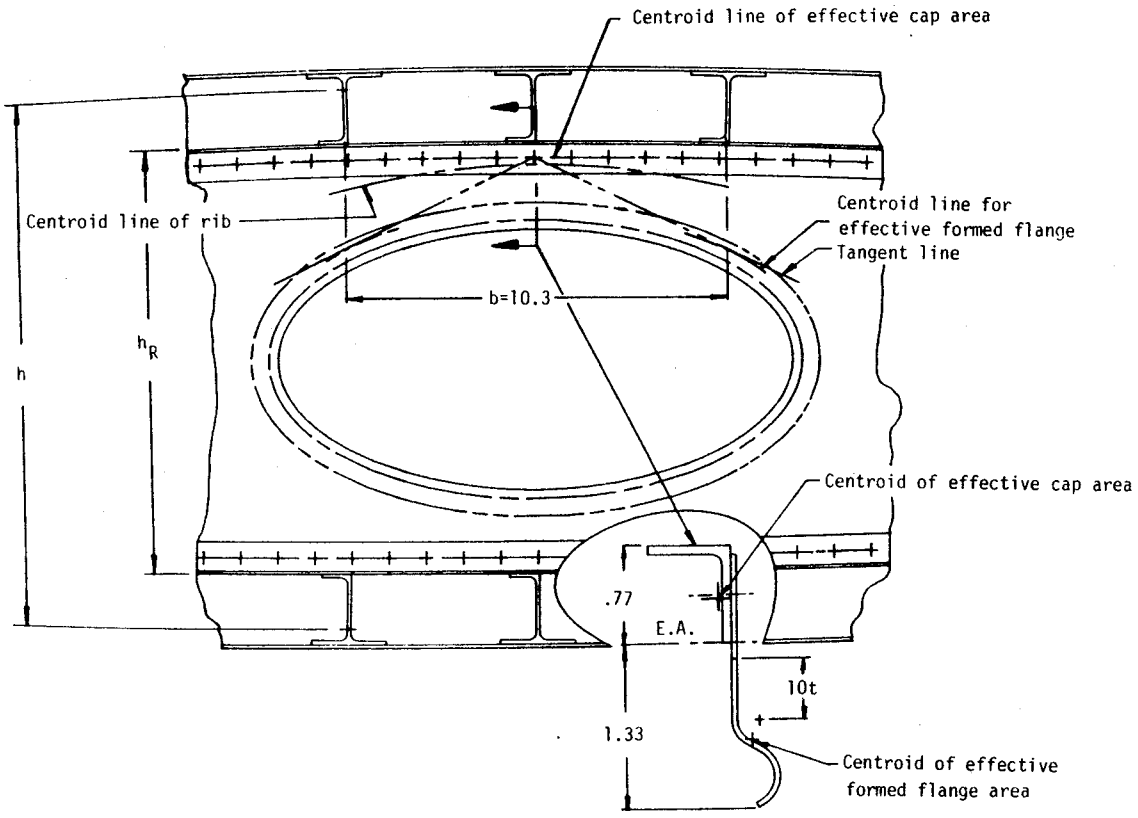


Figure B9.6.1-2 Rib With Cutout

## B9.6.2 Fuselage Structure

In Section B5.1.4.7, an aluminum fuselage frame ($E = 10.5 \times 10^6$ psi) is shown (Figure B5.1.4.7-1) which has properties

$$A = .329 \text{ in.}^2$$

$$\bar{y} = 1.391 \text{ in.}$$

$$I_{RG} = .308 \text{ in.}^4$$

Fuselage diameter is 2 (61.4 in.) = 122.8 in. and frame spacing is 19.0 inch. The maximum applied moment is $60 \times 10^6$ in.-lbs. Determine if the frame is stiff enough to support the fuselage compression panels.

1. From Equation B9-5, the required stiffness is

$$(EI)_f = \frac{MD^2}{16{,}000L} = \frac{60 \times 10^6 (122.8)^2}{16{,}000(19)} = 2{,}976{,}284 \text{ lb.-in.}^2$$

2. Actual stiffness is

$$(EI) = (10.5 \times 10^6)(.308) = 3{,}234{,}000 \text{ lb.-in.}^2$$

Thus, the frame is more than adequate to support the compression panel.

## REFERENCES

B9-1 Timoshenko, S. P. and Gere, J. M., Theory of Elastic Stability, 2nd Edition, McGraw Hill, New York, 1961.

B9-2 Seide, P. and Eppler, J. F., "The Buckling of Parallel Simply Supported Tension and Compression Members Connected by Elastic Deflectional Springs", NACA TN 1823, February 1949.

B9-3 Shanley, F. R., "Simplified Analysis of General Instability of Stiffened Shells in Pure Bending", Journal of Aerospace Sciences, Vol. 16, October 1949.

B9-4 Zahorski, A., "Efficiency of Lateral Stiffeners in Panels", Journal of Aeronautical Sciencies, October 1944, pages 299-306.

# COMPOSITE STRUCTURE

# TABLE OF CONTENTS

## B10.1.0 Introduction

A. Purpose This section presents current composite design information to assist the Structural Designer in determining efficient and reliable aircraft structural elements fabricated from composite material.

B. Concept of Structural Composites The basic concept of filamentary composite structural materials came into being because no single homogeneous structural material existed which was superior in all the desirable properties that dictate the selection of materials for specific applications. Improved homogeneous material systems are continually being developed, but their ultimate potential will always be limited by the fundamental inability to modify some key physical property, or the fundamental difficulty of improving simultaneously two or more contradictory characteristics. Hence, the concept of combining two or more materials to utilize jointly their desirable characteristics was born. Of particular interest are the composites which consist of fibers imbedded within a matrix of essentially homogeneous material (Figure B10.1.0-1).

What has given composite materials a new impetus toward competitive aerospace applications has been the development of new high-strength, high-modulus, low density, continuous filaments, such as graphite and organic aramid (Kevlar); the development of improved matrix materials; the concept of uniaxial, stabilized columnar filament arrays; and finally, the concept of cross plied laminates to tailor material strength and/or stiffness to specific envelopes of requirements (refer to Figure B10.1.0-2).

The incorporation of high-strength, high-modulus, and low-density filaments into a compatible matrix presents a composite material which offers the potential for major breakthroughs in aerospace vehicle design. These materials are classified as "advanced composites".

With advanced filamentary composites, increased design flexibility exists that is not possible with metal structures. Essentially, a new dimension in design has been added. In metal design, the design engineer is merely a material selector, whereas in composites, he becomes a material designer as well.

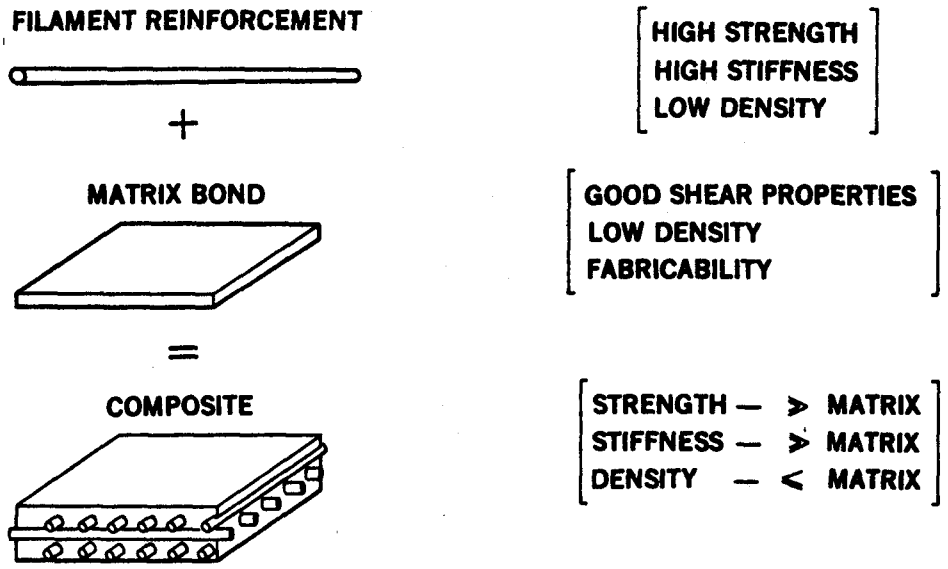


Figure B10.1.0-1 Filamentary Composites

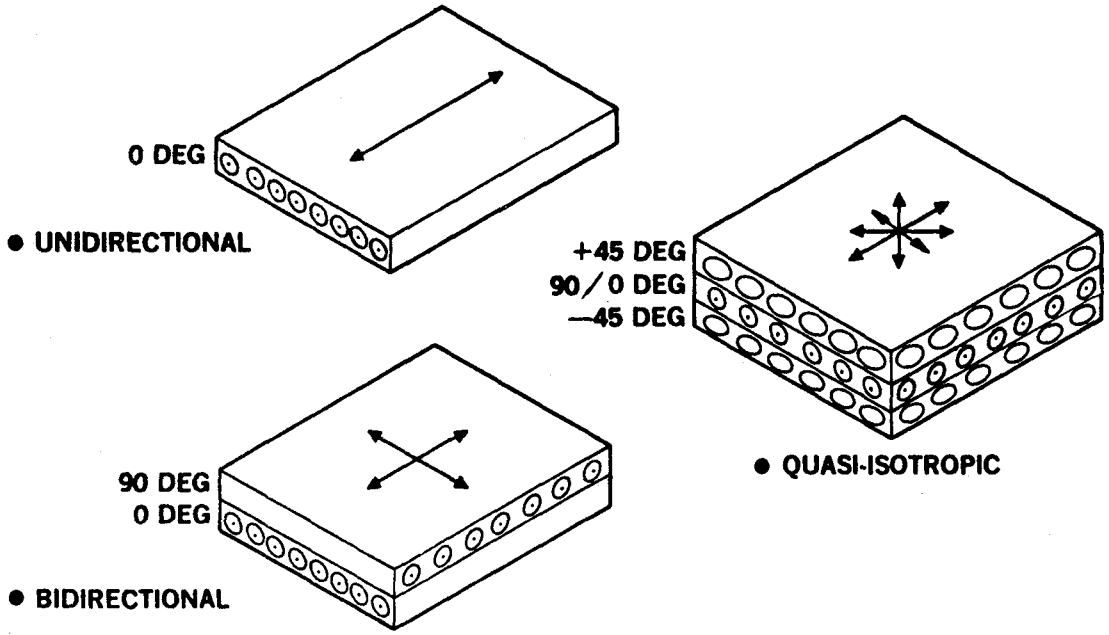


Figure B10.1.0-2 Concept of Cross Plied Laminates

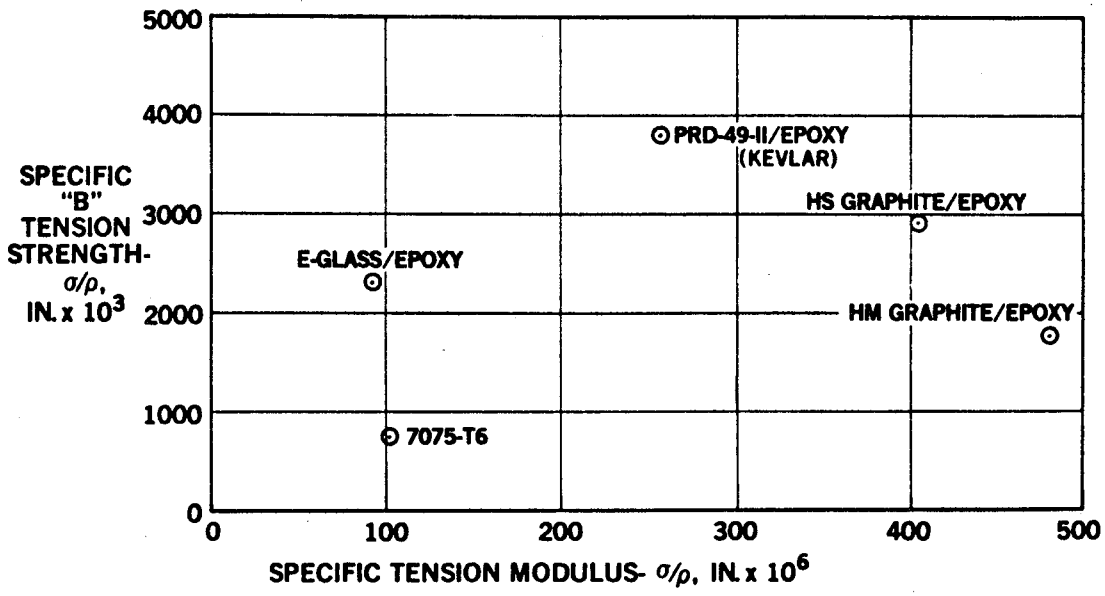


Figure B10.1.0-3 Specific Tension Strength and Modulus for Composite Materials

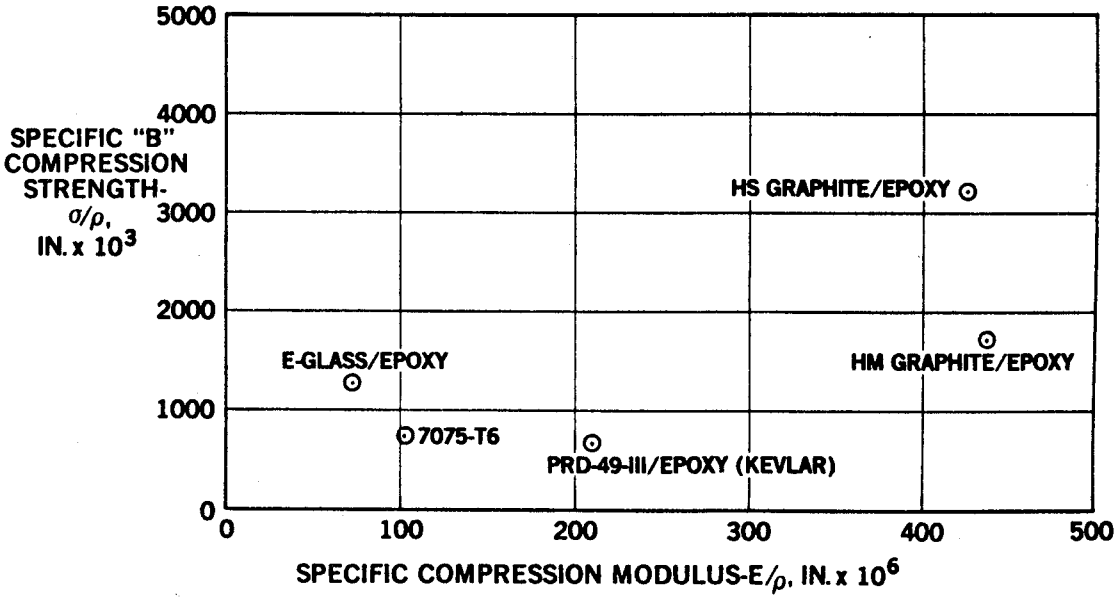


Figure B10.1.0-4 Specific Compression Strength and Modulus for Composite Materials

Composites provides the Structural Designer with the ability to construct a material which will meet specific loads and/or stiffness requirements, without wasting material (and weight), by providing strength and stiffness only where they are needed.

The attractive features of advance composites are:

1. High strength-to-weight and high stiffness-to-weight ratio, as shown in Figures B10.1.0-3 and -4.

2. Ability to tailor the material to minimize weight and meet specific strength or stiffness requirements.

3. Can be fabricated to finished shape and thickness dimensions which require minimal trimming.

4. Excellent fatigue characteristics.

5. Adapatability to integrally stiffened design, eliminating multiple parts and fasteners.

6. Suitability for fabrication of large parts with complex shapes.

## B10.1.1 Glossary of Terms

The following terms are necessary as a basis for understanding composite technology:

A. A-BASIS The "A" mechanical property value is the value above which at least 99 percent of the population of values is expected to fall, with a confidence of 95 percent.

B. ADHESIVE A substance capable of holding two materials together by surface attachment. The term is used specifically to designate structural adhesives, those which produce adhesion capable of transmitting significant structural loads.

C. ADHESION The state in which two surfaces are held together by interfacial forces, which may consist of valence forces, interlocking action, or both.

D. ADVANCED COMPOSITES Composite materials applicable to aerospace construction and made by imbedding high-strength, high-modulus fibers within an essentially homogeneous matrix.

E. ANISOTROPIC Not isotropic; having mechanical and/or physical properties which vary with direction relative to the natural reference axes inherent in the material.

F. AUTOCLAVE A closed vessel for producing an environment of fluid pressure (with or without heat) to an enclosed object while undergoing a chemical reaction or other operation.

G. AUTOCLAVE MOLDING A process similar to the pressure bag technique. The layup is covered by a pressure bag, and the entire assembly is placed in an autoclave capable of providing heat and pressure for curing the part. The pressure bag is normally vented to atmospheric pressure.

H. B-BASIS The "B" mechanical property value is the value above which at least 90 percent of the population of values is expected to fall, with a confidence of 95 percent.

I. B-STAGE An intermediate stage in the reaction of a thermosetting resin in which the material softens when heated and swells in contact with certain solvents, but does not entirely fuse or dissolve. Composites are often precured to this state to facilitate shipping, handling, and processing.

J. BALANCED LAMINATE A composite laminate in which all laminae at angles other than $0^{o}$ and $90^{o}$ occur only in ± pairs (not necessarily adjacent).

K. BLEEDER CLOTH A nonstructural layer of material used in the manufacture of composite parts to allow the escape of excess gas and resin during cure. The bleeder cloth is removed after the curing process and is not part of the final composite.

L. BOND The adhesion of one surface to another, with or without the use of an adhesive as a bonding agent.

M. BUCKLING (COMPOSITE) Buckling is a mode of failure characterized generally by an unstable lateral deflection due to compressive action on the structural element involved. In advanced composites, buckling may take the form not only of conventional general instability and local instability, but also a microinstability of individual fibers.

N. CAUL PLATES Smooth metal plates, free of surface defects, the same size and shape as a composite layup, used immediately in contact with the layup during the curing process to transmit normal pressure and to provide a smooth surface on the finished laminate.

O. CO-CURING The act of curing a composite laminate and simultaneously bonding it to some other prepared surface during the same cure cycle. (See SECONDARY BONDING.)

P. COMPOSITE MATERIAL Composites are considered to be combinations of materials differing in composition or form on a macro-scale. The constituents retain their identities in the composite; that is, they do not dissolve or otherwise merge completely into each other, although they act in concert. Normally, the components can be physically identified and exhibit an interface between components.

Q. CONTINUOUS FILAMENT YARN Yarn formed by twisting two or more continuous filaments into a single, continuous strand.

R. CRAZING The development of a multitude of very fine cracks in the matrix material.

S. CROSS PLY Any filamentary lamina which is not uniaxial.

T. CURE To change the properties of a thermosetting resin irreversibly by chemical reaction; i.e., condensation, ring closure, or addition. Cure may be accomplished by addition of curing (cross linking) agents, with or without catalyst, and with or without heat.

U. CURE STRESS A residual internal stress produced during the curing cycle of composite structures. Normally, these stresses originate when different components of a wet layup have different thermal coefficients of expansion.

V. DELAMINATION The separation of the layers of material in a laminate.

W. DENIER Abbreviation is den.; the weight in grams of 9,000 meters of fiber. This unit of measurement reflects both fiber size and density. For man-made fibers, one-den. fiber is considered "very fine"; 20- to 900-den. fibers are common apparel grades; while fibers in the 1,100-4,400-den. range are usually the high-strength, carpet and engineering grades. Yarn specifications usually include the number of fibers in the strand. A 50/20 yarn, for example, is a 50-den. yarn made from 20 fibers.

X. DISBOND A lack of proper adhesion in a bonded joint. This may be local or may cover a majority of the bond area. It may occur at any time in the cure or subsequent life of the bond area and may arise from a wide variety of causes.

Y. FABRIC A material constructed of interlaced yarns, fibers, or filaments, usually a planar structure. Nonwoven materials are sometimes included in this classification.

Z. FIBER A single homogeneous strand of material, essentially one-dimensional in the macro behavior sense, used as a principal constituent in advanced composites because of its high axial strength and modulus.

AA. FIBER CONTENT The amount of fiber present in a composite. This is usually expressed as a percentage volume fraction or weight fraction of the composite.

AB. FIBER DIRECTION The orientation or alignment of the longitudinal axis of the fiber with respect to a stated reference axis.

AC. FILAMENT A variety of fibers characterized by extreme length, such that there are normally no filament ends within a part except at geometric discontinuities. Filaments are used in filamentary composites and are also used in filament winding processes, which require long continuous strands.

AD. FILAMENTARY COMPOSITES A major form of advanced composites in which the fiber constituent consists of continuous filaments. Filamentary composites are defined here as composite materials composed of laminae in which the continuous filaments are in nonwoven, parallel, uniaxial arrays. Individual uniaxial laminae are combined into specifically oriented multiaxial laminates for application to specific envelopes of strength and stiffness requirements.

AE. FILAMENT WINDING An automated process in which continuous filament (or tape) is treated with resin and wound in a pattern on a removable mandrel.

AF. FILL Yarn oriented at right angles to the warp in a woven fabric.

AG. FILLER A second material added to a basic material to alter its physical, mechanical, thermal, or electrical properties. Sometimes used specifically to mean particulate additives.

AH. FLASH Excess material which forms at the parting line of a mold or die, or which is extruded from a closed mold.

AI. GELCOAT A quick-setting resin used in molding processes to provide an improved surface for the composite; it is the first resin applied to the mold after the mold-release agent.

AJ. GLASS CLOTH Conventionally woven glass fiber material.

AK. HAND LAYUP A process in which components are applied to the mold and the composite is built up and worked by hand.

AL. HOMOGENEOUS Descriptive term for a material of uniform composition throughout; a medium which has no internal physical boundaries; a material whose properties are constant at every point; i.e., constant with respect to spatial coordinates (but not necessarily with respect to directional coordinates).

AM. HORIZONTAL SHEAR The term "horizontal shear" is not an approved nomenclature, but it is included here for information only because of occasional encounters in the literature. Same as INTERLAMINAR SHEAR.

AN. HYBRID A composite laminate comprised of laminae of two or more composite material systems, sometimes integrally woven

AO. INTERFACE The boundary between the individual, physically distinguishable constituents of a composite.

AP. INTERLAMINAR Descriptive term pertaining to some object (e.g., voids), event (e.g., fracture), or potential field (e.g., shear stress) referenced as existing or occurring between two or more adjacent laminae.

AQ. INTERLAMINAR SHEAR Shearing force tending to produce a relative displacement between two laminae in a laminate along the plane of their interface.

AR. INTRALAMINAR Descriptive term pertaining to some object (e.g., voids), event (e.g., fracture) or potential field (e.g., stress) referenced as existing or occurring within a single lamina.

AS. ISOTROPIC Having uniform properties in all directions. The measured properties of an isotropic material are independent of the axis of testing.

AT. LAMINA A single ply or layer in a laminate made of a series of layers.

AU. LAMINATE A product made by bonding together two or more layers or laminae of material or materials.

AV. LAMINATE ORIENTATION The configuration of a cross plied composite laminate with regard to the angles of cross-plying, the number of laminae at each angle, and the exact sequent of the individual laminae.

AW. LAYUP A process of fabrication involving the placement of successive layers of materials.

AX. MACRO In relation to composites, denotes the gross properties of a composite as a structural element, but does not consider the individual properties or identity of the constituents.

AY. MANDREL A form fixture or male mold used for the base in the production of a part by layup or filament winding.

AZ. MATERIAL SYSTEM As used in this section, a specific composite material made from specifically identified fiber and matrix constituents in specific geometric proportions and arrangements and possessed of numerically defined properties.

BA. MICRO In relation to composites, denotes the properties of the constituents; i.e., matrix and reinforcement and interface only and their effect on the composite properties.

BB. MATRIX The essentially homogeneous material in which the fibers or filaments of composite are imbedded.

BC. MOLD RELEASE AGENT A lubricant applied to mold surfaces to facilitate release of the molded article.

BD. MOLDED EDGE An edge which is not physically altered after molding for use in final form.

BE. MOLDING The forming of a polymer or composite into a solid mass of prescribed shape and size by the application of pressure and heat.

BF. ORTHOTROPIC Having three mutually perpendicular planes of elastic symmetry.

BG. POROSITY A condition of trapped pockets of air, gas, or void within a solid material, usually expressed as a percentae of the total nonsolid volume to the total volume (solid + nonsolid) of a unit quantity of material.

BH. PREPREG, PREIMPREGNATED A combination of mat, fabric, nonwoven material, or roving with resin, usually advanced to the B-stage, ready for curing.

BI. QUASI-ISOTROPIC Having properties which are nearly uniform in all directions.

BJ. RESIN An organic material with indefinite and usually high molecular weight and no sharp melting point.

BK. RESIN CONTENT The amount of matrix present in a composite either by percent weight or percent volume.

BL. SANDWICH CONSTRUCTION A structural panel concept consisting in its simplest form of two relatively thin, parallel sheets of structural material bonded to and separated by a relatively thick, lightweight core.

BM. SCRIM (also called GLASS CLOTH, CARRIER) A reinforcing fabric woven into an open mesh construction, used in the processing of tape or other B-stage material to facilitate handling.

BN. SECONDARY BONDING The joining together, by the process of adhesive bonding, of two or more already cured composite parts, during which the only chemical or thermal reaction occurring is the curing of the adhesive itself (see CO-CURING).

BO. SHELF LIFE The length of time a material, substance, product, or reagent can be stored under specified environmental conditions and continue to meet all applicable specification requirements and/or remain suitable for its intended function.

BP. SYMMETRICAL LAMINATE A composite laminate in which the ply orientation is symmetrical about the laminate mid-plane.

BQ. TACK Stickiness of a prepreg.

BR. TOW A loose, untwisted bundle of filaments.

BS. VACUUM BAG MOLDING A process in which the layup is cured under pressure generated by drawing a vacuum in the space between the layup and a flexible sheet placed over it and sealed at the edges.

BT. WARP The longitudinally oriented yarn in a woven fabric (see FILL); a group of yarns in long lengths and approximately parallel.

BU. WET STRENGTH The strength of a composite measured after boiling the test specimen in water. Strength at the appropriate moisture content.

BV. WHISKER A single filamentary crystal. Whisker diameters range from 1 to 25 microns with aspect ratios between 100 and 15,000.

BW. WORK LIFE The period during which a compound, after mixing with a catalyst, solvent, or other compounding ingredients, remains suitable for its intended use.

BX. YARN Generic term for strands of fibers or filaments in a form suitable for weaving or otherwise intertwining to form a fabric.

BY. X-AXIS In composite laminates, an axis in the plane of the laminate which is used as the $0^{o}$ reference for designating the angle of a lamina.

BZ. XY PLANE In composite laminates, the reference plane parallel to the plane of the laminate.

CA. Y-AXIS In composite laminates, the axis in the plane of the laminate which is perpendicular to the X-axis.

CB. Z-AXIS In composite laminates, the reference axis normal to the plane of the laminate.

### B10.1.2 Laminate Orientation Code

It is recognized that one of the outstanding features of filamentary composite structure is its ability, through cross-plying, to be tailored to match individual loading requirements. This being so, it follows that large numbers of individually different cross-plied laminates are likely to be encountered from one application to the next. These laminates are uniquely distinctive in their properties and characteristics. They must be distinctly identified whenever they are to be associated with specific quantitative or numerical data.

A laminate orientation code has been devised for the USAF Advanced Composite Design Guide (Reference B10-1) which provides both concise reference and positive identification for the laminate. This coding system is used in most engineering communications and presentations.

The laminate orientation code, in general use, defines a laminate by indicating the specified orientation angle of each layer in the sequence of the layup through the total thickness of the laminate. For example:

The symmetrical balanced layup shown in B10.1.2-1 is denoted as $[0^{o}/-45^{o}/90^{o}/+45^{o}/0^{o}]_{s}$.

NOTE: The subscript "s" denotes a symmetry about the mid-plane. The use of parentheses in place of brackets is optional for convenience in typewritten text.

Where there is more than one lamina or layer at any given angle, the number of laminae at that angle is denoted by a numerical subscript:

$[0^{o}_{5}/90^{o}_{2}]$ = 5 layers of $0^{o}$ fibers and
2 layers of $90^{o}$ fibers

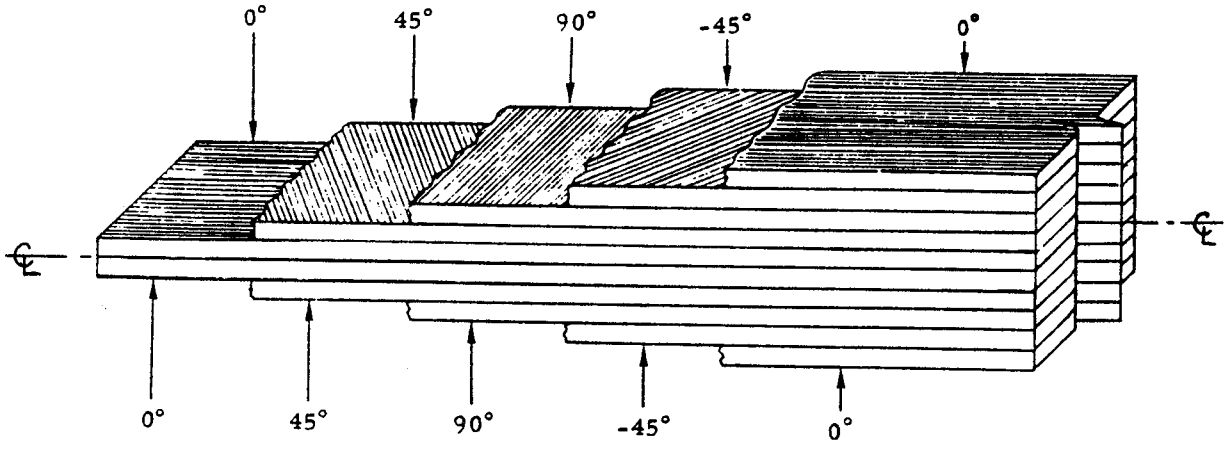


Figure B10.1.2-1 Symmetrical Balanced Layup

The appropriate laminate orientation coding at Douglas Aircraft Company is shown in Drafting Manual Section 11.448.

Note, also, that there is a difference in drawing procedure, depending on whether the part is to be manually or automatically cut and collated.

## B10.2.0 Composite Material Systems

### B10.2.1 Fiber Characterization

The fibers most commonly used in advanced composite structures are high-strength graphite and aramid (Kevlar). Other fibers, such as boron filaments, sapphire whiskers, high-modulus graphite fibers, and silicon carbide fibers have been or are being investigated.

A. Graphite Fibers Graphite filaments are made by graphitizing tows or bundles of organic precursor filaments; the most predominant fiber today is made from polyacrylonitrile (PAN), although rayon and pitch are used to some extent. The graphitizing process, which is schematically diagrammed in Figure B10.2.1-1, is currently conducted in three modes to produce the three types of graphite filaments currently in large-scale production. These filaments are designated herein as intermediate-strength, high-strength, and high-modulus. The processes may differ slightly for the new ultra-high-modulus filaments (E = 70 - 75 Msi). These are, however, still in the experimental or developmental stages.

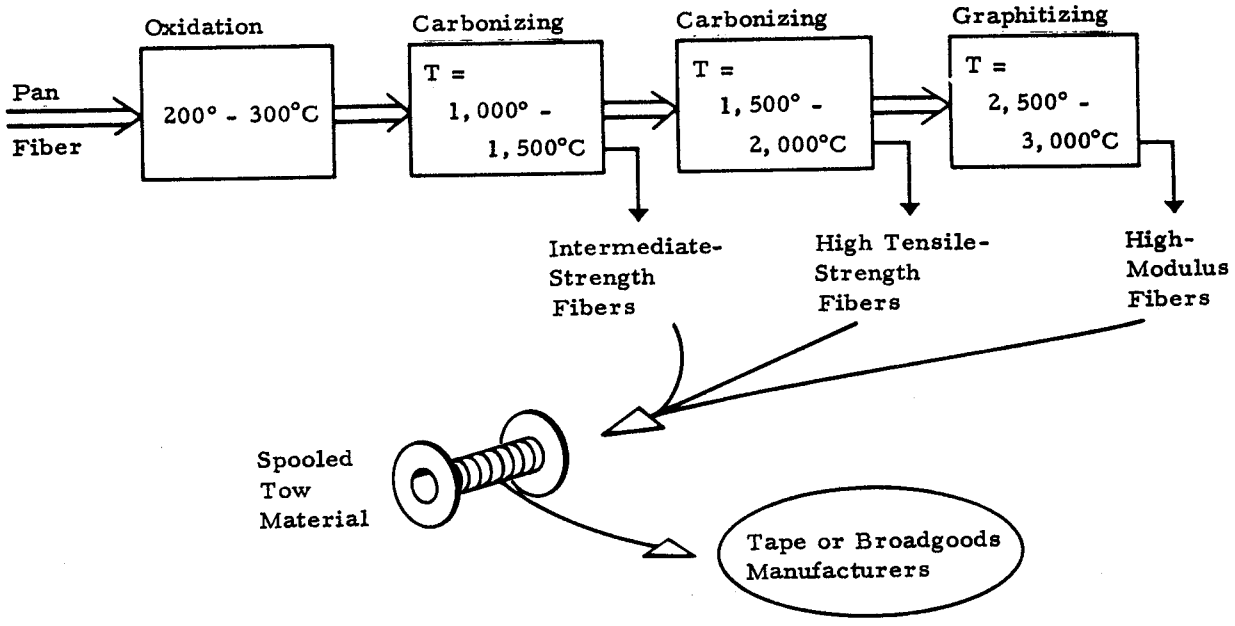


Figure B10.2.1-1 Graphite Filament Manufacture

Production graphite filaments are normally produced and furnished in twist-free tows of 10,000 fibers, both in batch or short staple form (48 inches) and continuous lengths (up to 3,000 feet). The properties of the three types of graphite filament are compared in Figure B10.2.1-2 where it should be noted that high-strength graphite fibers have the best compromise of properties. They are therefore used for aircraft structural design.

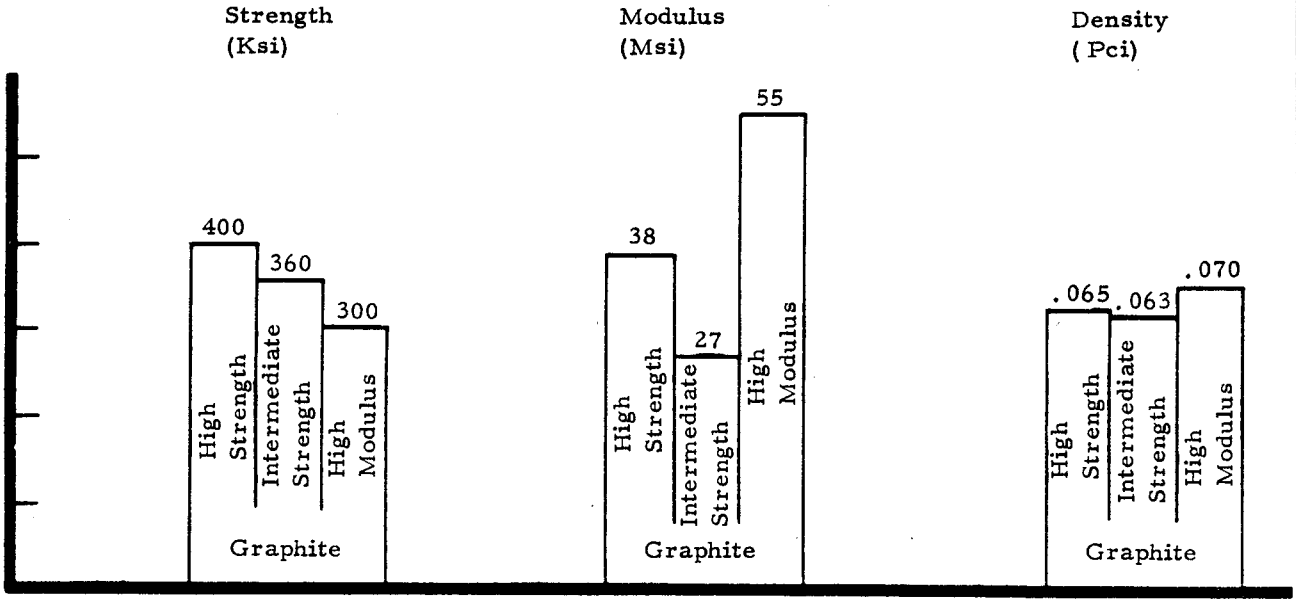


Figure B10.2.1-2 Fiber Properties (Typical)

A summary of properties for high-strength graphite fibers follows:

1. Graphite Fiber: graphitized from polyacylonitrile (PAN).
2. Nominal Fiber Diameter: 7-8 microns (.000295 in.).
3. Nominal Density: 1.74 specific gravity (0.0628 lbs./in.$^3$).
4. Tensile Strength: 400,000 psi.
5. Modulus: 35 x $10^6$ psi.
6. Elongation at Failure: 1.1%.

B. Aramid (Kevlar 49) Kevlar is DuPont's registered trademark for one member of its family of aramid fibers. It has a very high specific tensile strength (tensile strength divided by density). The specific tensile modulus of Kevlar 49 fiber is higher than that of fiberglass and aluminum, but not as high as for graphite or boron fibers. A summary of properties for aramid (Kevlar 49) fibers follows:

1. Fiber: made from polybenzimidozole (PBI), DuPont material.

2. Nominal Fiber Diameter: 12 microns (.0047 in.).

3. Nominal Density: 1.44 specific gravity (0.052 lbs./in.$^3$).

4. Tensile Strength: 400,000 psi.

5. Modulus: 18 x $10^6$ psi.

6. Elongation at Failure: 2.5%.

C. Fiberglass (Glass Compositions) E glass and S glass are the principal glass compositions for aerospace reinforcements. E glass, based on lime-alumina-borosilicate, is more common and most woven fabrics are made from this glass. S glass, a silica-alumina-magnesia composition developed for improved tensile properties, is used mainly as roving or other non-woven forms, and to a lesser extent as a woven fabric. Nearly all current glass filaments used to reinforce plastic moldings are drawn from a E glass melt composition. These continuous filaments (approximately 0.0003 inch in diameter) when twisted together into yarns for continuous winding or when woven into fabrics are treated (or finished) with surface active agents (silane complexes) to promote water resistance and adhesion to resin binders. The commercial numbers (e.g., 181, 143, etc.) assigned to glass fabric possess no material code significance and only identifies the weave pattern.

A summary of properties for E glass fibers follows:

1. Fiber: made from $SiO_2$ with $B_2O_3$ and other metallic oxides.

2. Nominal Fiber Diameter: 7-8 microns (.00030 in.).

3. Nominal Density: 2.54 specific gravity (.092 lb./in.$^3$).

4. Tensile Strength: 500,000 psi.

5. Modulus: $10.5 \times 10^6$ psi.

6. Elongation at Failure: 4.8%.

B10.2.2 Matrix Resin Material Characterization

The organic matrix resins most commonly used in aircraft structures are modified epoxy resins available as commercial formulations developed specifically for this purpose. For high-temperature applications (above 180°F), or where smoke or toxicity requirements exist, other organic resins such as polyimides and phenolics may be used. Thermoplastic resins such as polysulfones are being developed to take advantage of their post-forming capabilities. In the area of metal matrix, aluminum alloy and titanium matrix materials are the most likely choices for subsonic applications. The general characteristics for modified epoxy and polyimide matrix systems are tabulated in Table B10.2.2-1.

Table B10.2.2-1 Matrix Systems - General Characteristics

| Matrix Material | Maximum Service Temperature Range* | General Characteristics |
|---|---|---|
| Modified Epoxies | 120°F Continuous | Thermosetting resin utilized with very low laminating pressure (15 psi) and requiring a minimum of 250°F cure. |
| | 180°F | Thermosetting resin utilized for low laminating pressure (15 psi) requiring a minimum of 350°F cure. |
| Polyimide | 600°F Continuous<br>700°F Intermittent | Thermosetting resin requiring 350° to 600°F cure, plus an extended post-cure. The pressure required is usually about 200 psi. The polyimide resin family is characterized by high cost, difficult processing, good dielectric properties, and low cured laminate outgassing. |

*Minimum service temperature range is cryogenic.

B10.2.3 Laminate Fabrication

The preimpregnated raw material is manufactured by thoroughly coating or impregnating the properly spaced fiber tows with the matrix resin material. The basic sequence involved in the fabrication of tape and broadgoods, including laminate fabrication, is shown in Figures B10.2.3-1 and B10.2.3-2. The raw material forms and fabrication processes are defined in detail in DAC Process and Material Specifications (DPS and DMS). They are:

| | |
|---|---|
| DPS 1.04-14 | Instruction for Fabrication "B" Stage Control Flow Fiberglass or Kevlar Face Sheet with Honeycomb Core |
| DPS 1.621 | For Thermal Expansion Molded Parts |
| DPS 1.622 | For Autoclave Molded Parts |
| DMS 1926 | Material Spec for "B" Stage Control Flow Fiberglass or Kevlar Face Sheet with Honeycomb Core |
| DMS 1936 | Material Spec for Unidirectional Graphite Prepreg Tape and Epoxy |
| DMS 2163 | Material Spec for Prepreg Graphite Fabric and Epoxy |

B10.3.0 Applications

Composite structures are considered for new designs because of the high cost of fuel which has placed renewed emphasis on weight savings. Composite structures are also. Figure B10.3.0-1 indicates the composite applications to be considered for new DAC transport aircraft. Primary structures made from composites are still in the development stages. The usage of composites to replace production components on in-service DAC aircraft has been considered. Although the weight saving is good (15-25 percent), cost considerations have generally prevented the usage.

At DAC, the philosophy for the usage of composite structure has been to give priority development to secondary structure and control surfaces because of lower development costs, lower risk, favorable economic tradeoffs, and earlier commitment to production. Our plan has been to place in service a limited number of composite components in order to provide manufacturing cost data and provide the airlines with maintenance and repair experience. These data, which to date have been positive, will ensure the success of composite applications on new DAC aircraft.

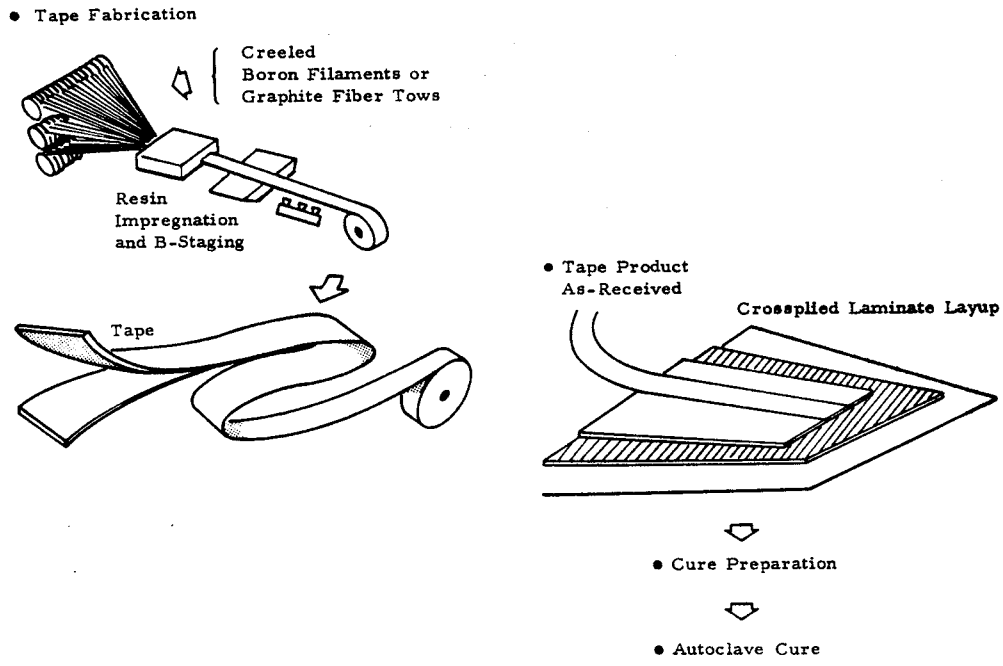


Figure B10.2.3-1 Graphite/Epoxy, Tape, and Laminate Fabrication Process

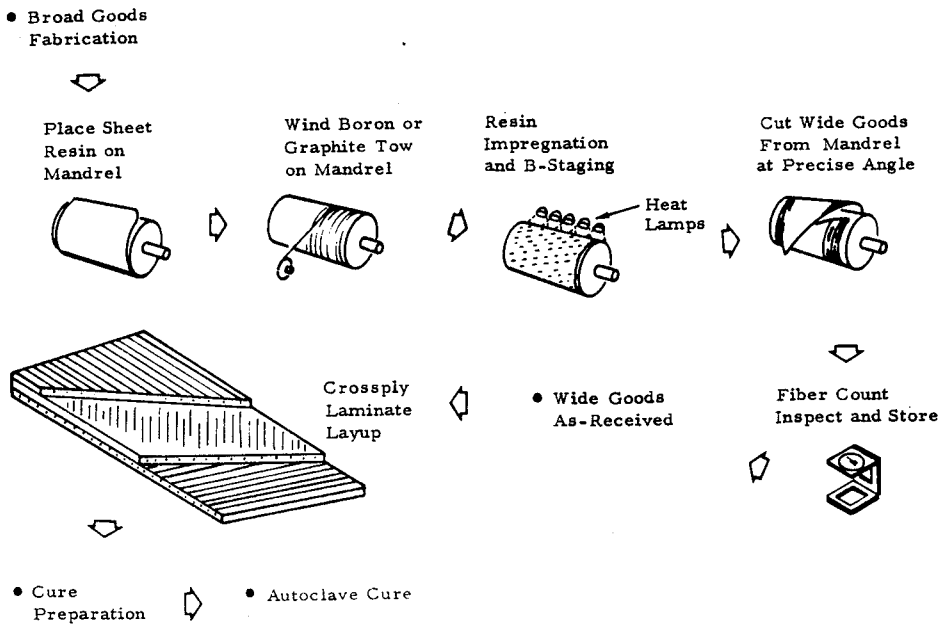


Figure B10.2.3-2 Graphite/Epoxy Fiber Broadgoods and Laminate Fabrication Process

Figures B10.3.0-2 and B10.3.0-3 show the composite structure which has been placed in service on the DC-9 and DC-10. On the DC-9, the Kevlar tailcone and Super 80 nacelles are production items. Figures B10.3.0-4 through B10.3.0-12 provide details of the various DC-9 and DC-10 composite structural components.

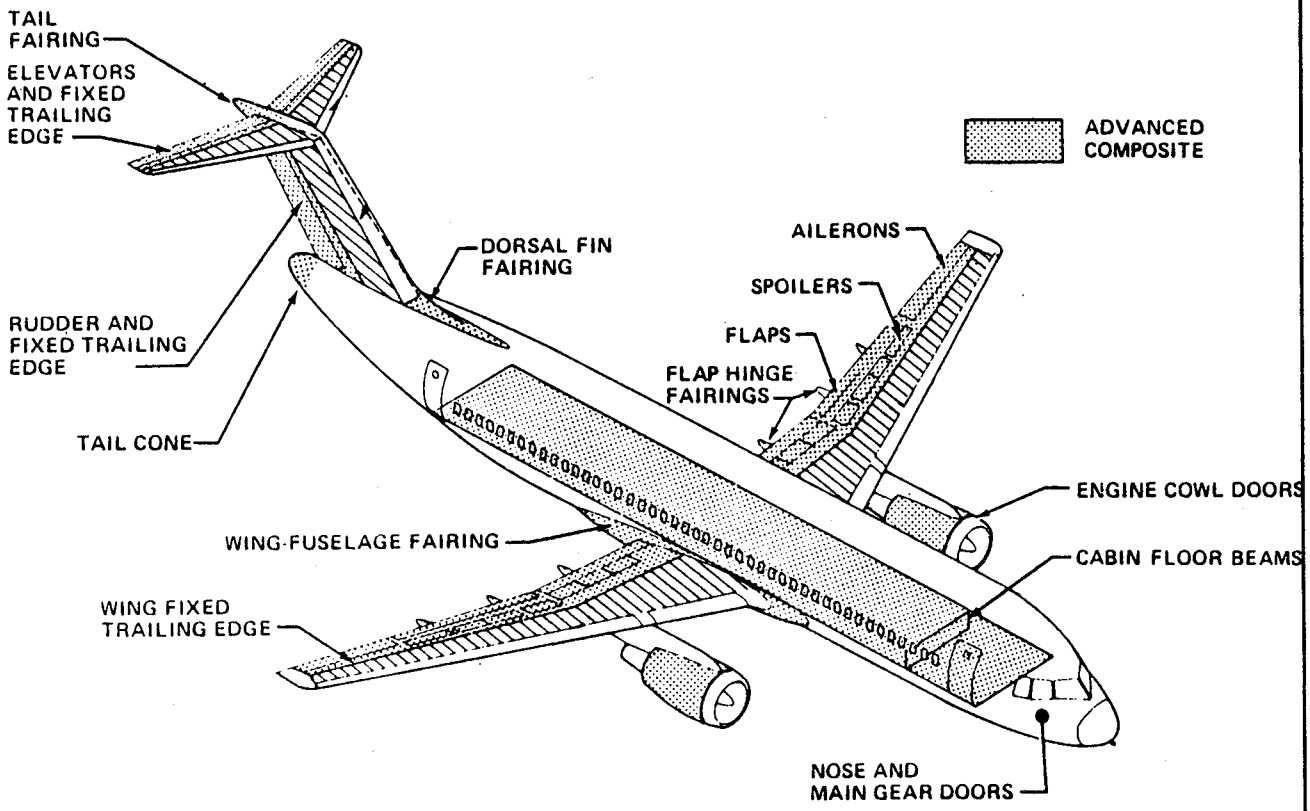


Figure B10.3.0-1 Advanced Composite Applications on New DAC Aircraft

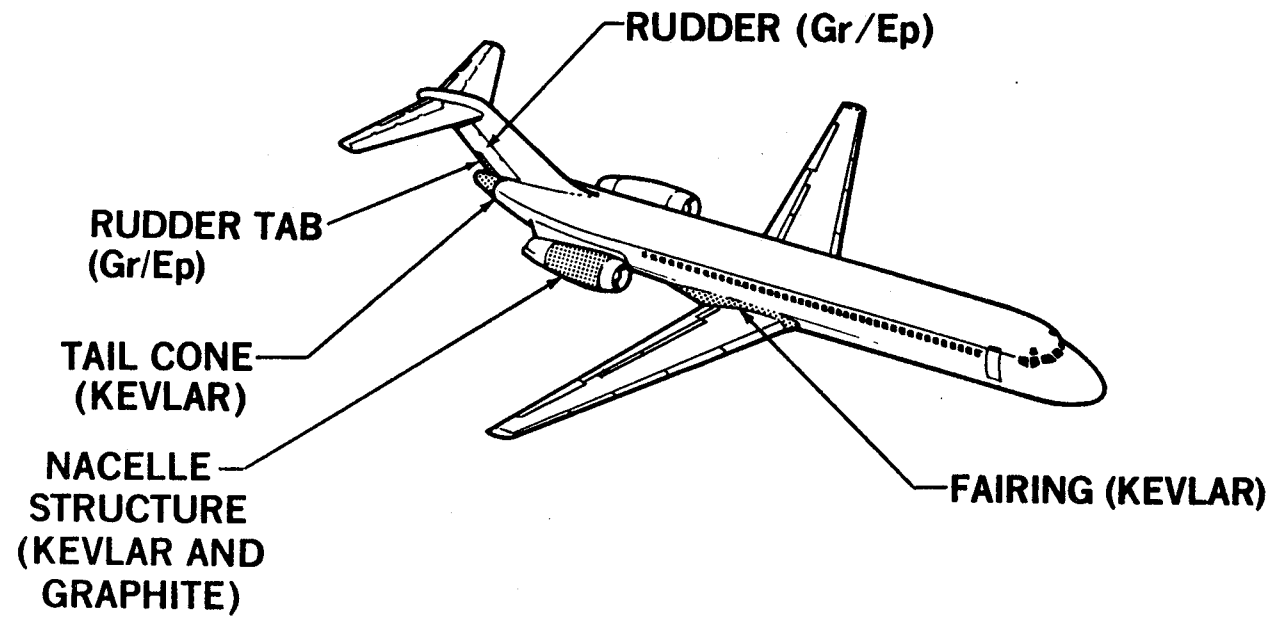


Figure B10.3.0-2 Composite Applications on the DC-9

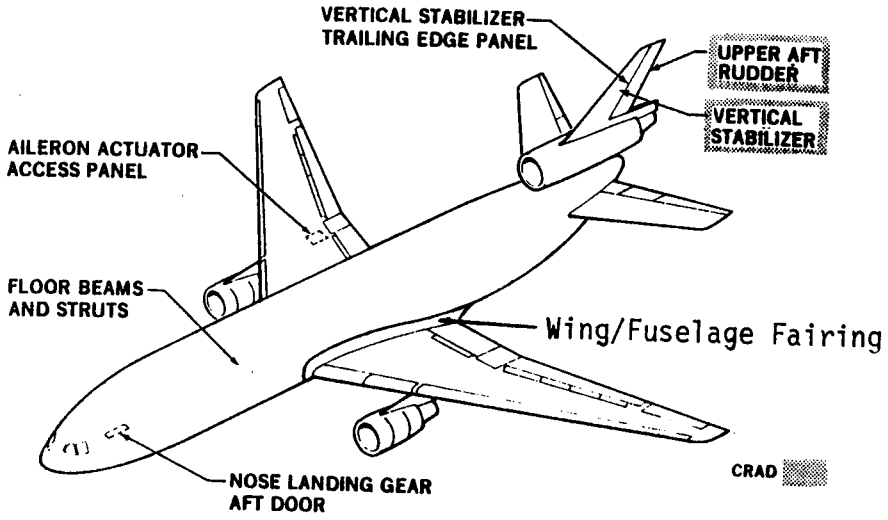


Figure B10.3.0-3 Composite Applications on the DC-10

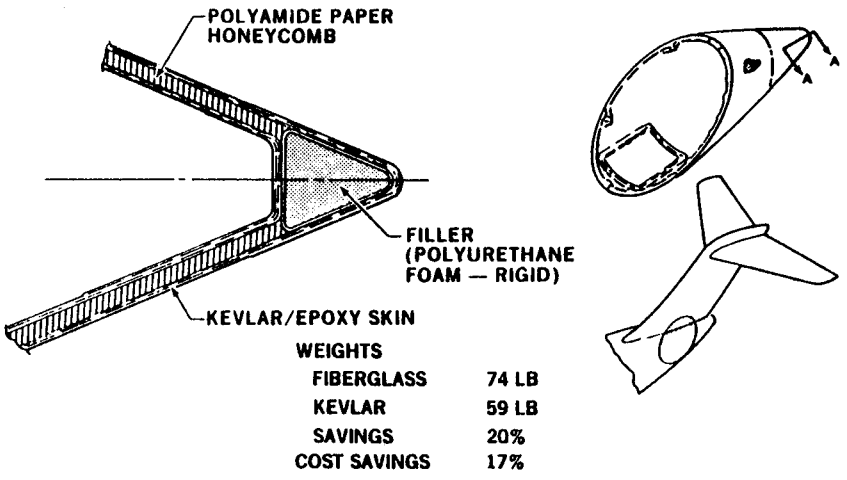


Figure B10.3.0-4 DC-9 Fiberglass Tailcone

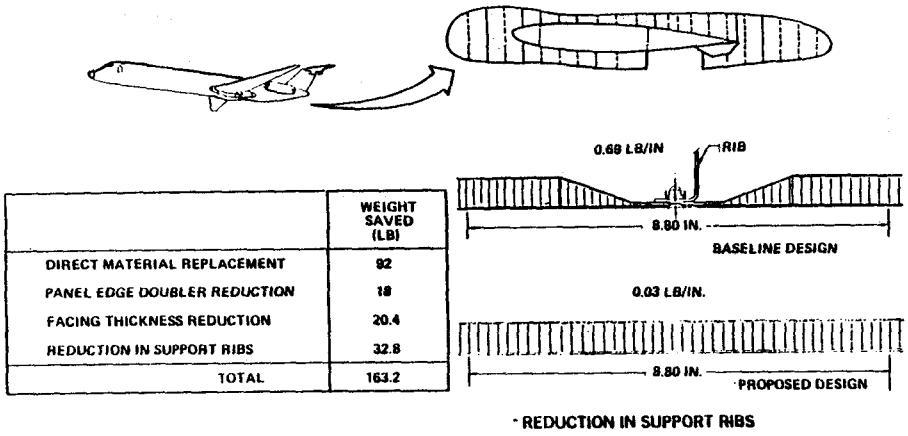


| | WEIGHT SAVED (LB) |
|---|---|
| DIRECT MATERIAL REPLACEMENT | 92 |
| PANEL EDGE DOUBLER REDUCTION | 18 |
| FACING THICKNESS REDUCTION | 20.4 |
| REDUCTION IN SUPPORT RIBS | 32.8 |
| TOTAL | 163.2 |

* REDUCTION IN SUPPORT RIBS

Figure B10.3.0-5 DC-9 Wing/Fuselage Kevlar Design

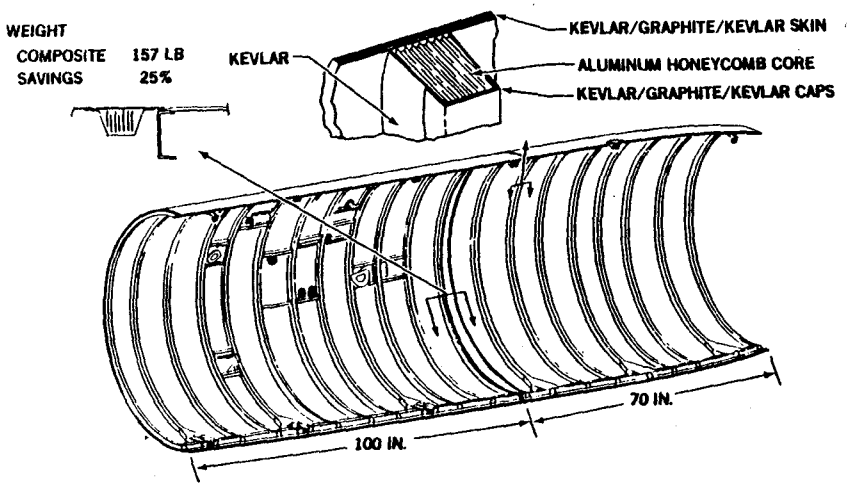


Figure B10.3.0-6 DC-9 Super 80 Lower Composite Access Doors

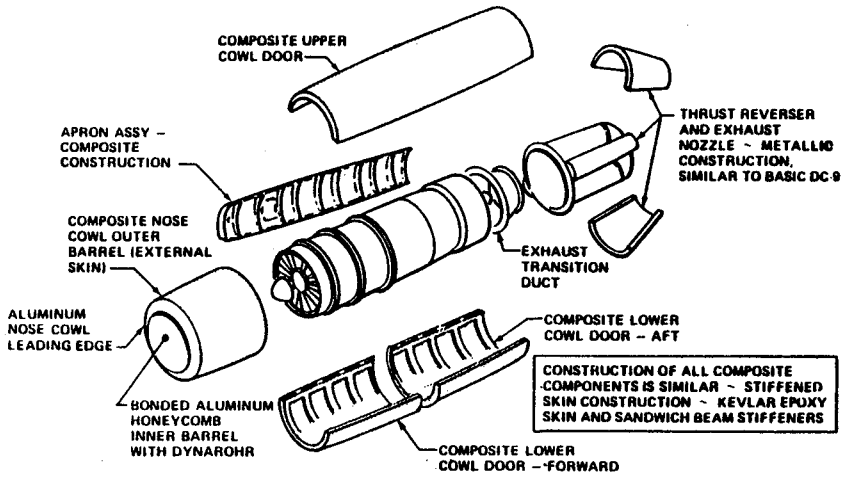


Figure B10.3.0-7 DC-9 Super 80 Composite Nacelle Construction

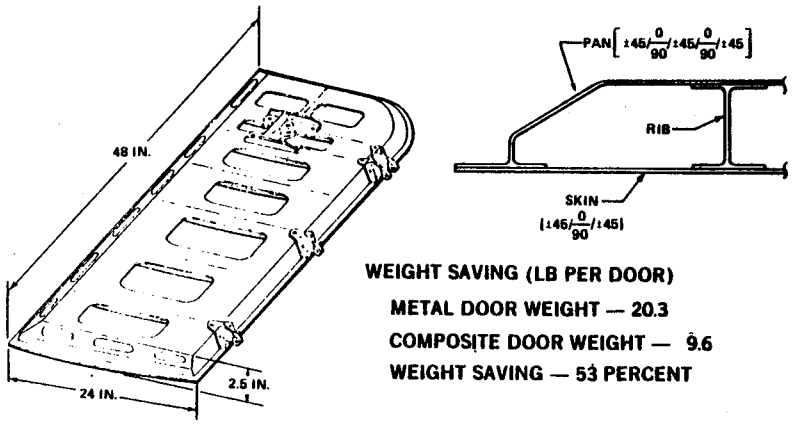


Figure B10.3.0-8 DC-10 Composite Nose Landing Gear Aft Door

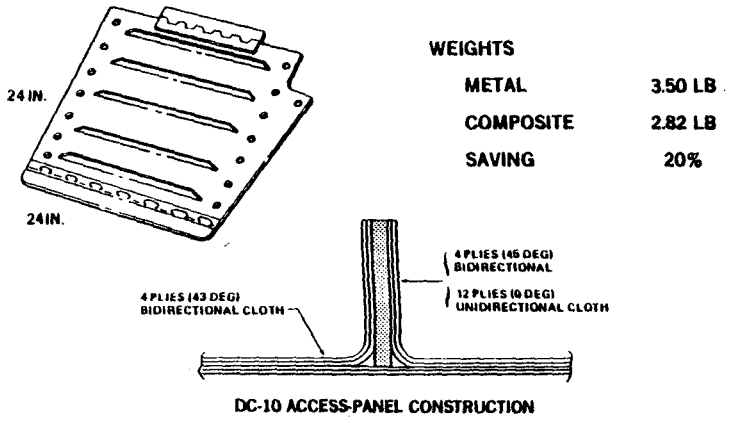


Figure B10.3.0-9 DC-10 Composite Aileron Actuator Access Panel

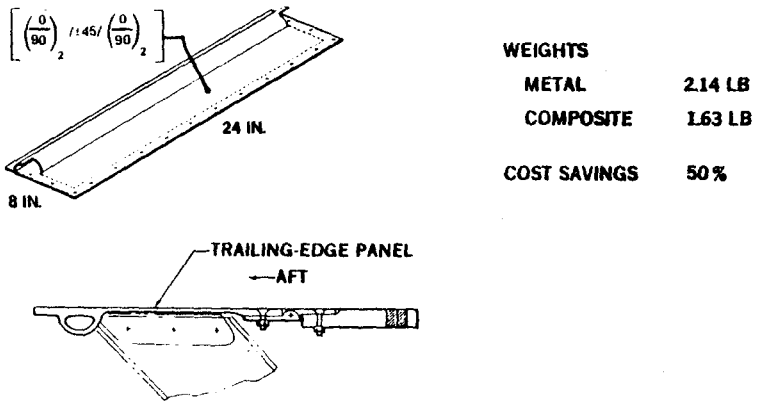


Figure B10.3.0-10 DC-10 Composite Vertical Stabilizer Trailing Edge Panel

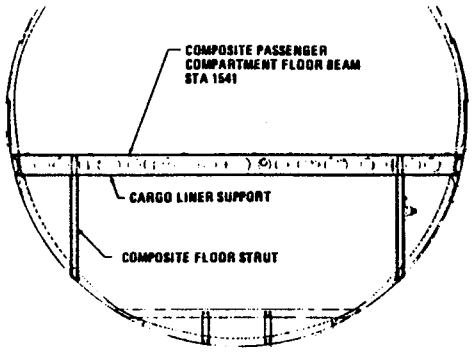


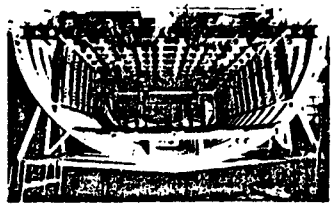

BEAM INSTALLATION IN AIRPLANE FUSELAGE

**WEIGHTS**

| | |
|---|---|
| **METAL** | **31.95 LB** |
| **COMPOSITE** | **23.50 LB** |
| **SAVINGS** | **26%** |

Figure B10.3.0-11 Composite Floor Beam and Strut

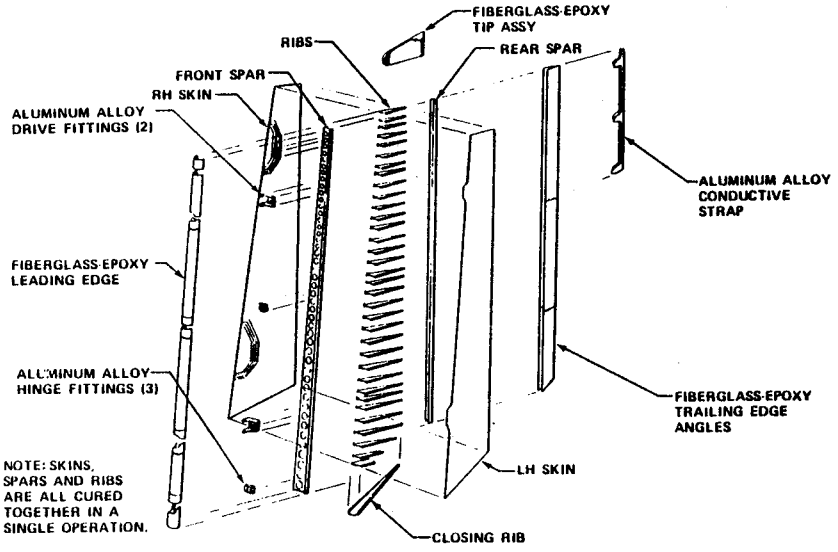


Figure B10.3.0-12 Graphite Rudder

## B10.4.0 Composite Design Consideration

### B10.4.1 Composite Laminate Characteristics

The advanced composite materials discussed in this section are uniaxial in their single-ply state. Their unidirectional states have very high mechanical properties along the longitudinal axis and low-to-moderate properties along the transverse axis. This is the primary difference, from a structural design standpoint, between advanced composites and metals. Fiberglass is not considered an advanced composite, but its characteristics, discussed in this section, are the same.

Metals are normally homogeneous and isotropic in nature, and their reaction to an applied load can be defined by knowing two of the three basic elastic constants (E, G and $\mu$). A basic unidirectional lamina, or any balanced symmetric laminate, on the other hand, is orthotropic in nature, having three mutually perpendicular planes of elastic symmetry. For planar applications, this type of material can be defined by four of the five basic elastic constants for orthotropic materials ($E_T$, $E_L$, $\mu_{LT}$, $\mu_{TL}$, $G_{LT}$). Note that $G_{TL} = G_{LT}$ and $\mu_{TL} = \frac{E_T}{E_L}\mu_{LT}$ for orthotropic materials.

There are twice as many independent planar elastic constants for orthotropic materials as for isotropic materials because of the different properties in the planes of symmetry. For many composite applications, the laminate is not even orthotropic, but is anisotropic. This happens when an orthotropic laminate is loaded in a direction which does not coincide with one of its principal axes, or when the laminate layup is symmetric, but not balance about its principal reference axis. A (0/±45/90) laminate is orthotropic and balanced when loaded in the $0^o$ or $90^o$ direction, while a (0/+45) laminate is not balanced and is anisotropic. This latter type of laminate requires six elastic coefficients for definition; $G_{TL} \neq G_{LT}$.

One other type of laminate is possible and occurs when the laminate is neither balanced nor symmetric about its mid-plane. This is called a coupled laminate because of the coupling of the shear stresses and the normal stresses (i.e., one will produce the other).

A coupled laminate requires 18 elastic coefficients for definition. In this type of laminate, in-plane applied loads produce out-of-plane distortions, which in turn cause the laminate to warp out of plane. As a general rule, all laminates should be symmetrically laid up about their mid-plane; coupled laminates should be avoided.

Unbalanced laminates are used beneficially in aeroelastic tailoring and should not be excluded. Figure B10.4.1-1 shows schematically the difference between the different types of laminates discussed, while B10.4.1-2 shows the differences between a symmetric laminate and one which is not symmetric. Refer to Section B10.7.2 for specific laminate orientation requirements.

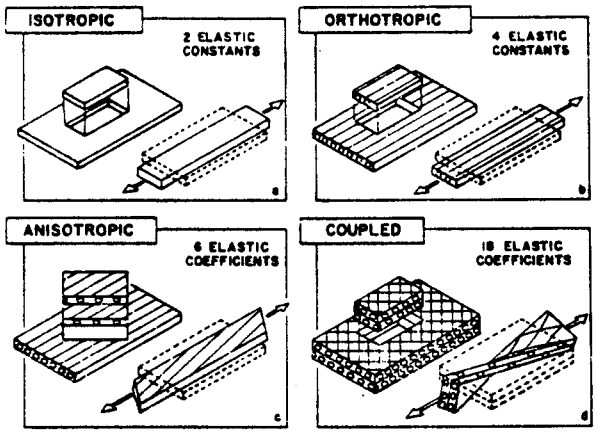


Figure B10.4.1.1 Composite Laminate Types

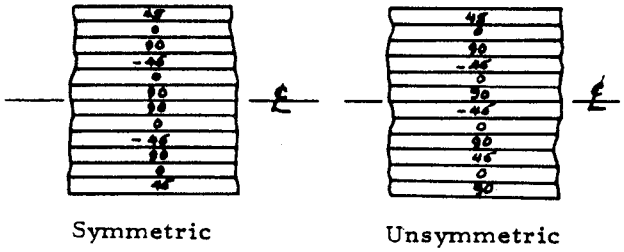


Figure B10.4.1-2 Laminate Symmetry

The directional nature of composite laminae provides the Structural Designer with the capability to construct a material which will meet specific loads and/or stiffness requirements by providing strength and stiffness only where they are needed. If the design requirement is simply to provide axial strength or stiffness, the majority of the material should be unidirectionally oriented. If this material is enclosed in some restraining member, such as shown in Figure B10.4.1-3, all of the material may be so oriented. If the composite material is unconfined, a nominal amount of transverse reinforcement must be provided to account for any off-axis loading that may occur, either

during fabrication or by applied loading. An example of such an unrestrained application would be any plate or skin, whether or not it is on an elastic base, or a stiffener application which is totally composite. A rule-of-thumb is to make the number of laminae in the transverse direction equal to 10 percent of the total number of laminae in the part. ($\pm 45^{o}$ shear panels are frequently an exception to this rule.)

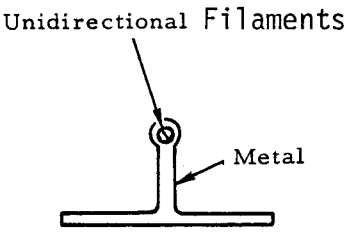


Figure B10.4.1-3 Restrained Unidirectional Applications

If shear loading or shear stiffness is the primary design consideration, then most of the material should be oriented at $\pm 45^{o}$ to the longitudinal axis, as this provides the highest shear properties. Care must be taken to evaluate any loading in the longitudinal or transverse directions, since the strength in these directions is quite low. Conditions, which would not normally be critical in metal design, may approach or exceed the strengths available in these directions when using a pure ($\pm 45$) layup. This consideration may necessitate the inclusion of $0^{o}$ and/or $90^{o}$ laminae.

In addition to the pure axial or pure shear cases there are many applications which require the ability to withstand a combination of loadings. Although it is possible to determine an optimum orientation sequence for any given loading condition, it is more practical to limit the number of orientations to a few specific families.

The only family that will be presented in this section is $[0_i/\pm 45_j/90_k]$. Members of this family will generally be able to match, with a reasonable degree of efficiency, any loading or stiffness requirements.

B10.4.2 Mechanical Property Considerations

A. Static Properties As with metals, static composite mechanical properties have been developed for the standard types of loading, such as tension, compression, and shear. Unlike metals, however, the anisotropy of advanced composite materials causes these properties to change with direction in respect to the major longitudinal axis. Test data are usually obtained for two directions: $0^{o}$ and $90^{o}$ to the principal axis of the laminate, with occasional testing at $45^{o}$. From these data, biaxial strength envelopes have been established analytically for any laminate orientation. These data are sufficient for a static, room temperature design. Static properties must include degradation due to environmental factors.

B. Elevated Temperature Properties The epoxy-based matrix materials are used in applications up to $180^{o}$F and it is these materials for which the greatest amount of data are available. For the temperature range above $180^{o}$F polyimide resins and phenolic aluminum resins are being used. These present greater fabrication problems, mainly because of outgassing during cure. They are, however, viable materials even though considerable development and data generation remain.

C. Fatigue Properties The fatigue data thus far generated on advanced composite materials have been mostly constant load amplitude data from which S-N curves have been developed. In most cases, these S-N curves are relatively flat, indicating a good resistance to fatigue damage, see Figure B10.4.2-1. This is generally attributed to the apparent crack-stopping ability of fiberous materials.

D. Damage Tolerance Properties The high-strength and stiffness properties of many composite materials make them very desirable for structural applications which require high structural efficiency. However, the material is brittle and has relatively low strength after being damaged. This low fracture strength is a serious consideration in the design and verification of structural integrity of advanced composite components. At present there is research being performed by many manufacturers of composites to develop a matrix material that will reduce this brittle nature. Different fiber material combinations are also being looked at. For design, it is normal practice to satisfy stringent damage tolerance requirements by limiting the design ultimate strain (refer to Section B10.6.0).

E. Thermal Coefficient of Expansion Aside from the standard reduction in mechanical properties at elevated temperature, composites also exhibit dimensional alterations with changes in temperature, as do isotropic metallic materials. The coefficient of thermal expansion $\alpha$ has different values for different directions within a laminate, as well as different values for different laminate orientations. The value of the coefficient, especially in organic matrix composites, is almost entirely filament-governed. For graphite/epoxy laminates, the coefficient approaches zero in filament directions; refer to Figure B10.4.2-2 for a general comparison of composite $\alpha$ to metal $\alpha$. Induced thermal stresses and deformations must be accounted for in designs which combine composites and metals and are expected to encounter elevated or reduced temperatures in service because of the large differences in thermal coefficient of expansion. (Refer to Section D6.0.0, Temperature Loads and Requirements.) Dimensional changes also occur with moisture, but these are not normally considered during early design phase.

In addition to the thermal stresses which are caused by temperature changes occurring in the normal service life of an aircraft, the thermal stresses caused by the actual fabrication of the part must be considered. These stresses can be caused either by the use of differing materials in a wet layup cure or by the difference in thermal properties between the tooling and the part material. These differences not only cause internal stresses, but can result in parts which have a significant amount of warpage even though the part itself may be a symmetrical layup.

F. Environmental Effects There are four (4) major differences between metal structures and advanced composite organic matrix materials with respect to their response to physical exposure.

1. Exposure of the matrix material to ultraviolet light results in chemical changes and usually leads to degradation of the mechanical properties of the composite. This problem can be greatly alleviated by painting the exposed surfaces.

2. Exposure of the matrix material to a number of physical agents, such as rain, hail, salt water, fuels, and other erosive or corrosive elements causes a loss in strength. Metals are also subject to some strength loss from this type of exposure, but the composite materials are affected to a much greater extent. The effectiveness of painting the exposed surfaces to reduce this degradation is still being investigated.

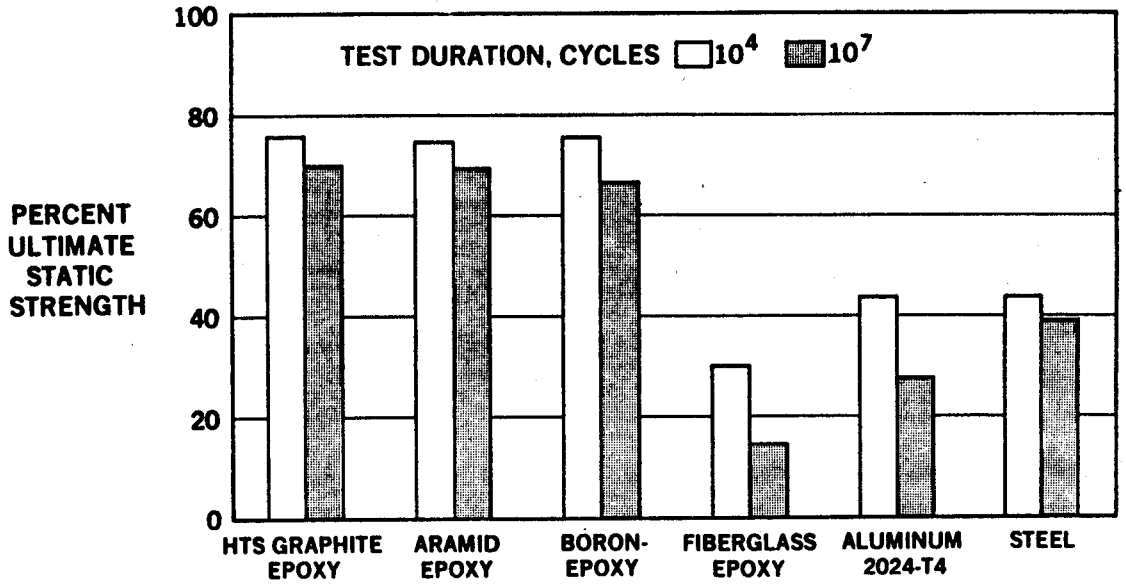


Figure B10.4.2-1 Fatigue Resistance of Materials

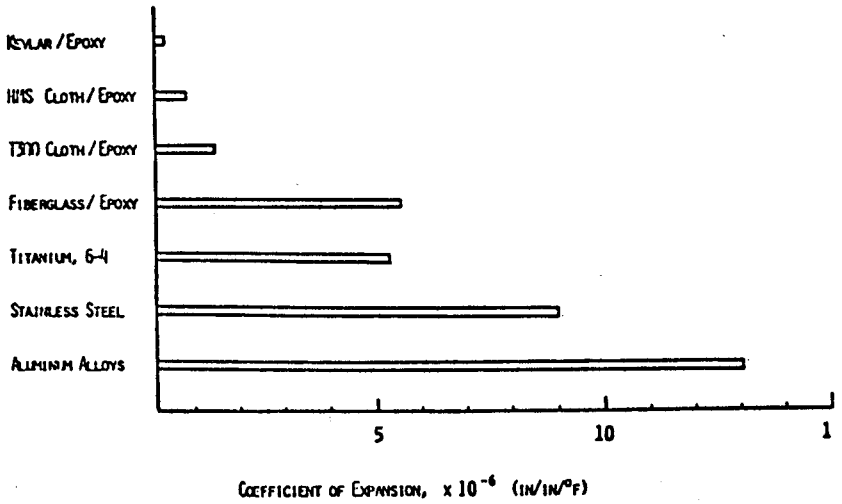


Figure B10.4.2-2 Thermal Expansion Characteristics

3. Graphite filaments are very low conductors, while Kevlar and fiberglass are non-conductors in comparison to metallic structures. This results in structures that are susceptible to severe damage from lightning strike, and also permits the buildup of dangerously large static charges. This low conductivity also presents a problem in the shielding of sensitive electronic equipment from electromagnetic interference.

   Several methods to protect composite structures are available. One such method is to coat the composite exterior surface with aluminum. The designer should become familiar with lightning problems, discussed in Section D8.0.0 and then contact the Atmospheric Physics group in Avionics for their assistance in evaluating the composite design with respect to lightning strikes and electrical static discharge.

4. There is the potential for galvanic corrosion between metals and composites. The magnitude of this corrosion potential with respect to the commonly used aircraft metals is shown in Figure B10.4.2-3. Galvanic corrosion must be evaluated with respect to the attachments used as well as with the adjoining metallic surface interface (refer to Section D7.0.0, DM 11.456, and consult with M&PE).

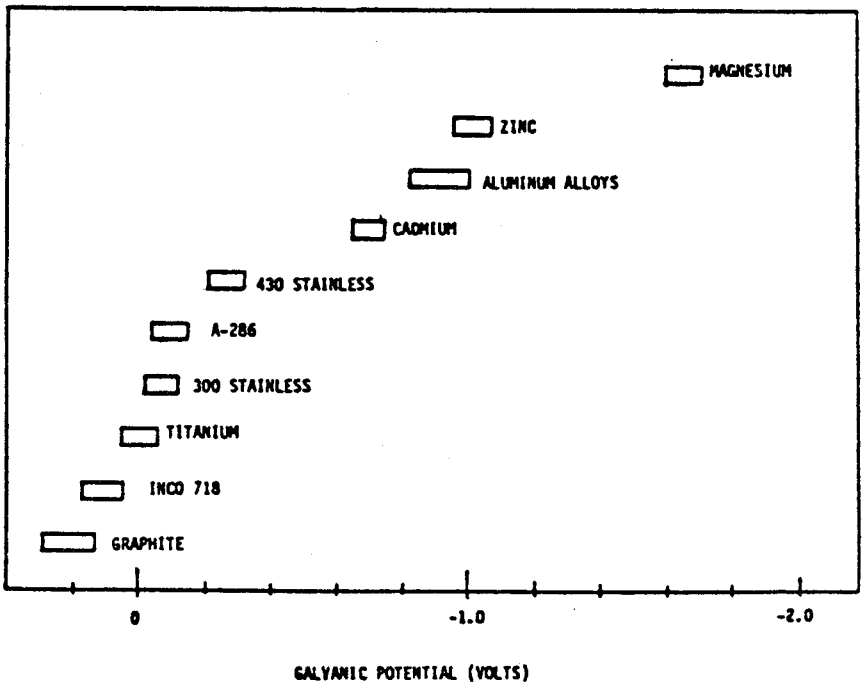


Figure B10.4.2-3 Galvanic Potential in Sea Water

B10.4.3 Characteristics of Joints

As with metal structure, two major joining techniques are employed to join advanced composite structure; mechanical fastening and adhesive bonding. The response of advanced composites to these methods is somewhat different from that of metal structures. In general, it is more structurally efficient to use bonded joints wherever possible because of the stress concentrations associated with fastener holes. However, there are many cases where the design requirements dictate a mechanical attachment, such as fail-safe and lightning protection. Considering the current state-of-the-art, there are situations where the inspectability of the bond is not adequate to provide a sufficient confidence level in the fabricated bonded joint. Therefore, the designer must be aware of the advantages and disadvantages of both adhesively bonded and mechanically fastened joints, in order to select the proper joining method for the specific application.

A. Adhesive-Bonded Joints (See Section C11.0.0 for Detailed Discussion.) There are a number of ways to bond two parts together. The most efficient methods always puts the adhesive bond surface in shear. The choice of type of joint to use is usually determined by physical constraints, the magnitude of the load to be transferred, and the manufacturing complexity that can be accepted. Those joints in which the adherends are tapered in some manner are more efficient than those, such as the single lap, which are not. In this respect, composites lend themselves to stepped joints or tapered joints because the built-up laminae can be ended very simply to form the step, whereas metal stepped joints require expensive machining.

B. Mechanically Fastened Joints Although many assembly problems can be solved by using adhesive bonding techniques, there are a number of cases where only mechanical joints are capable of meeting design requirements.

Unlike most metals, which are comparatively ductile, the majority of advanced composite materials and orientations are very brittle, being elastic almost to failure. This lack of ductility magnifies the local stress concentrations at the fastener holes and exerts a dominant influence on the magnitude of the allowable design tensile stress. Generally, only 35 to 50 percent of the basic laminate ultimate tensile strength is developed in the area of a mechanical joint. Methods of increasing this strength are available, depending on the strength required, and on whether the hole is a loaded or an unloaded hole.

In the unloaded hole case, the problem is to prevent the stress concentrations around the hole from adversely affecting the net tension strength of the skin. One method of doing this, when the load is uniquely in the $0^{o}$ direction and the line of holes is in the same direction, is to replace a composite strip of skin material locally along the line of holes with a material that is either ductile or has a stress-strain relationship such that a strain equal to that in the adjacent advanced composite will not cause a failure. For example, an open hole in graphite epoxy will locally reduce the longitudinal tension allowable by approximately 50 percent. By replacing the $0^{o}$ graphite plies in a strip along a line of unloaded holes with more ductile fiberglass, the net tension allowable can be increased to close to the original tension allowable. If a material replacement method is used to restore the longitudinal net tension strength; it is necessary to replace all of the $0^{o}$ plies, lest the remaining ones trigger a strain-induced failure.

In the case of loaded holes, the same problem exists as with unloaded holes, except that the fastener load produces bearing stresses which are superimposed upon the basic loads. This serves to decrease the net tension allowable even further by effectively increasing the $k_t$ of the section and adds several other failure modes which must be considered, such as bearing and shear-out. For loaded holes the method of replacing graphite plies with glass cloth, which was effective in relieving the stress concentration around open holes, must account for the bearing strength of the fiberglass. A method sometimes used to reinforce highly loaded holes involves the replacement of part or all of the composite material with some type of metal; the most common being titanium because of its thermal and galvanic compatibility. The amount of metal used depends on the magnitude of the load involved. Generally, however, the composite material is built up around the holes to account for the failure modes.

Another factor which must be considered when dealing with non-yielding (composite) materials is the effect non-yielding has on the bearing allowable in countersunk holes. In this situation, the fastener tends to bear on the lower edge of the countersink, which does not yield enough to let the countersunk fastener head bear in the hole. Therefore, only the shank part of the fastener is fully effective in bearing.

Mechanically fastened joints should be designed so that the critical failure mode is in bearing rather than shear-out or net tension in order to prevent catastrophic failure. This

will require edge distance and net areas relatively greater than those for conventional metallic materials. At relatively low edge distance to fastener diameter ratios (e/D) and low plate width distance to fastener diameter ratios (W/D), failure of the joint occurs in shear-out at the ends, or in tension at the net section. Multiple fastener rows are recommended for unsymmetrical joints, such as single shear lap joints, to minimize bending induced by eccentric loading. Local reinforcing of unsymmetrical joints by arbitrarily increasing laminate thickness should generally be avoided because the resulting increased eccentricity gives rise to greater bending stresses which counteract or negate the increase in material area.

### B10.4.4 Fabrication Considerations

The primary difference between advanced composite and conventional material construction from a fabrication viewpoint is that, with composites, the assembly can be formed much closer to the final configuration and dimensions. One principal benefit of this feature is the elimination of a great deal of final machining and its associated costs.

Since the composite part is fabricated basically in the final configuration, care must be taken in the design so that the configuration is compatible with the tooling used to produce the part. In particular, any part to be made in one piece must obviously be designed so that it will not lock itself on the tool because of closed angles. Tooling can be designed to accommodate such a part, but it is very expensive. It is much more economical to modify the part or fabricate it in stages.

Another major factor is the fact that the part must be cured at relatively high temperatures. The designer must be aware of this if his design includes several materials in the same layup which have different coefficients of thermal expansion. This could induce significant permanent internal stresses in the cured part. In addition, if even a one-system laminate is not symmetrical about its mid-plane, the part will be warped when removed from the tool, sometimes very severely.

It should be apparent from the foregoing discussion that, when designing with advanced composites, the Structural Designer must coordinate his design with Tooling and Manufacturing to determine the method which will be used to build the part.

## B10.5.0 Material Forms and Material Properties

The composite material properties presented in this section are for preliminary design purposes only. New and revised materials and material properties are continually being evaluated, so the engineer should contact the Composite Design Section in the Structural Design Group for advice on material selections and applications.

> CAUTION SHOULD BE EXERCISED WHEN USING THE PROPERTIES IN THIS SECTION. COMPOSITES ARE OFTEN STRAIN LIMITED BECAUSE OF THEIR BRITTLE NATURE (SEE SECTION B10.6.1) AND THE VALUES LISTED CAN NOT BE ATTAINED FOR PRACTICAL DESIGN APPLICATIONS.

## B10.5.1 Material Forms

Composites are utilized in various forms. A description of these forms follows:

A. Unidirectional Tape Prepreg All the filaments are orientated in one direction. The tape is fabricated in width ranging from 3 to 60 inches and is supplied in rolls.

Unidirectional tape works well when maximum performance is required in one direction. Tapes are made by careful alignment of side-by-side yarns; usually of 1420 or greater denier. Tapes are usually impregnated with resin and are available from many prepreg suppliers.

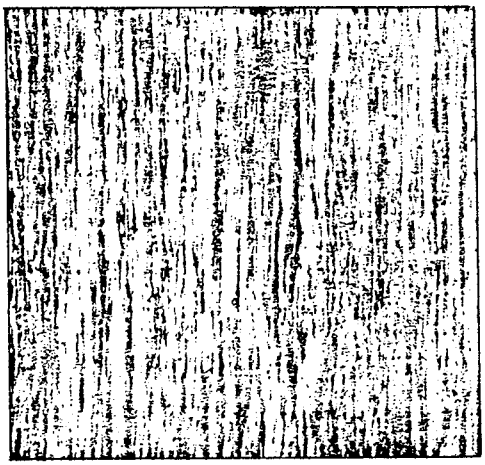

B. Unidirectional Weave Cloth Prepreg (95% - 0°, 5% - 90°) This cloth has 95% of its filaments in the warp direction (length direction) and 5% in the fill direction to facilitate material handling. Its strength is approximately equal to unidirectional tape. It is fabricated and available up to 72 inches in width.

A unidirectional weave is an adaptation of one of the basic textile weaves. It is a special case and can be produced using any of the basic weaves described. A greater number of relatively strong warp yarns and fewer, and generally weaker, filling yarns give this type of reinforcing fabric maximum strength in the warp direction only. This weave has the general characterstics: 1) maximum strength in one direction and 2) minimum strength in the transverse direction.

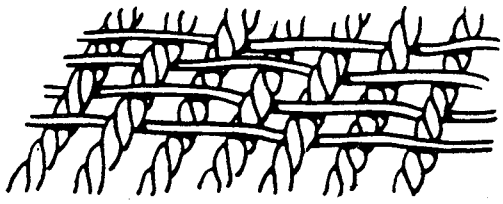

C. Bidirectional Weave Cloth Prepreg This cloth has close-to-equal proportions of filaments in the warp direction (length) and fill direction (width). Note that in satin weaves, the warp filaments are predominantly on one side and the fill is predominantly on the other. Hence, the cloth is not thermally balanced within itself and in thin laminates it may be necessary to specify on which side of the cloth the warp should be to prevent twisting of the laminates after curing. The cloth is fabricated in widths up to 72 inches.

Types of bidirectional weaves are:

1. Plain Weave - The oldest and most common basic textile weave in which one warp end (lengthwise thread) weaves over and then under one filling pick (crosswise thread). This weave has the general characteristics:

   a. Firmest and most stable of the industrial weaves

   b. Affords fair porosity with minimum yarn slippage

c. Uniform strength pattern in all surface directions

d. Affords ease of air removal in hand layup or molding.

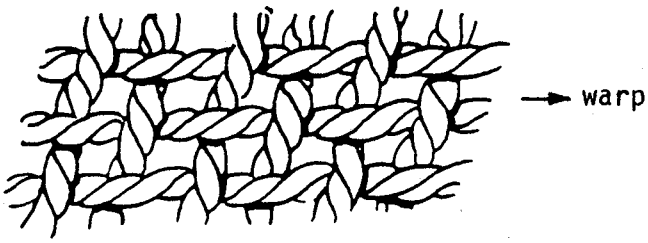


2. Basket Weave - This weave is similar to a plain weave, but it has two or more warp ends weaving as one end over and under two or more filling picks weaving as one pick. This weave has the general characteristics:

a. Less stable than a plain weave.

b. More pliable than a plain weave.

c. Flatter and stronger than an equivalent weight and count of plain weave.

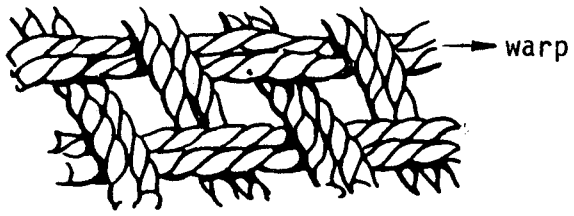


3. Crowfoot Satin or 4-Harness Satin - This weave is constructed with one warp end weaving over three and under one filling pick. It has the general characteristics:

a. More pliable than either a plain weave or a basket weave.

b. Specially designed to conform closely to complex or compound curved surfaces.

c. Makes possible the weaving of higher counts than plain or basket weaves.

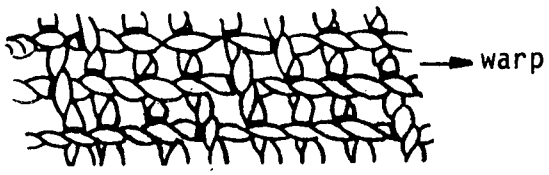


4. Long Shaft Satin - A long shaft satin construction has one warp end weaving over four or more and under one filling pick. This weave has the general characteristics:

   a. Most pliable and conforms readily to compound curves.

   b. Produces laminates and reinforced moldings with high-strength in all directions.

   c. Can be woven in the highest construction or density.

   d. Less open than other weaves.

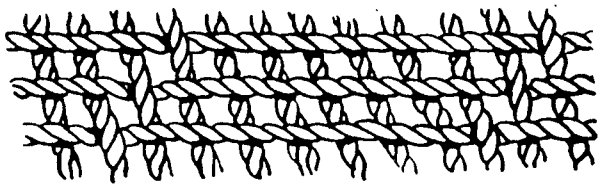

Typical bidirectional weave designs used in composites are:

5. Style 120 which is used where minimum thickness and a smooth surface are desired. It is a 4-harness satin weave. This construction has one warp end weaving over three and under one filling pick.

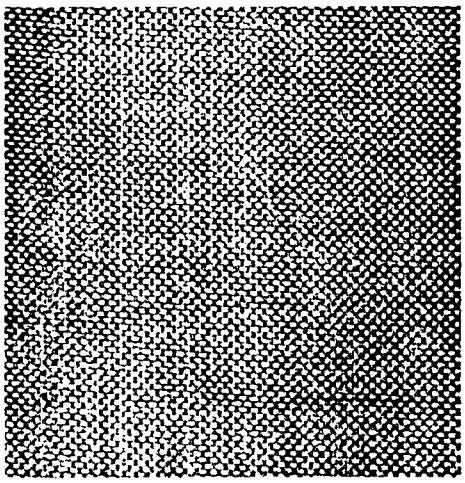

6. Style 181, Medium Weight which is an 8-harness long shaft satin weave; it conforms well to molds.

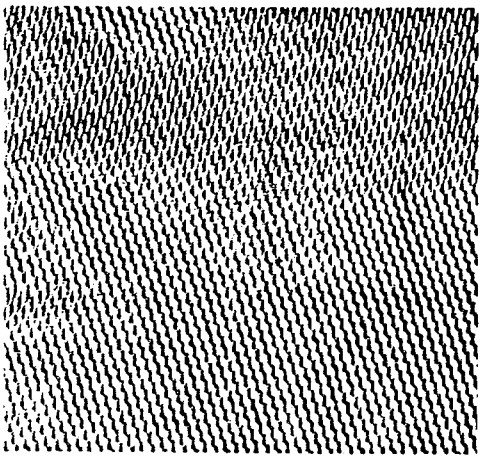

7. Style 220, which is used when economy is important; it provides minimum thickness and a smooth surface at lower cost than Style 120. Style 220 is made from 380 denier yarn, which increases the weight and thickness per ply slightly over Style 120.

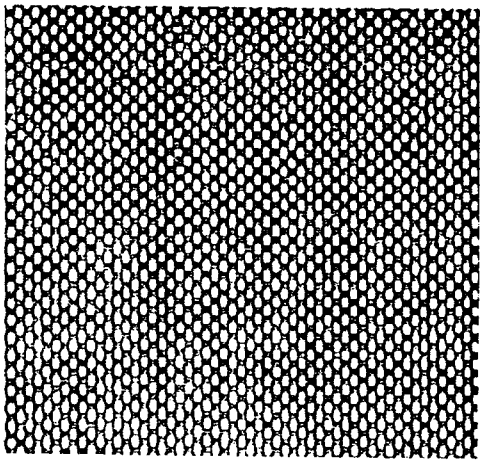

8. Styles 281 and 285 were both designed to be more economical versions of Style 181. Both take advantage of a heavier, 1140 denier, Kevlar yarn. Style 281 is a plain weave. Style 285 is a crowfoot, or 4-harness satin weave. Where a high degree of mold conformability is important, Style 285 is recommended.

Style 281

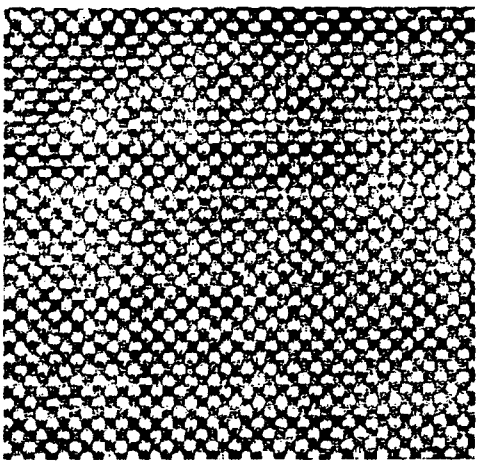

Style 205

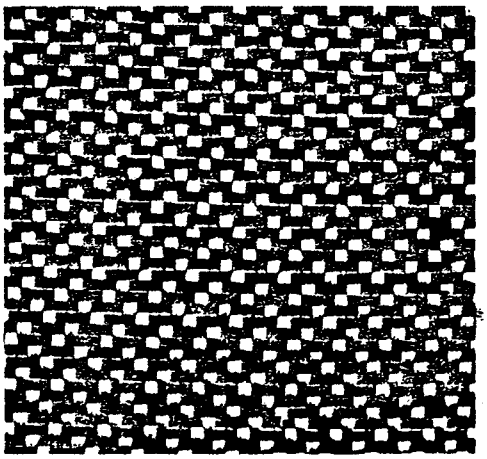

D. Rovings Continuous reinforcements formed by combining a number of strands (primarily used for filament windings).

B10.5.2 Material Properties

The purpose of this section is to provide the Structural Designer with the basic composite laminate properties necessary to size a structural component.

The laminate material properties are derived from DAC test data and from other industrial sources. They are for preliminary sizing only. Final analysis values will be determined by approved tests, as specified in FAR 25.602, 25.613 and 25.615 for commercial transports and Mil-A-00886 Series for military transports.

Three basic advanced composite material systems are presented: A) graphite/epoxy (GR/EP), B) Kevlar 49/epoxy (K-49/Epoxy), and C) fiberglass/epoxy (E-glass/Epoxy). For each system, key unidirectional or cross ply laminate properties (static design strengths, elastic properties, and physical constants) at room, elevated, and subzero temperatures are presented to the extent available. Fatigue and environmental effects are also presented.

The static design strengths are reported as "A" basis or "B" basis allowables, where a sufficient data base was available. Otherwise, the strengths are designated as "typical design allowables" and represent rational values which can be used for preliminary structural design. The elastic and physical properties are based on average or typical values, as is the practice in Mil-Hdbk-5C.

The following symbols are commonly used with respect to the material coordinate system shown:

| | | |
|---|---|---|
| Design Strength | $\varepsilon x_{tu}$ | Ultimate $0^o$ strain, in./in. |
| | $\varepsilon y_{tu}$ | Ultimate $90^o$ strain, in./in. |
| | $F_{bru}$ | Ultimate bearing stress, psi |
| | $F_{i_{su}}$ | Interlaminar shear ultimate, psi |
| | $F_{x_{cu}}$ | $0^o$ compression ultimate, psi |
| | $F_{x_{tu}}$ | $0^o$ tensile ultimate, psi |
| | $F_{xy_{su}}$ | In-plane shear ultimate, psi |
| | $F_{y_{cu}}$ | $90^o$ compression ultimate, psi |
| | $F_{y_{tu}}$ | $90^o$ tensile ultimate, psi |
| Elastic Properties | $E_{x_c}$ | $0^o$ compression modulus, psi |
| | $E_{x_t}$ | $0^o$ tension modulus, psi |
| | $E_{y_c}$ | $90^o$ compression modulus, psi |
| | $E_{y_t}$ | $90^o$ tension modulus, psi |
| | $G_{xy}$ | In-plane shear modulus, psi |
| | $\mu_{xy}$ | Major Poisson's ratio |
| | $\mu_{yx}$ | Minor Poisson's ratio |
| Physical Constraints | $\alpha_x$ | $0^o$ coefficient of thermal expansion, in./in./$^o$F |
| | $\alpha_y$ | $90^o$ coefficient of thermal expansion, in./in./$^o$F |
| | $\rho$ | Density, lb./in.$^3$ |

A. Graphite Epoxy Composite

1. Material Callout - T300/5208.

2. Material Specification - DMS 2163.

3. Qualified Materials -

   Fiber - T300, Thornel 300 Graphite Fiber
   Resin - 5208, Narmco 5208 Epoxy

4. Laminate Thickness After Cure -

   a. Tape: t = 0.0055 in.

   b. Bidirectional weave: t = 0.013 in. cloth (181 Style - 8-Harness Satin)

   c. Unidirectional weave: t = 0.006 inch cloth (95 - 5) [this material is little used at DAC at this time.]

5. Laminate Density After Cure - $\rho = 0.056$ lb./in.$^3$

6. Cure Requirements

   Autoclave cure
   Cure temperature - 350$^{o}$F
   Cure pressure - 100 psi

7. Material Usage - Primary and secondary structural components where strength or stiffness is required.

8. Material Strength, Properties, and Constraints - "B" basis allowable strengths, elastic moduli, and physical constants at room temperature, 250$^{o}$F and -65$^{o}$F conditions for T300/5208 composite material with any combination of 0$^{o}$, ±45$^{o}$, 90$^{o}$ fiber orientation are presented. An interactive computer program, "STRENGTH", is available to provide additional material allowables data (see Section E7 of this manual).

   The allowable data plots were compiled from monolayer coupon test data through the use of special properties program, "H1DA", reference B10-2. The plots are subjected to a limitation on the fraction of ultimate load below which transverse tensile failures are not allowed.

The limitation, $\phi$, is necessary because composites exhibit great longitudinal strengths due to the filaments, but very weak tensile strengths in the transverse directions due to the resin. If a laminate is layed up with a number of cross plies whose filaments compensate for the weak resin strengths in the transverse directions of certain lamina, then resin fracture of these lamina does not terminate the laminate's overall loading capacity. The criterion that transverse tensile failures in the resin can be accepted as long as they occur above a specified fraction of the ultimate load has become adopted. This specified fraction of the ultimate load is denoted as $\phi$.

The limits for $\phi$ are:

$\phi$ = 1.0 precludes transverse tensile failures in the resin (the material will develop the lowest possible allowables)

$\phi$ = 0.0 allows transverse tensile failures at any load (the material will develop the highest possible allowables)

A conservative value, $\phi$ = .667, means there will not be a transverse tensile failure in the resin at or below limit load.

The following plots (Figures B10.5.2-1 through B10.5.2-9) are "B" value allowables for the T300/5208 tape laminates at $\phi$ = 0, .667 and/or 1.0.

To obtain allowable data for bidirectional weave cloth (fabric prepreg) for T300/5208, use Douglas Report MDC J6990.

To obtain allowable data for 95% unidirectional weave prepreg for T300/5208, use Douglas Report MDC J6816.

In the absence of a full analysis for fastener load transfer use the following allowables: (see B10.7.3L for required laminate orientation):

$F_t$ = 40,000 (tension) net

$F_s$ = 20,000 psi (shear-out)

$F_{br}$ = 100,000 psi (double-lap)

$F_{br}$ = 80,000 psi (single-lap - no moment in joint)

$F_{br}$ = 60,000 psi (single-lap - moment in joint, constrained rotation)

$F_{br}$ = 25,000 psi (single-lap) - moment in joint, unconstrained rotation

Transverse Properties

Generally, shear in the transverse direction equals the interlaminar shear properties. For design, use:

$F_{isu}$ = 8,000 psi

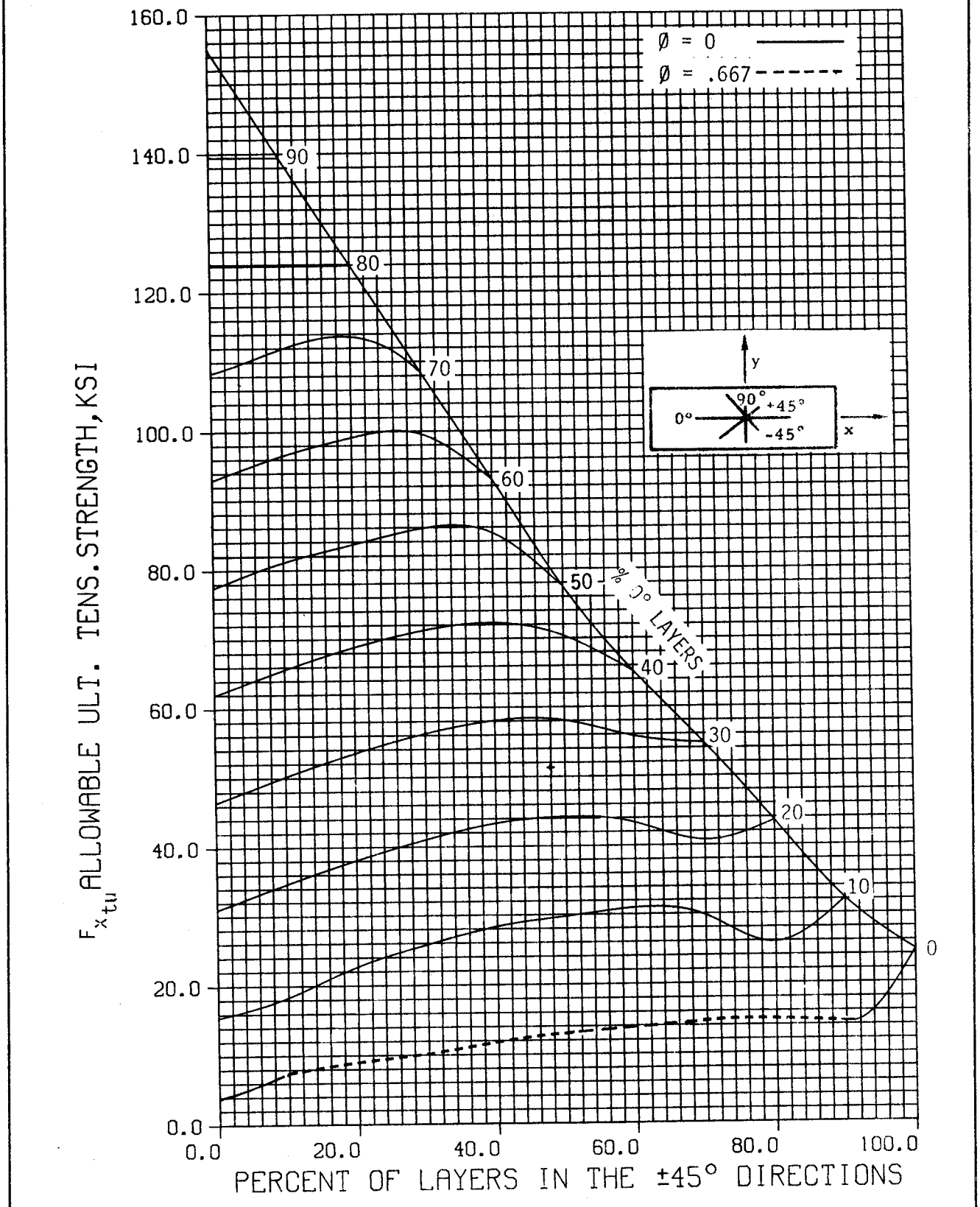


Figure B10.5.2-1 "B" Basis Ultimate Tensile Strength for $[0_i/\pm45_j/90_k]$ Family, T300/5208 Graphite/Epoxy Tape, RT/-65°F

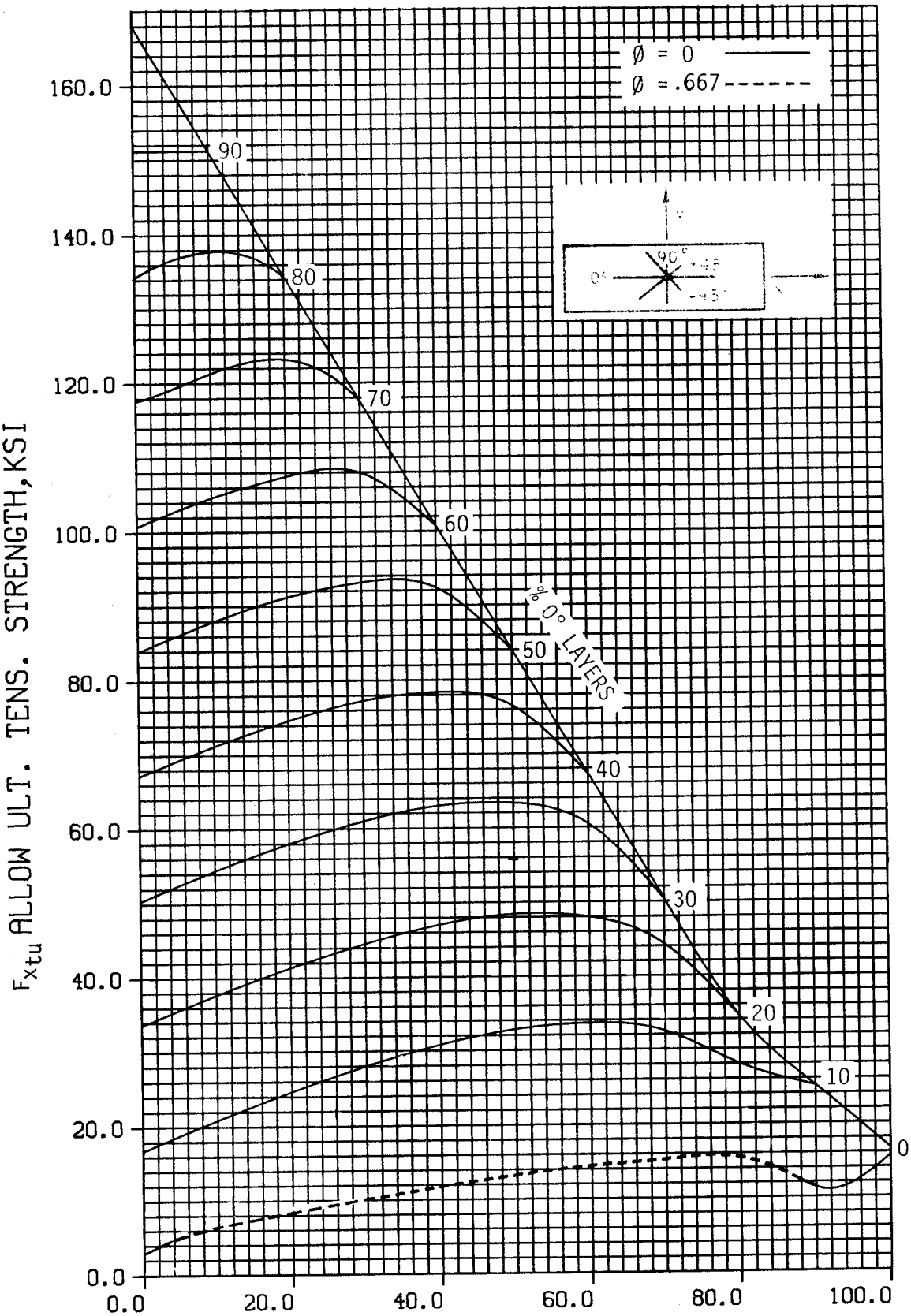


Figure B10.5.2-2 "B" Basis Ultimate Tensile Strength for $[0_i/\pm45_j/90_k]$ T300/5208 Graphite/Epoxy Tape, 250°F

DOUGLAS AIRCRAFT COMPANY

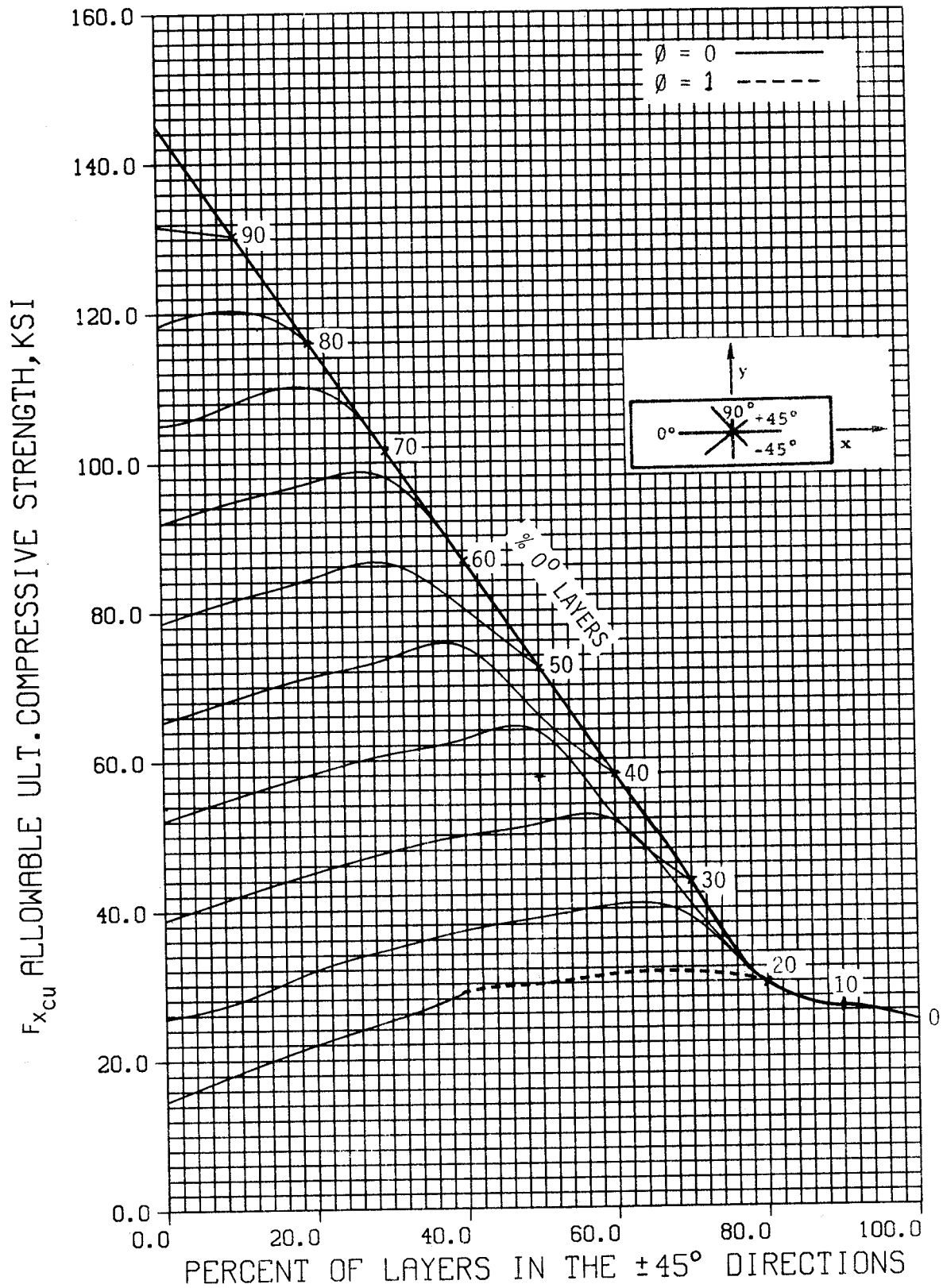


Figure B10.5.2-3 "B" Basis Ultimate Compressive Strength for $[0_i/\pm45_j/90_k]$ Family T300/5208 Graphite/Epoxy Tape, RT/-65°F

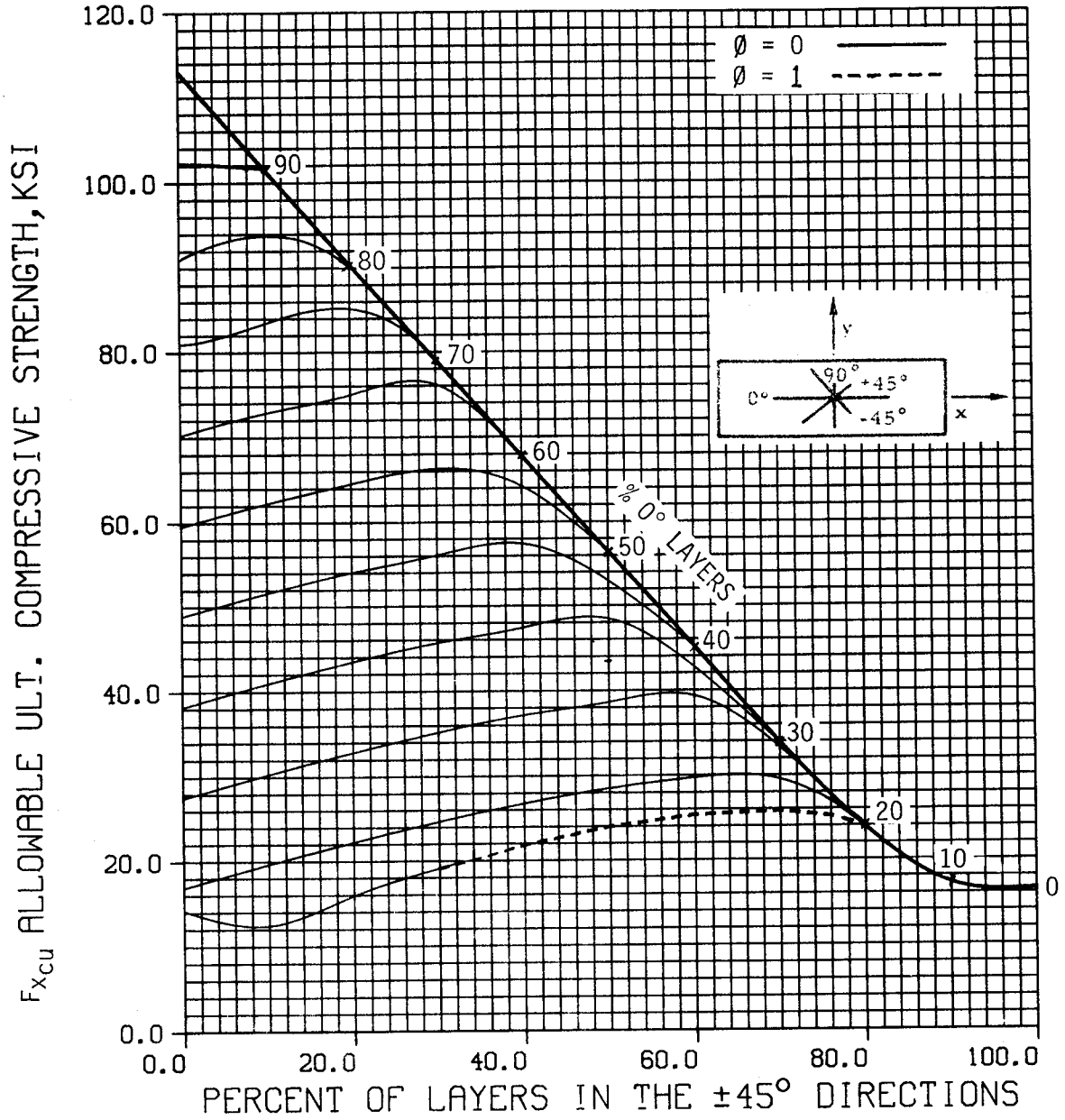


Figure B10.5.2-4 "B" Basis Ultimate Compressive Strength for $[0_i/\pm45_j/90_k]$ Family T300/5208 Graphite/Epoxy, 250°F

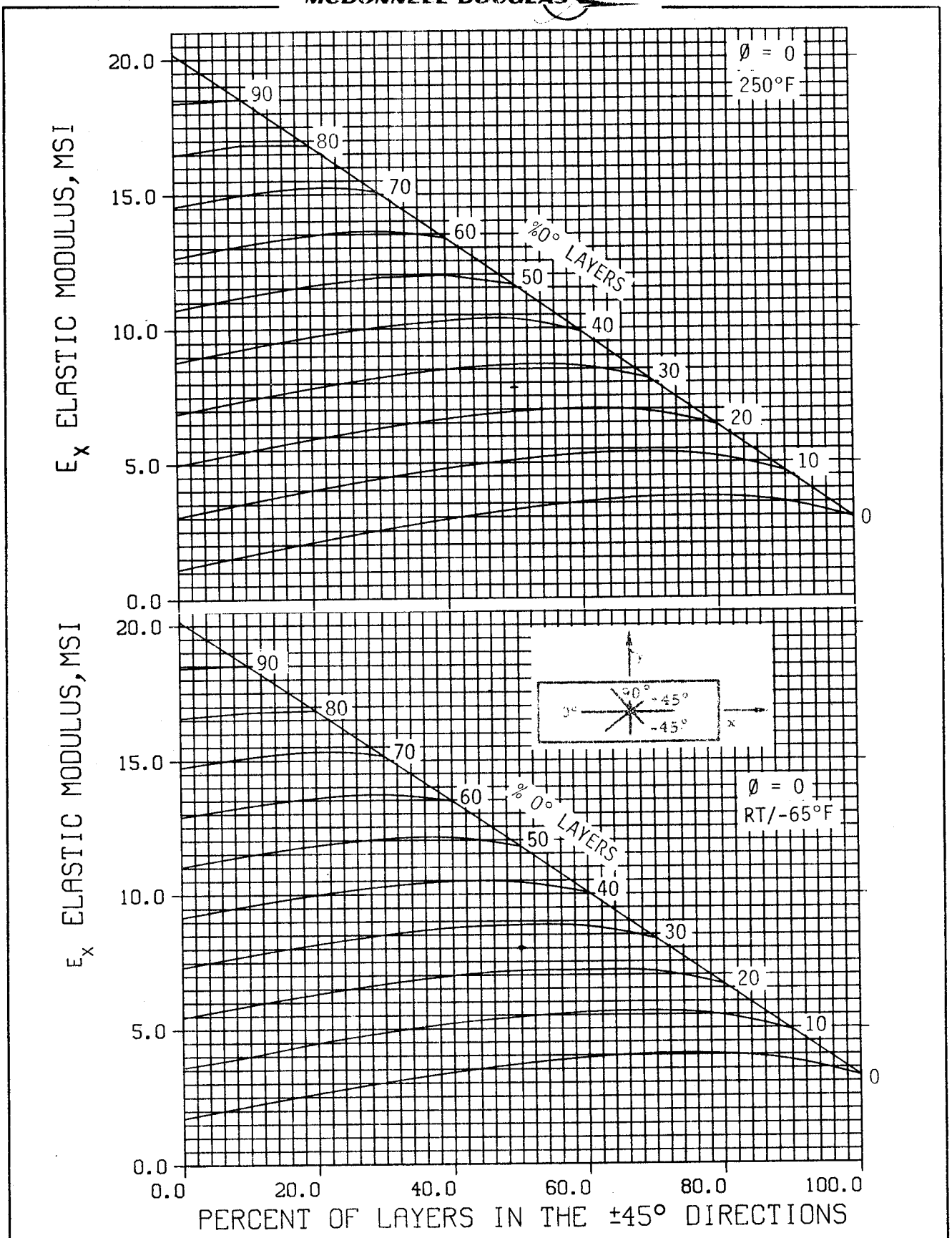


Figure B10.5.2-5 Elastic Modulus for $[0_i/\pm45_j/90_k]$ Family T300/5208 Graphite/Epoxy Tape

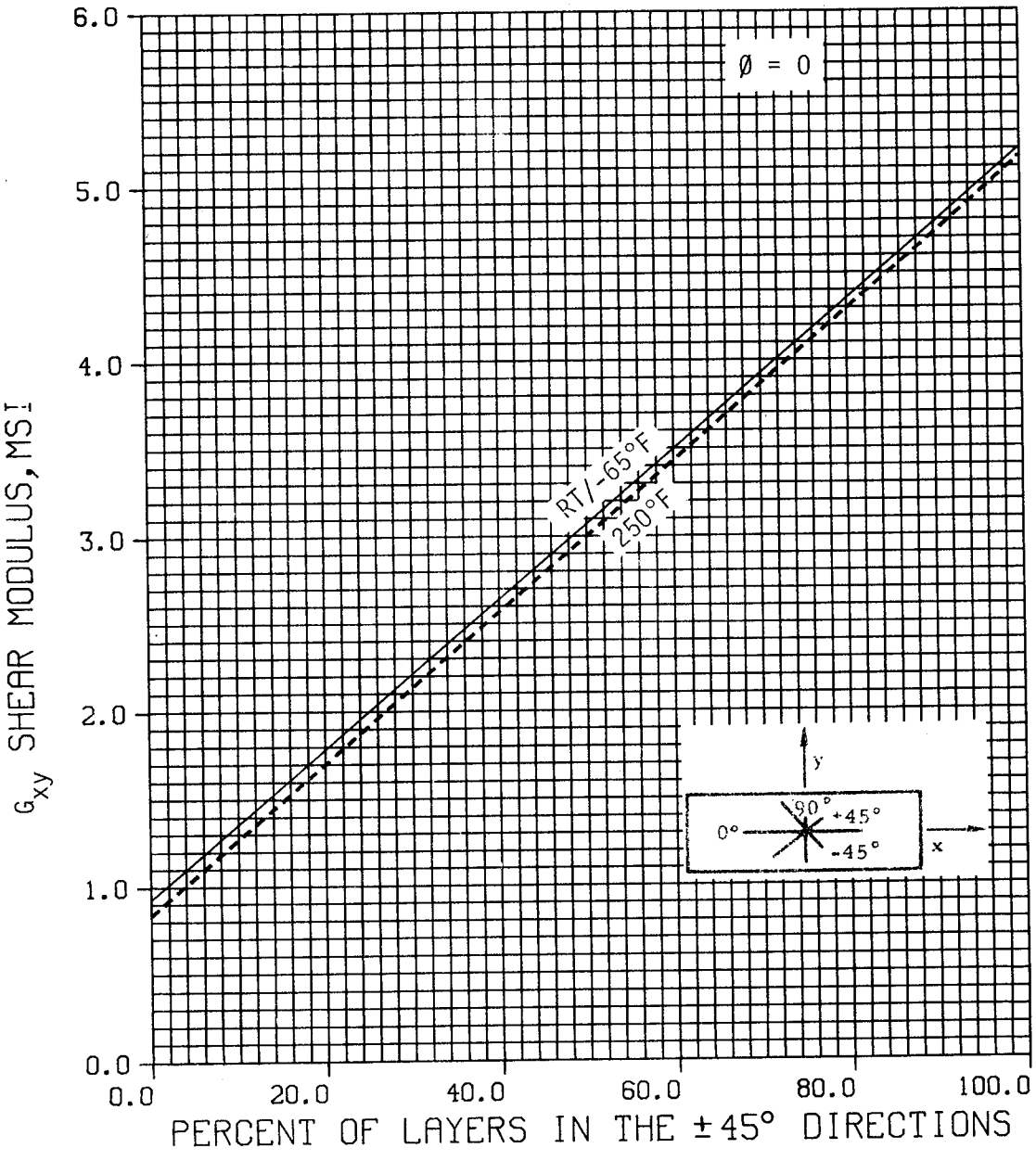


Figure B10.5.2-6 Shear Modulus for $[0_i/\pm45_j/90_k]$ Family T300/5208 Graphite/Epoxy Tape

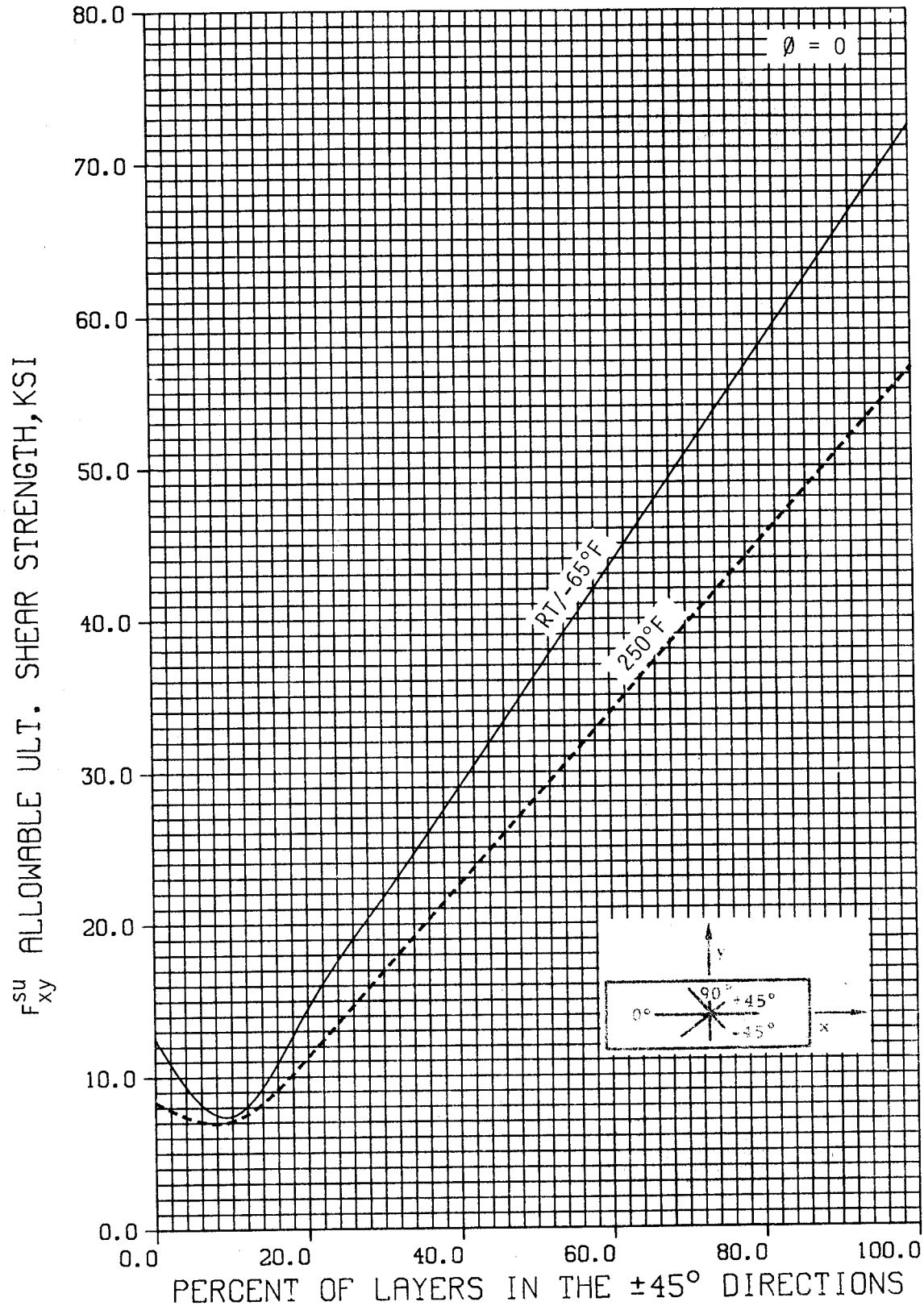


Figure B10.5.2-7 "B" Basis - Ultimate Shear Strength for $[0_i/\pm45_j/90_k]$ Family T300/5208 Graphite/Epoxy Tape

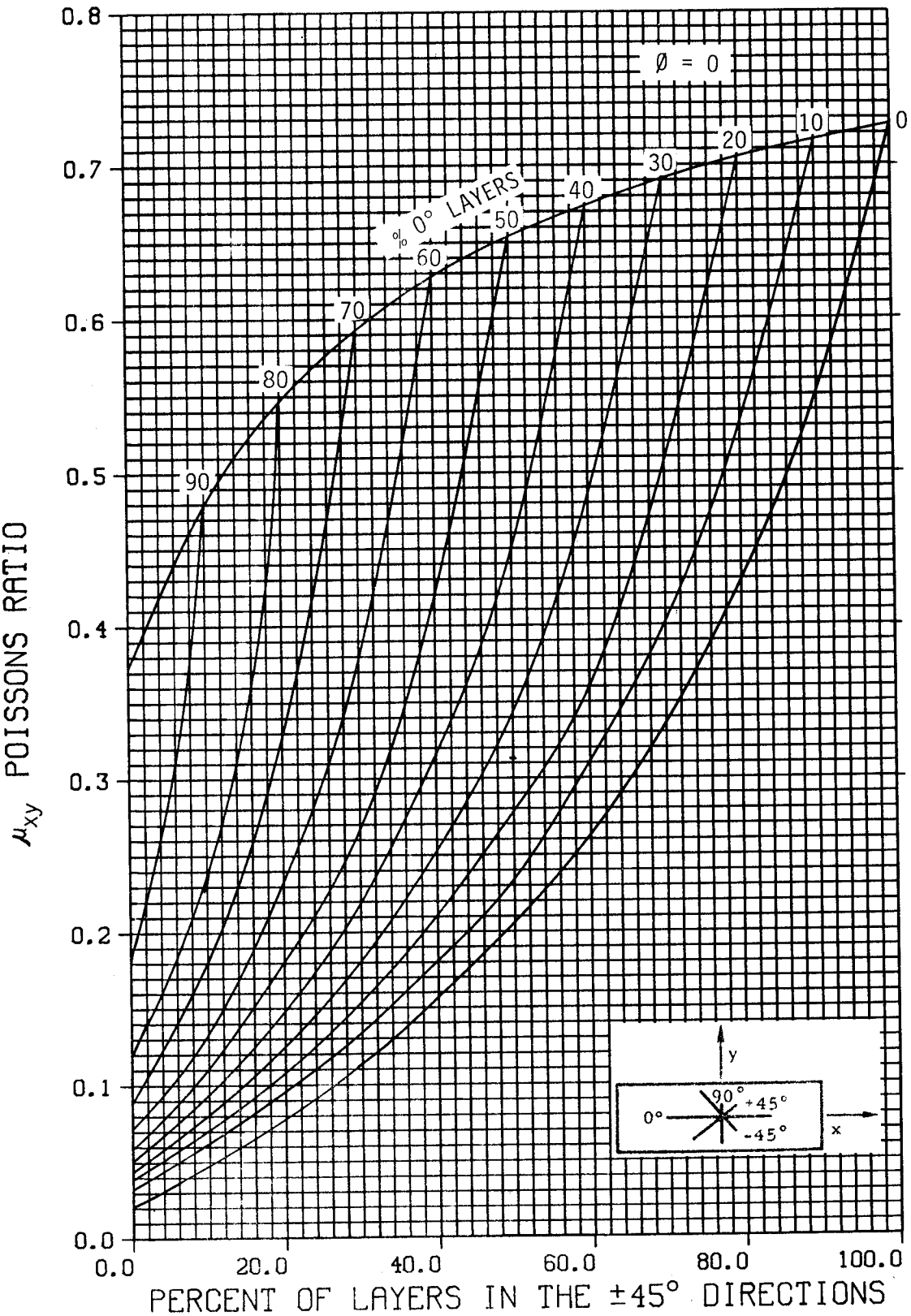


Figure B10.5.2-8 Poisson's Ratio for $[0_i/\pm45_j/90_k]$ Family T300/5208 Graphite/Epoxy Tape, RT/-65°F

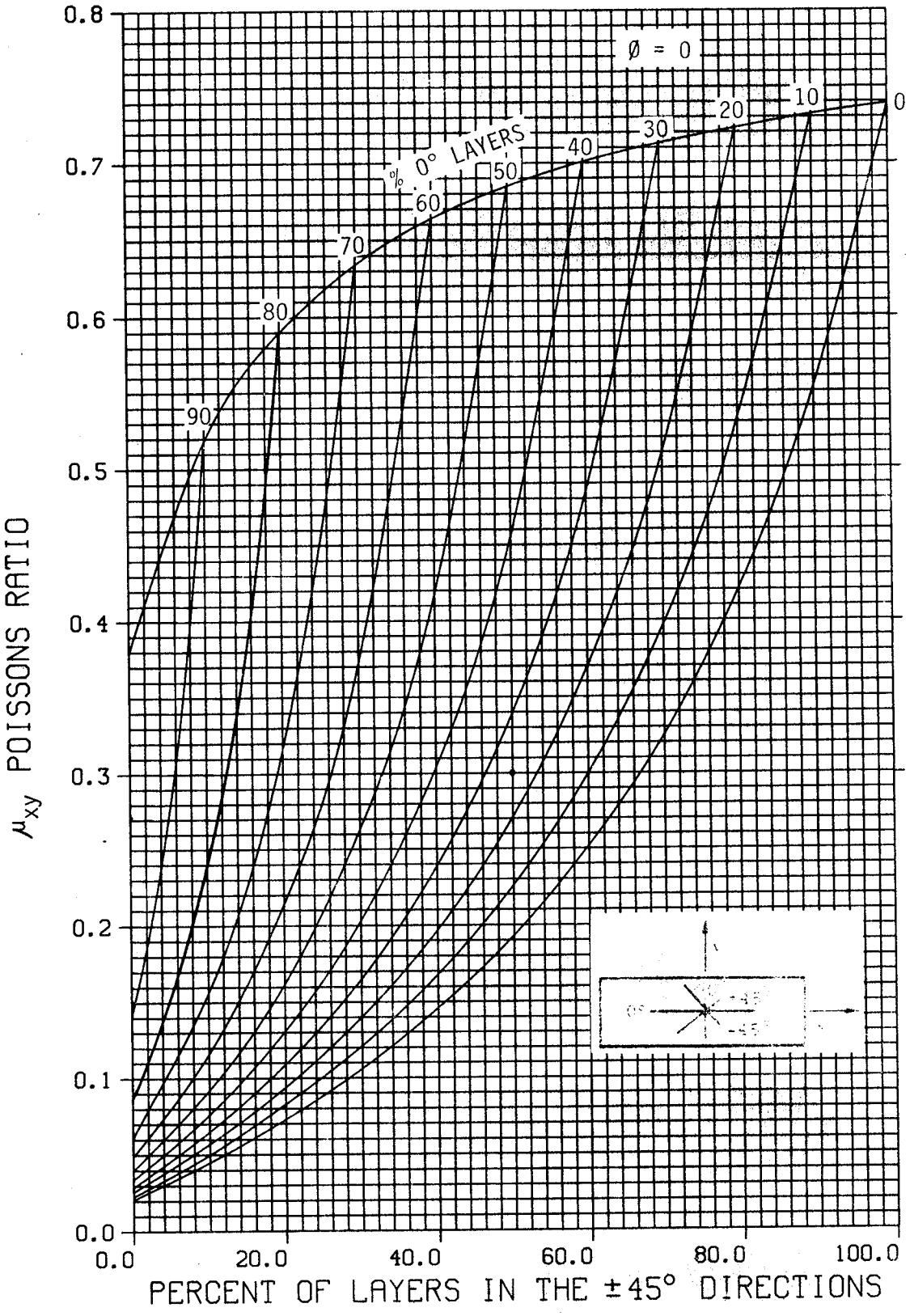


Figure B10.5.2-9 Poisson's Ratio for $[0_i/\pm45_j/90_k]$ Family T300/5208 Graphite/Epoxy Tape, 250°F

B. Kevlar Epoxy Composite

1. Material Callout - Kevlar 49/F155.

2. Material Specification - DMS 1926.

3. Qualified Materials -

Fiber - Kevlar 49 aramid fibers are manufactured by the DuPont Co. and is a registered trademark of that company (285 Style - 4-Harness Satin)

Resin - F155, a controlled flow "B" stage fiberite epoxy used primarily when laminating honeycomb core.

4. Laminate Thickness After Cure -

Tape: $t = 0.0050$ in.

Bidirectional weave: $t = 0.010$ in. cloth (at present, Kevlar is purchased in this form at DAC almost exclusively)

5. Laminate Density After Cure - $\rho = 0.049$ lbs./in.$^3$.

6. Cure Requirements -

Oven Cure - cure temperature - 250$^{o}$F
cure pressure - 14 psi (atmospheric)

Autoclave Cure - cure temperature - 250$^{o}$F
cure pressure - 25 to 35 psi

7. Material Usage - This material system is primarily used with Nomex honeycomb core because of the ability of the epoxy to provide good adhesion without the application of additional adhesive. It is also used for lightly loaded secondary structure.

8. Material Strength, Properties, and Constraints (Kevlar 49/F155 Kevlar Epoxy) - "B" basis allowable strengths, elastic moduli, and physical constants at room temperature conditions for Kevlar 49/F155 composite material with 0$^{o}$/90$^{o}$ cloth orientations are presented.

The interactive computer program named "STRENGTH" is available to provide material allowables in $0^o$, $90^o$ and $\pm 45^o$ orientations based on the $0^o/90^o$ material allowables (refer to Section E7).

Room temperature conditions - monolayer data t = .010 in.

$$*F_{bru} = 50{,}000 \text{ psi}$$

$$F_{x_{cu}} = F_{y_{cu}} = 24{,}700 \text{ psi}$$

$$F_{x_{tu}} = F_{y_{tu}} = 59{,}090 \text{ psi}$$

$$F_{xy_{su}} = 11{,}000 \text{ psi}$$

$$E_{x_c} = E_{y_c} = 4.35 \times 10^6$$

$$E_{x_t} = E_{y_t} = 4.98 \times 10^6$$

$$G_{xy} = G_{yx} = 0.25 \times 10^6$$

$$\mu_{xy} = \mu_{yx} = 0.13$$

*Calculated from tests with a .1875 inch diameter countersink bolts, single lap configuration, assuming fully effective skin thickness.

C. Fiberglass Epoxy Composites

1. Material Callout - E-glass/F155.

2. Material Specification - DMS 1926.

3. Qualified Materials -

Fiber - Style 120 crowfoot weave or Style 181, 8-Harness weave glass fiber cloth per MIL-C-0984

Resin - A controlled flow "B" stage fiberite epoxy used primarily when laminating honeycomb core.

4. Laminate Thickness After Cure -

   Bidirectional weave -
   120 Style - t = 0.005 in.
   181 Style - t = 0.010 in.
   (predominately used at Douglas Aircraft Co.)

5. Laminate Density After Cure - $\rho$ = 0.069 lbs./in.$^3$.

6. Cure Requirements -

   Oven Cure - cure temperature - 250°F
   cure pressure - 14 psi (atmospheric)

   Autoclave Cure - cure temperature - 250°F
   cure pressure - 25 to 35 psi

7. Material Usage - This material system is primarily used with Nomex honeycomb core because of the ability of the epoxy to provide good adhesion without the application of additional adhesive. It is used on lightly loaded secondary structure exclusively, especially when wear resistance is important.

8. Material Strength, Properties, and Constraints (E-glass/F155 120 or 181 Style Fiber Glass Epoxy) - Allowable data for 0°/90° cloth orientation are presented. The interactive computer program, "Strength", is available to provide material allowables in 0°, 90° and ±45° orientation based on the 0°/90° material allowables. Refer to Section E7.

   Room Temperature Allowables (0°/90° orientation)

   monolayer data for 120 cloth t = .005 in.
   monolayer data for 181 cloth t = .010 in.

   Note: Strength values shown in parentheses have been reduced 30 percent to allow for fabrication variables. These reduced values should be used for design.

| | | |
|---|---|---|
| $*F_{bru}$ | = 58,000 psi | (40,600 psi) |
| $F_{x_{cu}} = F_{y_{cu}}$ | = 53,000 psi | (37,100 psi) |
| $F_{x_{tu}}$ | = 50,400 psi | (35,280 psi) |

$F_{xy_{su}}$ = 14,000 psi ( 9,800 psi)

$F_{y_{tu}}$ = 56,000 psi (39,200 psi)

$E_{x_c} = E_{y_c} = 3.7 \times 10^6$ psi

$E_{x_t} = E_{y_t} = 3.6 \times 10^6$ psi

$G_{xy} = G_{yx} = 0.81 \times 10^6$ psi

$\alpha_x = \alpha_y = 5.5 \times 10^{-6}$ in./in./$^oF$

$\mu_{xy} = \mu_{yx} = 0.13$

300$^o$ F Temperature Allowables 0.5 Hour Exposure (0$^o$/90$^o$ orientation)

Note: Strength values shown in parentheses have been reduced 30 percent to allow for fabrication variable. These reduced values should be used for design.

$*F_{bru}$ = 25,000 psi (17,500 psi)

$F_{x_{cu}} = F_{y_{cu}}$ = 22,000 psi (15,400 psi)

$F_{x_{tu}}$ = 50,400 psi (35,280 psi)

$F_{xy_{su}}$ = 14,000 psi ( 9,800 psi)

$F_{y_{tu}}$ = 33,000 psi (20,790 psi)

$E_{x_c} = E_{y_c} = 2.04 \times 10^6$ psi

$E_{x_t} = E_{y_t} = 2.6 \times 10^6$ psi

$G_{xy}$ = -

$G_{yx}$ = -

$\alpha_x = \alpha_y = 2.3 \times 10^6$ in./in./$^oF$

$\mu_{xy}$ = -

$\mu_{yx}$ = -

B10.6.0 Design Strain Limitations

For any structure that is a Principal Structural Element (PSE) it is generally assumed that a crack will be initiated by inadvertent built-in preload stresses, manufacture, or service usage. (Refer to Section D10.0.0 Damage Tolerance). Such damage is not always obvious to the naked eye, but can sometimes be detected by normal Non-Destructive Inspection (NDI) techniques if the nominal diameter of the damage is greater than 0.5 inch. For damage which is smaller than this, it is assumed that the crack must not propagate during the service life (inspection period) of the aircraft.

Damage tolerance studies have shown that a plain hole is an approximate representation of the severity of other types of damage. For this reason, design allowable strain levels are often determined from coupon specimens with plain holes since these avoid dealing with the inexact nature of other types of damage. When such a specimen made from composites (particularly carbon/epoxy material) is tested in tension, it fails suddenly with no prior period of cracking. It is assumed, therefore, that if the design strain levels are kept below the failure strains (i.e., strain limited), that no cracks will propagate from an equivalent damaged region. While this approach imposes a severe weight penalty (relative to the composite potential), it has the advantage that there is little, if any, additional penalty required due to the presence of mechanical fasteners. At this time, the strain limitation approach appears reasonable, even though it is recognized that it is not a complete answer under all circumstances. It does provide a level of safety which is acceptable and which will be justified (or modified) by subsequent service experience with composite material. At the present time, a strain limitation of $\varepsilon$ = 0.004 in./in. at ultimate load will be applied as a design criteria when using composite material in this section as a PSE. This strain limitation value may change for different composite materials or as service experience dictates.

Figures B10.6.2-1 and B10.6.2-2 are design allowable charts that incorporate this strain limitation. They may be used directly to determine the allowable tension and shear stress for T300/5208 at any strain limitation. For any other composite material, determine the modulus from charts of percent ply orientation and multiply it by the strain limitation to determine the allowable tension stress:

$F_{x_t} = (E_{x_t})(\varepsilon)$. For shear allowable $F_{xy_s} = \frac{E_{x_t}}{\sqrt{3}}(\varepsilon)$

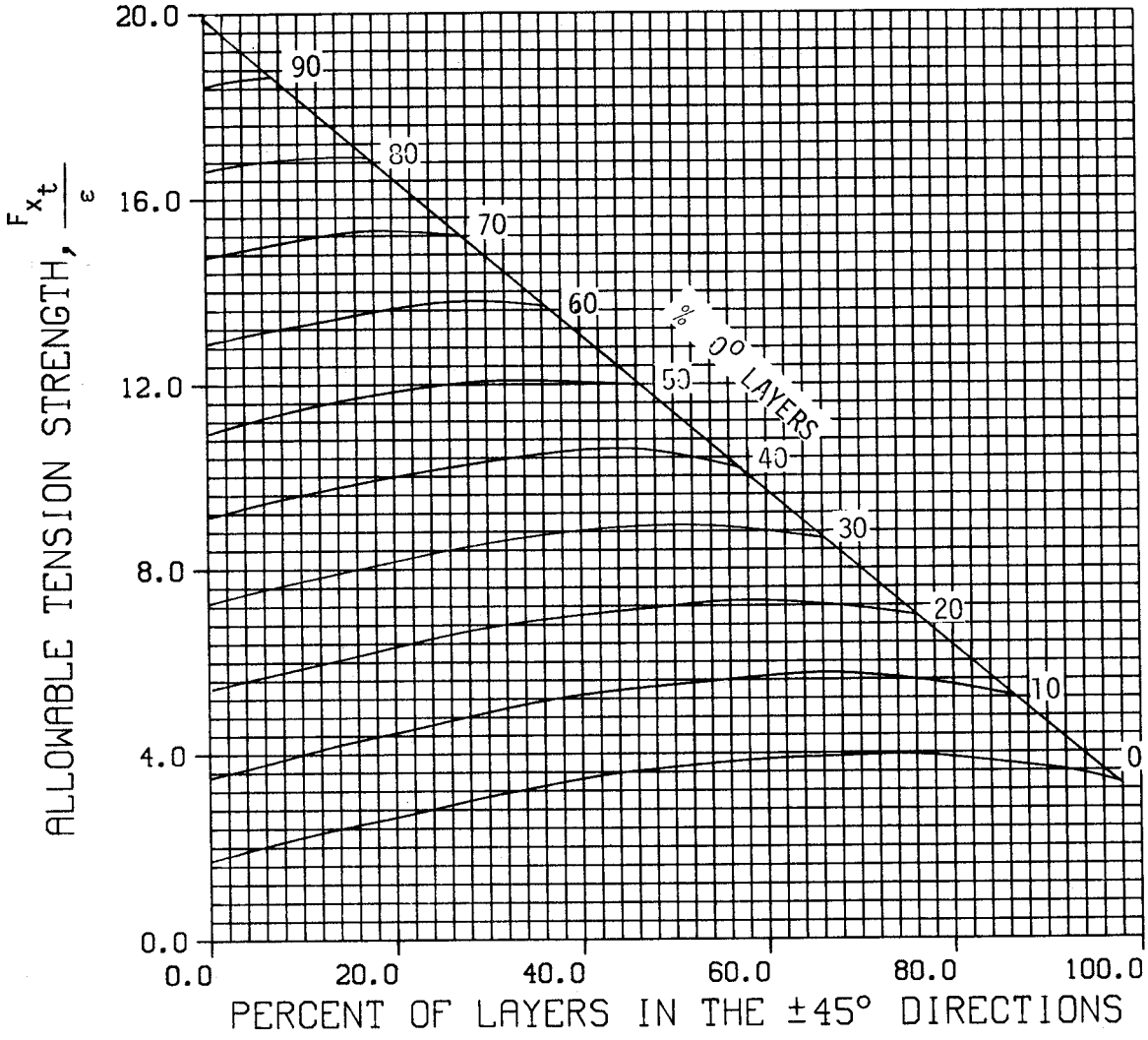


Figure B10.6.2-1 Strain Limited Tension (or Compression) Allowable Stress for T300/5208 Material

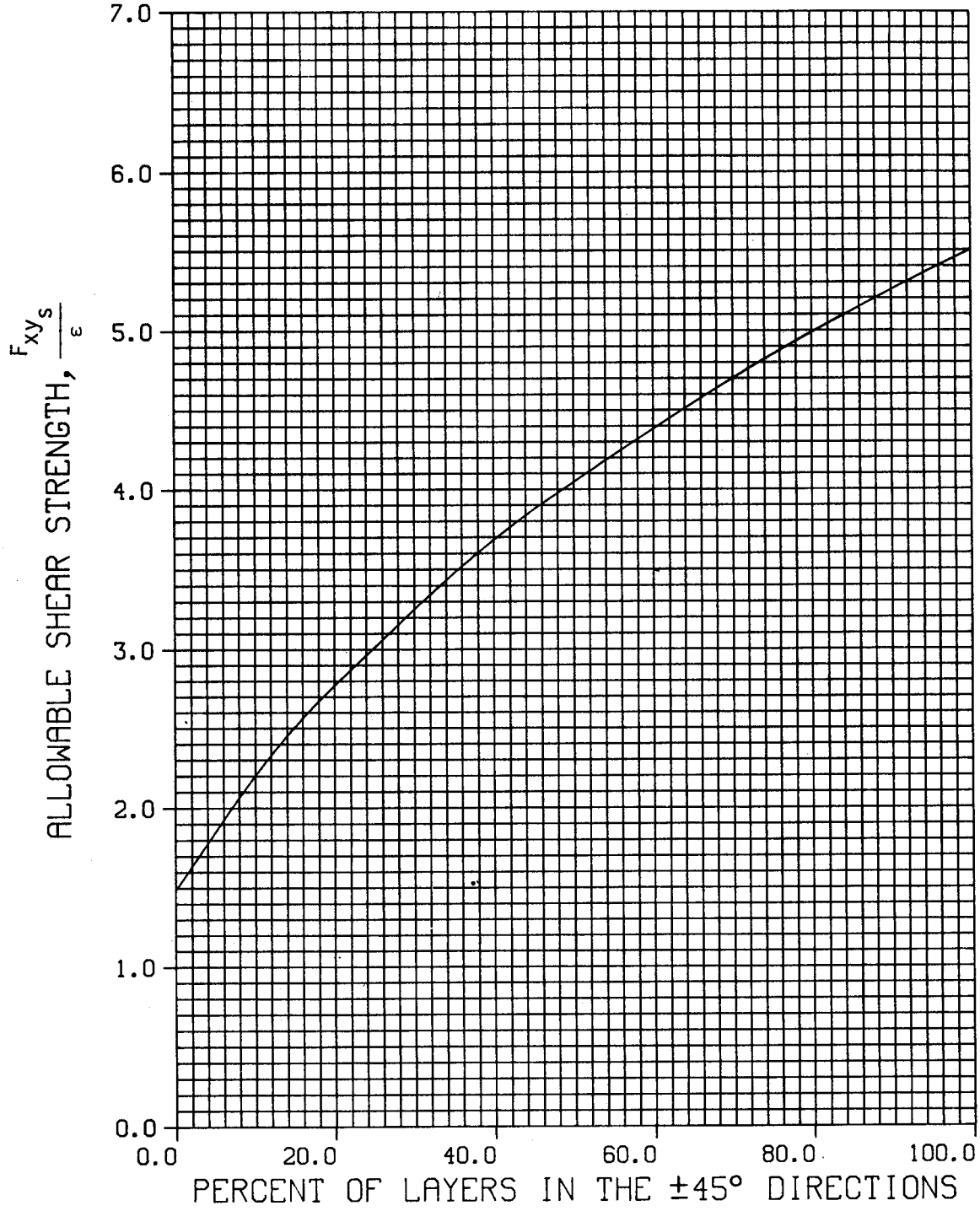


Figure B10.6.2-2 Strain Limited Shear Design
Allowable Stress for T300/5208 Material

The following problem illustrates composite design with the strain limitation:

Find the thickness which will sustain an ultimate applied tension load of

$N_x$ = 3000 lb./in. at room temperature

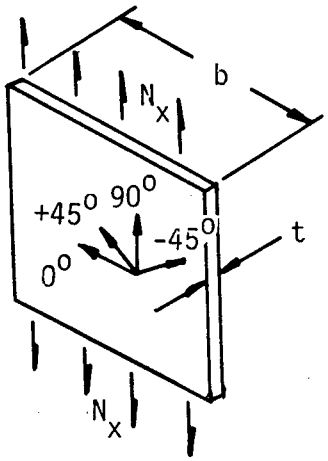


Material is T300/5208 graphite/epoxy tape for which the thickness/ply = 0.0055 inch.

Since $F_{x_{tu}}$ (the allowable ultimate tension stress in the x direction) is dependent on the ply orientation, assume an orientation of ($0^o/\pm45^o/90^o$). Thus

25% of the plies are $0^o$
25% of the plies are $90^o$
50% of the plies are $45^o$

From Figure B10.5.2-1 the "B" basic allowable with these percents, $F_{x_{tu}}$ = 51,000 psi, and the thickness required based on strength is determined as

$$t = \frac{N_x}{F_{x_{tu}}} = \frac{3,000}{51,000} = 0\ .0588 \text{ inch}$$

Next check for strain limitations of $\varepsilon$ = .004 in./in. allowable from Figure B10.6.2-1 or from the material property curve for $E_{x_t}$, Figure B10.5.2-5.

From Figure B10.6.2-1 the given ply percent,

$$\frac{F_{x_t}}{\varepsilon} = 8 \times 10^6 \text{ and}$$

$$F_{x_t} = \frac{F_{x_t}}{\varepsilon} \times \varepsilon = 8 \times 10^6 \times .004 = 32,000 \text{ psi}$$

The strain limited thickness is

$$t = \frac{N_x}{F_{x_t}} = \frac{3,000}{32,000} = .0938 \text{ inch}$$

The nominal ply thickness is 0.0055 in. (Reference Section B10.5.2.B) and the minimum number of plies is calculated as $\frac{.09375}{.0055}$ = 17.05. In order to maintain the same percentage of ply orientation ($0^o$, $\pm 45^o$, $90^o$), sets of 4 must be used. Therefore, the design requirements would be the nearest whole number, 5 sets of 4 plies, or 20 plies at a thickness of t = 20 x .0055 = 0.110 inch.

## B10.7.0 Structural Design Practices and Guidelines

Performance requirements will require the use of advanced composites in many structural components, since the density is approximately 1/2 the density of aluminum and its strength and stiffness is nearly equal to aluminum. However, the initial costs of fabrication and assembly will, in general, be higher than for the equivalent aluminum structure. Thus, when composites are being considered, Design Supervision approval must be obtained prior to initiation of detail design. Producibility Engineering must also be consulted during the preliminary design stages to assure that the costs of manufacturing are within reason.

In this section, design practices for the use of composites are specified and guidelines are presented to aid the designer in his selection.

Drawings and drawing dimensions for composite laminate structure shall be in accordance with the DM 11.444 - 11.461.

B10.7.1 Material Selection

A. At the present time only two material systems are FAA qualfied by DAC for flight structures: 1) Thornel T300 graphite fibers with the Narmco 5208 epoxy resin (T300/5208) and 2) Kevlar 49 with the Fiberite F-155 epoxy resin. These materials shall be used in collimated tape form or as woven fabric.

B. High modulus graphite filaments are available and may be used where required to enhance the structural stiffness.

C. Use of hybrids for obtaining special characterisitics must be reviewed with supervision before starting detail design.

D. Graphite or Kevlar laminate designs shall allow for reduced allowables resulting from moisture absorption. (The allowables in Section B10.5.2 do not account for this. However, to date the reduction has been found to be negligible.)

B10.7.2 Laminate Requirements

A. Orientations of $0^o$, $+45^o$, $-45^o$, and $90^o$ only shall be used for laminate layup.

B. Orientation from one layer to another layer should not be greater than $45^o$ if possible; for example: $0^o$, $+45^o$, $90^o$, $-45^o$, and $0^o$.

C. The stacking sequence shall be mid-plane symmetric (a symmetrical balance design) to prevent warping of the laminate after cure.

D. A minimum of $90^o$ cross plies equal to 10 percent of the total laminate thickness shall always be specified regardless of the load orientation.

E. Changes in laminate thickness should be gradual. This can be accomplished by stepping back or staggering the individual plies in the transition area. The slope formed by a thickness transition should be $30^o$ or less. The tolerance on the location of the transition should be as large as possible, preferably ±.10 inch or larger (see Figure B10.7.2-1).

F. The laminate thickness shall be specified by the number of layers. (Overall thickness is referenced.)

G. Four adjacent tape plies is the maximum laminate stackup allowed when these plies are orientated in the same direction in order to minimize edge delaminations.

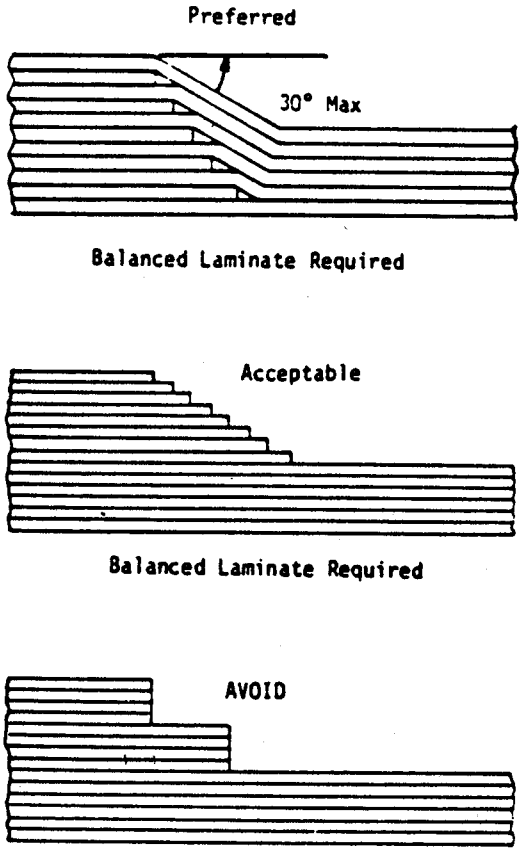


Figure B10.7.2-1 Laminate Thickness Transition

H. The maximum laminate strain in any fiber direction for composite laminate principal structural elements at ultimate design loads shall not exceed 0.004 in./in. to preclude fast fracture from unexpected damage (refer to Section B10.6.0). Structural Mechanics group should be consulted for up-to-date data.

I. Thin unstiffened composite laminates (0.040 inch thick or less shall not be allowed to buckle below 60% of limit load. Buckling is allowed above 60% limit load as cyclic tests have demonstrated that shear panels can be repeatedly buckled without causing any damage to the composite laminate (refer to Section B7.0.0 for Plate Buckling of Composites).

J. The laminate pattern at a joint should be as near isotropic as possible (quasi-isotropic).

B10.7.3 Fastener Requirements

A. Fastener usage shall be as specified in the Structural Fastener Usage Policy for the particular airplane. For new airplanes, when a fastener usage policy is not available, the guidelines of Reference B10-3 must be adhered to.

B. Unplated titanium, Inconel or Monel fasteners shall be installed in graphite laminates to prevent galvanic corrosion of the fastener.

C. Where mechanical fasteners are to be used in graphite/epoxy laminates, fiberglass surface layers shall be co-cured on both surfaces of the Gr/Ep laminate to prevent delamination from drill breakthrough and also to prevent galvanic corrosion of the mating aluminum or cadmium plated steel parts.

D. All shear carrying fasteners other than rivets, shall be installed with a tight fit hole, but not in an interference fit condition. Fasteners which would normally be interference fit in metal structures (lockbolts and Hi Loks) shall be installed in a Class V hole because delamination can occur if the fastener is forced through an interference hole.

E. Nuts shall be torqued to standard values.

F. Rivets shall be squeezed and not gun-driven into place.

G. Aluminum rivets shall not be used in graphite structure.

H. Fastener edge distance shall be 3D (not 2D) + 1/16 inch.

I. Optimum fastener spacing normal to the applied loads is 3 to 4D for Gr/Ep with a single row joint. Net tension stress increases for fastener spacings less than 4D. However, based on observed results in composites (Gr/Ep), the reduced stress concentration factor at closer spacings more than offsets the increased stress.

J. For two or more rows of bolts in Gr/Ep, the bolt pattern shall be staggered (not lined up one behind the other).

K. For countersunk holes, bearing area shall not include the countersink depth.

L. Where fasteners are installed in Gr/Ep, the following lamina direction percentages are recommended in order to have acceptable allowable strength:

$0^{o}$ - 25% to 50%
$90^{o}$ - Less than 25%
$45^{o}$ - 33% to 75%

B10.7.4 Fit Requirements

A. Composite components are stiff and cannot be post-formed to fit. Provisions shall be made to permit adjustments of mating parts.

B. Graphite/epoxy laminates shall not come in contact with aluminum mating parts (except aluminum honeycomb). A fiberglass surface layer is required to prevent galvanic corrosion.

B10.7.5 Sandwich Construction (Refer to Section B11.0.0)

Advanced composite laminates are frequently used as skins bonded to low density core, such as honeycomb materials. These skins may be precured and bonded with adhesives to the core to produce the final sandwich. Where structurally acceptable, one or both skins may also be cured during the skin to core adhesive bond cycle (co-cured assembly). In either case, it may be necessary to include an adhesive layer at the skin to core interface.

Analysis methods for preliminary sizing of composite sandwich structure are provided and/or referenced in Section B11.0.0.

B10.7.6 Stiffened Panel Construction

Advanced composite panels, flat and curved, may be designed with integral stiffeners. In this fabrication process, the tooling is configured to allow layup and subsequent simultaneous cure of the panel skin and the stiffening member. Figure B10.7.5-1 depicts section cuts of integrally stiffened panel configurations that have been produced. The stiffener members may also be laid up and cured as separate details and adhesively bonded or mechanically fastened to precured skins.

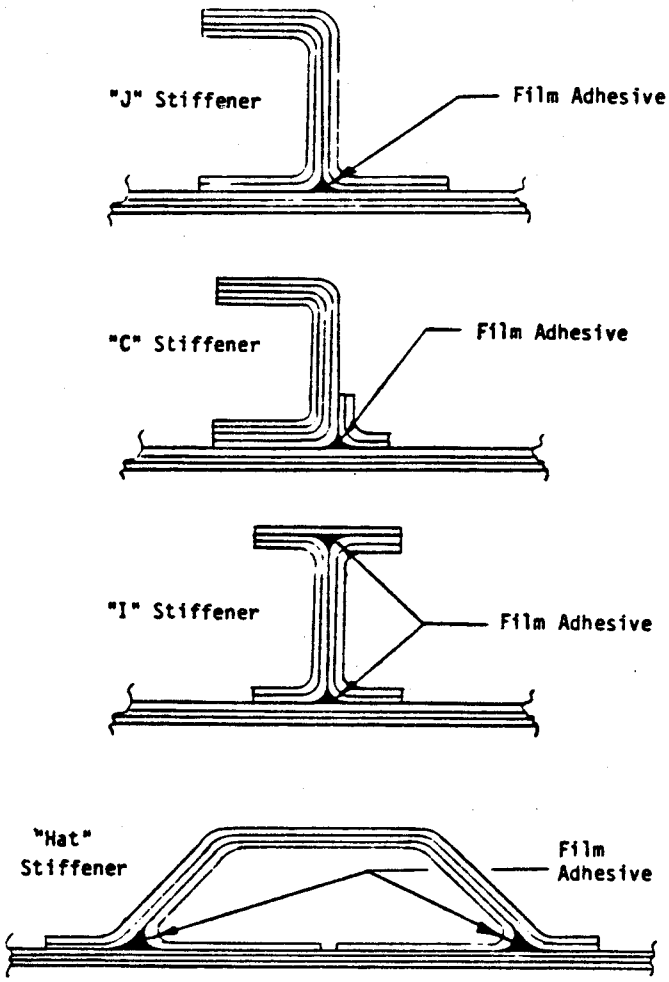


Figure B10.7.5-1 Stiffened Composite Sections

B10.7.7 Thermal Expansion

Thermal expansion differences between metal structure (especially aluminum) and the composite structure shall be accounted for to prevent unacceptable induced loads. The thermal expansion coefficient of graphite or Kevlar ranges between zero and 3 x $10^{-6}$ in./in./$^{o}$F depending on the orientation of fibers in the laminate. For pseudo-isotropic patterns, the typical value is 1.5 x $10^{-6}$ in./in./$^{o}$F. Thus, when graphite/epoxy or Kevlar/epoxy laminates are fastened to an adjoining aluminum structure, the expansion differences must be accounted for in the analysis of the fastener strength and included in determining the bearing load (refer to Section B10.5.2 for thermal coefficients of composites).

B10.7.8 Rain Erosion Protection

If a plane, tangent to the surface of the laminate is within 75$^{o}$ of being perpendicular to the boundary layer flow over the aircraft, as shown in Figure B10.7.8-1, that portion of the laminate requires rain erosion coating. Consult with M&PE for types of coatings.

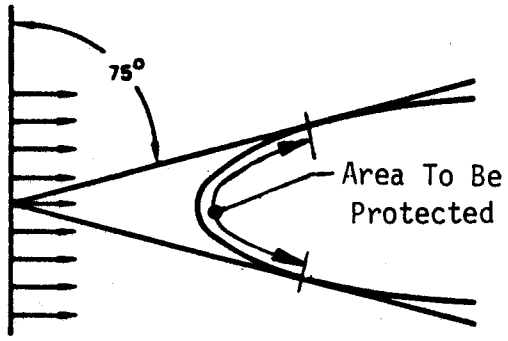


Figure B10.7.8-1 Rain Erosion Requirements

B10.7.9 Systems Interface

A. Special provisions shall be provided for graphite, Kevlar, and fiberglass structures to prevent damage from lightning and P-static discharge.

B. Provisions shall be provided for the grounding of electrical subsystems since neither graphite, Kevlar, or fiberglass will provide the necessary electrical path.

## REFERENCES

B10-1 "Advanced Composite Design Guide", Air Force Materials Laboratory (AFML/LC), Wright Patterson Air Force Base, Ohio 45433.

B10-2 "Plastic for Aerospace Vehicles, Mil-Hdbk-17A, Department of Defense, Washington, D.C., 20025

B10-3 Kam, C. Y., "Structural Fastener Usage Policy for Advanced Composite Structures, MDC J2277, July 1982.

# SANDWICH STRUCTURE

TABLE OF CONTENTS

## B11.0.0 Sandwich Structure

### B11.1.0 Introduction

Sandwich structure is a laminated construction formed by bonding a thin face sheet to each side of a thick, low density core as shown in Figure B11.1.0-1. It is a "stressed skin" construction. The basic concept is: 1) to space the strong, thin face sheets far enough apart with a thick core to assure that the construction will be stable, 2) to provide a core that is stiff and strong enough to stabilize the face sheets through a bonding medium (such as an adhesive layer or brazing alloy), and 3) to provide a core that is strong enough to resist the transverse shear loads. Sandwich structure in bending is analogous to an I-beam where the outer flanges carry the compression and tension loads, and the web supports the flanges and carries the shear loads. In the sandwich, the faces carry the compression and tension loads, while the core carries shear forces, provides continuous support to stabilize the faces, and is capable of bending about a common neutral axis. Proper choice of materials and thicknesses of faces, core, and adhesive results in a high strength and/or stiffness to weight ratio.

Sandwich structure uses relatively thin faces to carry loads. Therefore, consideration must be given to the following modes of failure which may occur under edge and/or normal loads.

#### B11.1.1 General Instability

General instability of the entire panel when subjected to edge compression.

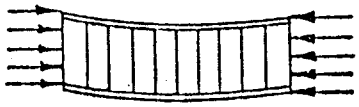

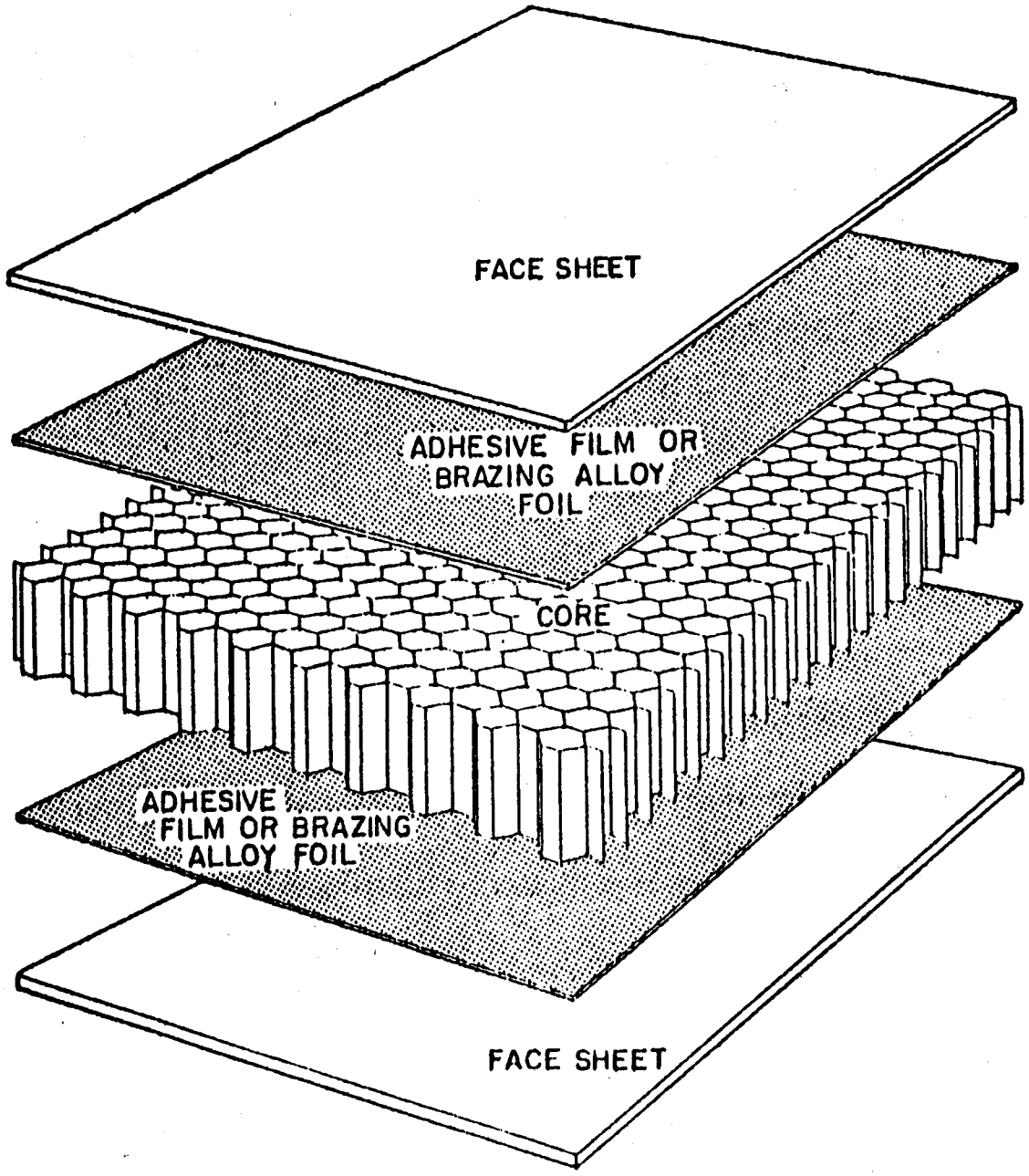


Figure B11.1.0-1 Sandwich Structure

### B11.1.2 Shear Crimping

Shear crimping of the panel due to low shear strength in the core. Shear crimping appears to be a local mode of failure, but is often a form of general overall buckling in which the wavelength of the buckles become very small because of low core shear modulus. The crimping occurs very suddenly and usually causes the core to fail in shear at the crimp, and may also cause shear failure in the bond between the core and face. Crimping may also occur in conjunction with overall buckling of the sandwich and in such cases, the overall buckle begins to appear, the crimp occurs suddenly because of severe local shear stresses at the ends of the overall buckle, and as soon as the crimp appears, the overall buckle may disappear. Therefore, although examination of the failed sandwich indicated crimping or shear instability, failure may have begun by overall buckling which finally caused crimping.

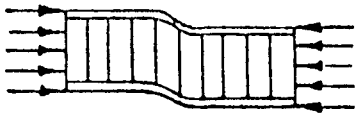

### B11.1.3 Intracell Buckling

Intracell buckling or dimpling of the faces into the core, due to cell size. This dimpling of the faces may not lead to failure, unless the amplitude of the dimples is large enough to cause a wrinkling of the faces if dimples grow across the core cell walls. Dimpling that does not cause total failure may be severe enough so that permanent dimples remain after removal of the load.

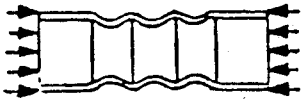

### B11.1.4 Face Wrinkling

Face wrinkling of the face across the panel width, due to either a weak bond, a low tensile or compressive strength core. Wrinkling may occur if a sandwich face subjected to edge compression buckles as a plate on an elastic foundation. The faces may buckle inward or outward, depending on the flatwise compressive strength of the core, relative to the flatwise tensile strength of the bond between the faces and core. If the bond between faces and core is strong, faces can

wrinkle and cause tension failure in the core. The wrinkling load depends then upon the elasticity and strength of the foundation system. That is the core and the bond between face and core. The wrinkling load will also depend upon the initial face eccentricity of waviness since the faces are never perfectly flat.

In addition to the overall buckling and local modes of failure, the sandwich shall be designed so that faces do not fail in tension, compression, shear, or combined stresses due to edge loads and/or normal loads, and cores do not fail in shear or flatwise compression due to normal loads.

B11.1.5 Basic Design Principles

A. Sandwich faces shall be thick enough to withstand stresses under static and fatigue loads at operating stresses and temperatures.

B. The core shall be thick enough and have sufficient shear modulus and strength so that overall sandwich buckling, excessive deflection, or shear failure will not occur under design loads.

C. The core shall have a sufficient modulus of elasticity and the sandwich shall have great enough flatwise compressive strength so that wrinkling of either face will not occur under design loads.

D. If face dimpling is not permissible, the cell size shall be small enough so that dimpling of either face into the core spaces will not occur under design loads.

B11.1.6 Symbols

The following symbols are used for the sandwich structure design. They are adopted in part from the Reference B11-9.

$a$ = Long edge panel dimension, in., or subscript denoting loaded edge

$A$ = Nondimensional parameter of material properties in both the elastic and plastic ranges, $\frac{F_c}{E_t}$

b = Short edge panel dimension, in., or subscript denoting loaded edge

c = Subscript denoting "core" or "compression"

d = Total sandwich depth or thickness, in.

D = Bending stiffness, $\frac{E_t t_f \left(t_f + t_c\right)^2}{2(1-\mu^2)}$, in.-lbs.

E = Young's modulus of elasticity (use with appropriate subscripts), psi

$E_t$ = Tangent modulus of elasticity, psi

f = Calculated stress, psi, or subscript denoting face

F = Allowable stress (use with appropriate subscripts), psi

$G_c$ = Core shear modulus, $\frac{E_t}{2(1+\mu)} \times \frac{t_w}{s}$, psi

H = Extensional stiffness $2t_f E_t$, lbs./in.

k = Nondimensional parameter, $t_f/t_c$

K = Buckling coefficient

m = Number of half-wave buckles ("b" direction)

n = Number of half-wave buckles ("a" direction)

p = Normal load, psi

P = Load, lbs.

q = Load intensity for compression and shear, lbs./in.

r = Radius, in.

$r_a$ = Bi-axial compression stress ratio, $f_a/f_b$

s = Core cell size (diameter of inscribed circle of honeycomb core), in.; subscript denoting shear when applied to stress; and "secant" when applied to moduli

t = Thickness (use with appropriate subscripts), in., or subscript denoting tangent

u = Subscript denoting ultimate

U = Transverse shear stiffness $\frac{E_t(t_f + t_c)^2}{2(1+\mu)t_c} \times \frac{t_w}{s}$, lbs.-in.

V = Panel shear and bending stiffness parameter (subscripts), psi

$$\frac{\pi^2 D}{b^2 U} = \frac{\pi^2 t_f t_c (1+\mu)}{(1-\mu^2)b^2} \left(\frac{s}{t_w}\right)$$

w = Subscript denoting honeycomb core cell wall. Density of material, lbs./in.$^3$

$\beta$ = Bending coefficient for normal loads P.

$\gamma$ = Shear coefficient for normal loads P.

$\mu$ = (mu) Poisson's ratio

The symbols will be defined more explicitly as they are used in the analysis section.

B11.1.7 Core Identification

A. Hexcel Expanded Aluminum Honeycomb Core is identified by the following code system:

1. First Number: Cell size, s, in fractions of an inch.

2. Second Number: The aluminum alloy used -
   3003 designates 3003 (or 3S) aluminum alloy H-19 temper.
   5052 designates 5052 (or 52S) aluminum alloy H-39 temper.

3. Third Number: The nominal foil thickness in inches.

4. First Letter: Perforations -
   P indicates that the cell walls are perforated.
   N indicates that the cell walls are nonperforated.

Example: 3/16 - 5052 - .002N
3/16 inch cell - 5052 aluminum alloy - .002 foil thickness - cell walls nonperforated.

B. Hexcel Unexpanded Aluminum Honeycomb Core Planks are available and are identified by the word "HOBE" (HOneycomb Before Expansion) and the code per A above.

C. Brazed Sandwich Core is identified by the following code system:

1. First Number: Cell size in sixteenths of an inch, 4 = 4/16, 5 = 5/16, etc.

2. Second Number: Foil thickness in ten thousandths of an inch, 10 = .0010, 15 = .0015, 10 = .0020, etc.

3. First Group of Letters: Core configuration -

S = Square cell 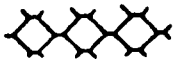

H = Hexagonal cell 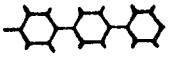

Si = Sine cell 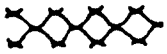

SC = Corrugated square cell 

SiC = Corrugated sine cell 

HC = Corrugated hexagonal cell 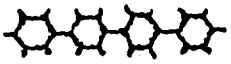

4. Second Group of Letters: Perforations -

NP = Nonperforated

P = Perforated

Example: 3-15-S-P, AMS350-.500 x 10 x 48R -
3/16" cell - .0015 foil-square cell-perforated.

AM350 precipitation hardening stainless steel alloy 1/2 inch thick x 10 inches wide x 48 inches long with ribbon direction parallel to the 48 inch dimension.

## B11.2.0 Present Applications

Honeycomb sandwich panels are currently used on the A-3D, A-4D, C-133, DC-8, DC-9, and DC-10 production airplanes.

The access doors and panels on the C-133 landing gear pods are constructed of aluminum honeycomb core with fiberglass faces. Figure B11.2.0-1 shows the relative positions of the doors on the pods and a view of a typical door. Figure B11.2.0-2 shows two typical cross sections of the internal structure showing the change of core densities, reinforcing channels, and other reinforcements.

The original A-4D rudder, designed with conventional construction, was redesigned to improve service life. The revised rudder is constructed of aluminum honeycomb with aluminum faces and external hat section reinforcements. Figure B11.2.0-3 shows the airplane and the rudder. Figure B11.2.0-4 shows details of the construction. Perforated core is used to allow for pressure tests and sealing checks.

The panels used on the A-3D airplane are similar in design to the DC-8 panels.

Figure B11.2.0-5 shows a perspective of the DC-8 jetliner and many of the nearly 170 metal faced, metal honeycomb panels used on this airplane.

The bonded assemblies in use today are grouped in the following types:

## B11.2.1 Flat Panels

Flat panels of constant thickness are used on the upper and lower wing surfaces aft of the rear spar in the flap region on the DC-8 and DC-10 because of superior resistance to sonic fatigue. The panel construction consists of:

A. An aerodynamically smooth external surface.

B. A doubler to reinforce the external face over supports and around the edges.

C. The hexagonal aluminum honeycomb core.

D. The attach spacers where required.

E. The internal face.

F. The internal face reinforcing pan doubler.

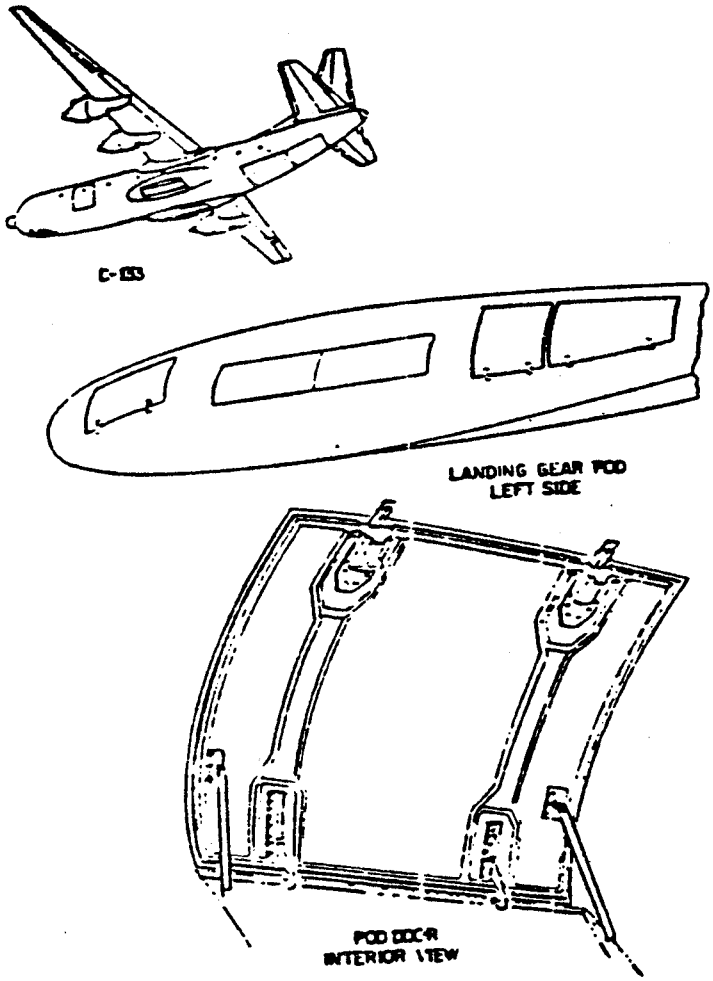


Figure B11.2.0-1 C-133 Landing Gear Pod Door

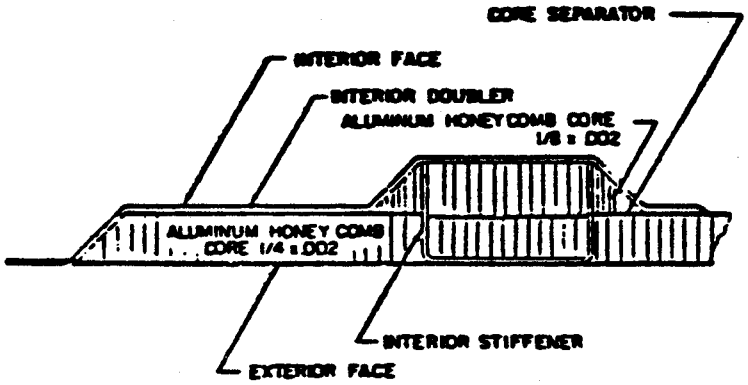


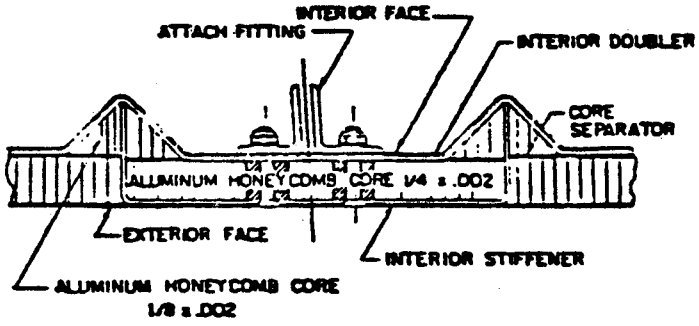


Figure B11.2.0-2 Cross Sections-Typical Door

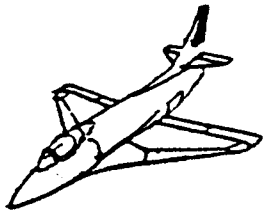

A4D

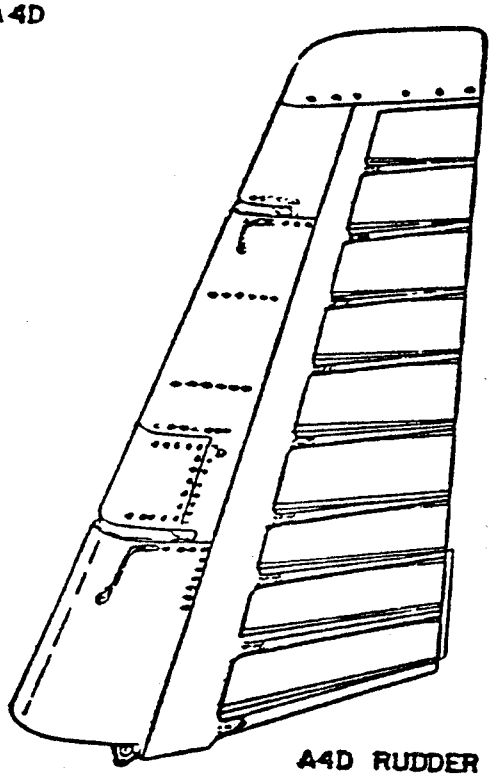

A4D RUDDER

Figure B11.2.0-3 A-4D Rudder

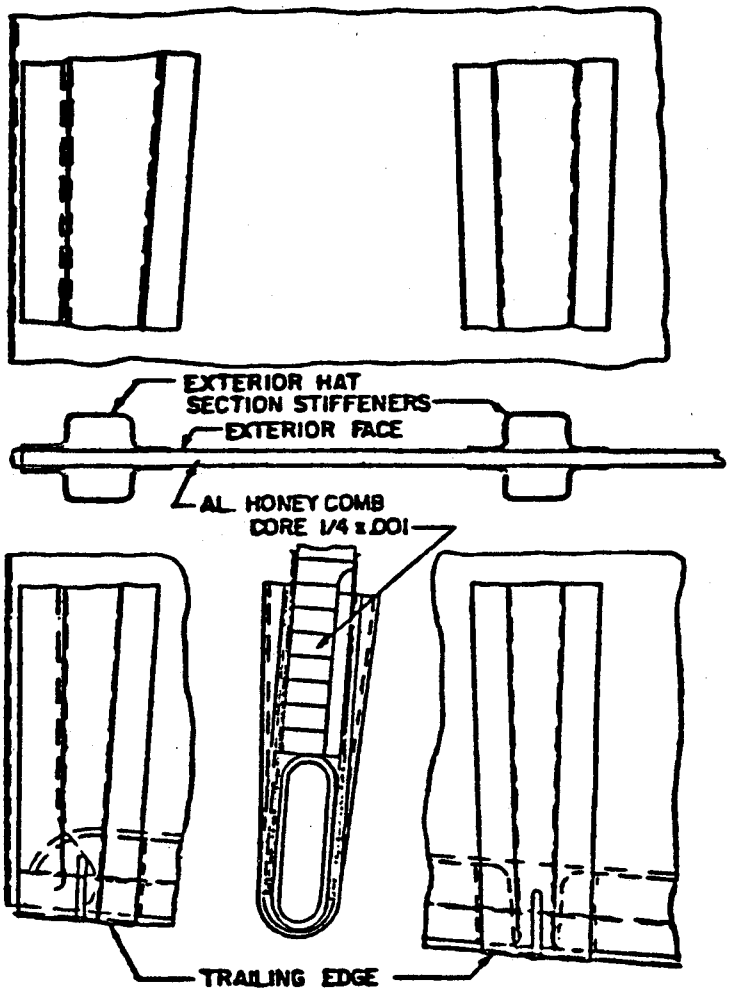


Figure B11.2.0-4 A-4D Rudder Construction

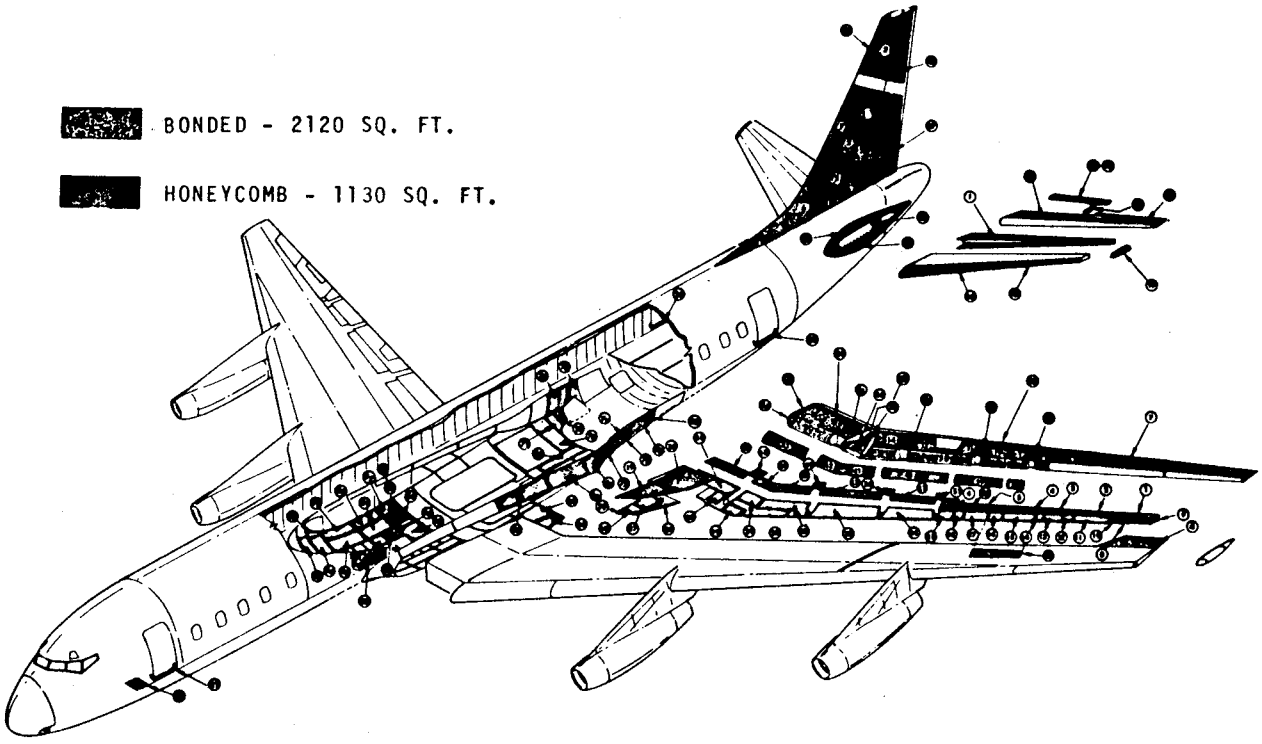


Figure B11.2.0-5 DC-8 Jetliner (Dark Area Indicates Location of Metal Honeycomb Panels

These panel configurations were developed from acoustic and fatigue tests. The face thickness was selected to the minimum gauge with doublers added where necessary. Panels continuing over multiple supports are continuous beams uniformly loaded and have maximum bending moments and shears at the supports. These maximum bending moments are approximately twice the maximum mid-span bending moments. For efficient lightweight structure, the panels are reinforced only over the supports with the reinforcements ending approximately at the points of inflection.

Abruptly ending doublers were tested and found to have poor fatigue life. As a result, a finger-type doubler was developed which gives a tapered effect by gradually picking up the loads in the faces, and at the same time, acting as doublers around the attach holes to reduce stress concentrations. Finger doublers on the external face doublers required excessive machining and prefitting of the core. Straight external face doublers were tested with finger-type internal face doublers. Fatigue life was very satisfactory when the straight type external face doubler ended midway of the length of the internal face doubler pan, as shown in Figure B11.2.1-1. The interior face doubler is a one-piece, deep-drawn pan. This construction allows unnecessary material to be removed from the center of the doubler, permitting the edge members to be integral with the finger-type support reinforcements, thus eliminating overlapping edge member joints.

Attachments must be made to and through the honeycomb panels for joining to other structure. Spacers are required to transfer the loads to the core and prevent the core from being crushed. Available commercial rivet and bolt spacers were evaluated for the DC-8, but none fully met the requirements. Solid bar type were investigated and finally chosen because they met the majority of the requirements and had other advantages. For the DC-8, DC-9 and DC-10 laminated fiberglass was selected as being lightweight and compatible with the bonding cycle. The geometry was determined by the requirements. Width was selected as one-half inch for three-sixteenth inch diameter fasteners. This width allows for enlargement to one-fourth inch attachments if oversize attachments are required. The laminations are normal to the attachment centerline to prevent splitting during installation of the fasteners. The height of the spacer was selected to the minimum tolerance of the mating parts, so laminations could be added to build up the spacer to the existing tolerances of the assembled parts to allow for manufacturing tolerances.

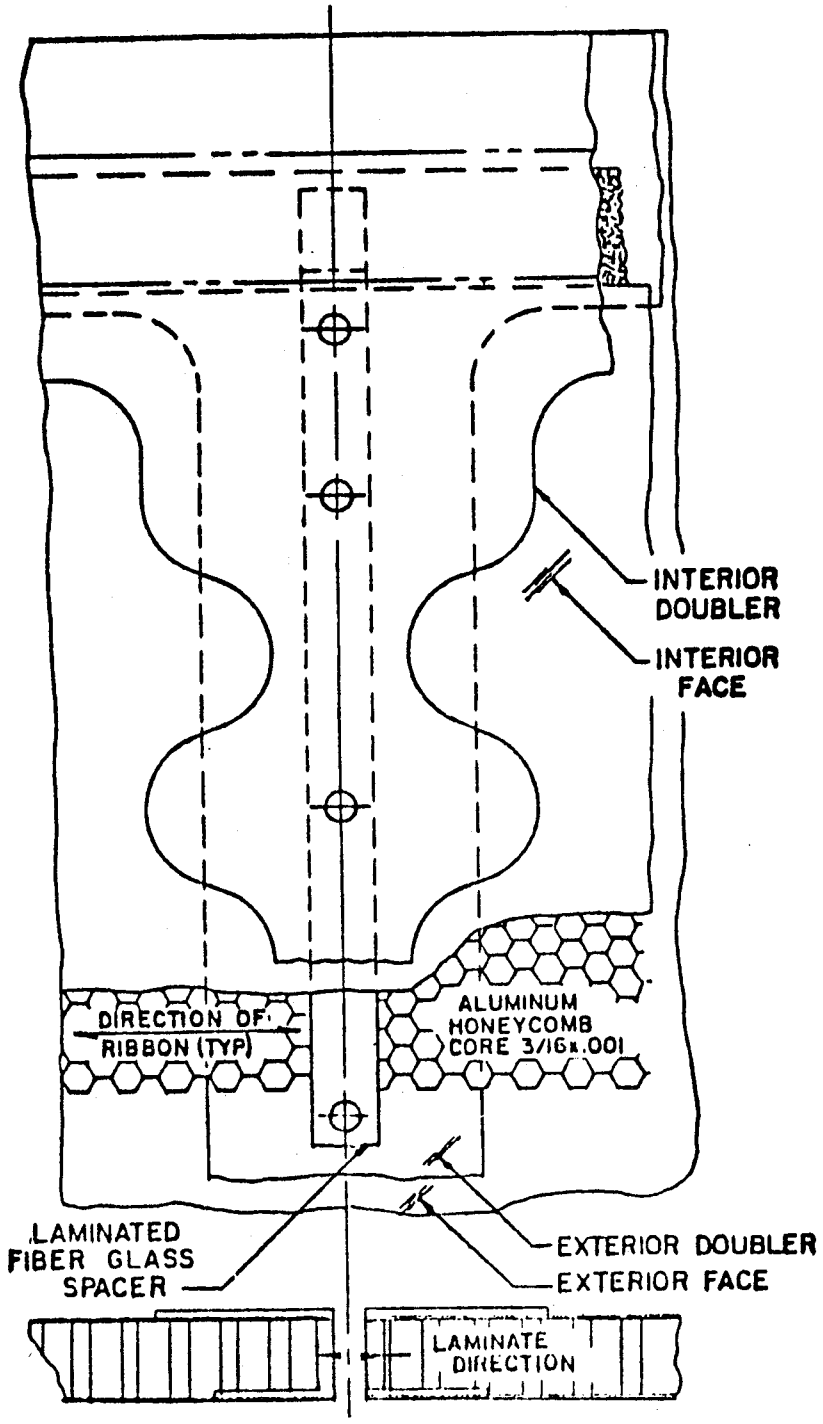


Figure B11.2.1-1 Panel Construction

The fiberglass spacer was required to resist the forces of installing quarter inch rivets, pulling, and breaking the shank of quarter inch steel lockbolts, and the over-torquing of quarter inch bolts. The spacers were made continuous to permit the addition of additional fasteners between existing fasteners if required. The pilot holes are #20 (.159 - .167) to assist in drilling the attachment holes through the glass laminate.

### B11.2.2 Single and Double Curved Panels

Single and double curved panels are used for wing-to-fuselage fillets They were chosen for resistance to sonic fatigue and to eliminate many intermediate support ribs. The design standards for flat panels apply to the curved panels. Fixtures are required to hold the parts during assembly and bonding. Aluminum detail parts must be formed to the contours required. The DC-8 uses aluminum faced panels and the DC-9 and DC-10 uses fiberglass faces. Figure B11.2.2-1 shows the cross section of a typical fillet panel.

### B11.2.3 Wedge Panels

Wedge panels of single and double taper are used on the upper and lower surfaces of the wing, aft of the rear spar in the region forward of the aileron. They are used for sonic fatigue reasons, but also eliminate some intermediate support ribs. Figure B11.2.3-1 shows a typical panel assembly.

Wedge panels are used for spoilers on the upper surface of the wing forward of the flaps. They were made of honeycomb for sonic fatigue resistance and rigidity in torsion. The spoilers are driven by one or two drive stations and twist deflections were required to be a minimum. The spoilers were designed with preload twist manufactured in the panels. The panels under normal flight loads deflect to give the proper slot lip gap for cruise speeds. Figure B11.2.3-2 shows a typical spoiler assembly. Ten of the spoilers are used, of which six are used at low speed in connection with the ailerons.

Wedge panels are used for trailing edges of the control surface tabs. Honeycomb was selected because it gave the greatest torsional rigidity for the weight. Any excess weight incurs greater weight penalty because all weight aft of the hinge must be dynamically and statically balanced. Honeycomb construction permits very thin faces and the elimination of all internal rib structure.

Non-perforated core is used in the panels to preclude the entrance and entrapment of moisture. Moisture changes the balance and introduces freezing problems.

Figure B11.2.3-3 shows a typical control tab assembly.

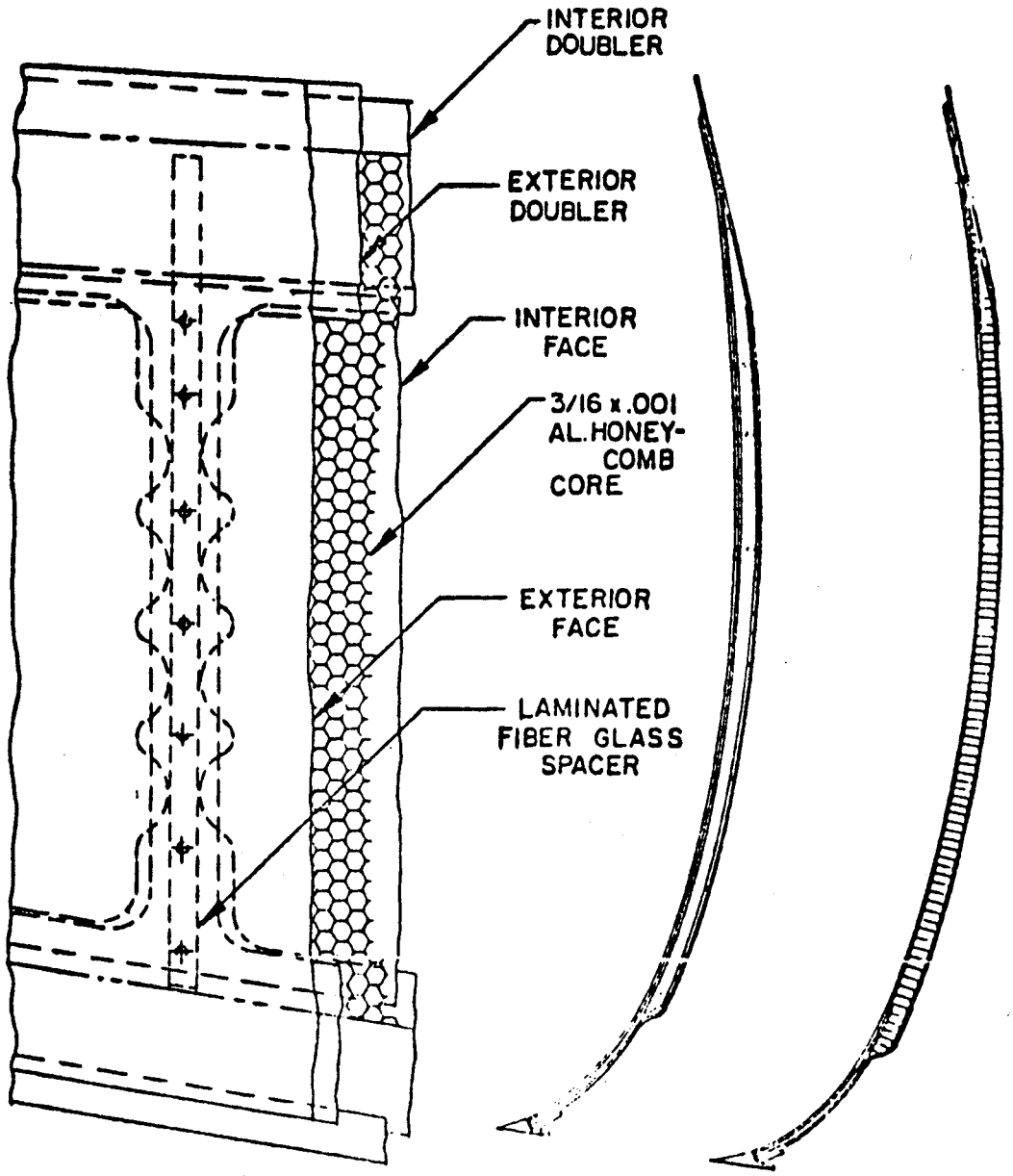


Figure B11.2.2-1 Fillet Panel

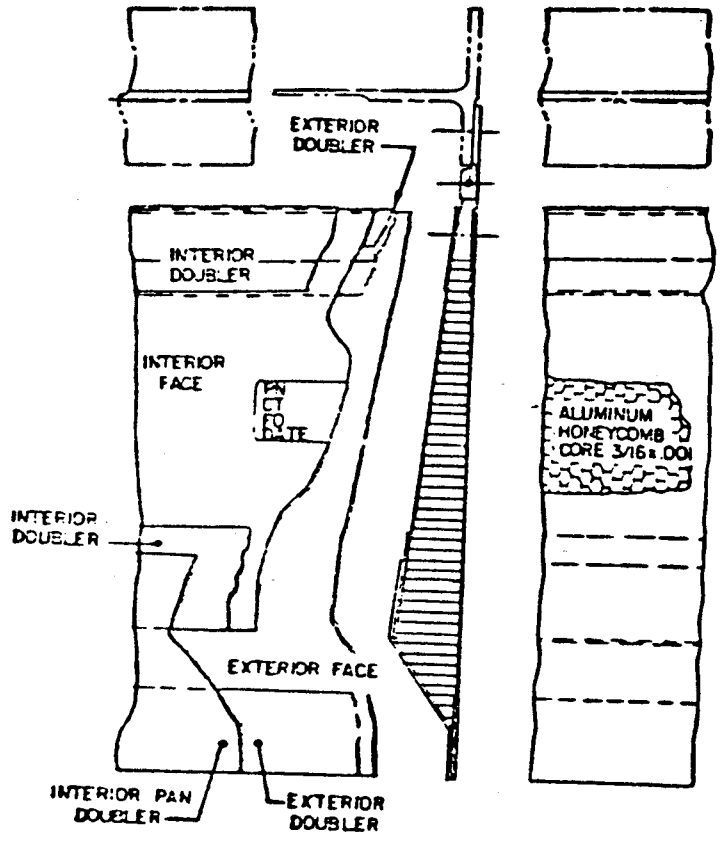


Figure B11.2.3-1 Wedge Panel

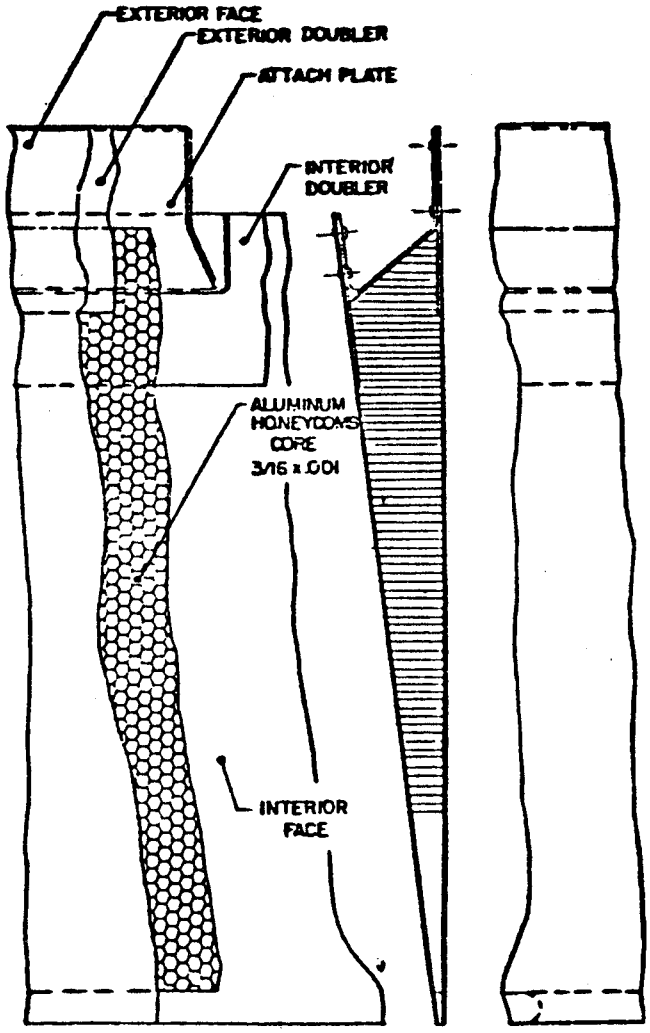


Figure B11.2.3-2 Typical Spoiler Assembly

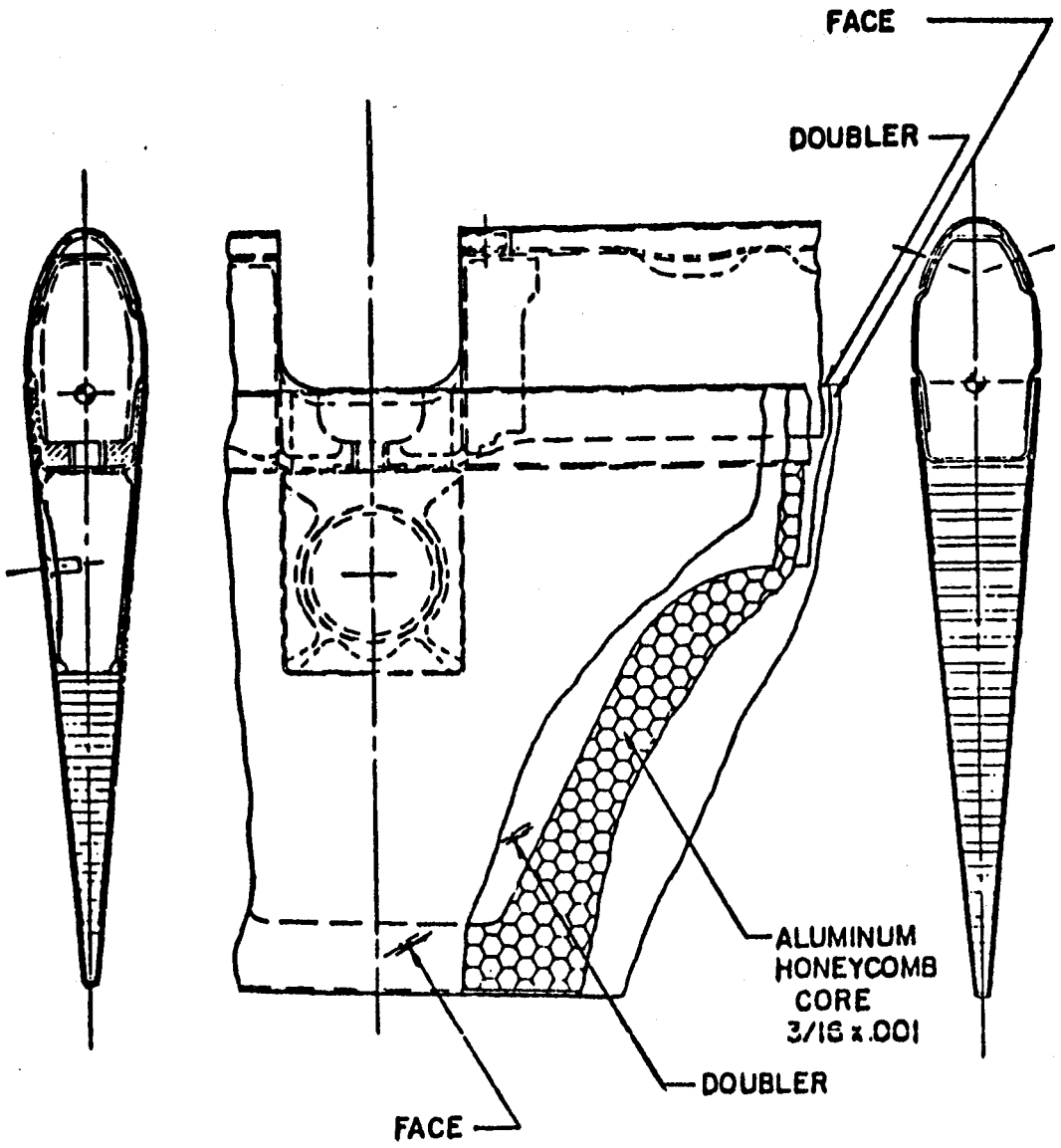


Figure B11.2.3-3 Control Tab Assembly

B11.2.4 Flap Vanes

Flap vanes are airfoil shaped panels with both twist and taper incorporated. Honeycomb was selected to obtain a lightweight, torsionally rigid structure, and eliminate internal ribs. The vanes are also in a region of high sonic forces and the honeycomb is superior for sonic fatigue. Figure B11.2.4-1 shows a typical flap vane assembly.

B11.3.0 Future Applications

High density materials, such as titanium and stainless steel, will be used more frequently for sandwich panel construction in future aircraft and missile design. Typical supersonic and hypersonic aircraft applications are cover panels for wing integral fuel tanks, wing tips, control surfaces, and trailing edges.

Sandwich cylinders made from high temperature materials will also find many applications in missile and space construction.

Composite sandwich structure is being considered more and more for secondary structure. Most new DAC commercial aircraft will have a great percentage of composite sandwich structure because it is both cost and weight effective.

When considering sandwich panel construction for future applications the following guidelines should be followed:

A. Use metal face sandwich structure only for parts which are easily removed and replaced in the event of damage to the thin face sheets or debonding of the face sheets from the core. Control surfaces and trailing edge structure are good applications.

B. Do not use sandwich structure for control surface which are unpowered and aerodynamically balanced. Damage to the thin face sheets can allow the entrance of moisture which can upset the balance requirements.

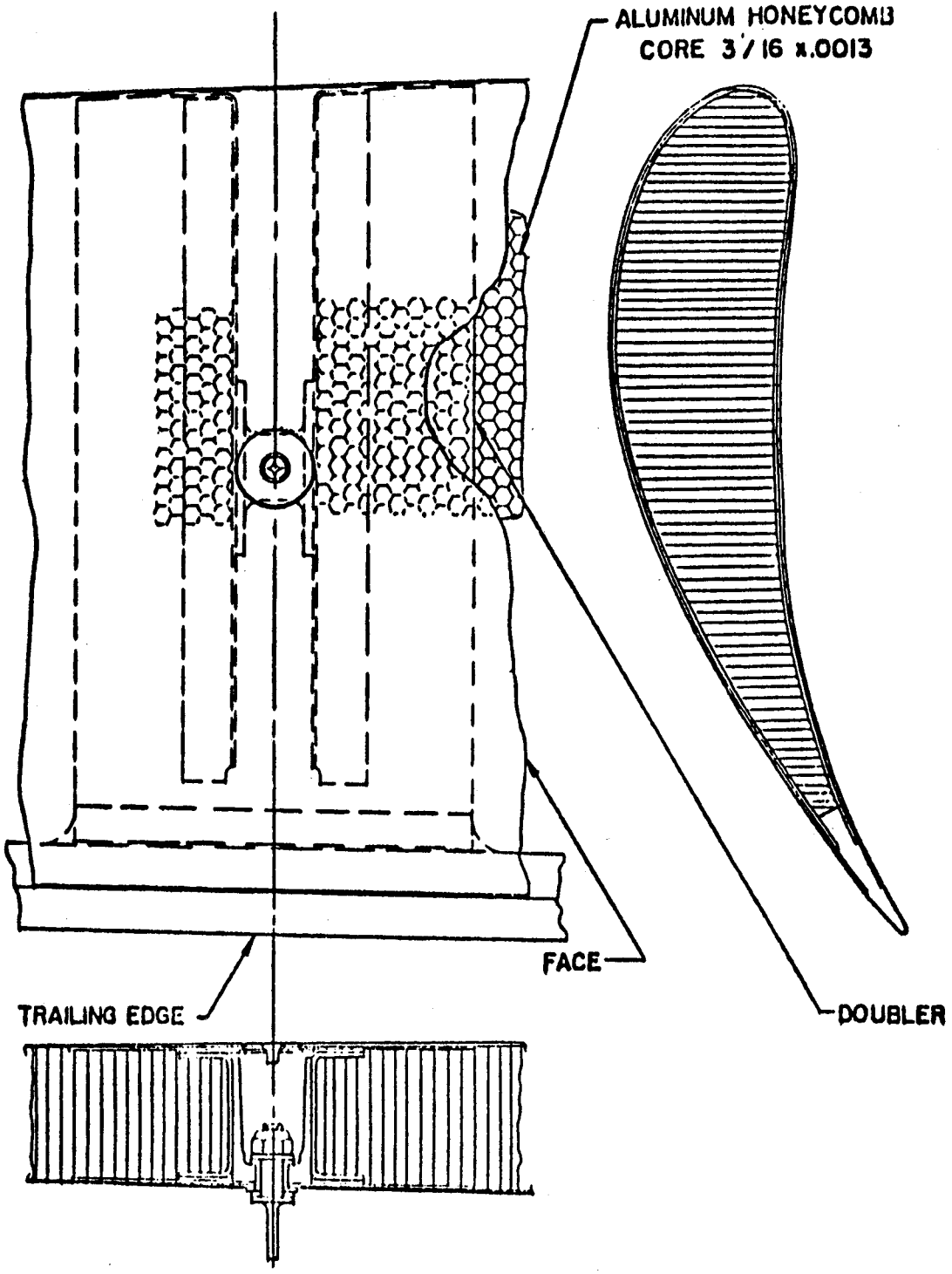


Figure B11.2.4-1 Typical Vane Assembly

## B11.4.0 Weight

A summation of the individual weights of the core, two face sheets, and the bonding material will give the basic panel weights. Doublers, edge members, and fitting weights must be added for the complete panel weight.

### A. Core Weights

| Cell Size (inch) | Foil Gauge (inch) | Core Density (lbs./ft.$^3$) | | |
|---|---|---|---|---|
| | | Honeycomb | | Sq. Cell Core |
| | | Aluminum | Stainless Steel | Stainless Steel |
| 1/8 | .0007 | 3.1 | | |
| 1/8 | .001 | 4.5 | | |
| 1/8 | .002 | 8.1 | | |
| 3/16 | .001 | 3.1 | 6.3 | 5.9 |
| 3/16 | .002 | 5.7 | 12.6 | 11.8 |
| 3/16 | .003 | 8.1 | | 17.8 |
| 1/4 | .001 | 2.3 | 4.8 | 4.3 |
| 1/4 | .002 | 4.3 | 9.6 | 8.5 |
| 1/4 | .003 | 6.0 | | 12.9 |
| 3/8 | .001 | 1.6 | 3.4 | 2.5 |
| 3/8 | .002 | | 6.7 | 5.1 |
| 3/8 | .005 | 6.5 | | |

### B. Face Sheet Weights

| Material | Density (lb./in.$^3$) | Sheet Weight per MIL Thickness (lb./ft.$^2$) |
|---|---|---|
| 2024-T4 Aluminum | .100 | .0144 |
| 7075-T6 Aluminum | .101 | .0145 |
| 6A1-4V Titanium | .160 | .0230 |
| PH15-7Mo (RH-950) | .179 | .0402 |
| 17-7PH (TH-1050) | .282 | .0406 |
| A-286 | .286 | .0412 |
| Rene 41 | .298 | .0429 |
| Kevlar-49/F155 | .049 | .00706 |
| Graphite T300/5208 | .056 | .00806 |
| Fiberglass E-glass/F155 | .069 | .00994 |

C. Bonding Material Weights

| Material | Density ($lb./in.^3$) | Avg. Weight/Bond ($lb./ft.^2$) |
|---|---|---|
| Lithobraze #925 (.002 in.) | 437 (5.25 troy oz./cu. in.) | .1255 |
| *FM-1,000 Adhesive | | .065 |
| DPS 1.99 Adhesive | | .0936 |
| *HT-424 Adhesive ($350^oF$) | | .130 |

D. Typical Aluminum Honeycomb Panel Weights

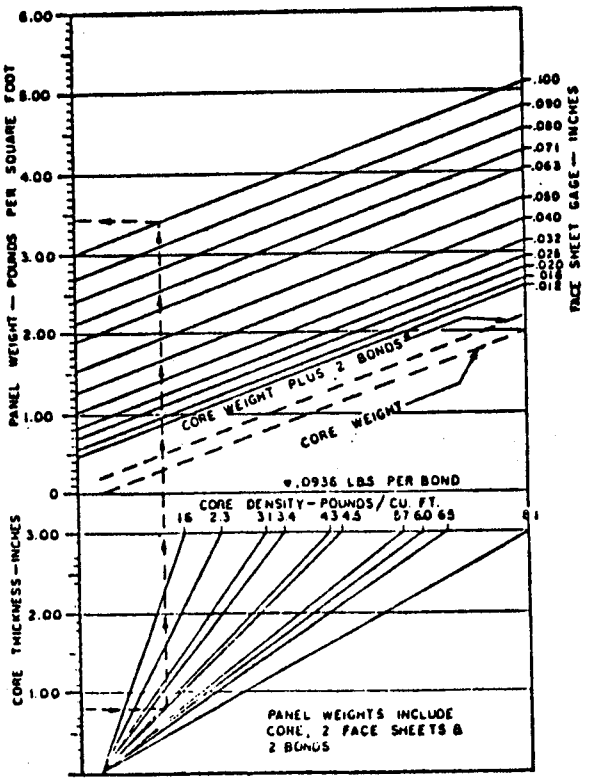


*Mfd. by the Bloomingdale Rubber Co.

## B11.5.0 Cost of Sandwich Construction

Sandwich construction is seldom the least expensive construction and a definite reason for using it must be indicated, such as superior resistance to sonic fatigue, minimum weight or stiffness and rigidity and least parts count. Costs or comparative costs are sometimes difficult to evaluate because of many variables based in the fabrication and bonding techniques. The following discussion of costs will give some basic ideas for consideration. Producibility Engineering and the Materials and Process Engineering Group (M&PE) should be consulted for definitive costs when considering honeycomb construction in new applications.

### B11.5.1 Aluminum Honeycomb Construction

The adhesive film used for aluminum bonding makes up a large portion of the honeycomb panel cost. A simple honeycomb panel uses two square feet of film per square foot of completed panel and an additional film for each doubler. A panel with two doublers would use four layers of film. Qualification tests required for each new shipment of adhesive film is an additional cost as is the cost of maintenance of refrigerators to store the adhesive before use. Epoxy foam and putty are additional cost items also.

Time standards have been established for various operations, such as machining and deburring the honeycomb core, crushing or machining edges, cleaning parts and subsequent protection priming before bond, prefitting of details, bagging of parts, and other operations described under fabrication methods. All of these standards are subject to modification due to the complexities of any particular part.

Many intangibles exist, such as costs of polyglycol used to hold the core during machining, maintenance of cleaning tanks, cleaning solvents, operation of the autoclaves, operation of air pressure and vacuum systems, and paper and cartons for protecting details and complete panels. Process monitoring costs must be considered and included. These costs include regulatory equipment for the autoclaves and control coupon tesing for each panel.

Special efforts must be made in the fabrication of details to insure that closer tolerances are held.

The choice of honeycomb for structure must justify the above mentioned costs and extra care handling required throughout the manufacture of a honeycomb panel.

B11.5.2 Brazed Sandwich Construction

Metallic sandwich construction for elevated temperature applications uses brazing alloys for bonding the face sheets to the core. Brazing is accomplished under heat and pressure in either a reducing atmosphere, inert atmosphere or in a vacuum. The cost of the brazing cycle used in this process must be ascertained to determine the overall cost. Tooling and equipment used for brazing include graphite or steel brazing fixtures, stainless steel retorts, inert gases, and evacuation equipment.

B11.6.0 Mechanical Properties

The properties in this section are provided as an aid in determining whether or not sandwich structure is a good choice for a particular design application. More definitive properties provided in MIL-Handbook-23A, Reference B11-9, should be used for detail design.

B11.6.1 Core Mechanical Properties

Table B11.6.1-1 shows typical core properties.

B11.6.2 Density

The density of hexagonal cell honeycomb is given by $w'_c = \frac{8}{3}\frac{t_w}{s} w_c$ and the density of square cell is given by $w'_c = \frac{2t_w}{s} w_c$ neglecting the weight of the bond at the nodes.

Actual measurements indicate that coefficients of 3 for hexagonal cells and 2.3 for square cells is a good approximation. Figure B11.6.2-1 gives the core density for several materials and cell sizes, based on these approximations.

# Table B11.6.1-1 Typical Core Properties
## Reference B11-9

| Core Material | Density Lbs./Ft.$^3$ | Test Environment: Temperature $^{o}$F | Test Environment: Humidity Percent | Elastic[2] Modulus, psi 1000 psi | Compression[2] Strength, psi 1000 psi | Shear Modulus 1000 psi: TL | Shear Modulus 1000 psi: TW | Shear Strength psi: TL | Shear Strength psi: TW |
|---|---|---|---|---|---|---|---|---|---|
| Balsa Wood | 5.0 | 70 | 64 | 222 | 670 | 9.8 | 12.2 | 160 | 150 |
| | 6.0 | 70 | 64 | 313 | 910 | 12.3 | 16.6 | 190 | 180 |
| | 7.0 | 70 | 64 | 404 | 1160 | 14.9 | 21.0 | 230 | 200 |
| | 8.0 | 70 | 64 | 495 | 1410 | 17.5 | 25.3 | 270 | 230 |
| | 9.0 | 70 | 64 | 586 | 1650 | 20.1 | 29.7 | 300 | 260 |
| | 10.0 | 70 | 64 | 678 | 1900 | 22.6 | 34.0 | 340 | 290 |
| | 11.0 | 70 | 64 | 769 | 2150 | 25.2 | 38.4 | 380 | 320 |
| Paper (Nomex)[1], Expanded-Hexagonal (DAC DMS 1974J $t_c$ = .270 in. | | | | | | | | | |
| 1/8 - Paper - .004 | 1.8 | 73 | 50 | - | 70 | 2.0 | 1.0 | 60 | 30 |
| 1/8 - Paper - .004 | 3.0 | 73 | 50 | - | 270 | 6.7 | 3.1 | 180 | 95 |
| 1/8 - Paper - .004 | 3.5 | 73 | 50 | - | 360 | 5.8 | 3.2 | 190 | 100 |
| 1/8 - Paper - .004 | 4.0 | 73 | 50 | - | 470 | 7.8 | 4.2 | 250 | 125 |
| 1/8 - Paper - .004 | 5.0 | 73 | 50 | - | 600 | 8.5 | 4.5 | 250 | 130 |
| 1/8 - Paper - .004 | 9.0 | 73 | 50 | - | 1600 | 14.5 | 8.0 | 340 | 220 |
| Aluminum, Expanded-Hexagonal | | | | | | | | | |
| 1/4 - 5052 - .007N | 2.0 | 75 | 50 | - | 140 | 20.4 | 10.2 | 140 | 80 |
| 1/4 - 5052 - .002N | 3.9 | 75 | 50 | 259 | 480 | 47.7 | 18.8 | 340 | 170 |
| 1/8 - 5052 - .001P | 4.5 | 75 | 50 | - | 580 | 57.7 | 29.4 | 390 | 230 |
| 1/4 - 5052 - .003N | 5.9 | 75 | 50 | 437 | 900 | 75.4 | 25.7 | 560 | 280 |
| 1/4 - 5052 - .004N | 7.7 | 75 | 50 | 535 | 1390 | 108.7 | 32.2 | 770 | 380 |
| Titanium - Square | | | | | | | | | |
| 1/4 - 75A - .003 | 6.7 | 75 | - | - | 900 | 79 | 61 | 420 | 350 |
| 1/4 - 75A - .003 | 6.7 | 600 | - | - | 420 | - | - | - | - |
| 1/4 - 75A - .003 | 6.7 | 1200 | - | - | 140 | - | - | - | - |
| Steel, Stainless - Square | | | | | | | | | |
| 1/4 - 17-7PHA - .002 | 8.9 | 75 | - | - | 540 | 99 | 57 | 300 | 260 |
| 1/4 - 17-7PHA - .002 | 8.9 | 600 | - | - | 420 | - | - | - | - |
| 1/4 - 17-7PHA - .002 | 8.9 | 1200 | - | - | 320 | - | - | - | - |

(1) Dupont registered trademark.
(2) Properties are parallel to the grain of balsa and parallel to the flutes of honeycomb cores.

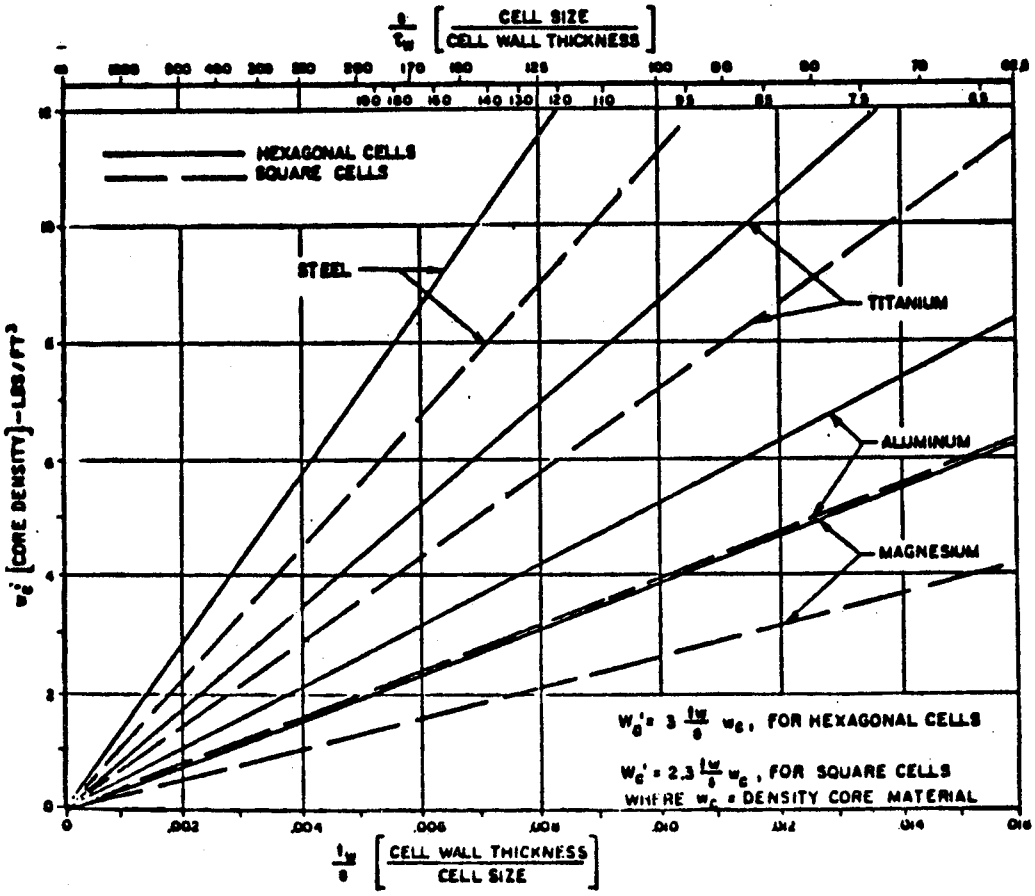


Figure B11.6.2-1 Core Density for Hexagonal and Square Cells

B11.6.3 Elastic Modulus in Direction of Cell Axis

The elastic modulus parallel to the cell axis in a honeycomb core is approximately given by $E'_c = \frac{w'_c}{w_c} E_c$. The elastic modulus of the core versus density for several core materials is shown in Figure B11.6.3-1.

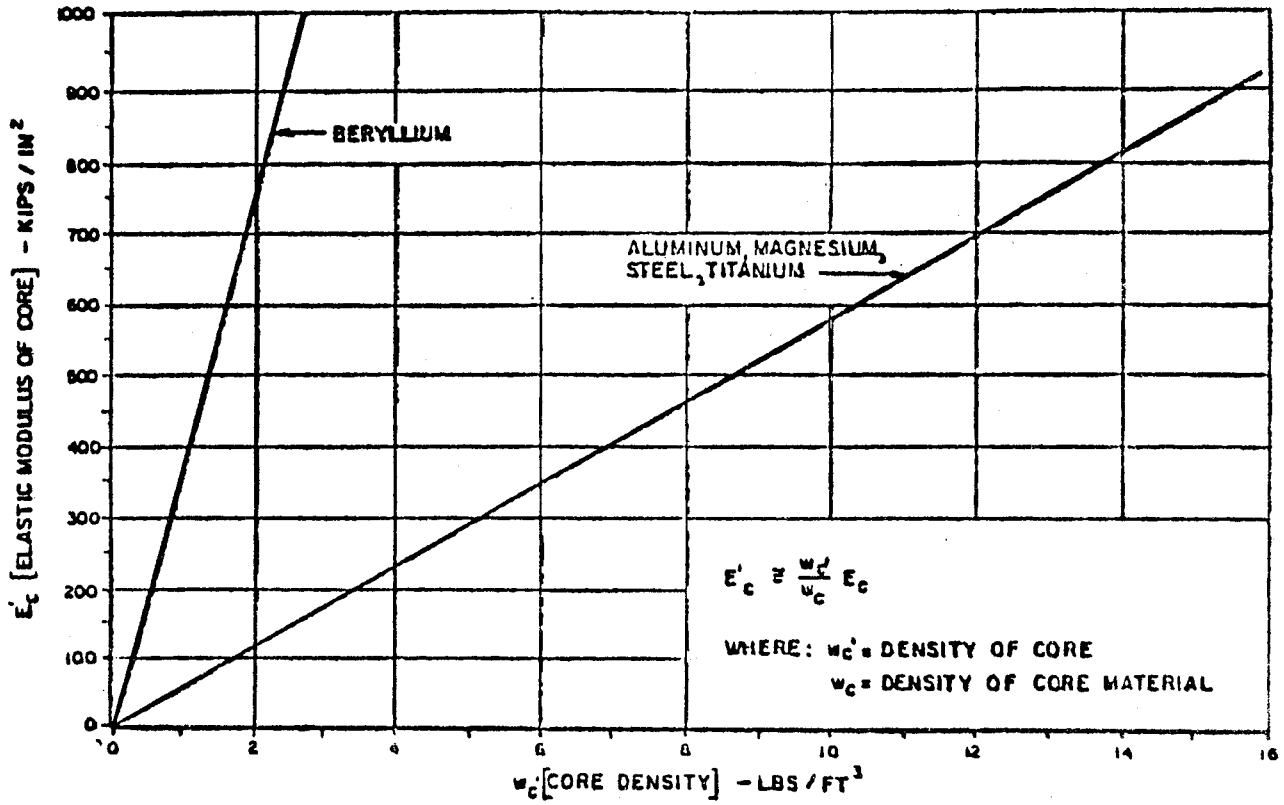


Figure B11.6.3-1 Elastic Modulus for Various Material

B11.6.4 Shear Modulus

The shear modulus for hexagonal cell honeycomb parallel to the nodes is given by $G_{TL} = \frac{5}{8} \frac{w'_c}{w_c} G_c = \frac{5}{3} \frac{t_w}{s} G_c$. Perpendicular to the nodes, the shear modulus is given by $G_{TW} = \frac{3}{8} \frac{w'_c}{w_c} = \frac{t_w}{s} G_c$ (Reference B11-1.)

Experimental results indicate these theoretical values are too high (see Table B11.6.1-1).

The empirical equations, $G_{TL} = \frac{5}{11} \frac{w'_c}{w_c} G_c$ and $G_{TW} = \frac{2}{11} \frac{w'_c}{w_c} G_c$ are a better approximation. They are shown graphically in Figure B11.6.4-1.

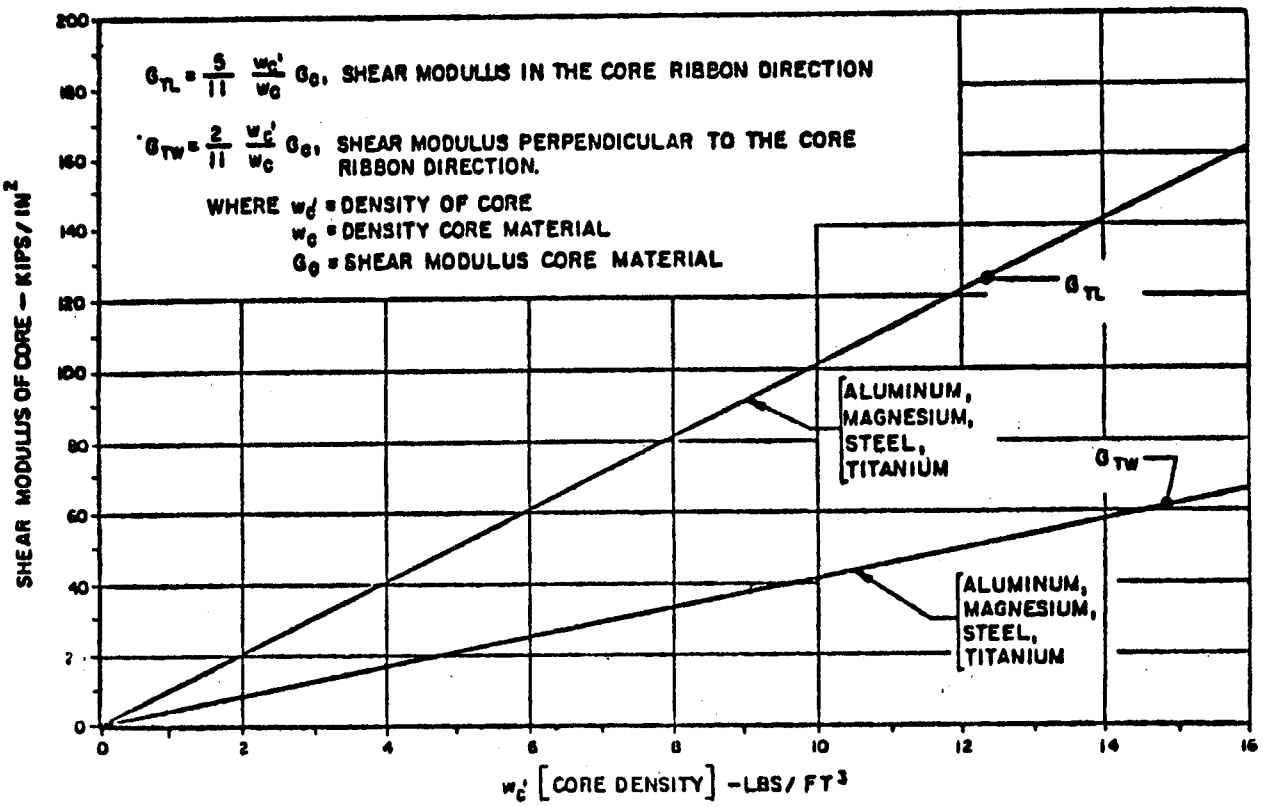


Figure B11.6.4-1 Shear Modulus for Various Materials

These equations are based on tests of aluminum hexagonal cell honeycomb cores and represent minimum values. (Reference B11-2.) For square cell honeycomb, the theoretical shear modulus in the two directions is equal; that is:

$$G_{TL} = G_{TW} = \frac{3}{8} \frac{w'_c}{w_c} G_c = \frac{t_w}{s} G_c$$

Experimental results show that $G_{TL}$ is actually greater than $G_{TW}$ For square cell test data, see Table B11.6.1-1.

B11.6.5 "A" Scale Charts

The "A" scale is a nondimensional parameter of material properties in both the elastic and plastic ranges of deformation. It is defined in this section as the allowable compressive stress divided by the tangent modulus, $E_t$, as shown in the following equation:

$$\text{"A" scale} = \frac{F_c}{E_t} \text{ (Reference B11-3).} \qquad \text{(B11-1)}$$

The tangent modulus, $E_t$, is the instantaneous slope of the stress strain curve at a given stress. In the elastic region $E_t$ = E. Thus the "A" scale method is applicable in both the elastic and the plastic ranges. This parameter is also valid at elevated temperatures as, $E_t$, can be calculated from elevated temperature stress-strain data. With this "A" scale parameter and a given loading environment, a sandwich panel can be designed when used with appropriate design charts.

Figures B11.6.5-1 and -2 are "A" scale charts for typical materials used at DAC (2024, 7075, and Ti 6Al-4V). If further "A" scale charts are desired, they may be constructed from the equation

$$E_t = \frac{E}{1 + \frac{.002\ En}{F_{cy}} \left( \frac{f}{F_{cy}} \right)^{n-1}} \qquad \text{(B11-2)}$$

where

$f$ = the variable stress, psi

$F_{cy}$ = the material compression yield stress, psi

$E$ = the material elastic modulus, psi

$n$ = the material stress-strain shape factor

Data for $F_{cy}$, E, and n should be obtained from Mil-Handbook 5C, Reference B11-10. If n values are not available, use n = 20.

The use of tangent modulus for correcting for plastic effects is probably conservative for honeycomb sandwich stability problems which are a plate buckling phenomenon as opposed to column buckling. The effective modulus used thoughout this manual for plate buckling problems is $\sqrt{E_t E}$ as opposed to $E_t$ used in this section. However, Mil-Hnbk-23A does not define the effective modulus and there is little test data available, so the conservative tangent modulus is used.

The "A" scale approach can also be adopted for composite materials even though they demonstrate a purely elastic behavior. In this case,

$$\text{"A" scale} = \frac{F_c}{\frac{\sqrt{E_x E_y}}{1-\mu_{xy}\mu_{yx}}} \qquad \text{(B11-3)}$$

where

$E_x$ = the material elastic modulus parallel to the "a" edge, psi

$E_y$ = the material elastic modulus parallel to the "b" edge, psi

$\mu_{xy}$ = Poisson's ratio parallel to the "a" edge

$\mu_{yx}$ = Poisson's ratio parallel to the "b" edge

Figures B11.6.5-3 through -5 are "A" scale charts for typical composite materials used at DAC (Fiberglass E-glass/F-155, Kevlar-49/F-155, and Graphite T300/5208). Further "A" scale charts may be constructed from properties ($E_x$, $E_y$, $\mu_{xy}$, $\mu_{yx}$) for a given material and ply orientation; refer to section B10.0.0.

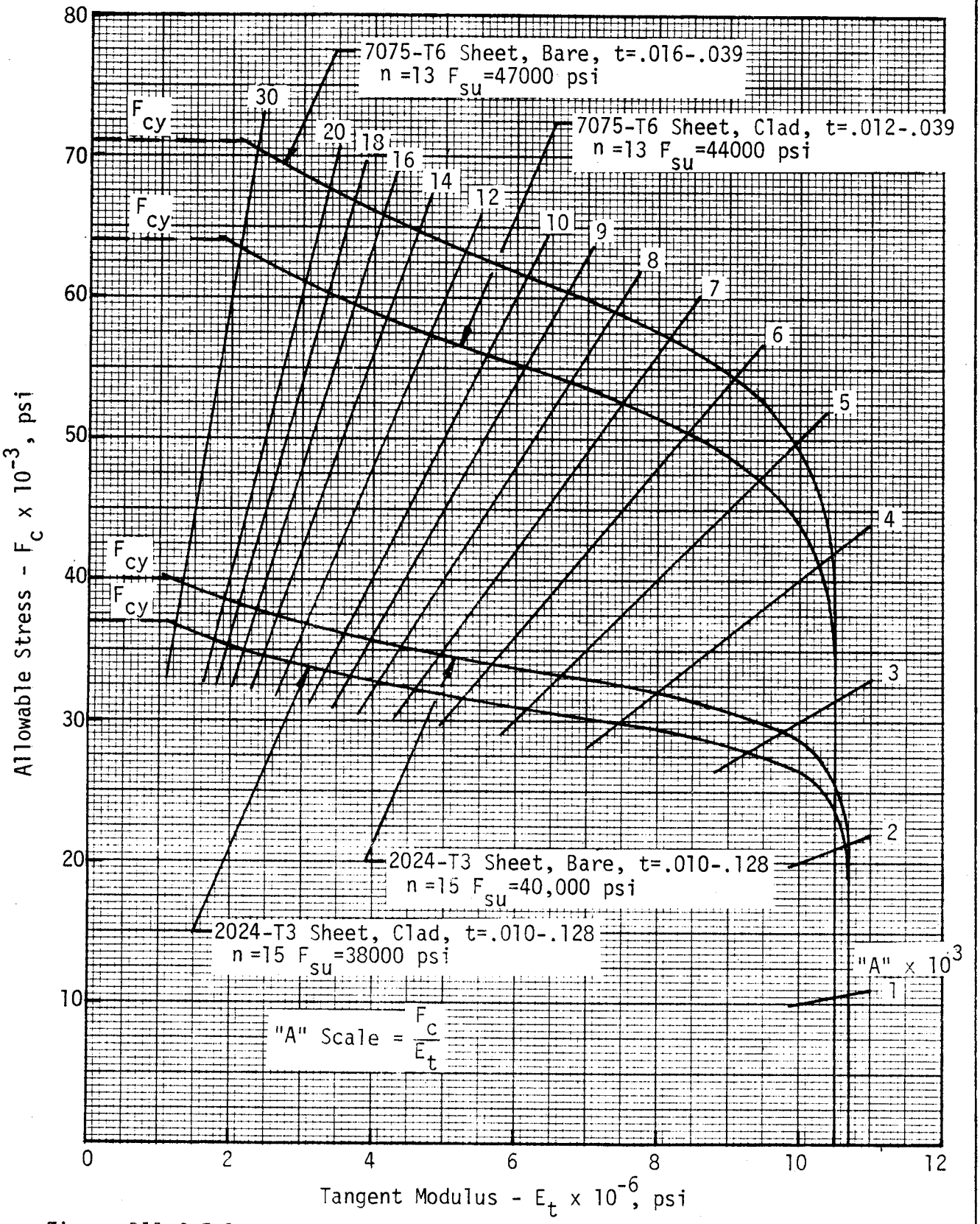


Figure B11.6.5-1 Minimum Guaranteed Compression Stress-Tangent Modulus Curves for 2024 and 7075 Alloy Aluminum at Room Temperature, Grain Direction-Longitudinal

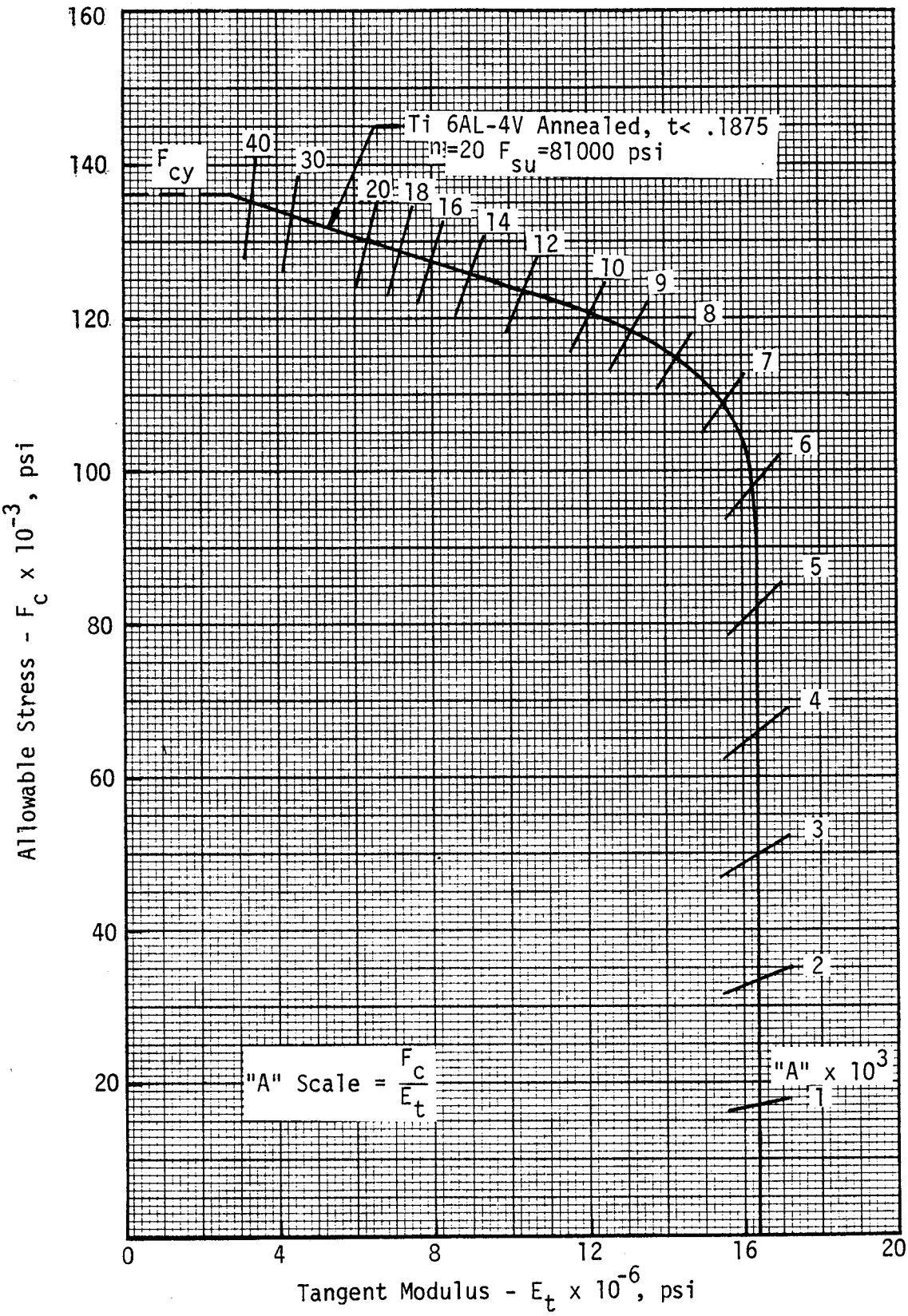


Figure B11.6.5-2 Minimum Guaranteed Compression Stress-Tangent Modulus Curve for Ti-6Al-4V at Room Temperature Grain Direction-Longitudinal

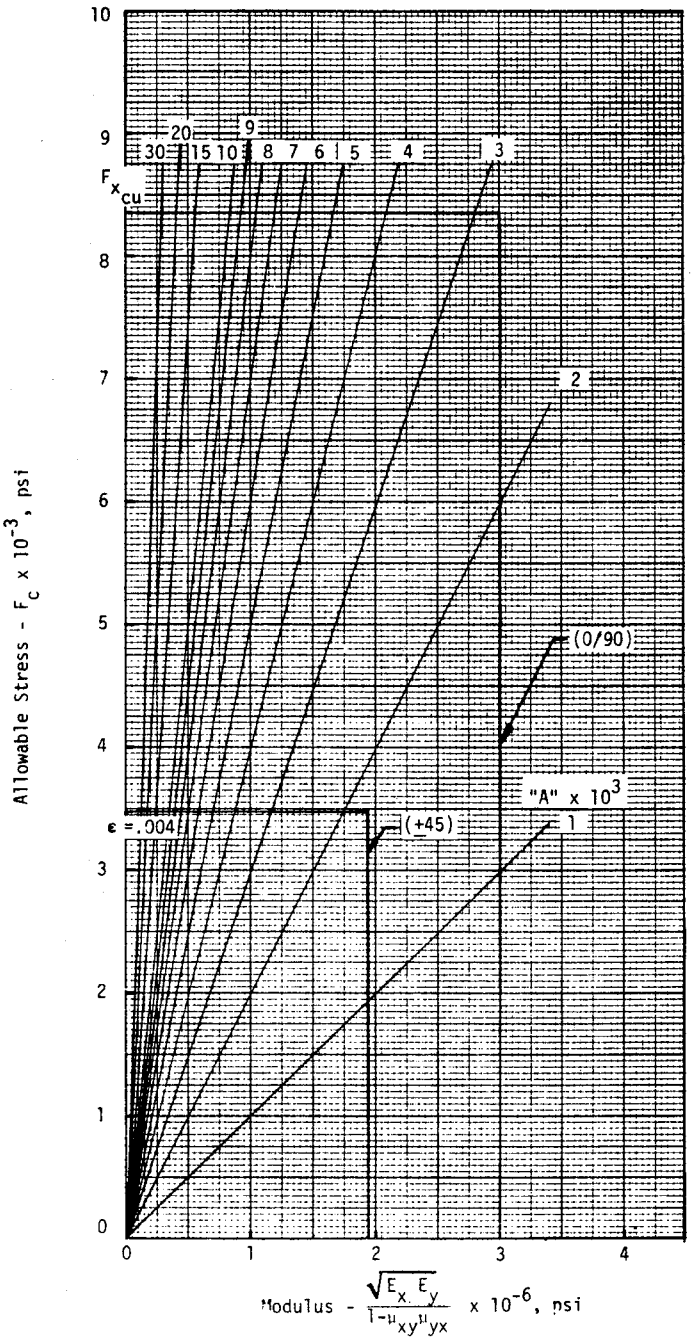


Figure B11.6.5-3 "B" Basis Compression Stress - Modulus Curves for E-Glass/F155 Cloth, 181 Style

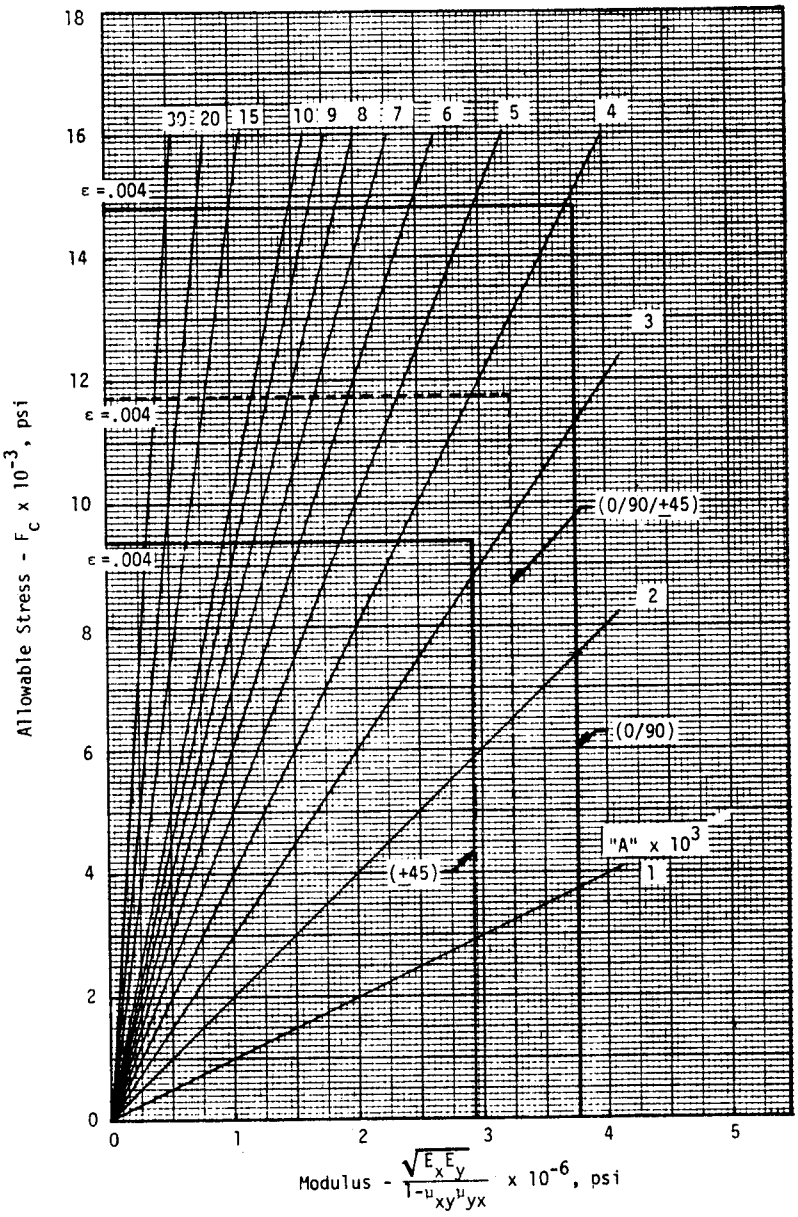


Figure B11.6.5-4 "B" Basis Compression Stress - Modulus Curves for Kevlar-49/F155 Cloth, 285 Style

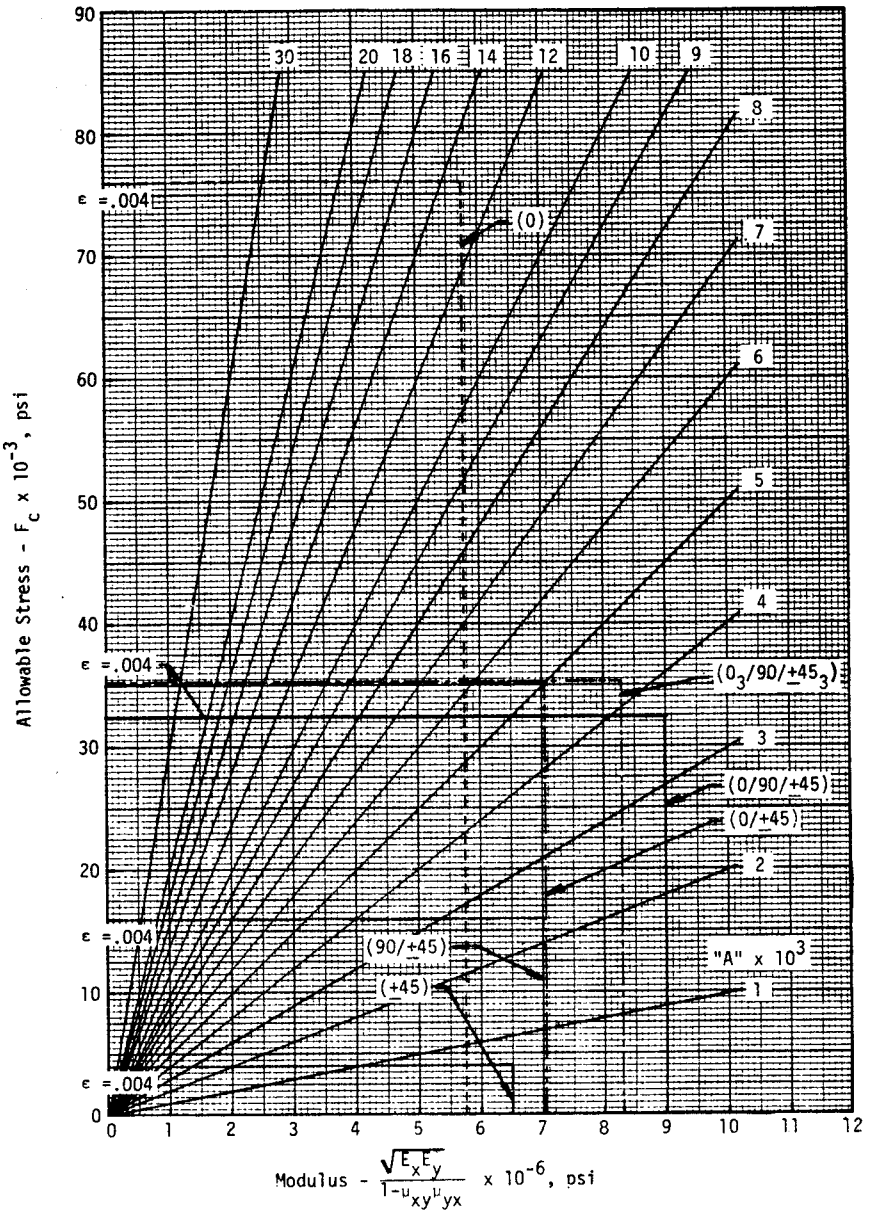


Figure B11.6.5-5 "B" Basis Compression Stress - Modulus Curves for T300/5208 Graphite/Epoxy Tape

## B11.7.0 Design Approach

Design information is available in Mil-Hdbk-23A, Reference B11-9, for analyzing flat sandwich panels (isotropic and orthotropic) under all kinds of load conditions and edge conditions. Similar information is available for cylinders. Computer programs are available for determing allowable loads on composite sandwich structure. These programs are listed in Section E7. The information presented in this section should be used for preliminary sizing of flat isotropic sandwich panels under axial compression, biaxial compression, shear loading, and normal loading. Data is provided, herein, to determine face wrinkling and intracell buckling of sandwich face sheets. Both of these failure modes are affected by the honeycomb cell size.

The equations used in this section do not agree exactly with Reference B11-9 equations, but they are close enough approximations to give quick preliminary sizing of any sandwich structure, including composites, for aircraft usage.

A. Isotropic Panels For analysis, an isotropic sandwich panel is considered a panel made of of isotropic parts; the faces and core.

Metal faces are isotropic, whereas fiberglass faces would be orthotropic due to their different strength properties in the three basic planes. Averages of these properties ($\sqrt{E_x E_y}$) will give a good representation for preliminary sizing.

Core material such as honeycomb (illustrated) is considered as isotropic in the XZ and YX planes, but orthotropic in the XY plane.

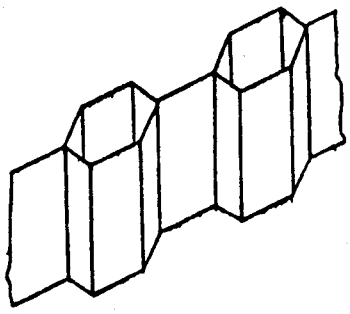

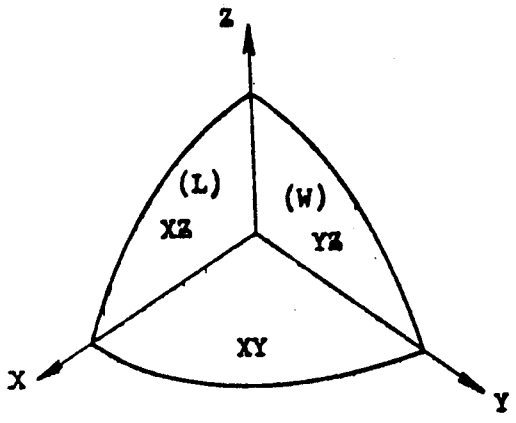


B. Flat Panels A flat sandwich panel shall have the following notations: a = long edge, b = short edge, $t_c$ = core thickness, $t_f$ = face thickness.

C. Simply Supported edges Simply supported panel edges will transmit edgewise compression loads and restrain lateral edge motion. They cannot resist bending moments.

D. Intracell Buckling The intracell buckling stress of a flat panel face sheet is given by the equation:

$$F = 0.943E_t\left[\frac{t_f}{s}\right]^{1.5} \qquad \text{(B11-4)}$$

This expression is plotted in Figure B11.7.0-1 in the form of "A" scale for direct correlation with the material design charts in Section B11.6.5.

E. Face Wrinkling The face wrinkling stress is given by the equation:

$$F = \frac{.461\ E_t}{(S/t_w)^{2/3}} \qquad \text{(B11-5)}$$

This expression is plotted in Figure B11.7.0-2 in the form of "A" scale for direct correlation with the material design charts in Section B11.6.5.

B11.7.1 Uniaxial Compression

A. Figure B11.7.1-1 is a design chart for uniaxial compression. It was derived from the equation:

$$\frac{t_f}{t_c} = K = \frac{\sqrt{Z}}{1-\sqrt{Z}} \times \left[1 - 1.27\ \text{"A"}\left(\frac{s}{t_w}\right)\sqrt{Z}\right] \qquad \text{(B11-6a)}$$

where

$$Z = 2.6614\left(\frac{q}{b}\right)^2\ \left(\frac{1}{\text{"A"}}\right)^3\left(\frac{1}{E_t}\right)^2 \text{ (see Ref. B11-1)} \qquad \text{(B11-6b)}$$

All edges are assumed to be simply supported.

The design chart is valid for all materials and temperatures when the proper "A" scale and $E_t$ is used.

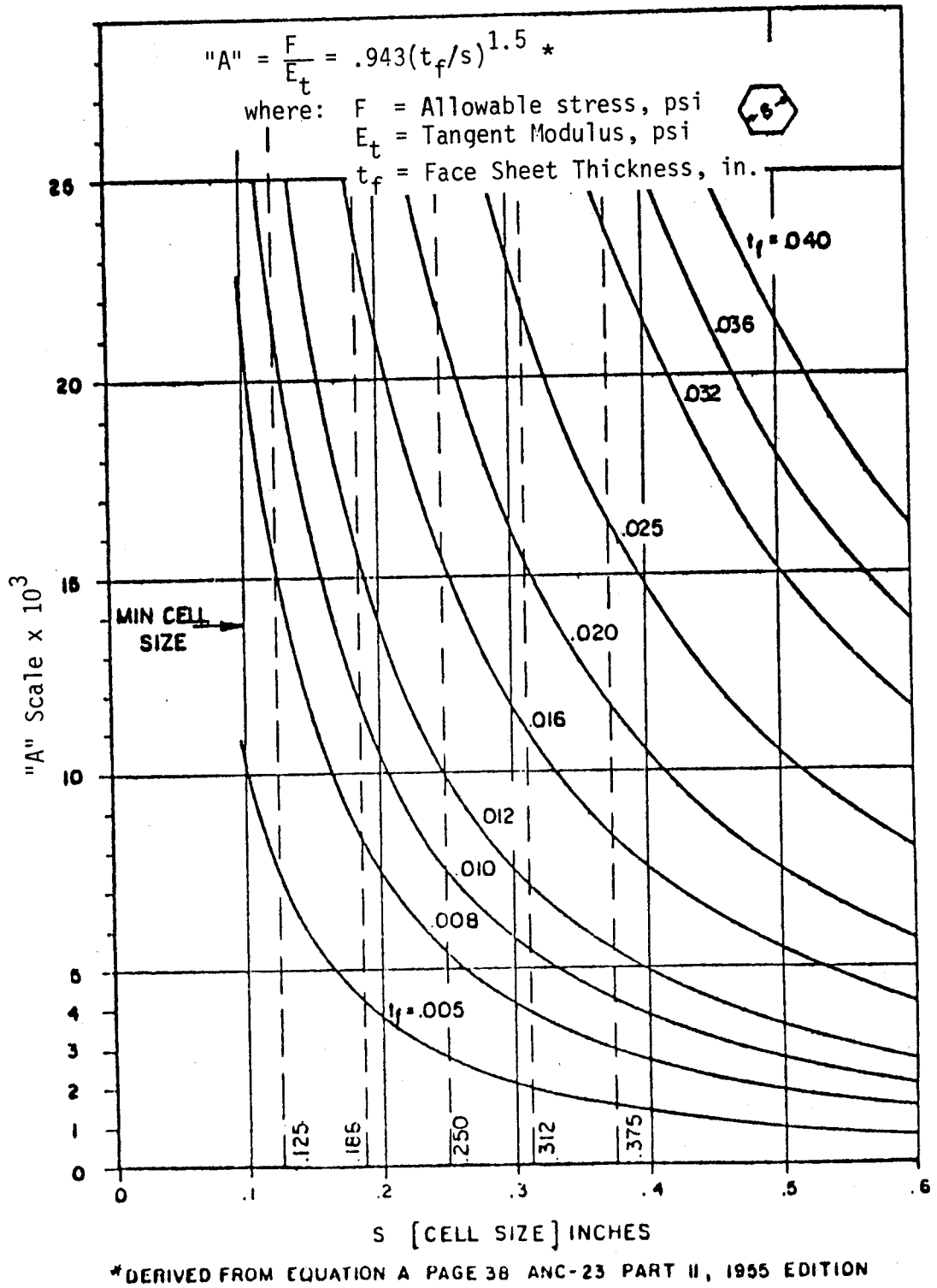


Figure B11.7.0-1 Intracell Buckling Design Curve

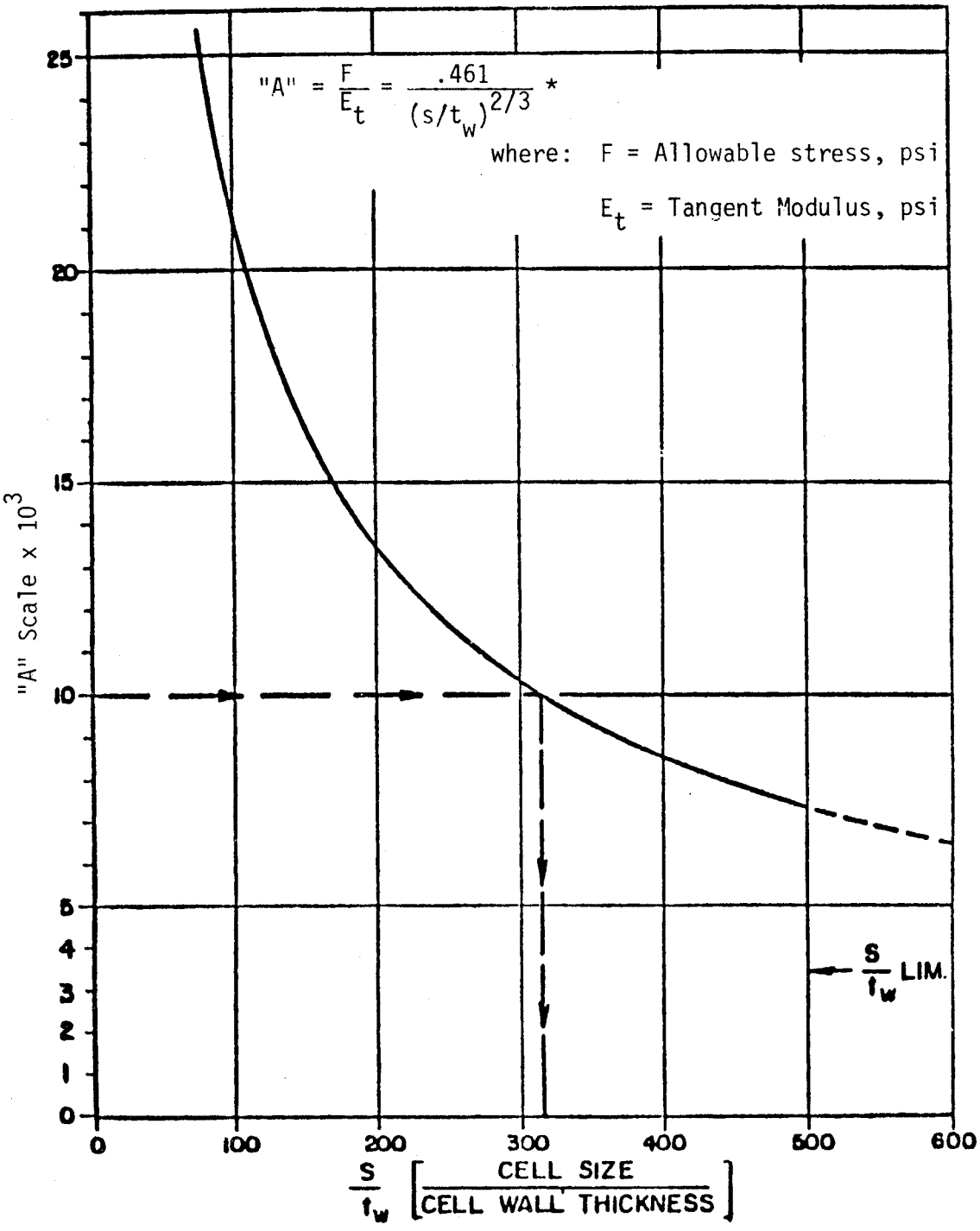


Figure B11.7.0-2 Face Wrinkling Design Chart

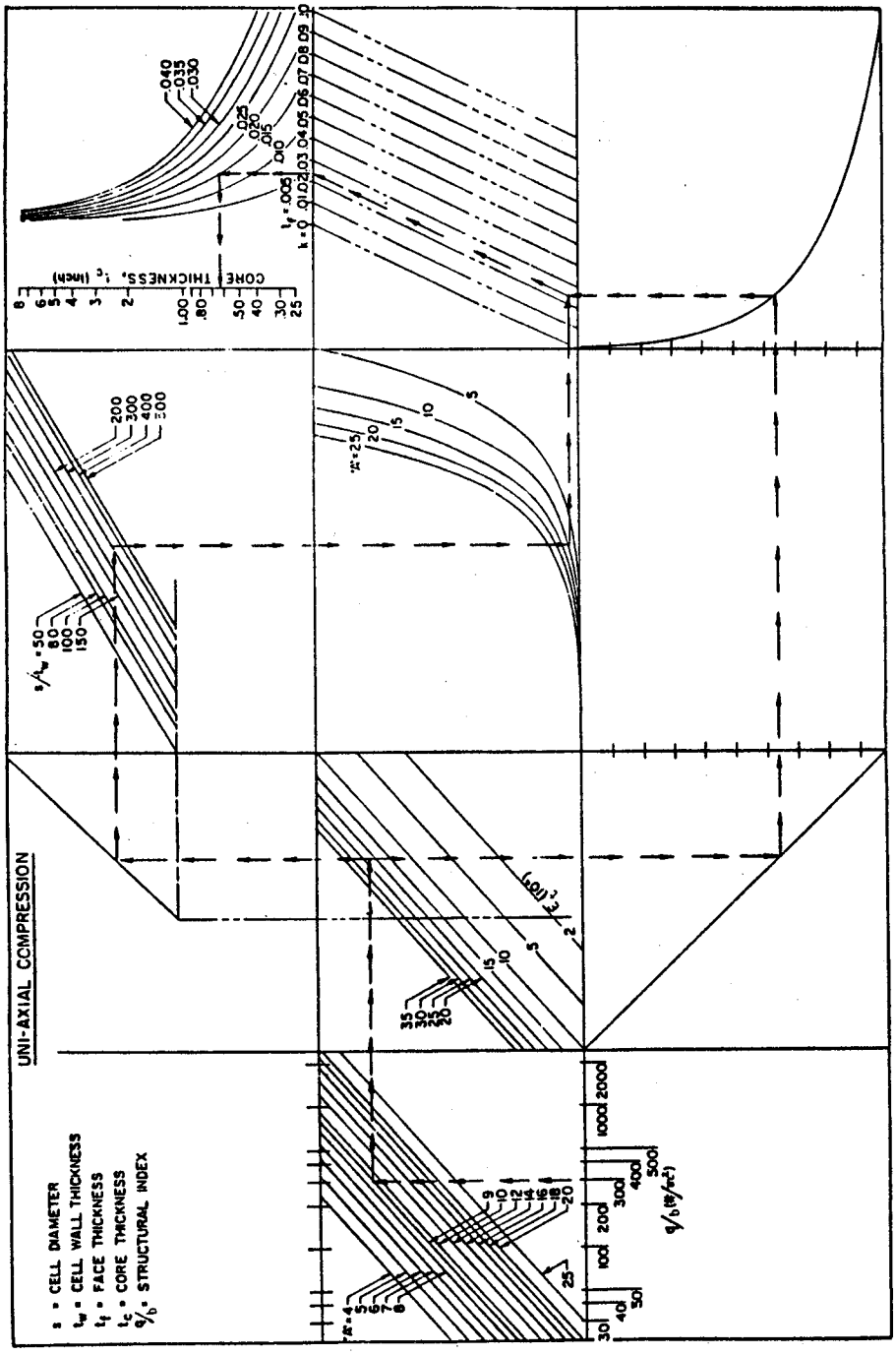


Figure B11.7.1-1 Uni-axial Compression Design Chart

B. Example problem using the design chart to find core thickness $t_c$. Given: The 7075-T6 bare aluminum panel shown below with a uniform 20,000 pound uniaxial compression loading.

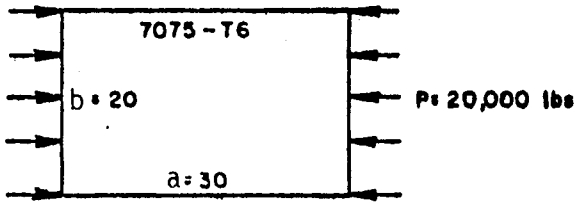


Step 1. Calculate the value of q/b.

$$\frac{q}{b} = \frac{P}{b^2} = \frac{20,000}{400} = 50 \text{ psi}$$

Step 2. Decide the working stress allowable for the material ($F_c$). Enter the "A" scale chart, Figure B11.6.5-1, 7075-T6 bare aluminum with this stress where

$$\text{"A"} = \frac{F_c}{E_t}$$

For this example:

$$F_c = 63,200 \text{ psi}$$

$$\text{"A"} = .012$$

$$E_t = 5.28\ (10^6) \text{ psi}$$

Step 3. Calculate the face thickness required to resist direct compression:

$$t_f = \frac{P}{2bF_c} = \frac{20,000}{2 \times 20 \times 63,200} = .00791 \text{ in.}$$

Note: Use the next larger standard gauge, .010 inch, and calculate the working stress f.

$$f = \frac{20,000}{2 \times 20 \times .01} = 50,000 \text{ psi}$$

For this stress, read off the tangent modulus from Figure B11.6.5-1 and calculate the "A" scale as

$$E_t = 8.55\ (10^6)\ \text{psi (Figure B11.6.5-1)}$$

$$\text{"A"} = \frac{(50{,}000)}{8.55\ (10^6)} = .00585$$

Step 4. Enter the intracell buckling chart, Figure B11.7.0-1 with the "A" value and face thickness, $t_f$ as in step 3 to find the cell sizes = .296 inch. (Use the next smaller standard size of .250 inch.)

Step 5. Enter the face wrinkling chart, Figure B11.7.0-2 with the "A" scale value from step 3 and find $s/t_w$ equal to 500. (Cutoff.)

Step 6. Calculate $t_w$ from $s/t_w$ = 500 as found in step 5. $t_w$ = .00050. (Use the next larger standard foil of .001 inch.)

Step 7. Follow the arrows through the chart as illustrated below or use Equation B11-6a and find the core thickness $t_c$ = 0.50 inch.

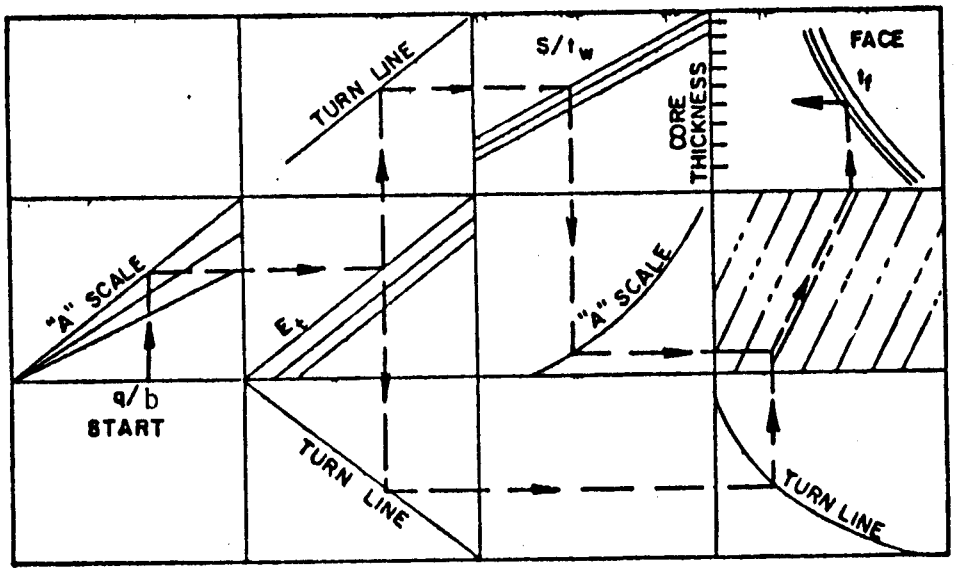

## B11.7.2 Biaxial Compression

A. Figure B11.7.2-1 is a design chart for biaxial compression. It was developed from the equation:

$$\frac{F_c}{E_t} = \text{"A" Scale} = \frac{2.6614(t_f + t_c)^2 \left(\frac{a}{b} + \frac{b}{a}\right)^2}{\left[1 + \left(\frac{a}{b}\right)^2 r_a\right]\left[b^2 + 13.52\, t_f t_c \left(\frac{s}{t_w}\right)\left(1 + \left\{\frac{b}{a}\right\}^2\right)\right]} \qquad \text{(B11-7)}$$

Where $r_a$ is the ratio $f_b/f_a$ and has the limits $1 \geq r_a \geq .4$

B. Example problem using the design chart to find the "A" scale values.

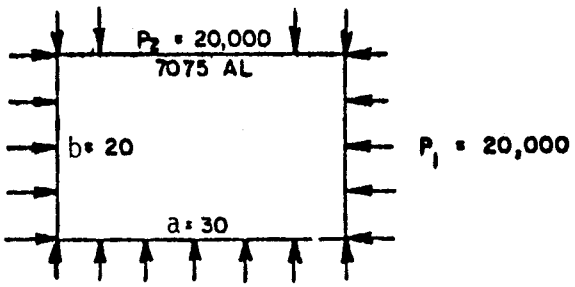


Step 1. Decide the working stress allowable for the material ($F_c$). Enter the "A" scale chart, Figure B11.6.5-1, with this stress, where "A" = $F_c/E_t$. For this example:

$F_c$ = 63,200 psi

"A" = .012

$E_t = 5.28\ (10)^6$ psi

Everything required for using the design chart (Figure B11.7.2-1) or Equation B11-7 is now known, except the core thickness. Assume a core thickness and find the "A" scale value. For the most efficient design, the "A" scale should be equal to the "A" scale value found in step 2. For example, assume $t_c$ = .700 inch, then from Figure B11.7.2-1 or Equation B11-4 for

$$t_f + t_c = .010 + .500 = .510$$

$$\frac{a}{b} = \frac{30}{20} = 1.5$$

$$r_a = .67 \text{ (step 5)}$$

$$t_f = .01 \text{ (step 2)}$$

$$\frac{s}{t_w} = 250 \text{ (step 6)}$$

"A" = .00579

The allowable "A" scale determined in step 2 was "A" = .00585. Thus, another iteration is required with $t_c$ greater than 0.70.

## B11.7.3 Shear Loading - Edgewise

A. Figure B11.7.3-1 is a design chart for edgewise shear loading. It was developed from the equation:

$$F_s = \frac{\pi^2 D}{2b^2 t_f} (K) \qquad \text{(B11-8)}$$

where

$$K = \frac{K_{V=0}}{1 + \left[K_{V=0} - \left(1 + \left\{\frac{a}{b}\right\}^2\right)\right]}$$

with

$$K_{V=0} = 5.35 + 4\,(b/a)^2$$

These equations can be put in the following form:

$$\frac{F_s}{E_t} = \text{"A"} = \frac{2.6614\left(t_f + t_c\right)^2 (5.35 + 4\,[b/a]^2)}{b^2 + 13.52\, t_f t_c \left(\frac{s}{t_w}\right)(4.35 + 3\,[b/a]^2)} \qquad \text{(B11-9)}$$

B. The procedure for using the design chart for shear buckling is shown below in a schematic presentation.

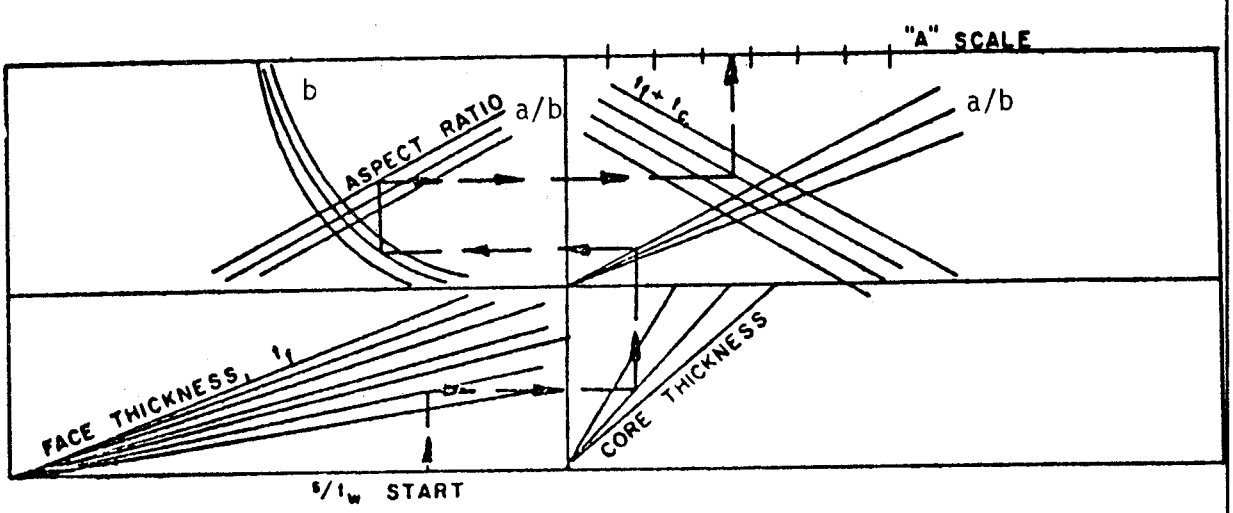

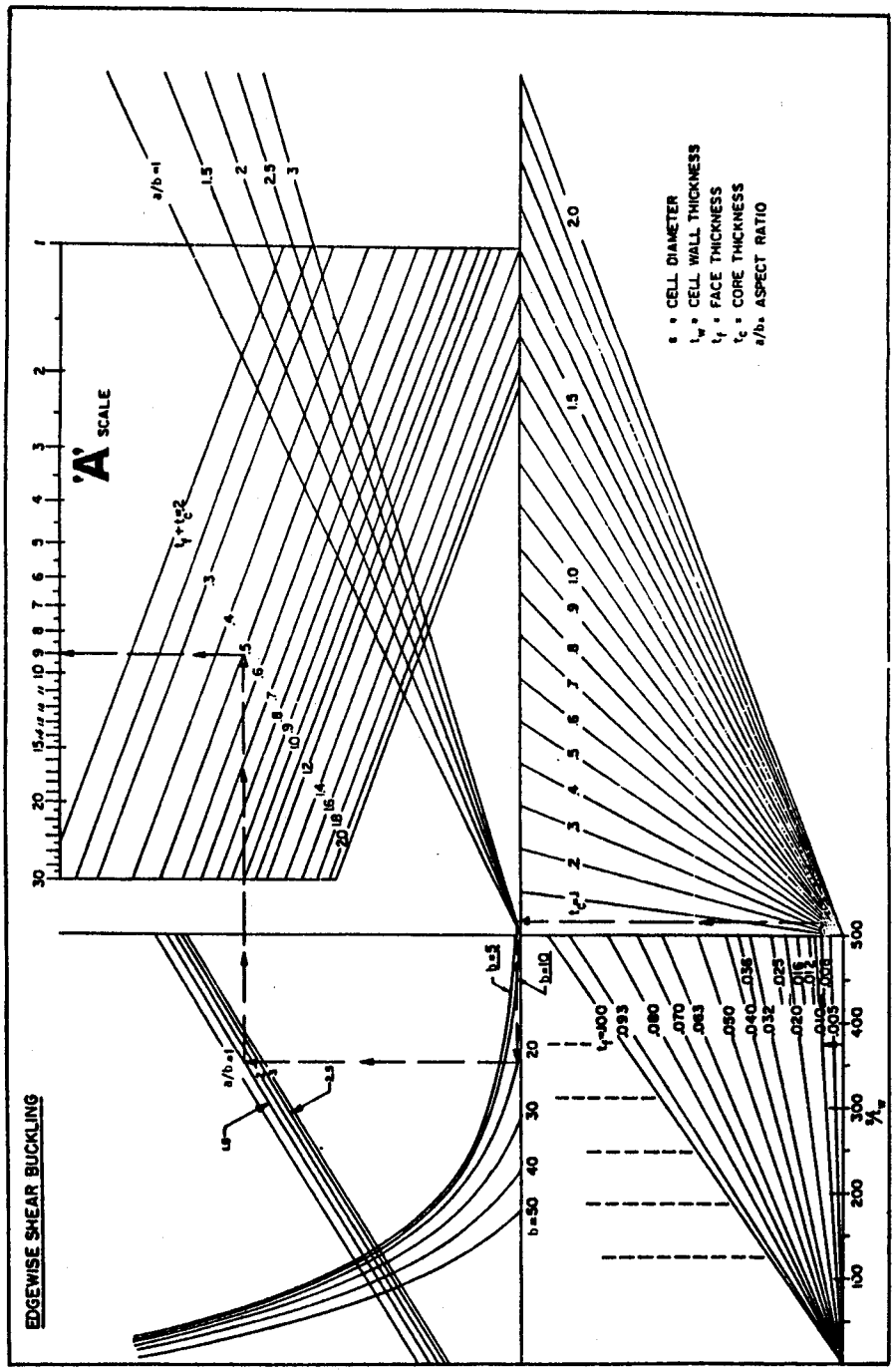


Figure B11.7.3-1 Edgewise Shear Design Chart

C. An example problem using the design chart to find an "A" scale at which shear buckling will not occur follows. Given: The aluminum panel shown below with a 15,000 pound edgewise shear load and simply support edges.

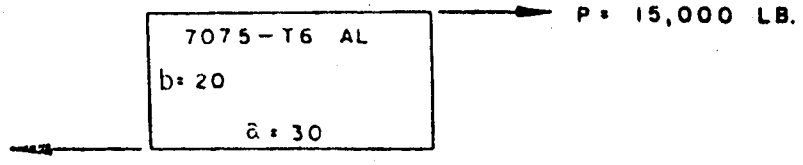


Step 1. Enter the ultimate shear allowable, $F_{su}$, into the "A" scale chart (Figure B11.6.5-1) for 7075-T6 bare aluminum at room temperature, for this example and find that $E_t = 10.2 \times 10^6$ psi. Then

$$\text{"A"} = \frac{47,000}{10.2 \times 10^6} = .00461$$

Step 2. Calculate the face thickness required from the direct shear load by assuming $F_{su}$ as the allowable stress.

$$t_f = \frac{P}{2b\,F_{su}} = \frac{15,000}{2 \times 20 \times 47,000} = .0080 \text{ in.}$$

Note: Use the next larger standard gauge of .010 inch and calculate the working stress, f

$$f = \frac{15,000}{2 \times 20 \times .01} = 37,500.$$

At this stress, $E_t = 10.5 \times 10^6$ psi from Figure B11.6.5-1 and

$$\text{"A"} = \frac{37,500}{10.5 \times 10^6} = .00357$$

Step 3. From the intracell buckling chart, Figure B11.7.0-1, enter with the "A" scale value and the face thickness, $t_f$, determined in step 2 to find the cell size, s = .412 inch.

Note: Use the next lower standard size of .375 inch.

Step 4. From the face wrinkling chart, Figure B11.7.0-2, enter with the "A" scale value from step 2 and find $s/t_w$ = to 500 (cutoff).

Step 5. Calculate $t_w$ from $s/t_w$ as found in step 4.

$$t_w = \frac{s}{500} = \frac{.375}{500} = .00075 \text{ in.}$$

Note: Use the next larger standard foil of .001 inch.

Step 6. Assume a core thickness, $t_c$ = .50 inch. Find true

$$\frac{s}{t_w} = \frac{.375}{.001} = 375$$ and enter the design chart.

Calculate

$$\frac{a}{b} = 1.5$$

$$t_f + t_c = .510 \text{ inch}$$

Follow the arrows through the chart as illustrated or use Equation B11-9 and find "A" scale .0091. Then $F_{s_{cr}}$ = 61,500 psi from Figure B11.6.5-1.

Note: This example panel will fail in direct shear of the faces (47,000 psi) before panel buckling (61,500 psi). The buckling allowable, $F_{s_{cr}}$, must be equal to, or greater than, the shear allowable $F_{su}$.

## B11.7.4 Normal Loading

### B11.7.4.1 Bending Stress in the Faces

A. The maximum bending stress (at the center of the panel) of a uniformly loaded sandwich panel, simply supported on all edges, is defined by the equation:

$$f_{max} = \frac{\beta p b^2}{t_f t_c}$$ (References B11-4, -5, -6) (B11-10)

Values for $\beta$ are plotted in Figure B11.7.4-1 as a function of panel aspect ratio a/b. Figure B11.7.4-2 is a design chart for this equation.

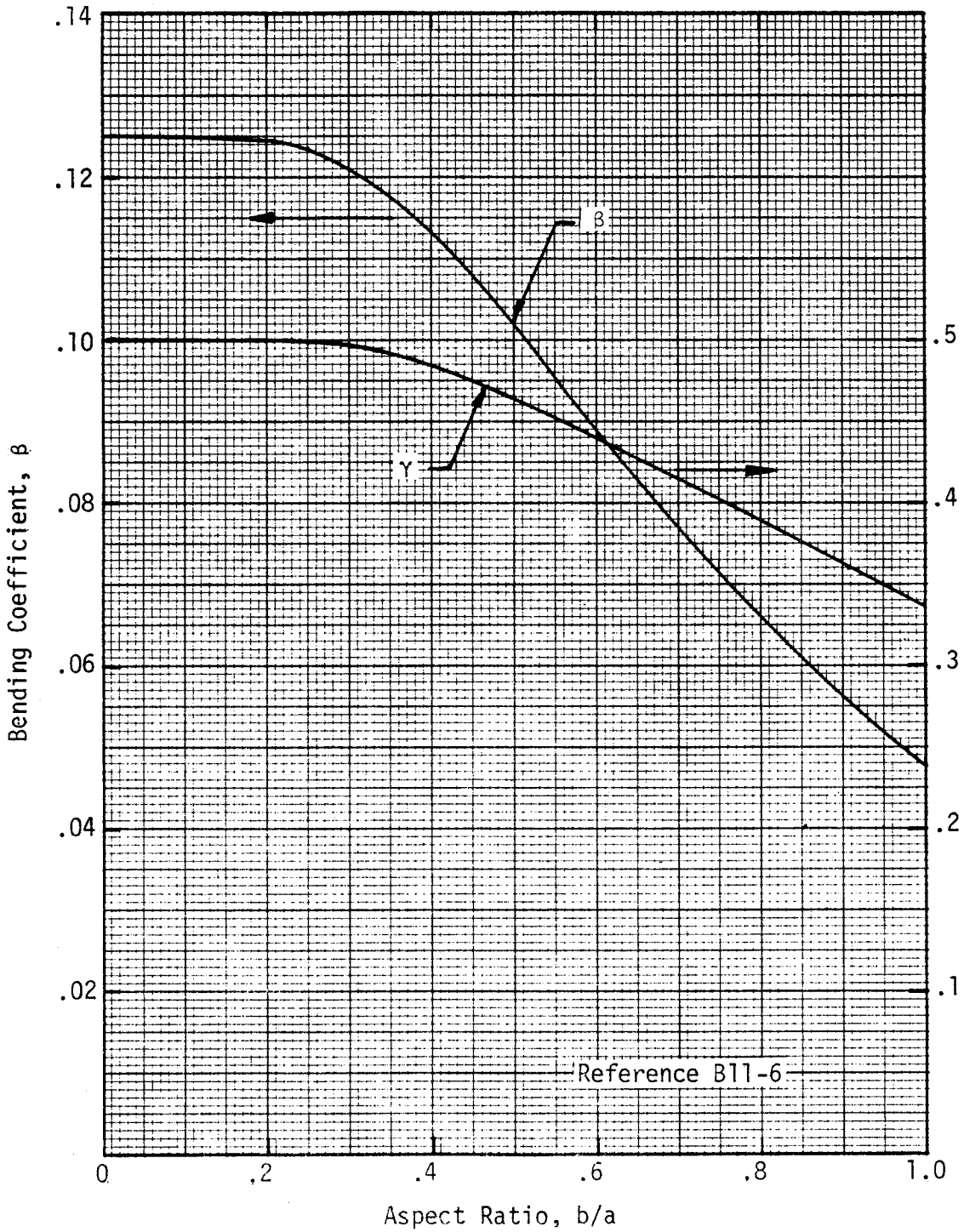


Figure B11.7.4-1 Coefficients for Plates Under Normal Loads

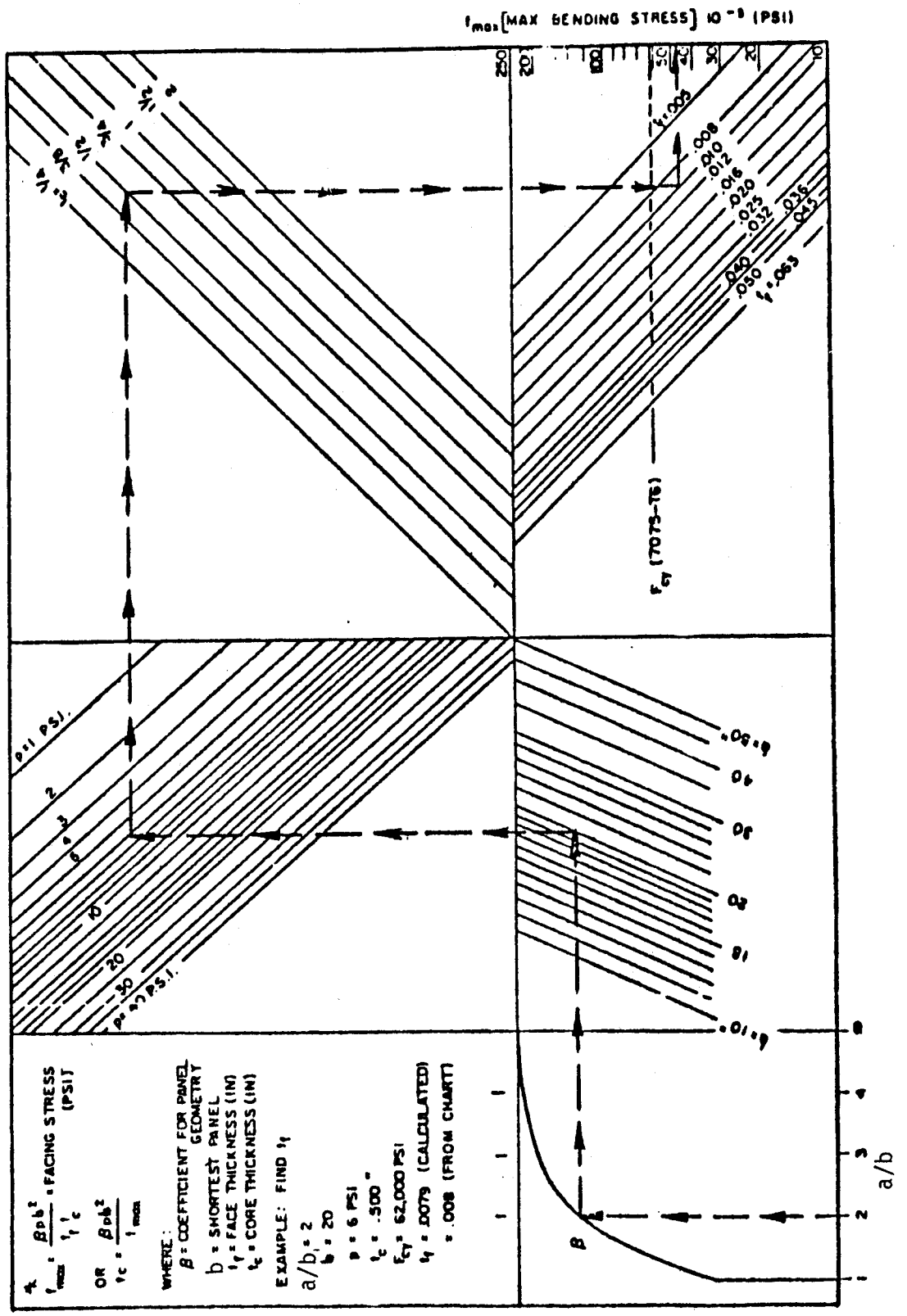


B11.7.4-2 Normal Loading Design Chart

B. A schematic diagram showing how to use the design chart for finding panel geometry, maximum face stress or the allowable normal load for given conditions follows:

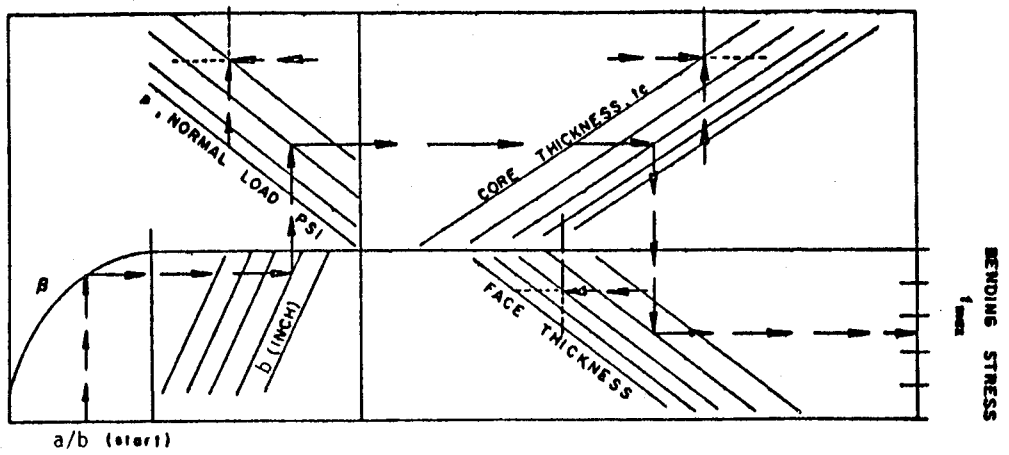


C. The following example problem for finding the maximum face stress in a uniformly loaded sandwich panel, simply supported on all edges illustrates the procedure for using the design charts

Given: $b = 20.0$ in.
$a = 40.0$ in.
$p = 6.0$ psi
$t_c = .500$ in.
$F_c = 63{,}200$ psi

Find: $t_f$, the face thickness required.

Follow the example through the chart, Figure B11.7.4-1, and find that .008 is the first line below $F_c$ = 63,200 psi, but the standard minimum gage for aluminum is .010 and should be used.

The actual stress for .010 faces is 48,816 psi.

If the problem is to find the required core thickness and the following data is known or assumed:

f = Material allowable or working stress, psi

a&b = Length of the sides, inches

$t_f$ = Face thickness, in.

p = Normal pressure on panel, psi

Then, $t_c$ can be obtained by starting at the a/b scale and working through the chart to the $t_c$ lines: start at the $f_{max}$ scale and work backwards in the chart to the $t_c$ lines. Where these two lines cross is the required core thickness.

A similar method can be used to find the allowable normal load p (psi).

The core shear allowable should now be checked on normal loading.

B11.7.4.2 Core Shear

A. The core shear stress is maximum along the longest edge (a) of a simply supported plate under normal load as defined by:

$$f_s = \frac{\gamma pb}{t_f + t_c} \text{ where } a > b \text{ (Ref. B11-4, -6, -7, -8)} \quad \text{(B11-11)}$$

Values for $\gamma$ are plotted in Figure B11.7.4-1. Figure B11.7.4-3 is a design chart for Equation B11-11.

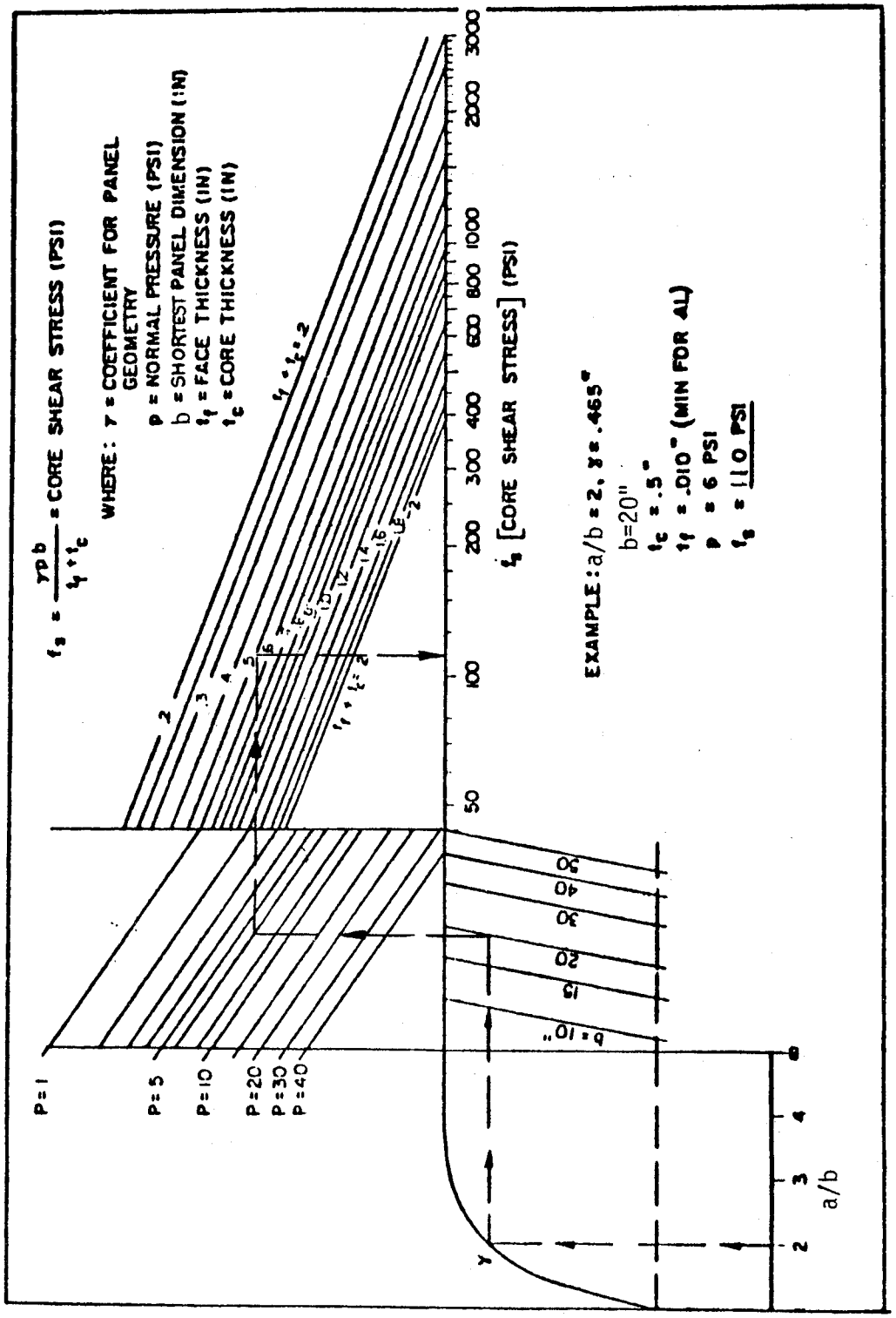


Figure B11.7.4-3 Core Shear Design Chart

B. A schematic design chart for core shear stress is shown below to illustrate the procedure for using the chart.

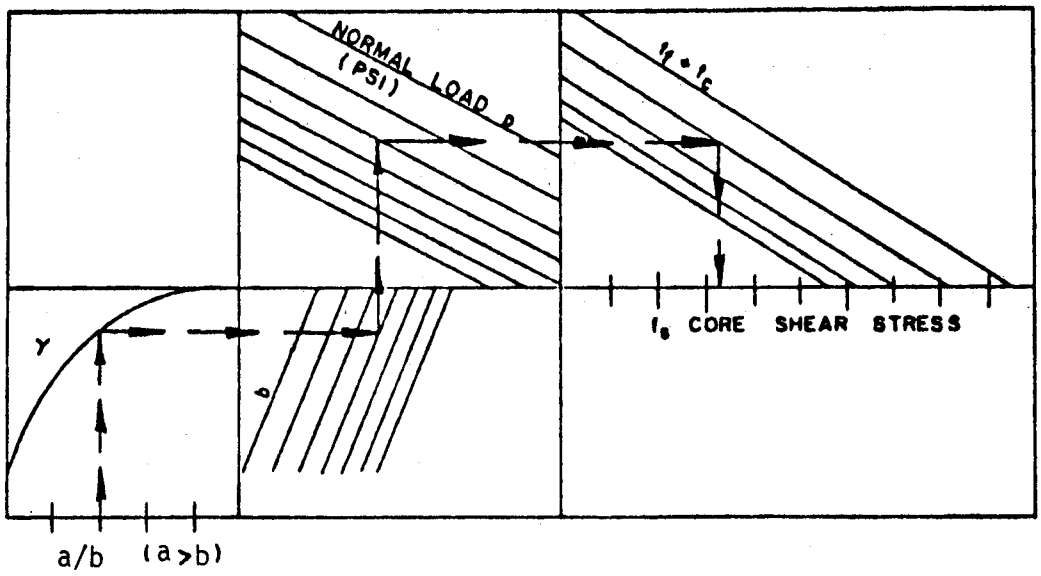


C. Example problem using the design chart -

The panel is loaded with a uniform normal load (psi) with the edges simply supported.

Given: a/b = 2
a = 40 in., b = 20 in.
$t_c$ = .500 inch
$t_f$ = .010 inch
p = 6 psi
$t_f + t_c$ = .510 inch

From the design chart follow through as in paragraph B and find the core shear stress. Select a core that has an allowable equal to, or greater than, the answer from the nomograph.

Another use for the chart is to select a core with a given shear allowable and the panel length and width with a given uniform load and solve for $t_f + t_c$.

Note: This method must be used in conjunction with bending stress.

## REFERENCES

B11-1 Kaechele, L. E., "Minimum Weight Design of Sandwich Panels", Report RM-1895, the Rand Corp., March 1957. (ASTIA Document No. AD 13 011; 3-22-57.)

B11-2 Kuenzi, E. W., "Mechanical Properties of Aluminum Honeycomb Core", Forest Products Laboratory Report No. 1849.

B11-3 Bockrath, G. E., "Allowable Stresses in Flat Square Cell Honeycomb Panels", Douglas Aircraft Company, Report No. SM-23567, May 1959.

B11-4 Trent, D. J., "Design of Optimum Honeycomb Panel Under Normal Pressure", Douglas Aircraft Company, Report No. SM-23747.

B11-5 Trent, D. J., "Design of Optimum Honeycomb Beam Under Normal Pressure", Douglas Aircraft Company, Report No. SM-23748.

B11-6 Timoshenko, S., "Theory of Plates and Shells", McGraw-Hill, New York, 1940.

B11-7 Lewis, W. C., "Deflection and Stresses in a Uniformally Loaded Simply Supported, Rectangular Sandwich Plate", Forest Products Laboratory Report No. 1847-A, December 1956.

B11-8 Raville, M. E., "Deflection and Stresses in a Uniformly Loaded Simply Supported, Rectangular Sandwich Plate", Forest Products Laboratory Report No. 1847, December 1955.

B11-9 Mil-Handbook-23A, Structural Sandwich Composites, December 30, 1968.

B11-10 Mil-Handbook-5C, Metallic Materials and Elements for Aerospace Vehicle Structure, Volumes I and II, September 15, 1976.

# TRANSPARENCIES

TABLE OF CONTENTS

A. Internal pressurization.
B. Extreme thermal regimes.
C. Pressurization cycles.
D. Thermal cycles.
E. Rain removal.
F. Anti-icing.
G. Defogging.
H. Precipitation static, RCS, EMP, and lightning protection.
I. Ingress/egress/escape.
J. Aircraft loading peculiarities.
K. Vision requirements.

### B12.2.2 Crew Accommodations

The selection of crew size and seating arrangement is based on aircraft type, mission, and anticipated task loading. The seating arrangement for a transport type aircraft is generally side-by-side. The design eye location for the pilot/co-pilot is derived from the location of: the seats, control column, rudder pedals, consoles, and instrument panels. Instructions for establishing the design eye location may be obtained from data contained in MIL-STD-850 (Reference B12-2), Society of Automotive Engineers, Inc. (SAE) Aerospace Standard AS580 (Reference B12-3), the FAA Civil Aeronautics Manual (CAM 4b) (Reference B12-4), or Federal Aviation Regulations (FAR 25) (Reference B12-5). The design eye location must provide for head movement about the spinal column for maximum vision. The pilot will not maintain a position representing the standard design eye location, but may move his head forward five inches or more to an alert eye position, or outboard as much as fourteen inches to increase his vision. Consideration must be given to external light ray traces through the transparency to minimize the effects of distortion or deviation when recieved by the pilot at an alternate head position. Normal vision is binocular rather than monocular as the design eye concept implies.

The designer must monitor the shaping of the front section and assure that adequate clearances are provided for: heads of crew members, ingress and egress under normal and emergency conditions, HUDS, glareshields, and growth in size of various electronic components. Additional head clearance might be considered to accommodate the amount of deflection that may occur as a result of bird impact on the transparencies.

It is recommended that a full size mockup be constructed to facilitate this design stage. A soft (foam board) type mockup is sufficient to meet this requirement.

B12.2.3 Optical Factors

The optical factors that must be considered include:

clear vision areas,

impairments to vision, and

optical properties.

A. Clear Vision Areas The clear vision area must be defined for both normal and extreme icing conditions. Anti-ice areas defined by a rectangular shape provide the maximum amount of cleared area. Such requirements dictate the type of anti-ice system that would be appropriate, which in turn often establishes the materials selection. The amount of clear vision area is further limited by the location of posts or structural members that automatically define the shape of the anti-ice pattern.

The method of rain removal, whether it is mechanical wipers, hot airblast, aerodynamic heating, or chemical rain repellants, must be defined in terms of clear vision area.

The clear areas of vision should be defined prior to aerodynamic shaping. As a basis for defining the clear areas of vision, there are certain existing specifications that may be utilized as minimum guides, such as: MIL-STD-850, CAM 4b, appropriate Federal Air Regulations (FAR 25) and SAE AS580B.

These specifications provide visibility guidance when considering the respective operational requirements of the aircraft. Under the "see and be seen" concept, the clear vision areas should be maximized. Maximum forward down-vision should always be provided for forward viewing transparencies, including the effects of an aircraft nose-up attitude, so that runways or runway lights may be seen without obstructions. Overhead vision may be required to monitor an in-flight refueling operation or to observe other aircraft when in airport patterns. In the event the aircraft is designed for aerial drops, consideration must be given to providing downward viewing transparencies to observe the target locations.

B. Impairments to Vision Certain components must interface and be coordinated with the development of the required clear vision areas and aerodynamic shaping. In many cases, the component locations are limiting factors in defining the required clear vision areas. A forward instrument panel and glareshield, required for most aircraft, could have an affect on limiting the amount of forward down-vision. Overhead consoles may limit the amount of overhead clear vision area. The placement of vertical posts and horizontal beams must be accomplished in such a manner to minimize the amount of obstruction to vision and the amount of distortion resulting from transparency manufacturing methods and not violate requirements for clear areas.

Consideration must be given to edge designs for interfacing the transparencies to the supporting structure. Allowances must be made for bus bars, chip retarders, opaque inserts, parked wipers, electrical connectors, and thermal conditions at the edges. If an electrical coating is used in the transparency, it would require thermal sensing elements which must be placed to minimize interference with the vision envelope.

To provide the crew the best possible vision, the lines of sight should always be normal to the transparency surface The transparencies would have to be flat slabs normal to the aircraft line of flight path, or the pilot eye location would have to be centered in a spherically shaped transparency. Both shapes are impractical from the standpoint of aerodynamic and structural requirements. Optimum vision would be obtained in a spherical enclosure where the walls were perpendicular to the lines of sight. This however is impractical. As a practical compromise, the angle of incidence should not exceed 60 degrees (measured from FRP); the contour of the transparency should not change so abruptly that it would create a distorted effect for binocular vision; and there should be no

abrupt changes in contour or thickness between adjacent transparency panels, which would allow differences in deviation and cause an image shift.

C. Optical Properties Aerodynamic and structural shaping will affect the optical properties of transparencies. Light rays will be refracted or reflected depending on the angle of incidence of the ray traces as dictated by the aerodynamic shape and the source of light. Expecting light rays from external objects to be efficiently transmitted through a transparency at high angles of incidence leads to other problems and will result in higher rejection rates and higher transparency costs. Coatings for anti-icing, defogging, radar cross section, precipitation static discharges, EMP and RF attenuations affect the light transmission and other optical characteristics of the transparency. Internal lights and instruments will reflect off the transparency surface during low ambient light operations if the light emitting sources are not properly shielded.

B12.2.4 Aerodynamics

Comprehensive studies must be conducted when developing the nose shape to provide maximum fields of view and acceptable optical performance of the transparencies. Aerodynamic drag must be held to a minimum so that the aircraft may perform efficiently. Consideration must be given to the amount of allowable drag and weight versus the energy efficiency of the aircraft.

Attention must be given to surface shape boundary conditions so that transition will be aerodynamically smooth. Protuberances that could cause whistling noises or optical aberrations that would be objectionable to the flight crew must be prevented.

The aerodynamic shape of the aircraft nose and forward fuselage affects: the optical characteristics and unit cost of the transparency, the potential for adequately anti-icing the forward facing transparencies by either electrical or hot air blast techniques, limits the applications of wipers for rain removal, and may even dictate the type of transparency materials used. A compound curved transparency increases costs, impaires the optical quality along the edges, and usually decreases reliability.

B12.2.5 Structural Design

Aircraft visual transparencies are subjected to a wide variety of loads, such as: internal pressure, aerodynamic pressure, bird impact, foreign object impact, inertia, thermal expansion and contraction, transverse thermal gradients (heated panels), airframe torsion and bending, fatigue, and in some cases, installation preload. Because of the large differences in load carrying capability between the transparency and airframe materials, and the optical degradation caused by loading the transparency, it is recommended that the loads introduced into the transparency should be kept to a minimum by carrying the load through the support structure. The geometric shape of the transparency determines whether the pressurization loads can be carried in hoop tension or flat panel membrane loading. These pressurization loads can be carried more effectively in hoop tension, but the optics normally deteriorate with the curvature of the transparency in relation to the conventional aircrew positioning. Fail-safe characteristics must be a prime consideration in the design of adjacent structure.

Edge design of any transparency is very important. Because the commonly used glazing materials possess much lower strength properties than metals, and the strength properties are more temperature dependent within the operational environment, the stresses developed in these materials must be distributed as evenly as possible. The large difference in the thermal expansion of some of the glazing materials can result in high thermal stresses. This is particularly true in a glass/plastic composite where the coefficient of thermal expansion ratio is on the order of ten to one. Edge attachment stresses are greatly influenced by the differences of the thermal expansion/contraction rates between the transparency materials and the supporting structure materials.

To allow normal maintenance actions, the transparency and supporing structure designs should be limited to a single row of attachments with sufficient hole size tolerances to allow maintenance personnel to readily align the transparency on the aircraft and maintain interchangeability. The attachments should be of one diameter for each length. For ease of maintenance, loose hardware, such as retainers, skins, fittings, and fasteners, that are difficult to account for during a transparency change-out should be kept to a minimum. Retainers and dry seals should be permanent parts of the transparency.

B12.2.6 Bird Strike Capability

All transparencies or supporting structure surrounding the aircrew, which could affect the aircrew safety or mission completion if struck by birds, should be designed to withstand the impact of a four-pound

bird at that aircraft's design cruise velocity up to an 8000 foot altitude (AGL) or as required by the certifying agency. This capability would also apply to the potential of transparency or support structure break-up as a primary result of the impact even if the bird does not penetrate the transparency. Secondary impact debris which could consist of such things as standby instruments and HUD components must also be considered and their effect minimized.

During the design integration of the transparency-to-structure, the support structure should not be considered expendable after a bird strike. There should be no abrupt changes in the shape of the support structure cross section, such as discontinuities or localized stress riser, particularly in the corner transitions. Adjacent structure should sufficiently resist bird impact to protect internal instruments or equipment.

Certification of a transparency system to meet the bird strike requirement is normally accomplished by testing. No acceptable analytical method exists. Reference B12-1 presents a compilation of available bird strike design methods.

B12.2.7 Environmental

Environmental factors include:

A. Hot and cold soak performance consistency.

B. Resiliency to thermal shock to ensure that internal stresses do not cause failure.

C. Humidity exposure under constant or repetitious electrolytic or hygroscopic conditions that could cause a transparency to fail.

D. Rain, snow, ice crystal, and hail impact or abrasion resistance.

E. Dust abrasion resistance.

F. Salt and fog resistance.

G. Chemical resistance to those materials which are commonly used on or around the aircraft.

H. Resistance to the effects of lightning and precipitation static (p-static) phenomena.

I. Aircrew and maintenance actions resulting in scratches, cuts, digs, and repeated cleaning cycles.

J. Long term resistance to total pressure changes across the transparency resulting from changes in altitude, explosions, and climatic conditions.

The general specification for transparency anti-icing, defrosting, and defogging system heating requirements are contained in MIL-T-5842 (Reference B12-6), FAR 25, or military handbooks.

The shaping of the forward fuselage section and the location and composition of the aircrew transparencies plays a large role in the susceptibility of that area to lightning effects. If coatings are used on these transparencies for anti-icing, defogging, or RCS suppression, then lightning, precipitation static, and nuclear electromagnetic pulse effects begin to play a potentially important role. These adverse environments may be approaching a critical importance level in the case of military aircraft which use pyrotechnic devices for escape (such as explosive cords that are used to separate the transparency or structure from the aircraft).

### B12.2.8 Combat Exposure

Technical considerations for a combat environment include: radar cross section reduction (which might be considered as a technology related to anti-ice and anti-fog coatings), ballistic impact and shrapnel protection (which requires a far different treatment than bird strike protection), laser and particle beam defense, and nuclear effects defense for thermal, flash (aircrew eye protection), blast over-pressure, and electromagnetic pulse.

### B12.2.9 Electrical

If energized electrical conductive coatings or imbedded wires are used for the anti-icing and defog systems, space must be allowed in the crew compartment for controllers, transformers, and electrical discharge suppressors. These electrical components must be accessible to perform periodic functional checks. Maintenance accessibility must be planned during the flight compartment layout phase.

The shape of the transparency and the selection of transparency materials limits the type of conductive circuits that can be used. The available coatings are gold, indium oxide, or stannic oxide, and these coatings have limitations regarding the amount of power that can be applied, as well as the type of materials they may be applied to.

B12.2.10 Material Selection

The options of transparent materials available for the design of crew compartment windows are limited. The adaptability of some of the available materials are further limited because some of the more environmentally desirable materials cannot be formed and applied in a cost effective manner, nor are they competitive from a weight standpoint.

The basic transparency materials available are categorized as structural, interlayers, and coatings. The transparency structural materials are used in a monolithic state, laminated or multiple laminated with interlayers, and coated as required.

A. Structural Materials The types of primary structural materials available are described in the monolithic state as:

1. As-cast acrylic (MIL-P-5425).
2. Modified as-cast acrylic (MIL-P-8184).
3. Stretched acrylic (MIL-P-25690).
4. Polycarbonate (MIL-P-893310).
5. Thermally strengthened glass (MIL-G-25667).
6. Chemically strengthened glass (MIL-G-25667).
7. Borasilicate glass (MIL-G-25667).

During the flight compartment layout phase, the forward facing transparencies must be developed conceptually, including the selection of materials. The selection of materials must be based on the formability of the material to fit the aerodynamic shape developed for the aircraft configuration. Material thickness sizing must be accomplished to meet the structural requirements of pressurization, aerodynamic loads, miscellaneous loads, and bird impact criteria.

B. Interlayer Materials There are a variety of interlayers that have been used to laminate transparency materials. They can be classified as sheet material and cast-in-place materials. Some of the interlayers have been in use for many years, while others are still in the development stages. These interlayers include:

1. Sheet Polyvinyl Butyral (PVB) (MIL-G-25871 and MIL-P-25374).
2. Sheet urethanes (vendor proprietary).
3. Cast-in-place silicones (vendor proprietary).
4. Cast-in-place urethanes (vendor proprietary).

C. Coating Materials Transparencies have required the utilization of electrical conductive coatings and protective coatings. Electrical conductive coatings are gold, indium oxide, or stannic oxide (tin oxide). To date, the gold and indium oxide coatings have been used to meet requirements for 100 to 200 volts and the stannic oxide coatings have been used for 100 to 400 volt systems.

The gold coatings have only been used as applied to the acrylic materials. The indium oxide coatings are applied to glass and limit the amount of tempering that can be accomplished for the glass. The stannic oxide can only be applied at high temperatures only on glass. The glass is tempered at the same time the stannic oxide coating is applied.

Protective hard coatings may be applied to the surfaces of plastic materials to improve the resistance to weathering, moisture, chemicals, and abrasion. These hard coatings are normally vendor proprietary materials and generally have not been reliable.

D. Material Applications As-cast and modified (partically cross linked) as-cast acrylics have been used for nonpressurized canopy and windshield designs, monolithic cabin windows, and face plies for simple or compound contoured laminated windshields/canopies.

Stretched acrylic materials have been used in simple or compound curved monolithic configurations for fighter type windshields and canopies and as a monolithic configuration for transport windows. Stretched acrylic has been laminated with variations of PVB (MIL-P-25374) or cast-in-place silicone materials. Stretched acrylic has been used as structural plies. Composite windshields in single curved applications have been comprised of stretched acrylic plies laminated with variations of PVB (MIL-P-25374) or cast-in-place silicone interlayer and chemically strengthened glass outer face plies. For this application, the embedded side of the glass face ply has been coated with an electrically conductive coating for a 200-volt electrical anti-icing system.

Polycarbonate material has been used in simple and compound curved monolithic configurations for fighter type windshields and canopies. Monolithic polycarbonate must have a protective coating applied to all surfaces to improve its environmental resistance. Polycarbonate has been used as structural plies for composite windshields and canopies comprised of two or more polycarbonate plies with cast-in place silicone or sheet

urethane interlayers and either as-cast acrylic or chemically strengthened glass outer face plies. For those applications utilizing a glass face ply, conductive coatings have been applied to the inside surface of the glass for meeting radar cross section or anti-icing requirements. Polycarbonate is not recommended for use on transport type aircraft.

Thermally and chemically tempered glass or semi-tempered and fully tempered glass has been laminated with PVB (MIL-G-25871 and MIL-G-5485) and used as forward facing windshields. In large transport aircraft, sheet urethane has been used as a laminating material. Laminated glass windshields have been used in flat and single curved configurations. Chemically strengthened glass has been used in the monolithic state as a thermal shield for supersonic transport applications and as face plies for composite windshields.

E. Transparency Fabrication The selection of the transparency materials should be made early in the development of the transparency system.

It is recommended that the shaping, selection of materials, and total systems requirements be established simultaneously, so that all requirements are considered when changes to the developed shapes are contemplated.

During these early development phases, potential transparency fabricators should be consulted regarding probable development and testing costs. Some design considerations include:

1. Glass cannot be compound contoured.

2. Glass may be formed to simple single curved shapes only.

3. There are limitations, as a result of furnace sizes, regarding the size and complexity of glass formed parts that can be tempered.

4. Some shapes may prevent the use of conductive coatings because of fabricating limitations.

5. Oversights and production problems result from finalizing the lofted shapes before systems requirements have been considered for rain removal, anti-icing, defogging, and weather sealing.

B12.2.11 Maintenance

The transparency designer should consider ease of maintenance. The removal and replacement of a transparency should not require more than two hours for two men. The number of extraneous parts that need to be removed or disconnected should be limited to electrical connectors, wiper blade removal, or a single row of loose fitting attachments. The replacement parts should have integral "dry-seals" so that "wet-sealant" is required only under the bolt heads for corrosion protection and pressure sealing. Hoisting provisions should be considered during the initial design.

B12.3.0 Design Methods

B12.3.1 Vision and Optical Design

B12.3.1.1 Introduction

The reason for outfitting the cockpit enclosure with transparencies is to allow the aircrew to directly view the exterior scene. The pilot and other aircrew members rely on visually acquired information from the external environment during many phases of flight.

The aircrew's view of the exterior scene is restricted to some degree by the transparencies used in the cockpit enclosure. The extent of interference or degradation induced by the transparencies depends on many design factors, including material composition, thickness, shape, installed angle, and others. One of the transparency design engineer's task is to minimize the adverse effects of these factors on visual performance. The goal is to achieve optimal aerodynamic efficiency and structural integrity without compromising vision to the extent that either aircrew safety or mission success would be unacceptably degraded.

The purpose of this section is to provide the design engineer with information regarding the variables involved with visual performance and the vision envelope.

B12.3.1.2 Factors Affecting Visual Performance

Factors which affect visual performance include:

A. Light transmission.
B. Deviation.
C. Distortion.
D. Orangepeel effects.
E. Light reflections.

These factors are described in detail in References B12-1 and B12-7.

B12.3.1.3 Crew Station Mockup

The crew enclosure geometric shape is determined by many factors, such as: visual requirements, mission and task loading requirements for space allocations, aerodynamic drag, structural arrangement, equipment accessibility, etc. It is imperative that the crew station envelope be defined and the airframe designed around it. In order to fully evaluate the crew station design, a full-scale mockup of the aircraft cockpit is normally required. The mockup should include sufficient detail to permit an evaluation of the configuration by an aircrew familiar with the specific mission requirements. This evaluation would be with respect to vision, arrangement, location, actuation clearances, equipment installation and accessibility, aircrew accommodations, and complete structural arrangement. The mockup windshield(s)/canopy should be manufactured from transparent material similar to the production part so that the vision limitation can also be evaluated.

B12.3.1.4 Design Requirements

Requirements for clear vision and optical requirements have been defined to some extent in MIL-STD-850, Civil Aeronautics Manual [CAM 4b], Aerospace Standard 580B [AS580B]. Standard practices of the aircraft industry have taken up most of the remaining slack, but as is evident in the "unavoidable" mid-air crashes which happened because neither crew was aware of the other craft, more effort is necessary.

B12.3.1.5 Vision Envelope Development

FAR 25, SAE AS580B, CAM 4b, and MIL-STD-850 are used as guides for the development of the crew compartment vision envelope. The use of these documents and actual dimensional details of components, such as seats, instruments, and instrument panels, provide background guidance in the development of space allocations for required systems that must be contained in the crew compartment.

The transparency designer is required to satisfy many requirements for areas of clear vision. To fully understand the requirement and provide a tool by which the requirement can be fulfilled requires the clear vision diagram and the analysis technique called ray tracing. Computer programs "Vision" and "Refract", described in Section E7.0.0, are available to make a clear vision diagram and account for index of refraction.

After all space allotments have been accounted for, the aerodynamic shaping may take place in conjunction with defining the vision envelope. This is probably the most important feature to be accomplished for a new aircraft design because of the many transparency subsystems' requirements that must be considered. These transparency subsystems are identified with noted acceptable methods for meeting the requirements, such as:

A. Rain removal - windshield wipers.

B. Anti-icing - windshield electrical system.

C. Defog - transparency electrical systems.

D. Demist - transparency electrical systems.

E. Visibility - visibility envelope and transparency component details.

F. Optics - aerodynamic shapes, transparent materials availability and suitability.

G. Clear vision (emergency) - openable window.

H. Escape - openable window.

I. Smoke evacuation - openable window.

As a general rule, transparencies are defined by specific loft dimensions that are approximately three inches outside of the daylight openings of the transparencies and must not be misused when defining the vision envelope. Within this three inches are retainers, seals, inserts, bus bars, and attachments.

Shown in Figure B12.3.1.5-1 is a ambinocular vision diagram for the DC-10 aircraft presented as a rectilinear plot. The vision envelope generally meets or exceeds the requirements of CAM 4b and SAE AS580B. The design eye location was initially established as being 21 inches from the airplane centerline or 42 inches between the pilot and co-pilot. These locations allow the pilot or co-pilot to reach common controls (throttles); otherwise, if the distance were greater, the controls would have to be duplicated for both sides of the aircraft. In addition to reaching common controls, the shape of the top of the fuselage and the design of the overhead electrical panel should be defined in terms of reach by both the pilot and co-pilot.

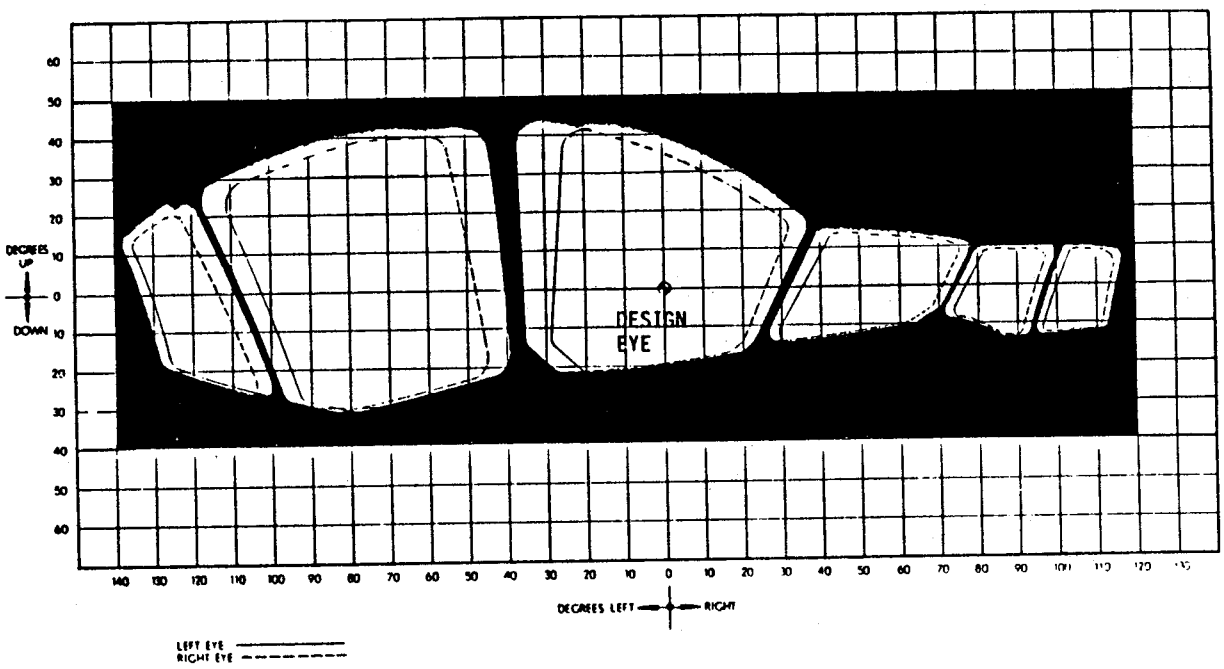


Figure B12.3.1.5-1 DC-10 Pilot's Ambinocular Vision

The windshields directly in front of the pilot/co-pilot should be flat whenever practicable, providing the aerodynamic drag is minimized. A wider choice of transparent materials, particularly glass outer panes, would be available for flat windshields; a rain removal wiper system could be more readily idealized; and the chances for optical distortion would be greatly reduced. The costs for flat windshields would be less that 50 percent of the costs for curved parts. The forward downward vision should be between 20 and 25 degrees between the airplane center post and the side post, providing the pilot can rotate his eyes to see the required instruments below the glareshield, thus providing the pilot a maximum over the nose view of the runway and runway lights during night landing approach. The forward up vision should be approximately 40 degrees with the intent of providing the pilot sufficient up visibility when banking the aircraft in congested air space and for potential in-flight refueling operations. By providing this additional up vision, it is intended to eliminate the need for overhead windows. The post between the windshield and the side window should provide the visibility boundary to the left of approximately 40 degrees for up vision and boundary to the left of 30 degrees for down vision if possible. However, the side post location must provide a landing surface for the openable window, such that, when the window is opened in flight it will provide visibility under restricted requirements, and wind and/or rain will not blow into the pilot's face. Currently, the maximum aft vision requirement is 120 degrees per AS 580B. If there is an advantage in increasing this angle to permit the pilot to see the wing tips or engines, the increased vision should be provided.

To obtain FAA certification, visibility plots are submitted early to the FAA for approval. The current requirements are specified by CAM 4b, but a proposed rule is being circulated within industry to modify the vision requirements. The proposed rule is FAR 25, paragraph 25.773X (proposed). When production airplanes are available, photographs are generally made with the FAA dual lens camera identified as the NAFEC camera and compared with CAM 4b requirements. The dual lens camera accurately depicts what is seen with two eyes when the camera is positioned at the design eye location. During flight tests, FAA pilots further evaluate the transparencies for vision, distortion and optical deviation that might be caused by transparency manufacturing problems.

## B12.3.2 Materials

### B12.3.2.1 Introduction

There is not a great variety of optically transparent materials available and when coupled with the requirement for optical quality, formability, and the resistance to the operational environment, the number of materials appropriate for use in aircraft visual transparencies is further limited. Although limited, three categories of materials must be considered for the design of transparencies. The three categories are:

A. Structural Materials.
B. Interlayer Materials.
C. Coating Materials.

While the number of available materials is limited, the state-of-the-art for new material development and new utilizations of existing material are continually in the research and development stages. Since the transparency fabricators are always attempting to improve their competitive positions they generally are aware of the availability and application of new materials and technologies. The transparency design engineer must continually coordinate with these potential sources and be on the alert for any new improved materials or processes as well as utilizing the information contained herein. The designer should cautiously use the fabricator's proposed technologies, otherwise wrong decisions can result in high costs for development and service problems.

### B12.3.2.2 Material Utilization

The selection of individual material for an aircraft transparency, whether the transparency is to be monolithic or laminated, is very important and the designer must consider the balance between functional requirements, design, fabrication, weight, and total cost. Material property data for trade studies may be obtained from sources such as Reference B12-8, published literature, other airframe manuacturers, material suppliers and fabricators. The designer should use the transparent material mechanical properties data cautiously. It must be noted that the data for transparent materials are usually based on only a few test specimens, the values are usually average values, and the data have not been treated statistically to ascertain miniminum guaranteed values.

Since the mechanical property values for transparent materials are not as accurate as those for metal, deficient materials have frequently been used for transparency design. Early failures have resulted particularly in the area of edge design. In an effort to minimize or eliminate early failures, it is recommended that the transparency be designed to reduced stress levels much in the same manner that metal components are designed to reduced stress levels for fatigue consideration.

Since plasic materials have a low modulus of elasticity, trade studies should be performed to optimize the design for weight and aerodynamic drag weight. To accomplish this, the maximum deflections of the transpancy under normal operating pressures should be evaluated against aerodynamic drag.

Polymeric (plastic) transparent materials are extremely sensitive to changes in ambient temperatures. The mechanical properties of these materials vary widely with temperature extremes, becoming stiffer, stronger, and brittle at low temperatures, and weaker and more flexible (ductile) at elevated temperatures. The temperature gradient created across the thickness of the material, such as aerodynamic heating or cooling on the outboard side, and enclosure heating or cooling on the inboard side, allows the material to operate at higher external temperatures than that which would cause failure in a soaked condition. Inorganic (glass) materials do not suffer strength changes with temperature variations to the same degress as plastics.

Transparency systems designed for the crew compartment of large size commercial transports and high performance aircraft are generally of laminated construction to minimize deflections, while passenger cabin windows and light aircraft (including helicopters and business jets) are generally monolithic construction to obtain low costs and minimum weight. The laminated design may be comprised of several different structural materials, as well as several different types of interlayer material. The primary negative factors for all glass laminated plies are weight and formability; whereas, the negative factors, when only plastic laminated plies are used, are low abrasion resistance, low chemical resistance, low thermal and electrical conductivities, and a lack of a compatible exterior, anti-static electrical conductive coating. Yet, weight is such an important factor that plastics should always be considered for the main structural plies for weight savings, but deflections and thermal conditions must be thoroughly studied to assure that service life will not be affected.

Laminated construction may be comprised of combinations of plastic or glass structural plies, interlayer materials, glass or plastic face plies, electrically conductive coatings, and other coatings from which to choose.

The outer ply of a transparency may generally have more requirements that have to be met than the other plies. These requirements may include abrasion resistance, chemical resistance, anti-icing, radar reflectance, precipitation static, and lightning protection, as well as foreign object impact. Particularly forward facing windshields are subjected to these conditions; thus, dictating the use of glass for reliability. The designer should be aware of service problems and service life of various combinations of materials. Usually, this type of information is obtainable from the users (airlines and military). Several different combinations may satisfy the requirements, however, it is the obligation of the designer to select the most cost-effective system.

The following steps outline a procedure to aid in the material selection process:

A. Define the operational and functional environment.

B. Determine the geometric shape requirements (for aerodynamics).

C. Make a list of candidate materials.

D. Thoroughly evaluate prior service problems for materials or combination of materials.

E. Analyze the results and compare against additional factors of cost, weight, geometric shape, anticipated reliability, life-cycle cost, and technical risk associated with proceeding with the design (especially if the design has not been previously proven).

B12.3.2.3 Proprietary Materials and Processess

Most of the transparent materials utilized for structural or face plies are controlled by Military Specifications or other nonproprietary documents, such as noted in Reference B12-8. The composition and method of preparation of these materials are either protected by patents or fabricator proprietary information.

All electrically conductive and abrasion resistant coatings are proprietary to the transparency fabricators.

Silicones, urethanes, and other types of interlayer material are proprietary to the transparency fabricator. Polyvinyl butyral used to laminate glass is described by MIL-G-25871, but the basic material and plasticizer content is developed and processed by the raw material

supplier; while the transparency fabricators control the methods during the laminating process. The fabricators of laminated plastic transparencies control the proprietary processes even though, when used, he purchases polyvinyl butyral with special plasticizer content from raw material suppliers.

It is evident then that the transparency designer must be knowledgeable of not only the properties of the structural materials, but must also have a familiarity and must assess the fabricator's products. Otherwise his design could become "locked in" with resultant poor service life where it would be virtually impossible to redesign the transparency without a complete redesign of the adjacent structure, which becomes extremely expensive.

After the requirements have been established, the designer should design a transparency that is optimum in terms of: (1) satisfying the requirements; (2) low weight and cost; (3) reliability; and (4) possessing the least technical risk associated with the end product. Once the design has been established, a determination must be made through negotiations with Procurement, Product Support and the fabricators whether a satisfactory warranty can be obtained. The transparency must be designed so that at least two fabricators can be qualified to produce end products.

B12.3.2.4 Manufacturing/Machining Requirements

Machining operations performed on transparent material, if not properly accomplished, may greatly reduce the service life of a finished transparency. It then becomes imperative that the designer become familiar with some of the basic machining techniques, even though the machining methods and processes remain proprietary to the fabricator, so that he may better define the end item product on his drawings and specifications.

Glass panes are cut to size from annealed sheets, then the edges are chamfered, seams are machine ground to a 180 grit, flat rock or equivalent finish prior to either semi or fully-tempering the pane. Once the tempering has been accomplished the glass cannot be machined in any way without catastrophic failure. Historically, the annealed sheets were plate glass that were extruded, ground and polished on both sides to obtain the required thickness and optical quality. The plate glass process has been abandoned in favor of "float glass". "Float glass" is produced by extruding glass through slits and floating it at predetermined speeds over molten tin to obtain the final thickness and optical quality. The "float glass" is generally smoother than plate glass and does not require additional surface machining.

Acrylic material can be machined, but the machine tools, such as drills, routers, and band saws, must be designed to reduce the amount of heat generated when machining at reduced speeds and the finished parts are usually annealed after machining. When the special machined tools are properly used, the finish does not require further polishing.

Polycarbonate requires that the machined surfaces be ground and polished to a 63 RMS finish, unless a proprietary protection technique is used that has been proven to be reliable. Many handbooks and Douglas Process Standards are available that describe these processes.

### B12.3.2.5 Structural Transparent Materials

The materials currently available for structural application in transparencies are chemically or thermally tempered glass (MIL-G-25667), as-cast acrylic (MIL-P-5425), stretched acrylic (MIL-P-25690), or polycarbonate (MIL-P-83310). The selection of the structural material will dictate the edge attachment design. Glass structural plies must be laminated with special fiber type or metallic reinforcing strips and fiber or phenolic edge members bonded to the assembly in order to drill holes for bolted attachment to the support structure. Stretched acrylic and polycarbonate materials may be drilled and bolted directly to the support structure. Material properties should be obtained from Mil-Handbook 17, Part II (Ref. B12-8). Additional data for polycarbonate may be obtained from Reference B12-9.

### B12.3.2.6 Interlayer Materials

Interlayer materials are used to laminate glass to glass, glass to plastic, or plastic to plastic. Interlayer materials are unique in that they must: be an adhesive; serve as an energy absorbing medium; accommodate the differential expansion/contraction rates between the laminated materials caused by thermal conditions; provide fail-safe features; and be of good optical quality and have low light transmission loss. Because of this, when an interlayer is used, the transparency is, by definition, a composite.

The choice of available interlayer material is limited to polyvinyl butyral, polyurethane, and silicone bases. The bases are proprietary to the various transparency fabricators. Material properties are available in Reference B12-8. Interlayers provide an optimum location to imbed electrical heating and temperature sensing elements. The materials to be laminated must have proprietary surface preparations and primers applied. Interlayers are available as either sheet material or as Cast-In-Place (CIP) compounds. The final thickness of an interlayer using sheet material is accomplished by a buildup of individual sheets, while the desired thickness of CIP must be accomplished by creating a measured void between two structural plies, sealing the edges and injecting the CIP under pressure to fill the void.

Interlayers are considered to be non-structural. However, they do become stressed as a result of differential thermal expansion/contraction between the adjacent panes. This stress is concentrated along the bondline and can cause delamination or glass "cold chipping" (in the case of a PVB/glass interface). Careful consideration must be given to the selection of thickness so that the material may deform without adhesive or cohesive failure. Thermal studies must be conducted to determine the amount of expansion or contraction of the adjacent plies and an evaluation made to determine the elongation required so that the thickness selection will reliably meet these requirements. The selection of a final interlayer thickness must also take into account bird impact requirements.

Edge chipping and/or cracking can be the result of contraction of the cold edges of a glass laminated transparency or contraction at the edges of glass face plies adjacent to metal structure. Generally when the outer ply is glass, it carries an electrical conductive coating for anti-icing. Between bus bars, where the electrical power is concentrated, the glass maintains a temperature above +32$^{o}$F on the exterior surface and as high as +110$^{o}$F next to the interlayer. The glass edges may get as low as -100$^{o}$F. In this area the interlayer is trying to contract, but it is tending to expand between bus bars, therefore, putting high tensile components on the edge of the face ply that can cause edge chipping or cracking of a PVB/glass interface or delamination for other laminated materials. The glass laminating fabricators install slip plane materials between the bus bars and the interlayers in an attempt to prevent cold chipping, but the slip plane material does not prevent delamination. Some research has been undertaken by several commercial airlines to install electrical heating devices around the entire periphery of glass laminated windshields to heat the edges. These devices have been installed on three different types of aircraft that represent three different designs. The results of these tests, to date, reveal that the frequency of cold chipping has been greatly reduced and the amount of delamination, which has always been a problem, has been reduced to an acceptable amount. More recently, urethane interlayers have been used because of the materials' pliability under more extreme temperature regimes.

If the edge attachment design is not symmetrical (e.g., not all structural plies bolted to structure) then uniform loading due to in-plane loads is not possible and tensile stresses at the edge tend to cause delamination, cracking, or edge chipping. The magnitude of the load differential on the individual plies is dependent upon the stiffness of the laminates. Another mode of introducing tensile stresses at the edge is during manufacture - the autoclave pressure used during lamination may squeeze the face plies together somewhat, and after the cure cycle, when the pressure is removed, the face plies tend to return to their original shape, but the cured interlayer resists this regression and tensile forces arise (curved surfaces).

The strength of an interlayer is dependent upon three variables:

A. Temperature which affects the basic physical properties of the interlayer material.

B. Geometry which is important because of the non-linear, large displacement characteristics of most interlayers.

C. Substrate Materials (including coatings and primers) which have an affect on the adhesive strength of the interlayer depending upon the basic structural material and coatings relative to the laminating processes.

The information and data supplied in this section should be supplemented with data from transparency fabricators, Mil Specs, and industry reports.

B12.3.2.7 Coatings

Transparent glazing materials may require the application of additional coatings to improve performance and/or for protection. These coatings fall into two general categories: conductive and protective. The conductive coatings are applied to the surfaces of the monolithic sheets before lamination and the protective coatings are applied to the finished parts.

Transparent coatings can provide a desirable way of altering physical characteristics of transparent materials because they are lightweight and can be applied selectively. The metallic coatings, however, usually require relatively high temperatures for application, and, therefore, may not be compatible with most plastics and some glasses. The one exception to this is the application of gold coatings to plastics which result in a low adhesion, but usable, metallic coating system. Also, the protective coating application may affect the base mechanical properties of the substrate. The need for one or more coatings must be carefully considered because, in addition to increasing the complexity and cost, each coating may decrease the luminous transmittance of the transparency.

Generally metallic coatings will reduce luminous transmittance, while protective coatings applied to plastics may cause an apparent slight increase in transmittance by decreasing the surface haze.

Many satisfactory coatings are available for specific applications. However, most are proprietary, either as to their composition or the process of adhesion to the substrate, or both. It is the responsibility of the designer to supply the fabricator with the

criteria that must be met by the finished product. In order to do this, the designer should be aware of the complexities and peculiarities of these coatings.

A. Protective Coatings As the name implies, these coatings are used to protect the transparency material and ranges from opaque through fully transparent. For opaque coatings, generally edge sealing or fungus resistant, the chemical compatibility with the substrate and durability are the primary concerns.

B. Abrasion Resistant Coatings Plastic materials are much softer than glass. Polycarbonate is particularly vulnerable to environmental exposure and must be protected in some manner. The acrylic materials historically have not had protective coatings applied. These coatings are somewhat susceptible to the following: dust and sand abrasion, solvent attack, and long term weathering.

Adequate protection against these variables is measured by how well the coating retains its optical qualities and, also, how well it adheres to the substrate during its design service life. First generation, abrasion resistant, surface coatings for polycarbonate have not been too satisfactory, in that exposure to ultra-violet radiation and high humidity weakened the bond between the coating and the substrate, resulting in the coating peeling, particularly at low temperature extremes.

A second generation coating system which was developed specifically for polycarbonates has shown improvements and has been utilized on the F-16 aircraft. Third generation coatings are being evolved which also show a high degree of promise.

C. Rain Repellent Coatings The purpose of these coatings is to assist in the removal of rain during approach, landing, and takeoff under the design conditions (usually "heavy rain" per Reference B12.8, Table 6.4-1).

The in-flight applied "coating" is complex because it requires an on-board distribution system (nozzles, manifold, etc.), a fluid reservoir, tubing, a pump, and an electrical circuit to activate the pump. This system is used in conjunction with a wiper system. Also, there must be some provision to service and refill the reservoir on the ground.

During a heavy rain, this material is squirted onto the windshield surface and mixes with water as mixed by the action of the wiper that tends to coat the surface so that water does not cling to the surface because of its inherent surface tension capability.

D. Conductive Coatings and Resistivity This category contains electrically conductive coatings that serve to maintain clear areas (as in defogging or anti-icing) or protect the transparency system from damage due to electric phenomena (such as static or lightning), or radar reflective coatings for military applications.

Reference B12-8 provides a good synopsis of coating resistivity measurements in so far as the measurement theory is concerned. It should be noted that some of the reported coating uniformity and consistency is a problem (Reference B12-10). To minimize this problem the shape of the heated area must be as close as possible to rectangular.

It should also be noted that relatively recent studies (Reference B12-11) have shown a need for appropriate shielding and grounding of these electrically conductive coating systems, such as has not been accomplished previously.

E. Anti-icing Coatings This is by far the most widely used type of coating on aircraft transparencies. The principle is to apply a thin metallic film to the transparency and supply it with electrical power through bus bars which is converted into heat due to the resistivity of the film. The heat then is conducted through the glazing to maintain an exterior surface temperature of approximately $+35^{o}F$, which is sufficient to prevent ice formation. This temperature is controlled by strategically placed heat sensors to limit the power supplied and prevent overheating.

The film is applied to the substrate using vacuum deposition techniques, except for a stannous oxide coating on glass, which requires a pyrolitic process. This film is usually placed on the inboard surface of the outer ply of a laminated design. This ply is then laminated to the main structural ply with an interlayer. The surface temperature ($+35^{o}F$) is dependent upon the thickness of the glass ply and the temperature of the film.

The design of the anti-ice system must utilize a total system approach involving the functional know-how of technical disciplines from Structural Design, Strength Analysis, Thermodynamicists, Aerodynamicists, and Electrical. The rate to be performed by these disciplines must be all inclusive for each technical area. The structural designers must define the shape of the transparency relative to the shape of the nose and provide surface areas, establish the material thicknesses required and specify the materials that will fulfill the requirements for structural integrity (including bird impact, fatigue, and fail-safe) as approved by strength analysts.

The materials for structural integrity then dictate the choices of electrical conductive coatings that may be used. Stannic oxide is used exclusively on tempered glass, indium oxide on glass, and gold coatings on either glass or acrylics. The electrical characteristics of these coatings, as well as limitations, densities, and operating requirements, are generally obtainable from the transparency fabricators. The thermodynamicists perform a complete thermal analysis for the design submitted, taking into account the aerodynamic shape of the nose relative to the transparency, the heat transfer coefficients of the materials, the extreme climatic conditions specified by the FAA or military agencies, and the limitations of the coatings. They establish the wattage required for an electrical system. They should determine the wattage required for the normal conditions when icing is most often expected to occur and the emergency condition when icing may or may not occur during the life of the aircraft. MIL-T-5842 is an aid in providing information for determining the amount of energy required to prevent the formation of ice or the transparency surface. The results of this analysis should show that about 4 watts/square inch of surface area is required to prevent the formation of ice on the transparency surface for most transport aircraft flight conditons which will provide the largest service life for the transparency. The analysis may show that a maximum of 8 watts/square inch is required for extreme icing conditions which should include the tolerance of the total electrical systems. This thermal analysis should also define the coating temperature to be not more than 90$^{o}$F to perform the required normal operation and a maximum of 115$^{o}$F for the extreme condition. Relative to the transparency coatings the bus-to-bus resistance can then be determined as the method of measuring the coating. From this analysis the electrical systems designers determines the power requirements, select a controller, and provide a decal position anti-ice electrical in the crew compartment that defines off, normal, and emergency use of the system. In prior applications the power has varied between 200 and 400 volts. The selection of a controller should take into account that sudden thermal shocks to the coating will result in failures of glass, therefore the controller should allow a minimum of three minutes for warm-up or before the full power is applied and ideally should maintain the required temperatures on the coating. Therefore, when the controller cycles on-off the temperature change should only be a few degrees.

Once the electrical coating requirements have been defined then the structural designer should determine from the potential transparency fabricators the effect the coating density may have on the light transmission requirements. The designer should investigate the vendor's capabilities and ability to deliver finished parts. In the event the light transmission is greatly affected it may be necessary to re-shape the transparency to alter coating requirements; thus, additional thermal studies would be required.

After the transparency electrical requirements have been finialized the structural designer may then finish his drawing. Even though the fabricator generally establishes how the wires are located within the laminate the drawing should specify a minimum of two attachments to each bus bar to prevent power surges that cause thermal shocks at the soldered connectors.

The Structures' design drawing should specify the following:

$$K_A = 0.75 \text{ or greater}$$

$$K_H = 1.3 \text{ or less}$$

$$K_M = 0.65 \text{ or greater}$$

These values take into account the uneveness of the conductive coating and the placement of the sensing element within the laminate. The fabricators have various inspection probes to establish these relationships with respect to the coating and sensing elements.

A windshield having perfectly uniform power dissipation would have all three power constants equal to unity. The power constant system of heating pattern quality control is sufficiently flexible so that manufacturing improvements can be reflected in power constant limits which become closer to unity as the heating pattern becomes more uniform.

The sensing elements are small, but must be located in the least objectionable vision area of the transparency. (See Ref. B12-12 for additional information on the design of the electrical system.)

F. Defogging Coatings The basic principles are exactly the same as for anti-icing, except that the power required is approximately 1 watt/in.$^2$, and the surface to be heated is the interior (versus exterior). The function of the coating is to keep the exposed inner surface of the transparency at a

temperature above the dew point of the cabin air. It is the thermodynamicist's responsibility to determine this dew point under the worst operational conditions. Because of the uncertainty of the variables involved in this determination, the design temperature must be specified slightly higher than the theoretical value.

These coatings also require the same kind of heat transfer calculations as for the anti-icing coatings, even though the coating is at or near the inner surface, because the cold exterior surface causes the heat to flow outboard also. The power required is generally 115 volts.

G. Radar Reflection Coatings The purpose of this coating is to minimize the return signal of a radar beam from any portion of the transparency - exterior surface, interior surfaces and corners. This is generally termed 'reducing the radar cross section of the aircraft' and is normally accomplished within the present state-of-the-art by coating the transparency with a metallic film that is optically transparent, but which also reflects an impinging radar beam and prevents it from entering the cockpit. It cannot be prevented 100 percent, but at least it will decrease the concentration (intensity) of the return signal. Even when some of the radar beam enters the cockpit and is reflected back, it is further attenuated as it is reflected and passes back out through the transparency and metallic film. A more detailed, unclassified discussion can be found on this subject in Reference B12-8.

The coating is a vacuum deposited, metallic film, which should be grounded for electrostatic purposes. However, if the transparency is equipped with an electrically conductive coating for the purpose of anti-icing (or anti-fogging) this will normally satisfy the criteria for radar reflection. Defensive search radar signals are present in a wide range of frequencies, therefore, the reflective coating should be effective over a broad band from 3,000 to 20,000 MHz. A coating which is of sufficient thickness to repel any particular radiation accomplishes two principal actions: (1) the majority of the signal is reflected at a non-returning angle to the generator/receiver, and (2) the coating plus the transparency is reacting as an inefficient radome having an extremely high dielectric constant.

NOTE: Since flying radar stations (AWACS) are becoming more numerous, there are no "non-returning angles" for signals reflected from curved surfaces.

Coating thicknesses must be kept to a minimum so as not to cause too great a loss in light transmission. Once coating thickness criteria are established a means of checking this thickness on the substrate is required. The simplest method is bus-to-bus resistance, but if the coating is only required for radar reflection, while ignoring the p-static and lightning requirements, it would be unnecessarily complex and expensive to fabricate bus bars into the system. (If the coating is also used for anti-icing then it already has bus bars included.) During production an economical method is to coat small witness samples having bus bars along with the transparency. This permits some degree of confidence in production quality control, but subsequent checking in the field for coating deterioration is still difficult.

H. Radiation Protection Coatings This is required to protect the pilot from radiations from his own electronic detection systems. It should cover the transparency as completely as possible to prevent high power signals from entering the cockpit. This is the same type of coating as for radar reflection, and where a radar reflective coating is used it might also be designed for use as a radiation protection for the aircrew (if necessary).

I. Anti-Static Coatings The purpose of these coatings is to prevent the buildup of electrostatic charges on the exterior surface of plastic enclosures, thereby, preventing damage to the transparency or injury to personnel by a discharge of the accumulated charge. Plastic materials have an affinity for electrostatic charges as a result of almost any frictional impingement, whether it be from rain, snow, dust, or even wiping during a cleaning operation. These charges can interfere with radio signals and, also, can attract dust particles, thus, obscuring vision. Further, when cleaning the glazing to remove this accumulation of dirt damage may occur as a result of abrasion (wiping).

An anti-static coating does not have to be grounded, but it allows the many charges (both positive and negative) to "flow" over the surface and effectively neutralize each other. This type of coating must be applied to the exterior surface of the plastic transparency, but it is not too durable and must be continually re-applied. A metallic coating would serve very well, but if there is another metallic coating on or within the transparency, the loss of light transmittance would be too great.

The best solution presently in use for plastic transparencies is to use a dielectric coating which has a polar mobility permitting oppositely charged areas to neutralize themselves. Hydrophyllic compounds and some silicone oils possess the necessary structure to perform the anti-static function. Charges on a plastic transparency will remain indefinitely until neutralized by a humid atmosphere, water film, or other agent.

None of the solutions to the anti-static problem are entirely satisfactory at the present time. However, if a glass outer ply is used in a laminated design this problem is eliminated, of course, at the expense of a complex and costly transparency system. If the coating is grounded to the airframe it may be considered as a static discharge coating.

B12.3.2.8 Sealing Materials and Applications

Sealing is an important factor in the design of a transparency system. The transparency installation to the structure must be sealed to protect the crew compartment from the exterior weather elements and to prevent pressurization leaks. To assure that a transparency system will attain the design required service life the components within a transparency must also be protected against various environmental elements.

Rubber seals of a solid material or inflatable fabric reinforced configurations have been used as weather and pressurization seals for permanently installed transparencies or openable canopies. Another approach to sealing against weather and pressure has been the use of either or both a pliable mastic tape or wet sealants. Various techniques and sealants have been used to protect the components of a laminated transparency against the environmental elements.

A. Weather Seals The function of a weather seal is to prevent water and solvents from finding entry between the transparency and the structure into the crew compartment or becoming trapped next to structure that could result in stress corrosion. Not only would solvents entering the crew compartment be an annoyance to the crew, but the solvents could easily cause electrical equipment malfunctions.

Permanently installed transparencies and openable transparencies are installed with "dry-seals".

B. Dry-Seal Applications Dry-seals are generally molded silicone rubber designs that are cemented to the transparency. The silicone is of a low Shore Durometer Hardness (SDH), described as DMS 2221, in the order of 20 to 35 SDH. The shape of the seal is designed to displace when a force is applied, in order to compensate for the fact that rubber does not compress under load and must be displaced or deflected. The maximum thickness of a molded seal is usually 0.100 to 0.150 inches. When the transparency is installed on the aircraft structure the seal displaces to a thickness of 0.060 to 0.090 inches when the attachments are torqued to 35-50 inch pounds. This displacement generally will flow into minor machined surface irregularities and prevent moisture or solvent ingress.

It must be noted that either a polysulfide or silicone wet sealant must always be applied around the bolt shank and attachment heads to prevent dissimiliar metal reactions and to prevent pressurization leaks around the bolt.

C. Wet-Sealant Applications Silicone and polysulfide wet sealants have been used to fill voids and gaps between the transparency and structure for weather sealing. The amount of sealant used must be based on preliminary estimates of gap dimensions and sealant then applied to structure approximately 25-50% thicker than the finished gap will be. The sealant materials are either applied with a spatula or under pressure from a sealing gun.

The use of wet sealants has many disadvantages even though the materials will perform the required sealing functions. Prior sealants installed must be removed before a new transparency is installed. In a timely manner, the sealants have to be available. Generally, all sealants are a two-part mix. After the two-part materials have been completely mixed the useful worklife is one-half to two hours depending on the mix. In the event the transparency installation is not as planned, it is possible that a lot of sealant may be scrapped for exceeding the useful worklife. The time required for the sealants to be completely cured requires 72 hours at temperatures above 70°F. These sealants are messy and difficult to clean from the adjacent areas after the transparency is installed. Silicone sealants are usually easier to clean up after after an installation than the polysulfides.

Prior to the use of any sealants the sealant materials should be tested for chemical compatibility to the transparency materials. Some sealants react with transparency materials

and cause crazing, particularly to polycarbonate. Generally, wet sealants for pressure and weather sealing are not recommended.

D. Pressure Seals The function of a pressure seal is to maintain cabin pressurization, even to the extent that small leak paths are not allowed. The noise or whistling created from a small leak is usually objectionable and very annoying to flight crew members. For those transparencies that are permanently installed, the weather and pressure seal should be one unit; preferably the molded silicone "dry-seal" concept and cemented to the transparency. The concept of a dry-seal is designed to facilitate transparency replacement in the field. It increases the reliability and decreases the skill level required of maintenance personnel and eliminates the time consuming cure cycle necessary with wet sealants. If necessary, the mastic tape or wet-sealant can be used since the concepts have previously been successful, but they are not recommended for a new design.

For openable windows, such as clearview windows on transport aircraft, the pressure seal best utilized is an extruded silicone, tubular section that is snapped into a retention ring on the structure. The seal has holes that are vented to the pressure side of the cabin so that it will inflate (after the window is closed against a portion of the seal) when the aircraft is pressurized.

It has been accepted design practice to design reinforced, inflatable seals for use with openable canopies. Canopies usually have a lot of movement in the direction of opening, closing, and translation to close and lock. The inflatable seals utilized usually collapse, so that when the vast amount of movement takes place they are hidden and cannot be damaged. The material is usually of silicone construction with several layers of dacron cloth embedded for reinforcement. The seals are automatically inflated with a special pneumatic system on the aircraft that pressurizes this seal only. The inflatable seal concept is somewhat complex which causes a lower reliability than a passive seal. This is an area where additional research is needed to determine if a solid material or some skinned foams could be designed to replace the inflatable seal concept. The design and the material selection should attempt to prevent easy puncture or tearing in service.

E. Transparency Component Protection There are several components within a laminated transparency that must be protected from external environmental elements. The edges

must be protected against the ingress of solvents to the interlayer materials because the material reactions will cause bubbling. The exterior edge of an outer ply must be protected to prevent solvents, including water, from entering the edge and causing coating depletion, bubbles, or delamination.

Several approaches have been used to protect the laminated transparency edges. Formed sheet metal pans have been used in combination with a polysulfide sealant applied between the pan and the transparency. Since there are several variations of polysulfide sealants, the selection should be made based on using the sealant with the least amount of solvents or plasticizers. In glass laminates it has been shown that in a polysulfide sealant with a high solvent content the solvent will migrate into the interlayer. Silicone or polysulfide sealants have been applied directly to the edges of laminated transparencies. When silicone is used the laminate must be thoroughly cleaned and a primer applied so that the silicone sealant will bond to the materials. Before any of these sealants are used a determination should be made regarding the compatibility of the materials so that stress cracking or crazing of the plastic materials will not occur. Adhesive backed tapes have also been applied to transparency edges.

Various techniques have been used to prevent solvent ingress into the laminated transparency next to the outer ply edge. Figure B12.3.2.8-1 shows a vulcanized, solid silicone material next to the outer ply. For subsonic aircraft this type of seal has proven to be very reliable. When wet sealants are substituted for this material the sealants do not seem to have the same service life. Figure B12.3.2.8-2 shows another approach to the proptection of the outer ply. The weather sealant used has been either silicone or polysulfide sealants. The silicone sealant is a popular and commonly used material. However, it has been replaced for advanced applications because it easily erodes due to the aerodynamic effects of air and particles in the air, such as dust, ice, and rain. Polysulfide is superior to silicone in resistance to erosion and moisture penetration, but is susceptible to deterioration due to aging effects, as evidenced by weather checking and crazing. This was determined to be caused by ultra-violet exposure, so carbon black (an ultra-violet screen material) was added to the polysulfide sealant material and resulted in a sealant that was resistant to aging. This improvement extended the service life; but erosion is still the final cause of failure. It is recommended that periodic applications of fresh sealant be applied to extend the service life.

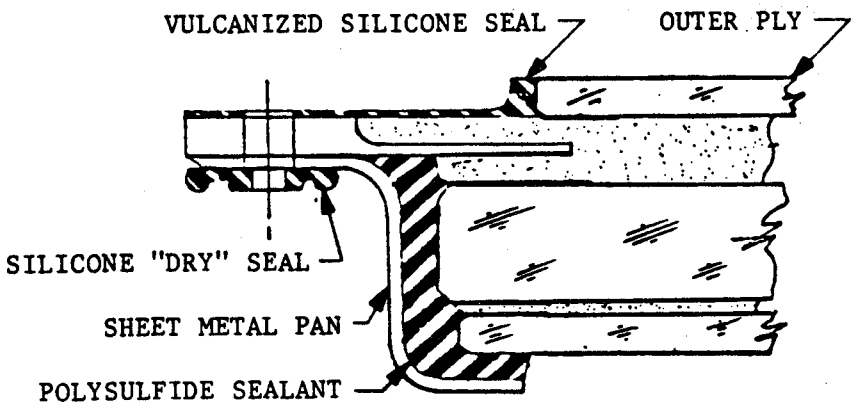


Figure B12.3.2.8-1 Application of a Vulcanized Seal

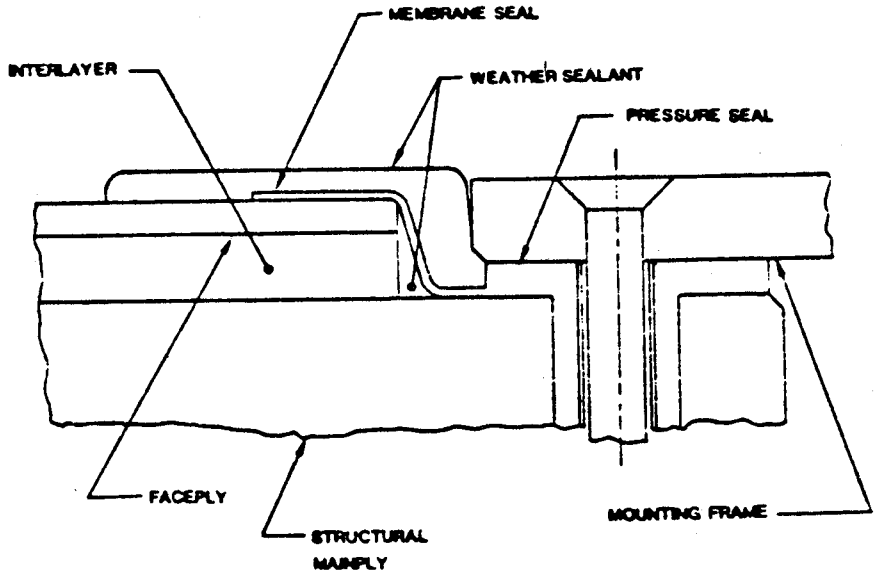


Figure B12.3.2.8-2 Example of Advanced Sealing System

B12.3.2.9 Laminated Transparencies

Historically, laminated glass windshields have been fabricated in accordance with MIL-G-25871, and laminated acrylic windows have been laminated in accordance with modified versions of MIL-P-25374. Since the introduction of chemically strengthened glass and polycarbonate transparent structural materials there have been many other approaches to laminating transparencies.

Generally, when glass and plastics are laminated they have been referred to as composite transparencies, but the combinations must be laminated with interlayer materials.

As new high-performance aircraft are conceived, the requirements for transparency subsystems are becoming more stringent. Several materials have been presented in prior sections that have desirable properties that will satisfy some of the criteria; however, no material will satisfy all requirements for structural, thermal, and electrical systems. When designing a transparency subsystem to accommodate these new high-performance criteria, combinations of these materials may be necessary. Therefore, the most desirable feature of several materials must be investigated, subsequently selected, and combined in a laminated composite transparency design. The detracting aspects of this type of design are high costs, reduced optical performance, and life expectancy. Increased weight may occur when compared to a monolithic plastic part, but when plastic can be substituted for glass in a laminate there is a considerable weight savings.

A. Structural Characteristics One of the functions of a laminated composite transparency is to enhance the mechanical characteristics of the overall assembly. One or more plies of structural materials form the structural core combined with abrasion resistant face plies connected by resilient interlayer to achieve a fail-safe assembly. When properly designed it may be possible to carry fuselage loads across the cutout for the transparency, thus, permitting a lighter more efficient transparency and support structure design. For this type of design care must be exercised to maintain fail-safe capabilities of the adjacent structure.

B. Optical Characteristics The optical characteristics of a laminated composite transparency subsystem are much more difficult to assess and maintain than for a monolithic transparency design. The laminate is always degraded because of light transmission loss due to increased thickness, reflections that result from dissimilar index of refraction for the various materials, and manufacturing associated problems.

Some optical problems that may become evident in a laminated composite transparency are:

1. The many surfaces existing within a laminated transparency combine to cause multiple images, depending on the slope of the transparency which can be very distracting, especially under low light or night time conditions.

2. The several different materials having differing indices of refraction lead to greater deviation.

3. Deviation or distortion is also potentially greater because of non-parallelism of the surfaces due to uneven compression, particularly at the edges, of the sheet interlayers, or tooling problems in the case of a Cast-In-Place (CIP) interlayer.

4. Light transmission is more a function of the material used than the fact that many materials are used. However, there is a loss of light transmittance due to the many interfaces of the various materials used.

5. Birefringency will be more prominent, especially in plastic laminates because some interlayer materials are good light analyzers, thereby, enhancing the natural birefringency of polycarbonates and acrylics.

C. Electrical Characteristics The requirements for anti-icing, defogging, or RCS are more efficiently met by utilizing electrical conductive coatings. The conductive coatings for anti-icing and defogging cannot be exposed; therefore, a face or face plies are required to be laminated to structural plies.

The RCS coating may be combined with the precipitation static coating or it may be embedded on the laminated side of either a glass or acrylic face ply. Whenever possible, when all four requirements must be met, as many requirements as possible should be combined so that the number of coatings are minimized.

D. External Defogging (Demisting) An electrical demisting system can be developed to provide enough heat to the outer surface of the transparency to keep the outer surface from fogging. The fog occurs when an aircraft makes a descent and landing from a cold cruise condition when the transparency is cold soaked to a humid condition on the ground. The design condition for demisting is to maintain the outer surface temperature above the ambient temperature. A transient heat transfer analysis is required to determine the adequacy of the

heat applied. Generally, this system is optional or by airline demand.

B12.3.3 Structural Design

B12.3.3.1 Transparency Thickness Sizing

The basic transparency thickness may be initially based on simple stress and deflection flat plate or curved plate equations that account for edge constraints. The loading is generally due to internal pressure combined with aerodynamic effects and is assumed to be uniformly distributed normal to the transparency surface.

In many aircraft, the factor which determines the thickness of a windshield transparency is the load due to a bird strike.

B12.3.3.2 Transparency Edge Design

An aircraft transparency system consists of two structural elements, the transparent material and the edge area. The edge area refers to the two or three inches of transparent material at the perimeter, the attachments and related hardware, and the support structure.

An ideal windshield design is one that would be a permanent installation and would not have to be removed for the life of the aircraft. Unfortunately, the electrical system within transparent materials are not as durable as the metal structure and must be removed and replaced from time to time. The number and types of fasteners should, therefore, be minimized.

The maintenance history of commercial and military aircraft show that normally about half of all windshield failures occur at the edge of the transparency, with the greater part of these failures resulting from delamination in multi-ply laminated windshields, or crazing and cracking in polycarbonate and acrylic windshields.

The design and analysis of the edge area of an aircraft windshield system involves many considerations. The following items and their effect on edge design are discussed in this section:

Transparency support structure.
Method of attachment.
Transparency material.
Laminated transparencies.
Load analysis.
Hole preparation.
Mechanical behavior of the material.
Temperature effects.
Sealing.

A. Transparency Support Structure The design of the structure that supports a windshield is a critical part of the overall system development. The support structure must be capable of sustaining fuselage loads that would have been carried by the frame, longerons and skin panels removed to accommodate the windshield, as well as the loads that result from aerodynamic, pressurization, and bird strike forces. Pressurization produces cyclic loads resulting in fatigue, while a bird strike produces the most severe load.

When a hole is cut in an aircraft shell to accommodate a windshield, the transparency is designed to resist the pressure, but it may or may not be designed to transmit loads across the hole. Utilization of a windshield to react primary aircraft loads may result in an efficient, lightweight design, but requires that the windshield be designed to react fuselage hoop stresses due to internal pressure, act as a bending member for continuity of the fuselage skin, frames and longerons, and act as a fuselage shear carrying member. An example of this concept, called a structural windshield, is the Air Force B-1 bomber, Figure B12.3.3.2-1, which utilizes a double row of tight fitting attachment holes. The load is transferred to the structure in double shear. It has been Douglas policy for commercial aircraft not to transmit loads from the structure to a transparency because of fail-safe requirements. In the event of structural component failure the damage would be minimized so that a catastrophic failure is not encountered.

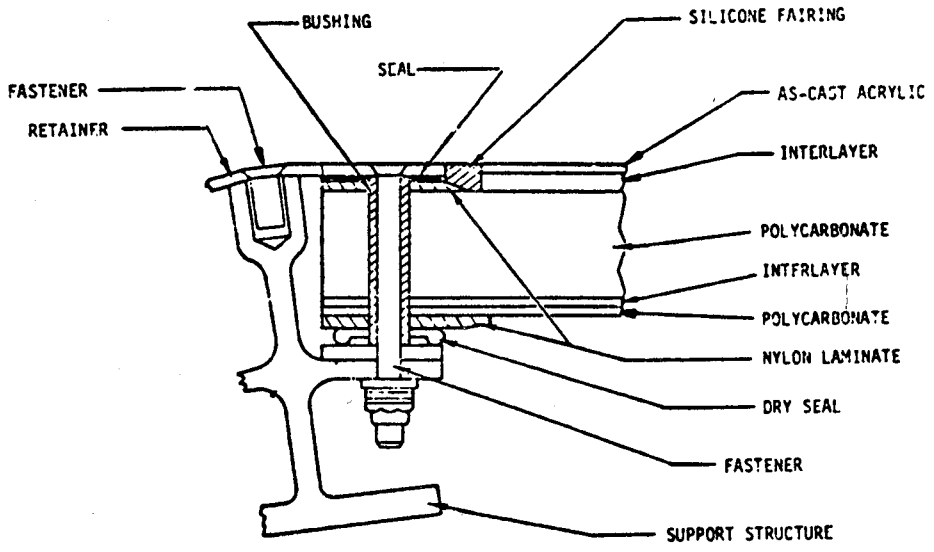


Figure B12.3.3.2-1 Edge Design in Double Shear for a Windshield

The non-load transfer windshield, while capable of resisting pressure and bird impact, does not transmit loads across the cutout. The adjacent structure must be sufficiently strong to carry the loads around the cutout. This type of windshield may be flat or curved. The DC-10 windshield, shown in Figure B12.3.3.2-2, isolates the glass from aircraft structural loads. This design utilizes a flat glass transparency and a single row of fasteners with oversize holes.

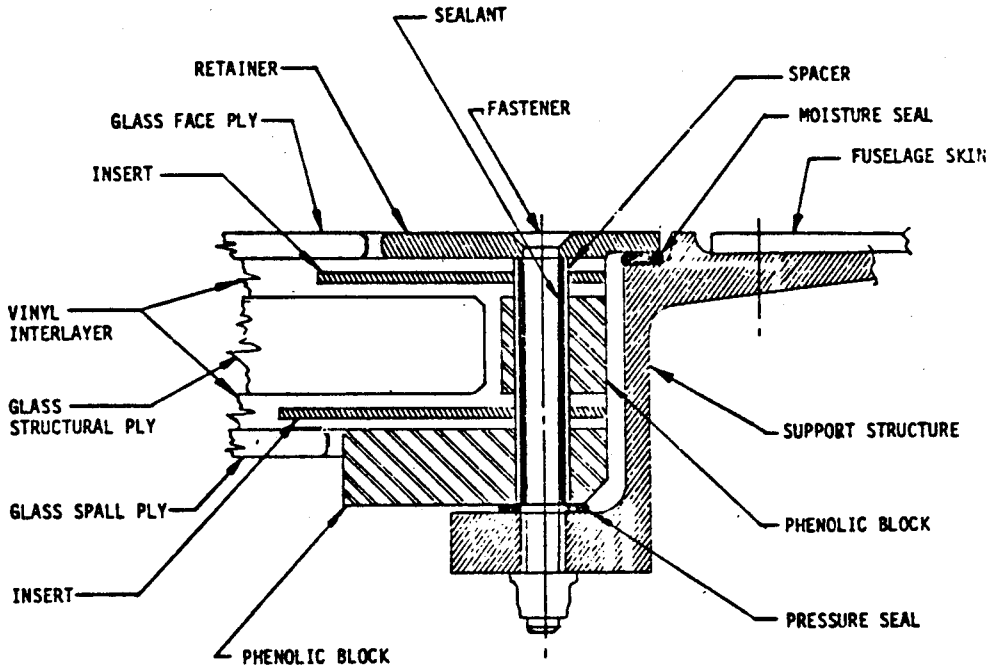


Figure B12.3.3.2-2 Edge Design for a DC-10 Windshield.

Many Air Force aircraft, such as F-16, employ a curved windshield and/or canopy. The internal pressure loads are transmitted to the surrounding structure by membrane action in the transparent materials. Localized bending stresses occur at the perimeter of the transparency. These aircraft typically utilize a single row of attachments with oversize holes, as shown in Figure B12.3.3.2-3. Other aircraft use a center beam and/or arch to provide stiffness at the junction of a fixed forward windshield and aft openable canopy. The stiffness of this type of support structure is usually determined by bird strike requirements.

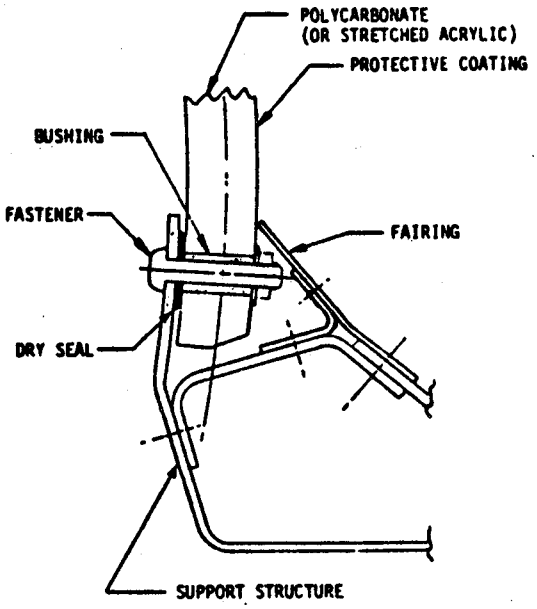


Figure B12.3.3.2-3 Edge Design for a Monolithic Canopy

Design for bird strike is an important consideration. The average impact force imparted to a windshield that is installed at a 30 degree slope would exceed 10,000 pounds if the bird weighed four pounds and if the aircraft were flying at 350 knots (Reference B12-13). This potential force has a severe influence on the support structure design. The main criteria for producing a windshield system that would survive this impact load is that the support structure stiffness be compatible with the stiffness of the transparency. Consideration must also be given to providing doublers and frames that will protect instruments and components that may be located in the overhead electrical panel and instrument panel.

Every detail in the choice of the support structure concept must be measured with respect to its impact on weight, strength (including fail-safe), maintainability, and reliability to achieve a cost effective design.

B. Method of Attachment At least three methods of transmitting load from a transparency to the supporting structure are possible: one method requires no fasteners, the second method requires loose fitting holes for fasteners, and the third method requires tight fitting holes for fasteners.

The quickest transparency to replace is one that does not require attachments, such as used for the DC-9 and DC-10 cabin windows. This slip joint installation transmits loads to the support structure in shear as shown in Figure B12.3.3.2-4. Its advantages are that in-plane stresses (and localized stress concentrations) caused by the fasteners are eliminated. Manufacturing of the transparency is simplified considerably. The inner pane for this design is the fail-safe member as shown in Figure B12.3.3.2-5.

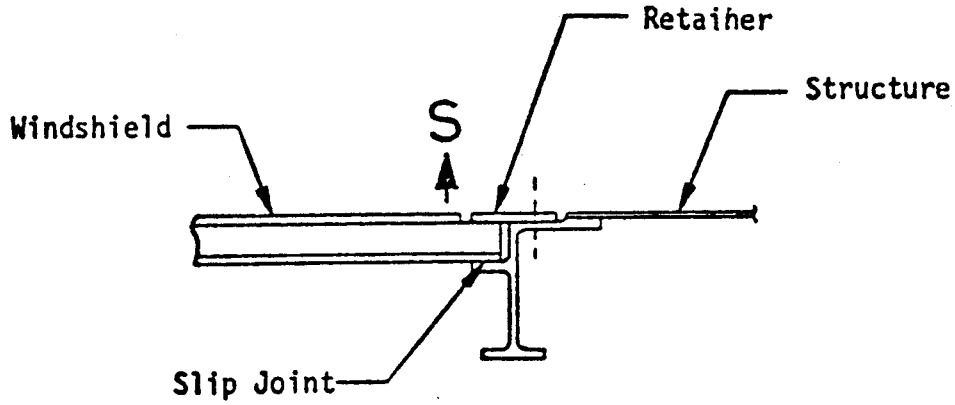


Figure B12.3.3.2-4 Slip Joint Transparency Installation

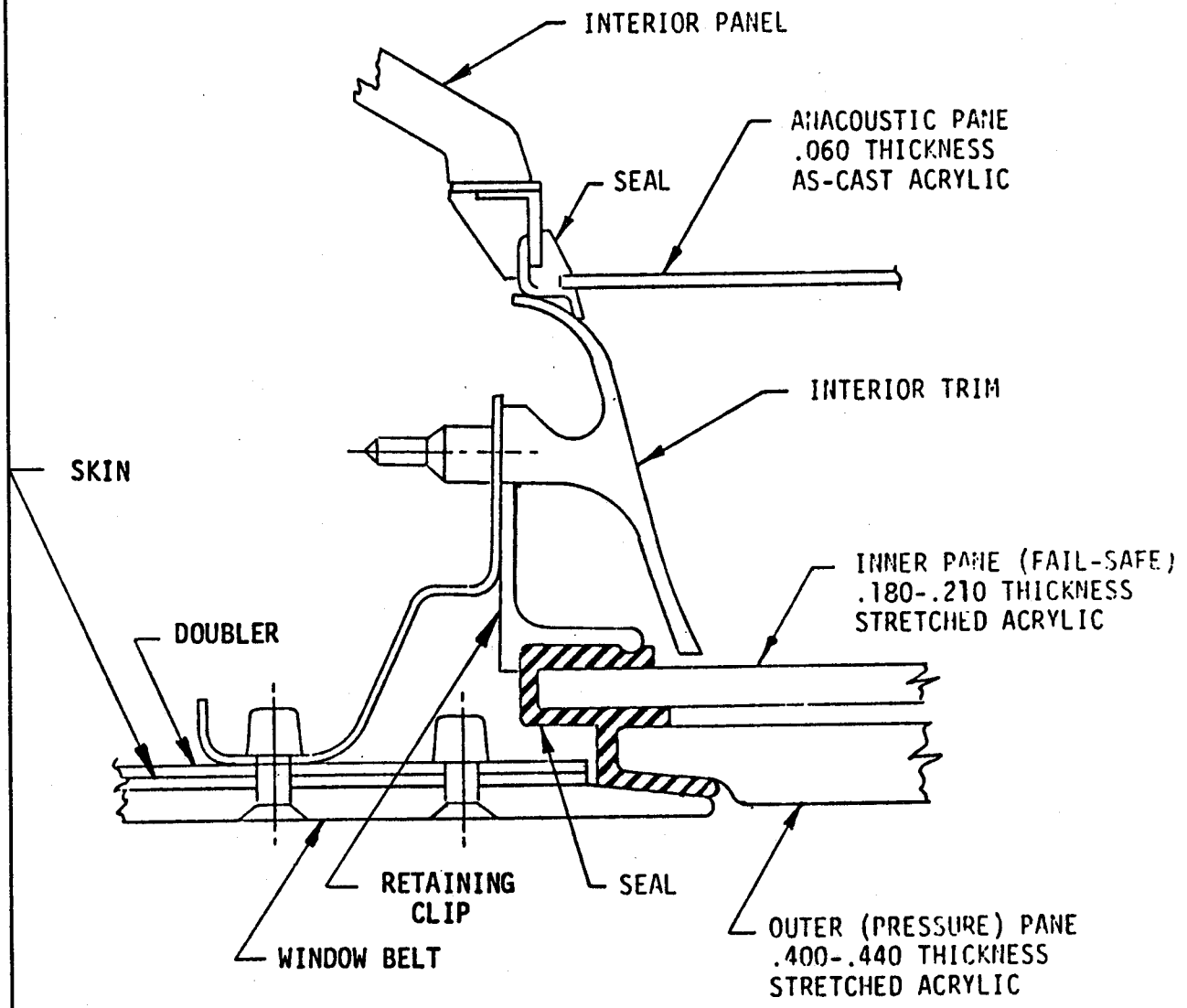


B12.3.3.2-5 Cross Section DC-10 Cabin Window Installation

A transparency installed with fasteners in oversize holes is generally associated with the type of windshield system that does not transfer primary aircraft loads across the cutout in the pressure shell. This system has the capability of transmitting loads developed in the transparency to the support structure in shear and tension as shown in Figure B12.3.3.2-6. Local bending moments may be developed in the fastener and the support flange. A method of utilizing this system is shown in Figure B12.3.3.2-7.

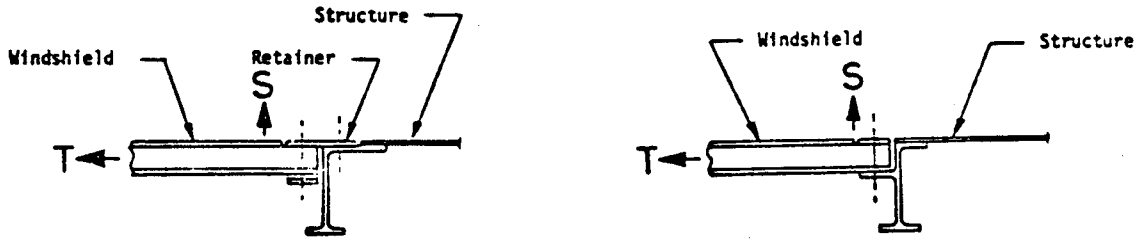


Figure B12.3.3.2-6 Transparency Installation with Single Row of Loose Fitting Fasteners

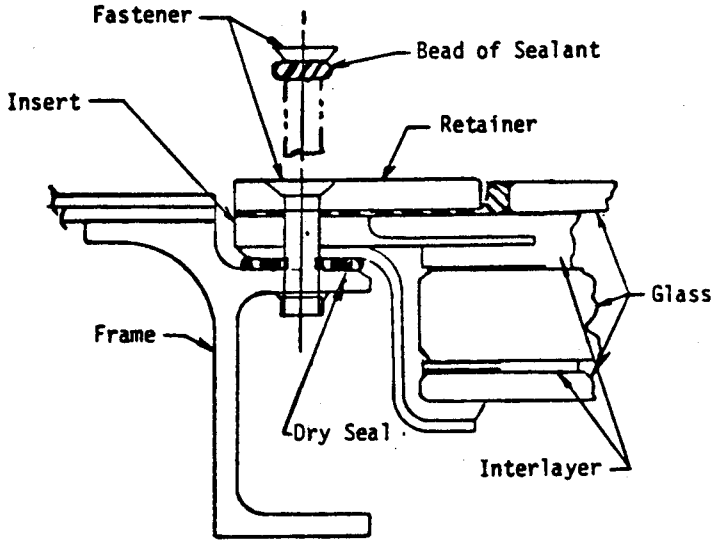


Figure B12.3.3.2-7 Edge Design for DC-9 Windshield

A transparency may be installed with fasteners in tight holes. This configuration generally reacts primary aircraft loads. This may be the lightest of configurations since it treats the transparency and surrounding structure as a single unit without the cutouts and discontinuities of other designs and transfers shear, tension, and bending moments. This configuration, shown in Figure B12.3.3.2-8, has two basic drawbacks: the comparatively large number of fasteners requires a high installation and removal time; and the fasteners need tight fitting holes to transfer a bending moment. This leads to additional installation and removal problems when the repairs are being accomplished in an environment other than existed in the aircraft manufacturer's factory. This type of installation may not meet the fail-safe requirements for commercial aircraft. The U.S. Air Force B-1 aircraft, Figure B12.3.3.2-1, uses this approach. An alternate one-bolt concept for the B-1 aircraft is reported in Reference B12-12.

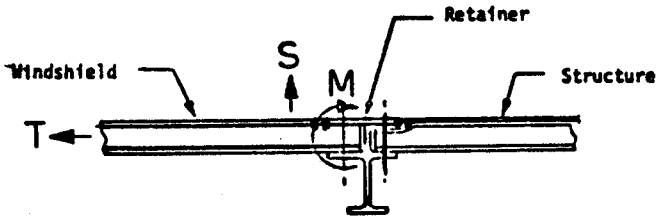


Figure B12.3.3.2-8 Transparency Installation with Double Row of Tight Fitting Fasteners

C. Transparency Material Current aircraft windshields are fabricated from either glass or plastic materials. The plastic materials currently in use are polycarbonate and stretched acrylic. The transparency material influences the edge design.

Glass transparencies are usually flat, multi-ply laminates consisting of a thick structural ply, an external face ply, and an internal ply, all separated by a soft interlayer. The configuration, shown previously in Figure B12.3.3.2-2, is a typical edge design.

Glass windshields are not bolt-through configurations. The structural glass ply is terminated short of the fasteners, and the load is transferred through the interlayer material, and metal inserts imbedded in the interlayer. A phenolic block replaces the structural glass ply in the area of the attachments.

An oversize, metal bushing is used to hold the plies apart. This prevents compression of the soft interlayer materials, especially at elevated temperatures.

The face ply stops short of the fasteners and is replaced by a metal retainer. The internal ply also terminates before the edge and is replaced with a phenolic block.

The configuration shown in Figure B12.3.3.2-2 is a single row, single shear attachment system. Pressurization loads are reacted by the fasteners in tension. Bending loads are minimal because of the high stiffness inherent in glass, the use of oversize holes, and the installation of a rubber seal between the transparency and support structure. Crazing is not a problem in this configuration, although edge delamination is.

Practically all current pressurized aircraft with plastic transparencies use either stretched acrylic or polycarbonate for their monolithic transparencies and as-cast or stretched acrylic and polycarbonate for their multi-ply transparencies. The reliability and service life for polycarbonate has not been established and should not be used until it is proven.

Plastic windshields are usually curved and may be cylindrical with a large radius, such as the B-1 bomber, or have a relatively small radius such as the F-15 and F-16. The stiffness of the plastic material is quite low when compared to glass or aluminum and the resultant deflection under pressure loading causes bending at the edge of the transparency.

D. Laminated Configuration The problems peculiar to a laminated, multi-ply configuration are different than those found in a monolithic configuration. The use of edge retainers, bushings and spacers, and the problem of delamination must be carefully considered in multi-ply laminated configurations. Glass configurations which utilize PVB as its interlayer have had a history of edge chipping where sealing and edge heating have not been incorporated.

Edge retainers should be flush with the face ply, as shown previously in Figure B12.3.3.2-2. The use of edge retainers that overlap the face ply and protrude into the airstream are not recommended for high performance aircraft, because of potential sealant erosion under the retainer as documented in Reference B12-14 and B12-15. The use of a Z-channel (Reference B12-16), as shown in Figure B12.3.3.2-9, has been used in the past to protect the edge from moisture incursion and has proven to be effective for subsonic aircraft when the outerply of a laminated configuration is thin (less than 0.08 in. thick).

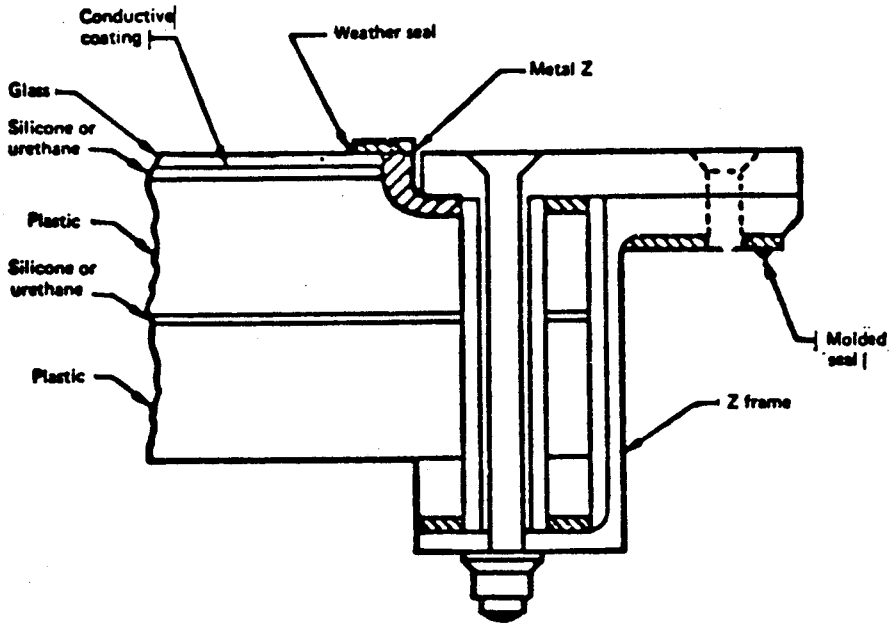


Figure B12.3.3.2-9 Edge Design for a Windshield Using Z-channel Sealing

Bushings are used in multi-ply configurations to hold the plies apart. This prevents compression of the soft interlayer during bolt torquing and at elevated temperatures.

Bushings are used in monolithic polycarbonate or acrylic transparencies, as well as multi-ply laminated transparencies, to increase the bearing area. These bushings should be bonded in the holes. It is recommended that those bushings installed in a single shear system have a shoulder to eliminate the possibility of the panel failing due to shearing of the adhesive between the panel and bushings. Asymmetrical loading by the single shear arrangement tends to exert a pullout force on the fastener and bushing as documented in a cyclic edge test reported in Reference B12-17.

E. Load Analysis Since the fastener system is inherently a structural weak point in the windshield design, careful consideration must be given to the stresses induced in the material by the fasteners. The load distribution and failure potential is effected by edge distance, fastener spacing, load distribution in multi-ply laminates, and whether or not the fasteners are reacted in single shear or double shear. For plastic materials consideration must be given to the critical stress for crazing.

It requires that the designer achieve: minimum edge distance in order to provide as much vision as possible for the pilot; and maximum bolt spacing in order to reduce the number of fasteners for better maintainability.

Step one in defining edge distance and hole spacing is to calculate edge load. The analysis varies depending on whether the transparency is curved or flat.

A curved shell resists internal pressurization as hoop tension where the axial edge load is a function of the transparency radius and pressure loading. In addition to an axial load, the edge of a transparency also transfers shear loads and bending moments to the fuselage support structure as shown in Figure B12.3.3.2-10. A curved shell with a large radius (approximately 100 in. and greater) is assumed to react the pressurization loading as a flat plate.

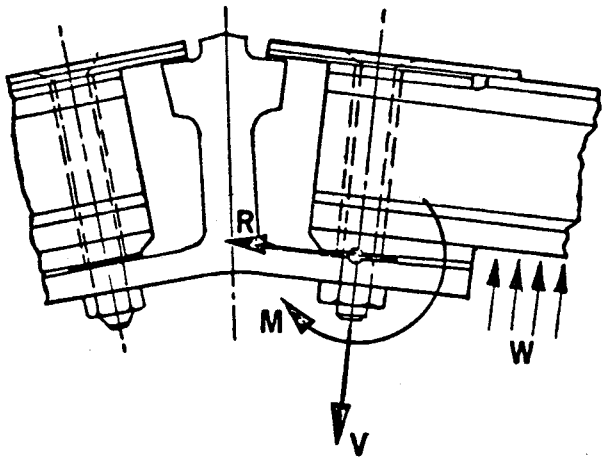


Figure B12.3.3.2-10 Edge Reactions Due to Pressurization Loading for a Curved Shell with Medium Radius

The magnitude of the localized edge bending moments depends on the stiffness of the edge attachments and support structure. The use of a computer program, such as CASD, is recommended to produce an accurate final analysis to account for the localized bending moments that result from the stiffness of the bolts and support structure and to account for the total edge reactions, axial, shear, and bending moments that might occur.

The primary mode of failure in the attachment area is bearing of the bolt or bushing against the transparent material. If the pressure is high enough the plastic material adjacent to the hole will start to crush and flow, thus, allowing the bolt or bushing to move and elongate the hole.

Bearing allowables for polycarbonate and stretched acrylic materials are given in Reference B12-8. Maximum operating temperatures should be considered in selecting the ultimate bearing allowable. For stretched acrylic and polycarbonate materials consideration must also be given to crazing when the materials are loaded in bearing above the critical stress level. Bearing allowables are not needed for glass, since glass windshields use inserts and the interlayers to transfer the transparency loads to the attachments.

The determination of stress distribution in a multi-ply, laminated transparency with a single shear attachment system is dependent on: the capability of the interlayer material to transfer shear between structural plies, material temperature, and the stiffness of the support structure and bolt. Maximum stress will occur in the structural ply closest to the support structure. The percentage of load carried by this ply may be calculated by use of the finite element stress analysis and a computer program. Reference B12-18 presents a computer program method that may be used to determine stress distribution in a multi-ply laminate.

The criterion for hole spacing in a flat glass windshield is generally based on the requirements for bird impact resistance and for the need to maintain a pressure seal between the transparency and the support structure.

Concern must be given to bolt strength. It is important that sufficient bending strength be provided to prevent permanent bending deformation of the attachments under limit load so that the bolts can be readily removed in maintenance operation.

F. Hole Preparation Hole drilling in acrylic and polycarbonate materials is a critical procedure for the life of the transparencies. If proper precautions are not taken, stress cracking or crazing will result in the loss of much of the impact resistance of the plastic material.

As noted in Reference B12-8 all of the transparent plastics materials currently available are susceptible to crazing, though in widely varying degrees. Crazing has been defined as fine cracks which may extend in a network over or under the surface or through a plastic. These fine cracks are often difficult to discern, because they are approximately perpendicular to the surface, very narrow in width, and usually not over 0.001 inch in depth. They can be seen by reflection from their surfaces and appear as bright lines when the specimen is viewed at varying angles to the incident light. Refer to Materials & Process Engineering for appropriate DPS callouts for the detail drawings.

Performance data published by General Electric Company (Ref. B12-19), a manufacturer of lexan polycarbonate resin, state that crazing of polycarbonate can be caused by a combination of tensile stress, heat and/or moisture. Where heat and moisture will be encountered, tensile loads should not exceed the 1500-2000 psi range.

The results of polycarbonate edge tests have been reported in Reference B12-13 as follows:

"At the conclusion of the tests very fine stress crazing was noted in the test section of the polycarbonate specimens. It was believed that contamination incurred from handling the specimens during the tests caused the stress crazing. Additional tests were conducted where the specimens were carefully cleaned and handled with clean cotton gloves. Stress crazing did not occur in these tests, which demonstrated that exposed surfaces of polycarbonate must be protected from contamination to prevent stress crazing when the material is subjected to tensile stresses.

"The results of these tests.....demonstrate the sensitivity of polycarbonate to contamination of many types. It is considered mandatory to protect the material from hostile environments to prevent crazing when the material is subjected to tensile stresses. A procedure has been established to preclude contamination in the edge attachment holes for the B-1 windshield. This procedure consists of thoroughly cleaning the bearing hole and bushing with aliphatic naphtha and

isopropyl alcohol, followed immediately by bonding the bushing in place with silicone sealant to preclude contamination of the polycarbonate prior to installation. After installation, the edge attachment area is considered adequately sealed."

Concerning crazing in stretched acrylic material, Reference B12-8 states that stretching of acrylic plastics represents the most effective preventive measure against crazing.

G. Mechanical Behavior of the Material Creep and fatigue are encountered in windshield transparencies. Creep is a time-dependent deformation produced normally at high temperatures in most metals, but in plastics it can occur at room temperature. Fatigue is associated with the cyclic loading conditions encountered throughout the life of an aircraft and must be considered for a long-life, cost effective system.

The following statement is contained in Reference B12-19, "As with all materials, the resistance of LEXAN (polycarbonate) to creep - permanent deformation under continued stress - changes with environmental and load variables. For long term service at room temperatures, loadings should not exceed 1,500-2,000 psi."

Cyclic creep tests and fatigue tests were performed on an edge attachment design concept for the B-1 bomber (Figure B12.3.3.2-1) as reported in Reference B12-13. Specific temperatures, stress levels, and time periods were based on typical B-1 mission profiles.

H. Temperature Effects Cyclic temperatures have a deleterious effect on the life of an aircraft windshield, especially at the edges of a multi-ply configuration where differential material expansion and contraction are more prominent.

Laminated, multi-ply transparencies, such as acrylic/interlayer/polycarbonate, must be designed for edge frame clearance. The face ply generally is not bolted, whereas, the structural ply is bolted. Differential expansion (or contraction) is stimulated by the temperature gradient that exists between exterior and interior surfces, as well as by the difference in the coefficients for thermal expansion. Bending in the transparency is also promoted by a temperature gradient and results in tension (or stretching) on the exterior surface and compression on the interior surface.

I. Sealing A seal is required for pressurized aircraft transparencies at the interface of the transparency and support structure and in the fastener holes in order to maintain pressurization and to prevent moisture ingress.

A dry seal is generally preferred to a wet seal for pressurization because of the problems associated with transparency replacement. A wet seal generally bonds the transparency to the frame making removal difficult. In addition, the sealing material requires several hours to cure, resulting in excessive down time.

The use of wet sealant is acceptable for the installation of the attachments. It may be injected into the space between the bolt and bushing as shown previously in Figure B12.3.3.2-2 or installed under the bolt head as shown in Figure B12.3.3.2-7.

B12.3.3.3 Bird Impact Design

Collisions between birds and aircraft have become one of the major flight safety problems of the jet age. Since approximately 75% of worldwide bird strikes on commercial aircraft and 50% on U.S. military aircraft occur on or near airports; every effort should be made to reduce and/or remove bird populations on and around airports. With the realization that aircraft and birds will always share the same sky, aircraft must be designed to resist the impact of a collision with a bird.

The response of an aircraft transparency to a bird strike may be characterized in several ways: penetration, bouncing, and bagging.

Bird penetration refers to a fracture of the transparent material and occurs with little or no deformation of the transparency. This condition can result in loss of the aircraft and has appeared to increase during the years following the transition from reciprocating power plants to jet engines accompanied by higher takeoff/landing velocities.

Bird bouncing refers to those transparency systems that rely on materials to repel a bird. The bird is deflected off the transparency and the deflected debris retains a high proportion of the initial energy.

Glass windshields may rely on the bird bagging concept. For this method the glass panes fracture at impact and allow the interlayer to deform and absorb energy. Deformation is permanent.

A. Design Requirements Bird impact requirements have been specified in AFSC DH2-1, MIL-A-008865, MIL-W-81752, and Federal Aviation Regulations (References B12-5 and B12-20 thru B12-21 and B12-22). Commercial aircraft must be certified to FAA bird impact requirements.

To ensure the completion of flight objectives following a bird strike all future aircraft (including helicopters and rotor craft) should satisfy the following requirements.

1. Internal panes must be made of non-splintering material.

2. The windshields, windows, canopy, all supporting structure, and latching mechanisms that are positioned ahead of and protecting the pilot and crew shall be designed to withstand the impact of a four-pound bird when the velocity of the airplane (relative to the bird along the airplane flight path) is equal to the maximum operational, true airspeed achievable in level flight at altitudes up to 8000 feet. The most adverse temperatures shall apply after considering: the maximum hot temperatures (including aerodynamic heating), anti-icing system, maximum temperature, coldest temperature expected on the windshields/windows up to 8000 feet (AGL) (Reference B12-22).

   Note: The coldest temperature should include a descent from a high altitude cruise condition (cold soak). The most critical maximum hot temperature for bird impact would be based on aerodynamic heating effects for supersonic aircraft and ground soak conditions or transparency heating system failure (if applicable).

3. As a minimum goal the selected materials for the transparencies and supporting structure must be capable of withstanding a bird impact with such a low order of fragmentation that the pilot or crew would not be injured. Head clearance must be taken into account to preclude the possibility of pilot or crew injury from excessive deflections during bird impact.

4. Transport type aircraft transparencies shall be designed to withstand a bird impact without penetration.

5. No additional cockpit equipment shall be permitted to become a "secondary impact" missile that could conceivably injure a crew member.

6. The design of windshields in front of the pilot and crew should be such that in the event of bird impact not more than 50 percent of the aircrew's forward visibility will be lost.

7. Canopy mechanisms that are important to ingress/egress or emergency escapes shall be designed to withstand bird impacts without jamming, and pyrotechnic systems utilized for emergency escapes shall be designed to withstand the effects of bird impacts without damage or activation.

B12.3.4 Testing

B12.3.4.1 Introduction

This section is directed toward defining the testing that must be performed to assure that a final transparency design will perform under all of the intended operational requirements of the aircraft.

Testing is costly. Before any testing is accomplished, careful consideration should be given to identifying meaningful tests. Oftentimes, existing data may be used to satisfy the design requirements; in some cases, it can be used for comparative purposes to aid in developing meaningful tests that are less costly.

Transparency testing may be divided into three categories:

A. Design development
B. Preproduction qualification
C. Production part acceptance

Light transmission, haze, deviation, and distortion should be evaluated on monolithic specimens, including specimens with appropriate coatings. Laminated specimens should be evaluated for all optical parameters, including the effects of index of refraction and reflections from the various surfaces.

B12.3.4.2 Design Development Testing

The design of a new transparency system involves a wide range of tests that may be conducted on full size windshields or canopies. These tests may be conducted for impact and structural integrity, to investigate cyclic pressure and thermal effects throughout a realistic service life, to define the transparency reaction to a high speed environment, to determine optical clarity or to substantiate reliability. Some of these tests may be repeated as part of a preproduction qualification program, and/or a production part and acceptance program.

B12.3.4.2.1 Bird Impact Testing

All new transparency designs, whether commercial or military, that are located in front or adjacent to the flight crew must be bird impact resistant. Generally, the transparencies tested must be full size representatives of production parts. The transparencies must be mounted on production representative support structure and sufficient surrounding structure must be provided to take into account the near-field and far-field effects of the bird impact forces. The tests should be conducted under environmental extremes. To accomplish this series of tests, generally three to five transparencies are required from each transparency manufacturer. Cost normally dictates that these parts are not processed for optical quality.

B12.3.4.2.2 Projectile Impact Testing

Projectiles can be categorized many ways: hail is a frequent occurrence, dropped tools or equipment impact the transparency, jet blast emanating from an aircraft in front of a transparency cause gravel, sand, or other small particles found on runways to hit the transparency. Many types of projectiles may be found under combat conditions, such as fragments, ballistics, and other foreign objects.

Usually, if a transparency meets bird impact requirements, it will also withstand hail impact and meet most safety requirements. Exceptions are: monolithic transparencies will not meet fail-safe criteria and a fully tempered glass, outer ply may be cracked thereby jeopardizing vision.

Jet blast may cause objects from the runway to hit the transparency and cause pitting of the outer surface, but the structural integrity is not seriously affected nor usually the optical quality. A sharp stone might break an outer glass ply, but it does not happen often, and testing for such conditions should not be a requirement.

Testing requirements for combat projectile impact conditions must be defined by the customer to fit the applicable aircraft.

B12.3.4.2.3 Endurance Testing

Full size transparency specimens should be tested under operational conditions to meet the minimum expected aircraft service life requirements. These tests can take two forms, simulated life testing, and flight testing. The simulated life endurance test should be developed to represent the mission profiles of the intended aircraft. The frequencies of cycling pressure and temperatures must be developed as a fail-safe test to meet the required service life of the transparency.

If possible, the effects of aerodynamics should also be duplicated. The number of cycles per service life should be repeated several times. By repeating the test four times, it is intended to compensate for aging and the effects of atmospheric conditions (such as ultra-violet, cleaning and sunlight that are difficult to duplicate in a test program), and to provide a statistically developed data base for reliability of the test.

Included in the test procedures should be the cold soak and the hot soak temperature conditions to represent operational conditions when the aircraft is sitting on the ground.

Before concluding the life cycle tests, one part from each of the transparency manufacturers should be subjected to design ultimate loads (two times normal pressure) at room temperature.

In the event that one or more of the parts survive the life cycle testing, it is recommended, if feasible, that the part be included in any on-going bird test program to determine if the materials have deteriorated because of cyclic fatigue.

B12.3.4.3 Preproduction Qualification Testing

Those tests that verify the design and manufacturing process and thus provide a baseline for subsequent acceptance tests are called qualification tests. Qualification testing is conducted to accomplish two functions: Preproduction Qualification Tests and Production Part Acceptance Tests.

Preproduction qualification tests are defined as a series of formal contractual tests that are conducted to insure design integrity over a specified operational and environmental range. The tests should be conducted on prototype or preproduction items fabricated to the proposed production design specifications and drawings. These tests are a constraint to production release on programs which involve volume acquisition. The preproduction qualification tests include those contractual reliability and maintainability demonstration tests required prior to production release.

Preproduction qualification testing includes all tests required to verify design requirements and encompasses the following areas:

Structural
Optical
Electrical
Environmental
Systems interface

Generally, these types of tests have been accomplished during the design and development stage and verification of performance is conducted to officially certify compliance with the operational requirements.

B12.3.4.4 Production Part Acceptance Testing

Production part acceptance tests are defined as a series of formal contractual tests that are conducted to insure the effectiveness of the manufacturing process, equipment, and procedures. These tests are conducted on a production part taken at random from the first production lot and are repeated if the process is changed significantly and when a second or alternate source is brought on line.

These non-destructive tests should be repeated on a sampling basis for some tests and on all parts for others. Suggested items to be tested would include the heating systems and electrical systems. Thermal effects, optical quality, dimensional fit, and workmanship should be verified thorughout the production process.

## REFERENCES

B12-1 Lawrence, J. H., Guidelines for the Design of Aircraft Windshield/Canopy Systems, AFWAL-TR-80-3003, February 1980.

B12-2 MIL-STD-850B, "Aircrew Station Vision Requirements for Military Aircraft", November 1970.

B12-3 Society of Automotive Engineer, Inc., "Pilot Visibility from the Flight Deck Design Objectives for Commercial Transport Aircraft", AS 580B, November 1978.

B12-4 Civil Aeronautics Manual 4b, "Airplane Airworthiness; Transport Categories", May 1960.

B12-5 Federal Aviation Regulations, Airworthiness Standards: Transport Category Airplanes, Part 25, Department of Transportation, June 1974.

B12-6 Transparent Areas, Anti-Icing, Defrosting and Defogging System, General Specification for, MIL-T-5842, Dept. of the Air Force, July 1953.

B12-7 Grether, W. F., Optical Factors in Aircraft Windshield Design as Related to Pilot Performance, AMRL-TR-73-57, July 1973.

B12-8 MIL-HDBK-17A, Part II, Plastics for Aerospace Vehicles, Part II, Transparent Glazing Materials, June 1977.

B12-9 Greene, F. E., Testing for Mechanical Properties of Monolithic and Laminated Polycarbonate Materials, Part I, Test Results and Analysis, AFFDL-TR-77-96, Wright-Patterson Air Force Base, Ohio, October 1978.

B12-10 Ward, John W., "Aircraft Windshields Heated by Means of Transparent Conductive Films", Applications and Industry, Number 16, American Institute of Electrical Engineers, pages 408-416, January 1955.

B12-11 Twomey, R. C., Effects of Laboratory Simulated Precipitation Static Electricity and Swept-Stroke Lightning on Aircraft Windshields, AFFDL-TR-76-75, Wright-Patterson Air Force Base, Ohio, July 1976.

B12-12 Lawrence, James H., Jr., Et al, Windshield Technology Demonstrator Program - Detail Design Options Study, AFFDL-TR-77-1, Wright-Patterson Air Force Base, Ohio 45433, September 1977

B12-13 Mahaffey, J. E., "Material Evaluation. B-1 Crew Module Windshield", Conference on Transparent Aircraft Enclosures, page 175, AFML-TR-23-126, Wright-Patterson Air Force Base, Ohio, June 1973.

B12-14 Hoffman, J. B., Evaluation of Windshield Materials Subjected to Simulated Supersonic Flight Environments, AFFDL-TR-77-92, Wright-Patterson Air Force Base, Ohio, September 1977.

B12-15 Hoffman, J. B., Evaluation of Aircraft Windshield in a Simulated Supersonic Flight Environment, AFFDL-TR-79-3058, Wright-Patterson Air Force Base, Ohio, June 1979.

B12-16 Beaumont, P. N. and Parker, S., "Windshield Design Concepts", Conference on Transparent Enclosures, AFML-TR-73-126, Wright-Patterson Air Force Base, Ohio, June 1973.

B12-17 Lawrence, J. H., Jr., Windshield Technology Demonstrator Program - Canopy Detail Design Options Study, AFFDL-TR-78-114, Wright-Patterson Air Force Base, Ohio, September 1978.

B12-18 Denke, P. H. and Hoffman, J. B., The Determination of Deflection and Stress Distribution for a Laminated Transparent Beam, AFFDL-TR-76-114, Wright-Patterson Air Force Base, Ohio, March 1977.

B12-19 Lexan Product Manual, General Electric Co.

B12-20 Air Force Systems Command Design Handbook, Airframe, DH2-1 Department of the Air Force, Andrews AFB DC, October 1978.

B12-21 Windshield Systems, Fixed Wing Aircraft - General Specification for, MIL-W-81752, 23 April 1970.

B12-22 Lawrence, J. H., Jr. and Coker, M. J., Windshield Bird Strike Structure Design Criteria, AFFDL-TR-73-103, October 1973.